The Roles of a Conserved MAP Kinase Pathway in the Regulation of Development and Secondary Metabolism in *Aspergillus* Species

Dean Frawley, B.Sc.

Maynooth University
National University
of Ireland Maynooth

Thesis submitted to Maynooth University for the degree of Doctor of Philosophy

October 2020

Supervisor:

Dr. Ozgur Bayram

Fungal Genetics & Secondary

Metabolism Laboratory

Biology Department

Maynooth University

Maynooth, Co. Kildare

Head of Department:

Prof. Paul Moynagh

Biology Department

Maynooth University

Maynooth, Co. Kildare

Table of Contents

Chapter 3: Results - Roles of the pheromone module kinases and the HamE scaffold in the regulation of *A. nidulans* development and secondary metabolism..59

Chapter 4: Results - The pheromone module is conserved in *A. flavus* and is required for regulation of sporulation, sclerotia formation and secondary metabolism 106

Chapter 5: Results - The pheromone module regulates sporulation, secondary metabolism and stress responses in the human pathogen *A. fumigatus* 147

Chapter 6: General Discussion and Overall Conclusions 189

Declaration of Authorship

This thesis has not previously been submitted, in whole or in part, to this, or any other University, for any other degree. This thesis is the sole work of the author, except where otherwise stated.

Dean Frawley, BSc.   *[signature]*   **Date:**   **24/09/2020**

Acknowledgements

Firstly, I would like to thank my supervisor Dr. Ozgur Bayram for providing me with the opportunity to perform my 4th year undergraduate and postgraduate research in his laboratory. I have learned a lot of useful skills over the years and I feel like this lab has made me more mature, both as a researcher and as a person.

I would like to also express my gratitude to the past members of the FGSM lab, who helped train me extensively and were always very helpful whenever I was struggling, especially when I first started in the lab.

I am thankful for my thesis committee advisor and assessor team, consisting of Dr. Paul Dowling and Prof. Kevin Kavanagh. I really appreciate the feedback you both have given me over the years and your guidance throughout the PhD.

Thank you to all of the postgraduates and staff in the biology department. You guys have all made the PhD experience easier and reminded me of the important things in life. I'd like to give a special mention to some people that have been particularly special to me. Dr. Anatte Margalit, Dr. Felipe Guapo de Melo, Dr. Sandra Murphy and Dr. Dearbhlaith Larkin. You guys always made me feel like I belonged in the department, especially when I was first starting out and I always loved having chats with you all.

I'd like to thank all of my undergraduate bio buddies: Luke Byrne, Kate Flynn, Ciara Gilmartin, Aisling Gilroy and Ryan Coyne. You guys made me love coming into college each day, especially seeing as I had no mates in 1st year! I loved our little trips together, whether we were going to Galway, Edinburgh or even just to the Maynooth playground when we went and acted like big kids for the day because we were all on the verge of mental breakdowns! I miss you all and I know that we don't get to see each other much but whenever we do, I know we'll always be close. Thank you all.

I would like to give a special thank you to the big dog Dr. Betim Karahoda. If it weren't for you, I don't think I would have ever been able to make it through the first year of this PhD. You have always been like a protective big brother to me and I have always been amazed at just how good you were in the lab, how much information you knew and how you always seemed to make experiments work first time (I'm still struggling to do that!). Thank you for all the long walks and €1 coffee breaks (which weren't as good when it was raised to €1.50). I also loved our lunch breaks and anytime we would end up getting free food together! I'd also like to say thank you to you and Melissa. You both have always been so nice to me over the years and I always wish the best for the both of you.

I'd like to thank some people who I didn't get to see often over the past few years but anytime I did see them, it would always make me happy. These are John Granahan, Olena Yavorska and Dylan Fitzgerald. You guys have always been some of my closest friends and anytime I'm with any of you, things just seem easier and I'm always able to take my mind off the PhD stresses and relax. John, thank you for all the drinks and chats over the years, including back when we were little band nerds having jamming sessions in Liam's house to when we were cute little undergrads going out for our Christmas parties and all of the years since then. Olena, thank you for all the long walks and gossip chats, all of our sushi lunches and all of our depressedarados/netflix sessions. Dylan, my main boi, thank you for supplying me with the occasional meme to get me through the day and then avoiding all forms of contact with me for months

on end. Half of the time I don't know if you're still alive but whenever you do appear, I know that things will always be the same with us. I miss the good ol' days sitting in Costa together for like 3 hours, doing absolutely nothing productive with our time and judging everybody.

Now a special mention for the big daddy himself Peter Lillis. Thank you for getting me through this PhD with your daily fun facts and your sassy attitude. I will miss the days when you would break excel, regularly manipulate your data and when you would somehow always find a way to automate your whole life. However, I still hate you because of the times when you would lower my chair and when you would tell me to change the colour on a powerpoint slide, just to then tell me it looks shit and to change it back to the way it was previously… But overall, thank you for all the support and for all the Eiffel towers over the years <3

As promised, I'd like to devote a paragraph thanking the best person/friend/girlfriend a guy could ask for, Dr. Ciara Tierney/Tierno/Toe. Thank you for everything. From the very start, I always knew we would be close. You've always been such a good support for me throughout this PhD and without you, I don't think I would have been able to get through this whole experience. Thank you for all the chats early on in the PhD where I would come into your lab and get hit by a wall of heat and when we would sit outside the common room and you would have to listen to me complain about literally everything and everyone. Who would have thought that we would go from you completely rejecting me at the summer party to being all loved up <3 Thank you for always making me laugh and for all of the adventures, I can't wait to have plenty more with you. Thank you especially for always putting up with me even when I get stressed over the most ridiculous things (eggs! I need eggs!). Thanks to you, I always want to be a better person and enjoy life properly. Now I can't imagine things without you. You've always been my rock, I love you.

I'd love to give a huge thank you to my amazing family, who have been such a good support for me my whole life. Mam and Dad, you have always made sure to raise me right and you both have made me into the man I am today. I couldn't be more grateful. Thank you for always trying to give me the best life possible while encouraging me to do well and to be a good person. You both have gone through some very tough challenges in life and I'd like you to know that I've always admired you both so much. I'd like to also say that my entire family have been amazing to me and I love you all, thank you for being great!

As a final mention, I'd like to dedicate this thesis to my Nanny Catherine Masterson, who sadly passed away on the 29th September 2016, a few days before I started this PhD. I would have loved to have you there on my graduation day and for many years after. I know you would have been so proud. Every time I miss you, I look at my arm and tell myself 'I'm fine'. You always made me appreciate the small, essential things in life. Thank you for everything. I love you.

Oral Presentations

- Maynooth University Postgrad/Postdoctoral Seminar Series, 17th October 2017: **'Analysis of HamE as a scaffold in the *Aspergillus nidulans* AnFus3 Module'.**

- Maynooth University Postgraduate/Postdoctoral Seminar Series, 20th September 2018: **'Characterising the roles of HamE in *A. nidulans* development and secondary metabolism'.**

- '3 minute thesis competition', Maynooth University, 11th October 2018: **'Investigating the control of toxin production in fungal species'.**

- Microbiology Society Annual Conference, 9th April 2019: **'The HamE scaffold positively regulates MpkB phosphorylation to promote development and secondary metabolism in *Aspergillus nidulans'*.**

- Maynooth University Postgraduate/Postdoctoral Seminar Series, 28th May 2019: **'Regulation of development and aflatoxin production in *Aspergillus flavus via* a conserved MAP kinase pathway'.**

- Maynooth University Biology Research Day, 5th June 2019: **'A conserved MAP kinase pathway regulates development and secondary metabolism in *Aspergillus* species'.**

- Maynooth University Biology Summer School, 12th August 2019: **'The use of genetic engineering techniques in microbiology-based research.'**

Poster Presentations

- Maynooth University Biology Research Day, 6th June 2017: **'The Potential Scaffolding Role of HamE in the *Aspergillus nidulans* AnFus3 Module'.**

- Maynooth University Biology Research Day, 5th June 2018: **'Characterising the role(s) of HamE, a potential scaffold in the *Aspergillus nidulans* AnFus3 module'.**

- 30th Fungal Genetics Conference, Asilomar, 13th March 2019: **'The HamE scaffold positively regulates MAP kinase signal transduction to promote development and secondary metabolism in *Aspergillus nidulans'.***

- 30th Fungal Genetics Conference, Asilomar, 14th March 2019: **'Assembly of a heptameric STRIPAK complex at the nuclear envelope is required for coordination of light-dependent multicellular fungal development with secondary metabolism in *Aspergillus nidulans'.***

- 15th European Conference on Fungal Genetics, 18th February 2020: **'A conserved mitogen-activated protein kinase pathway regulates development and secondary metabolism in three *Aspergillus* species.**

Publications (First author)

FRAWLEY, D., KARAHODA, B., SARIKAYA BAYRAM, O. & BAYRAM, O. 2018. The HamE scaffold positively regulates MpkB phosphorylation to promote development and secondary metabolism in *Aspergillus nidulans*. *Sci Rep,* 8**,** 16588, 10.1038/s41598-018-34895-6.

FRAWLEY, D., GRECO, C., OAKLEY, B., ALHUSSAIN, M. M., FLEMING, A. B., KELLER, N. P. & BAYRAM, O. 2020. The tetrameric pheromone module SteC-MkkB-MpkB-SteD regulates asexual sporulation, sclerotia formation and aflatoxin production in *Aspergillus flavus*. *Cell Microbiol*, 10.1111/cmi.13192.

FRAWLEY, D., STROE, M. C., OAKLEY, B. R., HEINEKAMP, T., STRASSBURGER, M., FLEMING, A. B., BRAKHAGE, A. A., BAYRAM, O. 2020. The pheromone module SteC-MkkB-MpkB-SteD-HamE regulates development, stress responses and secondary metabolism in *Aspergillus fumigatus*. *Front Microbiol,* 11:811, 10.3389/fmicb.2020.00811.

FRAWLEY, D. & BAYRAM. O. 2020. Identification of SkpA-CulA-F-box E3 ligase complexes in pathogenic *Aspergilli*. *Fungal Genet Biol,* doi.org/10.1016/j.fgb.2020.103396.

FRAWLEY, D. & BAYRAM. O. 2020. The pheromone response module, a mitogen-activated protein kinase pathway implicated in the regulation of fungal development, secondary metabolism and pathogenicity. *Fungal Genet Biol.*

Publications (Co-author)

ELRAMLI, N., KARAHODA, B., SARIKAYA-BAYRAM, O., **FRAWLEY, D.**, ULAS, M., OAKLEY, C. E., OAKLEY, B. R., SEILER, S. & BAYRAM, O. 2019. Assembly of a heptameric STRIPAK complex is required for coordination of light-dependent multicellular fungal development with secondary metabolism in Aspergillus nidulans. *PLoS Genet,* 15**,** 10.1371/journal.pgen.1008053.

SILVA, L. P., **FRAWLEY, D.**, JOSE DA SILVA., L., TIERNEY, C., FLEMING, A. B., BAYRAM, O., & GOLDMAN, G. 2020. Putative membrane receptors contribute to activation and efficient signaling of Mitogen-Activated Protein Kinase cascades during adaptation of *Aspergillus fumigatus* to different stressors and carbon sources.

BAYRAM, O., SARIKAYA-BAYRAM, O., KARAHODA, B., THIEME, S., ELRAMLI, N., **FRAWLEY, D.**, MCGOWAN, J., FITZPATRICK, D., ULAS, M., SCHMITT, K., JOSE DE ASSIS, L., VALERIUS, O., GOLDMAN, G & BRAUS, G. H. (**Manuscript prepared for submission**). Control of multicellular fungal development by F-box receptors of SCF type Cullin Ring Ligases.

Awards

- 'John and Pat Hume Postgraduate Scholarship': Maynooth University, 27th June, 2016.

- '1st place poster presentation prize': 6th Biology Research Day, Maynooth University, 6th June 2017.

- '2018 Government of Ireland Postgraduate Scholarship': Irish Research Council, 27th March, 2018

- 'Runner-up poster presentation prize': 7th Biology Research Day, Maynooth University, 5th June 2018.

- 'Society conference travel grant': Awarded by the Microbiology society to present at the annual conference in the ICC Belfast, UK.

- '1st place oral presentation prize': 8th Biology Research Day, Maynooth University, 5th June 2019.

Table of Abbreviations

Abbreviation	Full Name
˚C	Degree Celsius
Δ	Deletion
μ	Micro
aa	Amino acids
ASPGD	*Aspergillus* genome database
BIFC	Bimolecular fluorescence complementation
BLAST	Basic local alignment search tool
BSA	Bovine serum albumin
CC	Coiled coil
cDNA	Complementary deoxyribonucleic acid
CPA	Cyclopiazonic acid
CWI	Cell wall integrity
DAPI	4′,6-diamidino-2-phenylindole
DEPC	Diethylpyrocarbonate
DIC	Differential interference contrast
DIG	Digoxigenin-11-UTP
DMATS	Dimethylallyl tryptophan synthetase
DMSO	Dimethyl sulfoxide
DNA	Deoxyribonucleic acid
DTT	Dithiothreitol
EDTA	Ethylenediaminetetraacetic acid
EGF	Epidermal growth factor
ESID	Extracellular sporulation inducing factor
Fab	Antigen binding fragment
FOC	Fold of control
GDP	Guanosine diphosphate
GFP	Green fluorescent protein
GH	Glycine-Histidine
GMM	Glucose minimal medium
GPCR	G-protein coupled receptor

GTP	Guanosine triphosphate
HA	Human influenza hemagglutinin
HAM	Hyphal anastomosis mutant
HOG	High osmolarity gylcerol
HRP	Horseradish peroxidase
IgG	Immunoglobulin
JIP	JNK interacting proteins
JNK	c-Jun N-terminal kinases
Kb	Kilo basepairs
kDa	Kilo Daltons
KSR1	Kinase suppressor of Ras 1
LB	Lysogeny broth
LC	Liquid chromatography
M	Molar
MAPK	Mitogen-activated protein kinase
MAP2K	Mitogen-activated protein kinase kinase
MAP3K	Mitogen-activated protein kinase kinase kinase
ml	Millilitre
mm	Millimetre
mM	Millimolar
mRFP	Monomeric red fluorescent protein
mRFP-H2A	Monomeric red fluorescent protein-Histone 2A
mRNA	Messenger ribonucleic acid
MS	Mass spectrometry
NADPH	Nicotinamide adenine dinucleotide phosphate
NGF	Nerve growth factor
nm	nanometre
NRPS	Non-ribosomal peptide synthetase
ORF	Open reading frame
PAD	Photodiode array director
PAK	P21-activated protein kinase
PAS	Periodic acid-Schiff
PBS	Phosphate buffered saline

PC12	Pheochromocytoma
PCR	Polymerase chain reaction
PDA	Potato dextrose agar
PDZ	Postsynaptic density, Disc large, Zo-1
PH	Pleckstrin-homology
PIPES	Piperazine-N,N'-bis (2-ethanesulfonic acid)
PKC	Protein Kinase C
PKS	Polyketide synthase
PMSF	Phenylmethylsulfonyl fluoride
PN	Penicillin
PSD	Postsynaptic density
qPCR	Real time/quantitative polymerase chain reaction
RA	Ras-associated
RACK1	Receptor for activated C kinase 1
RCF	Relative centrifugal force
RP-HPLC	Reversed-phase high performance liquid chromatography
RPM	Revolutions per minute
RTK	Receptor tyrosine kinase
RT-PCR	Reverse-transcriptase polymerase chain reaction
SAM	Sterile alpha motif
SAPKs	Stress-activated protein kinases
s.d.	Standard deviation
SDS	Sodium dodecyl sulphate
SDS-PAGE	Sodium dodecyl sulphate polyacrylamide gel electrophoresis
sGFP	Synthetic green fluorescent protein
SM	Secondary metabolite
SOC	Super optimal broth with catabolite repression
SPK	Spitzenkorper
SS	Sequence similarity
ST	Sterigmatocystin
SSC	Saline sodium citrate

TAE	Tris:acetate:EDTA
TAP	Tandem affinity purification
TBST	Tris buffered saline with 0.1% Tween 20
TEV	Tobacco etch virus
TFA	Trifluoroacetic acid
Thr	Threonine
Thr-X-Tyr	Threonine-X-Tyrosine
TQ	Terrequinone A
Tyr	Tyrosine
UHPLC-HRMS	Ultra-high performance high resolution mass spectrometry
UTR	Untranslated region
UV	Ultraviolet
VSC	Vesicle supply centre
WD	Tryptophan-aspartate
WHM	Wickerham
WT	Wild type
YES	Yeast extract sucrose
YFP	Yellow fluorescent protein

Figure Lists

Chapter 1

Chapter 3

Chapter 4

Chapter 5

Chapter 6

Appendix A

Appendix B

Appendix C

Table Lists

Appendix A

Table Number	Table Name	Page Number
Table S1	SteC-TAP interacting proteins during 24 hours of vegetative growth.	229
Table S2	MkkB-TAP interacting proteins during 24 hours of vegetative growth	230
Table S3	MpkB-TAP interacting proteins during 24 hours of vegetative growth	231
Table S4	HamE-TAP interacting proteins during 24 hours of vegetative growth	233
Table S5	Phosphorylated residues detected for HamE during 24 hours of vegetative growth	234
Table S6	Phosphorylated residues detected for SteC during 24 hours of vegetative growth in the presence of HamE	234
Table S7	Phosphorylated residues detected for SteC during 24 hours of vegetative growth in the absence of HamE	235
Table S8	Phosphorylated residues detected for MkkB during 24 hours of vegetative growth in the presence of HamE	236
Table S9	Phosphorylated residues detected for MkkB during 24 hours of vegetative growth in the absence of HamE	237

Appendix B

Table S7	SteD-GFP (CADAFLAP00010300) interacting proteins at 24 hours of vegetative growth.	261
Table S8	HamE-HA (CADAFLAP00009262) interacting proteins at 24 hours of vegetative growth.	262

Appendix C

Table Number	Table Name	Page Number
Table S1	Fungal strains created or used in this study	269
Table S2	Plasmids created or used in this study	269
Table S3	Oligonucleotides created or used in this study	270
Table S4	SteC-GFP (Afu5g06420) interacting proteins at 24 hours of vegetative growth.	274
Table S5	MkkB-GFP (Afu3g05900) interacting proteins at 24 hours of vegetative growth.	276
Table S6	MpkB-GFP (Afu6g12820) interacting proteins at 24 hours of vegetative growth.	277
Table S7	SteD-GFP (Afu2g17130) interacting proteins at 24 hours of vegetative growth.	279
Table S8	HamE-HA (Afu5g13970) interacting proteins at 24 hours of vegetative growth.	280

Summary

In order for eukaryotes to efficiently detect and respond to environmental stimuli, a myriad of protein signalling pathways are utilised. An example of highly conserved signalling pathways in eukaryotes are the mitogen-activated protein kinase (MAPK) pathways. MAPK pathways are responsible for the regulation of a diverse array of biological processes, such as cell proliferation, immune responses and metabolism, to name a few. In fungal organisms, MAPK pathways have been shown to be involved in the modulation of cell fusion and mating, asexual and sexual reproduction, cellular stress responses and secondary metabolism. MAPK pathways have been extensively studied in yeast, a model organism for unicellular fungi. One MAPK pathway in particular is known as the pheromone module, which consists of three kinases (Ste11, Ste7, Fus3), the adaptor protein Ste50 and the scaffold protein Ste5. This pathway is critical for the response to pheromone signalling between neighbouring yeast cells, resulting in the regulation of cell fusion, otherwise known as mating or sexual reproduction. Orthologous MAPK pathways have been studied in fungal species such as the model ascomycete *Neurospora crassa*. In this species, the pheromone module pathway has been shown to be involved in the regulation of germling and hyphal fusion, which is critical for the establishment of the interconnected fungal mycelium.

With respect to the genus *Aspergillus,* information regarding the influence of MAPK signalling pathways in the regulation of fungal development is limited. Orthologs of the core pheromone module components in yeast have been identified previously in the model filamentous fungus *A. nidulans*. These include the three kinases SteC, MkkB and MpkB (orthologs of yeast Ste11, Ste7 and Fus3 respectively) and the adaptor protein SteD (ortholog of yeast Ste50). However, there are no orthologs of the Ste5 scaffold in filamentous fungal genomes, suggesting a unique mechanism of regulation exists for the pheromone module pathway in species like *A. nidulans*. This led to the first aim of this research thesis which was to identify and characterise a scaffold candidate for the pheromone module in *A. nidulans*. We identified the AN2701 gene which encodes a large protein consisting of multiple WD40 repeats, which is characteristic of scaffold proteins. This gene is orthologous to the *N. crassa ham5* gene which encodes a scaffold protein in the Mak-2 pheromone module pathway. For this reason, we named the protein product of the AN2701 gene 'HamE'. *Via* a genetic and proteomic approach, we provided evidence that the HamE scaffold physically interacts with the kinases MkkB and MpkB and that a pentameric complex is formed at the

hyphal tips and plasma membrane. HamE is essential for the regulation of kinase phosphorylation levels and a *hamE* mutant exhibits dramatically reduced levels of MpkB phosphorylation, signifying reduced MAP kinase signalling and transcription factor activation. Deletion of any of the five members of the complex results in reductions in asexual sporulation, as well as complete inhibition of sexual cleistothecia formation and dramatic decreases in the expression levels of various secondary metabolite genes.

The next aim of this research thesis was to further characterise the roles of the pheromone module in *Aspergillus* species. Due to the dramatic defects in development and secondary metabolism observed in pheromone module mutants in *A. nidulans*, it was decided to assess whether the pheromone module could be utilised by other *Aspergillus* species to regulate their development and secondary metabolism. We found that orthologs of the pheromone module genes are highly conserved in the genus *Aspergillus*. We identified orthologs of each of the five core pheromone module components in two pathogenic fungi, *A. flavus* and *A. fumigatus*. *A. flavus* is a prolific producer of secondary metabolites such as the highly carcinogenic compound aflatoxin B1. This species is considered a major global threat as it is capable of causing contamination of a wide variety of agricultural crops and ingestion of crops contaminated with aflatoxin can lead to the development of hepatocellular carcinomas. *A. fumigatus* is an opportunistic human pathogen and is a major risk to immunocompromised individuals. This species produces dangerous secondary metabolites such as the immunosuppressant gliotoxin, which promotes invasive pulmonary aspergillosis and this can lead to mortality rates as high as 95% in immunocompromised patients.

In *A. flavus,* we provided evidence of the existence of a tetrameric pheromone module pathway, which is made up of two sub-complexes. Initially, MkkB and MpkB form a dimer at the hyphal tips, potentially in response to chemotropic interactions between neighbouring hyphae. The SteC-SteD dimer then interacts with the MkkB-MpkB dimer in the cytoplasm and assembly of the complex results in phosphorylation and migration of MpkB into the nucleus, where it presumably interacts with various transcription factors. Interestingly, HamE was shown to localise to the hyphal tips but was not observed to interact with the pheromone module components, signifying a potentially unique mechanism of signalling in this species. Deletion of *steC, mkkB, mpkB* or *steD* results in inhibition of both asexual sporulation and sclerotia production.

Additionally, each of these mutants produced significantly lower levels of aflatoxin B1 and increased levels of other secondary metabolites, such as leporin B and cyclopiazonic acid. Deletion of *hamE* resulted in sexual sterility and reductions in aflatoxin B1 production, however, asexual sporulation was not hindered.

In *A. fumigatus, via* interactome data, we provided evidence of the existence of a pentameric pheromone module pathway, similar to what is observed in *A. nidulans*. The proteins of this pathway exhibited similar sub-cellular localisation patterns to those observed in *A. flavus*. HamE, MkkB and MpkB localise to the hyphal tips, suggesting that they form a trimeric complex. SteC interacts with SteD and this dimer associates with the trimeric complex in the cytoplasm to form a pentameric complex, allowing for kinase phosphorylation and translocation of MpkB into the nucleus. Deletion of any of the five pheromone module components results in dramatic reductions in asexual sporulation, vegetative growth rate and production of various secondary metabolites, particularly gliotoxin. Each mutant also exhibited increased sensitivity to both cell wall and oxidative stress agents.

Overall, this thesis provides a comprehensive analysis of the molecular roles of the pheromone module in *Aspergillus* species. These data suggest that this pathway is a conserved mechanism of signal transduction that is required for the regulation of fungal development and secondary metabolism. Findings from this thesis may contribute to the development of strategies which could involve targeting the components of the pheromone module in order to help prevent crop spoilage and infections caused by *Aspergillus* species.

Chapter 1

Introduction

1.1. Cell signalling pathways mediate appropriate cellular responses to stimuli

Eukaryotic organisms must be capable of constantly detecting and rapidly responding to a myriad of environmental stimuli in order to survive. To achieve this, an array of protein signalling transduction cascades are utilised, which allow cells to consistently detect, interpret and respond to signals in their environment (Elion, 2000, Dhanasekaran et al., 2007). Signalling transduction pathways are composed of intricate networks of proteins, enzymes and chemical messengers (**Figure 1.1.**). These proteins become active upon detection of specific signals at various cell receptors and result in signalling to the nucleus to elicit appropriate biological responses. These pathways are responsible for the regulation of a multitude of vital cell processes in eukaryotic organisms like proliferation, apoptosis, metabolism and differentiation, as well as stress, mating and immune responses (Pan et al., 2012, Good et al., 2011, Lim and Pawson, 2010).
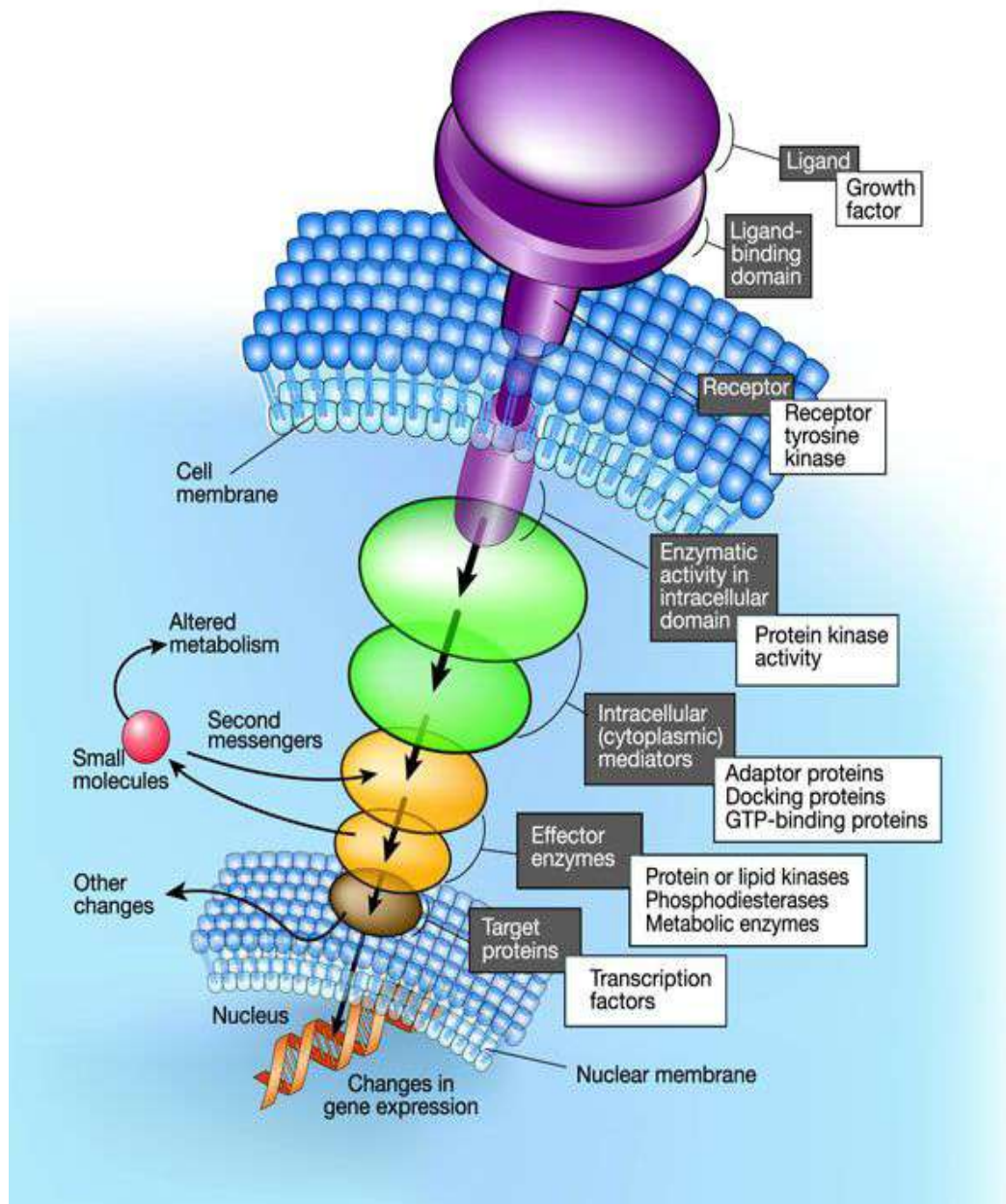
Figure 1.1. A schematic illustrating the general structure of signal transduction pathways. Receptors at sites like the plasma membrane detect a wide array of stimuli and in response, mediate the transduction of a signal downstream to the nucleus *via* a variety of primary and secondary messengers. This ultimately results in the regulation of a myriad of cell biological processes. Image taken from (Downward, 2001).

1.1.1. Stimulus detection at cell receptors triggers activation of signalling pathways

All cells contain a large repertoire of diverse receptors, which allow for the detection of changes in either the internal or external environment of the cell. These receptors commonly span the plasma membrane and are capable of binding ligands such as growth factors, peptide hormones and cytokines, to name a few. This often results in changes to the conformation of the receptor, which can lead to either formation of receptor dimers or the re-orientation of separate receptor domains. These changes in receptor structure can induce the generation of a signal, leading to the activation of various cell signalling pathways, such as Mitogen-Activated Protein Kinase (MAPK) pathways which will be discussed in the next section (Downward, 2001, Schlessinger, 2000).

There are many different categories of receptors in eukaryotes. For example, integrins are transmembrane receptors that bind the extracellular matrix and are capable of forming heterodimers, resulting in more than 20 different receptors. These receptors are responsible for the formation and maintenance of the cell architecture and for cell-cell communication (Schlaepfer and Hunter, 1998). The superfamily of G protein-coupled receptors (GPCRs) is the largest group of receptors ever discovered in mammals. These receptors contain a seven-transmembrane spanning region that undergo a conformational change when activated by a stimulus, which results in signal transduction throughout the cell (Cabrera-Vera et al., 2003). This ultimately regulates cell responses to a wide array of environmental stimuli, including neurotransmitters, pheromones, light and hormones (Katritch et al., 2013, Lagerstrom and Schioth, 2008, Steury et al., 2017, Takeda et al., 2002). Consequently, GPCRs are implicated in many biological processes, such as various cardiovascular, neurological and pulmonary disorders, to name a few (Skieterska et al., 2017). Receptor protein kinases are a group of receptors that are vital for the regulation of a variety of biological responses. Receptor tyrosine kinases (RTKs) are believed to be the largest family of catalytic membrane receptors. These receptors have a high binding affinity for stimuli such as growth factors and cytokines (Schlessinger, 2014) and defects in RTK signalling are often associated with diseases such as cancers (Templeton et al., 2014).

1.2. MAPK pathways

MAPK cascades are an example of highly conserved signalling pathways in eukaryotes from yeast to human (Widmann et al., 1999, Marshall, 1994, Schaeffer and Weber, 1999). These pathways become active upon detection of a stimulus at a receptor, often located at the plasma membrane of the cell. Common stimuli include growth factors, pheromones and cytokines, as well as oxidative, osmotic and cell wall stressors (Widmann et al., 1999). In a general MAPK pathway (**Figure 1.2.**), stimulus detection leads to the recruitment and assembly of protein kinases in a classic '3-tiered kinase' cascade. The three kinases are often termed: MAP3K (MAPKKK), MAP2K (MAPKK) and MAPK, which are co-localised and tethered in close proximity of the membrane,

enabling their phosphorylation in a sequential manner. The transfer of single phosphate groups primarily occurs on the hydroxyl groups of serine, threonine (Thr) and tyrosine (Tyr) residues (Brautigan, 2013, Jin and Pawson, 2012). Initial phosphorylation of the MAP3K, often *via* interactions with GTPases or kinases directly downstream of cell receptors (Cuevas et al., 2007), allows it to phosphorylate the MAP2K which then phosphorylates the MAPK. This terminal MAPK becomes dually phosphorylated at a conserved tripeptide Threonine-X-Tyrosine (Thr-X-Tyr) motif, allowing for it's activation. The MAPK then migrates to the nucleus where it interacts with transcription factors to influence gene expression, eliciting a characteristic response to the detected stimulus (Marshall, 1994, Widmann et al., 1999, Yoshioka, 2004, Saito, 2010).
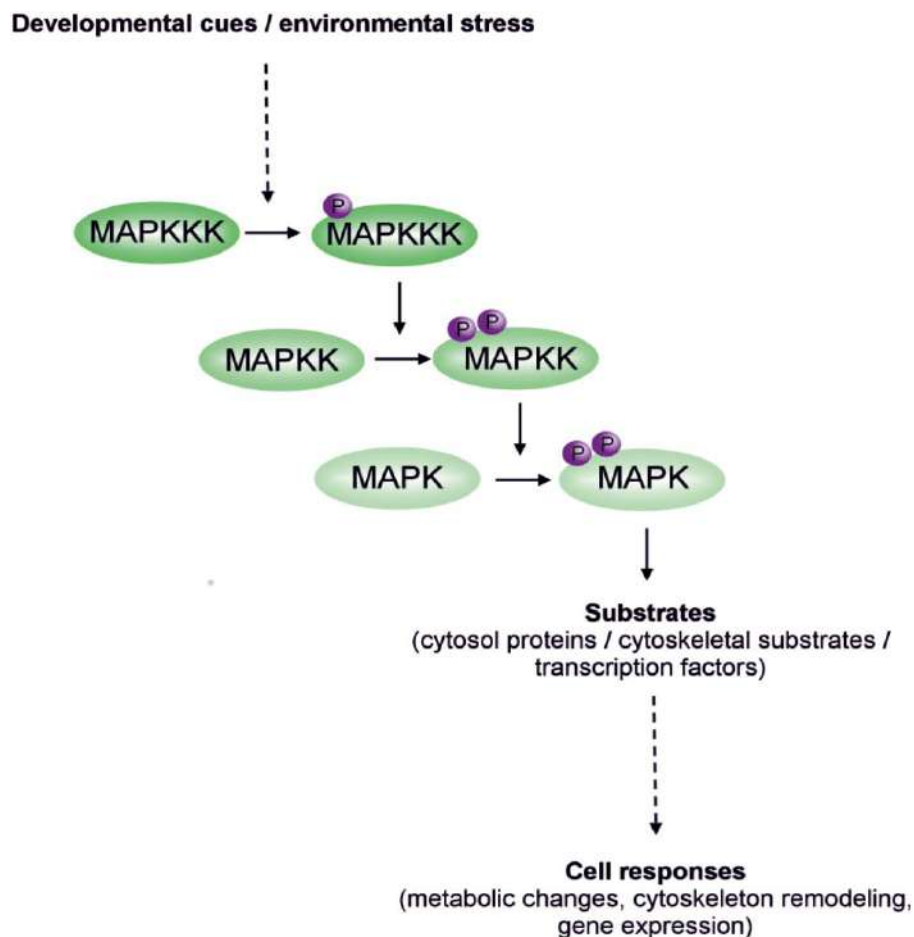
Figure 1.2. The general structure of a 'three-tiered' MAPK cascade. Stimulus detection at a receptor results in activation of the MAPKKK, which allows for sequential phosphorylation of both the MAPKK and MAPK. MAPK activation triggers changes in transcription factor activity, resulting in the regulation of a wide variety of biological responses, dependent on the stimulus detected. Image taken from (Jagodzik et al., 2018).

1.2.1. The roles of scaffold proteins in MAPK pathways

In order to regulate MAP kinase complexes spatially and temporally, as well as regulating signal propagation and intensity, cells utilise a unique class of highly diverse proteins known as scaffolds. These are large, multi-domain proteins that act as a physical platform and are capable of binding multiple members of a MAPK pathway. This, in turn, allows scaffolds to regulate processes such as (i) the localisations of kinases with respect to one another *via* tethering of proteins to locations like the plasma membrane, (ii) the assembly of macromolecular signalling complexes and (iii) signal propagation to the nucleus *via* sequential phosphorylation of each kinase (Buday and Tompa, 2010, Brown and Sacks, 2009, Good et al., 2011, Pan et al., 2012). The first scaffold to be identified was the Ste5 scaffold in yeast (Elion, 2001), which will be discussed in more detail in section 1.4.2. Since this discovery, many more scaffolds have been identified in a wide range of eukaryotes, including mammals (Morrison and Davis, 2003, Kolch, 2005, Sacks, 2006). Overall, scaffolds are critical for the regulation of signal specificity in MAP kinase pathways, allowing for the modulation of appropriate biological responses dependent on the specific stimulus detected at receptors (Bhattacharyya et al., 2006, Morrison and Davis, 2003, Shaw and Filbert, 2009). A schematic illustrating proteins in MAP kinase pathways binding to a generic scaffold protein is given in **Figure 1.3**.
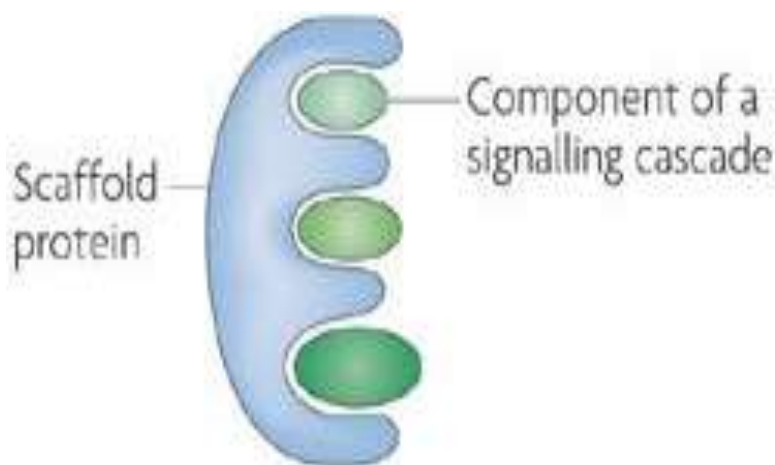
Figure 1.3. General schematic of a scaffold protein binding multiple members of a signalling cascade. Scaffolds are large multi-domain proteins capable of binding multiple proteins of a signalling cascade. These scaffold proteins can assemble large protein complexes to initiate kinase phosphorylation and signal transduction to the nucleus. Image taken from (Shaw and Filbert, 2009).

1.2.1.1. Scaffolds possess various protein domains that allow for the regulation of a myriad of biological responses

Scaffolds utilise a wide array of protein interaction domains to regulate MAP kinase binding, tethering and signalling (Good et al., 2011). Scaffolds also possess a high level of intrinsic structural disorder, which is often considered to provide flexibility for protein interactions and regulatory rearrangements (Buday and Tompa, 2010). Scaffolds are highly heterogeneous in structure and function and can possess different domains depending on the species and pathway the scaffold belongs to (Buday and Tompa, 2010).

For example, scaffold proteins belonging to the postsynaptic density (PSD) at the top of dendritic spines contain multiple well-folded domains, such as the PDZ (**P**ostsynaptic density, **D**isc large, **Z**o-1) domain (Feng and Zhang, 2009). PDZ domains are 80-90 amino acids in length (Feng and Zhang, 2009, Doyle et al., 1996, Magalhaes et al., 2012) and contain a conserved glycine-leucine-glycine-phenylalanine sequence which forms a cup-like structure (Harris and Lim, 2001). This allows for the binding of the distal regions of receptor carboxyl-terminal tails, which are known as the PDZ-binding motif (Harris and Lim, 2001, Magalhaes et al., 2012, Kornau et al., 1995). Many of these PSD scaffolds contain more than one PDZ domain, and thus, are capable of binding multiple proteins at once (Zhang and Wang, 2003, Feng and Zhang, 2009). Consequently, these scaffolds play roles in diverse biological processes, such as linking glutamate receptors with downstream signalling elements, constructing protein signalling complexes and regulating cytoskeletal structures (Elias and Nicoll, 2007, Kim and Sheng, 2004, Sheng and Hoogenraad, 2007).

The Receptor for activated C kinase 1 (RACK1) scaffold in mammals belongs to the tryptophan-aspartate repeat (WD-repeat) protein family (Adams et al., 2011). WD repeats are repetitive sequence motifs of 43 amino acids that contain highly conserved residues such as the glycine-histidine (GH) dipeptide and a conserved aspartic acid residue located before a characteristic WD dipeptide (Fong et al., 1986). WD repeats form 7-blade or 8-blade β-propeller structures which act as a binding platform for multiple proteins, allowing for the assembly of large signalling complexes (Adams et al., 2011, Paoli, 2001). These WD repeat scaffolds are often also involved in the anchoring and shuttling of proteins, modulating their sub-cellular localisations and tethering proteins at locations like the plasma membrane (Adams et al., 2011). RACK-1 has been implicated in cancer metastasis, as it is required for the regulation of cell migration and invasion and the reorganisation of cytoskeletal dynamics (Adams et al., 2011, Duff and Long, 2017).

1.2.1.2. Scaffold proteins are implicated in module crosstalk and complex regulatory feedback loops

While scaffolds are required for signalling specificity in MAP cascades, their large, multi-domain structures allow them to facilitate crosstalk between multiple pathways. This can either lead to the activation or suppression of more than one pathway in response to a given stimulus (Pan et al., 2012). For example, the Axin master scaffold in the highly conserved Wnt pathway contains multiple protein domains and thus is capable of interacting with a myriad of different signalling components (Luo and Lin, 2004). This pathway is critical for the regulation of processes like embryonic development and dysregulation of this pathway is implicated in the progression of various cancers (Pan et al., 2012, Song et al., 2014). In Wnt signalling, Axin interacts with a variety of proteins, including receptors, kinases and phosphatases (Mao et al., 2001, Rubinfeld et al., 2001, Hsu et al., 1999). However, this scaffold also interacts with proteins that are non-specific to the Wnt pathway, such as the MAPKKK MEKK1 and adaptor proteins, leading to the regulation of kinase signalling (Zhang et al., 1999, Cowan and Henkemeyer, 2001). Due to the wide variety of interaction partners that exist for Axin, this scaffold has been implicated in tumour suppression (Satoh et al., 2000), cytoskeletal rearrangements (Cowan and Henkemeyer, 2001, Luo and Lin, 2004) and the negative regulation of embryonic axis formation (Zeng et al., 1997), signifying the range of critical roles that scaffolds play in biological systems.

Aside from promoting signal specificity and propagation, scaffolds can also regulate MAP kinase signal duration and intensity, as they are implicated in complex positive and negative feedback loops (Brown and Sacks, 2009, Garrington and Johnson, 1999). The regulation of signal duration is critical as sustained or transient signals can elicit different biological outcomes. Also, dysregulation of signal propagation is implicated in cancer progression (Murphy and Blenis, 2006). The Ksr1 (Kinase suppressor of ras 1) scaffold in mammals interacts with the kinases Mek and Erk, to regulate proliferation and differentiation of neuronal PC12 (pheochromocytoma) cells (Muller et al., 2000). In response to epidermal growth factor (EGF), Mek/Erk signalling is transient, lasting only minutes and results in PC12 cell proliferation. However, in response to nerve growth factor (NGF), Mek/Erk signalling is sustained for hours and results in PC12 cell differentiation (Marshall, 1995). Overexpression of the KSR scaffold increases basal activated Erk levels, which can stimulate PC12 cell differentiation even when these cells are only stimulated with EGF (Muller et al., 2000). Thus, this provides evidence that scaffold proteins are crucial for regulating the signalling dynamics of kinases, modulating the duration of signal propagation. Consequently, scaffolds are capable of altering the outcomes of various biological processes.

1.2.2. MAPK cascades regulate a diverse array of processes in eukaryotes

1.2.2.1. The mammalian JNK and p38 kinases and JIP scaffolds

The mammalian JNK (c-Jun N-terminal Kinases) and p38 kinases are MAPKs that belong to a family known as the stress-activated protein kinases (SAPKs) (Davis, 2000). These MAP kinases become activated by a collection of MAP2K enzymes (**Figure 1.4.**), such as MKK4 and MKK7 for JNKs and MKK3, MKK4 and MKK6 for p38 kinases (Morrison and Davis, 2003). MAP3K enzymes that select for either JNKs or p38s or both include proteins belonging to the ASK1, MEKK and MLK families (Morrison and Davis, 2003). SAPK modules play important roles in the responses to various stimuli such as cytokines and growth factors (Davis, 2000) and can often be co-ordinated by scaffold proteins.
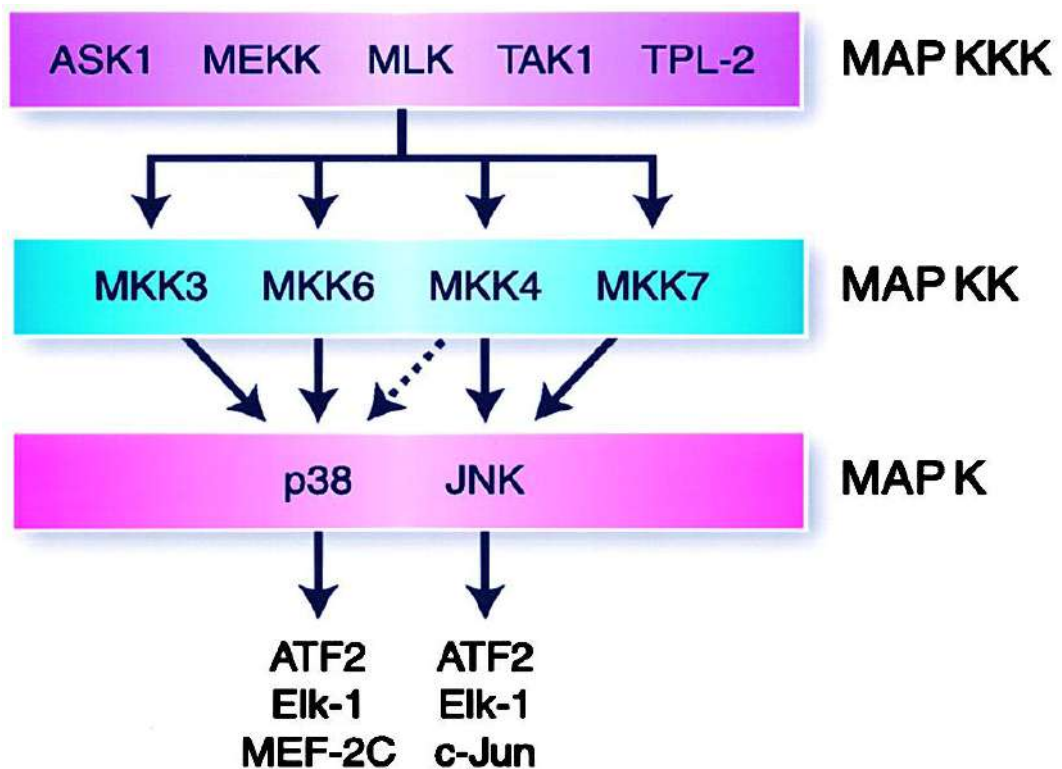
Figure 1.4. Activation of the p38 and JNK MAPKs. MAP3Ks (MAPKKKs) such as ASK1 and MEKK phosphorylate a variety of MAP2Ks (MAPKK) which can then lead to phosphorylation and activation of either p38 or JNK kinases. Image taken from (Davis, 2000).

9

The JNK interacting proteins (JIP) are a group of scaffolds that function as protein dimers in SAPK signalling modules and are required for the activation of both the JNKs and p38 kinases (Morrison and Davis, 2003, Kelkar et al., 2000, Yasuda et al., 1999). The JIP1 and JIP2 scaffolds can bind JNK, the MAP2K MKK7 and various MAP3Ks (**Figure 1.5.**) (Yasuda et al., 1999, Whitmarsh et al., 1998), while JIP2 can also interact with MKK3 and two p38 kinases (Buchsbaum et al., 2002, Schoorlemmer and Goldfarb, 2001). These JIP scaffolds are capable of positively and negatively regulating kinase activation, dependent on their interactions with other proteins and detection of stimuli. For example, when JIP1 binds the kinase AKT1, the JNK-JIP1 interaction is inhibited, resulting in termination of JNK activation. However, this can be reversed by excitotoxic stress, which causes a release of AKT1 from the JIP1 scaffold, resulting in increased JNK activation (Kim et al., 2002).
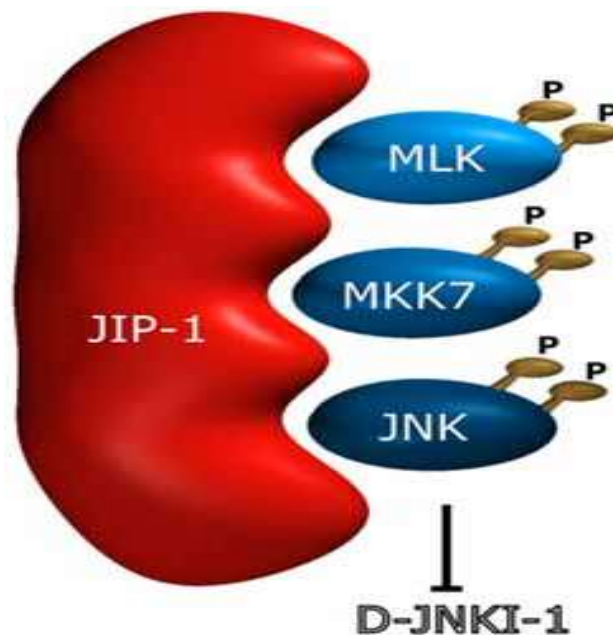
Figure 1.5. The JIP-1 scaffold in a JNK kinase pathway. The large JIP-1 scaffold protein is capable of binding a MAP3K (MLK), a MAP2K (MKK7) and a JNK MAPK, facilitating protein-protein interactions and sequential phosphorylation of each kinase. Image taken from (Borsello and Forloni, 2007).

The JNKs and p38 MAPKs and JIPs are triggered in response to various environmental and genotoxic stresses. These pathways are critical in the maintenance of biological processes such as inflammation, tissue homeostasis, cell proliferation, differentiation and migration. These pathways, when de-regulated, are also implicated in the development of various cancers as dysregulation of scaffold functionality and kinase signalling can lead to uncontrolled cell division and metastasis (Nebreda and Porras, 2000, Kyriakis and Avruch, 2001, Rincon and Davis, 2009). This highlights the necessity for scaffold-mediated regulation of MAP kinase signalling as well as the

critical roles that MAP kinase pathways play in the modulation of biological responses in eukaryotes.

1.3. The fungal kingdom

The fungal kingdom is one of the largest eukaryotic kingdoms, consisting of an estimated 1.5-5 million species, with only about 100,000 species being described in the literature so far (Dang et al., 2005, Choi and Kim, 2017). Species that belong to this kingdom include moulds, rusts, lichens, mushrooms, smuts and yeasts. Fungi are ubiquitous in the environment and are of critical importance to humankind as many species can be manipulated for use in agricultural, industrial and clinical settings and can be regarded as beneficial or detrimental with respect to human and plant health (Alazi and Ram, 2018). To date, approximately 10% of known fungal species have been classified as pathogens of animals, plants or humans (Ziaee et al., 2018).

For the most part, the relevance of fungi is due to the ability of many species, predominately filamentous fungi to undergo secondary metabolism. This is a process of producing a wide range of small, bioactive compounds, known as secondary metabolites (SMs), that exert a diverse array of properties, acting as cytotoxic agents, mutagens, immunosuppressants, antibiotics and carcinogens (Bok and Keller, 2004). Many significant SMs, both beneficial and harmful, have been isolated from fungal species. For example, the antibiotic penicillin is produced by species of *Penicillium* (Bills and Gloer, 2016)*,* while *Aspergillus* species such as *A. nidulans, A. flavus* and *A. fumigatus* produce toxic compounds like sterigmatocystin, aflatoxins and gliotoxin respectively (Hedayati et al., 2007).

Fungi share many similarities with higher eukaryotes and consequently are useful systems for studying eukaryotic biology. Many species of fungi are considered model organisms for research purposes, such as *Neurospora, Saccharomyces* and *Aspergillus* species which have allowed for the study of biological processes such as fungal growth, development, cell signalling and secondary metabolism, to name a few.

1.4. The use of *Saccharomyces cerevisiae* as a model system

The unicellular fungi *S. cerevisiae* (baker's yeast) has been adapted for extensive use as a model eukaryotic organism in many areas of molecular and cell biology research. Yeast possesses numerous characteristics that facilitate it's use as a model system. It is genetically well-defined, possessing a genome that has been fully sequenced and is widely accessible. It can be easily manipulated *via* gene mutations, gene disruptions, gene tagging and other genetic manipulations, making it suitable for studying various biological processes that can be applicable to human and fungal systems, such as cell division, cell death, signalling pathways and disease processes, to name a few

(Dikicioglu et al., 2013, Mager and Winderickx, 2005, Hartwell, 2002, Madeo et al., 2002).

Yeast has been widely used for both medical and industrial purposes. With regards to industry, the production of both wine and beer have been predominately performed by utilising yeast strains (Peris et al., 2018). However, yeast can also be implicated in the production of various biofuels such as cellulosic ethanol, which can act as a renewable substitute for fossil fuels (Peris et al., 2018). With respect to medicinal uses, yeast can be utilised for the screening of new compounds that are biologically active and the study of drug-induced molecular mechanisms (Mager and Winderickx, 2005). It has been shown *via* comparison of both yeast and human genomes that 30% of all known genes involved in disease in humans possess orthologs in yeast (Foury, 1997). This has resulted in the use of yeast to study protein functionality, protein-protein interactions and signalling pathways, such as MAPK pathways that contribute to the progression of various diseases.

1.4.1. MAP kinase pathways in yeast

The utilisation of yeast for studying protein interactions and signalling pathways has allowed for the extensive characterisation of many pathways that contribute to cell adaptation, survival, reproduction and apoptosis in eukaryotes, ranging from fungi to humans. This organism has been critical in the elucidation of MAPK signalling mechanisms across the entire eukaryotic kingdom (Chen and Thorner, 2007).

The yeast genome encodes 5 MAPKs that function in separate signalling pathways to module various biological responses (Qi and Elion, 2005). One MAPK is Mpk1, which becomes activated downstream of protein kinase C (PKC) signalling. Mpk1 is responsible for the regulation of cell wall remodelling, enabling cell growth (Mazzoni et al., 1993, Widmann et al., 1999). The second MAPK is Hog1 which promotes the survival of cells in hyperosmotic conditions by maintaining osmotic stability (Brewster et al., 1993). The third MAPK is Smk1, which is critical for the regulation of yeast sporulation, specifically the assembly of the spore wall (Krisak et al., 1994). The fourth MAPK is Kss1 which regulates the switch from the budding yeast cell form to the invasive filamentous growth programme (Ma et al., 1995). Lastly, the fifth MAPK Fus3 is responsible for the regulation of cell-cell fusion, otherwise known as sexual development, in response to pheromone signalling (Bardwell, 2005).

1.4.2. The yeast Fus3 pheromone module mediates cell mating

The yeast Fus3 MAPK mating pathway is the most extensively studied MAPK pathway to date in any eukaryotic organism. Yeast have two opposite mating types, known as 'a' and 'α' genotypes. Both of these cell types exist as haploid cells and the fusion of two opposite mating types results in the formation of diploid cells. In order

for two yeast cells to fuse, they release opposite pheromone mating signal peptides. 'a' cells respond to 'α' factor pheromone produced by 'α' cells and vice versa. This results in cells undergoing various physiological changes such as cell cycle arrest in the G1 phase of growth, oriented growth towards the neighbouring cell and plasma membrane and nuclear fusion of the two mating partners (Bardwell, 2005).

In order to transduce a signal downstream to the nucleus in response to pheromone detection and to regulate morphological changes, the Fus3 MAPK signalling cascade, otherwise known as the pheromone module is utilised. Once pheromones are released by neighbouring cells, they are detected by GPCRs, like Ste2 and Ste3 at the plasma membrane. When activated, these receptors undergo a conformational change. The Gα subunit of the GPCR then exchanges guanosine diphosphate (GDP) for guanosine triphosphate (GTP), which triggers dissociation of the Gβγ heterodimer from the Gα subunit. The Gβγ heterodimer then recruits the large, multi-domain Ste5 scaffold protein to the membrane, as well as the p21-activated protein kinase (PAK) Ste20 (Pryciak and Huntress, 1998, Bardwell, 2005, Leeuw et al., 1998). Ste5 is essential for assembling a three-tiered kinase cascade as it possesses a binding site for the Gβγ heterodimer as well as sites for binding three separate kinases (Choi et al., 1994, Whiteway et al., 1995). The activation of the kinase cascade commences upon phosphorylation of the MAPKKK Ste11. This is dependent on the cooperation of Ste5, Ste20 and the adaptor protein Ste50. Ste5 and Ste50 bind Ste11 *via* Sterile Alpha Motif (SAM) domain interactions, localising it to the membrane and Ste20 phosphorylates the N-terminal regulatory domain of Ste11, resulting in it's activation (Pryciak and Huntress, 1998, Wu et al., 1999, Xu et al., 1996). By binding of each kinase to sites on the Ste5 scaffold, Ste11 is then capable of phosphorylating the MAPKK Ste7, which then phosphorylates the terminal MAPK Fus3 on both a threonine and tyrosine residue (Hao et al., 2008, Kranz et al., 1994, Saito, 2010). Once activated, Fus3 is then capable of migrating to the nuclear envelope where it translocates into the nucleus to interact with the Ste12 transcription factor (van Drogen et al., 2001). This results in the regulation of sexual mating between two neighbouring yeast cells, allowing them to fuse (Wong Sak Hoi and Dumas, 2010, Bardwell, 2005). An overview of the Fus3 pheromone module is illustrated in **Figure 1.6.**

Since the discovery and characterisation of the Fus3 pheromone module in yeast, many homologous proteins and signalling pathways have been discovered in eukaryotes, ranging from filamentous fungi to humans. Homologous pheromone module pathways will be discussed in filamentous fungal species like *Neurospora crassa* and *Aspergillus nidulans* in later sections.
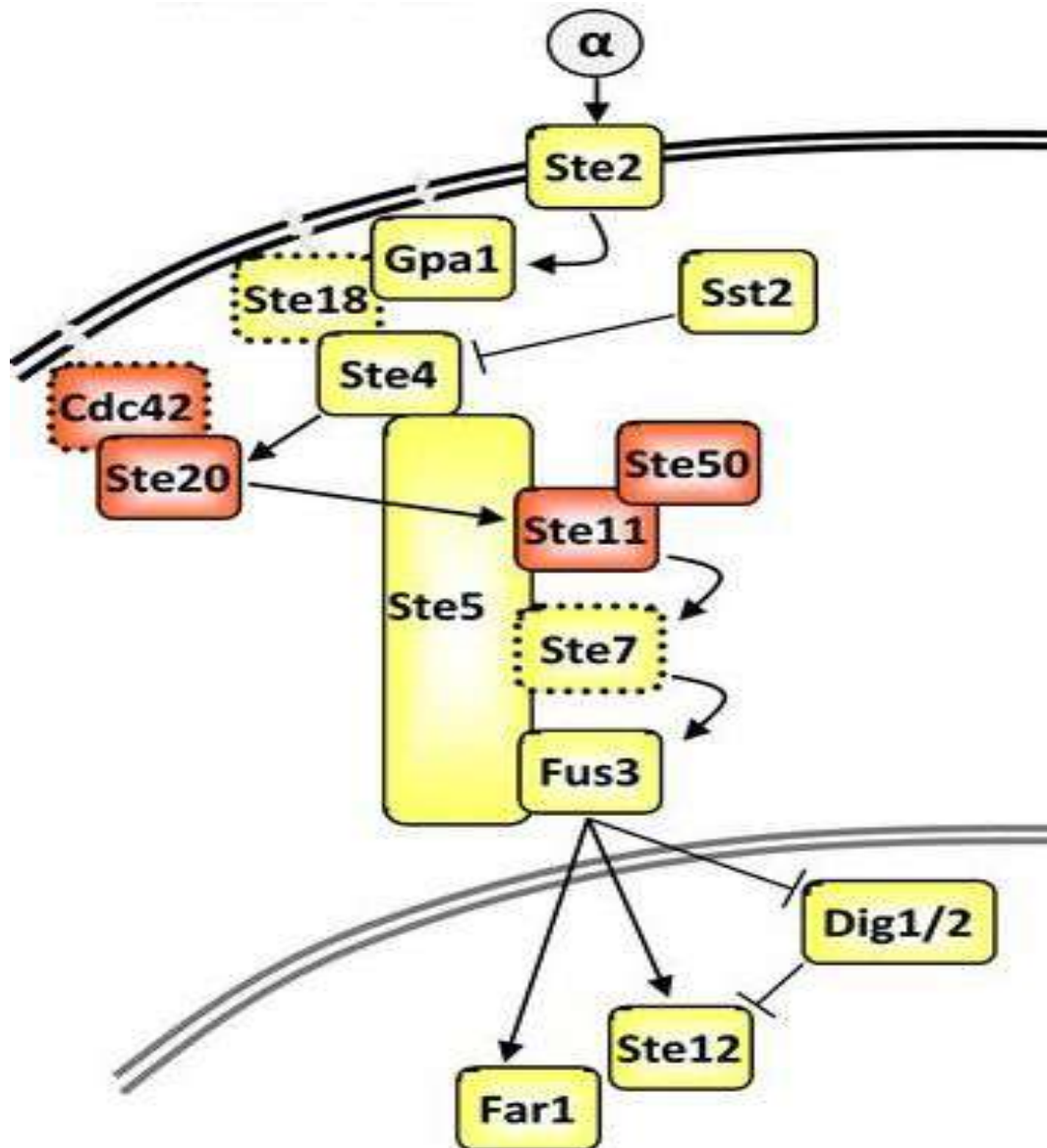
Figure 1.6. The Fus3 pheromone module in *S. cerevisiae*. Detection of either 'a' or 'α' pheromones by GPCRs like Ste2 result in the assembly of the three tiered kinase cascade consisting of the MAP3K Ste11, the MAP2K Ste7 and the MAPK Fus3. These kinases bind to the scaffold Ste5 and phosphorylate one another to enable Fus3 activation and translocation into the nucleus. This results in activation of transcription factors like Ste12 which regulates cell fusion. Image taken from (Vaga et al., 2014).

1.5. Use of the filamentous fungus *A. nidulans* as a model organism for studying fungal development and secondary metabolism

Since the incorporation of unicellular yeasts in fungal research, there has been an increasing focus on the use of filamentous fungi as these species are of high agricultural, medical and industrial importance. The filamentous ascomycete fungus *A. nidulans* has been used extensively in research as a model organism for eukaryotic biology. This species has been implicated in various fields such as cell biology, biochemistry, secondary metabolite biosynthesis, fungal genetics and development, to name a few (Dasgupta et al., 2016, Morris and Enos, 1992, Harris, 1997).

This fungus possesses numerous characteristics that have allowed for its use as a model system. It contains a fully sequenced haploid genome, carrying only a single copy of each of its genes. Because of this, relatively simple deoxyribonucleic acid (DNA)-mediated transformation methods and tools have been developed to allow for gene disruptions, gene deletions, gene tagging and other genetic modifications in this organism *via* homologous recombination. Subsequently, this has led to the extensive use of *A. nidulans* for studying gene and protein functions, protein-protein interactions and signalling pathways that contribute to the regulation of various biological processes (Adams et al., 1998, Miller et al., 1985). This fungus is also safe to use in laboratory research environments and is easy to culture. *A. nidulans* is capable of producing a range of bioactive SMs and undergoes three different methods of reproduction, which are vegetative hyphal growth, asexual conidiation and sexual reproduction (Yu, 2010) which will be discussed in later sections. This has allowed for the use of *A. nidulans* in researching the genes and proteins that contribute to the regulation of developmental programmes as well as secondary metabolism in filamentous fungi.

1.5.1. Vegetative growth of *A. nidulans*

Filamentous fungi like *A. nidulans* can undergo multiple modes of reproduction. Initially, following the germination of a unicellular fungal spore, an axis of polarity is defined which dictates the direction of growth (Dorter and Momany, 2016). Continuous growth along this axis results in the emergence of a germ tube. This germ tube is then capable of making the transition to become a multicellular vegetative hypha **(Figure 1.7.)**, which is an elongated tube-like structure and is the basic growth unit of most fungi (Bayram and Braus, 2012, Harris, 2019). Each fungal spore is capable of producing multiple hyphae which become interconnected *via* hyphal fusion to form the mycelium (**Figure 1.7.**). These hyphae can also undergo hyphal branching, which involves the establishment of a new axis of polarity on an existing hypha. Consequently, a new secondary hypha can grow from this point and can lead to the formation of tertiary hyphae and so on, increasing the density of hyphae within the mycelium (Harris, 2019, Harris, 2008). Fungal hyphae usually contain cross-walls which are known as septae that extend along the length of the hyphae, spaced at regular intervals **(Figure 1.7.)**. These septae contain pores and allow for the transport of

cytoplasm, nuclei and other cellular units throughout the growing hyphae (Steinberg, 2007). This allows for the development of a sophisticated communication system in fungal mycelia.
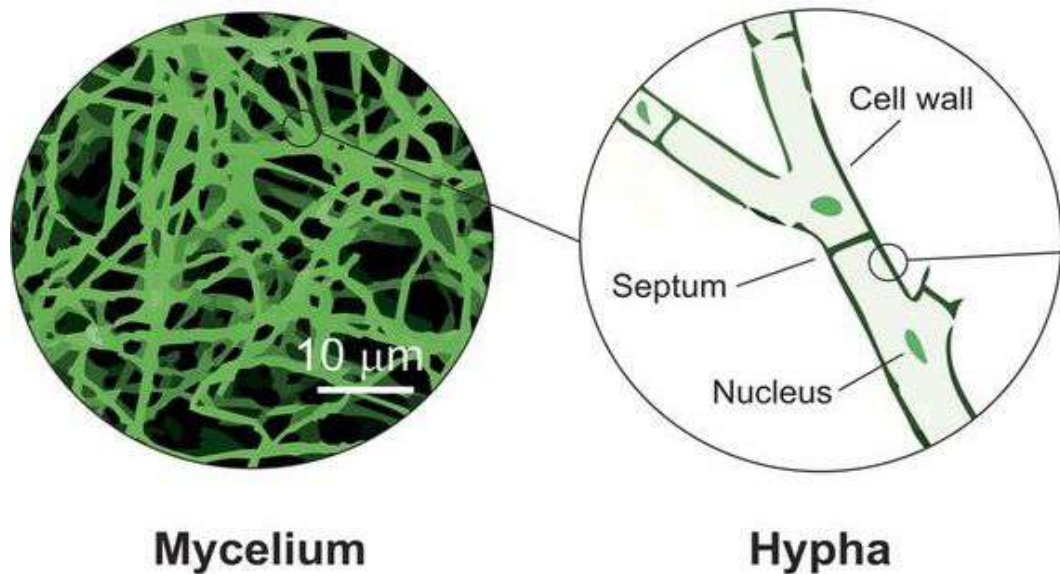
Figure 1.7. Illustration of the fungal hypha and interconnected mycelium. An optical microscopy image depicting the fungal mycelium composed of individual interconnected hypha. The fungal hypha consists of cells that are separated by porous cross walls known as septae, allowing for communication and transport of cellular components like nuclei. Image taken from (Haneef et al., 2017).

In order for hyphae to grow and obtain nutrients, polar extension at the hyphal tips must occur. This requires continuous expansion of the plasma membrane, along with the biosynthesis of new cell wall components. This is facilitated by the Spitzenkorper (SPK), which is an apical body located at hyphal apices that functions as a Vesicle Supply Centre (VSC). In this structure, exocytic vesicles containing enzymes for cell wall synthesis accumulate at the hyphal apex (Riquelme and Sanchez-Leon, 2014, Harris, 2009, Steinberg, 2007). This leads to the fusion of these vesicles with the hyphal tip, resulting in the deposition of new plasma membrane and cell wall material (**Figure 1.8.**) (Riquelme et al., 2018). Hyphae often extend outwards from the germinating spore, in search of nutrients. Various extracellular signals can be detected by the hyphal tips and they are also capable of transporting nutrients towards the interior regions of the mycelium to facilitate the growth of new spores (Harris, 2019).
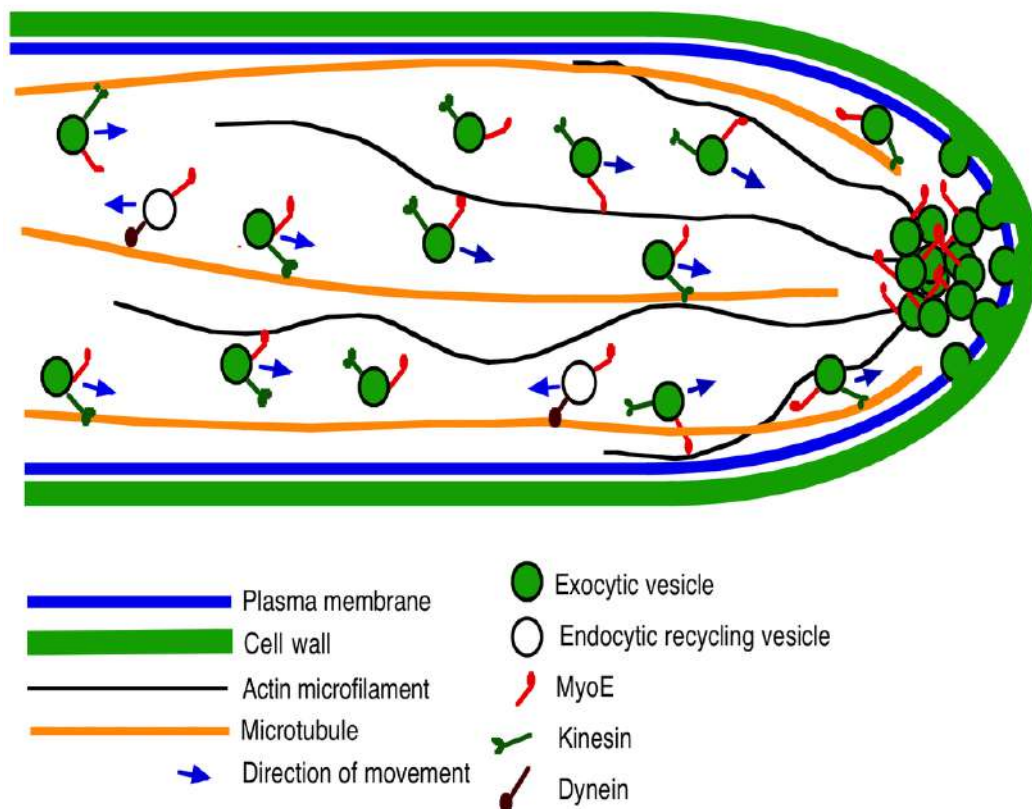
Figure 1.8. Schematic of the Spitzenkorper. Exocytic vesicles containing enzymes essential for cell wall synthesis are transported to the growing hyphal apex. These vesicles fuse with the hyphal tip and deposit new cell wall and plasma membrane material, allowing for continuous expansion of the hypha. Image taken from (Taheri-Talesh et al., 2012).

1.5.2. Asexual sporulation of *A. nidulans*

1.5.2.1. Formation of the conidiophore

The majority of filamentous fungi will reproduce predominately *via* asexual sporulation. This method of growth commences following the establishment of the mycelium. Vegetative hypha then become competent to detect environmental signals such as light, which triggers the formation of a foot cell. This is a basal cell that arises due to thickening of the fungal hypha and consists of a two-layered wall. The inner wall is specific to the basal cell, while the outer layer is continuous with the mycelium (Adams et al., 1998, Etxebeste et al., 2010). The formation of the foot cell leads to the emergence of the stalk, which is an aerial branch of 4-5µm diameter and 100µm length that extends *via* negative geotropism from the foot cell (Etxebeste et al., 2010). Once stalk expansion terminates, the tip of the stalk begins to bulge, forming a globular structure of 10µm in diameter known as the vesicle. Within each vesicle, multiple nuclear divisions occur, resulting in 60-70 nuclei (Mims et al., 1988). On the vesicle

surface, multiple cells, termed metulae begin to bud. The nuclei formed will then begin to migrate, with one nucleus entering each developing metulae. This is followed by the formation of a septum at the base of each metulae, separating them from the vesicle (Kues and Fischer, 2006). Metulae then undergo a specialised type of division, each generating two apical buds which mature to become phialides. Phialides, *via* mitosis, then produce long chains of roughly 100 asexual haploid spores, termed conidia, which are clones of the parent organism. At this stage, the entire developmental structure is known as the condiophore which is formed after a total of 15 hours following developmental induction (Sewall et al., 1990a, Etxebeste et al., 2010). An overview of the steps involved in mature conidiophore development are illustrated in **Figure 1.9.**
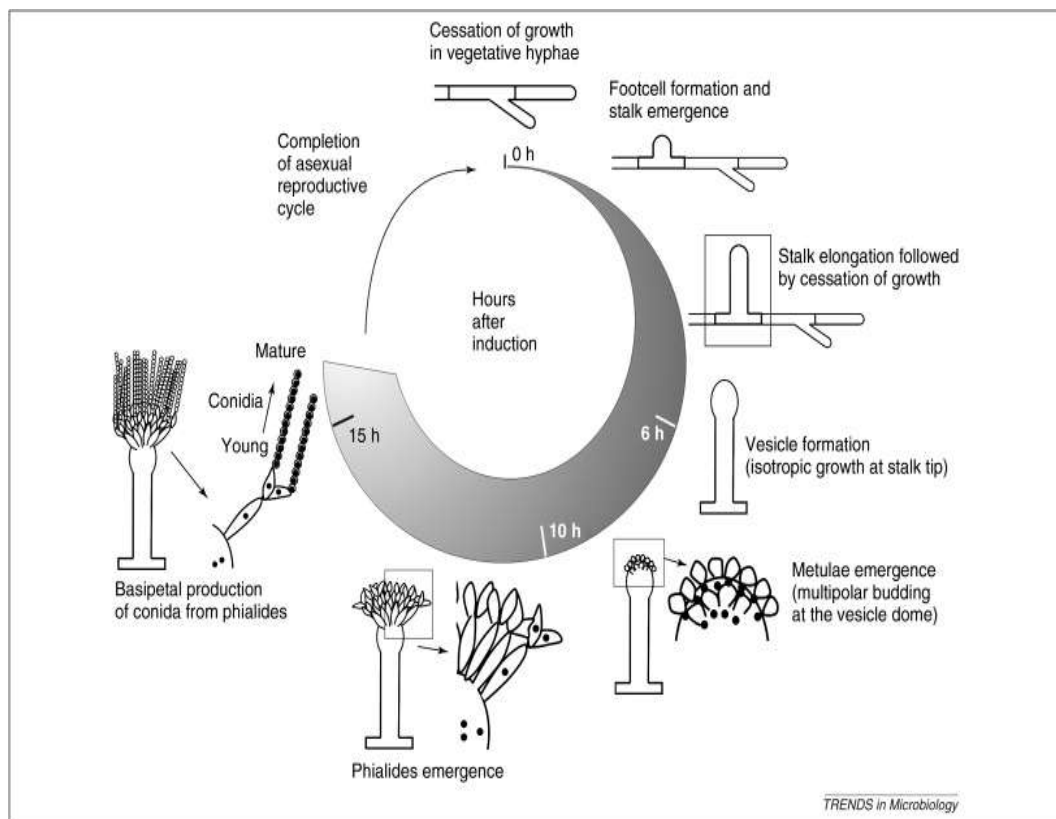
Figure 1.9. Formation of the asexual conidiophore. Illustrated are the morphological changes that occur upon detection of light *via* competent vegetative hypha. Time points of each developmental stage are provided. Mature condiophores are produced roughly 15 hours following detection of environmental signals. Image taken from (Etxebeste et al., 2010).

1.5.2.2. Genetic regulation of asexual conidiation

In order to respond to light and to trigger morphological changes leading to conidiophore development, many genetic regulators must be activated (**Figure 1.10.**). FluG is an essential upstream regulator of conidiation as it is required for the production of an extracellular sporulation inducing factor (ESID) (Lee and Adams, 1994). FluG activates multiple transcription factors, such as FlbB, FlbC, FlbD and FlbE, which contribute to conidiophore development (Park and Yu, 2012). FlbB is located in close proximity to the SPK where it forms a complex with FlbE (Garzia et al., 2009). The FlbB-FlbE heterodimer is required for the activation and binding of FlbD. FlbB-FlbD heterodimers then bind to the promoter region of the BrlA transcription factor (Garzia et al., 2010). This, together with the actions of FlbC, which binds to the *cis*-regulatory elements of *brlA*, allow for activation of BrlA. This occurs after about 6 hours of developmental induction, marking the end of the stalk elongation phase (Kwon et al., 2010, Mah and Yu, 2006).

BrlA is required for the expression of an array of genes specific to the conidiation process. One of which is the transcription factor AbaA, which is activated following establishment of the metulae and is required for the regulation of phialide differentiation (Andrianopoulos and Timberlake, 1991, Sewall et al., 1990a). AbaA is also essential in the regulation of various other downstream genes, such as *wetA,* which is activated during the late stages of conidiation and is necessary for the regulation of both conidial pigmentation and synthesis of cell wall layers that contribute to spore integrity and impermeability (Sewall et al., 1990b, Marshall and Timberlake, 1991). Another transcription factor that is activated downstream of BrlA is VosA, which is required for the regulation of spore maturation and synthesis of trehalose, which is a sugar that enables stabilisation of both membranes and proteins (Ni and Yu, 2007). Deletion of any of these genes results in developmental effects at various stages of condiophore establishment. For example, *brlA* mutants form bristle-like structures that form elongated stalks and are incapable of progressing to the vesicle stage of development (Clutterbuck, 1969, Boylan et al., 1987). This, along with the fact that these genes are highly conserved in the majority of *Aspergillus* species (Yu, 2010), indicate that they are critical for the establishment of asexual differentiation in response to light detection.
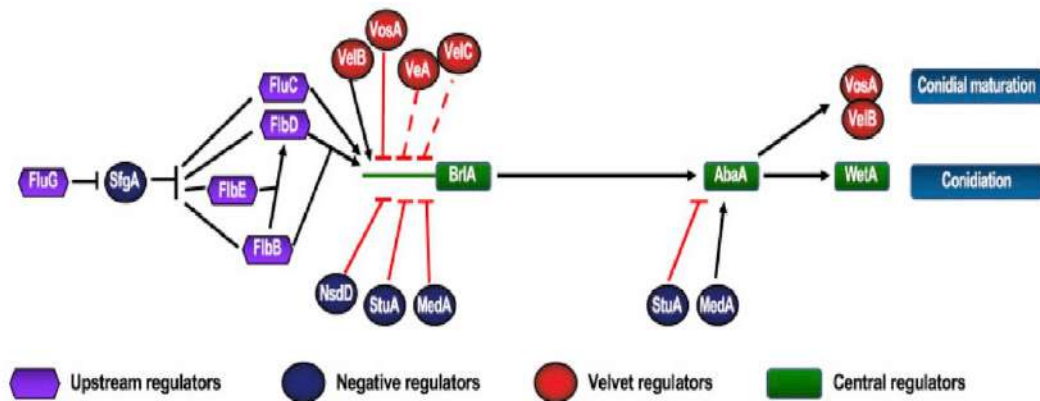
Figure 1.10. The positive and negative regulators that contribute to asexual differentiation. The upstream regulator FluG regulates production of the transcription factors FlbB-FlbE to promote activation of BrlA. This, in turn, promotes activation of AbaA WetA and VosA, which contribute to spore maturation. Various negative regulators and velvet regulators are also shown. The velvet regulators will be discussed in more detail in a later section with respect to their involvement in sexual development. Image taken from (Ojeda-Lopez et al., 2018).

1.5.3. Sexual development of *A. nidulans*

1.5.3.1. Mating and sexual cleistothecia formation

While the majority of *Aspergillus* species reproduce predominately *via* asexual sporulation, only a small percentage of species (36%) are capable of undergoing sexual reproduction, which occurs mostly in the absence of light (Dyer and O'Gorman, 2012). Reproduction *via* sexual means is the main cause of genetic recombination and diversity in the genus *Aspergillus*, and it can potentially generate species that possess increased fitness and adaptability to their surrounding environments (Dyer and O'Gorman, 2011, Geiser, 2009). Like asexual differentiation, a prerequisite for sexual reproduction is the establishment of the mycelium and competent hyphae which undergo hyphal fusion. Mating in *Aspergillus* species requires crossing of two opposite mating type genes, known as either *MAT1-1* and *MAT1-2*, which are transcription factors that regulate sexual development and identity (Turgeon and Yoder, 2000, Varga et al., 2014). Species can either be heterothallic, meaning they possess only one of these mating type genes or they can be homothallic, where the one species possesses both mating types. Homothallism is the predominant form of sexuality in *Aspergillus*. Species such as *A. nidulans* are homothallic and can thus undergo sexual differentiation without the need for a mating partner but still retain the ability to outcross and so are not limited to self-fertilisation (Paoletti et al., 2007, Czaja et al., 2011).

The sexual cycle in many *Aspergillus* species, including *A. nidulans,* involves the production of sexual ascospores. Ascospores are harboured within closed spherical fruiting bodies known as cleistothecia. These reproductive structures are surrounded by external thick-walled globose cells termed Hulle cells, which are considered to

protect cleistothecia as they develop (Dyer and O'Gorman, 2012, Sarikaya Bayram et al., 2010, Wei et al., 2001). Initially, four meiotic ascospore progeny are produced within structures known as asci. These undergo another round of mitotic division, resulting in 8 spores in each ascus. In general, cleistothecia have the potential to possess as many as 100,000 asci. However, on average for *A. nidulans*, a cleistothecium will harbour 80,000 viable ascospores (Braus et al., 2002). Ascospores become dispersed during the degradation of the ascus and cleistothecium walls, rather than forceful discharge which is observed during asexual sporulation (Dyer and O'Gorman, 2012). A schematic illustrating the general structure of an *A. nidulans* cleistothecium is provided (**Figure 1.11.**).
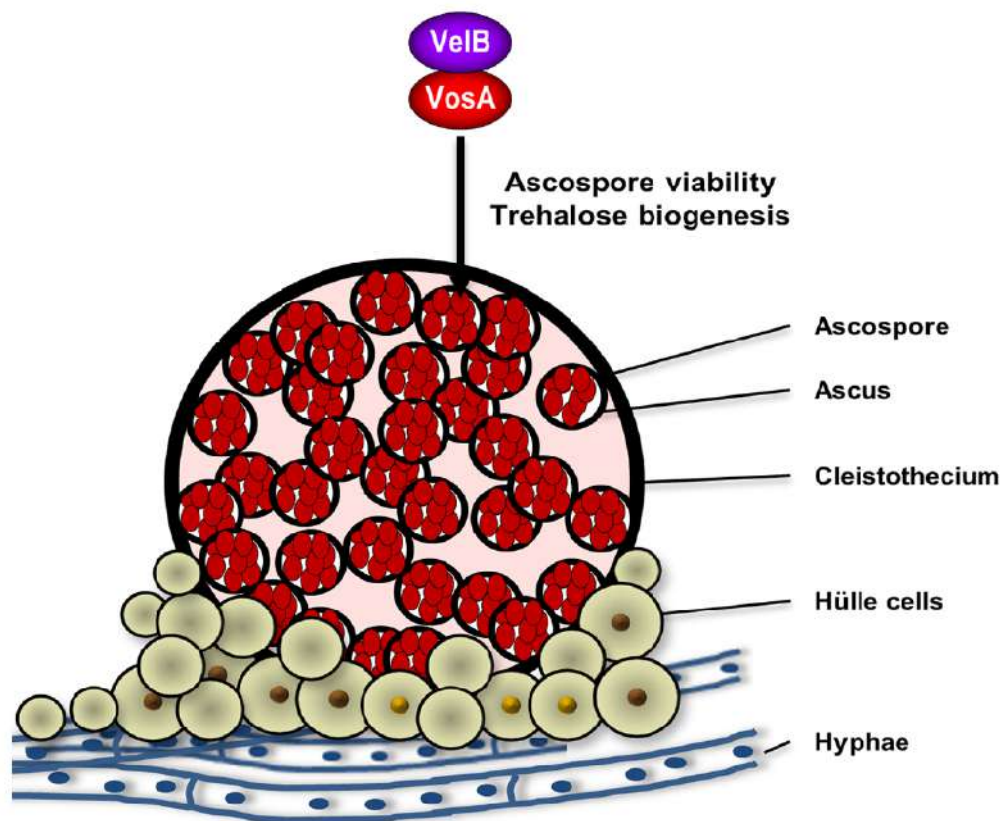
Figure 1.11. The *A. nidulans* cleistothecium. Following hyphal fusion, sexual ascospores develop within vesicle-like structures known as asci. The asci are surrounded by the sexual fruiting body which is known as the cleistothecium. Collections of Hulle cells are at the periphery of each developing cleistothecium and provide nourishment and protection to the fruiting bodies as they mature. Image taken from (Park et al., 2014)

1.5.3.2. The velvet complex

Like asexual differentiation, the sexual reproductive cycle is a highly regulated process and requires an array of proteins in order to respond to stimuli and to trigger morphological transitions. The major proteins that contribute to the regulation of both asexual and sexual development are the velvet proteins, which are fungal specific proteins that are highly conserved among the ascomycetes (Ni and Yu, 2007). The velvet family of proteins consists of four members, with VeA being the founding member of the group. Other proteins in this family include VelB, VosA and VelC (Bayram et al., 2008). VeA is a light-responsive protein that represses asexual conidiation in the absence of light (Mooney and Yager, 1990). VelB is also a light-dependent regulator of fungal development and it interacts with VeA in the cytoplasm (Bayram et al., 2008). VosA interacts with VelB and VosA-VelB heterodimers are required for the negative regulation of conidiation, as well as the accumulation of trehalose in both asexual and sexual spores (Ni and Yu, 2007, Sarikaya Bayram et al., 2010). Lastly, VelC is a positive regulator of sexual cleistothecia production and a negative regulator of asexual sporulation (Park et al., 2014).

In the absence of light, VeA-VelB heterodimers can translocate into the nucleus and interact with the methyltransferase LaeA (Bok and Keller, 2004) to form the trimeric velvet complex, with VeA acting as the light-responsive bridging factor, linking VelB to LaeA (Bayram et al., 2008). This complex has been shown to be essential for regulating sexual development and the process of secondary metabolism (Bayram et al., 2008) which will be discussed in section 1.6.2. Both VeA and VelB are required for the regulation of sexual fruiting body formation, while LaeA is necessary for the production of Hulle cells as well as the regulation of asexual sporulation in the presence of light (Bayram et al., 2008, Sarikaya Bayram et al., 2010). Assembly of the velvet complex is inhibited in the presence of light, with VeA expression and nuclear import being reduced. Because VelB translocation into the nucleus is VeA-dependent, the formation of the trimeric velvet complex in the nucleus is thus reduced (Bayram and Braus, 2012). An overview of the roles of velvet complex and various heterodimers formed by the velvet proteins are illustrated in **Figure 1.12.**
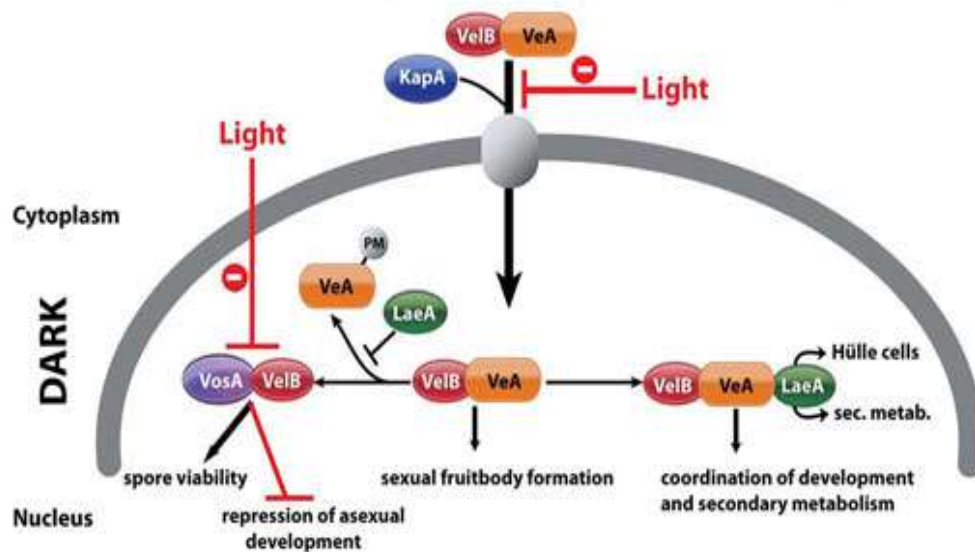
Figure 1.12. Individual velvet protein interactions and complex formation. In the absence of light, the VelB-VeA heterodimer is translocated into the nucleus. The dimer can positively regulate sexual fruiting body formation and can also interact with the methyltransferase LaeA to regulate both Hulle cell formation and secondary metabolism. VelB can also interact with VosA to promote spore viability and to repress asexual development. Image taken from (Sarikaya Bayram et al., 2010).

1.6. Secondary metabolism in filamentous fungi

As mentioned earlier, filamentous fungi are of significant importance as they have the potential to produce a wide range of bioactive SMs. These SMs can be used for example as pharmaceuticals, antibiotics and pesticides but can also pose threats to human and plant health by exerting carcinogenic and mutagenic effects (Yaegashi et al., 2014). While many compounds of interest have been isolated and characterised from filamentous fungal species, genome sequencing suggests that fungal species are capable of producing SMs well in excess of previously predicted numbers as they possess a myriad of dormant SM gene clusters that are not activated under standard laboratory conditions (Sanchez et al., 2012). Due to this, fungal secondary metabolism has become an attractive field of study, with extensive research being performed in attempt to characterise the metabolite profile of filamentous fungal species and to identify new novel SMs.

1.6.1. Classifications and uses of SMs

The production of SMs is dependent on individual sets of genes that are organised in gene clusters and are co-ordinately regulated by specific transcription factors (Brakhage and Schroeckh, 2011, Evans et al., 2011). Fungal SMs are heterogenous, diverse in structure and function and belong to various classes such as polyketides,

non-ribosomal peptides, indole alkaloids and terpenes. Polyketides are the most abundant fungal SMs and are synthesised by type I polyketide synthases (PKSs), which are large, multi-domain proteins (Keller et al., 2005). Polyketides are made up of short chain carboxylic acids like malonyl coenzyme A and acetyl coenzyme A which become condensed to form carbon chains of various lengths. Examples of well-known polyketides include the carcinogenic compound aflatoxin and the cholesterol-lowering drug lovastatin (Keller et al., 2005, Kennedy et al., 1999). Non-ribosomal peptides represent a diverse group of SMs that are derived from either proteinogenic or non-proteinogenic amino acids and are synthesised by large multidomain enzymes known as non-ribosomal peptide synthetases (NRPSs) (Finking and Marahiel, 2004). Examples of well-known non-ribosomal peptides include the β-lactam antibiotics cephalosporin and penicillin (Smith et al., 1990, Keller et al., 2005). Indole alkaloids are primarily synthesised from tryptophan and dimethylallyl pyrophosphate building blocks by the enzyme dimethylallyl tryptophan synthetase (DMATS). The most well characterised indole alkaloid is ergotamine, produced by *Claviceps purpurea,* which can be used to treat migraines (Keller et al., 2005, Tudzynski et al., 1999). Lastly, terpenes are typically odoriferous compounds and are composed of multiple isoprene units. They are synthesised by the enzyme terpene cyclase and examples of terpenes include carotenoids which are believed to act as protective agents against UV radiation and gibberellins, which stimulate excessive plant growth, leading to cell death (Keller et al., 2005, Avalos and Carmen Limon, 2015, Salazar-Cerezo et al., 2018).

1.6.2. Fungal development and secondary metabolism are co-regulated

The process of secondary metabolism is highly regulated and is often co-ordinated with the regulation of fungal growth and development (Calvo et al., 2002, Yu and Keller, 2005). As mentioned earlier, the velvet complex is critical for the modulation of both asexual and sexual differentiation in response to light, as well as secondary metabolism. The main protein of the complex that contributes to secondary metabolism is the highly conserved methyltransferase LaeA, which has been shown to be involved in chromatin remodelling and acts as a global regulator of SM biosynthesis in filamentous fungi (Bok and Keller, 2004, Keller et al., 2005, Bok et al., 2006, Reyes-Dominguez et al., 2010). This protein has been shown to exert a modulatory role, *via* an epigenetic control mechanism on a wide array of SM gene clusters. For example, LaeA is required for the regulation of the sterigmatocystin gene cluster, a carcinogenic compound produced by *A. nidulans* (Bayram and Braus, 2012, Bok et al., 2006). LaeA is also required for the biosynthesis of penicillin by *Penicillium chrysogenum*, gibberellin production by *Fusarium fujikuroi,* gliotoxin production by *A. fumigatus* and aflatoxin production by *A. flavus,* to name a few (Hoff et al., 2010, Wiemann et al., 2010, Kale et al., 2008, Bok and Keller, 2004).

By coupling the processes of development and secondary metabolism, filamentous fungal species possess the ability to conquer new environments and to adapt to new ecological niches, as the majority of SMs enable protection of the parent

organism from competitors as they develop and reproduce (Bayram and Braus, 2012). The co-regulation of these two processes is governed by a multitude of environmental factors and signalling pathways that act upstream of the velvet complex. MAPK pathways are critical for signal transduction downstream to the nucleus, modulating velvet complex functionality and acting as control elements at the interface of both fungal differentiation and SM biosynthesis (Bayram et al., 2012). A MAPK pathway, which is homologous to the yeast Fus3 pheromone module, will be discussed in detail in the next section with regards to its roles in the regulation of both development and secondary metabolism in *A. nidulans*.

1.7. The *A. nidulans* pheromone module

As discussed earlier in **section 1.4.2.**, *S. cerevisiae* utilises a MAPK pathway known as the Fus3 pheromone module to regulate cell fusion and sexual reproduction. Since the discovery of this pathway, multiple MAP kinases and pathways have been identified and characterised in filamentous fungi. These pathways have been shown to be responsible for the regulation of a wide variety of biological processes in fungal species, including asexual conidiation, sexual development, pathogenesis and SM biosynthesis (Li et al., 2005, Lev et al., 1999, Zhao et al., 2005). Orthologs of various proteins belonging to the Fus3 pheromone module pathway have been identified and characterised in *A. nidulans*. These include SteC (Ste11 ortholog), MkkB (Ste7 ortholog), MpkB (Fus3 ortholog), SteD (Ste50 ortholog) and the SteA transcription factor (Ste12 ortholog) (Wei et al., 2003, Vallim et al., 2000, Teague et al., 1986, Bayram et al., 2012).

In *A. nidulans,* the three kinases SteC, MkkB and MpkB interact with the adaptor protein SteD at the plasma membrane in response to pheromone signalling to form the *A. nidulans* pheromone module (**Figure 1.13.**). This results in the sequential phosphorylation of each kinase and the activation of MpkB. Upon activation, the entire tetrameric complex migrates from the plasma membrane to the nuclear envelope and MpkB is translocated into the nucleus. MpkB is then capable of interacting with and phosphorylating both the SteA transcription factor and VeA to promote velvet complex assembly and the subsequent regulation of both fungal development and secondary metabolism (Bayram et al., 2012, Bayram et al., 2008, Atoui et al., 2008, Sarikaya Bayram et al., 2010).

Interestingly, despite the similarities of this pathway to the yeast Fus3 pheromone module (**Figure 1.13.**), no Ste5 scaffold ortholog has been identified in *A. nidulans*. It has also been shown that Ste5 orthologs are absent from filamentous fungal genomes (Rispail et al., 2009). This suggests a unique method of MAP kinase signalling regulation is utilised in filamentous fungi which will be discussed in the next section.
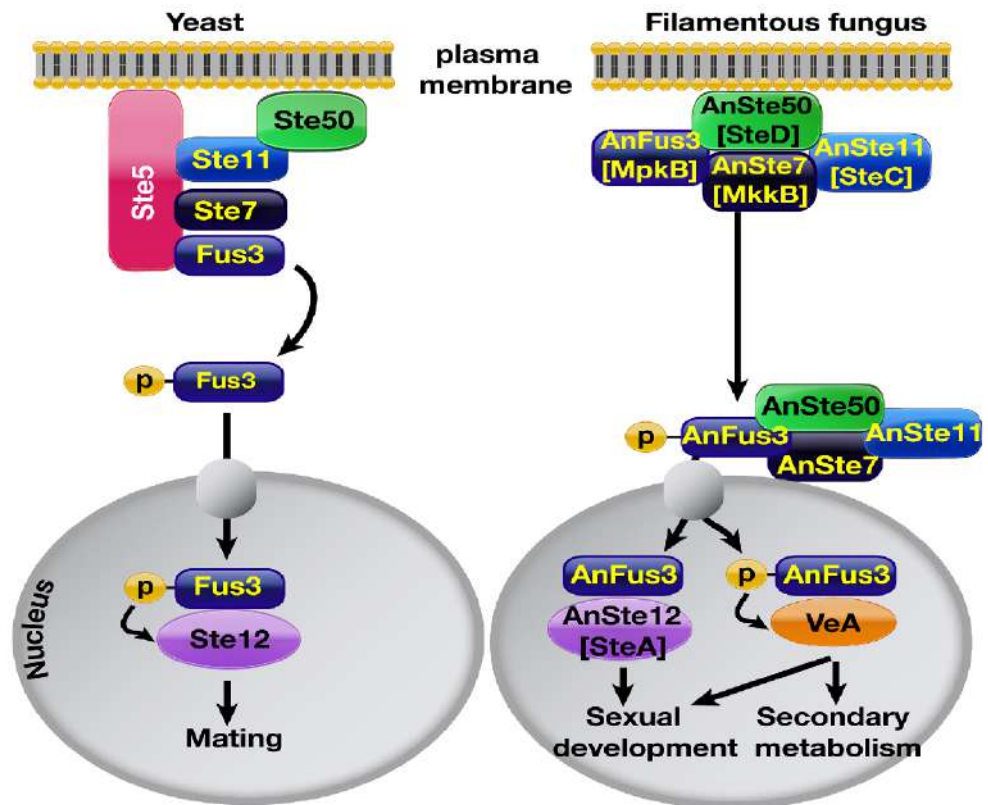
Figure 1.13. Comparison of the yeast and *A. nidulans* Fus3 pheromone modules.
The *A. nidulans* pheromone module consists of the three kinases SteC, MkkB and MpkB which bind to the SteD adaptor at the plasma membrane. Migration of the tetrameric complex to the nuclear envelope results in MpkB translocation into the nucleus. MpkB then activates SteA and VeA to regulate both fungal development and secondary metabolism. Image from (Bayram et al., 2012).

1.8. The *N. crassa* Mak-2 pathway and Ham5 scaffold

A MAP kinase pathway homologous to the yeast Fus3 pheromone module has also been identified and characterised in the ascomycete fungus *N. crassa*, which has been widely used as a model system for studying fungal genetics and development (Roche et al., 2014, Berlin and Yanofsky, 1985). The MAP kinase pathway in this organism consists of the three kinases Nrc-1 (MAPKKK), Mek-2 (MAPKK) and Mak-2 (MAPK) which are crucial for the regulation of both germling and hyphal fusion, as well as sexual development and SM production (Li et al., 2005, Pandey et al., 2004). These three kinases associate with the Ste-50 adaptor protein which promotes Nrc-1 activation (Dettmann et al., 2014), similar to what is observed in *A. nidulans*.

Another similarity to the *A. nidulans* pathway is that no Ste5 ortholog exists in *N. crassa*. However, a protein that was shown to possess typical scaffold characteristics and is crucial for the regulation of cell fusion was identified in this species. This protein was named Ham-5 (Hyphal anastomosis mutant), as the respective mutant strain was

26

incapable of forming interconnected hyphae (Aldabbous et al., 2010, Fu et al., 2011). Ham-5 is highly conserved and unique in filamentous ascomycete fungi and does not exist in yeast (Jamet-Vierny et al., 2007). However, Ham-5 orthologs are mostly uncharacterised and information on their biological roles is sparse. This proposes the question of whether Ham-5 and it's orthologs are required for kinase signalling regulation in filamentous fungal species, as opposed to Ste5 orthologs. Characterisation of the Ham-5 protein by two independent research groups led to the determination that Ham-5 is a large protein of 1,686 amino acids and seven putative WD40 repeats exist at the N-terminus, which are characteristic scaffolding domains. This protein was also shown to be highly phosphorylated, containing 16 putative phosphorylation sites, mostly in the middle section of the protein. This is indicative of proteins that are highly regulated, which is often the case for proteins implicated in cell signalling pathways. Most importantly, Ham-5 was shown to act as a scaffold in the Mak-2 kinase cascade as it was shown to physically associate with Nrc-1, Mek-2 and Mak-2, as well as the Ste-50 adaptor (**Figure 1.14.**). (Dettmann et al., 2014, Jonkers et al., 2014).

It was observed that this entire pentameric complex is localised to small puncta in opposing hyphal tips which grow towards one another during chemotropic interactions. During this polarised growth, the MAP kinase complex undergoes repeated cycles of assembly and disassembly, in which the complex assembles in one hyphal tip, disassembles and then assembles in the opposite hyphal tip (Jonkers et al., 2014). The assembly of this complex results in the sequential phosphorylation of each kinase, resulting in activation of Mak-2. Mak-2 then translocates into the nucleus and activates the PP-1 transcription factor (Dettmann et al., 2014), which is similar to yeast Ste12. This, in turn, leads to the regulation of cell fusion, fungal development and the production of SMs (Li et al., 2005, Leeder et al., 2013).
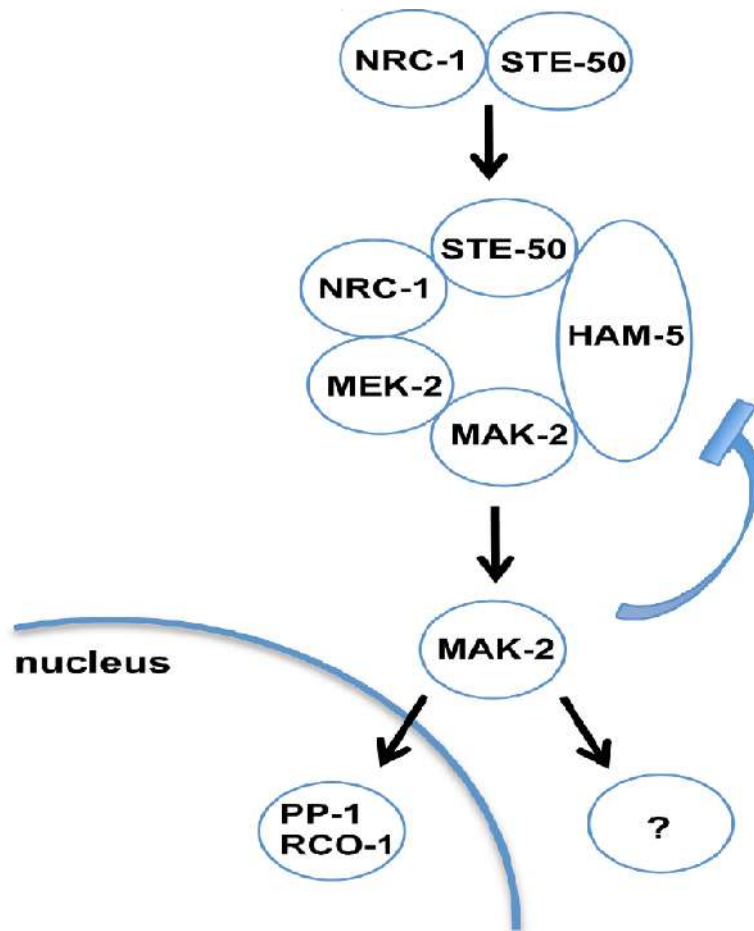
Figure 1.14. Composition of the *N. crassa* Mak-2 cascade. Unknown upstream signals trigger the activation of the kinase Nrc-1, *via* Ste-50 interactions. This results in the recruitment of Ham-5 which mediates the assembly of the pentameric complex. Phosphorylation of each kinase results in Mak-2 activation and translocation into the nucleus. Mak-2 interacts with transcription factors like PP-1 and RCO-1 to promote cell fusion, sexual development and SM production. Mak-2 is also capable of phosphorylating the Ham-5 scaffold, triggering complex disassembly (depicted as a blue arrow). Image taken from (Dettmann et al., 2014).

1.9. The plant pathogenic fungus *A. flavus*

A. flavus is a saprophytic filamentous fungus that inhabits soils worldwide and is considered to be significantly relevant with regards to human and animal health, as well as agriculture. Like *A. nidulans,* this fungus reproduces predominately *via* asexual sporulation, producing conidiophores and haploid conidia (**Section 1.5.2.**) (Amaike and Keller, 2011). Another similarity to *A. nidulans* is that *A. flavus* produces a wide array of SMs and this process is coupled to its development. The genome of *A. flavus* is predicted to contain at least 56 SM gene clusters, with only 8 of these being described in detail in the literature to date (Georgianna et al., 2010, Marui et al., 2011). Certain metabolites produced by this fungus are highly dangerous, such as the aflatoxins which are a group of potent carcinogenic compounds (Amaike and Keller, 2011). Due to the production of aflatoxins, *A. flavus* is classified as a major global threat as it is capable of causing contamination of a wide variety of agricultural crops (**Figure 1.15.**), such as maize, peanuts, corns, cereals and cottonseed, to name a few (Rushing and Selim, 2019, Yu et al., 2005, Lewis et al., 2005). This results in the estimated economic loss of roughly $1 billion annually in the US alone (Amare and Keller, 2014). Ingestion of aflatoxin contaminated crops can pose significant threats to humans and animals and can result in the development of hepatocellular carcinomas or aspergillosis (Bhatnagar-Mathur et al., 2015, Hedayati et al., 2007, Kew, 2013). As of 2016, it was estimated that roughly five billion people are susceptible to the threat of aflatoxins (Faustinelli et al., 2016).
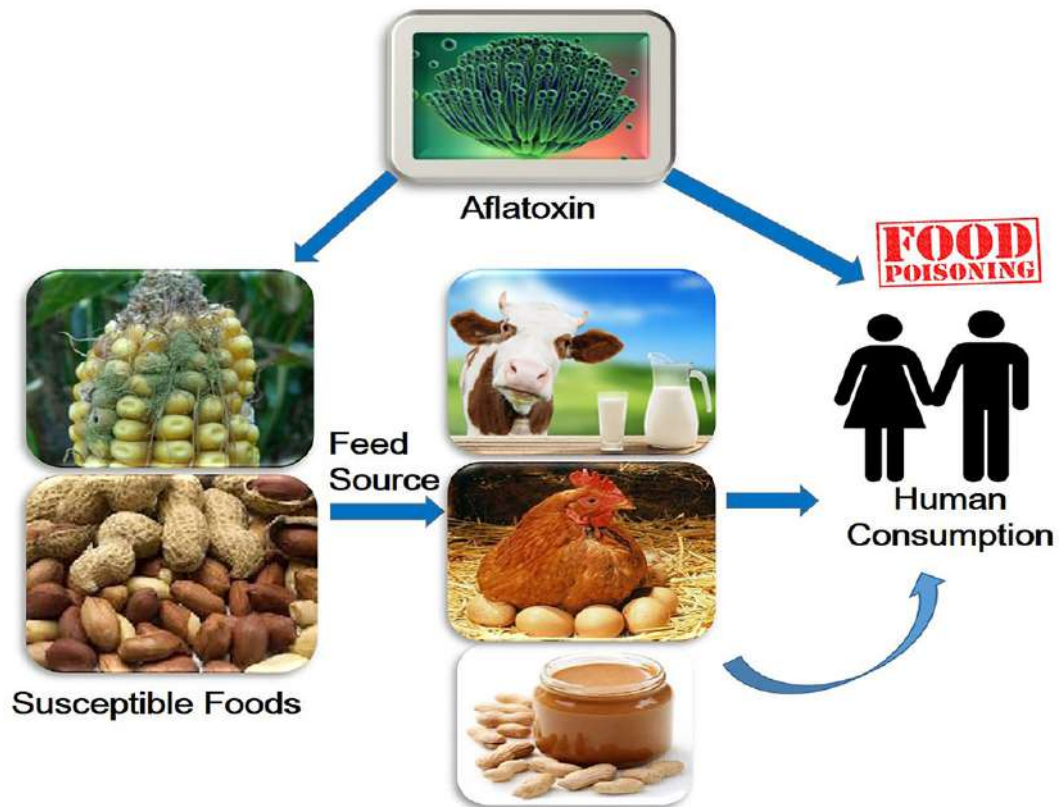
Figure 1.15. Aflatoxin contamination of various crops results in food poisoning and development of hepatocellular carcinomas. *A. flavus* germination on agricultural crops like corn and peanuts can lead to the production of carcinogenic aflatoxins and contamination. Consumption of these contaminated crops either by livestock or directly by humans can lead to food poisoning, aspergillosis and hepatocellular carcinomas. Image taken from (Kumar et al., 2016).

1.9.1. Sexual sclerotia development in *A. flavus*

In order to survive extreme environmental conditions such as starvation, *A. flavus* produces large, multicellular structures known as sclerotia, which are hardened masses of hyphae and are vestigial cleistothecia (McAlpin, 2004, Wicklow and Shotwell, 1983). The formation of sclerotia requires three developmental events to occur. The first stage is known as 'initiation', during which fusion occurs between hyphae to form small initials. The second stage is termed 'development'. It is during this stage that the sclerotia form and enlarge, adopting a white coloration. The final stage of development is known as 'maturation', where the sclerotial surface becomes hardened and pigmented (Willetts and Bullock, 1992).

Sclerotia are also produced as a means of sexual reproduction for various *Aspergillus* species. Under appropriate environmental conditions, if the two opposite mating types *MAT1-1* and *MAT1-2* are present, the sclerotia of most fungal species are capable of developing sexual spores (Horn et al., 2016, Terhem and van Kan, 2014).

However, sclerotia formation does not require the presence of two mating types as sterile sclerotia, devoid of ascospores can be produced by individual mating types (Horn et al., 2009, Horn et al., 2014). When favourable conditions arise, sclerotia can also act as a primary source of inocula for various fungal species, allowing for direct germination to form infective hyphae and conidia which can then infect plant tissues. It has been shown that in some cases, such as for *A. parasiticus,* that sclerotium inoculum is a more efficient means of invasion during peanut pod infection than conidial inoculum (Horn et al., 1994). This, coupled with the longevity of sclerotia in soils, results in sclerotia being considered a major concern with regards to crop health and fungal spread in agricultural environments (Jurick and Rollins, 2007, Coley-Smith and Cooke, 1971).

1.9.2. Global genetic regulators of *A. flavus* development and secondary metabolism

It has been shown that both conidia and sclerotia are capable of containing aflatoxin, as well as many other SMs and that sclerotial development is positively correlated with aflatoxin production (Wicklow and Shotwell, 1983, Brown et al., 2009, Gloer, 1995). However, these two processes are not necessarily dependent on one another and there is limited information regarding the genetic regulation of sclerotia development and how the production of these structures is linked to SM production (Chang et al., 2016, Chang et al., 2017). It has been noted that the development of both *A. flavus* sclerotia and *A. nidulans* cleistothecia share a common origin. This has led to the proposal of a multitude of conserved genetic regulators and pathways for the regulation of both sclerotia development and SM production in *A. flavus* (Calvo and Cary, 2015, Dyer and O'Gorman, 2012, Calvo et al., 2002).

As is the case for *A. nidulans*, the velvet protein VeA acts as a major regulator of *A. flavus* development and SM production. It has been shown that the *veA* gene is required for sclerotia formation and the production of aflatoxins, as well as various other SMs. These include the indole-tetrameric acid mycotoxin cyclopiazonic acid (CPA) and the indole diterpene tremorgenic mycotoxin aflatrem (Duran et al., 2007, Calvo et al., 2004). The *A. flavus laeA* ortholog has also been shown to be critical for both the production of a wide variety of SMs, including aflatoxins and the development of sclerotia (Kale et al., 2008, Georgianna et al., 2010). Studies have also indicated that *laeA* acts as a negative regulator of *veA* expression (Georgianna et al., 2010). *A. flavus* possesses orthologs of both *velB* and *velC* (Chang et al., 2013). *velB* mutants exhibited similar phenotypes to the *veA* mutants, producing reduced levels of aflatoxin and impaired sclerotia formation, whereas the *velC* mutant did not display this phenotype (Duran et al., 2007). (Chang et al., 2013) described interactions of LaeA and VelB with both VeA and FluG and proposed that a fine balance of these interactions is critical for the regulation of sclerotia formation, sporulation and SM production (**Figure 1.16.**). FluG acts in an antagonistic manner with respect to the other velvet members with regards to regulating sclerotia production. A *fluG* mutant displays an increase in

sclerotia formation and does not affect the levels of aflatoxin produced (Chang et al., 2012).

Various other genetic regulators have been found to be involved in *A. flavus* development and secondary metabolism. These include *nsdD* and *nsdC* which encode a GATA-type zinc finger transcription factor and C2H2 zinc finger-type transcription factor, respectively. Both of these genes have been shown to be required for sclerotia production and aflatoxin production in a *veA*-independent manner (Cary et al., 2012, Han et al., 2001, Kim et al., 2009). It is likely that many other genetic regulators exist in *A. flavus*. This species has been shown to possess the *mpkB* ortholog which is essential for the phosphorylation of VeA and velvet complex assembly in *A. nidulans*. However, to date, the roles of *mpkB* in *A. flavus* sclerotia development and secondary metabolism have not been elucidated. It is also known that *A. flavus* contains orthologs of SteC, MkkB, SteD and HamE (Frawley et al., 2020a), suggesting that a MAP kinase pathway may be assembled in this species, similar to what is observed in *A. nidulans*. This could provide a mechanism of velvet complex regulation, allowing for the subsequent regulation of development and SM production in this species.
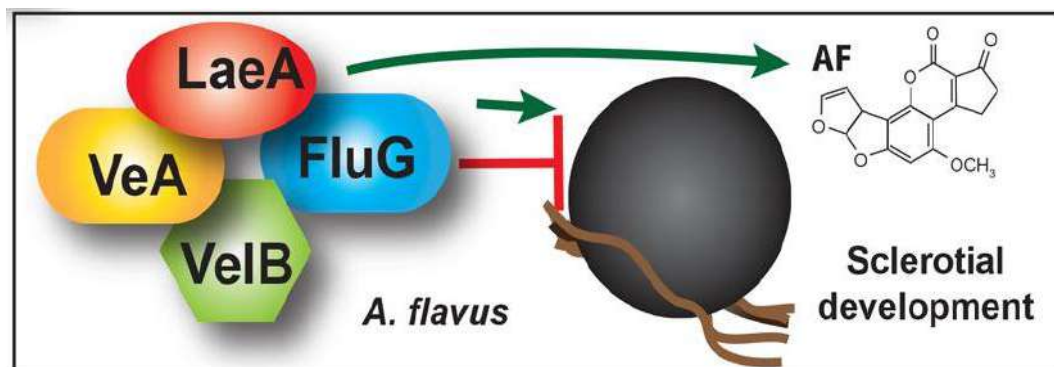
Figure 1.16. The velvet complex is conserved in *A. flavus* and is responsible for the regulation of sclerotia formation and SM production. The trimeric velvet complex (VeA-VelB-LaeA) is highly conserved in *A. flavus*. This complex interacts with FluG and a coordinated balance between these interactions is critical for the regulation of both sclerotia development and the production of various SMs, including aflatoxins. Image taken from (Calvo and Cary, 2015).

1.10. The opportunistic human pathogen *A. fumigatus*

A. fumigatus is a saprophytic fungus that is ubiquitous in the environment (Latge, 1999) and reproduces predominately *via* the production of hydrophobic conidia, in a similar manner to both *A. nidulans* and *A. flavus*. These conidia can easily spread throughout the air, allowing for the colonisation of new environments and the rapid spread of this species (Dagenais and Keller, 2009). The conidia of this fungus can pose severe threats to human health, as these spores are commonly inhaled daily and can germinate in the alveoli in the lungs due to their small size of 2-3μm (Latge, 1999). Within 4-6 hours of colonisation, conidia can produce short hyphae known as germ tubes (van de Veerdonk et al., 2017) and can spread throughout the lungs, resulting in the development of invasive pulmonary aspergillosis (**Figure 1.17.**). Immunocompromised individuals, such as patients that are undergoing chemotherapy or organ transplantations for example, have a much higher risk of developing pulmonary aspergillosis and the mortality rate in these individuals is generally over 50%, reaching as high as 95% in specific situations (Latge, 1999, Latge, 2001, McCormick et al., 2010, Balloy and Chignard, 2009, Maschmeyer et al., 2007).
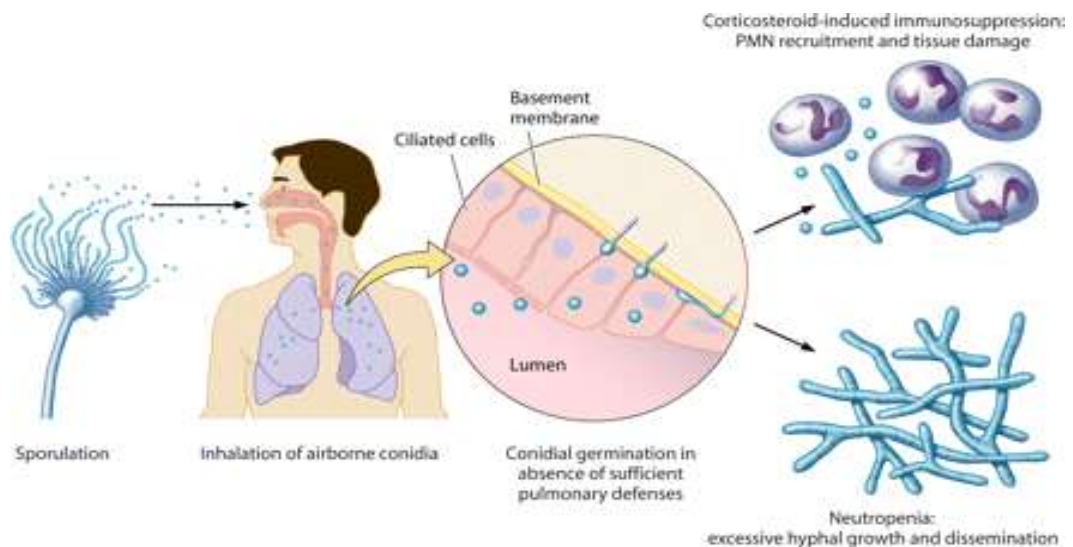
Figure 1.17. Colonisation of the human lung by *A. fumigatus* conidia leads to pulmonary aspergillosis. Inhaled conidia reach the alveoli of the human lungs and are capable of germinating and disseminating throughout the lung tissue in immunocompromised individuals. Image taken from (Dagenais & Keller, 2009).

1.10.1. Factors that contribute to *A. fumigatus* pathogenicity

A myriad of factors contribute to the survival and spread of *A. fumigatus* spores in the human body. For example, *A. fumigatus* is capable of adapting it's metabolism to a wide range of environmental conditions. *A. fumigatus* has the ability to produce various proteases and enzymes that possess broad biological activity. These proteases and enzymes are utilised to degrade lung tissue, resulting in the liberation of macromolecules and organic compounds for metabolism (de Vries and Visser, 2001, van de Veerdonk et al., 2017). A major contributor to *A. fumigatus* virulence is the production of various SMs, most notably the immunosuppressive mycotoxin gliotoxin (Hof and Kupfahl, 2009), which is implicated in 96% of cases of *A. fumigatus* infection (Ghazaei, 2017). Gliotoxin inhibits the activity of various enzymes including nicotinamide adenine dinucleotide phosphate (NADPH) oxidases and alcohol dehydrogenases and is also capable of inducing apoptosis and inhibiting various functions of macrophages and neutrophils (Gardiner et al., 2005, Spikes et al., 2008). As a result, gliotoxin production enables fungal growth and colonisation of host tissue *via* suppression of the immune system (Ghazaei, 2017).

MAPK pathways are also implicated in *A. fumigatus* pathogenicity. For example, *A. fumigatus* utilises various MAPK pathways to regulate cellular responses to a myriad of stresses that it encounters when infecting a human host. The main defence and source of structural integrity for *A. fumigatus* cells as they colonise the lungs is the fungal cell wall (Abad et al., 2010). The cell wall retains high plasticity and its composition is readily altered to adapt to various environmental conditions and cell stressors, allowing for *A. fumigatus* spores to avoid the body's natural defence mechanisms (van de Veerdonk et al., 2017). Stressors that target the fungal cell wall activate a MAPK pathway known as the cell wall integrity (CWI) pathway, which signals *via* the MAPK MpkA. This pathway is essential in regulating detection and appropriate responses to cell wall perturbing agents, allowing for fungal survival and spread throughout the host (van de Veerdonk et al., 2017). *A. fumigatus* also utilises MAP kinases to regulate responses to other cell stresses like osmotic and oxidative stressors. In response to hyperosmotic conditions, the high osmolarity glycerol (HOG) pathway becomes activated, which signals to the nucleus *via* the MAPK SakA (Martinez-Montanes et al., 2010, de Nadal and Posas, 2015). It has been shown that the kinases SakA, along with MpkC, are essential in regulating the adaptation of *A. fumigatus* spores to osmotic stresses as well as various oxidative and cell wall stresses (Bruder Nascimento et al., 2016). The utilisation of a myriad of MAPK pathways allows for the efficient detection and adaptation of *A. fumigatus* to the human host environment, promoting cell survival and pathogenicity.

1.10.2. Regulators of *A. fumigatus* development and secondary metabolism

As mentioned in section 1.10, *A. fumigatus* reproduces *via* the production of conidiophores and haploid conidia (Dagenais and Keller, 2009). The main regulators of asexual sporulation discussed for both *A. nidulans* and *A. flavus* are also conserved

in *A. fumigatus.* These include the central regulatory pathway proteins BrlA, AbaA and WetA (Yu, 2010, Adams et al., 1998), the upstream regulators of conidiation FluG, FlbA, FlbB, FlbC, FlbD and FlbE (Wieser et al., 1994) and the velvet complex components VeA, VelB, VelC, VosA and LaeA (Bayram and Braus, 2012, Ni and Yu, 2007). With regards to sexual development, it was proposed originally that *A. fumigatus* does not have a natural sexual life cycle. However, it has been shown *via* Basic local alignment search tool (BLAST) analysis that the *A. fumigatus* Af293 genome contains at least 215 functional genes that have been linked to sexual development (Dyer and O'Gorman, 2012, Galagan et al., 2005, Fedorova et al., 2008). It was also shown that *A. fumigatus* contains the pheromone precursor (*ppgA*), pheromone receptors (*preA* and *preB*) as well as both mating type genes (*MAT1-1* and *MAT1-2*) in near-equal proportions, suggesting that sexual reproduction occurs between *A. fumigatus* isolates in the wild (Paoletti et al., 2005). In 2009, it was discovered that *A. fumigatus* is capable of producing asci, ascospores and cleistothecia under very specific laboratory conditions (O'Gorman et al., 2009). However, despite these discoveries, information regarding the genes and proteins that contribute to the regulation of sexual reproduction in *A. fumigatus* is limited. Also, the environmental conditions required to induce sexual development, as well as the evolutionary significance of this developmental programme in *A. fumigatus* are also not fully understood.

Like *A. nidulans* and *A. flavus, A. fumigatus* is capable of producing a wide range of SMs. *A. fumigatus* has 40 predicted SM core synthase enzyme-encoding genes, 19 of which have been shown to produce downstream products (Romsdahl and Wang, 2019). Examples of SMs produced by *A. fumigatus* include gliotoxin (discussed in section 1.10.1), as well as endocrocin, trypacidin, fumagillin and many others. Endocrocin contributes to fungal pathogenicity *via* inhibition of neutrophil recruitment (Berthier et al., 2013). Trypacidin is a spore metabolite that exerts cytotoxic activity against lung cells (Gauthier et al., 2012). Fumagillin exhibits antibiotic properties and has been studied extensively for use in cancer treatments as it also exerts anti-angiogenic activity (Sin et al., 1997, Mc et al., 1951).

As mentioned above, orthologs of the velvet complex proteins exist in *A. fumigatus* and these proteins have been shown to regulate both development and secondary metabolism in this species (Park et al., 2012). VeA mutants exhibit significant differences in gene expression in comparison to a wild type strain, with 453 genes being upregulated and 1,137 genes being downregulated (Dhingra et al., 2013). VeA is required for the positive regulation of an array of secondary metabolism genes. The SMs under VeA control include gliotoxin, (Dhingra et al., 2012), fumagillin, fumitremorgin G, fumigaclavine C and glionitrin A (Dhingra et al., 2013). LaeA acts as a global regulator of various SM gene clusters and deletion of the *laeA* gene results in reduced virulence as well as the loss of gliotoxin production (Bok et al., 2005). Microarray analysis has also shown that the loss of LaeA results in significant changes in expression in as many as 13 SM gene clusters, with the majority of these clusters being significantly downregulated (Perrin et al., 2007).

Despite the knowledge of various regulators of development and secondary metabolism in *A. fumigatus,* information regarding the mechanisms of signal detection and transduction is limited. Interestingly, it has been shown that *A. fumigatus* possesses orthologs of each of the five *A. nidulans* pheromone module proteins (Frawley et al., 2020b). With the exception of *mpkB,* which has recently been studied (Manfiolli et al., 2019), these proteins are mostly uncharacterised and very little information is known regarding their biological roles in *A. fumigatus.* It is possible that these proteins could form a complex, similar to what is observed in *A. nidulans.* This could suggest that the pheromone module is utilised to regulate development and secondary metabolism in *A. fumigatus,* perhaps *via* interactions with the velvet complex proteins.

1.11. Aims of this study

MAPK pathways are highly conserved signal transduction cascades in eukaryotic organisms and are required for the regulation of a wide array of biological processes (Schaeffer and Weber, 1999). In fungi, these pathways are utilised to regulate a myriad of cellular responses such as asexual sporulation, sexual reproduction, stress responses and secondary metabolism (Li et al., 2005, Lev et al., 1999, Zhao et al., 2005). The regulation of MAPK signalling is a highly dynamic process that requires the coordination of a variety of chemical messengers and signalling elements. In many cases, large multi domain proteins known as scaffolds are incorporated in MAPK cascades to spatially and temporally regulate MAPK signalling (Good et al., 2011). For example, the MAPK cascade known as the pheromone module in yeast requires the Ste5 scaffold to bind three kinases and to promote signal propagation to the nucleus, inducing sexual development and cell fusion (Bardwell, 2005, Pryciak and Huntress, 1998). A homologous MAPK pathway has been discovered in the filamentous ascomycete fungus *A. nidulans* and has been shown to consist of four proteins. These proteins are the three kinases SteC, MkkB and MpkB, as well as the SteD adaptor. This pathway was shown to regulate asexual sporulation, sexual cleistothecia development and the production of various SMs (Bayram et al., 2012). However, the mechanism of signal regulation and the composition of the complex were not considered to be fully understood. This is because no scaffold protein was shown to be interacting with the members of this pathway.

As a result, this led to the first aim of this thesis which was to identify a scaffold candidate for the *A. nidulans* pheromone module and to characterise its roles within this pathway and its interactions with each member of the complex. Consequently, the purpose of this work is to provide insight into both the regulation of MAPK signalling in this fungus, as well as the influence of this MAPK cascade in the modulation of fungal development and secondary metabolism. The second and third aims of this project were to identify homologous members of the pheromone module complex in the pathogenic filamentous fungi *A. flavus* and *A. fumigatus* respectively. Once identified, a genetic and proteomic approach would be utilised to allow for the determination of whether or not these proteins form a complex, similar to what is

observed in *A. nidulans*. The roles of this complex with respect to the regulation of fungal development, stress responses and secondary metabolism would then be determined.

Overall, this thesis aims to provide a detailed characterisation of the composition and regulation of the pheromone module in three *Aspergillus* species. This thesis also aims to provide insight into how these fungi utilise this MAPK pathway to control their asexual and sexual development and production of various SMs. As a result, this study may contribute to the understanding of how fungal species like *A. flavus* and *A. fumigatus* are capable of producing dangerous mycotoxins like aflatoxins and gliotoxin respectively. By understanding the regulation of fungal development and SM production, strategies may be developed that could result in the prevention of crop spoilage due to mycotoxin contamination and infections caused by *Aspergillus* species.

Chapter 2

Materials and Methods

2.1. Strains, growth media and culturing conditions

2.1.1. Fungal and Bacterial Strains

Fungal strains used in this study are listed in **Appendix A:Table S14** for *A. nidulans*, **Appendix B:Table S1** for *A. flavus* and **Appendix C:Table S1** for *A. fumigatus*. The *A. nidulans* AGB551 strain, the *A. flavus* TJES19.1 strain and the *A. fumigatus* CEA17 (*pyrG+*) and CEA17 (*pyrGΔ*) strains served as wild type hosts for all deletions and epitope taggings. Various plasmids used for the knock-out and epitope tagging experiments are listed in **Appendix A:Table S15** for *A. nidulans*, **Appendix B:Table S2** for *A. flavus* and **Appendix C:Table S2** for *A. fumigatus*. All plasmids used for transformation of fungal cells were initially cloned into either Stellar (Clontech) and MACH-1 (Invitrogen) competent *Escherichia coli* cells.

2.1.2. Growth Media for Bacterial and Fungal Strains

Both bacterial strains listed in **2.1.1** were cultured in lysogeny broth (LB) medium (1% tryptone, 0.5% yeast extract, 1% NaCl), which was supplemented with 100μg/ml ampicillin and super optimal broth with catabolite repression (SOC) medium (2% tryptone, 0.5% yeast extract, 10mM NaCl, 2.5mM KCl, 10mM $MgCl_2$, 10mM $MgSO_4$, 20mM glucose).

For the growth of fungal strains, Glucose Minimal Medium (GMM) was used: (6g/L $NaNO_3$, 0.52g/L KCl, 1.52g/L KH_2PO_4, 10g/L Glucose, 0.24g/L $MgS0_4$), supplemented with 0.1% trace element solution (76μM $ZnSO_4$, 178μM H_3BO_3, 25μM $MnCl_2$, 18μM $FeSO_4$, 7.1μM $CoCl_2$, 6.4μM $CuSO_4$, 6.2μM Na_2MoO_4, 174μM ethylenediaminetetraacetic acid (EDTA)). Other supplements and selection markers included biotin (25μg/L), pyridoxine (10mg/L), uracil (1g/L), uridine (0.25g/L), pyrithiamine (0.1mg/L) (Sigma), nourseothricin sulphate (100mg/L) (Gold Bio) and phleomycin (100μg/ml for *A. flavus* strains and 30μg/ml for *A. fumigatus*).

For the growth of Green Fluorescent Protein (GFP), Human influenza hemagglutinin (HA) and Tandem Affinity Purification (TAP)-tagged fungal strains which were used for protein purifications, followed by mass spectrometry, liquid Sabouraud (CMO147 Oxoid, 30g/L) and complete media (GMM medium ingredients with the addition of 1g/L tryptone, 2g/L peptone and 1g/L yeast extract) were used.

For asexual development growth tests of *A. flavus,* Potato Dextrose Agar (PDA) medium was used (P6685 Sigma, 24g/L), with required supplements. For sclerotia induction, Wickerham (WHM) medium was used (2g/L yeast extract, 3g/L peptone, 5g/L corn steep solids, 2g/L dextrose, 30g/L sucrose, 2g/L NaNO$_3$, 0.76g/L K$_2$HPO$_4$, 0.24g/L MgS0$_4$, 0.2g/L KCl, 0.1g/L FeSO$_4$.7H$_2$O). For the cultivation of *A. flavus* strains for HPLC analysis, Yeast Extract Sucrose (YES) medium was used (20g/L yeast extract, 150g/L sucrose, 0.5g/L MgS0$_4$), while Czapek-Dox liquid medium (233810 BD, 35g/L) was used for *A. fumigatus* strains.

For testing the stress responses of *A. fumigatus* strains, strains were inoculated on GMM agar plates containing appropriate supplements and the following stress agents were used: Congo Red (20μg/ml, 30μg/ml, 50μg/ml), H$_2$O$_2$ (2mM, 3mM, 4mM) and NaCl (0.5M, 1M, 1.5M).

2.1.3. Culturing conditions for fungal cells

To induce vegetative growth, fungal spores were added to either GMM, complete, Sabouraud or Czapek-Dox liquid media and left to incubate for at least 24 hours on a shaker at 180 revolutions per minute (RPM). All *A. nidulans* and *A. fumigatus* cultures were incubated at 37˚C, while all *A. flavus* cultures were incubated at 30˚C. For asexual spore propagation, strains were inoculated on GMM agar plates, containing 2% agar and incubated at either 30 or 37 degrees in the presence of light. For sexual reproduction, *A. flavus* and *A. nidulans* were inoculated on WHM and GMM agar plates respectively and incubated in the absence of light. These plates were completely covered in aluminium foil. For asexual and sexual induction of vegetatively grown mycelia, fungal strains were initially cultured in liquid GMM for 24 hours and then the mycelia were filtered through miracloth and transferred to either solid GMM or PDA plates containing 2% agar. For asexual induction, strains were then incubated in the light, while strains were incubated in the dark to induce sexual development. Plates to be incubated in the dark were completely covered in aluminium foil. For all TAP-MS (Mass spectrometry) experiments, fungal strains were cultured in liquid complete medium overnight on a shaker, while all GFP and HA-tagged strains were cultured in either liquid complete medium or Sabouraud medium and incubated overnight on a shaker.

2.2. Plasmid Construction

Details of all plasmids and all oligonucleotide sequences used in this study are given in **Appendix A:Tables S15 and S16** for *A. nidulans*, **Appendix B:Tables S2 and S3** for *A. flavus* and **Appendix C:Tables S2 and S3** for *A. fumigatus*. The Lasergene Seqbuilder software was used to design all plasmid maps *in silico*. For all cloning experiments, pUC19 (Fermentas) digested with a *Sma*I restriction enzyme (Thermo Scientific), pAN8-1 digested with a *Stu*I restriction enzyme (Thermo Scientific) and pOSB113 digested with a *Swa*I restriction enzyme (Thermo Scientific) were used. For the construction of all deletion fragments, 1-1.5 kilo base pairs (Kb) from the 5' untranslated region (UTR) and 3' UTR flanking regions of the gene of interest were polymerase chain reaction (PCR)-amplified using the Q5 High Fidelity DNA Polymerase kit (New England Biolabs) from genomic DNA with respective oligonucleotides. These UTR fragments were fused by fusion PCR to a selection marker (*ptrA, pyroA, pyrG, phleO*) that was PCR-replicated from a plasmid containing the marker of interest. These three fragments were then cloned into the *Sma*I site of pUC19 by the In-Fusion HD Cloning enzyme (Clontech, 121416) to create a circular plasmid, that would then be transformed into competent bacterial cells.

To create the *sgfp, 3xha* and *ctap* fusion constructs, 1.5-2Kb of the gene open reading frame (ORF) (with stop codon removed) and 1-1.5Kb of the 3' UTR sequence were PCR-amplified from genomic DNA and fused to either *sgfp*, *3xha* or *ctap* epitope tags connected to various selection markers (*natR, ptrA, phleO, pyrG, pyroA*). All epitope tags were fused to the gene ORFs at the C-terminal ends. These three fragments were then cloned into the *Sma*I site of pUC19. Each ligated plasmid was then transformed into competent bacterial cells.

To generate the complementation plasmids, primers were created to replicate DNA fragments containing an entire gene ORF and 1.5-2Kb of both the 5' and 3' UTRs from a genomic DNA template. These genomic fragments were then cloned into plasmids that contain various selection markers. The *A. flavus hamE* complementation construct was cloned into the *Stu*I site of the pAN8-1 plasmid which contains a phleomycin resistance cassette (*phleO*), while the *A. flavus steC, mkkB, mpkB* and *steD* complementation constructs were cloned into the *Swa*I site of the pOSB113 plasmid, which contains a *pyrG* marker. The *A. fumigatus hamE* complementation construct was cloned into the *Swa*I site of the pOSB113 plasmid. To generate the *steC, mkkB, mpkB*

and *steD* complementation constructs, the entire ORFs excluding the UTR sequences were cloned into the *Pme*I site of the pSK379 plasmid, which contains a *ptrA* marker and a *gpdA* promoter. All ligated complementation plasmids were then transformed into competent bacterial cells. 10-15μg of each plasmid was transformed ectopically into fungal deletion recipient strains. For details of the construction of *A. nidulans* complementation strains, see (Bayram et al., 2012).

2.3. Transformation of bacterial cells and plasmid isolation

2.3.1. Bacterial cell transformation and confirmation

150μl of competent Stellar/MACH-1 *E. coli* cells were added to ligated circular plasmid constructs on ice and left to incubate for 30 minutes. Samples were heat shocked at 42˚C for 1 minute and immediately put back on ice. 800μl SOC medium was added and samples were left to incubate on a shaker (180 RPM, 1 hour, 37˚C). Samples were centrifuged for 1 minute (13,000 RPM), the supernatant was removed and bacterial cells were spread on LB agar plates containing ampicillin. Plates were left to incubate at 37˚C for 16 hours. The next day, colony PCR experiments using *Taq* polymerase were performed to verify positive colonies that would be selected for plasmid isolation.

2.3.2. Miniprep protocol for small scale plasmid isolation

For the small scale isolation of plasmids from positive colonies, the 'QIAprep spin miniprep kit' (Qiagen) was used. A single positive colony was inoculated in 5ml of LB medium containing ampicillin (1:1,000) and incubated on a shaker at 180 RPM for 16 hours at 37˚C. The next day, the bacterial culture was transferred to a Falcon tube and centrifuged for 10 minutes at 5,000 RPM. The supernatant was disposed and the pellet was resuspended in 250μl of P1 buffer, containing RNase A and LyseBlue. The resuspended pellet was then transferred to a microcentrifuge tube and 250μl of P2 lysis buffer was added. Samples were mixed well by inverting and left to incubate for 2-3 minutes. 350μl of N3 neutralisation buffer was then added and samples were inverted immediately, until the solution turned clear. Samples were centrifuged at 13,000 RPM

for 10 minutes and the supernatant was added to a QIA prep spin column in a collection tube. Samples were centrifuged at 13,000 RPM for 1 minute and the flowthrough was discarded. 500µl of PB buffer was added to the column and samples were centrifuged for 1 minute at 13,000 RPM. The flowthrough was discarded and 750µl of PE buffer was added to the columns. Samples were centrifuged for 1 minute at 13,000 RPM, the flowthrough was discarded and samples were centrifuged for another 1 minute to remove residual wash buffer. Columns were transferred to 1.5ml microcentrifuge tubes and 30-50µl of elution buffer was added directly to the columns. Samples were centrifuged at 13,000 RPM for 1 minute and eluted DNA was quantified using a Nanodrop.

2.3.3. Midiprep protocol for large scale plasmid isolation

For the large scale isolation of plasmids, the 'Plasmid Plus Maxi Kit' (Qiagen) was used. A single positive colony was inoculated in 50ml of LB medium containing ampicillin (1:1,000) and incubated on a shaker at 180 RPM for 16 hours at 37°C. The next day, the bacterial culture was transferred to 50ml Falcon tubes and centrifuged at 5,000g for 15 minutes at 4°C. The supernatant was removed and the bacterial pellet was resuspended in 8ml P1 buffer. 8ml of P2 lysis buffer was then added and the sample was mixed by inversion and left to incubate at room temperature for 3 minutes. 8ml of S3 buffer was added to the sample and was mixed well by inversion. The sample was transferred to a QIAfilter cartridge and left to incubate at room temperature for 10 minutes. During this incubation, a Qiagen plasmid plus spin column was connected to a QIAvac 24 Plus suction pump *via* a tube extender. A plunger was inserted into the QIAfilter cartridge and the bacterial sample was filtered into a new 50ml Falcon tube. 5ml BB buffer was added to the Falcon tube and sample was mixed well by inversion. The sample was then filtered through the Qiagen plasmid plus spin column by applying a 300 mbar vacuum until all of the liquid had been drawn through the column. 700µl of ETR buffer was then added to the columns, followed by 700µl of PE buffer. All liquid was drawn through the column. To remove residual PE wash buffer, the column was centrifuged at 10,000g for 1 minute. The column was then transferred to a 1.5ml microcentrifuge tube and 250µl of EB buffer was added. The sample was centrifuged at 10,000g to elute the DNA. All DNA samples were quantified *via* a Nanodrop.

2.4. Transformation of fungal cells

For transformation of fungal cells, strains were cultured for 24 hours at 37˚C in liquid GMM. Mycelia were filtered through sterile miracloth and washed three times with citrate buffer (150mM KCl, 580mM NaCl, 50mM sodium citrate, pH5.5). Mycelia were transferred to sterile flasks and incubated in 20ml citrate buffer containing 500mg glucanase (Novozymes) and 240mg lysozyme (Serva) for 100 minutes at 30˚C (50-60 RPM). Protoplasts were filtered through sterile miracloth into a 50ml Falcon tube and pre-chilled STC1700 (1.2M sorbitol, 10mM Tris pH5.5, 50mM $CaCl_2$, 35mM NaCl) was used to make the volume up to 50ml. Samples were inverted multiple times and left on ice for 10 minutes. Samples were centrifuged at 2,600 RPM for 15 minutes at 4˚C. Supernatant was removed and pellet was resuspended in 1ml STC1700 buffer. The volume was made up to 50ml with STC1700 buffer and samples were centrifuged using the same settings. Supernatant was removed and pellet was resuspended in 1ml STC1700. Protoplasts were separated into two 150µl aliquots, with 1-1.5µg of linear DNA or 10-15µg of circular plasmid DNA being added to one and no DNA being added to the other, to act as a negative control. Samples were incubated on ice for 30 minutes. PEG4000 (60% PEG4000, 10mM Tris pH7.5, 50mM $CaCl_2$) was added to each sample three times (2 x 250µl and 1 x 850µl aliquots). Following each addition, samples were inverted 15-20 times. Samples were left to incubate in a rack on top of ice for 30 minutes. STC1700 was added to each Falcon tube to make the volume up to 15ml and samples were inverted. Falcon tubes were centrifuged at 2,600 RPM for 15 minutes at 4˚C. Supernatant was discarded, the pellet was resuspended and protoplasts were inoculated on GMM agar plates containing 1.2M sorbitol.

2.5. Hybridization techniques

The Lasergene SeqBuilder software was used to design the 5' and 3' UTR probes for hybridisation and allowed for selection of appropriate restriction enzymes for digesting genomic DNA. Probes were synthesised and labelled with (DIG) Digoxigenin-11-UTP (PCR DIG Probe Synthesis Kit: Roche, 11093657910), using either 5' or 3' UTR fragments as templates and the respective oligonucleotides. Fungal genomic DNA was isolated from mycelia using the 'Zymo Research Fungal/Bacterial Miniprep Kit'. 700ng was digested overnight with a suitable restriction enzyme and was separated on

a 0.7% agarose gel at 100 Volts for 90 minutes. The gel was washed 3 times on a shaker at room temperature in the following solutions (0.25M HCl for 10 minutes, 0.5M NaOH/1.5M NaCl for 25 minutes and 1.5M NaCl/0.5M Tris for 30 minutes). The DNA fragments were transferred and ultraviolet (UV) cross-linked (UV Stratalinker 1800) to a nylon membrane (Amersham Hybond™-N+, GE Healthcare). The membrane was washed twice with 2x saline sodium citrate (SSC) buffer (NaCl 17.53g/L, Na-citrate 8.82g/L, pH7) and dried for 5 minutes at 70˚C. The membrane was incubated in a rotating tube at 42˚C in pre-hybridisation buffer (5x SSC, 50% formamide, 50mM pH7 sodium phosphate buffer, 7% sodium dodecyl sulphate (SDS), 2% blocking reagent (Roche 11096176001) and 0.1% lauroylsarcosine) for 1 hour on a rotator. The probe was then added and left to incubate overnight.

The next day, the membrane was left on the rotator and was washed with 2x SSC/0.1% SDS solution for 5 minutes, followed by 2 washes with pre-heated 0.1x SSC/0.1% SDS, each for 20 minutes. The membrane was washed with 20ml DIG buffer 1 (0.1M maleic acid, 150mM NaCl, pH7.5), followed by incubation in 15ml DIG buffer 2 (1:10 dilution of DIG buffer 1 in blocking reagent) for 30 minutes. Alkaline phosphatase conjugated anti-DIG antigen binding fragment (Fab) (Roche 11093274910) was then added to the DIG buffer 2 (1:10,000 dilution) and left to incubate for 1 hour. 2 washes with 20ml wash buffer (DIG buffer 1 with 0.3% Tween 20) were performed for 15 minutes, followed by an incubation in 10ml DIG buffer 3 (100mM Tris-base, 100mM NaCl, 50mM $MgCl_2$, pH9.5) for 5 minutes. For chemiluminescent detection, CDP Star substrate (Roche) was added to the membrane and the membrane was exposed using the G:BOX Chemi XRQ (Syngene).

2.6. Phenotypic assays

All strains were point inoculated on agar plates at a spore density of $5x10^3$ spores in triplicate. GMM agar plates were used for *A. nidulans* and *A. fumigatus*, while PDA and WHM agar plates were used for *A. flavus* strains. All plates contained appropriate supplements. Plates were incubated in the presence of light for 4-5 days (depending on the species) to induce asexual conidiation. Plates were incubated in the absence of light for 5 days (*A. nidulans*) and 2 weeks (*A. flavus*) to induce sexual cleistothecia and sclerotia development respectively. All *A. nidulans* and *A. fumigatus* incubations were performed at 37˚C, while all *A. flavus* incubations were performed at 30˚C.

Stereomicroscopic images of the colonies were captured using the Olympus szx16 microscope with an Olympus sc30 camera. Digital pictures were taken and processed with the Cell Sens Standard software (Olympus). Quantifications of colony diameter, asexual conidiation, cleistothecia production and sclerotia production were performed using three independent biological replicates. To determine asexual conidiation levels, 0.5cm diameter agar cores were removed from the centre of colonies that were spot inoculated ($5x10^3$ spores) on agar plates. These agar cores were resuspended in 500μl of Phosphate buffered saline (PBS) solution in 1.5ml microcentrifuge tubes and put on a shaker for 30 minutes. These spore solutions were then diluted 1/100 and haemocytometer slides were used for counting spores. To determine the quantities of cleistothecia produced, images at 2x magnification were taken of the spot inoculated strains using the Olympus szx16 microscope and cleistothecia were counted manually. WHM agar plates were washed with 70% ethanol to reveal sclerotia which were then counted manually without the need for magnification. Bar charts represent the mean values ± s.d. *P*-values were calculated by performing unpaired Student's *t*-tests (*$P<0.05$; **$P<0.01$; ***$P<0.001$), using the Graphpad Prism Version 6.

2.7. Protein extraction methods

2.7.1. Crude protein isolation

Protein crude extracts were isolated from either vegetative cultures or mycelia that had been transferred to solid agar plates. All mycelia were filtered and washed with 1x PBS and was broken using liquid nitrogen. Protein extracts were prepared by re-suspending the broken mycelia in 300-400μl protein extraction buffer (300mM NaCl, 50mM Tris-HCl pH 7.5, 10% glycerol, 1mM EDTA, 0.1% NP-40) that had been supplemented with 1mM dithiothreitol (DTT), 1X cOmplete EDTA-free protease inhibitors (Roche), 1mM benzamidine, 0.5mM PMSF and 1X phosphatase inhibitors (1mM NaF, 0.5mM sodium orthovanadate, 8mM β-glycerol phosphate), immediately prior to use. Samples were mixed vigorously by vortexing and centrifuged at 13,000 RPM for 10-15 minutes at 4˚C. 50μl of the supernatant was transferred to a new 0.5ml microcentrifuge tube to be used to determine protein concentration *via* a Bradford assay. Another 200μl of the supernatant was transferred to a new 1.5ml microcentrifuge tube and to this, 100μl of

3X SDS loading dye was added. These samples were then boiled at 95˚C for 10 minutes and stored at -80˚C until further use.

2.7.2. Nuclear protein isolation

Nuclear protein extracts were isolated from either vegetative cultures or mycelia that had been transferred to solid agar plates. All mycelia were filtered and washed with 1x PBS and was broken using liquid nitrogen. 5-6ml of broken mycelial powder was collected per strain in 50ml Falcon tubes. The mycelia were resuspended in 20ml nuclei isolation buffer (1M sorbitol, 10mM pH 7.5 Tris-HCl, 10mM EDTA), supplemented with 0.15mM spermine dihydrate, 0.5mM spermidine, 25mM phenylmethylsulfonyl fluoride (PMSF), 1mM DTT and 1x Roche protease inhibitors immediately before use. Resuspended samples were kept on ice for 5 minutes. Samples were centrifuged at 1,000g for 10 minutes at 4˚C. The supernatant was filtered through two layers of miracloth into SS34 tubes. These filtered samples were then centrifuged at 10,000 RPM for 15 minutes at 4˚C. The supernatant was removed and pellets were resuspended in 1.5ml of pre-cooled resuspension buffer (1M sorbitol, 10mM pH 7.5 Tris-HCl, 1mM EDTA), supplemented with 0.15mM spermine dihydrate, 0.5mM spermidine, 25mM PMSF and 1mM DTT, immediately prior to use. Samples were then transferred to 2ml microcentrifuge tubes and kept on ice. These samples were then centrifuged at 12,000 RPM for 15 minutes at 4˚C. The supernatant was removed and the crude nuclei samples were resuspended in 400µl of ST buffer (1M sorbitol, 10mM pH 7.5 Tris-HCl), supplemented with 10mM PMSF, 0.1mM DTT and 1x Roche protease inhibitors, immediately prior to use. Samples were centrifuged at 4,800 RPM for 30 seconds at 4˚C. 50µl of the supernatant was added to a new microcentrifuge tube and used to determine protein concentration *via* a Bradford assay. Another 200µl of the supernatant was added to a separate microcentrifuge tube and 100µl of 3X SDS loading dye was added, followed by an incubation at 95˚C for 8 minutes. These samples were then stored at -80˚C until further use.

2.8. Immunoprecipitation of fusion proteins

2.8.1. GFP/HA Trap

For the immunoprecipitation of GFP and HA fusion proteins, 1ml protein crude extracts were isolated from vegetative cultures grown for 24 hours in either liquid GMM, complete or Sabouraud media. Per protein sample, 10μl GFP-Trap sepharose (Chromotek) or anti-HA magnetic beads (Pierce) were washed twice with 190μl protein extraction buffer (as described in section **2.7.1.**). The GFP/HA-Trap beads were then isolated by placing samples on a magnetic rack (DynaMag™-2 Magnet) and then resuspended in 50μl protein extraction buffer. The resuspended beads were then added to 1ml crude protein extract. This mixture was left to incubate on a rotator for 3 hours at 4˚C. Samples were placed in a magnetic rack and the supernatant was discarded. Beads were washed twice with 1ml protein extraction buffer (without supplements) and were then washed for a third time with the same buffer containing 1mM DTT. All liquid was removed and the beads were stored at -80˚C until further use.

2.8.2. Tandem Affinity Purification (TAP)

2.8.2.1. Immunoglobulin (IgG) immobilization onto NHS-activated magnetic beads

2.5mg of IgG (Sigma, I4506) was dissolved in 1.5ml coupling buffer (50mM borate) and mixed well by vortexing. 300μl of NHS-activated magnetic bead solution (Pierce) was added to a 1.5ml microcentrifuge tube. Beads were collected by placing samples on a DynaMag™-2 Magnet (ThermoFisher, 12321D) and the supernatant was discarded. Beads were washed with 1ml pre-cooled wash buffer A (1mM HCl) and samples were vortexed for 15 seconds. Samples were placed on the magnetic rack and the supernatant was removed. 300μl of dissolved IgG was then added to the beads and samples were vortexed for 30 seconds. Samples were incubated on a rotator at room temperature for 2 hours. During the first 30 minutes of this incubation, samples were vortexed vigorously every 5 minutes for 15 seconds. After the initial 30 minutes, samples were vortexed every 15 minutes for 15 seconds. After the 2 hour incubation, the beads were collected and the supernatant was discarded. Samples were washed with 1ml wash buffer B (0.1M glycine, pH 2) and vortexed for 15 seconds. Beads were

collected again and the supernatant was discarded. This washing step was then repeated once more. 1ml of ultrapure water was added to the beads and samples were vortexed for 15 seconds, followed by collection of the beads and removal of the supernatant. 1ml of quenching buffer was added to the beads and samples were vortexed for 30 seconds, followed by an incubation on a rotator for 2 hours at room temperature. After this incubation, the beads were collected and the supernatant was discarded. 1ml of ultrapure water was added to the beads and samples were mixed well by vortexing. The beads were collected and 1ml of storage buffer was added. Samples were vortexed and beads were collected again. This wash with storage buffer was repeated two additional times. Beads were resuspended in 300μl of storage buffer and stored at 4˚C until further use.

2.8.2.2. Purification of TAP-tagged proteins

For TAP-tagged proteins, strains were cultured vegetatively for 24 hours in flasks (2 litre volume) containing 800ml complete medium and were then transferred to GMM agar plates for asexual and sexual induction. The mycelia were filtered through miracloth and washed three times with harvest solution (1x PBS, 1mM PMSF, 1% dimethyl sulfoxide (DMSO)). The mycelia were then dried and broken using liquid nitrogen. B250 buffer (250mM NaCl, 100mM Tris-HCl pH7.5, 10% glycerol, 1mM EDTA and 0.1% NP-40), supplemented with 1mM DTT, 1X cOmplete EDTA- free protease inhibitors (Roche), 1mM benzamidine, 0.5mM PMSF and 1X phosphatase inhibitors (1mM NaF, 0.5mM sodium orthovanadate, 8mM β-glycerol phosphate) immediately prior to use was used to extract proteins from the broken mycelia. Approximately 12-15ml of B250 buffer was used to resuspend 30ml of ground mycelial powder and samples were kept on ice for 10 minutes. Samples were then centrifuged for 25 minutes at 16,000 RPM at 4˚C. The protein supernatants were transferred to new Falcon tubes and 200μl of NHS-activated magnetic beads (Pierce), coupled to IgG from rabbit serum (Sigma) was added to each sample. Samples were left to incubate on a rotator at 4˚C for 4 hours. Samples underwent three washes with the following buffers: WB250 (250mM NaCl, 40mM Tris-HCl pH8, 0.1% NP-40), WB150 (150mM NaCl, 40mM Tris-HCl pH8, 0.1% NP-40) and TCB (WB150 with 500mM EDTA). To WB250 and WB150 buffers, supplements were added prior to use as described for B250 buffer, while the only supplements added to TCB before use

were 1mM DTT and 0.5mM PMSF. After the three washes, all liquid was removed and beads were resuspended in 1ml TCB buffer and transferred to 1.5ml microcentrifuge tubes. 20μl of tobacco etch virus (TEV) protease (AcTEV[TM]: Invitrogen) was added to the samples and left to incubate on a rotator at 4°C overnight.

The next day, 50μl Magnezoom[TM]-CAM beads (Bioworld, 20162002-1) was resuspended in 200μl CBB buffer (WB150 with 1mM MgOAc, 2mM CaCl$_2$, 1mM imidazole, 10mM β-mercaptoethanol) per sample. In 15ml Falcon tubes, 6ml CBB buffer was added, followed by 200μl CAM bead solution, 8μl CaCl$_2$ and 1ml of the TEV-treated protein supernatants that had been separated from the NHS-activated magnetic beads by using the magnetic rack. These mixtures were then left to incubate on a rotator at 4°C for 2 hours. Beads were then placed on a magnetic rack and the supernatant was discarded. Beads were washed with CBB and transferred to 1.5ml microcentrifuge tubes. Beads were collected again, followed by another wash with CBB. All liquid was removed and beads were stored at -80°C until further use.

2.9. Sample preparation for LC-MS/MS protein identification

Isolated GFP, HA and TAP-tagged proteins were resuspended in 50mM ammonium bicarbonate. 1μl of 0.5M DTT was added and samples were incubated at 56°C for 20 minutes. 2.7μl of iodoacetamide (0.55M) was added and samples were incubated in the dark for 15 minutes. 1μl of 1% (w/v) ProteaseMAX (Promega, V5111) was added followed by addition of 1μl trypsin (1μg/μl) (Promega). Samples were left to incubate overnight at 37°C. The next day, 1μl of Trifluoroacetic acid (TFA) was added to each and samples were vortexed briefly and left to incubate for 5 minutes at room temperature. Beads were collected on a magnetic rack and the supernatant was transferred to new tubes. The supernatants were centrifuged at 13,000 relative centrifugal force (RCF) for 10 minutes and dried in a Speed-Vac for 3 hours. Samples were stored at -20°C until further use.

Peptide samples were resuspended in 20μl resuspension buffer (0.5% TFA) and sonicated for 3 minutes, followed by a brief centrifugation. ZipTip C$_{18}$ pipette tips (Millipore, ZTC18S096) were used to purify peptide samples prior to mass spectrometric analysis. To equilibrate the ZipTips, a wetting solution (0.1%, 80%

acetonitrile) was aspirated 5 times, followed by aspiration of an equilibration buffer (0.1% TFA) 5 times. ZipTips were then used to pipette the peptide samples up and down 15-20 times. Then, the equilibration buffer was aspirated again 5 times, followed by elution of the peptides *via* aspiration of an elution buffer (0.1% TFA, 60% acetonitrile) 5 times into a new 1.5ml microcentrifuge tube. This solution was dried in a Speed-Vac for 2 hours and peptide samples were stored at -20˚C.

Immediately prior to loading, peptide samples were resuspended and solubilised in 10μl of Q-Exactive loading buffer (2% acetonitrile, 0.5% TFA) and 8μl was added to mass spectrometry vials (VWR). Samples were loaded on a high resolution quantitative LC-MS mass spectrometer (Thermo Fisher Q-Exactive). LC-MS identifications of peptides and their phosphorylation sites were performed using the Proteome Discoverer Daemon 1.4 software (Thermo Fisher) and organism-specific taxon-defined protein databases. Unique peptides were determined by isolating only those that do not appear in any of the wild type controls.

2.10. Immunoblotting

For all immunoblots, protean membranes (0.45μm pore size, GE Healthcare) were incubated in blocking solution [(5% (w/v) non-fat dry milk solution in 1X TBST (Tris buffered saline with 0.1% Tween 20)] for 1 hour at room temperature with gentle shaking. For the detection of GFP-tagged proteins, mouse α-GFP antibody (SC-9996, SantaCruz) was used at 1:1,000 dilution in blocking solution for 2 hours at room temperature. For HA-tagged proteins, mouse α-HA antibody (H3663, Sigma) was used at 1:2,000 dilution in blocking solution for 2 hours at room temperature. Secondary goat α-mouse (170-6516, Biorad) was used at 1:2,000 dilution in blocking solution for 1 hour at room temperature. For the detection of SkpA, custom made rabbit α−SkpA was used at 1:1,000 dilution in blocking solution for 2 hours at room temperature. For the detection of phosphorylated MpkB, rabbit α−phospho p44/42 (Cell Signalling Technology) was used at 1:1,000 dilution in 5% bovine serum albumin (BSA) solution for 2 hours at room temperature. For the detection of Histone 3, rabbit α-H3 antibody (AB1791, Abcam) was used at 1:4,000 dilution in blocking solution for 2 hours at room temperature. Goat α-rabbit (Biorad) was used as a secondary antibody for SkpA, phosphorylated MpkB and H3 detection at 1:2,000 dilution in blocking solution for 1

hour at room temperature. After each antibody incubation, membranes were washed three times with 1X TBST for 5 minutes. For visualisation of all membranes, Luminata Crescendo Western Horse radish peroxidase (HRP) Substrate (Millipore) was added and membranes were exposed using the G:BOX Chemi XRQ (Syngene). For all membranes, 80-100μg of protein was loaded in each lane of SDS gels with various acrylamide percentages (10-15%). For coomassie staining loading controls, proteins were run on 10% SDS gels and incubated in fixing solution (50% methanol, 10% glacial acetic acid) for 1 hour with gentle shaking. Gels were then incubated in staining solution (0.1% Coomassie Brilliant Blue R-250, 50% methanol, 10% glacial acetic acid) for 20 minutes, followed by incubation in de-staining solution (40% methanol, 10% glacial acetic acid) solution. This solution was renewed 3 times before exposure of gels using the G:BOX Chemi XRQ (Syngene).

2.11. Messenger ribonucleic acid (mRNA) extractions and quantitative PCR (qPCR) analysis

A. nidulans strains were inoculated in duplicate in 40ml of liquid GMM at a concentration of 5 million spores/ml and incubated for 48 hours on a shaker at 37˚C. *A. flavus* strains were inoculated either in liquid complete medium or liquid PDA medium at a concentration of 2×10^6 spores/ml and were incubated on a shaker at 30˚C. Liquid complete medium cultures were left to incubate for 24 hours while liquid PD medium cultures were left to incubate for either 48 or 72 hours. After 24 hours of incubation in complete medium, the mycelia were filtered and transferred onto PDA plates and samples were left to incubate in the presence of light at 30˚C for 24 hours.

For mRNA extractions, all fungal mycelia were filtered through miracloth and washed with diethylpyrocarbonate (DEPC) buffer (0.1% DEPC in 1X PBS) three times. 100mg of mycelia was collected in RNAse-free 1.5ml microcentrifuge tubes and mRNA was isolated according to the 'RNeasy Plant Mini Kit' protocol (Qiagen). mRNA was quantified according to the 'Qubit RNA BR Assay Kit' Protocol (Thermo Fisher). To synthesise complementary deoxyribonucleic acid (cDNA), 1μg of mRNA was used for each strain and the 'Transcriptor First Strand cDNA Synthesis Kit' (Roche) was used. The final 20μl cDNA solutions were made up to either 100μl or 200μl with PCR-grade water and stored at -20˚C until further use.

For qPCR experiments, cDNA of each duplicate strain was inoculated in triplicate in 96-well plates (Life Science Products). Plates were loaded in a LightCycler 480 qPCR machine (Roche) and the cycle parameters were as follows: Pre-incubation (95˚C, 10 minutes), Amplification [40 cycles] (95˚C-10 seconds, 60˚C-20 seconds, 72˚C-10 seconds), Melting curve (65˚C to 97˚C with continuous fluorescence readings). Advanced relative quantification was used to determine the levels of gene expression in each strain, using a Beta-tubulin (*benA*) control gene as a reference for all *A. nidulans* strains and a *skpA* control gene as a reference for all *A. flavus* strains. Relative expression analysis was performed by using the LightCycler 480 software. Bar charts represent the mean data of two combined biological replicates and 6 combined technical replicates per strain, ± s.d.

2.12. Reverse Phase-High Performance Liquid Chromatography (RP-HPLC) analysis of SM levels

For the determination of sterigmatocystin levels, *A. nidulans* strains were inoculated in triplicate in 40ml of liquid GMM at a concentration of 5 million spores/ml and incubated for 48 hours on a shaker at 37˚C. Mycelia were filtered through miracloth and 25ml of the liquid medium was collected in a 50ml Falcon tube. 25ml of chloroform was added to each and samples were briefly vortexed, followed by incubation on a rotator at 4˚C for 1 hour. Samples were centrifuged at 4,000 RPM for 15 minutes at 4˚C. 20ml of the lower phase of each sample was transferred to new 50ml Falcon tubes and left to evaporate in a fume hood. Samples were resuspended in 2ml chloroform, transferred to 2ml microcentrifuge tubes and dried in a Speed-Vac for 1 hour. Samples were resuspended in 200μl methanol and were loaded on a Shimadzu RP-HPLC with a photodiode array detector (PAD). 20μl of samples were injected onto a Luna®Omega 5μm Polar C18 (LC column 150 x 4.6m.m) and separated across a water:acetonitrile gradient with 0.1% (v/v) TFA. A sterigmatocystin standard (Sigma) was used at 12.5μg/ml concentration. Gradient conditions of 5-100% acetonitrile over 30 minutes with a flow rate of 1ml/minute were used with a PAD detection at 254nm. 3 biological replicates were prepared for each strain and the data is presented as a bar chart, with the bars representing the mean ± s.d. *P*-values were calculated by performing unpaired Student's *t*-tests (*$P<0.05$), using the Graphpad Prism Version 6.

To determine aflatoxin levels, *A. flavus* strains were point inoculated (5×10^3 spores) in triplicate on YES agar plates and incubated in the dark for 1 week at 30˚C. 15ml Falcon tubes were used to remove agar cores from the centre of each colony and a sterile scalpel was used to cut the agar cores into pieces. 3ml of deionised water was added to each sample and samples were vortexed vigorously for 10 seconds. 3ml of chloroform was then added to each sample, followed by vigorous vortexing for 10 seconds. The samples were then left to incubate on a rotator at 4˚C for 1 hour. Following this incubation, samples were centrifuged at 4,000 RPM for 15 minutes at 4˚C. A total of 2.5ml of the chloroform layer was transferred to 2ml microcentrifuge tubes and left to evaporate. Samples were resuspended and prepared for HPLC analysis as described for *A. nidulans* samples. An aflatoxin B1 standard (Sigma) of 10μg/ml concentration was used as a reference.

To determine gliotoxin levels, *A. fumigatus* strains were inoculated (10^7 spores/ml) in triplicate in 40ml Czapek-Dox medium and left to incubate on a shaker at 37˚C for 72 hours. The mycelia were filtered and 25ml of the supernatant was collected in Falcon tubes and mixed with 25ml of chloroform. The remaining steps performed are as described for the *A. nidulans* samples. A gliotoxin standard (Sigma) of 10μg/ml was used as a reference.

2.12.1. Sample preparation and UHPLC-HRMS of *A. flavus* metabolites

Strains were spot inoculated (5×10^3 spores) in triplicate on GMM and PDA plates containing supplements and were left to incubate in the presence of light at 30˚C for 2 weeks. Half of each agar plate was cut into small pieces using a scalpel and placed into 40ml glass vials. 10ml ethyl acetate was added to each vial and samples were sonicated for 90 minutes. 10ml water was then added to each sample and the vials were shaken for 5 seconds. Samples were left at room temperature for 10 minutes to allow for separation of the two layers. 10ml of the ethyl acetate layer was removed, using a glass pipette and was transferred to pre-weighed 12ml glass vials. Samples were left to dry in a fume hood and the crude extracts were weighed.

The crude extracts were resuspended in acetonitrile (10 mg/mL) and filtered through an Acrodisc syringe filter with a nylon membrane (Pall Corporation) (0.45μm pore size). Ultra-high-performance high resolution mass spectrometry (UHPLC-

HRMS) was then performed on a Thermo Scientific-Vanquish UHPLC system connected to a Thermo Scientific Q Exactive Orbitrap mass spectrometer in ES$^+$ mode between 200 m/z and 1000 m/z to identify metabolites. A Zorbax Eclipse XDB-C18 column (2.1 × 150 mm, 1.8 μm particle size) was used with a flow rate of 0.2 mL/min for all samples. LCMS grade water with 0.5% formic acid (solvent A) and LCMS grade acetonitrile with 0.5% formic acid (solvent B) were used with the following gradient 0 min, 20% Solvent B;2 min, 20% Solvent B; 15 min, 95% Solvent B; 20 min, 95% Solvent B; 20 min, 20% Solvent B; 25 min, Solvent B. Nitrogen was used as the sheath gas. Data acquisition and procession for the UHPLC-MS were controlled by Thermo Scientific Xcalibur software. Files were converted to the .mzXML format using MassMatrix MS Data File Conversion, and analyzed in MAVEN and XCMS (Clasquin et al., 2012). The peak area (from 3 biological replicates per strain) is presented as a bar chart, with the bars representing the mean ± s.d. *P*-values were calculated by performing unpaired Student's t-tests using the Graphpad Prism Version 6.

2.12.2. Extraction of compounds from *A. fumigatus* and LC-MS analysis

Strains were inoculated in triplicate in 40ml of liquid GMM and Czapek-Dox medium at a concentration of 5 million spores/ml and incubated for 48 hours on a shaker at 37˚C. The culture broth containing fungal mycelium was homogenized using an ULTRA-TURRAX (IKA-Werke, Staufen, Germany). Homogenized cultures were extracted twice with a total of 100 ml ethyl acetate, dried with sodium sulfate and concentrated under reduced pressure. For LC-MS analysis, the dried extracts were dissolved in 1ml of methanol and loaded onto an ultrahigh-performance LC–MS system consisting of an UltiMate 3000 binary rapid-separation liquid chromatograph with PAD (Thermo Fisher Scientific, Dreieich, Germany) and an LTQ XL linear ion trap mass spectrometer (Thermo Fisher Scientific, Dreieich, Germany) equipped with an electrospray ion source. The extracts (injection volume, 10 μl) were analyzed on a 150 mm by 4.6-mm Accucore reversed-phase-MS column with a particle size of 2.6 μm (Thermo Fisher Scientific, Dreieich, Germany) at a flow rate of 1 ml/min, with the following gradient over 21 minutes: initial 0.1% (v/v) HCOOH-MeCN/0.1% (v/v) HCOOH-H$_2$O 0/100, which was increased to 80/20 in 15 min and then to 100/0 in 2 min, held at 100/0 for 2 min, and reversed to 0/100 in 2 minutes.

2.13. Confocal Microscopy

2.13.1 Confocal imaging of *A. nidulans* strains

GFP and mRFP-tagged strains were inoculated ($5x10^3$ spores) in 500µl liquid GMM with supplements and cultured in Lab-Tek Chambered Coverglass W/CVT (Thermo Scientific) for 16 hours at 30°C. Localisations of the proteins were captured using either the Zeiss LSM 510 META inverted confocal microscope or the Olympus FluoView1000 laser scanning confocal microscope.

2.13.2. Confocal imaging and DAPI staining of *A. flavus* and *A. fumigatus* strains

For confocal microscopy imaging, conidia were cultured in eight-chambered cover glasses (Lab-Tek; Thermo Fisher Scientific). Strains were incubated at 30ºC for various durations in 400µl of liquid GMM, containing appropriate supplements.

For 4′,6-diamidino-2-phenylindole (DAPI) staining experiments, germlings were initially fixed in the wells of the chambered cover glasses. To ensure fixation, the liquid medium was removed and 400µl of fixative solution was added [8 % formaldehyde in 50 mM piperazine-N,N'-bis(2- ethanesulfonic acid) (PIPES), pH 6.7; 25 mM EGTA, pH 7.0; 5 mM $MgSO_4$; and 5 % DMSO, pre-warmed to the culture temperature]. Samples were left to incubate for 30 min at 30°C. Following this incubation, the fixative solution was removed and replaced with 400µl of 0.015µg/ml DAPI solution.

To capture images, an UltraView VoX spinning disk confocal system (PerkinElmer) mounted on an Olympus IX71 inverted microscope was utilized. This confocal system is equipped with a piezoelectric stage which is software-controlled to enable rapid Z-axis movement. To collect images, a 60X/1.42 numerical aperture Olympus Plan Apo objective and an ORCA ERAG camera (Hamamatsu Photonics) were used. Solid state 405-nm and 488-nm lasers were used for excitation of DAPI and GFP respectively. For live imaging, the specimen temperature was maintained at 30ºC using a temperature-controlled chamber. For DAPI experiments, fluorochrome-specific emission filters were used to prevent emission bleed through between fluorochromes. The system was controlled by Volocity software (PerkinElmer) running on a Power Mac computer (Apple). A stage micrometer was used to calibrate

magnifications. After the adjustment of both minimum and maximum intensity levels (black and white levels) for each channel, the images were exported directly from Volocity.

2.13.3. Immunostaining

Coverslips were soaked in 100% ethanol for 10 seconds and flame sterilised. Sterile coverslips were then added to a 6-well macrotitre tray and 450µl of Sabouraud medium (containing supplements) was added to each coverslip. $5x10^3$ spores of each strain were used to inoculate the medium and strains were left to incubate at 30°C for 14-16 hours.

The next day, fixation solution was freshly prepared by adding 0.6g paraformaldehyde to 15ml PME buffer (50mM PIPES, 25mM EGTA, 5mM $MgSO_4$, pH adjusted to 6.7 with NaOH). The solution was left to incubate at 68°C for 45 minutes until paraformaldehyde had fully dissolved and then solution was left to cool to room temperature before use. All medium was removed from wells by using a vacuum pump and 2ml of fixation solution was added to each coverslip. Samples were left to incubate at room temperature for 30 minutes. All fixation solution was removed using a vacuum pump and coverslips were washed three times for 5 minutes with 2ml PME buffer, with the liquid being removed after each wash. Lysing enzyme solution was prepared fresh by adding 400mg of lysing enzymes from *Trichoderma harzianum* (Sigma-L1412) to 20ml PME buffer. 10ml of this solution was added to 10ml egg white and 2ml of this solution was added to each coverslip. Samples were left to incubate at 25°C for 50 minutes while shaking slowly (50 RPM). Lysing enzyme solution was then removed and samples were washed three times for 10 minutes with 2ml PME buffer. 1.5ml extraction buffer (100mM PIPES, 25mM EGTA, 0.1% NP-40) was added to each coverslip and samples were left to incubate for 9 minutes at room temperature. Liquid was removed and samples were washed once with 1.5ml PME buffer. 1.5ml of ice-cold methanol was then added to each coverslip and samples were left to incubate for 10 minutes at room temperature. Samples were then washed twice with 1ml PME buffer for 5 minutes. 2ml of TBST (3% BSA) solution was added to each coverslip and samples were left to incubate for 30 minutes at room temperature.

200µl of primary antibody solutions (1:50 mouse α-GFP or 1:100 mouse α-HA) were added to the coverslips and samples were left to incubate for 1 hour at room

temperature. Samples were then washed three times with 250μl TBST for 5 minutes. 200μl of secondary antibody solution (1:100 goat anti-mouse Alexa fluor 594-Abcam:ab150120) was added to each coverslip and samples were left to incubate at room temperature for 1 hour in the dark. Samples were washed with 250μl TBST 3 times for 5 minutes. All liquid was removed and one drop of mounting medium (ProLong gold antifade mountant with DAPI-ThermoFisher Scientific:P36941) was added to a microscope slide. Each coverslip was placed germling side down on the microscope slide and the excess mounting medium was removed using filter paper. Nail polish was added to the microscope slides and was left to dry for 10 minutes at room temperature. Samples were stored overnight at 4˚C in the dark. Localisations of proteins were detected using the Olympus FluoView1000 laser scanning confocal microscope.

2.14. Protein domain searches

Detection of protein sizes and domains were performed using a combination of ScanProsite (de Castro et al., 2006) and InterPro (Mitchell et al., 2019) software. Detection of protein orthologs was performed by reciprocal BLAST searches (Altschul et al., 1990).

Chapter 3: Results

Roles of the pheromone module kinases and the HamE scaffold in the regulation of *A. nidulans* development and secondary metabolism

3.1. The absence of a Ste5 scaffold ortholog in *A. nidulans* suggests a unique method of MAP kinase signalling is utilised by filamentous fungal species

As discussed in **Section 1.7.**, the *A. nidulans* pheromone module consists of the MAP3K SteC, MAP2K MkkB, MAPK MpkB and adaptor protein SteD (Bayram et al., 2012). In this study, it was proposed that this tetrameric complex assembles at G-protein coupled receptors at the plasma membrane in response to pheromone detection, similar to the yeast pathway (Pryciak and Huntress, 1998, Hao et al., 2008). This results in sequential kinase phosphorylation and migration of the entire complex to the nuclear envelope. Phosphorylated MpkB is then capable of translocating into the nucleus, where it phosphorylates transcription factors like SteA and VeA, a velvet complex member, to regulate both sexual development and secondary metabolism (Bayram et al., 2008, Atoui et al., 2008, Sarikaya Bayram et al., 2010).

While this pathway exhibits many similarities to the yeast Fus3 module, it can be noted that there is no Ste5 scaffold ortholog in the *A. nidulans* genome. Additionally, there are no Ste5 scaffold orthologs in any filamentous fungal genomes (Rispail et al., 2009), suggesting a unique method of signalling in these species. In this study by (Bayram et al., 2012), it was suggested initially that the adaptor protein SteD may be acting as a scaffold for the pheromone module kinases to regulate signalling. However, SteD does not exhibit typical scaffold protein characteristics. Scaffolds are large, multi-domain proteins that have specific protein motifs, such as tryptophan aspartate (WD40) domains, that allow for protein-protein interactions (Xu and Min, 2011). SteD is a smaller protein of 494 amino acids with a molecular weight of 54.3 kilodaltons (kDa). It possesses sterile alpha motif (SAM) domains and a Ras-associated (RA) domain but does not contain any typical scaffolding domains (http://www.aspergillusgenome.org). It is known that the SteD ortholog in yeast functions as an adaptor, rather than a scaffold (Wu et al., 1999, Xu et al., 1996). This suggests that SteD may associate with all members of the pheromone module in *A. nidulans* but it is not required for the regulation of complex assembly.

With the absence of a scaffold protein in the pheromone module, this proposes the question of how these kinases are assembled in the correct orientation at the membrane, allowing for MpkB phosphorylation and signal propagation to the nucleus. The following work in this results chapter aims to provide insight on the composition of the pheromone module and to characterise a newly identified scaffold candidate.

Additionally, this chapter provides a comprehensive overview of the individual protein-protein interactions in the pheromone module, the mechanism of signalling and the subsequent effects of the individual module proteins in regulating *A. nidulans* development and secondary metabolism.

3.2. A scaffold candidate known as HamE (AN2701) interacts with the pheromone module proteins

In an attempt to characterise the composition of the pheromone module and it's individual protein-protein interactions, a combination of TAP pulldowns and MS/MS was performed. The *A. nidulans* pheromone module proteins SteC (AN2269), MkkB (AN3422) and MpkB (AN3719) were initially epitope tagged, each at the C-terminal of the gene ORF with TAP tags, connected to *natR* selective markers. Each TAP-tagged protein was expressed using the respective genes native promoter. No inducible promoters were used in this study, with the exception of the nitrate-inducible *niiA/niiD* promoter being used for Bimolecular fluorescence complementation (BIFC) experiments. For details of the generation and confirmation of these TAP-tagged strains, see (Bayram et al., 2012).

Immunoprecipitation of the TAP-tagged proteins was performed in duplicate. Strains were cultured vegetatively for 24 hours in complete medium and liquid chromatography-tandem mass spectrometry (LC-MS/MS) was performed to detect the potential *in vivo* interaction partners of each tagged protein. Details of sample preparation for mass spectrometry analysis are in section 2.9. Mass spectrometry data (**Figure 3.1. (a))** revealed that SteC co-purified MkkB and SteD **(Appendix A: Table S1)**, MkkB co-purified SteC, MpkB and SteD **(Appendix A: Table S2)** and MpkB co-purified MkkB **(Appendix A: Table S3),** providing more evidence of the assembly of a tetrameric complex as proposed by (Bayram et al., 2012).

3.2.1. Identification of HamE (AN2701) and characterisation of its structure and interaction partners

Interestingly, in purifications of each TAP-tagged kinase, an uncharacterised protein, denoted as AN2701 according to (http://www.aspergillusgenome.org) was detected in

high abundance in all replicates (**Figure 3.1. (a), Appendix A: Table S1-3).** As stated by (http://www.aspergillusgenome.org), the specific roles of this protein are unknown. However, it is known that orthologs of this protein play roles in conidiophore development, hyphal growth, sexual reproduction and plasma membrane fusion. AN2701 is a large protein with a molecular weight of 171.8 kDa and consists of 1,570 amino acids (**Figure 3.2 (c)**). By performing a domain search of AN2701 using the WDSPdb database (http://wu.scbb.pkusz.edu.cn/wdsp/), it was found that AN2701 contains 6 WD40 repeats at it's N-terminus, between amino acid residues 18-329 (**Figure 3.2 (a) and (c)**). These repeats are characteristic of scaffold proteins and allow for protein-protein interactions (Xu and Min, 2011). A coiled-coil domain was also identified between amino acid residues 1205-1225 and a region of intrinsic protein disorder was identified at the C-terminus between amino acid residues 1479-1570 (**Figure 3.2 (c)**). Many coiled-coil domains exhibit the capability to scaffold large protein complexes (Truebestein and Leonard, 2016), while regions of intrinsic disorder are thought to increase the functional versatility of proteins as they can provide conformational heterogeneity between protein domains and can enable the construction of large interaction networks (Buljan et al., 2013). Reciprocal BLAST searches were performed to identify orthologs of AN2701 in other fungal species. It was found that AN2701 exhibits 51.2% similarity to the *N. crassa* Ham-5 scaffold (discussed in **Section 1.8.**) of the Mak-2 module (Dettmann et al., 2014, Jonkers et al., 2014), with most of this conserved identity existing at the N-terminus. Because of this high similarity to Ham-5, it was decided to name the AN2701 protein 'HamE' and to test whether HamE acts as a scaffold in the *A. nidulans* pheromone module.

To test this, the AN2701 gene was tagged at the C-terminus of the ORF with a TAP tag, connected to a *natR* marker and prepared for MS analysis as described for the pheromone module kinases. MS allowed for the determination of HamE interaction partners and it's phosphorylation sites. MS data revealed that HamE is a highly phosphorylated protein that becomes phosphorylated on at least 8 amino acid residues (**Appendix A: Table S5, Figure 3.2 (b) and (c)**), between amino acids 425-1202. This data complements the findings of (Jonkers et al., 2014), who determined that Ham-5 contained similar domains at similar positions to HamE and contained 16 putative phosphorylation sites, suggesting complex methods of regulation exist for Ham proteins, which is characteristic of scaffold proteins. MS data also revealed that HamE co-purifies MkkB and MpkB (**Figure 3.1 (a), Appendix A: Table S4**). This suggests

that HamE directly interacts with the kinases MkkB and MpkB and may transiently interact with SteC and SteD to form a pentameric complex in response to pheromone detection **(Figure 3.1 (b)).**

a

	SteC-TAP		MkkB-TAP		MpkB-TAP		HamE-TAP	
	% Coverage	Unique Peptides	% Coverage	Unique Peptides	% Coverage	Unique Peptides	% Coverage	Unique Peptides
SteC	68.28	45	54.18	36				
MkkB	19.67	6	72.17	29	56.96	21	28.39	10
MpkB			78.53	18	82.20	25	4.52	2
SteD	73.48	27	69.03	22				
HamE	25.22	30	39.04	43	46.56	50	46.5	45

b
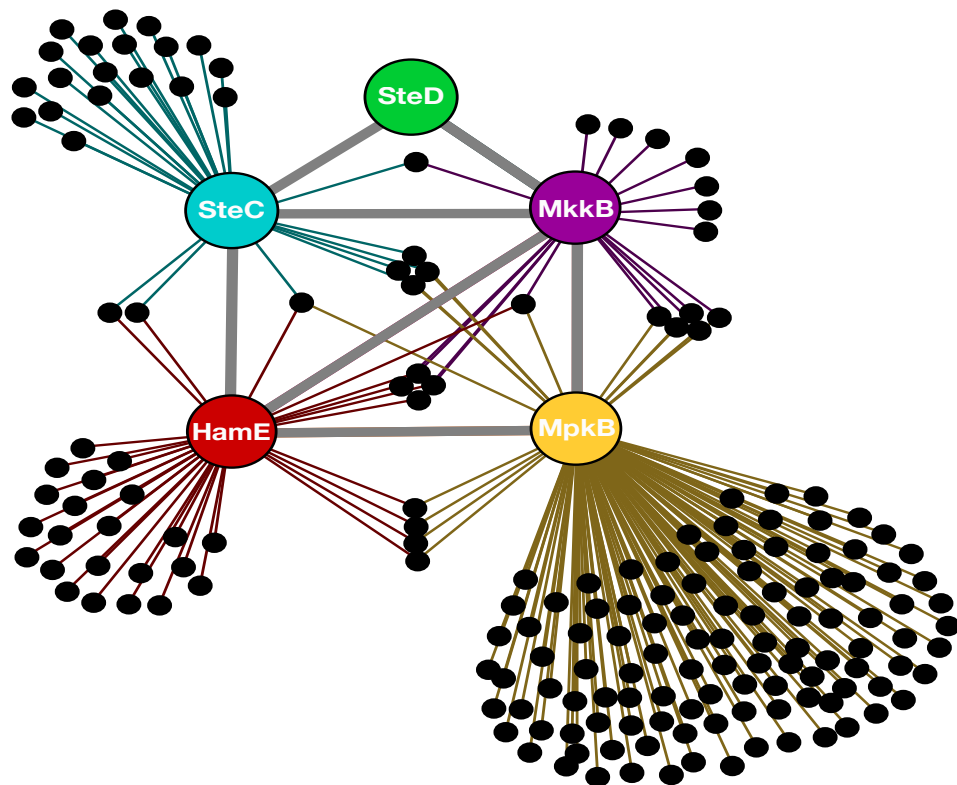
Figure 3.1. Discovery of the HamE scaffold and it's interactions with the pheromone module kinases (a) TAP pulldowns and LC-MS/MS analysis of the pheromone module kinases and HamE. cTAP-tagged proteins are given at the top of the table and co-purified proteins are given on the left-hand side. The percentage of coverage and unique peptides of each detected protein are displayed. 2 biological replicates of each strain were used. Strains were cultured vegetatively at 37˚C in complete medium for 24 hours. Supplementary mass spectrometry tables for this figure are provided in **Appendix A: Tables S1-4.** (b) Interaction network of the pheromone module components based on the unique peptides detected in each TAP pulldown. The interaction network was generated using the Gephi 0.9.2 software. Each black dot represents a protein detected in two independent biological replicates but not in any of the wild type samples.

a

Repeats	Score	Start	End	Strand_d	Loop_da	Strand_a	Loop_ab	Strand_b	Loop_bc	Strand_c	Loop_cd	H_bonds	Hotspots_on_the_top_face
WD1	20.77	18	63	KIVSVP	PPMPSRTQ	GAVARF	EACA	STASLF	LYAQGS	AILCLH	HDTL	NA	Q31
WD2	74.82	64	110	ALERRF	ENHKDD	IIFISV	DNVSERGAGR	LVISYD	ASK	TAIIWD	LFTG	triad	D75 I77
WD3	52.25	111	151	SVIARF	ASFEQ	LKAASW	MRNG	NVAFGN	EKG	DVILFE	PSTSE	NA	Q121 K123
WD4	37.11	152	193	HVSCRT	IFDP	ITALAP	ASDCR	TYAIGY	QNG	SILIAT	LLPTFT	NA	Q179
WD5	74.52	194	272	ILHTMT	TSRGPSP	IVSLAW	HASSSKQKSD	MLATMS	AIG	DLRVWS	IAKPPGKDVPRVIRVLKRSDTSSPSEPKWMAWSKN	NA	NA
WD6	34.75	273	329	GKIIQY	LDGETW	AWDVKT	KHITYEPVPTIDNPLGIANYGPTA	TLFTLG	PQF	TVQQYD		NA	W284 W286

b

HamE-TAP			
Position	Target	Peptide confidence	Sequence Motif
425	S	High	RYKPPYsPPTRSA
707	S	High	DMIPGRsPVGSPE
711	S	High	GRSPVGsPEPAYQ
786	S	High	AGSSALsPGGFGS
881	S	High	EEGFKPsPQTAVQ
973	S	High	PSVSGRsIDQYIN
1199	S	High	EANHNVsPATAEM
1202	T	High	HNVSPAtAEMRRK

c
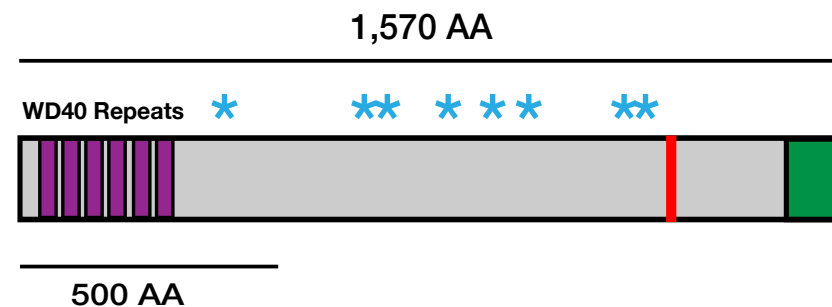
Figure 3.2. **HamE is a multi-domain scaffold protein that is highly phosphorylated** (a) Determination of the presence of 6 WD40 repeats in the N-terminus of HamE. Detection of these scaffolding domains was performed by using the WDSPdb database (http://wu.scbb.pkusz.edu.cn/wdsp/) (b) Detected phosphorylated residues of HamE, determined by TAP pulldowns coupled to Mass spectrometry. S (serine), T (Threonine). Supplementary MS table of results is provided in **Appendix A: Table S5.** (c) Schematic overview of the protein structure of HamE. HamE is a large, multi-domain protein that consists of 6 WD40 repeats at it's N-terminus (aa residues 18-329). The red bar represents a coiled-coil domain (aa residues 1205-1225) and the green shaded area (1479-1570) represents a region of intrinsic protein disorder. Blue stars represent the phosphorylation sites detected by MS analysis of TAP-tagged HamE.

To further confirm whether HamE associates with the pheromone module, BIFC experiments were performed to test whether or not HamE interacts with SteC *in vivo* and if so, at what sites in the fungal hyphae do they interact. C-YFP-HamE (yellow fluorescent protein) and N-YFP-SteC strains that contained nuclei tagged with monomeric red fluorescent protein (mRFP-H2A) were inoculated in liquid GMM and cultured at 30°C for 16 hours. BIFC experiments revealed that the two proteins interact and co-localise at the hyphal tips, plasma membrane and nuclear envelope (**Figure 3.3.**). Separate BIFC experiments performed by Bayram *et al.* (2012) revealed that SteC also co-localises with the remaining pheromone module proteins at these same sites. This suggests that HamE may interact with the entire tetrameric complex at the septa, plasma membrane, hyphal tips and nuclear envelope during vegetative hyphal growth to regulate signalling to the nucleus in response to pheromone detection.

C-YFP-HamE with N-YFP-SteC
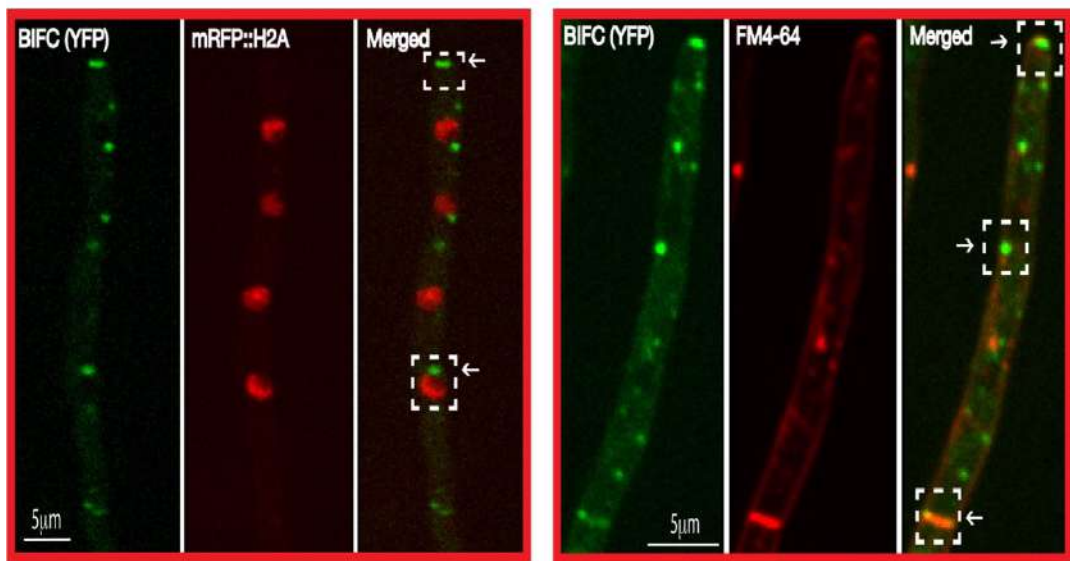
Figure 3.3. Bimolecular fluorescence complementation analysis showing the interaction of C-YFP-HamE and N-YFP-SteC. Images were captured from vegetative hyphae incubated for 16 hours at 30ºC under illumination. White arrows indicate co-localisation of these two proteins at the hyphal tips, septa, plasma membrane and nuclear envelope. Scale bar represents 5µm. mRFP::H2A (monomeric red fluorescent protein, histone 2A). FM4-64 is used to stain the plasma membrane and septa.

3.2.2 Determination of the localisation and relative abundance of HamE

Because data suggested that HamE is a member of the pheromone module, it was decided to determine when this protein is produced during development and where it localises to in the vegetative hyphae. To detect HamE production during different developmental stages **(Figure 3.4 (a)),** HamE was fused to a synthetic GFP (sGFP) epitope tag, connected to a *natR* marker at the C-terminal of the gene ORF. Time course immunoblotting was performed using this strain, incorporating time points across all developmental stages. Crude protein extracts were isolated from fungal mycelia that were either grown vegetatively in liquid GMM for 24 and 36 hours, asexually (12 and 24 hours) or sexually (12, 24 and 48 hours). For details on asexual and sexual induction of vegetative mycelia, see section 2.1.3. These protein extracts were run on SDS gels, transferred to protean membranes and probed with a mouse α-GFP antibody. It was found that the production of HamE is highly dynamic as the abundance of this protein is increased during the late stages of vegetative growth (36 hours) and early stages of asexual and sexual development (12 hours). HamE appears to be degraded at the late stages of asexual and sexual reproduction **(Figure 3.4. (a)),** suggesting that it may be required for regulation of the early phases of asexual conidiation and sexual cleistothecia development.

The HamE-GFP strain was also used to visualise the sub-cellular localisations of HamE *in vivo via* confocal microscopy. In this strain, Histone 2A was tagged with monomeric mRFP to allow for visualisation of the nuclei. It was observed that the HamE-GFP protein is dispersed throughout the cytoplasm but becomes enriched at the membrane, hyphal tips and nuclear envelope after 16 hours of vegetative growth **(Figure 3.4. (b)).** In **Figure 3.3.,** it can be observed that HamE co-localises with SteC at these same sites, providing further evidence that HamE interacts with the pheromone module at specific sites in the fungal hyphae to regulate cell signalling in response to pheromone detection.
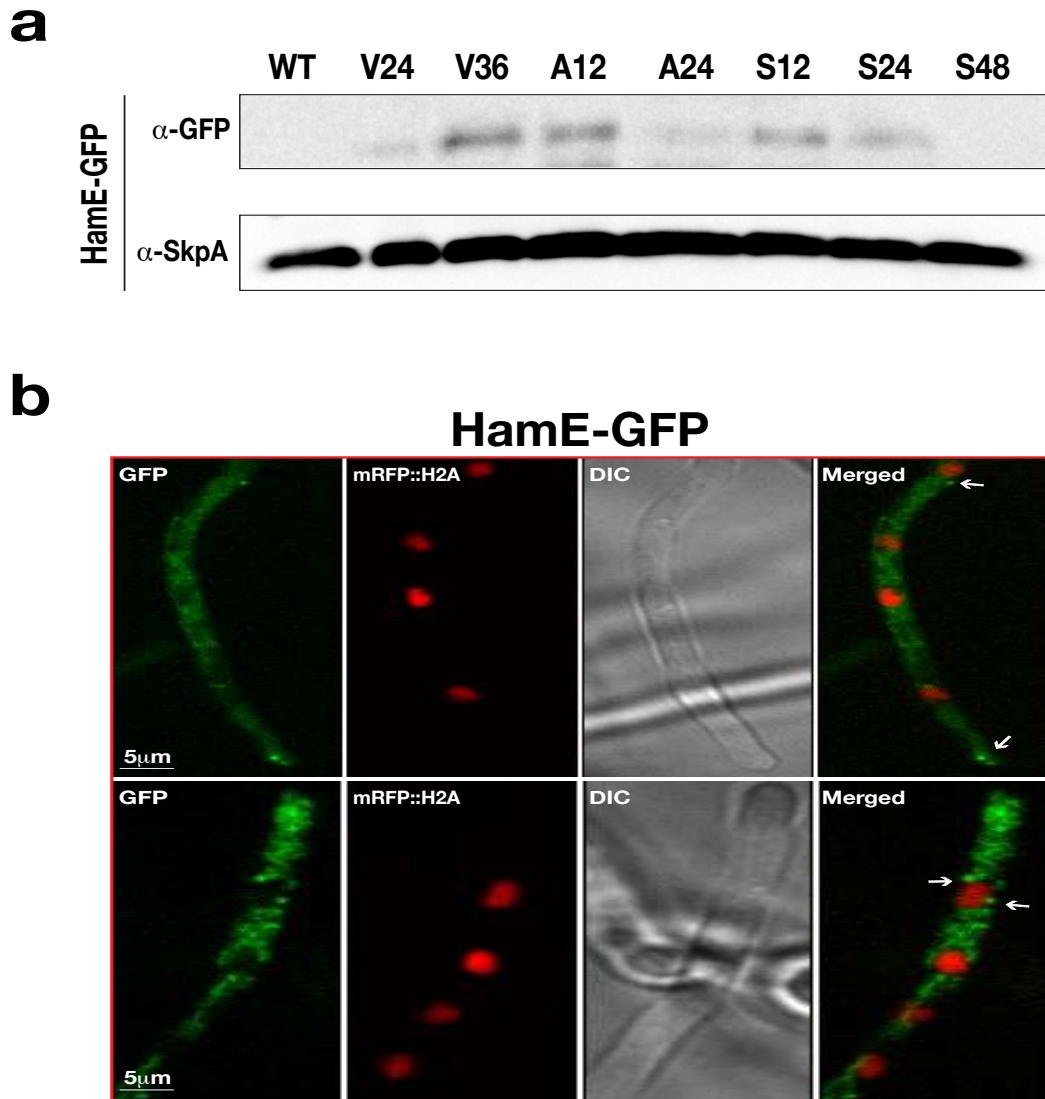
Figure 3.4. Time course abundance and localisation of HamE (a) Time course immunoblotting of HamE::sGFP at various stages of development. WT (wild type), V (vegetative), A (asexual), S (sexual). For asexual and sexual induction, the HamE::sGFP strain was cultured vegetatively for 24 hours in liquid GMM, with required supplements and transferred to GMM plates to be incubated in the light and dark respectively. The housekeeping protein SkpA is used as a loading control. 100µg of crude protein extracts were loaded in each lane on 10% SDS gels and proteins were transferred to protean membranes overnight. The full length blots used to generate this image are provided in **Appendix A: Figure S2**. (b) Localisation of HamE::sGFP *in vivo* at 16 hours of vegetative growth. The HamE::sGFP strain was inoculated (5x10³ spores) in 500µl of GMM, with required supplements in Lab-Tek Chambered Coverglass W/CVT for 16 hours at 30°C. The GFP fusion protein is dispersed

throughout the cytoplasm and localises at the hyphal tips, cell membrane and nuclear envelope, indicated by white arrows. mRFP::H2A, DIC (differential interference contrast). Scale bar represents 5μm.

3.3. HamE and the pheromone module proteins contribute to the regulation of asexual and sexual development

It has been shown previously (Bayram et al., 2012, Wei et al., 2003, Paoletti et al., 2007) that when the *steC, mkkB, mpkB* and *steD* genes are deleted, each respective mutant displays reduced levels of conidiation and are sterile, completely incapable of producing mature sexual cleistothecia, which are the fruiting bodies of *A. nidulans* (Dyer and O'Gorman, 2012). Because data suggested that HamE functions in the same pathway as the pheromone module, it was decided to test whether a *hamE* mutant would also exhibit these defects and whether double mutants would show similar phenotypes. A *hamE* mutant was created by replacing the gene ORF with a *pyroA* marker, an auxotrophic marker for pyridoxine. The *hamE* deletion cassette was also transformed into pheromone module protein deletion host strains to create double deletion strains. For detailed descriptions of how all mutant strains were generated, see sections 2.2., 2.4. and Bayram *et al.* (2012). Double deletion strains were confirmed by southern blotting (**Appendix A: Figure S1**).

3.3.1. The *hamE* mutant exhibits reductions in conidiation, but vegetative growth rate is not hindered

To determine the influence that HamE and the pheromone module double deletion strains have on the vegetative growth rate and asexual conidiation in *A. nidulans*, strains were point inoculated ($5x10^3$ spores) in triplicate on GMM agar plates, with required supplements and incubated in the presence of light at 37˚C for 4 days (**Figure 3.5. upper panel**). HamE-TAP and HamE-GFP fusion proteins (which are also HamE complementation strains) were also point inoculated to show that these proteins are functional. All strains were compared to the AGB551 wild type strain.

After 4 days of growth, the colony diameters were measured to assess the influence of each protein in the regulation of vegetative growth rate. The averages of

three replicates per strain were compared to the wild type average which was chosen to represent 100% growth (**Figure 3.7.**). Both the HamE-TAP and HamE-GFP strains exhibited a growth rate higher than the WT (105.9% and 112.8%, respectively), proving that these strains are functional and that the *hamE* gene complementation was successful. It was found that all mutants except the *hamE* deletion strain exhibited reduced colony diameters in comparison to the WT strain. All pheromone module single deletions exhibited similar vegetative growth rate reductions ranging from 23-26%. This provides evidence that the pheromone module proteins may be required in the hyphal extension stage of vegetative growth, while HamE appears to not be vital for this process. Double deletion strains also showed similar phenotypes to the single deletion mutants, suggesting that the deletion of *hamE* does not impose any extra defects in vegetative growth.

These asexually-induced strains were also used to determine the influence of these mutants in regulating conidiation. Stereomicroscopic images taken at 5x magnification (**Figure 3.6. upper panel**) of the colonies made it apparent that both the HamE-TAP and HamE-GFP strains produced large clusters of conidia, similar to that observed for the WT, while the *hamE* and pheromone module mutants showed very sparse conidiation. To quantify the levels of sporulation in each strain, agar cores from each of the three independent biological replicates per strain were removed and spores were counted using haemocytometer slides. Detailed methodology of these phenotypical tests is provided in **section 2.6**. All strains were compared to the respective WT average which was chosen to represent 100%. It was evident in each single and double mutant that the levels of asexual sporulation were significantly reduced, with values ranging from 50-64% reduction (**Figure 3.8**). These data provide evidence that these proteins, including HamE, function in a similar manner or pathway to regulate the asexual developmental programme.

3.3.2. The *hamE* and pheromone module mutants are incapable of producing sexual cleistothecia

To assess the roles of HamE and the pheromone module proteins in sexual development, strains were inoculated as described in **section 3.3.1** and these plates were completely wrapped in aluminium foil to be incubated in the dark at 37˚C for 5 days (**Figure 3.5. lower panel**). It was found that the WT, HamE-TAP and HamE-GFP

strains all exhibited a similar orange-yellow phenotype, which is characteristic of Hulle cells that surround developing fruiting bodies (Hermann et al., 1983). All single and double deletion strains displayed a pale white phenotype, indicating the loss of Hulle cells. To determine the presence of underlying mature cleistothecia, stereomicroscopic images were taken at 5x and 8x magnification (**Figure 3.6.**). It was apparent that individual fruiting bodies, surrounded by clumps of Hulle cells, could be visualised in the WT, HamE-TAP and HamE-GFP strains. The levels of cleistothecia production in the HamE-TAP and HamE-GFP strains were 97% and 98% respectively, in comparison to the WT, which was chosen to represent 100% production. All single and double deletion strains showed a complete loss of cleistothecia formation (**Figure 3.6. and Figure 3.9.**). All mutants were sterile and only capable of forming premature nests of Hulle cells. This data suggests that HamE and the pheromone module proteins may function in a similar manner or pathway to regulate the early stages of sexual development, cleistothecia formation and hyphal fusion.
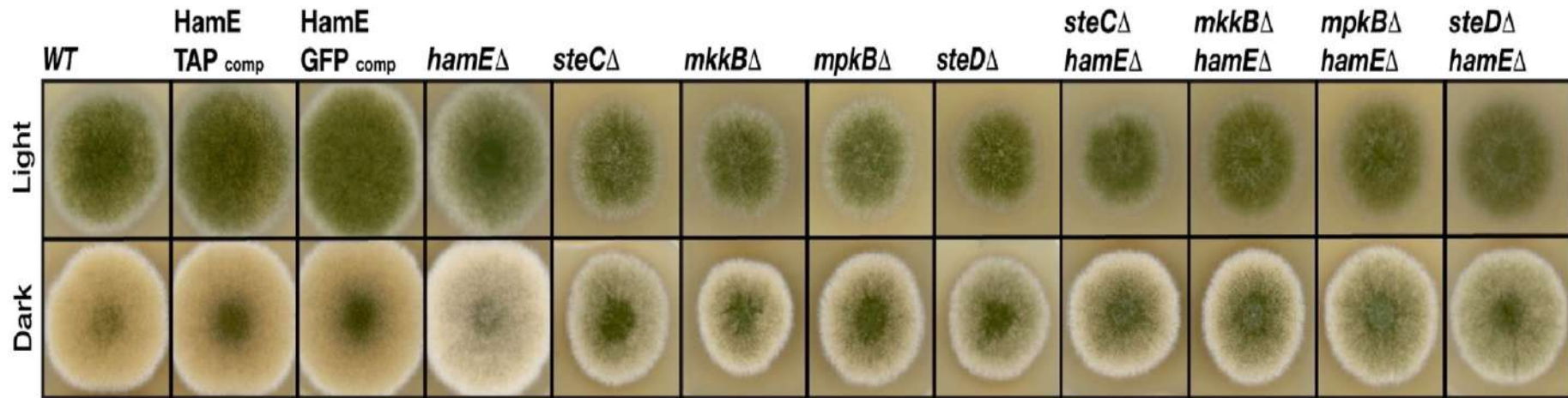
Figure 3.5. Vegetative, asexual and sexual phenotypes of complementation strains, as well as single and double deletion strains. The *hamE* and pheromone module kinase deletion strains, as well as double deletion strains and HamE complementations were spot inoculated (5×10^3 spores) in triplicate on GMM plates containing supplements. Wild type (WT) is the AGB551 strain. These plates were incubated for 4 days in the light at 37°C to induce asexual development and 5 days in the dark at 37°C to induce sexual development. Plates incubated in the dark were completely covered in aluminium foil. Plates were scanned using the Epson perfection V600 photo scanner.
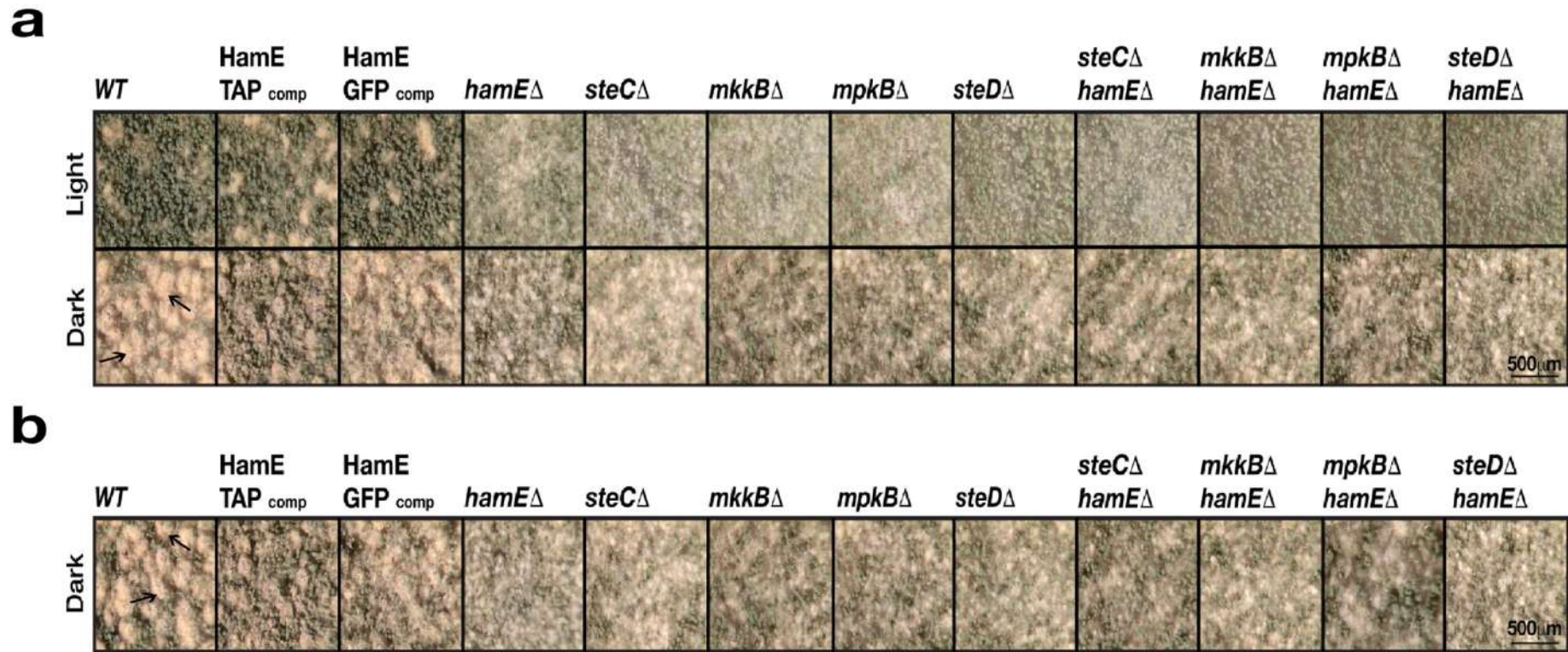
Figure 3.6. Close-up stereomicroscopic images of the strains from Figure 3.5. (a) Images were taken at 5x magnification. Black arrows represent mature fruiting bodies surrounded by Hulle cells, scale bar represents 500μm. (b) Stereomicroscopic images of sexually induced strains taken at 8x magnification.
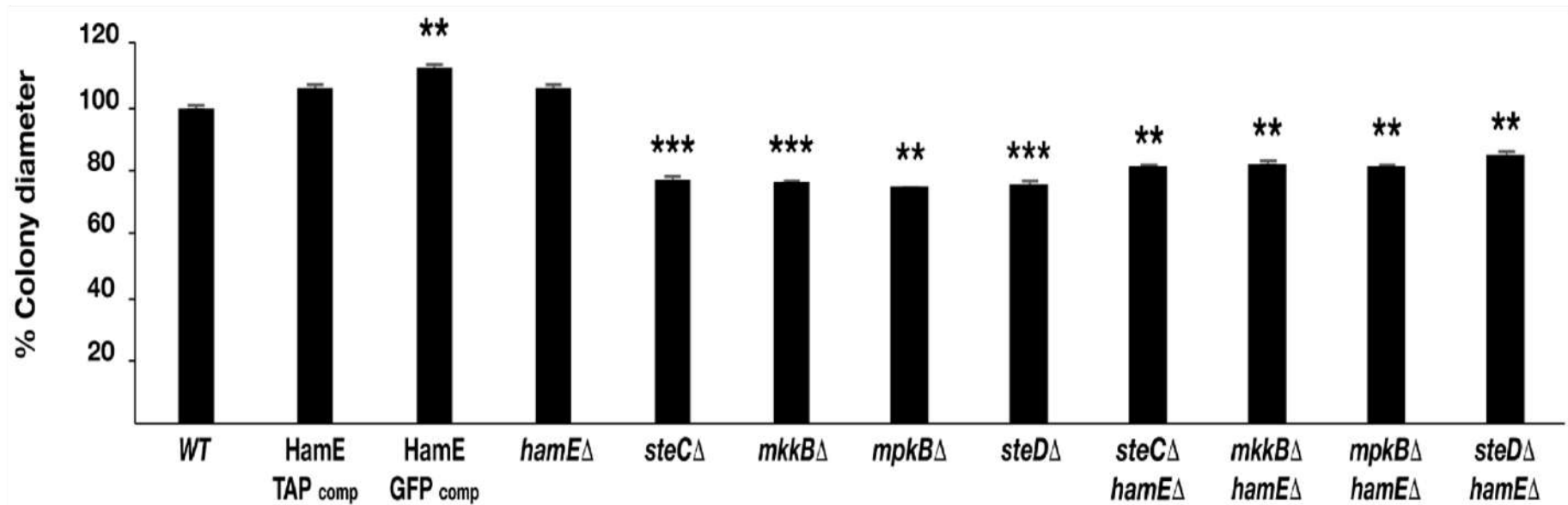
Figure 3.7. Graphical representation of the colony diameters of each asexually induced strain from Figure 3.5 with respect to the AGB551 wild type strain. Measurements were taken from three independent biological replicates for each asexually induced strain and the averages were plotted ± s.d. *P*-values were calculated by performing unpaired Student's *t*-tests (**P<0.01; ***P<0.001).
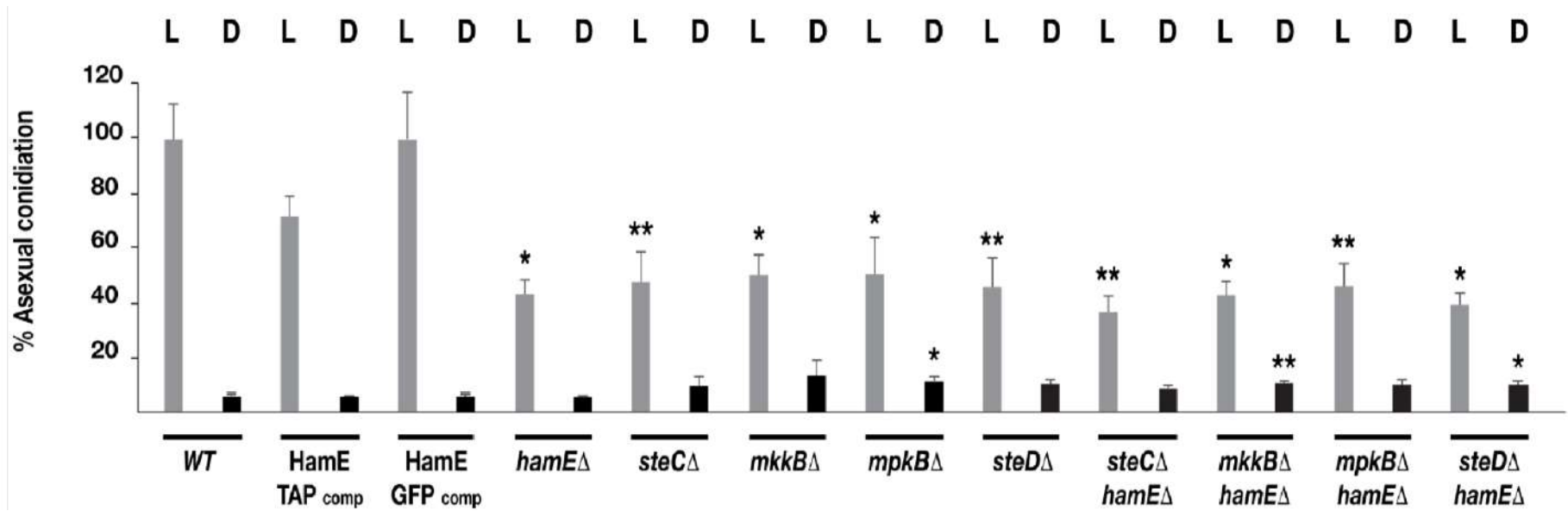
Figure 3.8. Quantification of asexual conidiation in each strain, induced in both asexual and sexual conditions. L=light, D=dark. The average sporulation value produced by the asexually-induced wild type strain was chosen to represent 100%. Mean values of all other strains (N=3) were plotted $\pm$ s.d. as a percentage of the WT. P-values were calculated by performing unpaired Student's t-tests (*P<0.05; **P<0.01), with light and dark-induced colonies being compared to the respective light and dark-induced wild type colonies.
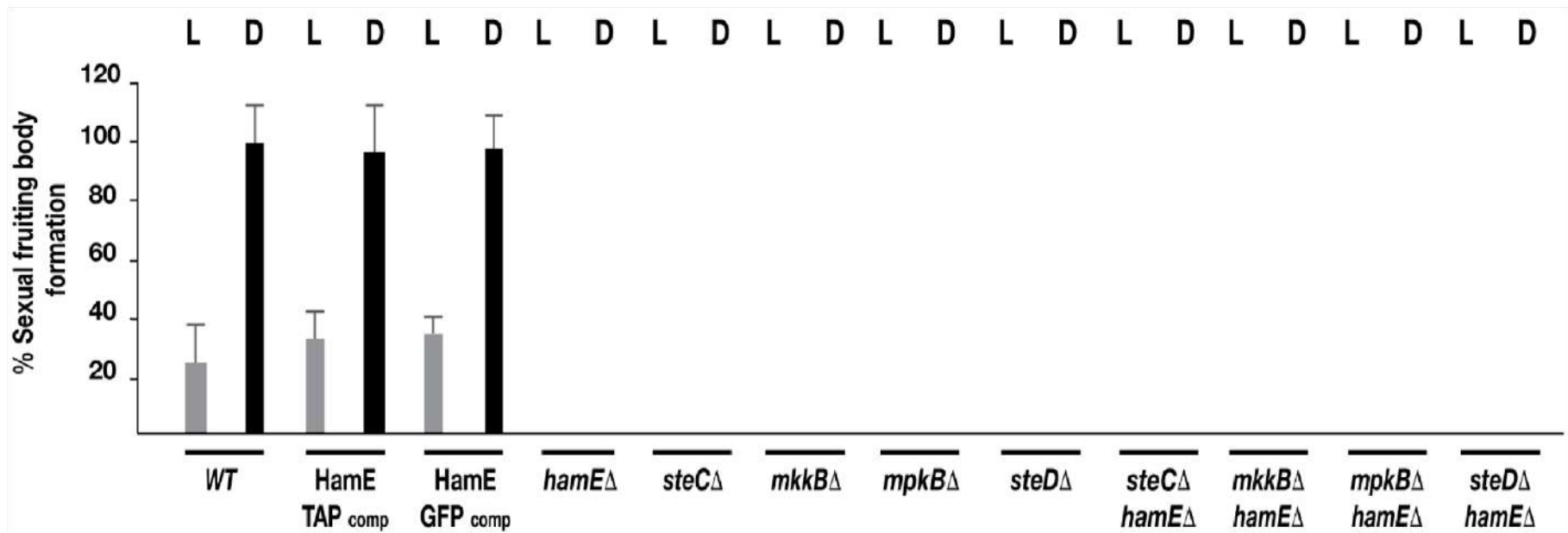
Figure 3.9. Quantification of cleistothecia production in each strain, induced in both asexual and sexual conditions. L=light, D=dark. Three 2x magnification images of each asexual and sexual replicate from **Figure 3.5**. were taken and the cleistothecia were counted manually (*N*=9). The average cleistothecia value produced by the sexually-induced wild type strain was chosen to represent 100%. The averages of each strain were plotted ± s.d. as a percentage of the WT

77

3.4. Expression of various sexual development and SM genes is dependent on the pheromone module proteins and HamE

Given that the pheromone module mutants and the HamE mutant exhibited defects in sexual development, it was decided to determine the influence of these proteins in the regulation of various sexual development and SM genes. In *A. nidulans,* sexual reproduction is co-ordinated with SM production by the heterotrimeric velvet complex (VeA-VelB-LaeA) (Bayram et al., 2008). *A. nidulans* is capable of producing over 40 SMs, that can exhibit beneficial as well as deleterious effects. Examples of SMs produced by *A. nidulans* include the carcinogenic compound sterigmatocystin, the antibiotic penicillin and the anti-tumour agent terrequinone A (Inglis et al., 2013).

3.4.1. Expression levels of the velvet complex genes are downregulated in all mutant strains

qPCR analysis was performed to determine the relative expression levels of the velvet complex genes *veA*, *velB* and *laeA* in each single and double deletion strain, with respect to the AGB551 WT strain. For details of sample preparation and qPCR analysis, see **section 2.11.** It was evident that there were significant reductions in gene expression for all three genes in each mutant, when compared to the wild type (**Figure 3.10**). For the *veA* gene, all mutants displayed similar levels of reduction, ranging from 58%-72%. Expression levels of the *laeA* gene were decreased, with mutants exhibiting reductions of 47%-64%. Lastly, the *velB* gene also displayed reduced expression levels, ranging from 32%-61%. These data suggest that HamE and the pheromone module kinases are required for the regulation of velvet complex gene expression, which could explain why these mutants display sterile phenotypes and are incapable of undergoing sexual development. Similar levels of reduction in each strain also signify that these proteins function in the same manner or pathway to regulate gene expression. Double deletion strains displayed comparable patterns of expression, with respect to the single mutants. This provides evidence that the deletion of *hamE* does not impose any subsequent effects when it is combined with another gene deletion, further suggesting that HamE functions in the same pathway as the pheromone module kinases to regulate gene expression.
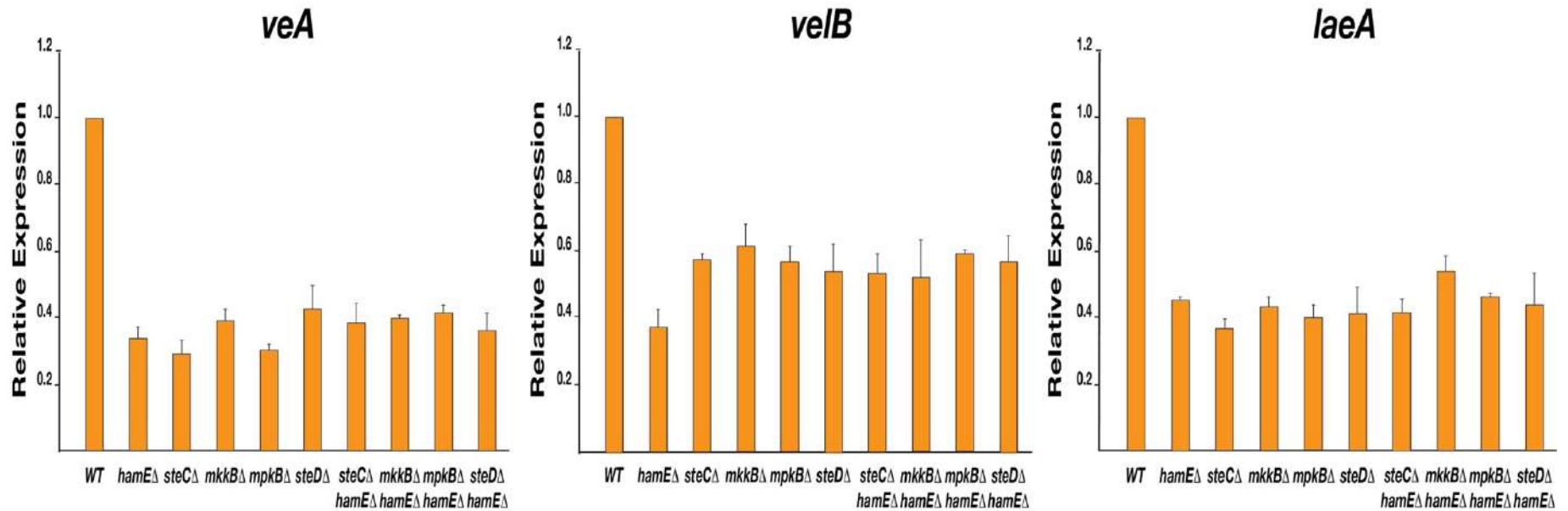
Figure 3.10. Expression levels of the *veA, velB* and *laeA* genes belonging to the velvet complex in all single and double deletion strains. Strains were inoculated (5×10^6 spores/ml) in 40ml of GMM and incubated for 48 hours at 37°C on a shaker. mRNA was isolated from 2 independent biological replicates per strain. This mRNA was converted to cDNA and used for qPCR analysis. 3 technical replicates per biological replicate were used (*N*=6). The average expression level values were plotted ± s.d. as a percentage of the wild type average, which was chosen to represent 100% expression.

3.4.2. HPLC experiments show reductions in sterigmatocystin production in all mutants

Sexual development in *A. nidulans* is coupled to secondary metabolism, a process of producing a myriad of SMs (Bayram et al., 2008). Due to the fact that all mutants exhibited impaired sexual reproduction and reductions in expression of the velvet complex genes, it was decided to assess whether these mutants would also be hindered in the production of various SMs. To determine the levels of production of the carcinogenic aflatoxin precursor sterigmatocystin (ST) in each mutant strain, RP-HPLC experiments were performed. The levels of ST in each mutant were measured and compared to the AGB551 WT strain. It was found that each single and double deletion strain produced significantly reduced levels of ST, with values ranging from 87.5%-97% reduction (**Figure 3.11.**). Double deletion strains displayed similar levels of reduction, in comparison to the respective single mutants. These data together suggest that HamE and the pheromone module kinases are crucial in the regulation of ST production and that these proteins all function in the same pathway to regulate secondary metabolism.
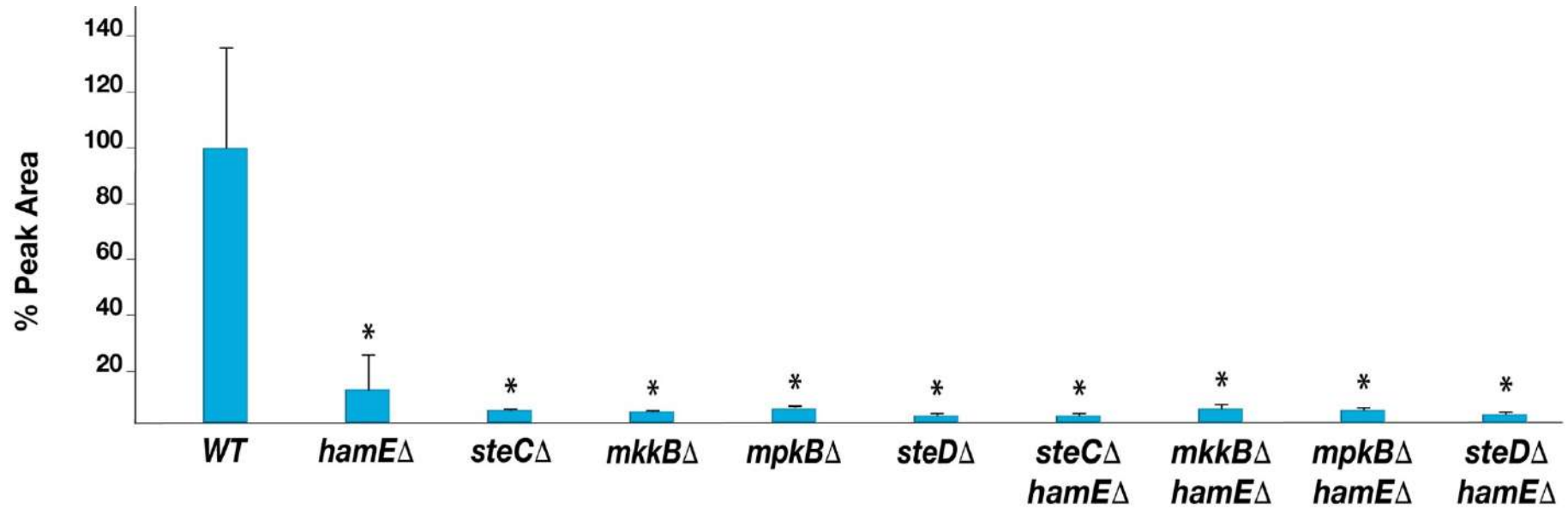
Figure 3.11. HPLC detection of sterigmatocystin levels in single and double deletion strains. Strains were inoculated (5×10^6 spores/ml) in 40ml of GMM and incubated for 48 hours at 37°C on a shaker. 25ml of supernatant was filtered and mixed with 25ml of chloroform on a rotator for 1 hour. The chloroform layers were separated and evaporated and the resulting pellets were resuspended in methanol and used for HPLC analysis. A ST standard was used as a reference. Average peak area values were plotted as a percentage of the wild type ± s.d. *P*-values were calculated by performing unpaired Student's *t*-tests (*P<0.05).

3.4.3. Expression levels of genes of the sterigmatocystin gene cluster are downregulated in all mutant strains

In attempt to complement the HPLC results from **Figure 3.11.,** which show reductions in the levels of ST production in all mutants, it was decided to test the gene expression levels for various genes belonging to the ST gene cluster. Expression of the transcriptional activator gene *aflR* and the two structural genes *stcQ* and *stcE* was assessed in all strains (**Figure 3.12.**). *aflR* transcript levels were significantly reduced in all mutants, with reductions in expression ranging from 63%-86%. Likewise, *stcQ* also exhibited significantly reduced expression levels (59%-91% reduction). Lastly, the levels of *stcE* expression showed a similar trend to the other two genes, displaying reductions ranging from 65%-88%. These data support the HPLC findings and together suggest that HamE and the pheromone module kinases are required for the regulation of ST production, likely *via* the regulation of expression of various genes belonging to the ST cluster.
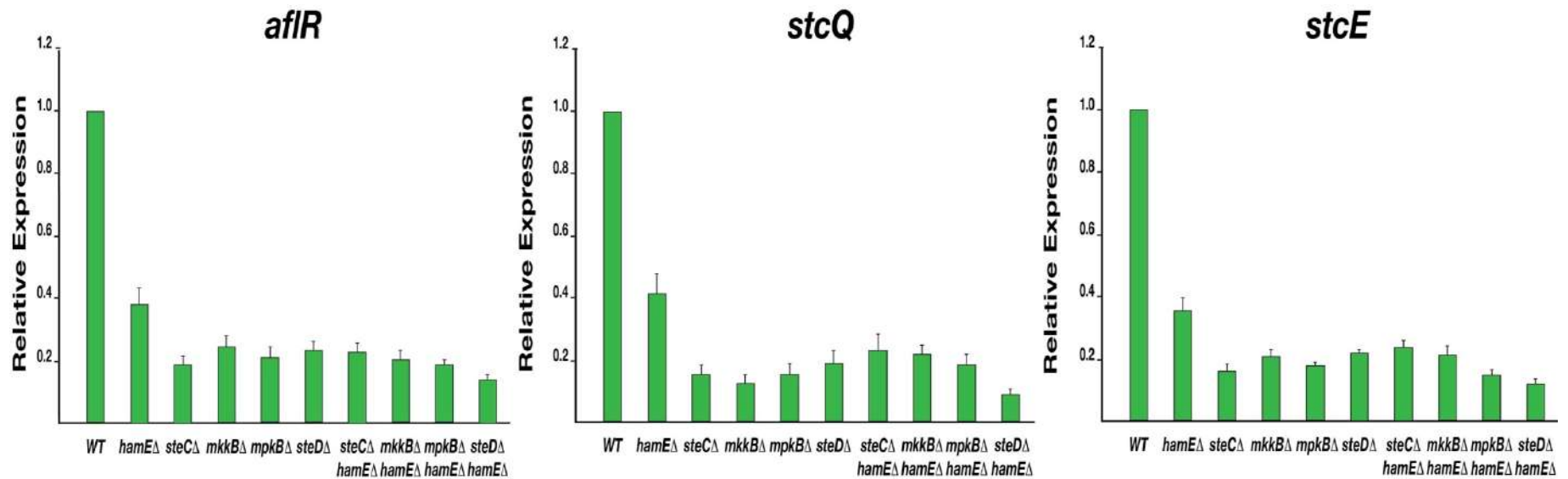
Figure 3.12. Expression levels of the *aflR, stcQ* and *stcE* genes belonging to the sterigmatocystin gene cluster in all single and double deletion strains. Strains were inoculated (5×10^6 spores/ml) in 40ml of GMM and incubated for 48 hours at 37°C on a shaker. mRNA was isolated from 2 independent biological replicates per strain. This mRNA was converted to cDNA and used for qPCR analysis. 3 technical replicates per biological replicate were used (*N*=6). The average expression level values were plotted ± s.d. as a percentage of the wild type average, which was chosen to represent 100% expression.

3.4.4. Expression levels of genes of the penicillin gene cluster are downregulated in all mutant strains

Because LaeA is a global regulator of secondary metabolism (Bok and Keller, 2004) and velvet complex gene transcript levels were reduced in all strains tested (**Figure 3.10.**), it was decided to test whether expression of other metabolite gene clusters is affected in each mutant strain. The *acvA*, *aatA* and *ipnA* genes of the penicillin (PN) gene cluster, a commonly used antibiotic, were tested. It was observed that the expression of each gene was considerably decreased in all single and double deletion strains (**Figure 3.13**). *acvA* levels showed significant reductions ranging from 62-85%. The transcript levels of *aatA* also exhibited dramatic reductions, which ranged from 56-77%. Lastly, the *ipnA* gene expression levels displayed the most considerable reduction range of 71%-89%. All single and double deletion strains behaved similarly, with reductions in expression remaining consistent throughout the 3 genes tested. These data suggest that HamE functions in the same pathway as the pheromone module to regulate velvet complex gene expression. In turn, these proteins are capable of regulating expression of metabolite gene clusters such as genes of the PN cluster.
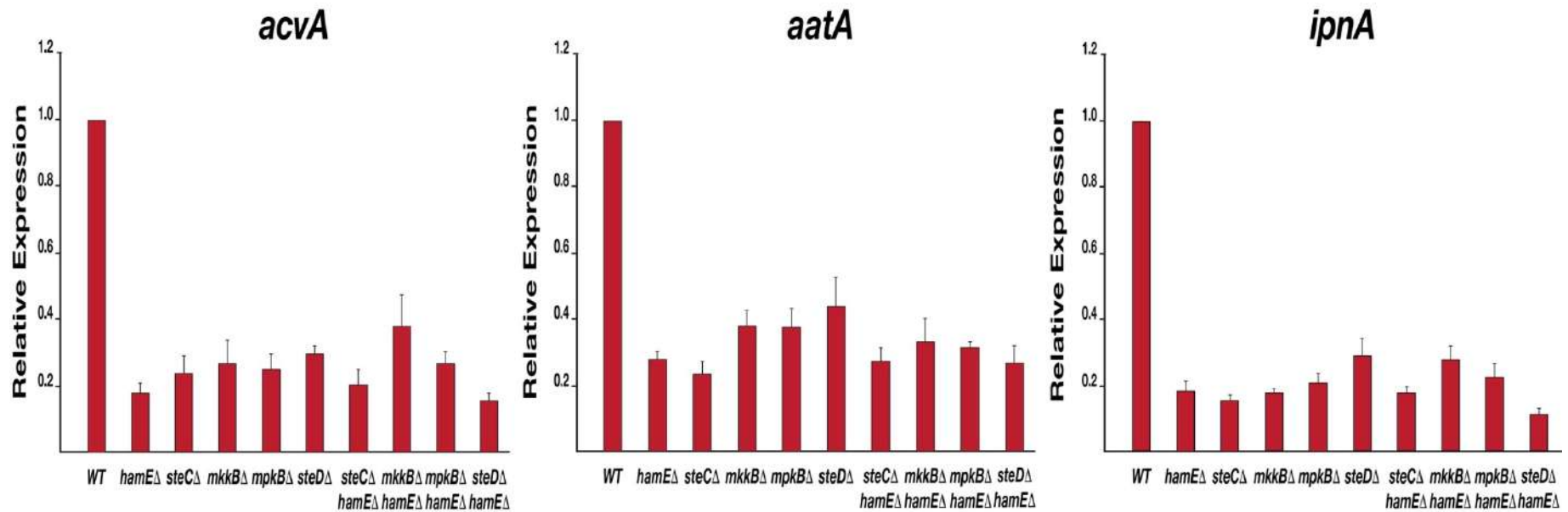
Figure 3.13. Expression levels of the *acvA*, *aatA* and *ipnA* genes belonging to the penicillin gene cluster in all single and double deletion strains. Strains were inoculated (5×10^6 spores/ml) in 40ml of GMM and incubated for 48 hours at 37°C on a shaker. mRNA was isolated from 2 independent biological replicates per strain. This mRNA was converted to cDNA and used for qPCR analysis. 3 technical replicates per biological replicate were used (*N*=6). The average expression level values were plotted ± s.d. as a percentage of the wild type average, which was chosen to represent 100% expression.

3.4.5. Expression levels of genes of the terrequinone A gene cluster are downregulated in all mutant strains

Lastly, the genes belonging to the anti-tumour compound terrequinone A (TQ) gene cluster were tested in all mutants. The genes *tdiA* and *tdiB* were chosen and these genes displayed the most considerable reductions in expression in comparison to all metabolite genes tested. *tdiA* exhibited dramatic reductions in expression, which ranged from 88%-95%. Similarly, levels of *tdiB* expression were also significantly reduced, ranging from 90-94%. Overall, these qPCR and HPLC data suggest that HamE and the pheromone module proteins function together to regulate MpkB-dependent regulation of the velvet complex. Deletion of any of these proteins results in reduced LaeA activity and subsequent decreased regulation of various metabolite gene clusters, which can range from carcinogenic compounds like ST to beneficial antibiotics and anti-tumour compounds like PN and TQ, respectively.
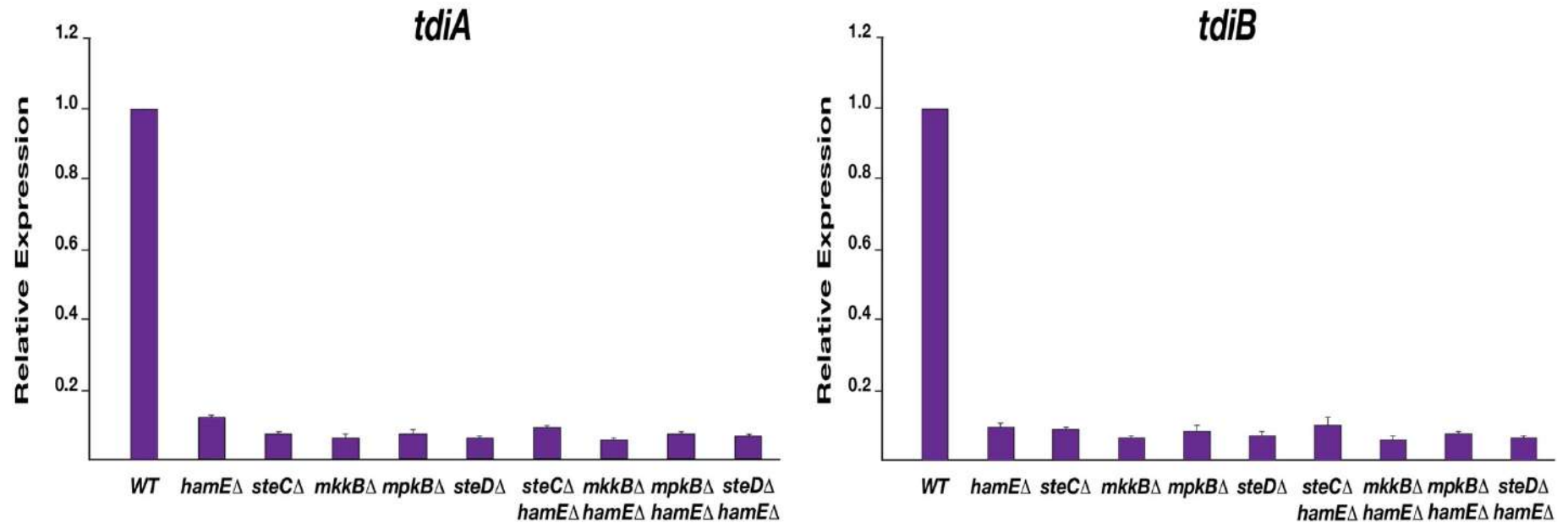
Figure 3.14. Expression levels of the *tdiA* and *tdiB* genes belonging to the terrequinone A gene cluster in all single and double deletion strains. Strains were inoculated (5×10^6 spores/ml) in 40ml of GMM and incubated for 48 hours at 37°C on a shaker. mRNA was isolated from 2 independent biological replicates per strain. This mRNA was converted to cDNA and used for qPCR analysis. 3 technical replicates per biological replicate were used (*N*=6). The average expression level values were plotted ± s.d. as a percentage of the wild type average, which was chosen to represent 100% expression.

3.5. HamE influences the production and phosphorylation of the pheromone module proteins

Given that evidence suggests HamE plays a role in the pheromone module pathway to regulate both development and SM, it was decided to determine the specific role(s) that HamE plays in this pathway. To assess the influence of HamE with regards to the production of the pheromone module proteins, *steC, mkkB, mpkB* and *steD* were fused to *sgfp* epitope tags and were expressed in strains that either harboured a functional copy of the *hamE* gene or had the *hamE* gene deleted. These tagged strains were cultured for various time points and were either grown vegetatively or induced for asexual or sexual development. Details of all culturing steps can be found in section 2.1.3. To determine if HamE influences the phosphorylation statues of the pheromone module proteins, *steC, mkkB* and *mpkB* were coupled to *ctap* epitope tags and expressed in either *hamE*$^+$ or *hamE*$^-$ background strains. These strains were immunoprecipitated by performing TAP pulldowns and samples were prepared for MS analysis. MS was used to identify the phosphorylated residues on each TAP-tagged protein and to compare the differences in these residues when the *hamE* gene is deleted.

3.5.1. The pheromone module proteins display changes in abundance throughout development in the absence of HamE

GFP-tagged strains were cultured vegetatively for both 24 hours and 36 hours. Vegetatively cultured mycelia were transferred to agar plates and induced either asexually for 12 hours and 24 hours, or induced sexually for 12 hours, 24 hours or 48 hours. Crude protein extracts were isolated from each sample and time course immunoblotting was performed to determine and compare the relative abundance levels of each GFP-tagged protein in the presence and absence of HamE (**Figure 3.15.**). An anti-GFP antibody was used for detection of each tagged protein and coomassie staining was performed to act as loading controls, showing equal loading in each well. Protein crude extract isolated from the AGB551 WT strain cultured vegetatively for 24 hours acted as the negative control, as this strain contains no GFP-tagged proteins.

3.5.1.1. Relative abundance of SteC-GFP

Immunoblots of SteC-GFP revealed a dynamic relative abundance profile for this protein. At 24 hours of vegetative growth, SteC is abundantly produced in the *hamE*$^+$ strain. When *hamE* is deleted, it can be observed that SteC shows a slight increase in abundance at 24 hours. At 36 hours of vegetative growth, SteC shows a faint band, signifying considerably reduced abundance at this time point. This could be due to a negative feed-back loop which serves to terminate the MAP kinase signal. In the *hamE* mutant, interestingly, SteC abundance is maintained and resembles the intensity observed at 24 hours of growth. Increased abundance of SteC in the *hamE* mutant is also evident during 12 and 24 hours of asexual induction. However, at 12 hours of sexual induction, SteC is highly abundant in the *hamE*$^+$ strain, whereas, in the *hamE* mutant, it is clear that SteC production is considerably reduced. At 24 and 48 hours of sexual induction, SteC is not produced in high abundance in either the *hamE*$^+$ or *hamE*$^-$ backgrounds.

3.5.1.2. Relative abundance of MkkB-GFP

The MkkB-GFP relative abundance profile displayed less varied results. At 24 hours of vegetative growth, the fusion protein is abundantly produced in both *hamE*$^+$ and *hamE*$^-$ backgrounds. However, at 36 hours of vegetative growth, it can be observed that MkkB abundance is decreased in the *hamE*$^+$ strain, but abundance is maintained in the *hamE* mutant, which is also the case for SteC. At 12 hours of asexual induction, MkkB production is very faint in both backgrounds but is completely reduced in the absence of HamE. At 24 hours of asexual growth, MkkB is not detected in either strains. At 12 and 24 hours of sexual induction, it is apparent that the abundance of MkkB is weak, with slightly reduced production being evident in the *hamE* mutant at 24 hours of growth. At 48 hours of sexual induction, MkkB is not detectable in either backgrounds.

3.5.1.3. Relative abundance of MpkB-GFP

MpkB-GFP production remained fairly constant in both backgrounds throughout each vegetative and asexual induction time point. At 24 hours of vegetative growth, MpkB

is detectable in high abundance in both the *hamE⁺* and *hamE⁻* strains. At 36 hours of vegetative growth, it can be seen that MpkB production shows a slight increase in the absence of *hamE*. At 12 hours of asexual induction, MpkB abundance remains constant in both backgrounds, while there is a slight increase at the 24 hour time point in the *hamE* mutant. MpkB levels were slightly reduced during the sexual induction time points in both strains. At 12 and 24 hours of induction, MpkB levels remain constant in both backgrounds. Interestingly, it can be observed that at 48 hours of sexual induction, MpkB levels increase significantly in the presence of HamE, however, in the *hamE* mutant, it is clear that these levels do not increase and resemble the levels of abundance observed at the 12 and 24 hour time points.

3.5.1.4. Relative abundance of SteD-GFP

Lastly, SteD-GFP production was also constant in both backgrounds at both vegetative growth incubations and the 12 hour asexual induction time point. At 24 hours of asexual growth, it can be observed that SteD abundance is decreased in both strains, however, it displays a slightly higher decrease in the *hamE* mutant. At 12 hours of sexual induction, production of SteD is low but constant in both backgrounds. Interestingly, SteD production becomes upregulated at the 24 hour sexual induction time point in both strains. At 48 hours, the abundance again decreases but is completely undetectable in the *hamE* mutant.

Together, these data underline complex modes of regulation for the pheromone module proteins and highlight potential roles of HamE in the regulation of kinase production. The highly varied relative abundance profiles of each protein could suggest that each pheromone module kinase undertakes unique functional roles outside of the roles they play within the context of the pheromone response.
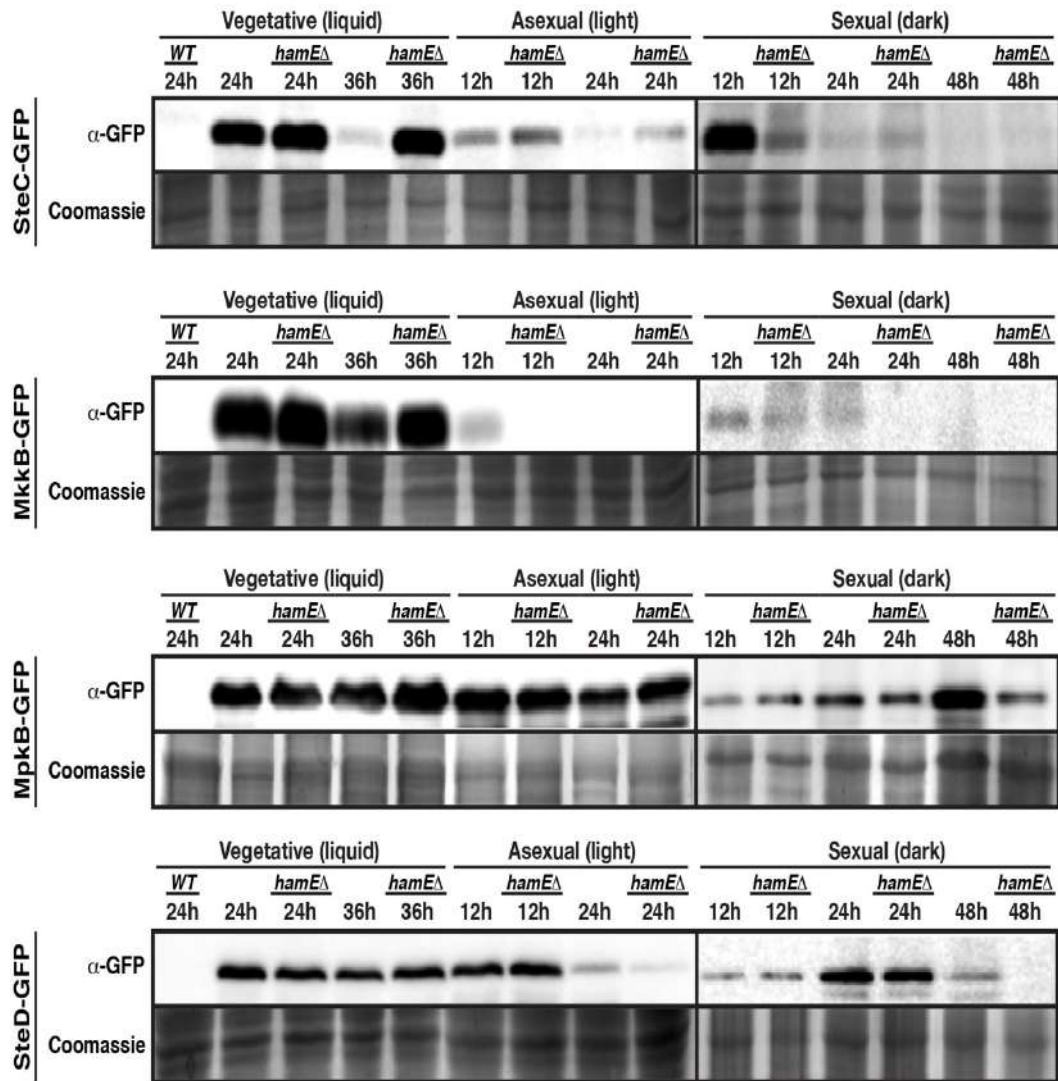
Figure 3.15. Relative abundance levels of GFP-tagged SteC, MkkB, MpkB and SteD fusion proteins at various stages of development in the presence and absence of *hamE*. Vegetative cultures were grown in liquid GMM. For asexual and sexual cultures, strains were grown for 24 hours vegetatively in liquid GMM and mycelia were transferred to GMM plates to be incubated in the light and dark respectively. 80μg of each protein sample was loaded on 10% acrylamide gels and for loading controls, gels were stained in 0.1% Coomassie Brilliant Blue R-250 dye and exposed using the G: BOX Chemi XRQ (Syngene). Details of antibodies used for detection of GFP-tagged proteins are described in section 2.10. Full length blots and gels used to generate this figure are in **Appendix A: Figures S3 and S4.**

3.5.2. The pheromone module kinases show significantly reduced levels of phosphorylation in the absence of HamE.

It was apparent that HamE plays a role in the regulation of kinase production. This led to the question of whether or not HamE has any influence over the regulation of kinase signalling. To gain insight into how HamE may alter the signalling dynamics of the pheromone module complex, TAP-tagged kinases in *hamE*$^+$ and *hamE*$^-$ backgrounds were immunoprecipitated *via* TAP pulldowns and prepared for MS analysis. MS data revealed the phosphorylated residues detected on each kinase in the *hamE*$^+$ and *hamE*$^-$ strains. Combined data from 4 independent biological replicates per strain were tabulated and are presented in **Figure 3.16 (b).** Supplementary mass spectrometry tables for this figure are provided in **Appendix A: Tables S6-S10.**

3.5.2.1. Phosphorylation of SteC

It was apparent that, in the *hamE*$^+$ strain, SteC becomes highly phosphorylated on a wide range of serine (S), threonine (T) and tyrosine (Y) residues (26 amino acid sites in total) (**Appendix A: Table S6**). However, in the *hamE* mutant, only 19 phosphorylated residues were detectable in total (**Appendix A: Table S7**). The 7 sites that were absent were the following: 42(Y), 153(S), 309(S), 418(S), 426(S), 464(S) and 575(S), revealing losses of phosphorylation throughout the protein sequence, rather than at a localised area. Currently, the significance of each phosphorylated residue on SteC is not known. These sites could be implicated in kinase signalling or protein ubiquitination and degradation (Martin, 2014). Due to protein coverage detected by MS being a huge factor in the detection of these phosphorylation sites, it cannot be claimed conclusively that HamE directly influences the phosphorylation states of SteC. In the *hamE*$^+$ strain, the protein coverage of the 4 replicates of SteC-TAP ranged from 64.67%-70.65%, while in the *hamE* mutant strain, these values ranged from 57.56%-70.88%. It is possible that if this protein coverage could be increased, that the number of detectable phosphorylated amino acid residues could also increase. However, it could be suggested that the deletion of *hamE* may potentially cause a decrease in SteC phosphorylation either directly or indirectly, which could explain the altered levels of abundance for SteC that were detected in **Figure 3.15.**

3.5.2.2. Phosphorylation of MkkB

Due to evidence that HamE interacts directly with both MkkB and MpkB (**Figure 3.1.**), it was predicted that HamE would influence MkkB and MpkB phosphorylation levels to a higher degree than that observed for SteC. The detectable phosphorylated residues for 4 replicates of MkkB-TAP were combined and it was apparent that there were significant differences in the *hamE*[+] and *hamE*[-] backgrounds. Like SteC, MkkB also displayed a high degree of phosphorylation on serine, threonine and tyrosine residues. 18 residues were detected in total for MkkB in the *hamE*[+] strain (**Appendix A: Table S8**), whereas only 5 residues were detected in total in the *hamE* mutant (**Appendix A: Table S9).** The following phosphorylated sites were not detectable in the *hamE* mutant: 26(S), 27(T), 28(S), 29(T), 31(S), 35(S), 213(T), 215(T), 218(S), 222(T), 359(S), 360(Y), 372(T) and 375(S). Like SteC, it was also apparent that these losses of phosphorylated residues are present throughout the length of the protein, rather than at specific segments. Protein coverage for MkkB in the *hamE*[+] background ranged from 58.07%-72.73%, while the values for protein coverage were higher for MkkB in the *hamE* mutant, ranging from 64.75%-77.18%. Like SteC, the biological significance of these phosphorylated residues is not known. However, these data provide evidence that in the absence of HamE, MkkB phosphorylation is considerably decreased, which could explain the defects in MAP kinase signalling observed in the *hamE* mutant.

3.5.2.3. Phosphorylation of MpkB

Lastly, the phosphorylated residues detected for MpkB in *hamE*[+] and *hamE*[-] backgrounds were combined across 4 replicates and tabulated. MpkB is the terminal kinase of the pheromone module and it is characteristic for these specific kinases to become phosphorylated mainly on two amino acid residues. This dual phosphorylation of MpkB occurs at a conserved Thr182-X-Tyr184 motif, which allows for activation of the MAP kinase to promote cell signalling (Widmann et al., 1999, Yoshioka, 2004, Saito, 2010). It was found that in both *hamE*[+] and *hamE*[-] backgrounds, only two and three phosphorylated residues were detected for MpkB, respectively (**Appendix A: Table S10).** In the *hamE*[+] strain, the protein coverage of MpkB ranged from 79.38%-86.44% and the phosphorylated sites detected were 15(S) and 184(Y). The protein coverage for MpkB in the *hamE* mutant ranged from 74.29%-85.31% and the sites detected were 15(S), 182(T) and 184(Y). It is apparent from these data that the protein

coverage values for MpkB were significantly high, revealing that the majority of peptides of the protein could be detected by MS. However, this MS data is not conclusive to determine if HamE exerts a modulatory effect on MpkB phosphorylation levels.

Because of this, it was decided to assess whether HamE instead influences the intensity of MpkB phosphorylation. To test this, we cultured both a WT and *hamE* mutant strain vegetatively and induced the vegetative mycelia either asexually or sexually. These cultures were incubated for different periods of time and crude protein extracts were isolated from each culture. Time course immunoblotting was performed using an α-phospho-p44/42 MAPK antibody which detects phosphorylation at the conserved Thr182-X-Tyr184 motif of MpkB (**Figure 3.16. (a)**). Interestingly, it was found that at all stages of development, MpkB phosphorylation at this motif is significantly reduced when *hamE* is deleted. The most considerable reductions are evident at 36 hours of vegetative growth and 12 and 24 hours of asexual induction. Together, these data provide evidence that HamE is essential for the regulation of kinase phosphorylation, specifically MkkB and MpkB. This could explain the impaired MAP kinase signalling and subsequent defects in development and SM observed in the *hamE* mutant.

SteC-TAP

Position	Target	Peptide confidence	Sequence Motif
30	S	High	HTTTQKsSTFSES
31	S	High	TTTQKSsTFSESQ
32	T	High	TTQKSStFSESQT
42	Y	High	SQTGTVyISPTKS
43	T	High	QTGTVYtSPTKSE
44	S	High	TGTVYTsPTKSEF
46	T	High	TVYTSPtKSEFSE
48	S	High	YTSPTKsEFSEAD
51	S	High	PTKSEFsEADDGL
150	S	High	AAHQQAsPDSARS
153	S	High	QQASPDsARSYSA
181	T	Middle	YSYGRPtSRPGSP
182	S	Middle	SYGRPTsRPGSPL
186	S	Middle	PTSRPGsPLRPHR
197	S	High	HRYVANsPMDSGR
233	S	High	HSRQNPsLDGMTM
309	S	High	SNCRRLsDHELME
398	T	High	SSRHNTtPSDHEI
400	S	High	RHNTTPsDHEIRP
418	S	High	RVSKLRsFFGARP
426	S	High	FGARPPsEMIIHE
464	S	High	RLSRAAsRLSVVS
467	S	High	RAASRLsVVSNTS
535	S	High	HPLQEEsPVEPNR
575	S	High	AATDGGsFNERLS
784	S	High	GHIHRPsLQGSVY

SteC-TAP(hamEΔ)

Position	Target	Peptide confidence	Sequence Motif
30	S	High	HTTTQKsSTFSES
31	S	High	TTTQKSsTFSESQ
32	T	High	TTQKSStFSESQT
43	T	High	QTGTVYtSPTKSE
44	S	High	TGTVYTsPTKSEF
46	T	High	TVYTSPtKSEFSE
48	S	High	YTSPTKsEFSEAD
51	S	High	PTKSEFsEADDGL
150	S	High	AAHQQAsPDSARS
181	T	High	YSYGRPtSRPGSP
182	S	High	SYGRPTsRPGSPL
186	S	High	PTSRPGsPLRPHR
197	S	High	HRYVANsPMDSGR
233	S	High	HSRQNPsLDGMTM
398	T	High	SSRHNTtPSDHEI
400	S	High	RHNTTPsDHEIRP
467	S	High	RAASRLsVVSNTS
535	S	High	HPLQEEsPVEPNR
784	S	High	GHIHRPsLQGSVY

MkkB-TAP

Position	Target	Peptide confidence	Sequence Motif
26	S	High	LNAAPKsTSTLSN
27	T	High	NAAPKStSTLSNG
28	S	High	AAPKSTsTLSNGD
29	T	High	APKSTStLSNGDS
31	S	High	KSTSTLsNGDSQV
35	S	High	TLSNGDsQVPGAA
213	T	High	CDFGVAtETVNSI
215	T	High	FGVATEtVNSIAD
218	S	High	ATETVNsIADTFV
222	T	High	VNSIADtFVGTST
268	S	High	PFDTTDsAAGDRA
275	S	High	AAGDRAsAGPMGI
359	S	High	ERHNRKsYLAPPA
360	Y	High	RHNRKSyLAPPAP
372	T	High	PKSLKEtRESPSP
375	S	High	LKETREsPSPAQA
383	S	High	SPAQAPsPVQKHG
470	S	High	RPTRRPsRTPLGD

MkkB-TAP(hamEΔ)

Position	Target	Peptide confidence	Sequence Motif
268	S	High	PFDTTDsAAGDRA
275	S	High	AAGDRAsAGPMGI
383	S	High	SPAQAPsPVQKHG
470	S	High	RPTRRPsRTPLGD
472	T	High	TRRPSRtPLGDSS

Figure 3.16. HamE influences the phosphorylation states of the pheromone module kinases (a) Determination of the phosphorylation status of MpkB in the presence and absence of *hamE* during different stages of development using an anti-phospho-p44/42 antibody. 80μg of each protein sample was loaded on 10% acrylamide gels and for loading controls, these gels were stained in 0.1% Coomassie Brilliant Blue R-250 dye and exposed using the G: BOX Chemi XRQ (Syngene). Full length blots and gels used to generate this figure are in **Appendix A: Figure S5.** (b) Comparison of the phosphorylated residues of SteC and MkkB in the presence and absence of *hamE*. The tables represent the total phosphorylated residues and their amino acid positions detected by MS using 4 independent TAP-tagged biological replicates of each strain. S (Serine), T (Threonine), Y (Tyrosine). Supplementary MS tables for this figure are in **Appendix A: Tables S6-S10.**

3.6. Assembly and localisation of the pheromone module is not HamE-dependent

In attempt to further characterise the role of HamE in the pheromone module, it was decided to assess whether HamE exerts any influence over the localisations of the module proteins and the assembly of the complex. To determine whether the *in vivo* sub-cellular localisations of the pheromone module proteins are influenced by HamE, strains expressing GFP-tagged proteins in *hamE*$^+$ and *hamE*$^-$ backgrounds were cultured vegetatively for 16 hours and visualised *via* confocal microscopy. To assess whether HamE facilitates complex assembly, strains harbouring TAP-tagged pheromone module proteins in *hamE*$^+$ and *hamE*$^-$ backgrounds were cultured vegetatively. TAP pulldowns were performed and the immunoprecipitated proteins were prepared for MS analysis.

3.6.1. The localisations of GFP-tagged pheromone module proteins do not differ in the presence or absence of HamE

The *in vivo* sub-cellular localisations of each of the pheromone module proteins are displayed in **Figure 3.17.** Each strain expressing GFP-tagged fusion proteins also expressed nuclei tagged with mRFP. The green and red signals were overlapped to determine the localisation of each protein with respect to the nucleus. It is evident in the work performed by Bayram *et al.* (2012) that each pheromone module protein localises to specific areas in the hyphae. These sites include the hyphal tip, nuclear envelope and plasma membrane, while MpkB is the only protein found to localise in the nucleus. However, these precise localisation patterns are brief and fluctuate quickly, making them difficult to detect. It can be observed in **Figure 3.17.** that localisation of each fusion protein was not detected at specific sites. Instead, each protein displayed mostly cytoplasmic localisation and it is evident that the deletion of *hamE* does not appear to have a significant influence on the localisation of any of the fusion proteins, as these proteins also display cytoplasmic localisation in this background.
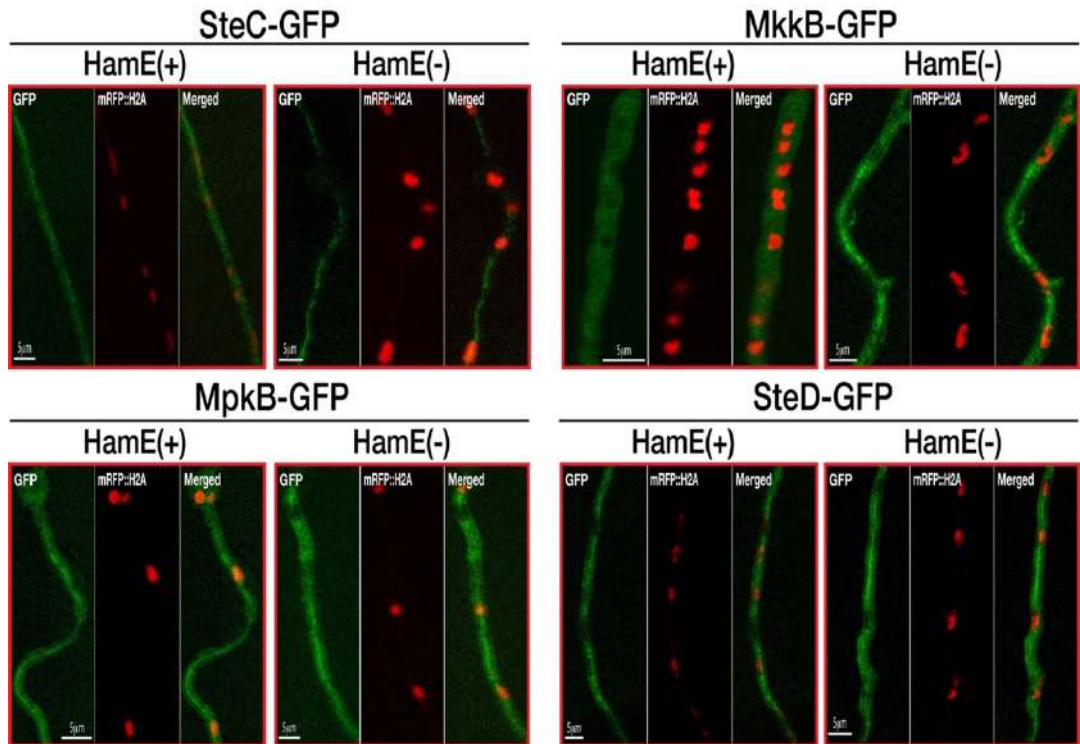
Figure 3.17. Sub-cellular localisations of the GFP-tagged pheromone module proteins in the presence and absence of HamE. Strains were inoculated (5x10^3 spores) in 500μl liquid GMM with supplements and cultured in Lab-Tek Chambered Coverglass W/CVT (Thermo Scientific) for 16 hours at 30˚C.

3.6.2. Assembly of the pheromone module complex is not HamE-dependent

To determine whether the complex is capable of assembling in the absence of HamE, TAP-tagged pheromone module proteins were immunoprecipitated in *hamE*$^+$ and *hamE*$^-$ backgrounds after 24 hours of vegetative growth. Interestingly, MS analysis of these proteins revealed that in the absence of the HamE scaffold, these proteins are still capable of assembling, as the entire tetrameric complex is detected (**Figure 3.18.**). SteC-TAP purifications (42 peptides, 62.08% coverage) in a *hamE* deletion background co-purified MkkB (8 peptides, 20.96%) and SteD (25 peptides, 64.78%) (**Appendix A: Table S11**). This is comparable to SteC-TAP purifications (45 peptides, 68.28% coverage) in a *hamE*$^+$ background (**Figure 3.1 (a)**), which co-purified MkkB (6 peptides, 19.67% coverage) and SteD (27 peptides, 73.48%).

MkkB-TAP purifications (29 peptides, 74.77% coverage) in the *hamE* mutant co-purified SteC (44 peptides, 71.9% coverage), MpkB (10 peptides, 36.44% coverage) and SteD (24 peptides, 72.06% coverage) (**Appendix A: Table S12**). In the *hamE*$^+$ background (**Figure 3.1 (a)**), MkkB-TAP purifications (29 peptides, 72.17% coverage) co-purified SteC (36 peptides, 54.18% coverage), MpkB (18 peptides, 78.53% coverage) and SteD (22 peptides, 69.03% coverage).

MpkB-TAP purifications (23 peptides, 80.51%) in the *hamE* mutant co-purified SteC (3 peptides, 5.87% coverage), MkkB (15 peptides, 35.25% coverage), SteD (5 peptides, 15.79% coverage) and the SteA transcription factor (22 peptides, 50.72%) (**Appendix A: Table S13**). In the *hamE*$^+$ background (**Figure 3.1 (a), Appendix A: Table S3**), MpkB-TAP purifications (25 peptides, 82.2% coverage) only co-purified MkkB (21 peptides, 56.96% coverage) and SteA (21 peptides, 56.96% coverage). SteC and SteD were not detected in these purifications, however, it can be noted that these proteins are only detected in low abundance in MpkB-TAP purifications in the *hamE* mutant and so, it cannot be deduced that the absence of *hamE* plays a role in these protein interactions.

Overall, it is evident from these data that the HamE scaffold is not required for the assembly of the tetrameric pheromone module complex and the individual protein-protein interactions. Interestingly, MpkB-TAP co-purifies the transcription factor SteA in both backgrounds, signifying that MpkB is capable of translocating into the nucleus in a HamE-independent manner.

TAP pulldowns in *hamE*Δ mutants

	SteC-TAP		MkkB-TAP		MpkB-TAP	
	% Coverage	Unique Peptides	% Coverage	Unique Peptides	% Coverage	Unique Peptides
SteC	62.08	42	71.90	44	5.87	3
MkkB	20.96	8	74.77	29	35.25	15
MpkB			36.44	10	80.51	23
SteD	64.78	25	72.06	24	15.79	5
HamE						

Figure 3.18. TAP pulldowns of the pheromone module kinases in *hamE*Δ backgrounds. Strains were cultured as described for Figure 3.1. TAP-tagged proteins are given at the top of the table and co-purified proteins are given on the left-hand side. 2 biological replicates of each strain were used. Supplementary mass spectrometry tables for this figure are given in **Appendix A: Tables S11-13.**

3.7. Summary of main findings and chapter conclusions

3.7.1. Identification of the HamE scaffold in *A. nidulans*

In this chapter, an ortholog of the *N. crassa* Ham5 protein, which functions as a scaffold in the Mak-2 kinase cascade (Jonkers et al., 2014, Dettmann et al., 2014) was identified in the filamentous fungus *A. nidulans*. This protein (gene reference: AN2701) had previously been uncharacterised according to the online Aspergillus genome database (ASPGD) (http://www.aspgd.org) and has been named 'HamE' in this study. Reciprocal BLAST searches and protein domain analysis revealed that HamE exhibits 62% similarity to Ham5 and contains similar domains at similar positions. HamE contains scaffolding domains such as WD40 repeats, localised to the N-terminus and at least 8 phosphorylation sites (**Figure 3.2.**), providing evidence that HamE is a highly-regulated scaffold protein.

3.7.2. HamE interacts with the pheromone module proteins

The HamE protein was initially detected in TAP pulldowns of the pheromone module kinases. MS experiments (**Figure 3.1.(a)**) revealed that HamE interacts with the proteins of the pheromone module, specifically MkkB and MpkB, while BIFC experiments (**Figure 3.3.**) provided evidence that HamE co-localises with SteC at specific sites in the hyphae such as the hyphal tips, plasma membrane and nuclear envelope. Together, this data suggests that HamE acts as a scaffold for the pheromone module, forming a pentameric complex (**Figure 3.1.(b)**).

3.7.3. HamE abundance and localisation

Western blotting was performed to determine the abundance of HamE throughout development. HamE abundance is increased at 36 hours of vegetative growth, 12 hours of asexual induction and 12 hours of sexual induction (**Figure 3.4. (a)**). This suggests that HamE could be implicated in the regulation of the early stages of sporulation and cleistothecia formation. Confocal microscopy experiments revealed that HamE localises to the nuclear envelope, plasma membrane and hyphal tips (**Figure 3.4. (b)**), similar to the localisation patterns observed in BIFC experiments with SteC. Taken

together, this data provides evidence that HamE co-localises with the entire pheromone module at these sites.

3.7.4. HamE is required for asexual sporulation and sexual cleistothecia production

The *hamE* gene was deleted in a WT background and pheromone module gene deletion backgrounds to create single and double deletions strains respectively. The *hamE* mutant strain exhibited defects in asexual sporulation and sexual development, which correlated with the phenotypes observed for mutants strains of the pheromone module proteins. Likewise, the double deletion strains exhibited similar reductions. Sporulation was reduced by 50-64% in all strains (**Figures 3.5. and 3.8.**), while all mutants were also sterile, completely incapable of producing mature sexual cleistothecia (**Figures 3.5. and 3.9.**). Together, these data suggest that HamE functions in the pheromone module pathway to regulate asexual and sexual development in *A. nidulans*.

3.7.5. Each mutant strain exhibited defects in secondary metabolism

All single and double deletion strains were tested *via* qPCR to determine the expression levels of various secondary metabolite genes. It was found that all mutants exhibited significantly reduced levels of expression of each gene tested. These genes included the velvet complex genes *veA, velB* and *laeA* (**Figure 3.10**)*,* which regulate sexual development and secondary metabolism, the *aflR, stcQ* and *stcE* genes of the carcinogenic ST gene cluster (**Figure 3.12**), the *ipnA, acvA* and *aatA* genes of the antibiotic PN gene cluster (**Figure 3.13**) and the *tdiA* and *tdiB* genes of the anti-tumour compound TQ gene cluster (**Figure 3.14**). This data provides strong evidence that HamE and the pheromone module proteins co-operate to regulate secondary metabolism, likely *via* the regulation of velvet complex activation or assembly.

3.7.6. HamE regulates the relative abundance of the pheromone module proteins

The proteins of the pheromone module were tagged with GFP tags and expressed in both a WT and *hamE* deletion background. To compare the levels of abundance of each protein throughout different developmental stages and to determine the influence of HamE in the regulation of protein abundance, time course immunoblotting was performed. It was evident that in the absence of HamE, each pheromone module protein exhibits either an increase or decrease in abundance during at least one time point (**Figure 3.15.**). This suggests that HamE-dependent regulation of the pheromone module proteins may implicate complex regulatory feedback loops. These data also provide evidence that each pheromone module protein possesses unique functionality outside of the complex, as each protein displays highly dynamic and dissimilar protein abundance profiles to one another.

3.7.7. HamE is not required for localisation or assembly of the complex but is essential for regulating the phosphorylation of the MAP kinases

To elucidate the specific roles of HamE within the pheromone module complex, the *in vivo* sub-cellular localisations of the proteins, the assembly of the complex and the phosphorylation states of the kinases were determined in both a WT and *hamE* deletion background. GFP-fused proteins in both backgrounds were visualised *via* confocal microscopy (**Figure 3.17.**). It was observed that HamE does not exert any clear influence over the localisations of the pheromone module proteins. TAP-tagged proteins in both backgrounds were immunoprecipitated and analysed by MS (**Figure 3.18.**). This revealed that the complex is capable of assembling in the absence of HamE. Lastly, the phosphorylation states of each kinase were identified in both backgrounds *via* TAP pulldowns coupled to MS (**Figure 3.16. (b)**), while the intensity of phosphorylation of MpkB was determined *via* time course immunoblotting (**Figure 3.16. (a)**). Together, these data provide evidence that HamE is capable of regulating the phosphorylation levels of each kinase, to promote kinase activation and signalling to the nucleus.

3.7.8. Overall conclusions

In conclusion, this study has identified and characterised the HamE scaffold protein for the pheromone module pathway and has provided evidence that this scaffold regulates asexual and sexual development as well as secondary metabolism. It has also been shown that HamE does not act as a passive scaffold, regulating complex assembly or localisation but instead exerts an active regulatory role, modulating the phosphorylation states of the kinases to regulate MAP kinase signalling and MpkB-dependent activation of transcription factors. An illustrated summary of this pathway can be seen in (**Figure 3.19.**). This study provides new insight into the regulation of MAP kinase signalling and the structure of MAP kinase pathways in filamentous fungal species.
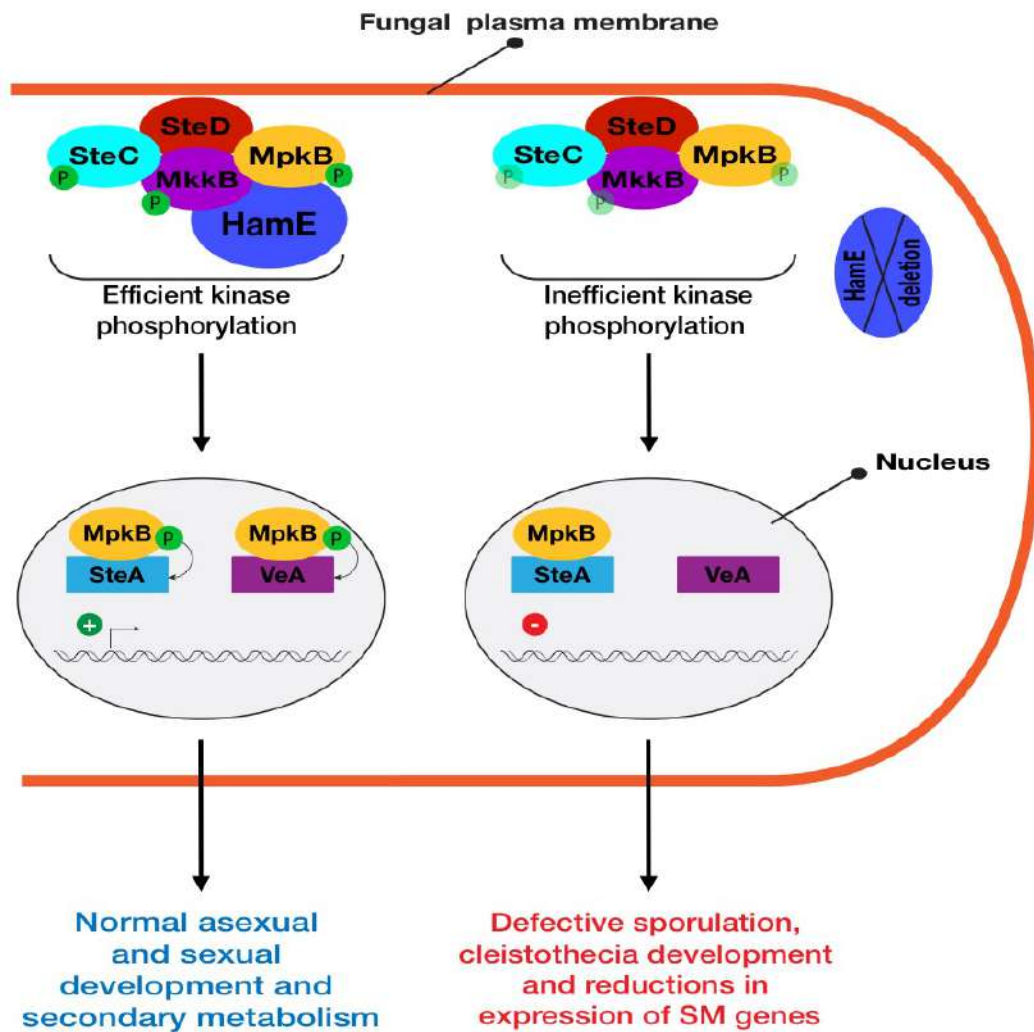
Figure 3.19. Schematic model of the pheromone module and the regulatory roles of HamE in kinase signalling, fungal development and secondary metabolism. HamE binds the kinases MkkB and MpkB and co-localises with the tetrameric complex of SteC-MkkB-MpkB-SteD at the plasma membrane, hyphal tips and nuclear envelope. HamE is required for efficient kinase phosphorylation, specifically MpkB. 'P' represents phosphate groups and inefficient kinase phosphorylation in the *hamE* mutant is represented by transparent phosphate groups. Efficient MpkB phosphorylation allows for MpkB to activate SteA and VeA to regulate both development and secondary metabolism, respectively.

3.8. Author contributions and declarations

All data from this chapter has been taken from Frawley et al. (2018) and the authors declare that there is no conflict of interest. The majority of experiments were performed by Dean Frawley. Exceptions are the following: (i) Initial TAP-MS experiments in $hamE^+$ backgrounds which were performed by Dr. Betim Karahoda. (ii) Initial generation of tagged kinase strains and mutants which were generated by Dr. Ozlem Sarikaya-Bayram and Dr. Ozgur Bayram. (iii) HamE-GFP sub-cellular localization experiments and BIFC experiments of HamE and SteC, which were performed by Dr. Ozgur Bayram.

Chapter 4: Results

The pheromone module is conserved in *A. flavus* and is required for regulation of sporulation, sclerotia formation and secondary metabolism

4.1. Characterisation of the *A. nidulans* pheromone module proposes the question of whether this pathway is conserved in *Aspergillus* species

Chapter 3 focused on the identification of a scaffold protein, which we named HamE (Frawley et al., 2018). HamE was shown to function as a regulatory scaffold within the pheromone module in *A. nidulans*. Data suggested that this scaffold associates with the kinases MkkB and MpkB to promote kinase phosphorylation and to regulate the intensity of MpkB phosphorylation throughout various stages of development. This allows MpkB to activate transcription factors and to subsequently regulate both development and secondary metabolism in this species. This chapter also focused on further characterising the roles of the pheromone module, with relation to asexual sporulation, vegetative growth and the production of specific SMs like the antibiotic PN, the anti-tumour compound TQ and the carcinogenic compound ST.

The significance of this MAP kinase pathway in *A. nidulans* led to the question of whether or not a similar mechanism is utilised in other *Aspergillus* species to regulate their reproductive programmes and SM biosynthesis, in response to environmental cues. For this chapter, the knowledge from the *A. nidulans* data was applied to the agriculturally-relevant *Aspergillus* species *A. flavus*. The main aims of this chapter are to identify a homologous MAP kinase pathway in this species and to establish the composition of the complex by determining individual protein-protein interactions. The roles of this complex with regards to the regulation of asexual sporulation, sexual sclerotia production and SM biosynthesis will also be addressed. Overall, this chapter aims to provide evidence that the pheromone module is a conserved mechanism of regulation utilised by *Aspergillus* species to control their development and secondary metabolism.

4.1.1. Orthologs of each of the pheromone module proteins exist in *A. flavus*

In order to identify whether orthologs of the pheromone module proteins exist in *A. flavus,* reciprocal BLAST searches were performed (Altschul et al., 1990). It was found that orthologs of all 5 members of the *A. nidulans* pheromone module exist in *A. flavus.* The *A. flavus* SteC ortholog (AFLA_048880) exhibits 87% sequence similarity to *A. nidulans* SteC, while the percentages of similarity for MkkB (AFLA_103480), MpkB (AFLA_034170), SteD (AFLA_002340) and HamE (AFLA_095770) orthologs are 85.2%, 99.7%, 83% and 75.2% respectively. Once these orthologs were detected,

'ScanProsite' (de Castro et al., 2006) and 'InterPro' (Mitchell et al., 2019) software were used to determine the sizes of these proteins and the domains they possess in comparison to the *A. nidulans* proteins (**Figure 4.1. (a) and (b)**). This revealed that the SteC protein in both *A. nidulans* (**Figure 4.1. (a)**) and *A. flavus* (**Figure 4.1. (b)**) possesses a SAM domain at the N-terminal between amino acids (aa) 63-126, as well as an RA domain at aa 248-351 for *A. nidulans* and aa 253-343 for *A. flavus*. Both proteins also possess a protein kinase domain at the C-terminal spanning a similar range of aa residues. MkkB and MpkB in both *A. nidulans* and *A. flavus* possess a protein kinase domain between the same aa residues. The SteD adaptor in both species contains a SAM domain at the N-terminus and a RA domain at the C-terminus at similar aa positions. Lastly, the HamE protein in both species contains WD40 repeats at the N-terminus, which are characteristic scaffolding domains (Frawley et al., 2018, Xu and Min, 2011).
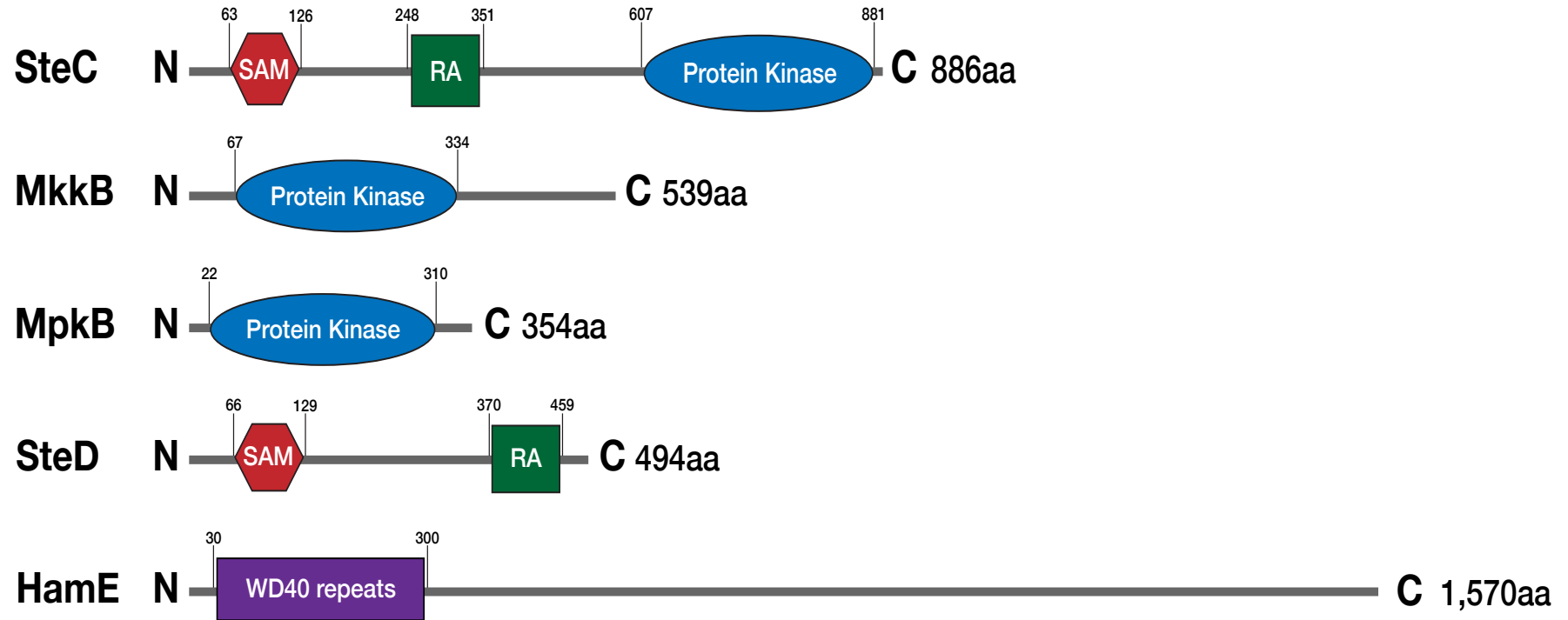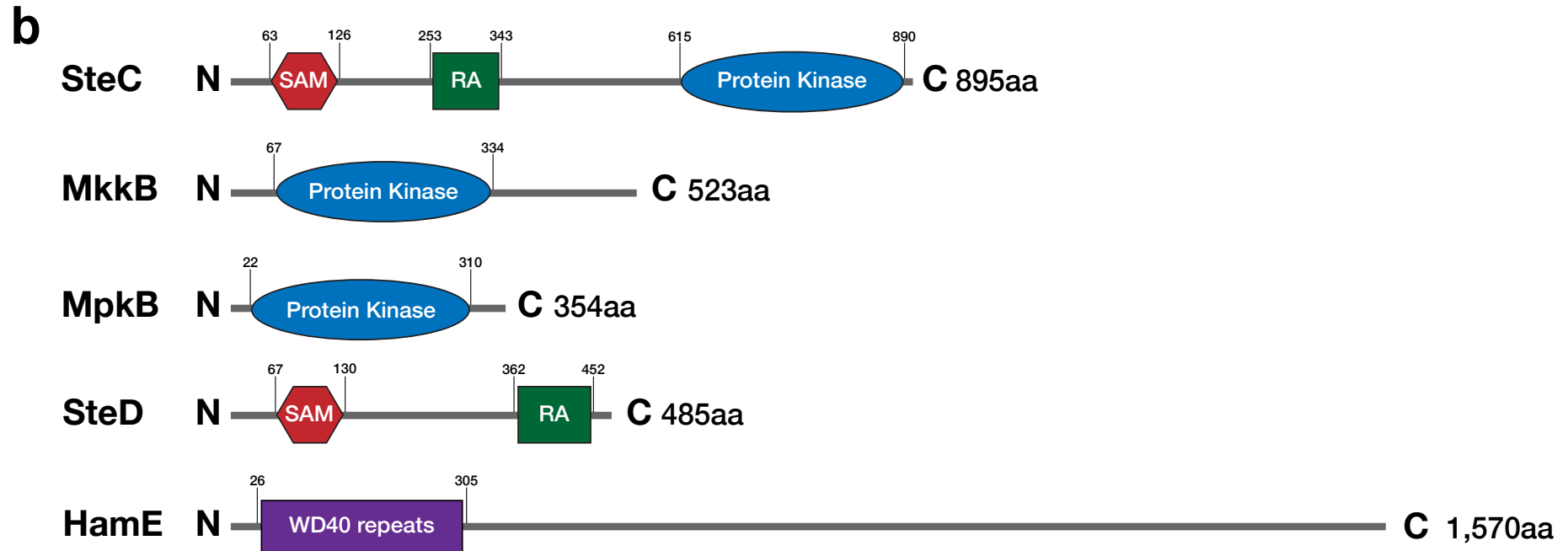
Figure 4.1. Domain architectures of the pheromone module proteins. (a) The domains and motifs of the pheromone module proteins in *A. nidulans*. 'aa' represents the size of the proteins in amino acids. 'N' and 'C' refer to the N and C protein terminals. Numbers surrounding the domains represent their amino acid locations. SAM (Sterile alpha motif) RA (Ras Association domain). (b) The domains and motifs of the homologous pheromone module proteins in *A. flavus*. Detection of protein sizes and domains were performed using a combination of ScanProsite (de Castro et al., 2006) and InterPro (Mitchell et al., 2019) software.

4.1.2. SteC, MkkB, MpkB and SteD form a tetrameric protein complex

To determine whether these homologous proteins form a complex in *A. flavus,* similar to what is observed in *A. nidulans* (Frawley et al., 2018, Bayram et al., 2012), a *sgfp* epitope tag was coupled to the C-terminals of the *steC, mkkB, mpkB* and *steD* genes. (**Appendix B: Figure S1**) All attempts to detect the *hamE* gene tagged with *sgfp* failed and so, the *hamE* gene was coupled to a *3xha* epitope tag at the C-terminus. (**Appendix B: Figure S2**). The fusion proteins were immunoprecipitated from vegetative cultures grown for 24 hours and were run on a MS to detect the tagged proteins and their interaction partners, which are listed in (**Figure 4.2. (a)**). It was found that SteC-GFP pulldowns co-purified MpkB and SteD (**Appendix B: Table S4**), MkkB-GFP pulldowns co-purified SteC and SteD (**Appendix B: Table S5**), MpkB-GFP pulldowns co-purified MkkB and SteD (**Appendix B: Table S6**) and SteD-GFP pulldowns co-purified SteC, MkkB and MpkB (**Appendix B: Table S7**). Unlike in *A. nidulans* (Frawley et al., 2018)*,* pulldowns of HamE did not result in detection of any of the pheromone module proteins (**Appendix B: Table S8**) and HamE was not detectable in any purifications of SteC, MkkB, MpkB or SteD. Together, these interactome data provide evidence of the existence of a tetrameric MAP kinase pathway consisting of SteC-MkkB-MpkB-SteD in *A. flavus* (**Figure 4.2. (b)**). Also, this data suggests that HamE may not be directly interacting with the members of this pathway.

a

GFP pulldowns

	SteC-GFP		MkkB-GFP		MpkB-GFP		SteD-GFP	
	% Coverage	Unique Peptides	% Coverage	Unique Peptides	% Coverage	Unique Peptides	% Coverage	Unique Peptides
SteC	51.96	30	66.93	46	/	/	62.57	42
MkkB	/	/	73.80	29	59.22	15	24.09	8
MpkB	7.63	2	/	/	79.38	21	14.69	4
SteD	48.25	15	70.93	21	18.56	6	54.02	17

b
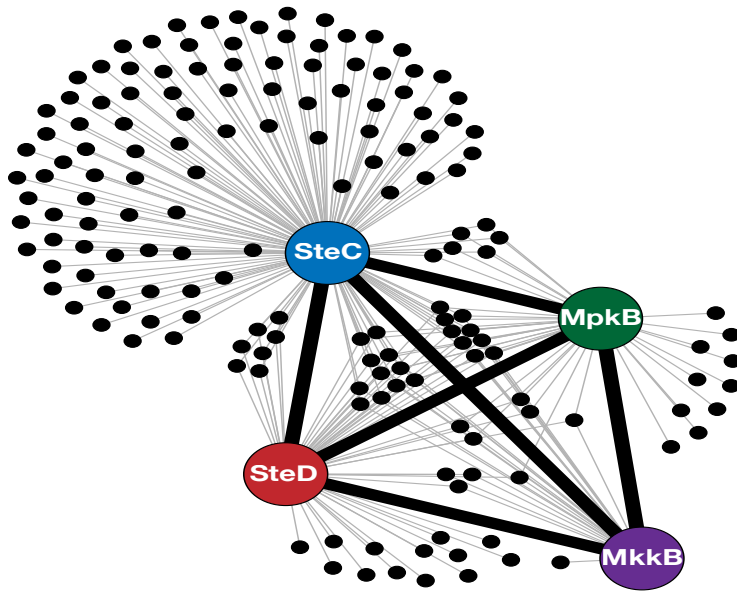
Figure 4.2. The interaction network of the pheromone module in *A. flavus.* (a) GFP pulldowns and LC-MS/MS analysis of the pheromone module proteins. Tagged proteins are given at the top of the table and co-purified proteins are given on the left-hand side. Strains were cultured vegetatively in duplicate at 30°C in complete medium for 24 hours. Supplementary MS tables for this figure are provided in **Appendix B: Tables S4-7.** (b) Interaction network of the pheromone module components based on the unique peptides detected in each GFP pulldown. The interaction network was generated using the Gephi 0.9.2 software. Black circles represent proteins detected in two independent biological replicates but not in any of the wild type samples.

4.2. The pheromone module proteins, with the exception of HamE, contribute to the regulation of asexual development, but not vegetative growth

To determine whether the pheromone module proteins contribute to the regulation of asexual sporulation in *A. flavus*, the genes encoding each protein of the complex were deleted (**Appendix B: Figure S1 and S2**) to monitor the phenotypes of the mutants. The *steCΔ, mkkBΔ, mpkBΔ* and *steDΔ* strains were generated by replacing the gene open reading frames with the phleomycin resistance cassette (*phleO*), while the *hamEΔ* strain was created by replacing the ORF with the *pyrG* gene. Complementation strains for each mutant were also generated by reinserting a functional copy of the gene ORF into the respective mutant strains.

Each mutant and complementation strain were spot inoculated on PDA plates in triplicate and incubated in the presence of light for 5 days to promote asexual conidiation (**Figure 4.3. (a) and (b)**). It was observed that the deletion of *steC, mkkB, mpkB* or *steD* dramatically influences sporulation (**Figure 4.4.**). Each one of these mutants exhibited a completely pale white phenotype and were unable to undergo asexual conidiation. The average percentage range of sporulation for the mutant strains was between 2.46%-3.84%, in comparison to the TJES19.1 wild type strain average, which was chosen to represent 100%. However, the *hamE* mutant phenotype resembled the wild type and was capable of producing asexual spores. The complementation of each gene successfully restored the levels of conidiation, with each strain resembling the wild type phenotype. The levels of sporulation for each complementation strain were between 66.54%-120.36%, with respect to the wild type strain. qPCR analysis was performed to assess the relative expression levels of asexual development genes in an *mkkB* mutant, in comparison to a wild type strain (**Figure 4.6.**). Strains were inoculated ($2x10^6$ spores/ml) in liquid complete medium and left to incubate on a shaker at 30˚C for 24 hours. Following this incubation, the mycelia were shifted onto PDA plates and left to incubate in the presence of light at 30˚C for 24 hours. It was found that expression of the *flbC* and *abaA* genes were significantly decreased in the mutant strain (0.67 and 0.46 fold of control respectively), while expression of the *flbB, flbD, brlA* and *wetA* genes did not exhibit any significant differences.

The colony diameters of each asexually-induced strain were measured and the averages of three independent replicates for each strain were plotted as a percentage of the respective wild type average (**Figure 4.5.**). Apart from the *hamE* mutant, which

displayed a slightly reduced colony diameter, no significant differences were observed in the rates of vegetative growth in any of the mutants, unlike the reduced rates of growth observed in *A. nidulans* (Frawley et al., 2018). These results indicate that the SteC, MkkB, MpkB and SteD proteins all contribute to the regulation of asexual sporulation in *A. flavus,* similar to what is observed in *A. nidulans.* However, this data suggests that these proteins are not required for the regulation of hyphal growth and also that HamE is not involved in the regulation of conidiation.
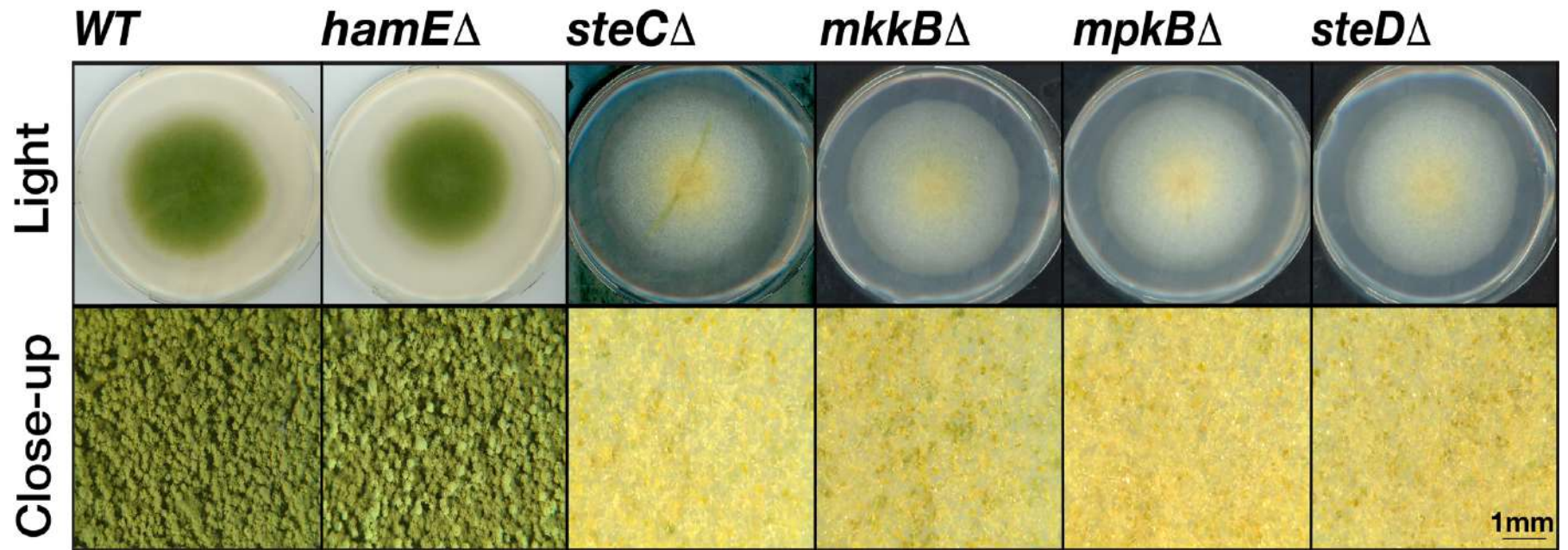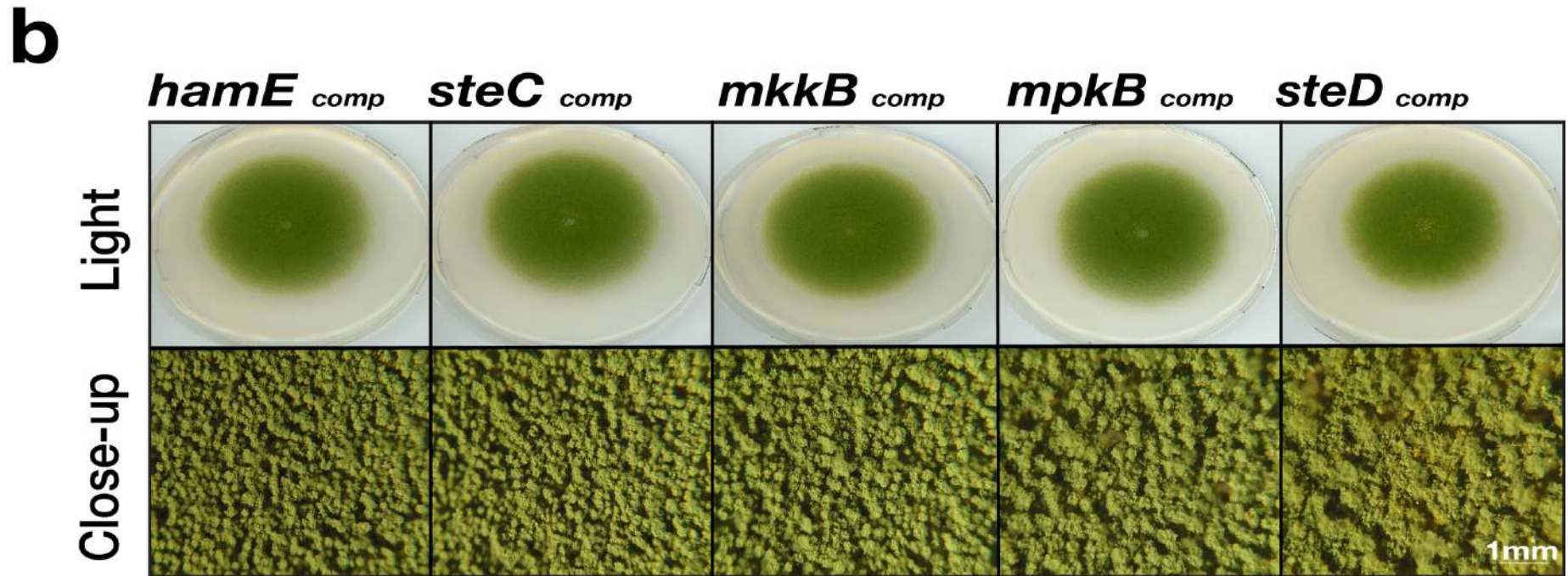
Figure 4.3. Asexual phenotypes of deletion and complementation strains. (a) The pheromone module deletion strains were spot inoculated (5×10^3 spores) in triplicate on PDA plates containing supplements. Wild type refers to the TJES19.1 strain. These plates were incubated for 5 days in the light at 30°C to induce asexual development. Plates were scanned using the Epson perfection V600 photo scanner. Close-up images were taken at 2x magnification using the Olympus szx16 microscope with an Olympus sc30 camera. (b) Asexual phenotypes of the complementation strains.
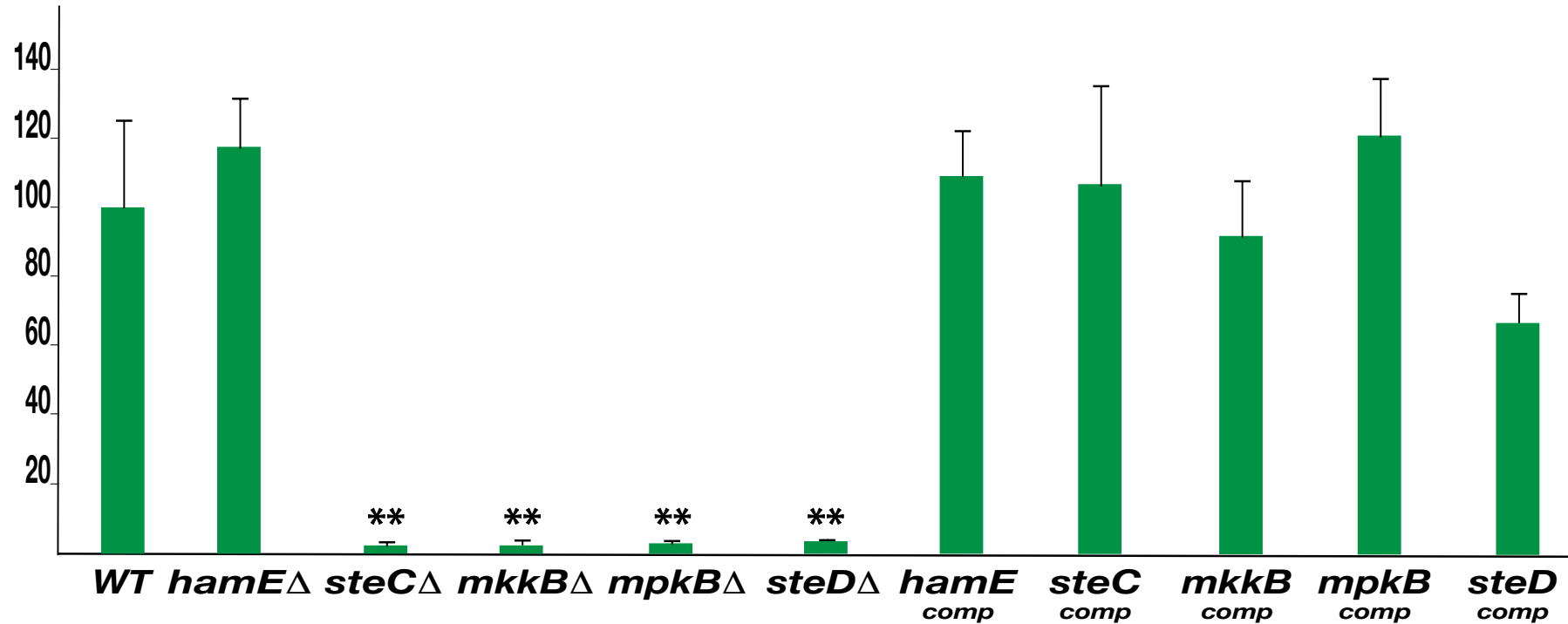
Figure 4.4. Quantification of asexual conidiation in deletion and complementation strains. The average sporulation value of the wild type strain was chosen to represent 100%. Mean values of all other strains (*N*=3) were plotted ± s.d. as a percentage of the WT. *P*-values were calculated by performing unpaired Student's *t*-tests (**P<0.01).
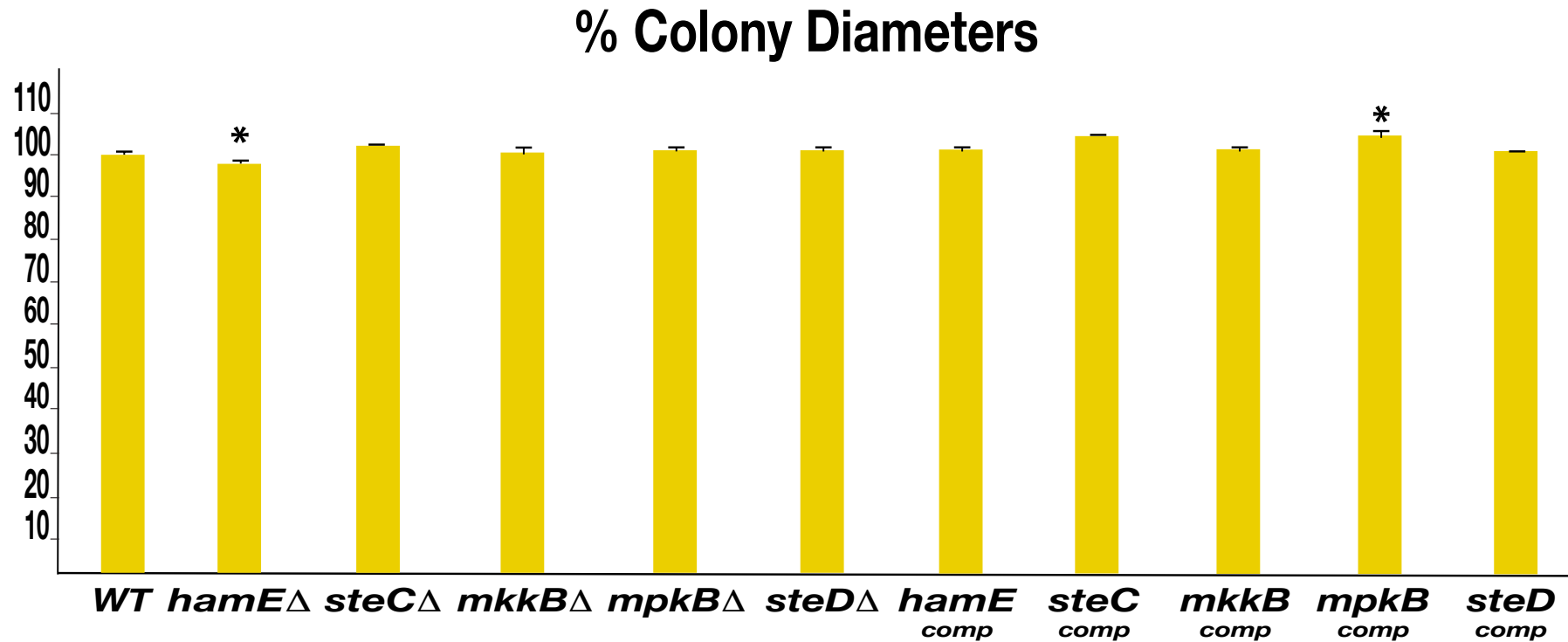
% Colony Diameters

Figure 4.5. Graphical representation of the colony diameters of each asexually induced strain from Figure 4.3. with respect to the TJES19.1 wild type strain. Measurements were taken from three independent biological replicates for each asexually induced strain and the averages were plotted ± s.d. as a percentage of the WT strain. *P*-values were calculated by performing unpaired Student's *t*-tests (*$P<0.05$).
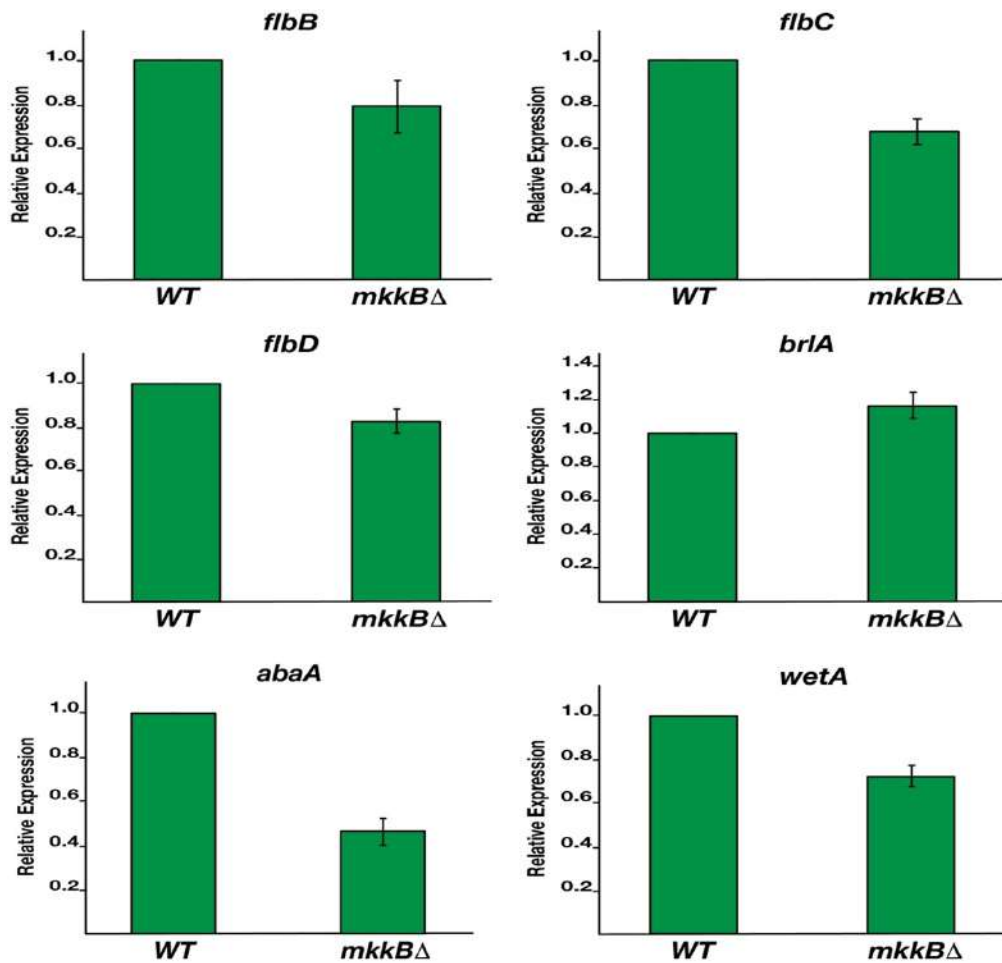
Figure 4.6. Relative expression levels of genes involved in the regulation of asexual development. The TJES19.1 strain and *mkkB*Δ mutant strain were inoculated (2×10^6 spores) in liquid complete medium and left to incubate on a shaker at 30°C for 24 hours. The mycelia were then shifted onto PDA plates and incubated in the presence of light at 30°C for 24 hours. mRNA was isolated from 2 independent biological replicates per strain. 1μg mRNA was converted to cDNA and used for qPCR analysis. 3 technical replicates per biological replicate were used. (N=6). The average expression level values were plotted ± s.d. as a percentage of the wild type average, which was chosen to represent 100% expression (1.0 relative expression). *skpA* was used as a reference gene to obtain relative expression levels of corresponding genes using the $2^{-\Delta\Delta Ct}$ method.

4.3. All pheromone module orthologs are essential for the regulation of sclerotia formation

The mutant and complementation strains were also tested to determine whether they play a role in the regulation of sexual development. Each strain was spot-inoculated on WHM agar plates in triplicate. These plates were completely covered in aluminium foil to simulate a dark environment and strains were cultured for 2 weeks to induce sexual development and sclerotia formation (**Figure 4.7. (a) and (b)**). Plates were scanned before and after washes with 70% ethanol which were performed to remove the asexual conidia and to reveal the sexual sclerotia underneath.

It was evident that the deletion of *steC, mkkB, mpkB* and *steD* resulted in a very clear change in phenotype, with each mutant displaying a pale white phenotype, devoid of asexual conidia. However, the *hamE* mutant displayed normal conidiation, with respect to the wild type strain. When each plate was washed with ethanol, the asexual conidia were removed and black, spherical sclerotia were visible on the wild type plates. However, there were no sclerotia produced by any of the mutant colonies, including the *hamE* mutant. Complementation of each gene resulted in the restoration of the wild type phenotype, as each of these strains were capable of undergoing normal asexual conidiation and sexual sclerotia formation. The average percentages of sclerotia production for each complementation strain in comparison to the wild type average were between 71.24%-132.42% (**Figure 4.7. (b) and Figure 4.8.**).

qPCR analysis was performed to assess the relative expression levels of various sexual development genes in an *mkkB* mutant, in comparison to a wild type strain (**Figure 4.9.**). Strains were inoculated ($2x10^6$ spores) in liquid PD medium and left to incubate on a shaker at 30°C for 72 hours. It was found that expression of the *veA* and *nsdD* genes were significantly decreased in the mutant strain (0.5 and 0.62 fold of control respectively), while expression of the *velB* and *laeA* genes did not exhibit any significant differences. This data suggests that each member of the pheromone module pathway is essential for the regulation of sexual development and sclerotia formation, similar to how these proteins regulate sexual development and cleistothecia formation in *A. nidulans* (Frawley et al., 2018). While HamE was also shown to be critical for sclerotia production, perhaps this protein does not directly function within the pheromone module pathway to regulate this process.

a

| | *WT* | *hamE∆* | *steC∆* | *mkkB∆* | *mpkB∆* | *steD∆* |

Dark (before wash)

Dark (after wash)

Close-up

1mm
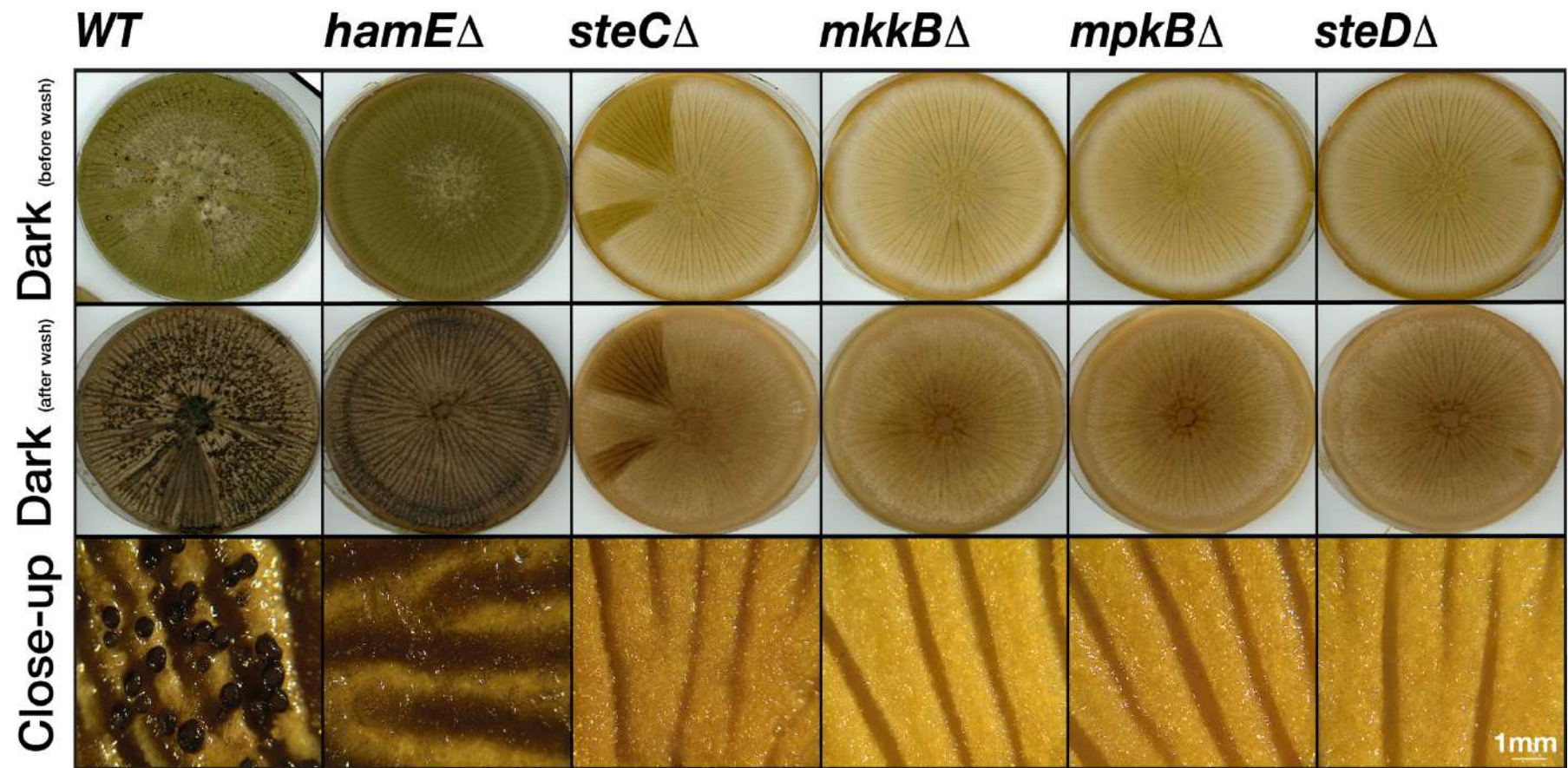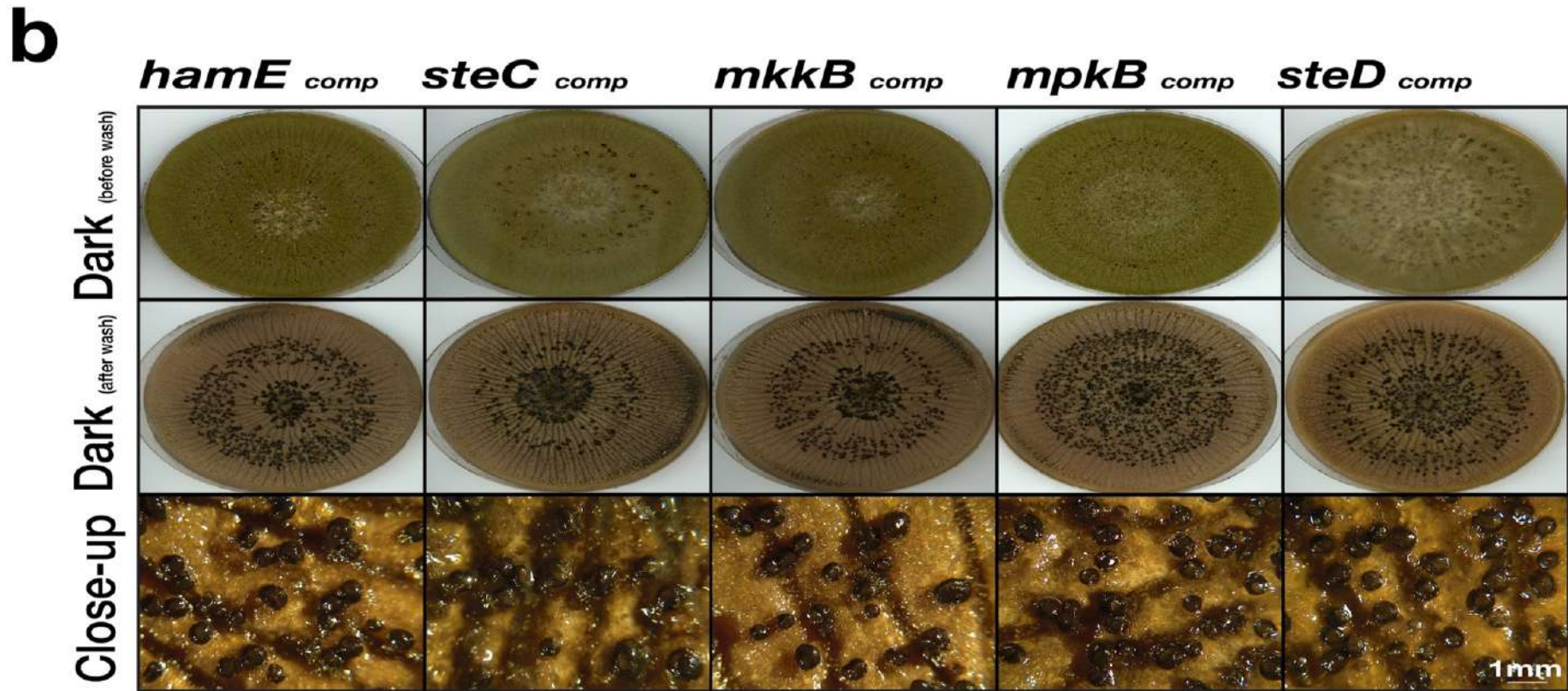
Figure 4.7. Sexual phenotypes of deletion and complementation strains. (a) The pheromone module protein deletion strains were spot inoculated (5×10^3 spores) in triplicate on WHM plates containing supplements. These plates were completely covered in aluminium foil and incubated for 2 weeks in the dark at 30˚C to induce sexual development. Prior to scanning, plates were washed with 70% ethanol to remove conidia and to reveal underlying sclerotia. Close-up images were taken at 1x magnification using the Olympus szx16 microscope with an Olympus sc30 camera. (b) Sexual phenotypes of the complementation strains.
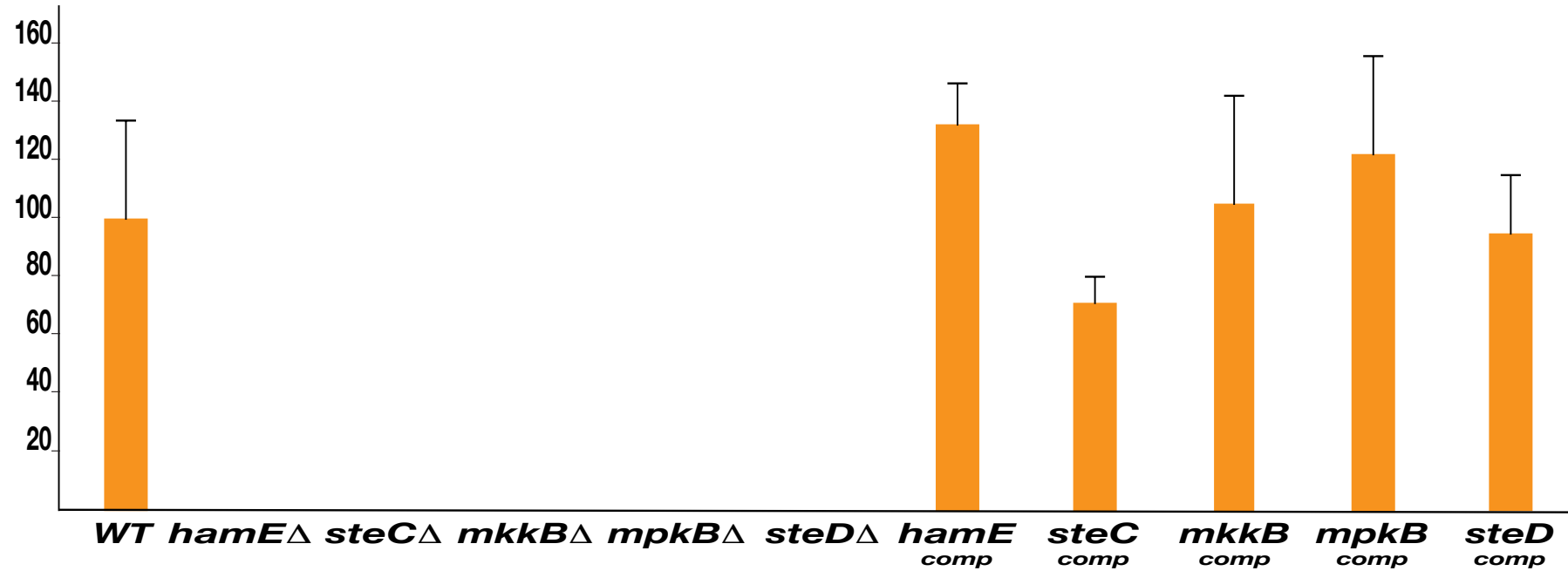
Figure 4.8. Quantification of sexual sclerotia formation in deletion and complementation strains. The average quantity of sclerotia produced by the wild type strain was chosen to represent 100%. Mean values of all other strains (N=3) were plotted ± s.d. as a percentage of the WT.
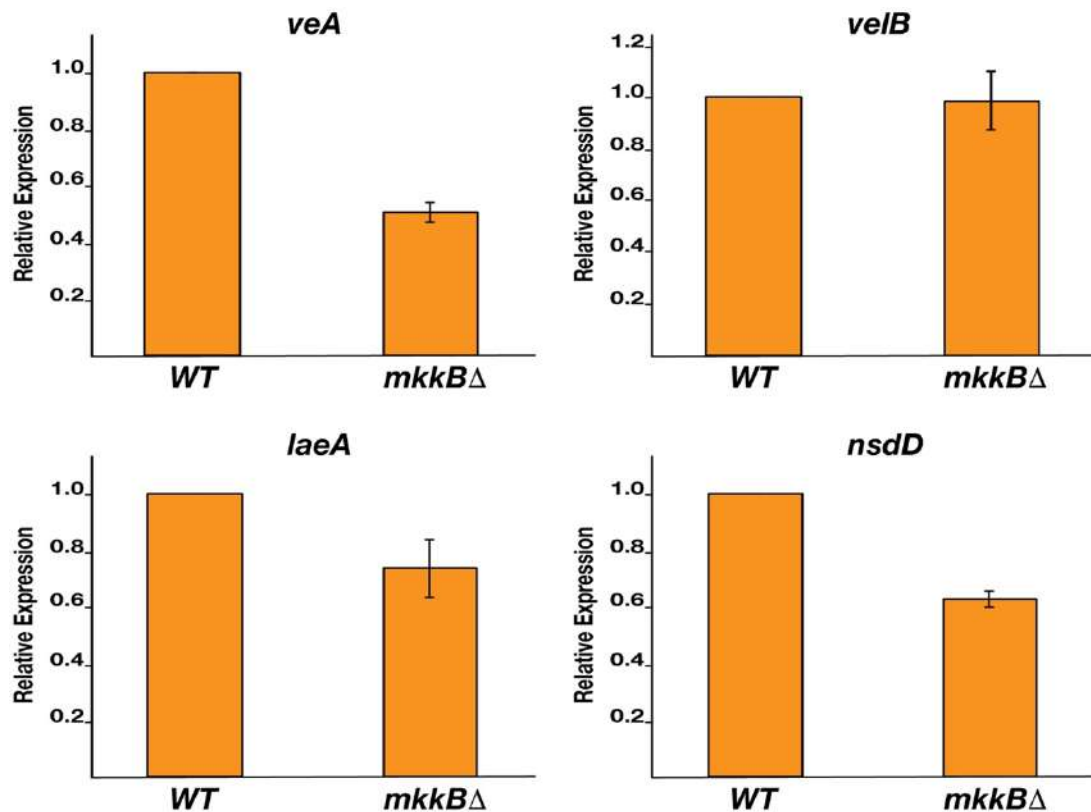
Figure 4.9. Relative expression levels of genes involved in the regulation of sexual development. The TJES19.1 strain and *mkkB*Δ mutant strain were inoculated (2×10^6 spores) in liquid PD medium and left to incubate on a shaker at 30˚C for 72 hours. mRNA was isolated from 2 independent biological replicates per strain. 1µg mRNA was converted to cDNA and used for qPCR analysis. 3 technical replicates per biological replicate were used. (N=6). The average expression level values were plotted ± s.d. as a percentage of the wild type average, which was chosen to represent 100% expression (1.0 relative expression). *skpA* was used as a reference gene to obtain relative expression levels of corresponding genes using the $2^{-\Delta\Delta Ct}$ method.

4.4. Production of various SMs is dependent on the pheromone module proteins

Due to the defects in development observed in the pheromone module mutant strains, it was decided to assess whether these proteins contribute to the regulation of secondary metabolism, similar to what is observed in *A. nidulans* (Frawley et al., 2018, Bayram et al., 2012). *A. flavus* is capable of producing a plethora of SMs including the carcinogenic aflatoxin B1 (Klich, 2007), the antiinsectan/antifeedant leporin B (Cary et al., 2015), the indole-tetramic acid mycotoxin cyclopiazonic acid (CPA) (Chang et al., 2009), the innate immunity modulators aspergillicin A and F (Kikuchi et al., 2015, Capon et al., 2003, Greco et al., 2019) and the analgesic/anti-inflammatory agent ditryptophenaline (Barrow and Sedlock, 1994, Saruwatari et al., 2014).

Strains were point inoculated ($5x10^3$ spores) on PDA plates and left to incubate for 2 weeks in the dark to induce SM production. Ultra-high-performance high resolution mass spectrometry (UHPLC-HRMS) analysis was performed on these samples to test whether the deletion of any of the pheromone module proteins influences the production of the six metabolites mentioned above. Interestingly, it was found that the *steC, mkkB, mpkB* and *steD* mutants exhibit very similar metabolic profiles that vary significantly with respect to the wild type and *hamE*Δ strain (**Figure 4.13.**). It was observed that each of the five mutants were incapable of producing aflatoxin B1 (**Figure 4.10. (a)**). The production of leporin B (**Figure 4.10. (d)**), CPA (**Figure 4.11. (a)**), aspergillicin A (**Figure 4.11. (d)**) and aspergillicin F (**Figure 4.12. (a)**) was increased in the *steC, mkkB, mpkB* and *steD* mutants, whereas the deletion of *hamE* did not result in any significant differences. With regards to ditryptophenaline production (**Figure 4.12. (d)**), there were no significant changes observed in any of the mutants with respect to the wild type strain.

a

Peak Area

WT   *hamEΔ* *steCΔ* *mkkBΔ* *mpkBΔ* *steDΔ*

**** n.d.   **** n.d.   **** n.d.   **** n.d.   **** n.d.

b

Aflatoxin B1

c

Aflatoxin B1
$[M+H]^+$

d

Peak Area

WT n.d.   *hamEΔ* n.d.   *steCΔ* ***   *mkkBΔ* **   *mpkBΔ* *   *steDΔ* *

e

Leporin B

f
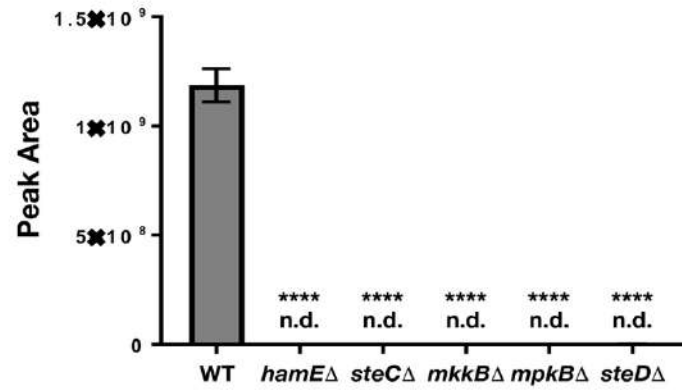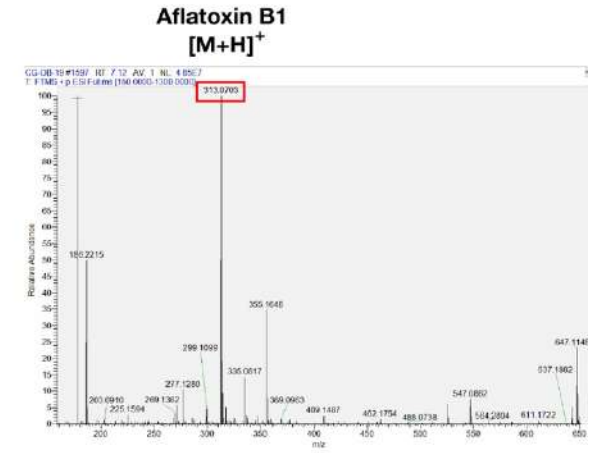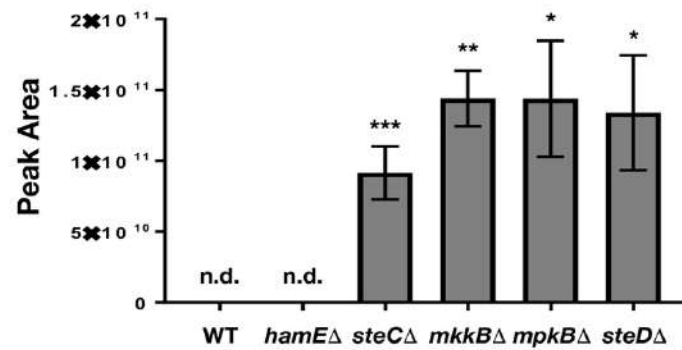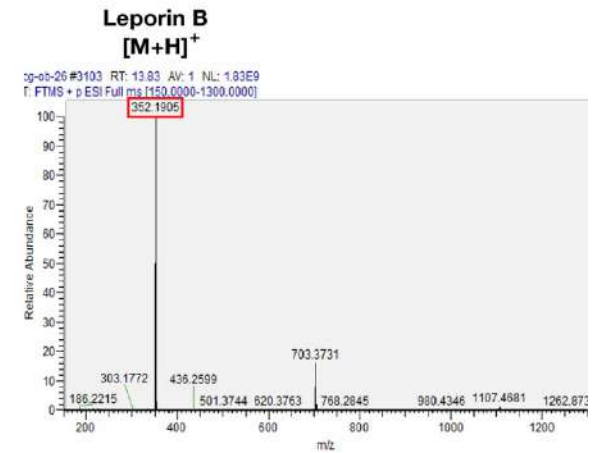
Leporin B
$[M+H]^+$

Figure 4.10. Levels of aflatoxin B1 and leporin B production in mutant strains. (a) Peak area values of aflatoxin B1 detected by UHPLC-HRMS in the TJES19.1 wild type strain and mutant strains. Strains were point inoculated in triplicate ($5x10^3$ spores) on PDA plates and incubated in the presence of light for 14 days at 30˚C. Crude extracts prepared from PDA plates were resuspended in acetonitrile (10 mg/mL) and filtered through an Acrodisc syringe filter with a nylon membrane (0.45μm pore size). UHPLC-HRMS was then performed on a Thermo Scientific-Vanquish UHPLC system connected to a Thermo Scientific Q Exactive Orbitrap mass spectrometer in ES^+ mode between 200 m/z and 1000 m/z to identify aflatoxin B1 in each strain. The bars represent the mean values of three biological replicates per strain ± s.d. *P*-values were calculated by performing unpaired Student's t-tests using the Graphpad Prism Version 6 (*****P*<0.0001). n.d. (not detected). (b) Chemical structure of aflatoxin B1. (c) HRMS spectrum of aflatoxin B1. (d) Peak area values of leporin B detected by UHPLC-HRMS. (**P*<0.05;***P*<0.01; ****P*<0.001). Experimental conditions are as described for **Figure 4.10. (a).** (e) Chemical structure of leporin B. (f) HRMS spectrum of leporin B.
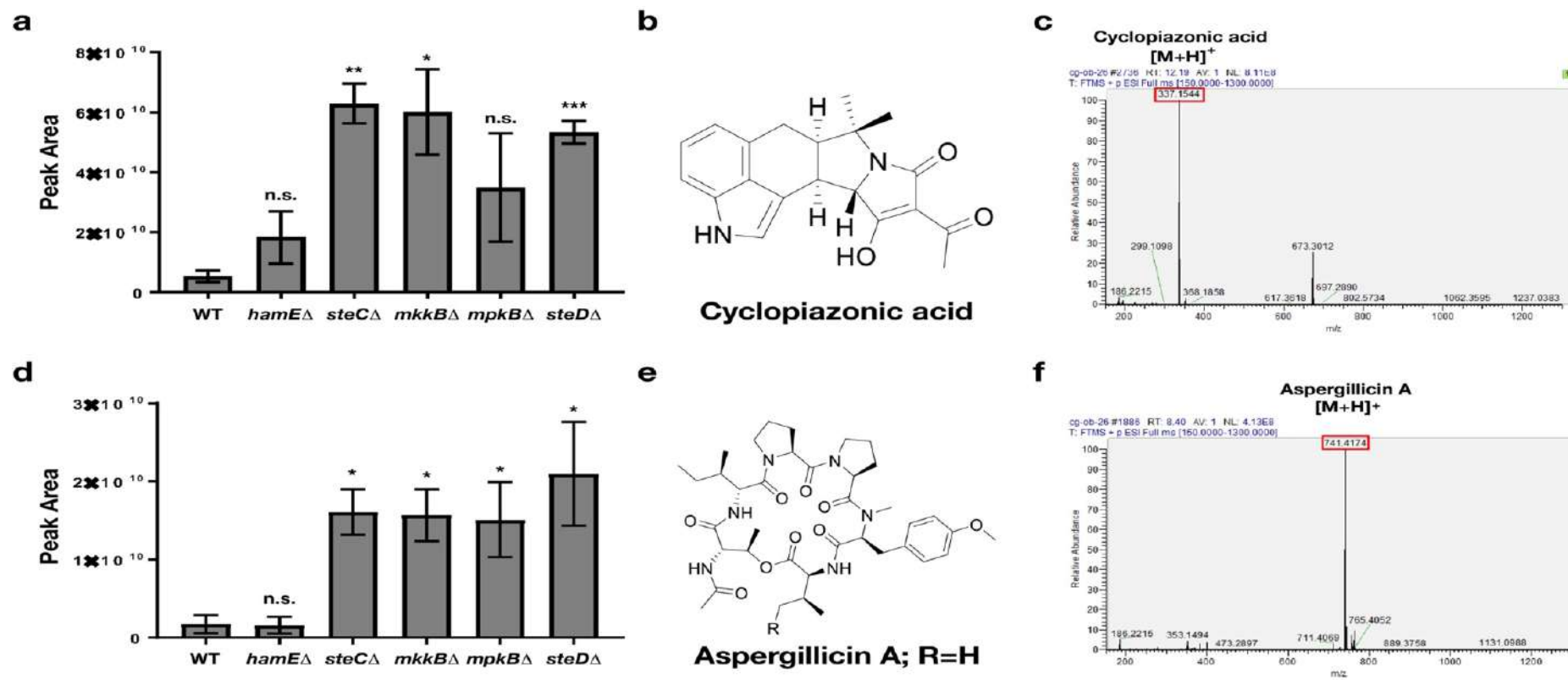
Figure 4.11. Levels of cyclopiazonic acid and aspergillicin A production in mutant strains. (a) Peak area values of cyclopiazonic acid detected by UHPLC-HRMS. (*$P<0.05$;**$P<0.01$; ***$P<0.001$). Experimental conditions are as described for **Figure 4.10. (a).** n.s. (non-significant). (b) Chemical structure of cyclopiazonic acid. (c) HRMS spectrum of cyclopiazonic acid. (d) Peak area values of aspergillicin A detected by UHPLC-HRMS. (*$P<0.05$). Experimental conditions are as described for **Figure 4.10. (a)**. (e) Chemical structure of aspergillicin A. (f) HRMS spectrum of aspergillicin A.

128
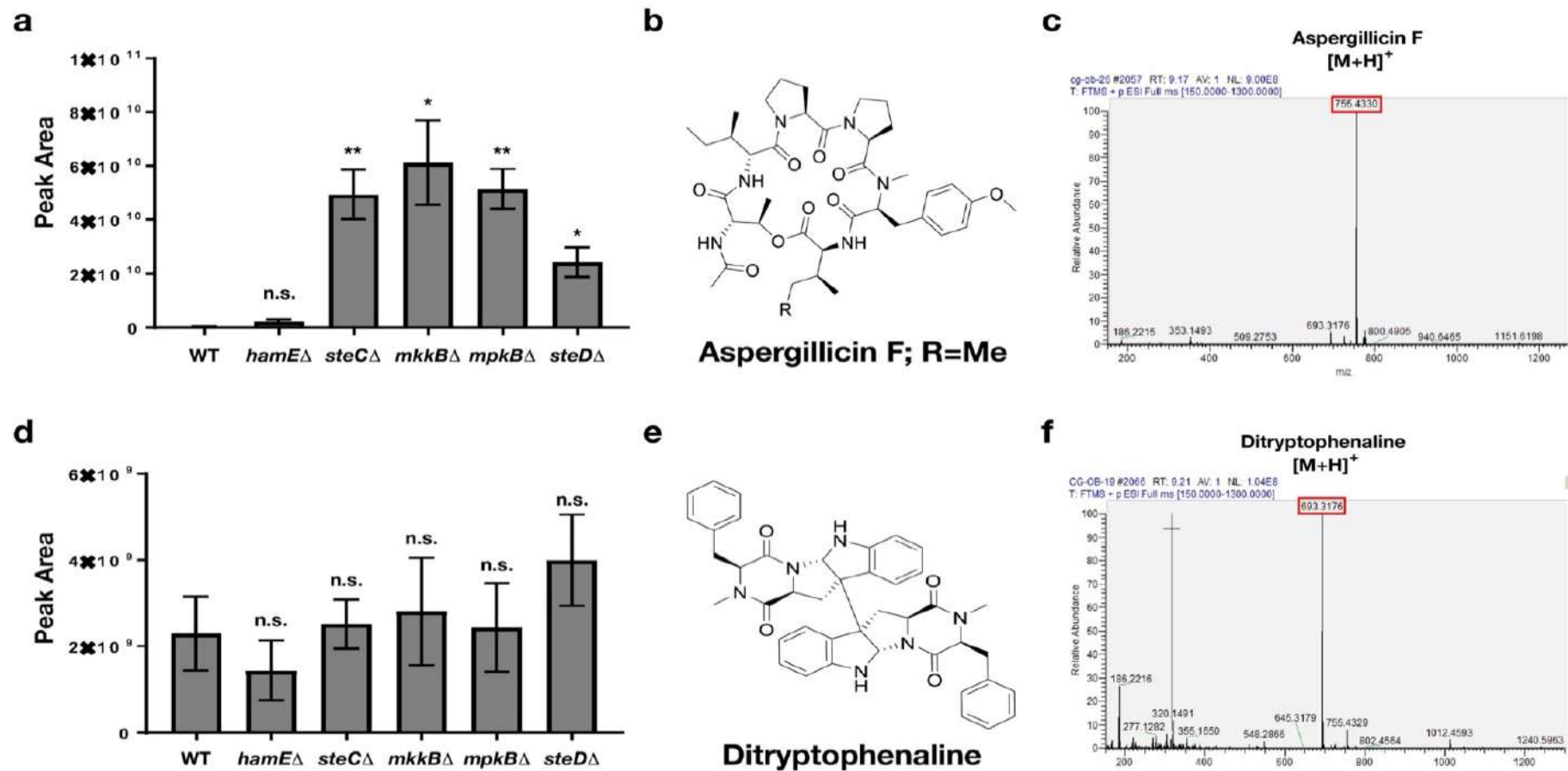
Figure 4.12. Levels of aspergillicin F and ditryptophenaline production in mutant strains. (a) Peak area values of aspergillicin F detected by UHPLC-HRMS. (*$P<0.05$;**$P<0.01$). Experimental conditions are as described for **Figure 4.10. (a)**. (b) Chemical structure of aspergillicin F. (c) HRMS spectrum of aspergillicin F. (d) Peak area values of ditryptophenaline. Experimental conditions are as described for **Figure 4.10. (a).** (e) Chemical structure of ditryptophenaline. (f) HRMS spectrum of ditryptophenaline.
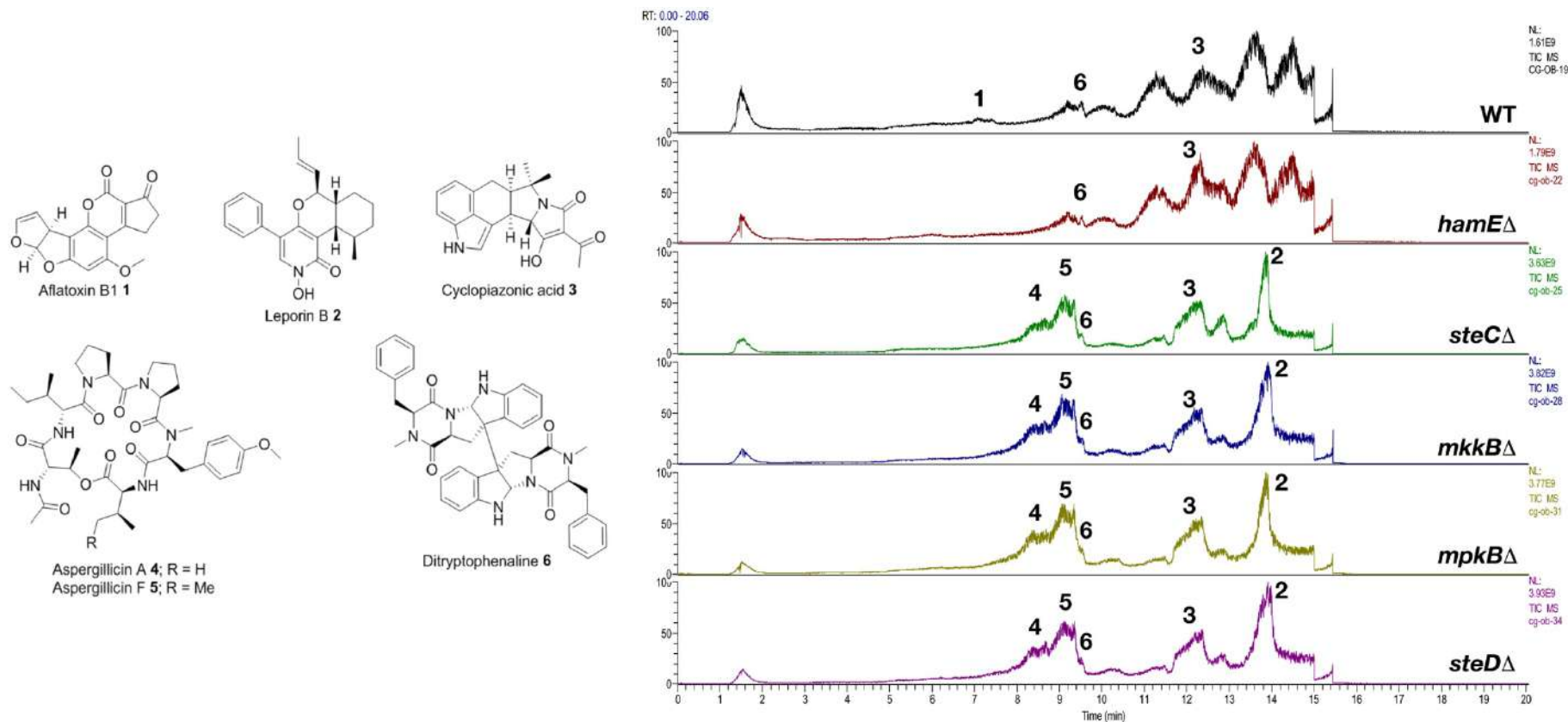
Figure 4.13. UHPLC-HRMS chromatograms of the TJES19.1 wild type strain and mutant strains. Resulting spectra obtained following UHPLC-HRMS analysis of the TJES19.1 wild type strain and mutant strains cultured on PDA plates for 14 days at 30˚C. Compounds detected are listed 1-6 and the respective chemical structures of each compound are presented.

4.4.1. The pheromone module proteins influence expression levels of SM genes

To determine the relative gene expression levels of genes that contribute to the biosynthesis of the SMs tested by UHPLC-HRMS, qPCR analysis was performed (**Figures 4.14., 4.15. and 4.16.**). The *aflR* (AFLA_139360)*, aflC* (AFLA_139410)*, aflM* (AFLA_139300)*, aflP* (AFLA_139210)*, aflA* (AFLA_139380) and *aflD* (AFLA_139390) genes belonging to the aflatoxin B1 gene cluster were tested in the wild type and *mkkB* mutant strain at various times of incubation. The backbone genes of leporin B (AFLA_066840-*lepA*)*, CPA (AFLA_139490-*cpaA*)*, aspergillicin A/aspergillicin F (AFLA_010580-*agiA*) and ditryptophenaline (AFLA_005440-*dtpA*) were also tested in these strains. Strains were inoculated ($1x10^6$ spores/ml) in either liquid PD or complete media. Strains inoculated in PD medium were left to incubate on a shaker at 30˚C for either 48 or 72 hours. Strains inoculated in complete medium were left to incubate on a shaker at 30˚C for 24 hours and were then filtered and transferred to PDA plates to be incubated in the dark at 30˚C for 6 days.

After 48 hours incubation in liquid PD medium, it was observed that the relative expression levels of the aflatoxin genes were similar in both the wild type and *mkkB* mutant (**Figure 4.14. (a)**). With respect to the relative expression values detected in the wild type, which are chosen to represent a value of 1 fold of control (FOC), the expression of *aflR* was 0.89 FOC*, aflC* was 0.75 FOC*, aflM* was 0.61 FOC*, aflP* was 1.04 FOC*, aflA* was 0.84 FOC and *aflD* was 0.76 FOC in the *mkkB* mutant. The *lepA, agiA* and *dtpA* genes were significantly upregulated in the *mkkB* mutant after 48 hours of incubation in PD medium (**Figure 4.14. (b)**), while the *cpaA* gene was not detectable at this time point. The expression of *lepA* was 1.78 FOC, *agiA* was 2.18 FOC and *dtpA* was 4 FOC.
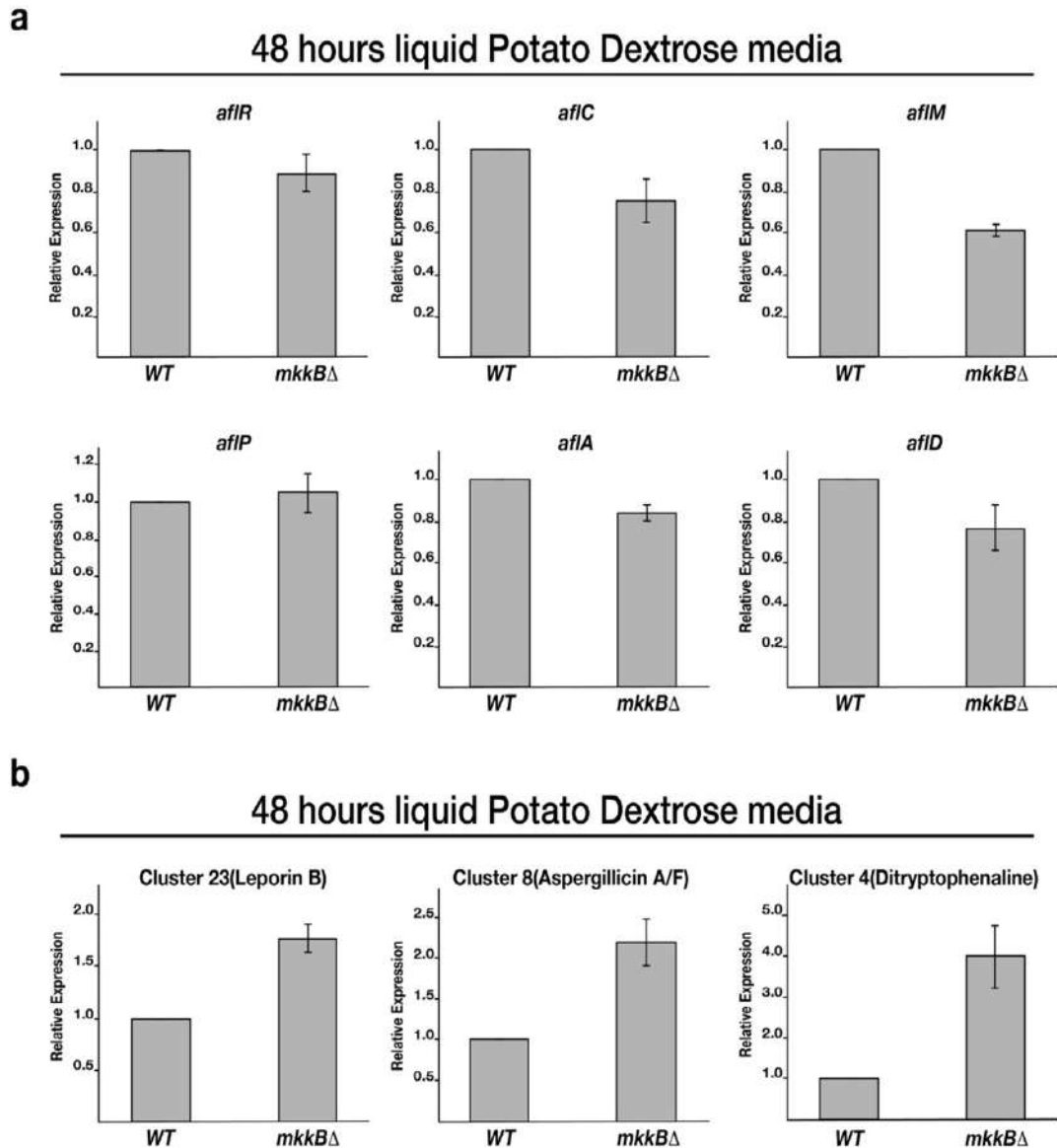
Figure 4.14. Relative expression levels of SM genes in strains cultured in liquid PD medium for 48 hours. (a). Relative expression levels of the *aflR, aflC, aflM, aflP, aflA* and *aflD* genes. The TJES19.1 strain and *mkkB*Δ mutant strain were inoculated (1×10^6 spores) in liquid PD medium and left to incubate (30˚C for 48 hours). mRNA was isolated from 2 biological replicates per strain. 1μg mRNA was converted to cDNA for qPCR analysis. 3 technical replicates per biological replicate were used. (N=6). Average expression level values were plotted ± s.d. as a percentage of the wild type average, which was chosen to represent 1.0 relative expression. *skpA* was used as a reference gene to obtain relative expression levels of corresponding genes using the $2^{-\Delta\Delta Ct}$ method. (b) Expression levels of genes corresponding to the leporin B, aspergillicin A/F and ditryptophenaline gene clusters in both TJES19.1 and *mkkB*Δ.

After 72 hours incubation in liquid PD medium, it was observed that multiple aflatoxin genes were downregulated in the *mkkB* mutant (**Figure 4.15. (a)**). The expression of *aflR* was 0.8 FOC, *aflC* was 0.79 FOC, *aflM* was 0.7 FOC, *aflP* was 1.3 FOC, *aflA* was 0.58 FOC and *aflD* was 0.42 FOC in the *mkkB* mutant. The expression of *lepA* was 0.72 FOC, *cpaA* was 0.94 FOC, *agiA* was 0.73 FOC and *dtpA* was 2.72 FOC (**Figure 4.15. (b)**).
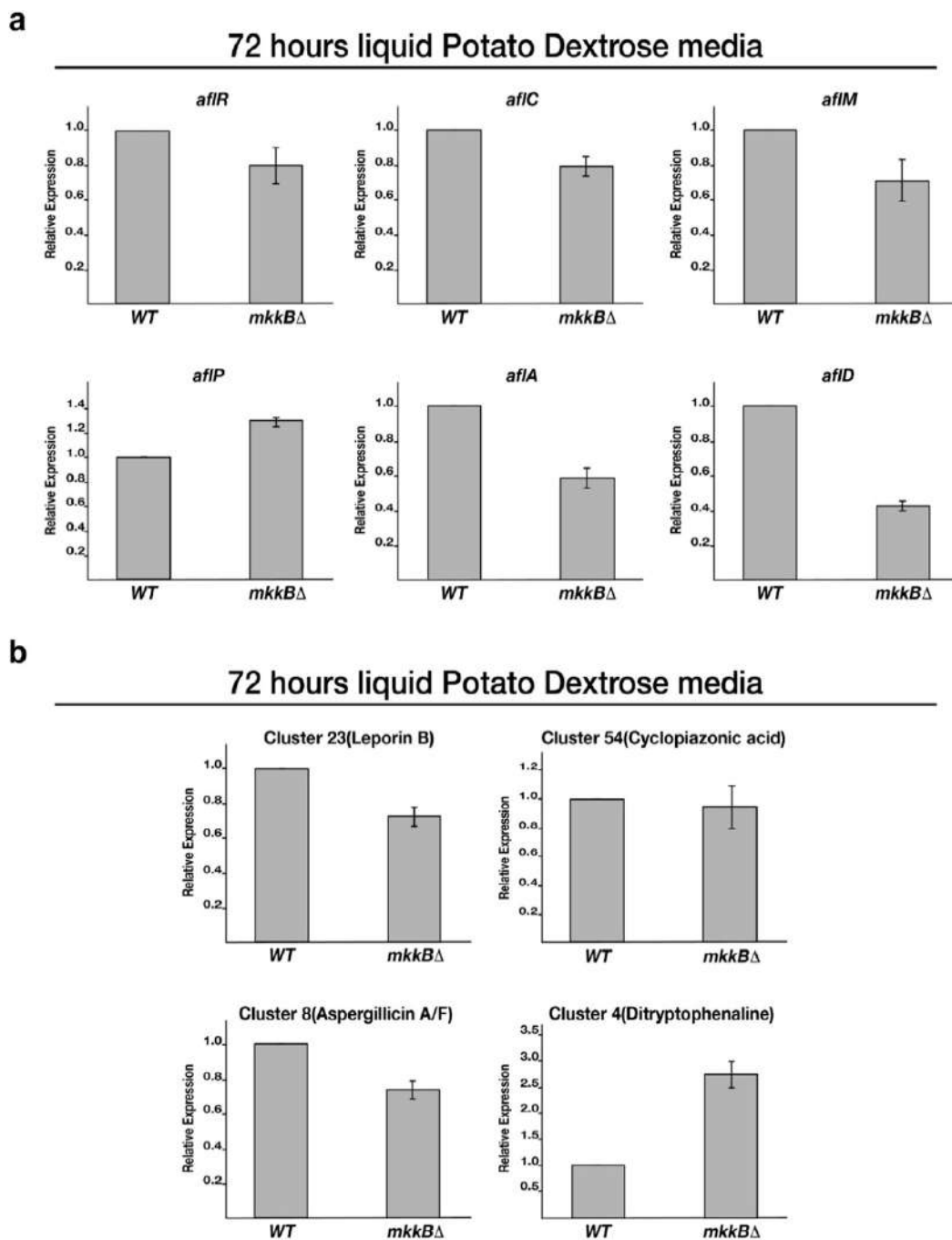
Figure 4.15. Relative expression levels of SM genes in strains cultured in liquid PD medium for 72 hours. (a) Relative expression levels of the *aflR, aflC, aflM, aflP, aflA* and *aflD* genes belonging to the aflatoxin B1 gene cluster. The TJES19.1 strain and *mkkB*Δ mutant strain were inoculated (1×10^6 spores) in liquid PD medium and left to incubate on a shaker at 30°C for 72 hours. (b) Relative expression levels of genes corresponding to the leporin B, CPA, aspergillicin A/F and ditryptophenaline gene clusters in both TJES19.1 and mkkBΔ.

After 24 hours incubation in liquid complete medium, followed by 6 days incubation in the dark on PDA plates, it is shown that the relative expression levels of the aflatoxin genes are mostly similar in both the wild type and *mkkB* mutant, with the exception of *aflM,* which is downregulated (**Figure 4.16. (a)**). The expression of *aflR* was 0.96 FOC, *aflC* was 1.07 FOC, *aflM* was 0.45 FOC, *aflP* was 0.83 FOC, *aflA* was 0.76 FOC and *aflD* was 0.97 FOC in the *mkkB* mutant. Expression of *lepA* was 1.15 FOC, *agiA* was 1.41 FOC and *dtpA* was 0.78 FOC, while the *cpaA* gene was not detectable at this time point. (**Figure 4.16. (b)**).
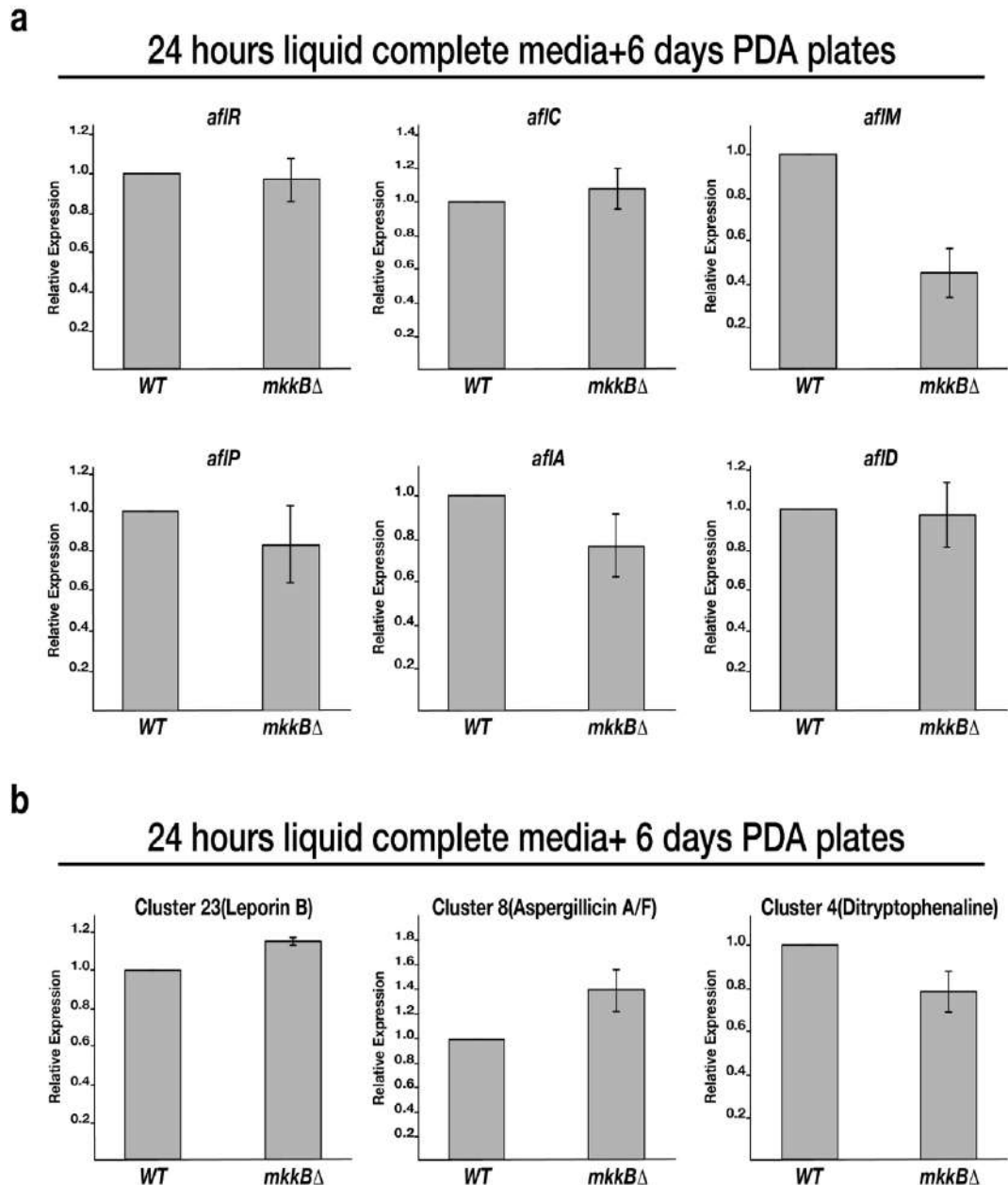
Figure 4.16. Expression levels of SM genes in strains cultured in complete medium for 24 hours, followed by incubation on PDA plates for 6 days. (a) Relative expression levels of the *aflR, aflC, aflM, aflP, aflA* and *aflD* genes belonging to the aflatoxin B1 cluster. The TJES19.1 strain and *mkkBΔ* mutant strain were inoculated (1×10^6 spores) in liquid complete medium and incubated on a shaker at 30°C for 24 hours. The mycelia were then filtered and shifted onto PDA plates to be incubated in the presence of light for 6 days at 30°C. (b) Relative expression levels of genes corresponding to the leporin B, aspergillicin A/F and ditryptophenaline gene clusters in both TJES19.1 and *mkkBΔ*.

This data provides evidence that MkkB may be involved in the positive regulation of various genes belonging to the aflatoxin gene cluster, such as *aflM, aflA* and *aflD*. MkkB may also be required for the negative regulation of the backbone genes of various SMs. In combination with the UHPLC-HRMS analysis, these data suggest that the deletion of either *steC, mkkB, mpkB* or *steD* results in complete inhibition of Aflatoxin B1 production and an increase in leporin B, CPA, aspergillicin A and aspergillicin F production. However, while the deletion of *hamE* results in complete inhibition of aflatoxin B1 production, it exhibits no significant differences with respect to production of the five other compounds tested. This could suggest that HamE does not function as a member of the pheromone module in *A. flavus* to regulate SM production but it may independently regulate aflatoxin production *via* a separate mechanism.

4.5. The pheromone module proteins localise to the hyphal tips and MpkB translocates into the nucleus

To determine the sub-cellular localisations of the pheromone module proteins *in vivo*, confocal microscopy imaging was performed, using the GFP-tagged proteins and a DAPI stain for the nuclei (**Figure 4.17.**). The green GFP signals and blue DAPI signals were overlapped to determine the localisation of each protein with respect to the nucleus. Each strain was inoculated in 400µl of liquid GMM, containing appropriate supplements and left to incubate at 30°C for various durations (24 hours or less). It was observed that SteC-GFP exhibited uniform cytoplasmic fluorescence throughout hyphae and is excluded from interphase nuclei. It was also evident that SteC-GFP localises to some but not all septa (**Figure 4.17. (a)**). MkkB-GFP displayed a uniform distribution throughout fungal hyphae. It was observed that this fusion protein is excluded from nuclei but is enriched at the septa and hyphal tips (**Figure 4.17. (b)**). Imaging of MpkB-GFP revealed that this fusion protein is localised throughout the fungal hyphae, exhibiting a uniform distribution. MpkB was also observed to be slightly more concentrated in the nuclei and at the hyphal apices (**Figure 4.17. (c)**). SteD-GFP fluorescence was faint, cytoplasmic and non-uniform. This fusion protein was observed to accumulate at some but not all septa and it appears that it is excluded from nuclei (**Figure 4.17. (d)**).
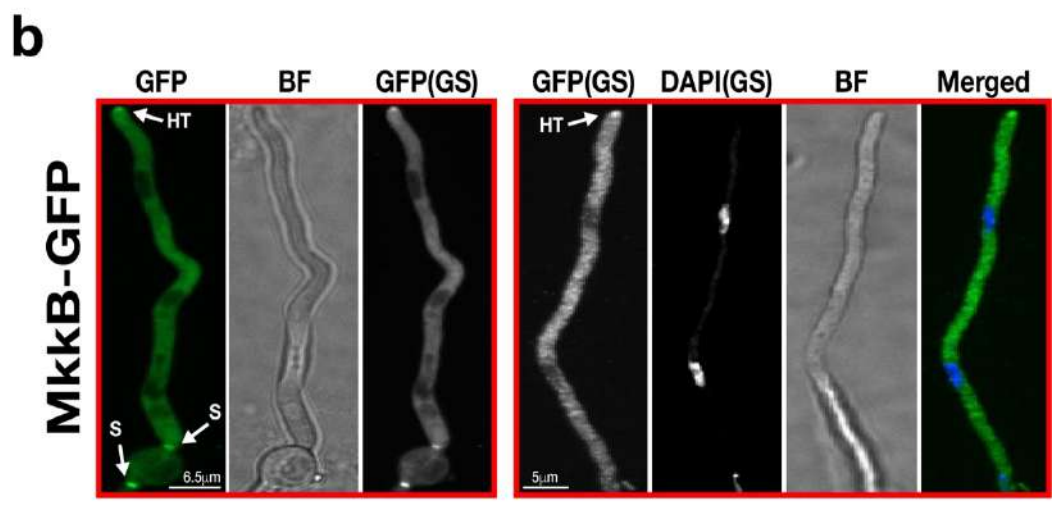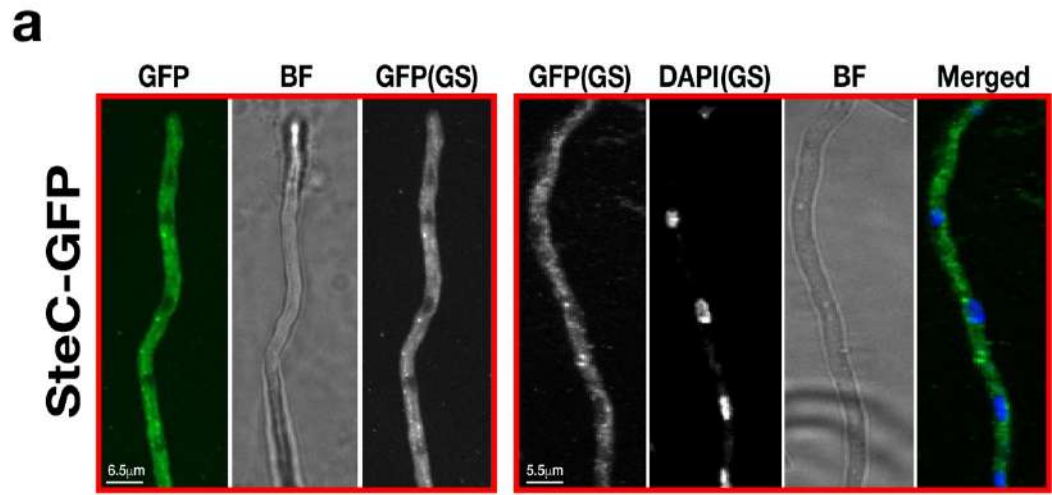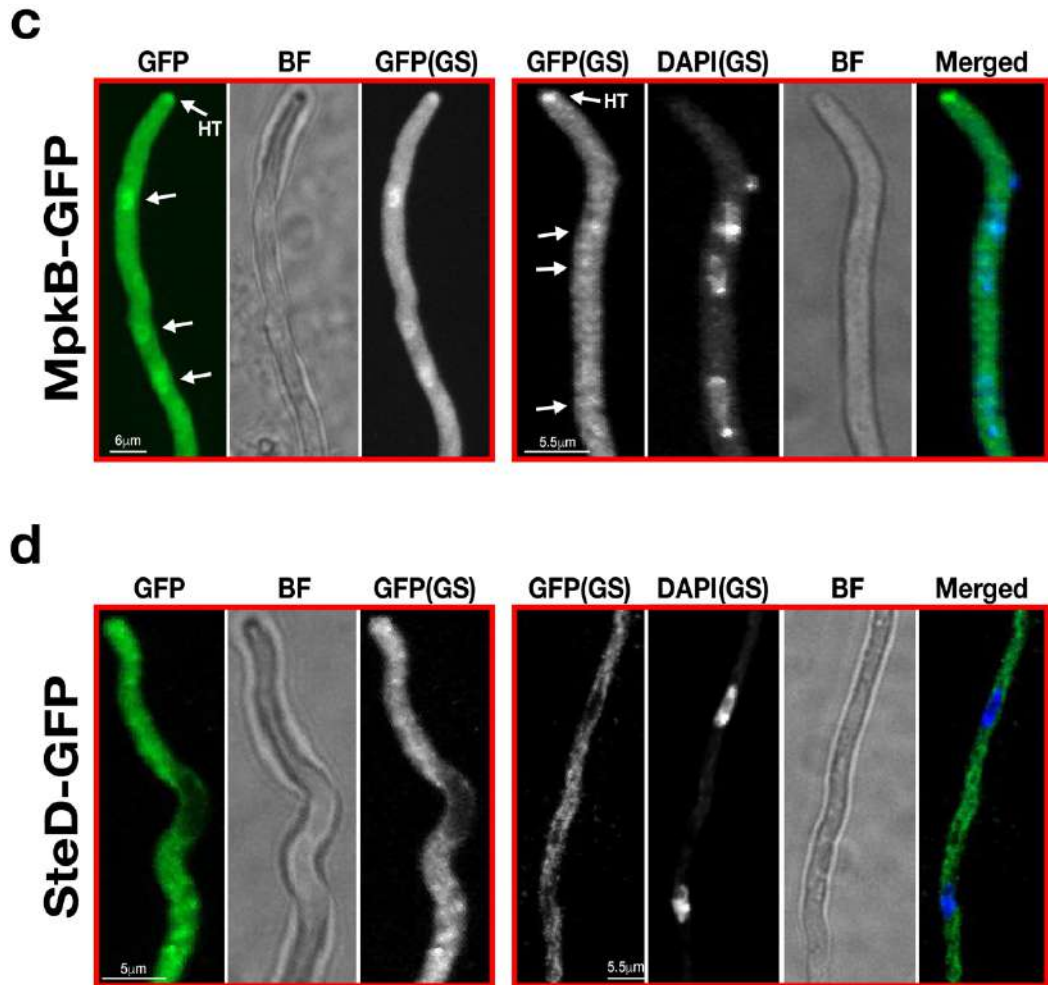
Figure 4.17. Localisation of the pheromone module proteins *in vivo*. (a) Sub-cellular localisations of SteC-GFP. All strains (panels a-d) were incubated at 30ºC for various durations in 400μl of liquid GMM, containing appropriate supplements. (BF) refers to brightfield images. (GS) refers to grayscale images. DAPI was used to stain the nuclei. Merged images are the overlap of the GFP and DAPI images. White arrows refer to accumulation of protein in the nuclei. (HT) refers to accumulation of protein at hyphal tips. (S) refers to accumulation of protein at septa. (b) Sub-cellular localisations of MkkB-GFP (c) Sub-cellular localisations of MpkB-GFP (d) Sub-cellular localisations of SteD-GFP.

4.5.1. Determination of the localisation and abundance of HamE

All attempts to successfully tag the *hamE* gene with the *sgfp* epitope tag failed. Consequently, a *hamE::3xha* strain was generated and immunostaining was performed to determine the sub-cellular localisation of this protein *in vivo*. The HamE-HA strain was cultured on sterile coverslips submerged in Sabouraud medium with required supplements. The strain was left to incubate at 30°C for 16 hours without agitation. DAPI staining was used to stain the nuclei blue and the two images were merged to show the localisation of the HamE protein with respect to the nuclei in the fungal hyphae. It was observed that the HamE protein is dispersed throughout the hyphae but becomes enriched at the hyphal tips and is absent from the nuclei (**Figure 4.18. (a)**). This pattern of localisation is similar to that observed for *N. crassa* Ham5 which was shown to localise at opposing hyphal tips during cell-cell communication (Dettmann et al., 2014, Jonkers et al., 2014).

To determine when the HamE protein is produced during different developmental stages, time course immunoblotting was performed. Crude protein extracts were isolated from fungal mycelia which were cultured for various lengths of time and were induced for either vegetative, asexual or sexual development. For the vegetative growth incubations, the HamE-HA strain was cultured in Sabouraud medium with required supplements for 20, 36 and 48 hours. For asexual and sexual induction, the HamE-HA strain was initially cultured in Sabouraud medium for 24 hours. Following this incubation, the mycelia were filtered and shifted to GMM agar plates to be incubated for 12 and 24 hours in the presence and absence of light to induce asexual and sexual development, respectively. These crude protein extracts were run on SDS gels, transferred to protean membranes and probed with a mouse α-HA antibody. The housekeeping protein SkpA was used as a control to ensure equal loading of samples. It was found that the production of HamE is highly dynamic as this protein was detectable at the late stages of vegetative growth (48 hours) and early stages of asexual development (12 hours) and sexual development (24 hours) (**Figure 4.18. (b)**). These data suggest that HamE is involved in all stages of *A. flavus* growth, however, the *hamE* mutant only exhibits impairment with regards to sexual reproduction. Therefore, more experiments are required to understand the roles that HamE may play in the processes of vegetative growth as well as asexual sporulation.
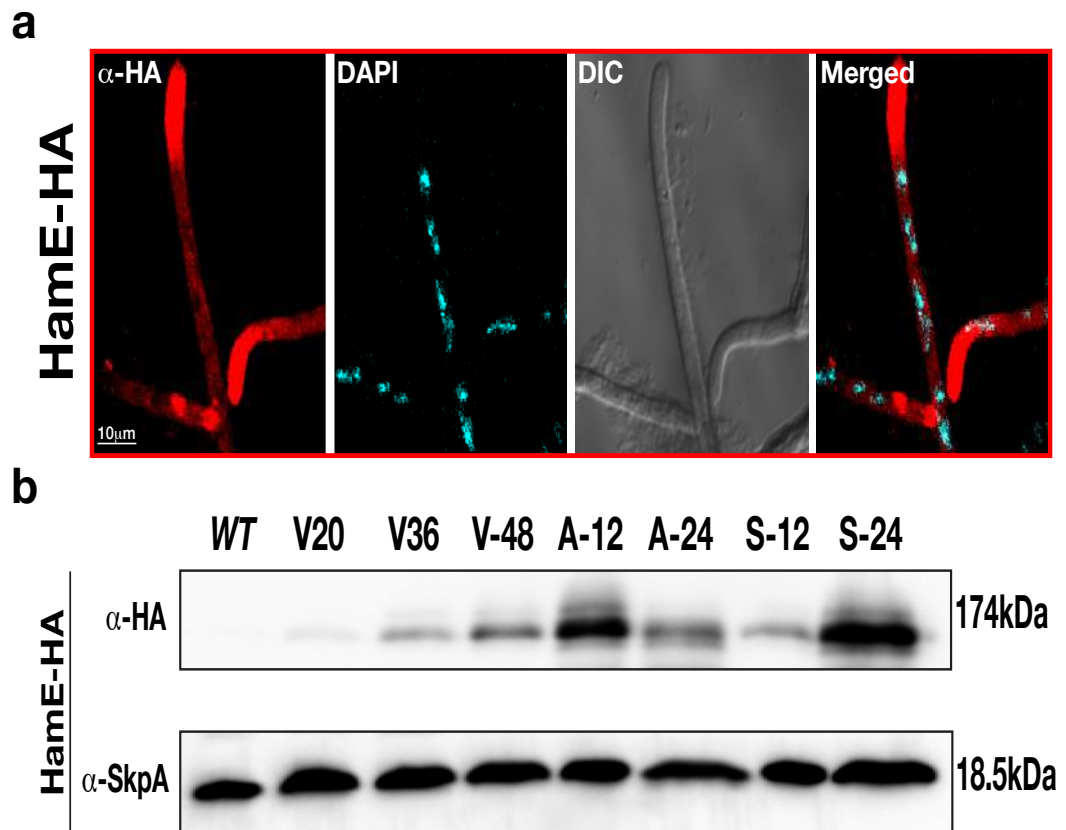
Figure 4.18. Localisation and time course abundance of HamE. (a) Localisation of HamE-HA *in vivo*. The HamE-HA strain was inoculated (5×10^3 spores) on sterile coverslips, covered in 450μl of Sabouraud medium, containing supplements. Strains were left to incubate at 30˚C for 14-16 hours. DIC (Differential Interference Contrast). Scale bars represent 10μm. DAPI was used to stain the nuclei. (b) Time course immunoblotting of HamE-HA at various stages of development. WT (wild type), V (vegetative), A (asexual), S (sexual). For asexual and sexual induction, the HamE-HA strain was cultured vegetatively for 24 hours in liquid Sabouraud medium, with required supplements and transferred to GMM plates to be incubated in the light and dark respectively. The housekeeping protein SkpA is used as a loading control. 50μg of crude protein extracts were loaded in each lane on 10% SDS gels and proteins were transferred to protean membranes overnight. The full length blots used to generate this image are provided in **Appendix B: Figure S3.**

4.6. Summary of main findings and chapter conclusions

4.6.1. The pheromone module is conserved in *A. flavus* and exists as a tetrameric complex

In this work, orthologs of all five members of the *A. nidulans* pheromone module were found to exist in *A. flavus*. These proteins exhibit high similarity to the *A. nidulans* proteins (**Figure 4.1.**), signifying their evolutionary conservation and importance. It was also shown that a tetrameric complex is formed in *A. flavus* (**Figure 4.2.)**. This complex consists of the MAP3K SteC (AFLA_048880), the MAP2K MkkB (AFLA_103480), the MAPK MpkB (AFLA_034170) and the adaptor protein SteD (AFLA_002340). Interestingly, the HamE ortholog (AFLA_095770) was not shown to be interacting with the members of this pathway.

4.6.2. The *A. flavus* pheromone module is required for the regulation of asexual sporulation

In *A. flavus,* the *steC, mkkB, mpkB, steD* and *hamE* genes were deleted to monitor the influence of the respective proteins in the regulation of asexual sporulation. It was observed that each mutant, with the exception of *hamEΔ,* exhibited significant defects in asexual reproduction, as these strains displayed a completely pale white phenotype (**Figures 4.3. and 4.4.**). The *hamE* mutant however, resembled the wild type strain and produced asexual conidia in similar quantities. Each gene was complemented to restore gene functionality and to confirm whether the defects observed in the mutant strains were directly due to the deletion of these genes. It was observed that complementation of each gene restored the ability to undergo normal asexual sporulation, as each strain resembled the wild type with regards to phenotype and quantities of conidia produced. It was also observed that the deletion of *mkkB* results in the downregulation of various genes involved in asexual sporulation such as *flbC* and *abaA* (**Figure 4.6.)**. Overall, these data provided evidence that the tetrameric complex of SteC-MkkB-MpkB-SteD is required for the regulation of asexual sporulation and that HamE is not required for the regulation of this pathway.

4.6.3. The pheromone module is essential for regulating sclerotia production

The pheromone module mutant strains were also assessed to test whether or not these proteins contribute to the regulation of sexual sclerotia formation. It was observed that each of the five mutant strains were completely incapable of producing sclerotia and these mutants were sterile (**Figures 4.7. and 4.8.**). Complementation of each gene restored the ability to produce sclerotia, with the quantities of sclerotia produced resembling the wild type levels. It was also observed that the deletion of *mkkB* results in the downregulation of various genes involved in sexual development, such as *veA* and *nsdD* (**Figure 4.9.**). Taken together, these data provide evidence that the pheromone module SteC-MkkB-MpkB-SteD, as well as HamE are all essential for regulating sclerotia production in *A. flavus*. However, the mechanism by which HamE exerts it's regulatory role may be independent of the pheromone module.

4.6.4. The pheromone module modulates the production of various SMs

To test whether the *A. flavus* pheromone module contributes to the regulation of secondary metabolism, as is the case in *A. nidulans* (Frawley et al., 2018, Bayram et al., 2012), UHPLC-HRMS and qPCR analysis was performed. It was observed that each of the five mutants were completely incapable of producing the carcinogenic compound aflatoxin B1 (**Figure 4.10. (a)**). Interestingly, it was also observed that the *steC, mkkB, mpkB* and *steD* mutants exhibited increased levels of leporin B (**Figure 4.10. (d)**), CPA (**Figure 4.11. (a)**), aspergillicin A (**Figure 4.11. (d)**) and aspergillicin F (**Figure 4.12. (a)**), proposing that these proteins are required for the negative regulation of these compounds. It was also found that the deletion of *hamE* does not exert any influence over the levels of production of these four compounds. Lastly, it was shown that deletion of any of these five genes does not result in a change in ditryptophenaline production (**Figure 4.12. (d)**). Overall, these data suggest that the SteC-MkkB-MpkB-SteD tetrameric complex is essential in positively regulating aflatoxin B1 production and negatively regulating production of various other SMs. Interestingly, HamE is also required for the regulation of aflatoxin B1 production, however, the mechanism by which HamE regulates production of this compound may be independent of the pheromone module mechanism of regulation.

4.6.5. The pheromone module complex is assembled in the cytoplasm and MpkB translocates into the nucleus

Confocal microscopy imaging was utilised to visualise the sub-cellular localisations of the pheromone module proteins *in vivo.* It was observed that the SteC-GFP and SteD-GFP fusion proteins exhibited mostly cytoplasmic localisation and both were excluded from interphase nuclei (**Figure 4.17. (a) and (d)**). The MkkB-GFP (**Figure 4.17. (b)**) and MpkB-GFP (**Figure 4.17. (c)**) fusion proteins displayed uniform cytoplasmic localisations and both were found to be enriched at the hyphal tips. MkkB-GFP was also found to accumulate at the septa, while MpkB-GFP was the only protein of the complex observed to localise to the nuclei. Taken together, these data suggest that both MkkB and MpkB accumulate at the hyphal tips, perhaps forming a dimer in response to pheromone signalling between neighbouring hyphae. Both SteC and SteD were dispersed throughout the hyphae and so, it is possible that these two proteins form a dimer in the cytoplasm. Perhaps the SteC-SteD dimer then interacts with the MkkB-MpkB dimer to form a cytoplasmic tetrameric complex. Assembly of the complex could allow for kinase phosphorylation and translocation of MpkB into the nucleus.

4.6.6. HamE localises to the hyphal tips and is produced during all stages of fungal development

It was observed that HamE is dispersed throughout the fungal hyphae but also becomes enriched at the hyphal tips (**Figure 4.18. (a)**), perhaps due to points of contact between hyphae, initiating cell-cell communication. It was also found that HamE is detectable during all stages of *A. flavus* growth. The abundance of HamE was increased during 48 hours of vegetative growth, 12 hours of asexual induction and 24 hours of sexual induction (**Figure 4.18. (b)**). This suggests that HamE may be required for the regulation of each method of development tested. However, it is not fully understood whether or not HamE is required for the regulation of asexual sporulation.

4.6.7. Overall conclusions

In conclusion, this study has identified orthologs of the pheromone module proteins in the filamentous fungus *A. flavus*. Data from this study provides evidence to support the assembly of a tetrameric MAPK signalling pathway in the cytoplasm. This protein complex consists of the three kinases SteC, MkkB and MpkB, as well as the adaptor protein SteD (**Figure 4.19**). We propose that this MAPK complex is likely made up of two sub-complexes. MkkB and MpkB possibly form a dimer that becomes enriched at the hyphal tips and these proteins may then interact with the SteC-SteD dimer to form a cytoplasmic tetrameric complex, perhaps in response to chemotropic interactions between hyphae. This may result in kinase phosphorylation and MpkB activation, allowing for it's translocation into the nucleus where it interacts with various transcription factors to positively regulate asexual sporulation, sexual sclerotia formation and aflatoxin B1 production.

These data also suggest that this complex does not require HamE to regulate MAPK signalling, unlike what is observed in other fungal species like *A. nidulans* (Frawley et al., 2018) and *N. crassa* (Jonkers et al., 2014, Dettmann et al., 2014). However, HamE was observed to accumulate at the hyphal tips and is critical for sclerotia formation and aflatoxin B1 production. Perhaps HamE is also required for the response to chemotropic signals, however, the mechanism of signalling to the nucleus is not fully understood. By characterising the molecular roles of the pheromone module in *A. flavus,* this may provide insight on how filamentous fungi regulate their development and secondary metabolism. This, in turn, may allow for strategies to be established that could result in the prevention of crop spoilage due to mycotoxin contamination and infections caused by *Aspergillus* species.
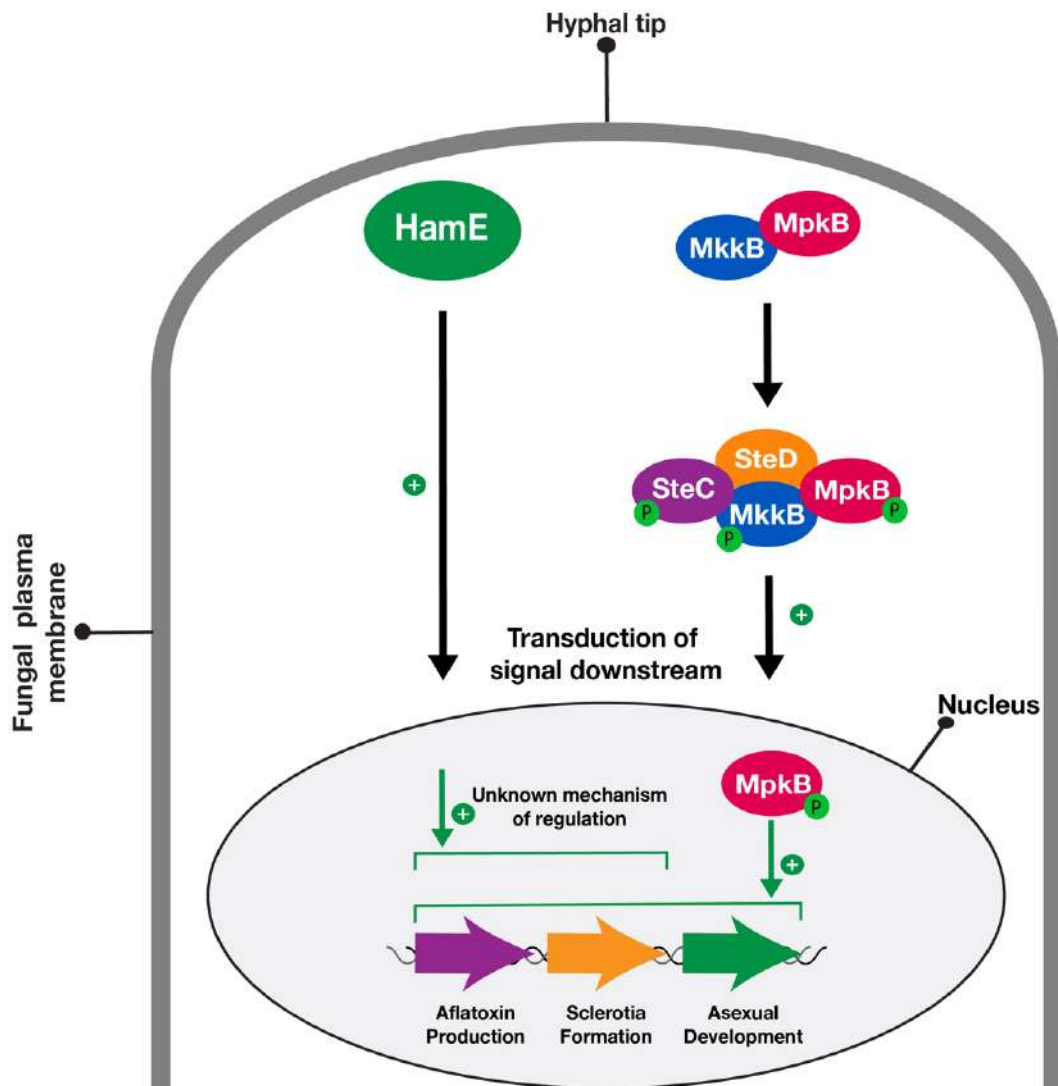
Figure 4.19. Schematic model of the *A. flavus* pheromone module and it's roles in regulating development and secondary metabolism. The MkkB-MpkB dimer, as well as HamE, localise to the hyphal tips. The MkkB-MpkB dimer likely interacts with the SteC-SteD dimer in the cytoplasm to form a tetrameric complex. Both HamE and the tetrameric complex signal downstream to the nucleus independently. Assembly of the complex leads to activation of MpkB, possibly by phosphorylation, which then results in translocation of MpkB into the nucleus. Presumably, MpkB then interacts with transcription factors to positively regulate asexual sporulation, sexual sclerotia formation and aflatoxin B1 production. HamE positively regulates sclerotia formation and aflatoxin B1 production *via* an unknown mechanism. 'P' represents phosphate groups.

4.7. Author contributions and declarations

All data from this chapter has been taken from (Frawley et al., 2020a) and the authors declare that there is no conflict of interest. The majority of experiments were performed by Dean Frawley. Exceptions are the following: (i) UHPLC-HRMS analysis of *A. flavus* crude extracts. This was performed by Dr. Claudio Greco, under the supervision of Prof. Nancy Keller at the Department of Medical Microbiology and Immunology, Madison, Wisconsin, United States. (ii) Confocal microscopy imaging of GFP-tagged *A. flavus* strains. This was performed by Prof. Berl Oakley at the Department of Molecular Biosciences, University of Kansas, United States of America.

Chapter 5: Results

The pheromone module regulates sporulation, secondary metabolism and stress responses in the human pathogen *A. fumigatus*

5.1. Identifying the pheromone module in *A. fumigatus*

Chapter 3 of this thesis focused on characterising a scaffold protein for the pheromone module in *A. nidulans,* whilst also providing more evidence of the roles of this protein complex in the regulation of asexual sporulation, sexual cleistothecia development and the production of various SMs. Chapter 4 of this thesis concentrated on the identification and characterisation of the pheromone module in the crop contaminating fungus *A. flavus.* This chapter provided insight on the composition and localisation of the complex. In conjunction with this, this chapter elucidated the roles of this complex in the regulation of asexual sporulation, sexual sclerotia formation and the production of various SMs, including the highly carcinogenic compound aflatoxin B1.

There is a high degree of conservation between the pheromone module proteins in these two *Aspergillus* species. Consequently, this led to the question of whether the human opportunistic pathogen *A. fumigatus* also utilises MAP kinase signalling *via* the pheromone module to regulate it's development and production of SMs, including the immunosuppressive agent gliotoxin. The main aims of this chapter are to identify a homologous MAP kinase pathway in this species. The composition of the complex will be established by determining individual protein-protein interactions *via* MS/MS experiments. The localisation of the complex components will be determined *via* generation of *sgfp* epitope tagged strains and confocal microscopy. The roles of this complex with regards to the regulation of asexual sporulation and SM biosynthesis will also be addressed. Overall, this chapter aims to provide evidence that the pheromone module is conserved in *A. fumigatus* and is highly important for the regulation of fungal growth, development and SM production.

5.1.1. *A. fumigatus* contains orthologs of each of the pheromone module proteins

To determine whether *A. fumigatus* possesses orthologs of the pheromone module proteins that are present in *A. nidulans,* reciprocal BLAST searches (Altschul et al., 1990) were performed and the ASPGD website was utilised. It was found that the *A. fumigatus* genome contains orthologs of all five members of the *A. nidulans* pheromone module. According to the Smith-Waterman algorithm (Madeira et al. 2019), the *A. fumigatus* SteC ortholog (Afu5g06420) exhibits 85.8% sequence similarity to the *A. nidulans* protein, while *A. fumigatus* MkkB (Afu3g05900), MpkB (Afu6g12820), SteD

(Afu2g17130) and HamE (Afu5g13970) exhibit 84.1%, 99.2%, 85.3% and 75.5% sequence similarity respectively.

Once detected, the 'ScanProsite' (de Castro et al., 2006) and 'InterPro' (Mitchell et al., 2019) software were used to determine the sizes of these *A. fumigatus* proteins and the domains they possess in comparison to the *A. nidulans* proteins (**Figure 5.1. (a) and (b)**). This revealed that the SteC protein in both *A. nidulans* and *A. fumigatus* possesses a SAM domain at the N-terminal. In *A. nidulans,* this SAM domain is located between aa 63-126, while for *A. fumigatus*, it is present between aa 98-161. The SteC protein in both species also contains a RA domain and a protein kinase domain. The RA domain in *A. nidulans* is located between aa 248-351, while the RA domain in *A. fumigatus* is located at aa 311-414. The protein kinase domain is located at aa 607-881 in *A. nidulans,* while the protein kinase domain in *A. fumigatus* is located at aa 672-947. According to ASPGD, the sequence provided for *A. fumigatus* SteC is 1,007 aa in length, considerably larger than the *A. nidulans* sequence. However, attempts at tagging this sequence with various epitope tags proved to be unsuccessful. This led to the proposal that the sequence provided on ASPGD is incorrect. Pair-wise sequence alignment of the *A. nidulans* and *A. fumigatus* protein sequences using the Smith-Waterman algorithm (Madeira et al. 2019) led to the determination of the extent of homology (**Appendix C: Figure S3**). This alignment revealed the presence of an alternate stop codon, premature of the stop codon provided on ASPGD. Consequently, tagging of the SteC sequence from this stop codon proved to be successful (**Appendix C: Figure S1 (b)**). This led to the proposal that the *A. fumigatus* protein sequence is instead 952 aa in length, as opposed to 1,007 aa.

The *A. nidulans* and *A. fumigatus* MkkB proteins both possess a protein kinase domain. This domain is present at aa 67-334 in both of these species, signifying high conservation between these two orthologs. The MpkB protein in both species also possesses a protein kinase domain at very similar residues. In *A. nidulans,* this domain is present at aa 22-310, while in *A. fumigatus,* this domain exists at aa 21-309. The SteD adaptor in both species contains SAM and RA domains. The SAM domains in *A. nidulans* and *A. fumigatus* are located at aa 66-129 and 67-130 respectively. The RA domains are located at aa 370-459 and 365-455 in *A. nidulans* and *A. fumigatus* respectively. Lastly, the HamE protein consists of WD40 repeats at the N-terminus of both proteins between aa 30-300 and 38-348 in *A. nidulans* and *A. fumigatus* respectively.
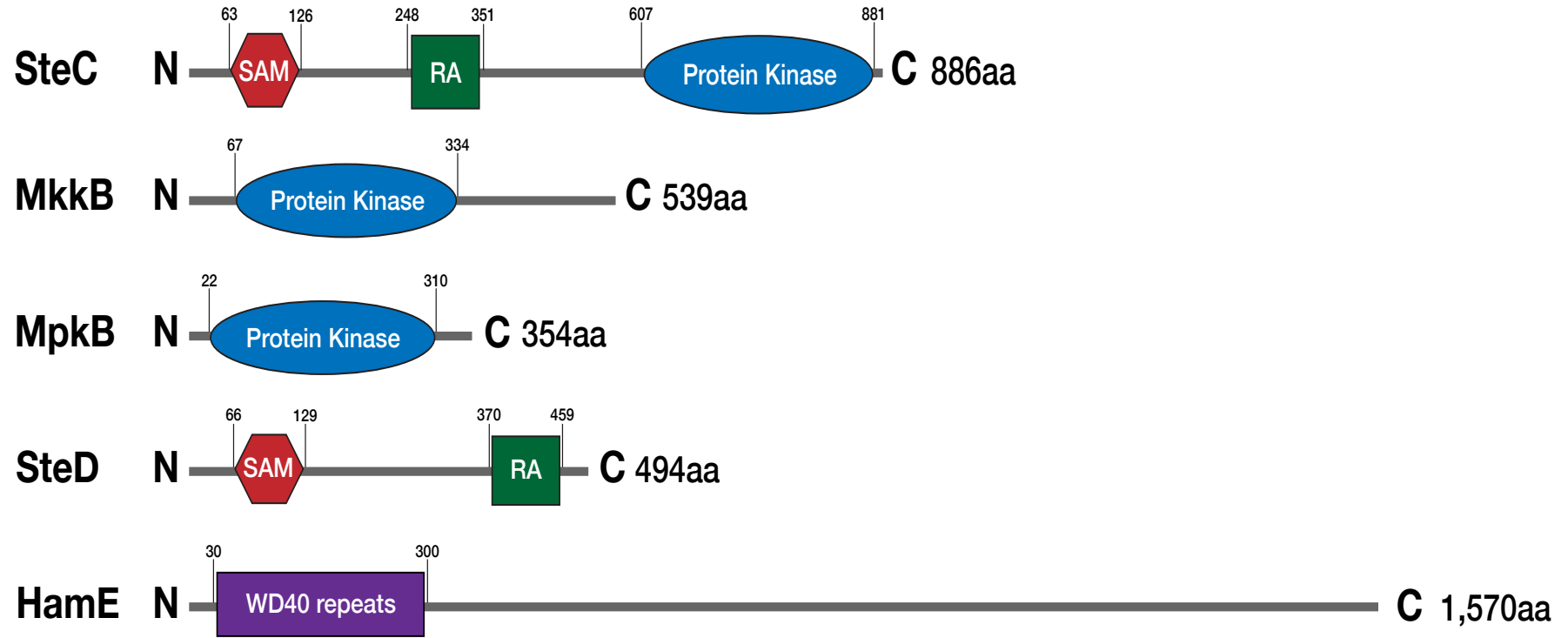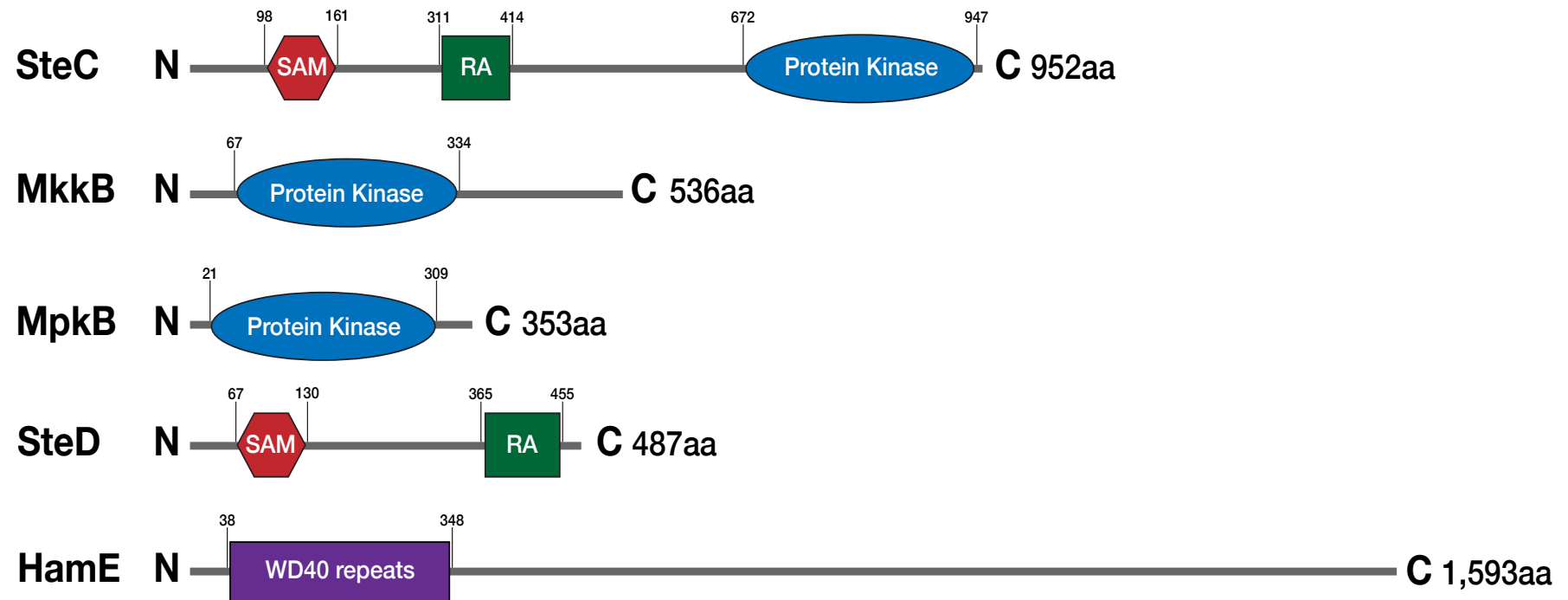
Figure 5.1. Domain architectures of the pheromone module proteins in *A. nidulans* and *A. fumigatus* (a) The domains and motifs of the pheromone module proteins in *A. nidulans*. 'aa' represents the size of the proteins in amino acids. 'N' and 'C' refer to the N and C protein terminals. Numbers surrounding the domains represent their amino acid locations. SAM (Sterile alpha motif), RA (Ras Association domain). (b) The domains and motifs of the homologous pheromone module proteins in *A. fumigatus*. Detection of protein sizes and domains were performed using a combination of ScanProsite (de Castro et al., 2006) and InterPro (Mitchell et al., 2019) software.

5.1.2. SteC, MkkB, MpkB, SteD and HamE may form a pentameric complex in *A. fumigatus*

Due to the fact that the pheromone module proteins form a pentameric complex in *A. nidulans* (Frawley et al., 2018) and a tetrameric complex in *A. flavus* (Frawley et al., 2020a) the question of whether or not these proteins form a complex in *A. fumigatus* was proposed. To assess protein-protein interactions, a *sgfp* epitope tag was coupled to the C-terminals of the *steC, mkkB, mpkB* and *steD* genes (**Appendix C: Figure S1**). All attempts to detect the *hamE* gene tagged with *sgfp* failed and so, the *hamE* gene was coupled to a *3xha* epitope tag at the C-terminus. (**Appendix C: Figure S2**). The fusion proteins were immunoprecipitated from vegetative cultures grown for 24 hours and were run on a MS to detect the tagged proteins and their interaction partners, which are listed in (**Figure 5.2. (a)**). It was found that SteC-GFP pulldowns co-purified the adaptor protein SteD (**Appendix C: Table S4**), MkkB-GFP pulldowns co-purified SteC, MpkB, SteD and HamE (**Appendix C: Table S5**), MpkB-GFP pulldowns co-purified MkkB and SteD (**Appendix C: Table S6**) and SteD-GFP pulldowns co-purified SteC (**Appendix C: Table S7**). Despite HamE being detectable in purifications of MkkB-GFP, HamE-HA pulldowns did not co-purify any pheromone module components (**Appendix C: Table S8**) and so this interaction may be transient or is readily terminated. Taken together, these interactome data provide evidence that a complex of at least four proteins is assembled in *A. fumigatus* (**Figure 5.2. (b)**). This complex consists of the three kinases SteC, MkkB and MpkB, as well as the adaptor protein SteD. It is possible that HamE is a member of this pathway, however, this would require further testing to prove that HamE physically interacts with the members of this pheromone module.

a

GFP pulldowns

	SteC-GFP		MkkB-GFP		MpkB-GFP		SteD-GFP	
	% Coverage	Unique Peptides	% Coverage	Unique Peptides	% Coverage	Unique Peptides	% Coverage	Unique Peptides
SteC	31.58	22	63.26	50			31.68	23
MkkB			71.08	29	14.74	5		
MpkB			18.13	5	77.34	20		
SteD	29.16	9	62.42	22	7.60	2	53.18	16
HamE			13.12	12				

b
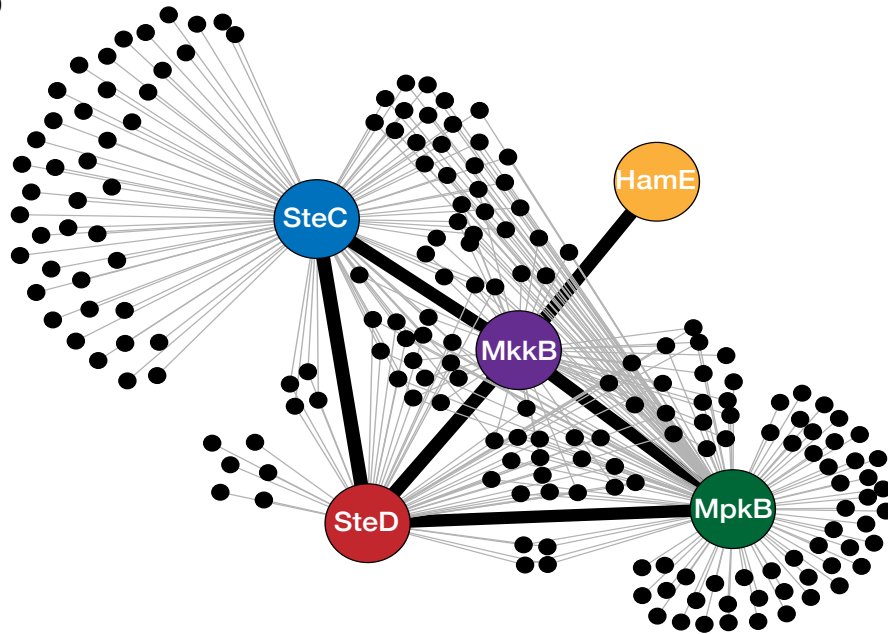
Figure 5.2. The interaction network of the pheromone module in *A. fumigatus.* (a) GFP pulldowns and LC-MS/MS analysis of the pheromone module proteins. Tagged proteins are given at the top of the table and co-purified proteins are given on the left-hand side. 2 biological replicates of each strain were used. Strains were cultured vegetatively at 37˚C in complete medium for 24 hours. Supplementary MS tables for this figure are provided in **Appendix C: Tables S4-7. (b)** Interaction network of the pheromone module components based on the unique peptides detected in each GFP pulldown. The interaction network was generated using the Gephi 0.9.2 software. Each black dot represents a protein detected in two independent biological replicates but not in any of the wild type samples.

5.2. The pheromone module proteins are required for the regulation of *A. fumigatus* development.

In order to assess whether the pheromone module protein orthologs in *A. fumigatus* contribute to the regulation of asexual sporulation and vegetative growth, mutant strains were generated. The respective *steC, mkkB, mpkB, steD* and *hamE* gene ORFs were deleted (**Appendix C: Figure S1**) by replacing these genomic regions with either the pyrithiamine resistance gene (*ptrA*) or the *pyrG* gene. To determine whether phenotypic differences observed in the mutant strains were due to the deletion of specific genes and not secondary abnormalities, complementation strains were made. A functional copy of each gene ORF, including the promoter and terminator regions were reinserted into the respective mutant strains to restore the wild type phenotype.

5.2.1. Each of the pheromone module proteins are critical for the regulation of asexual sporulation

Each mutant and complementation strain were spot inoculated in triplicate on GMM agar plates. These plates were incubated in the presence of light for 4 days to induce asexual reproduction and production of conidia (**Figure 5.3.**). For each of the five mutant strains, a dramatic reduction in sporulation was observed, similar to what is observed in both *A. nidulans* (Bayram et al., 2012, Frawley et al., 2018) and *A. flavus* (Frawley et al., 2020a) with the exception of the *A. flavus hamE* mutant, which did not show any defects in asexual reproduction. For the *A. fumigatus* mutants, the average values of conidia produced were expressed as a percentage of the CEA17 wild type average, which was chosen to represent 100% production (**Figure 5.4.**). The average percentage range for these mutants was between 10.16%-27.02%. The complementation of each gene restored the ability of these strains to undergo asexual sporulation to a similar degree to that of the wild type. The average percentage range of sporulation for the complementation strains was between 63.06%-102.89%.
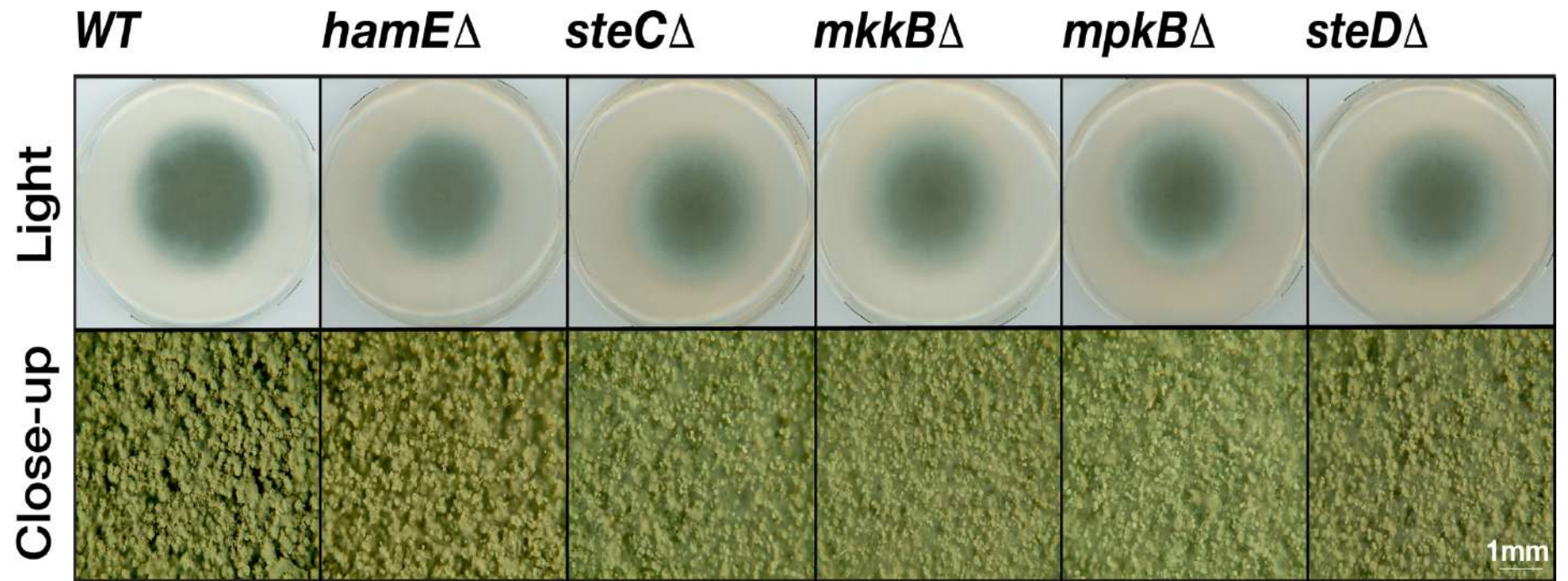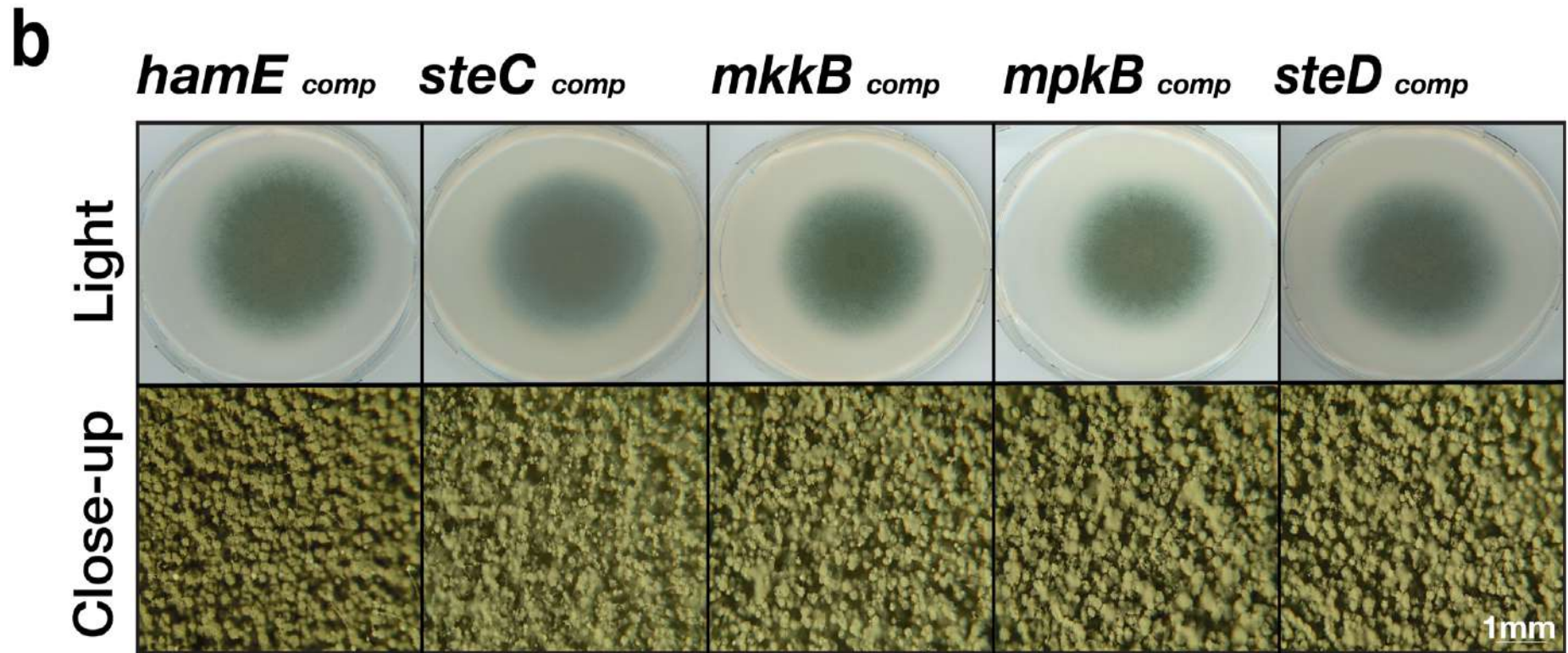
Figure 5.3. Asexual phenotypes of deletion and complementation strains. (a) The pheromone module protein deletion strains were spot inoculated $(5 \times 10^3$ spores) in triplicate on GMM agar plates containing supplements. Wild type refers to the CEA17 strain. These plates were incubated for 4 days in the light at 37°C to induce asexual development. Plates were scanned using the Epson perfection V600 photo scanner. Close-up images were taken at 4x magnification using the Olympus szx16 microscope with an Olympus sc30 camera. (b) Asexual phenotypes of the complementation strains.
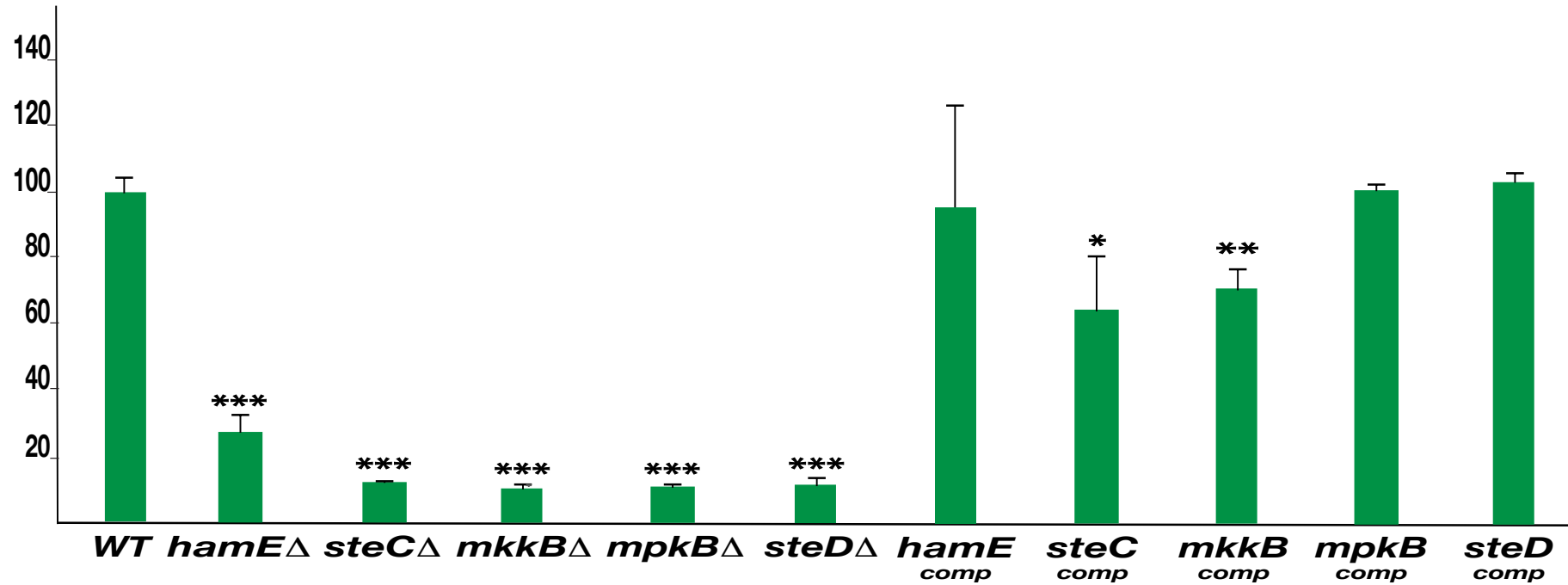
**Figure 5.4. Quantification of asexual conidiation in deletion and complementation strains**. The average sporulation value of the wild type strain was chosen to represent 100%. Mean values of all other strains (N=3) were plotted ± s.d. as a percentage of the WT. P-values were calculated by performing unpaired Student's t-tests (*$P<0.05$;**$P<0.01$; ***$P<0.001$).

5.2.2. Deletion of any of the pheromone module genes results in reductions in vegetative growth.

To determine whether the pheromone module proteins contribute to regulating vegetative growth in *A. fumigatus*, the colony diameters of each strain were measured and the averages of three biological replicates per strain were expressed as a percentage of the wild type average (**Figure 5.5**). It was observed that each mutant exhibited a significantly smaller colony diameter in comparison to the CEA17 strain, with the *hamE* mutant displaying the highest degree of reduction. Aside from the *hamE* mutant phenotype, these data support the findings in *A. nidulans,* where the deletion of either *steC, mkkB, mpkB* or *steD* results in a dramatic reduction in vegetative growth (Frawley et al., 2018). However, these results contradict the findings in *A. flavus* as no reductions in the rates of hyphal extension were observed in any of these mutants (Frawley et al., 2020a). For the *A. fumigatus* deletion strains, the average percentage range of colony diameters was between 83.22%-94.61%. Complementation of each gene restored the wild type phenotype and the average percentage range of hyphal extension was 98.2%-111.37%.

Taken together, these data suggest that the pheromone module proteins are essential for the regulation of both asexual sporulation and vegetative hyphal growth. These findings also suggest that these five proteins may act as a complex to regulate these processes due to the similarities of the mutant phenotypes.
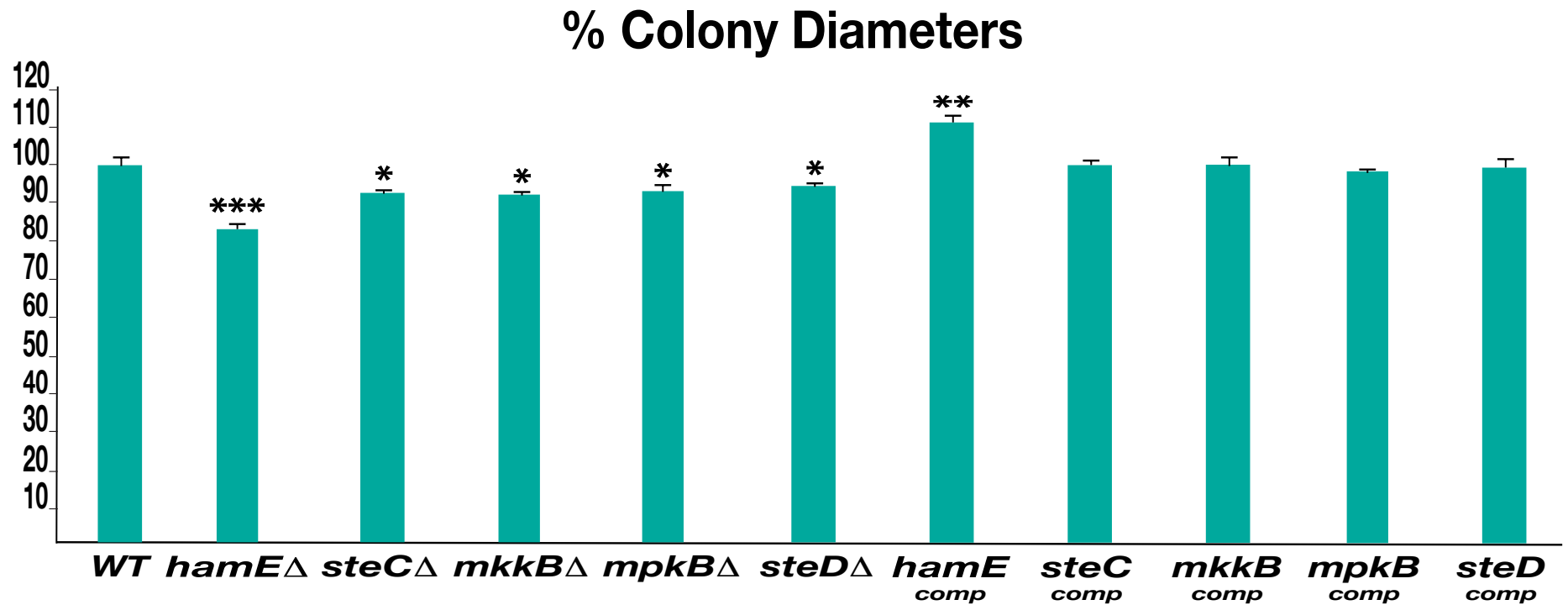
Figure 5.5. Graphical representation of the colony diameters of each asexually induced strain from Figure 5.3. with respect to the CEA17 wild type strain. Measurements were taken from three independent biological replicates for each asexually induced strain and the averages were plotted ± s.d. as a percentage of the WT strain. *P*-values were calculated by performing unpaired Student's *t*-tests (*$P<0.05$;**$P<0.01$; ***$P<0.001$).

5.3. The pheromone module proteins contribute to the regulation of various cell stress responses

As discussed in section 1.10.1., fungi like *A. fumigatus* utilise multiple MAPK pathways to respond to various cell stressors, such as cell wall, osmotic and oxidative stresses (Rispail et al., 2009, Hamel et al., 2012). Three main MAPK pathways become activated in *A. fumigatus* in response to stress. The CWI pathway is activated in response to cell wall stress agents and signals *via* the MAPK MpkA (van de Veerdonk et al., 2017, Valiante et al., 2015). The HOG pathway is required for the response to osmotic stressors and signals *via* the MAPK SakA (Martinez-Montanes et al., 2010, de Nadal and Posas, 2015, Du et al., 2006). Lastly, the HOG pathway, in cooperation with the MAPK MpkC have been shown to regulate cellular responses to osmotic, oxidative and cell wall stresses (Bruder Nascimento et al., 2016).

Despite MAPK modules achieving high signalling specificity in response to stimuli, many MAPK pathways incorporate multiple common proteins, leading to module cross-talk (Saito, 2010). In yeast, it has been shown that module cross-talk exists between various pathways, such as the pheromone module and HOG pathway. The HOG pathway incorporates the adaptor Ste50, the MAP3K Ste11, the MAP2K/ co-scaffold Pbs2 and the MAPK Hog1. In the pheromone module pathway, Ste11-mediated activation of the Fus3 kinase is regulated by the Ste5 scaffold, whereas Ste11-mediated activation of Hog1 in the HOG pathway is dependent on Pbs2. (Zarrinpar et al., 2004, Tatebayashi et al., 2006). These two pathways are not capable of being active at any one time, signifying that these pathways are insulated from one another. This was demonstrated by stimulating yeast cells simultaneously with both pheromones and osmostress stimuli and observing that cells could only respond to one stimulus at any given time (McClean et al., 2007). It was also shown that when the *fus3* gene is deleted, Hog1 is capable of becoming activated by pheromone stimuli. These findings emphasise how individual MAPK pathways can be interconnected and regulate one another. Due to this, the influence of the *A. fumigatus* pheromone module proteins in the modulation of various MAPK pathways was assessed.

5.3.1. Each mutant strain exhibited defects in growth in the presence of Congo Red.

To determine the relevance of the pheromone module proteins with respect to the responses to cell stressors, each mutant and complementation strain was spot inoculated on GMM agar plates containing various exogenous stress agents. The radial growth phenotypes of each strain were compared to the wild type phenotypes. To assess the influence of the pheromone module proteins in the response to cell wall stress, each strain was inoculated on plates containing various concentrations (20μg, 30μg and 50μg/ml) of the cell wall stressor Congo Red (**Figures 5.6. and 5.7.**). It was observed that the CEA17 wild type strain exhibited significant sensitivity to Congo Red at higher concentrations (50μg/ml). However, it was evident that the deletion of *steC, mkkB, mpkB, steD* and *hamE* resulted in increased sensitivity to Congo Red. Each of these mutant strains displayed significant growth defects in the presence of each concentration of Congo Red, suggesting that these proteins may play a role in cell wall biosynthesis. Complementation of each gene resulted in increased radial growth when compared to the respective mutants and the phenotypes of each complementation strain more closely resembled the wild type phenotypes.
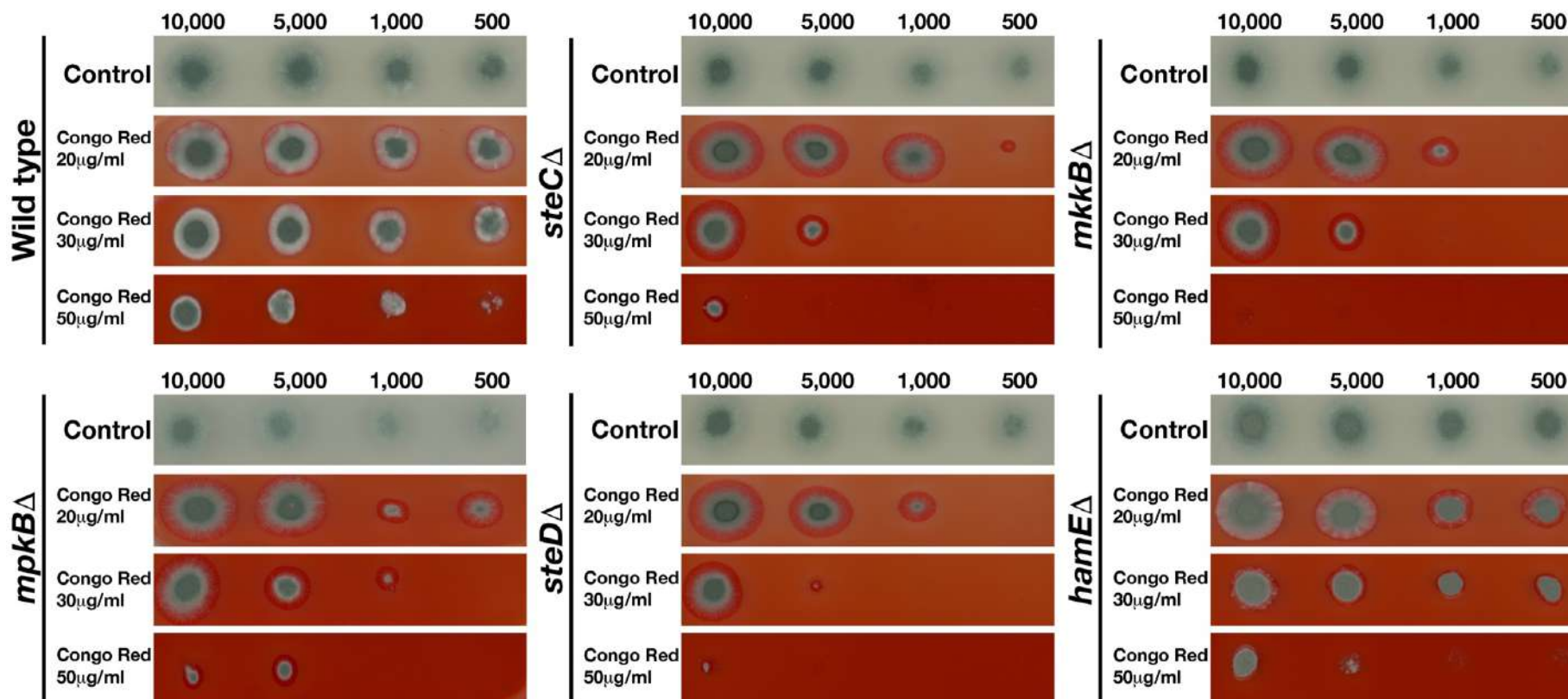
Figure 5.6. Growth phenotypes of the CEA17 wild type and mutant strains in the presence of various concentrations of Congo Red. Strains were point-inoculated on GMM agar plates containing either 20μg, 30μg or 50μg Congo Red and left to incubate at 37˚C for 3 days. The number of spores used for inoculation are listed above each panel. 'Control' refers to strains point inoculated on GMM agar plates that did not contain any stress agents.
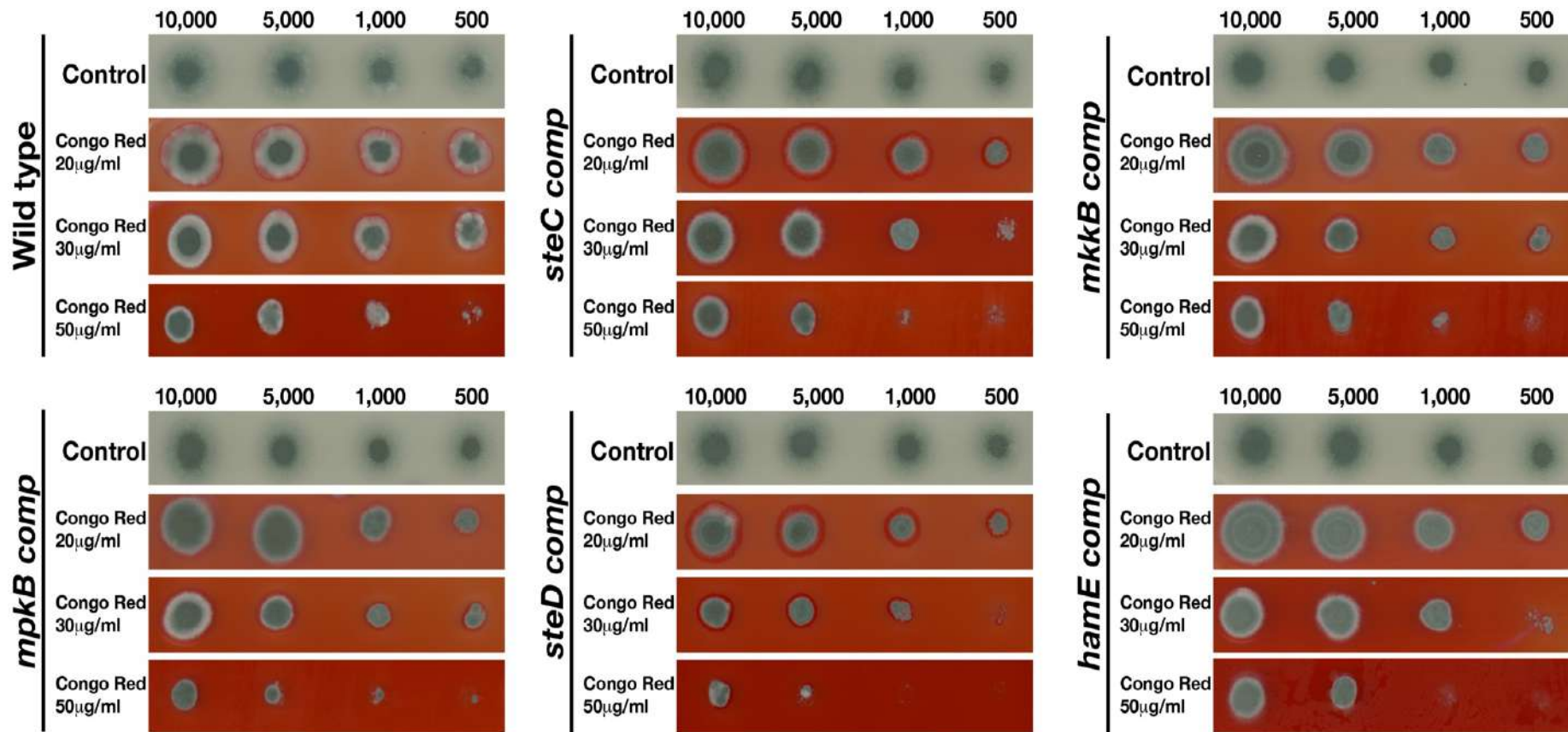
Figure 5.7. Growth phenotypes of the CEA17 wild type and complementation strains in the presence of various concentrations of Congo Red.
Strains were point-inoculated on GMM agar plates containing either 20μg, 30μg or 50μg Congo Red and left to incubate at 37˚C for 3 days.

5.3.2. Each mutant strain exhibited reduced radial growth in the presence of H_2O_2.

To determine whether or not the pheromone module proteins contribute to the response to oxidative stress, each strain was inoculated on plates containing various concentrations (2mM, 3mM and 4mM) of the oxidative stress agent H_2O_2 (**Figures 5.8. and 5.9.**). It was observed that the CEA17 wild type strain did not exhibit any significant growth impairments in the presence of any of the H_2O_2 concentrations tested. The radial growth of each inoculated CEA17 colony in the presence of H_2O_2 was similar to the growth on the control plates. However, it was observed that the wild type colonies inoculated in the presence of H_2O_2 displayed significantly reduced sporulation levels in comparison to colonies on the control plates.

For each of the mutant strains, it was apparent that the presence of H_2O_2 significantly impaired radial growth. The growth of each strain was reduced in the presence of all H_2O_2 concentrations tested and minimal growth was observed for each strain in the presence of 4mM H_2O_2. The complementation of each gene resulted in the restoration of radial growth, comparable to the rates observed for the wild type colonies, albeit slightly smaller. In the presence of each H_2O_2 concentration, these complementation strains closely resembled the wild type colonies with regards to both radial growth and levels of sporulation.
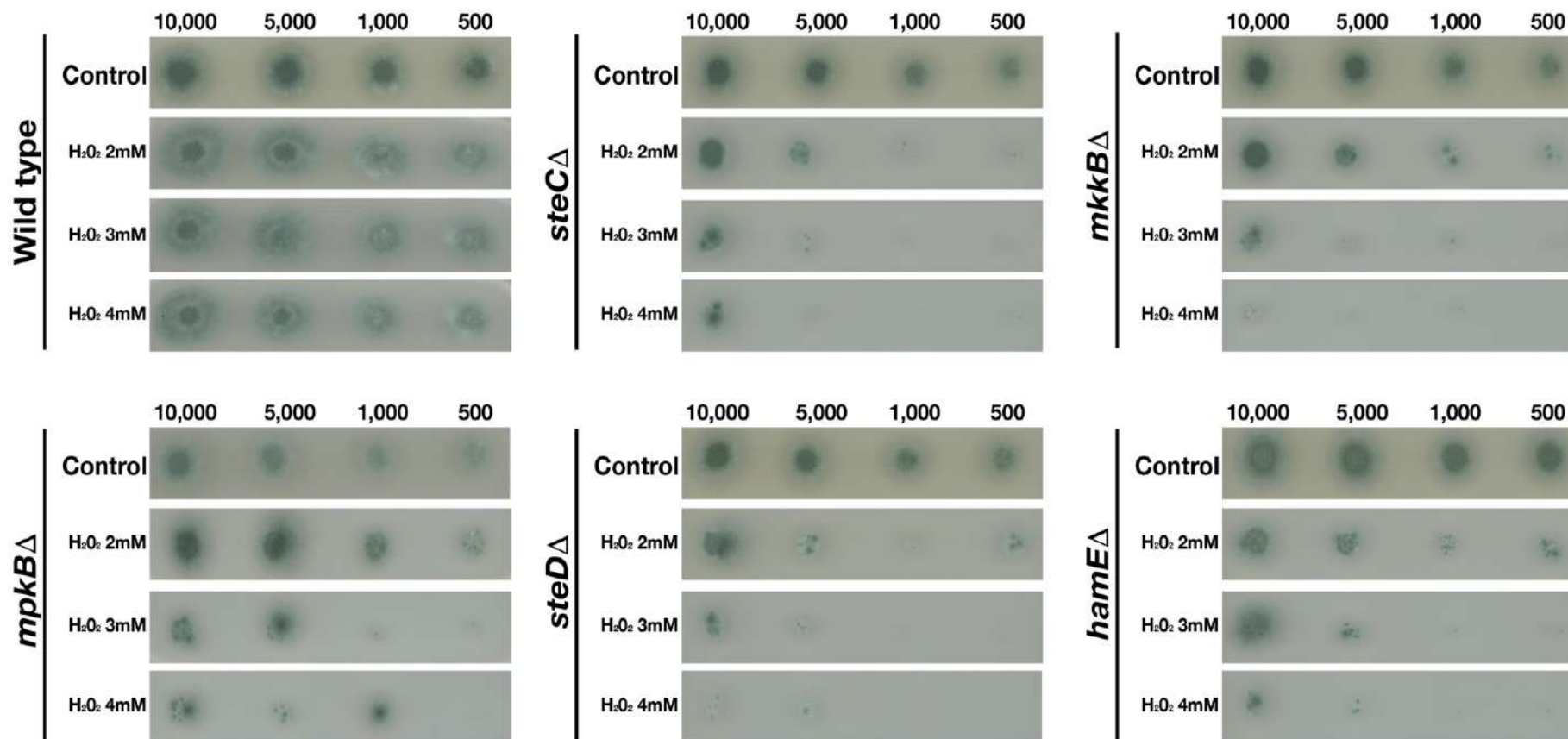
Figure 5.8. Growth phenotypes of the CEA17 wild type and mutant strains in the presence of various concentrations of H_2O_2. Strains were point-innoculated on GMM agar plates containing either 2mM, 3mM or 4mM H_2O_2 and left to incubate at 37˚C for 3 days.
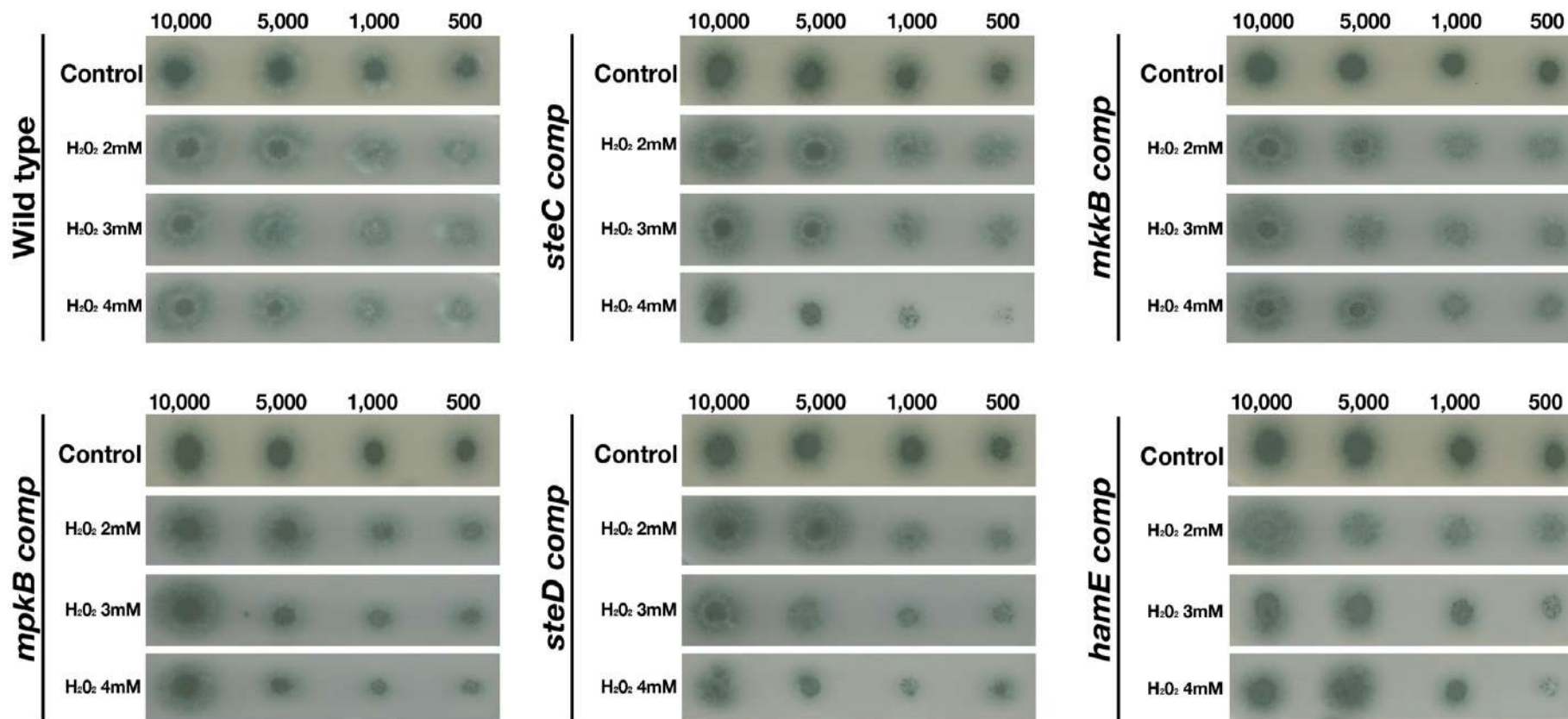
Figure 5.9. Growth phenotypes of the CEA17 wild type and complementation strains in the presence of various concentrations of H_2O_2. Strains were point-innoculated on GMM agar plates containing either 2mM, 3mM or 4mM H_2O_2 and left to incubate at 37°C for 3 days.

5.3.3. Deletion of *steC, mkkB, mpkB* or *steD* results in increased sporulation in the presence of NaCl.

In order to assess whether the pheromone module proteins play a role in the response to osmotic stress, each strain was inoculated on plates containing various concentrations of the osmotic stress agent NaCl (**Figures 5.10. and 5.11.)**. It was observed that in the presence of 0.5M NaCl, the radial growth of all strains, including the wild type was not inhibited (**Figure 5.10)**. At higher concentrations of NaCl (1M and 1.5M), the radial growth of all strains, including the wild type was significantly reduced. At 1.5M NaCl, growth of all strains was minimal but overall, no differences were observed between strains with regards to the rates of vegetative growth in the presence of osmotic stress. The complementation of each gene resulted in similar phenotypes as those observed for the mutant strains and wild type (**Figure 5.11.**).

Interestingly, in the presence of 0.5M and 1M NaCl, it was apparent that each strain, with the exception of the *hamE* mutant produced more spores and displayed a darker pigmentation in comparison to the wild type and the respective strains cultured on GMM without added stressors (**Figures 5.10. and 5.12.**). To visualise the differences in sporulation more efficiently, the undersides of each plate were imaged, using a dark background (**Figures 5.12. and 5.13.**). Imaging from the undersides of each colony revealed dramatic differences in sporulation between each strain. The wild type and *hamE* mutant colonies appeared white in the presence of all NaCl concentrations. However, in the presence of 0.5M and 1M NaCl, the *steC, mkkB, mpkB* and *steD* mutants exhibited increased levels of sporulation (**Figures 5.12.**). In the presence of 1.5M NaCl, each colony displayed a white phenotype and were all similar to the wild type. The complementation of each gene resulted in the restoration of the wild type phenotype, with each strain exhibiting a pale white phenotype in the presence of all NaCl concentrations tested (**Figures 5.13.**).

Taken together, the results of these stress tests indicate that the pheromone module proteins contribute to the regulation of cellular responses to cell wall stress and oxidative stress. The deletion of any of the five members of the pheromone module complex results in increased sensitivity to both the cell wall stress agent Congo Red and the oxidative stressor H_2O_2. The roles of the pheromone module complex in response to osmotic stress are less clear. It appears that the deletion of these genes does not influence sensitivity of NaCl. However, it is apparent that in the presence of an osmotic stress agent, the deletion

167

of *steC, mkkB, mpkB* or *steD* results in increased sporulation. This could indicate that these four proteins play a role in negatively regulating sporulation in the presence of osmotic stressors. This could be similar to the mechanism described for yeast Hog1, whereby it becomes activated in the response to pheromone signals in the absence of *fus3*. Interestingly, it has been shown previously in both *A. fumigatus* (Manfiolli et al., 2019) and *A. nidulans* (Paoletti et al., 2007, Kang et al., 2013) that an *mpkB* mutant induces formation of conidiophores in submerged cultures, indicating that the other members of the pathway could also contribute to this method of both positively and negatively regulating conidiation under specific circumstances, although this would require further testing to confirm these claims.
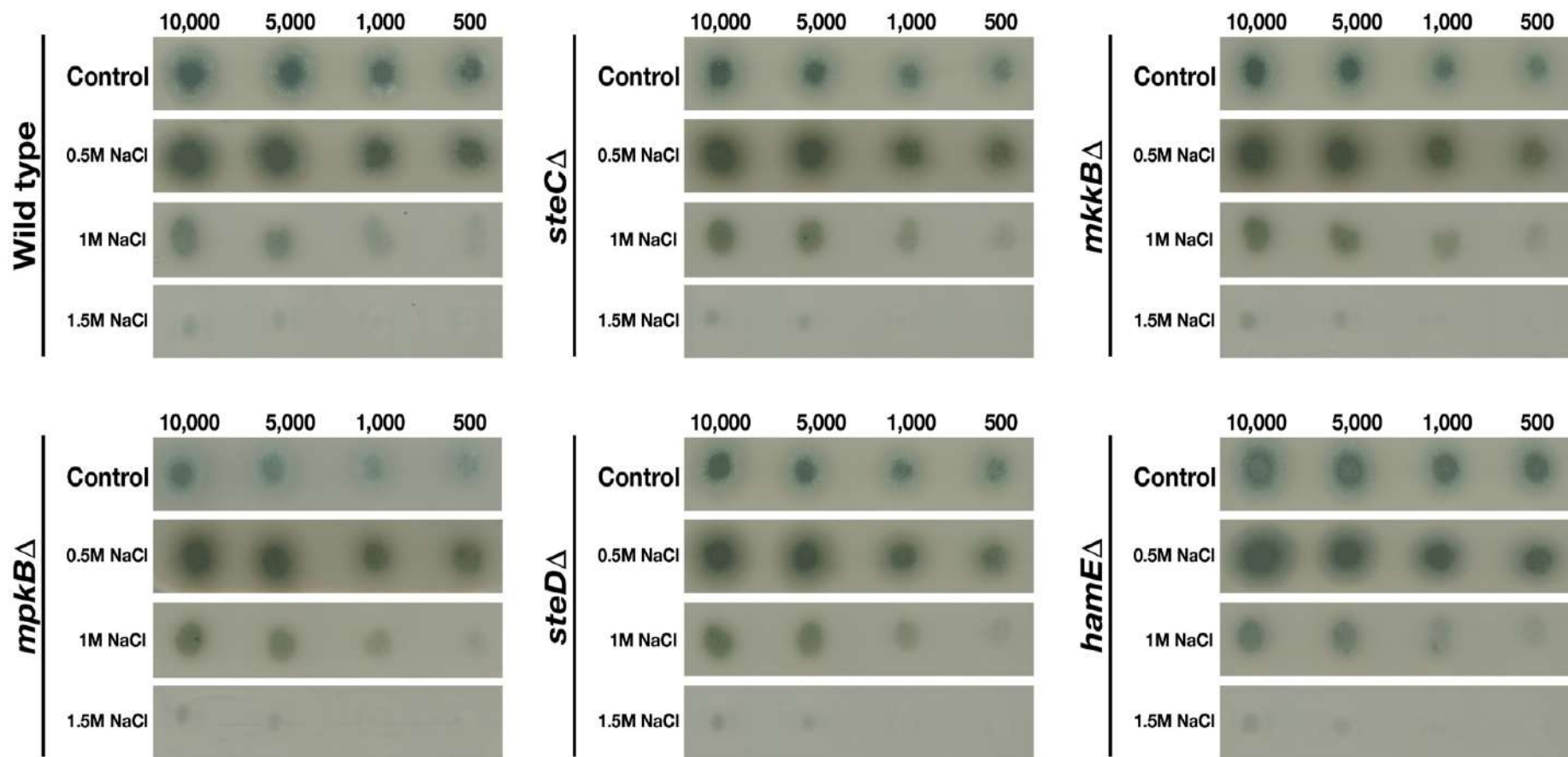
Figure 5.10. Growth phenotypes of the CEA17 wild type and mutant strains in the presence of various concentrations of NaCl. Strains were point-innoculated on GMM agar plates containing either 0.5M, 1M or 1.5M NaCl and left to incubate at 37˚C for 3 days.
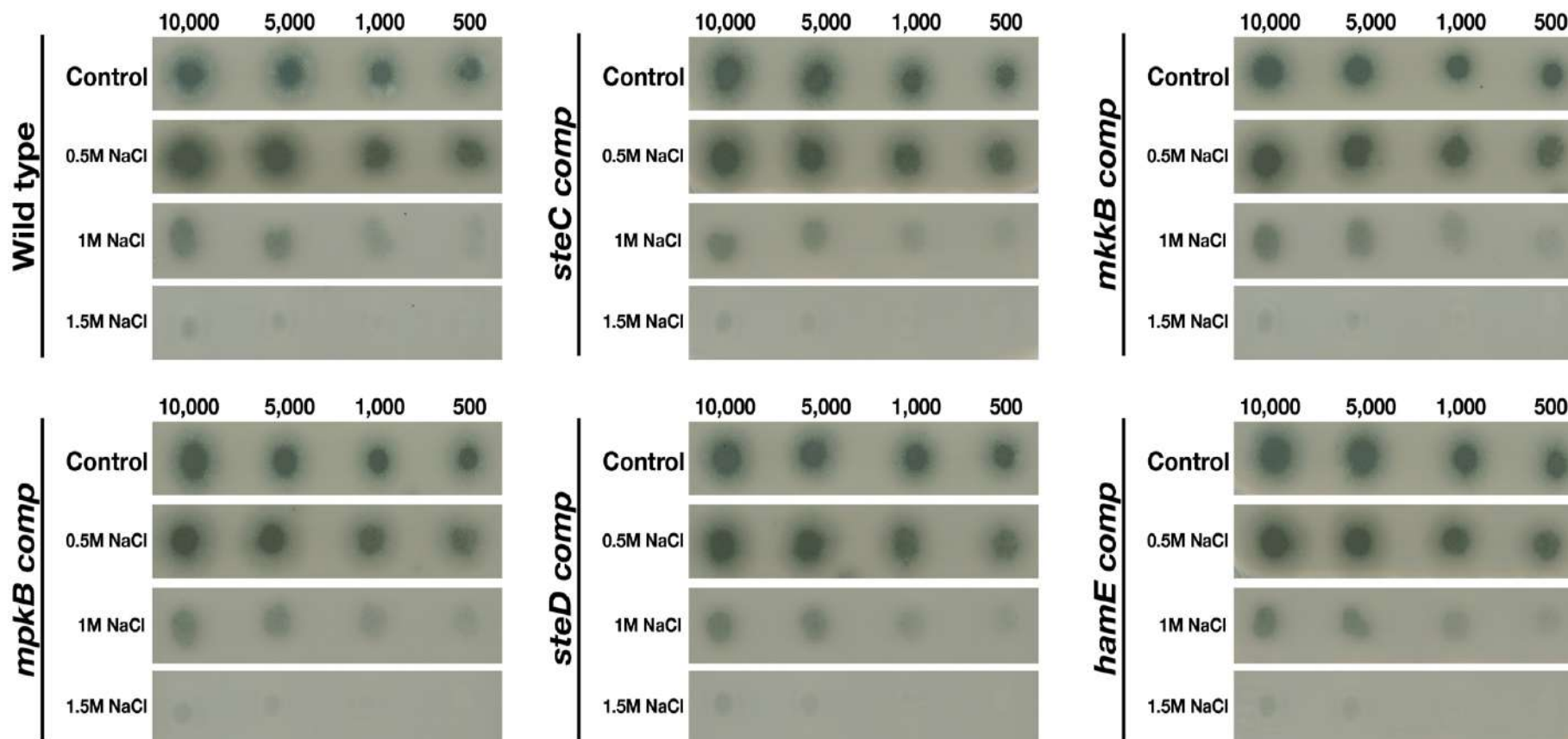
Figure 5.11. Growth phenotypes of the CEA17 wild type and complementation strains in the presence of various concentrations of NaCl.
Strains were point-innoculated on GMM agar plates containing either 0.5M, 1M or 1.5M NaCl and left to incubate at 37°C for 3 days.
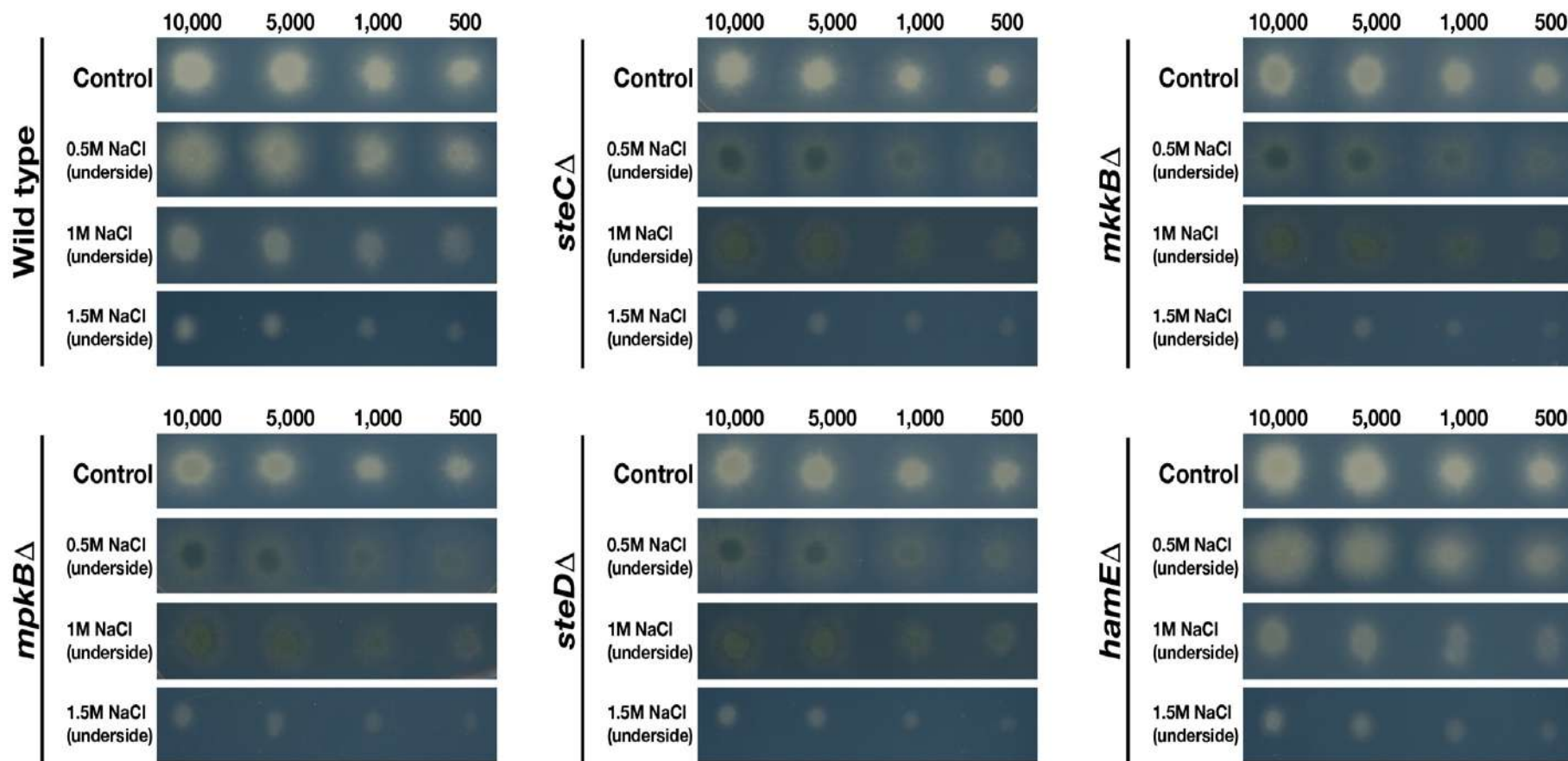
Figure 5.12. Images of the undersides of the CEA17 wild type and mutant strains in the presence of various concentrations of NaCl. The undersides of the colonies from **Figure 5.10.** were imaged to visualise the pigmentation of each stain.
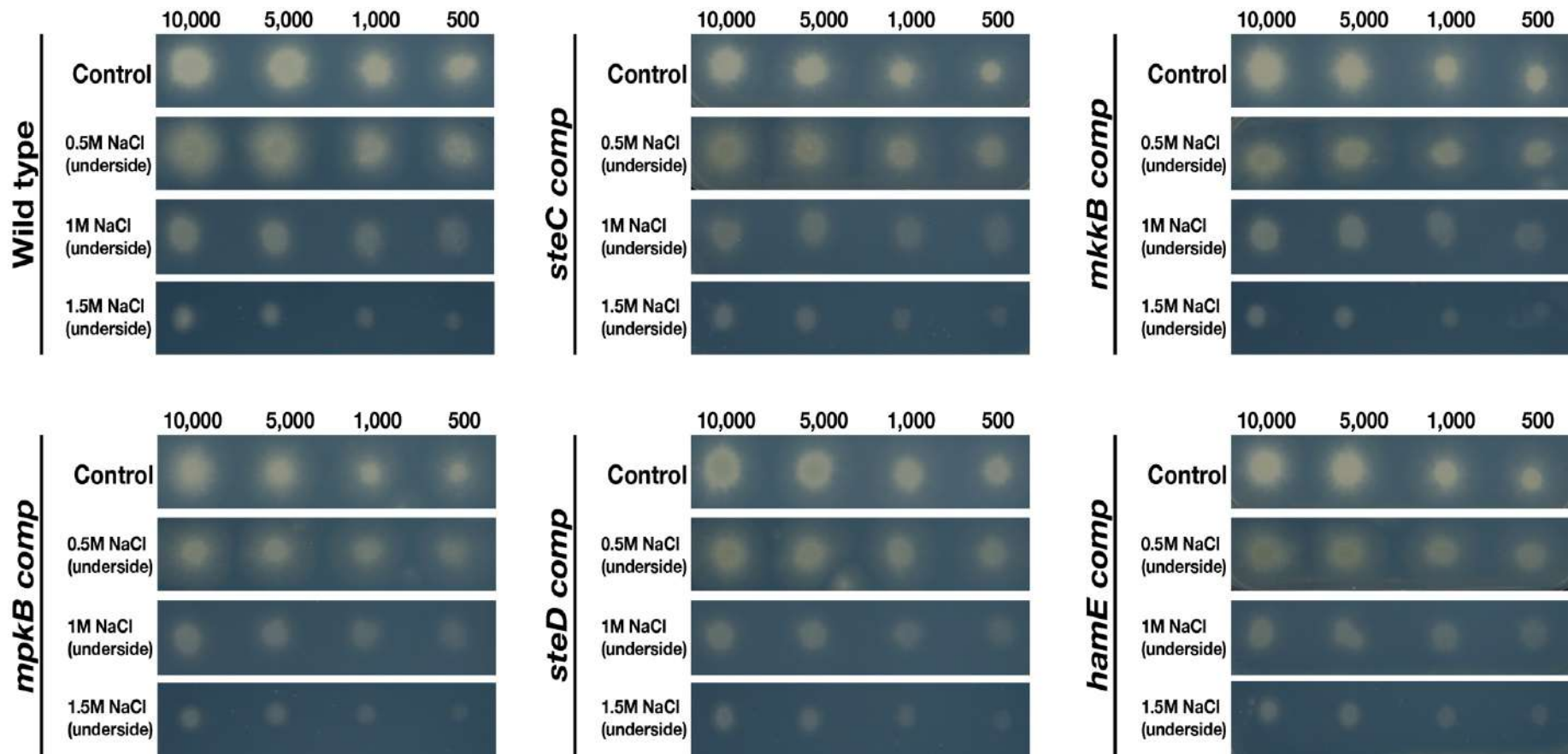
Figure 5.13. Images of the undersides of the CEA17 wild type and complementation strains in the presence of various concentrations of NaCl.
The undersides of the colonies from **Figure 5.11.** were imaged to visualise the pigmentation of each stain.

172

5.4. The production of various SMs is dependent on the pheromone module proteins

In order to determine the roles of the pheromone module proteins with regards to the regulation of secondary metabolism in *A. fumigatus*, the levels of various SMs produced by the pheromone module mutants were determined by LC-MS analysis. *A. fumigatus* is capable of producing a myriad of SMs, most of which are uncharacterised. Of the 40 predicted SM clusters in *A. fumigatus,* 19 of these have been linked to functional products (Romsdahl and Wang, 2019). The most notable SM is the immunosuppressive agent gliotoxin, which is a major contributor to *A. fumigatus* virulence (Hof and Kupfahl, 2009, Ghazaei, 2017). Other notable SMs produced by *A. fumigatus* include (i) fumagillin, an anti-angiogenic compound (Sin et al., 1997, Mc et al., 1951), (ii) pseurotin A, a competitive inhibitor of chitin synthase which is also an inducer of nerve cell proliferation and acts as an immunosuppressive agent (Maiya et al., 2007, Ishikawa et al., 2009), (iii) pseurotin D, which exhibits apomorphine-antagonistic activity (Ishikawa and Ninomiya, 2008), (iv) cyclotryprostatin, which is a compound that inhibits the mammalian cell cycle at the G2/M phase (Cui et al., 1997) and (v) pyripyropene A, which exhibits insecticidal properties (Horikoshi et al., 2017).

5.4.1. Gliotoxin production is significantly decreased in each of the pheromone module mutants

To quantify the levels of gliotoxin production in each mutant, each strain was inoculated (10^7 spores/ml) in triplicate in 40ml Czapek-Dox medium and left to incubate on a shaker at 37°C for 72 hours. Crude metabolite extracts were isolated and HPLC analysis was performed to detect the levels of gliotoxin. The average peak area values were plotted as a percentage of the wild type average which was chosen to represent 100% production (**Figure 5.14.**). It was found that each mutant produces significantly less gliotoxin in comparison to the wild type. The average reductions in gliotoxin production for the mutant strains were between 63-80%. Crude metabolite extracts were also isolated from each complementation strain to determine if the reductions in gliotoxin production were a direct cause of these gene deletions. It was observed that the complementation of each gene restored the ability of these strains to produce gliotoxin to a similar degree as that observed for the wild type strain. The average levels of gliotoxin production for the complementation strains ranged between 87%-145% of the wild type average. Statistical

173

tests showed no significant differences between the wild type and complementation strain averages.
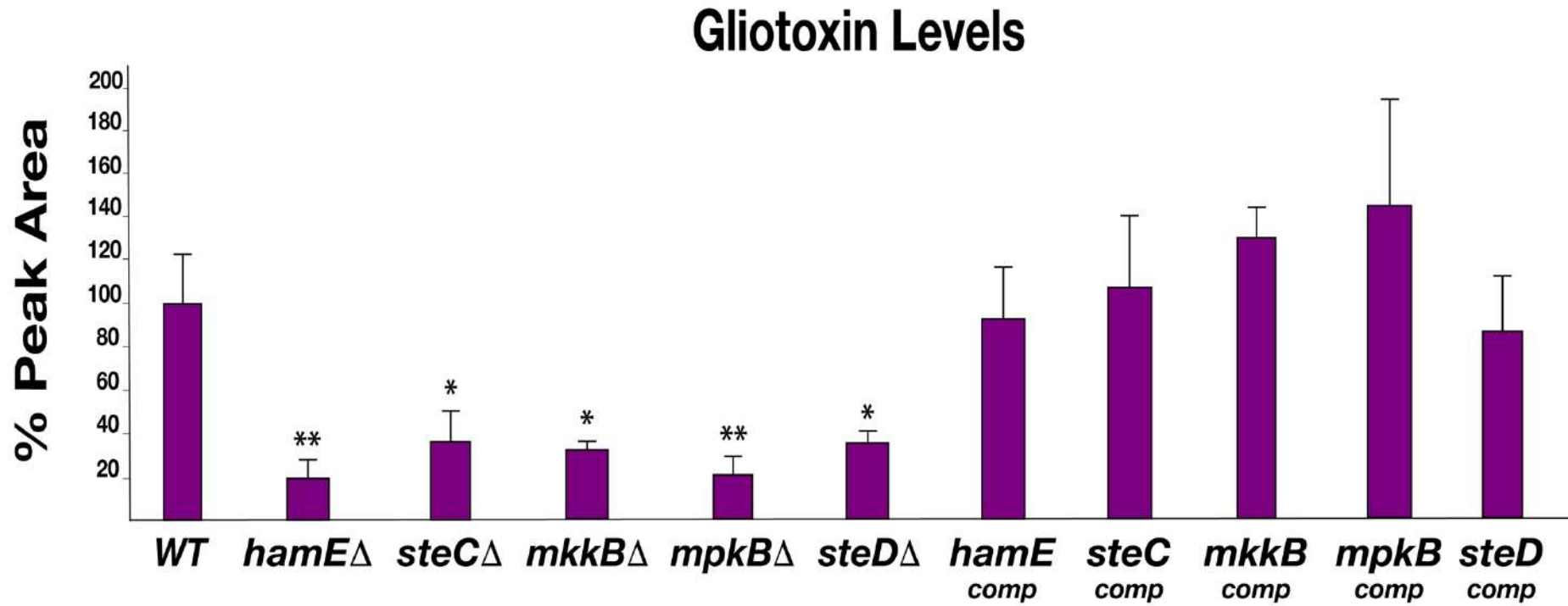
Figure 5.14. HPLC detection of the levels of gliotoxin produced by deletion and complementation strains. Strains were inoculated (10^7 spores/ml) in triplicate in 40ml Czapek-Dox medium and left to incubate on a shaker at 37˚C for 72 hours. A gliotoxin standard was used as a reference. Average peak area values were plotted as a percentage of the wild type ± s.d. *P*-values were calculated by performing unpaired Student's *t*-tests (*$P<0.05$; **$P<0.01$).

5.4.2. An *mkkB* mutant exhibits decreased levels of SM production

To determine the levels of pseurotin A, pseurotin D, fumagillin and pyripyropene A in the wild type, *hamE* mutant, *mkkB* mutant and respective complementation strains, LC-MS analysis was performed. Each strain was inoculated in triplicate in 40ml of liquid GMM and incubated for 48 hours on a shaker at 37˚C.

Interestingly, the *hamE* mutant and the *mkkB* mutant exhibited different trends in production of all four metabolites tested. It was observed that pseurotin A production (**Figure 5.15. (b)**) is increased in the *hamE* mutant (63% increase) and significantly decreased in the *mkkB* mutant (65% decrease). For pseurotin D (**Figure 5.15. (d)**), the levels showed a similar trend, with an increase in production being observed in the *hamE* mutant (37% increase) and a significant decrease being evident in the *mkkB* mutant (69% decrease). Fumagillin production (**Figure 5.16. (b)**) shows no significant difference between the wild type and *hamE* mutant, whereas in the *mkkB* mutant, the levels of production are dramatically reduced (31% decrease). Lastly, the levels of pyripyropene A (**Figure 5.16. (d)**) were slightly increased in the *hamE* mutant (20% increase), whereas production of this compound was significantly decreased in the *mkkB* mutant (50% decrease).

Overall, these data suggest that MkkB is critical for the positive regulation of gliotoxin, pseurotin A, pseurotin D, fumagillin and pyripyropene A. However, HamE is required for the positive regulation of gliotoxin and negative regulation of pseurotin A, pseurotin D and pyripyropene A, whilst having no apparent effects in the regulation of fumagillin production. This could suggest that HamE may also act independently of the pheromone module to regulate secondary metabolism, perhaps in a similar manner to what is observed in *A. flavus* (Frawley et al., 2020a).

a
Pseurotin A peak area values

Sample	Apex RT	Start RT	End RT	Area	%Area	Height	%Height
WT-1	8.71	8.65	8.78	2252906.93	28.26	695533.555	20.4
WT-2	8.71	8.65	8.79	2116475.82	28.53	667283.74	19.9
WT-3	8.72	8.66	8.79	2242612.04	28.07	685847.275	20.04
hamE deletion-1	8.71	8.65	8.78	3647660.02	36.85	1023676.33	25.25
hamE deletion-2	8.71	8.65	8.79	3341503.15	34.22	966780.892	23.28
hamE deletion-3	8.72	8.66	8.79	3793050.83	32.91	1099636.92	23.86
mkkB deletion-1	8.72	8.66	8.8	716519.044	14.9	201551.552	8.9
mkkB deletion-2	8.72	8.66	8.79	800232.225	14.62	222597.854	8.78
mkkB deletion-3	8.72	8.67	8.8	812913.339	13.53	228178.69	8.64
hamE comp-1	8.71	8.67	8.79	3756278.58	34.36	1096887.25	23.66
hamE comp-2	8.71	8.65	8.79	4024133.08	35.05	1128846.87	23.37
hamE comp-3	8.72	8.66	8.78	3658469.04	31.54	1096503.41	21.93
mkkB comp-1	8.71	8.66	8.79	3850922.75	36.17	1127132.86	25
mkkB comp-2	8.71	8.65	8.79	4009090.75	35.79	1137257.86	24.22
mkkB comp-3	8.72	8.66	8.79	3712897.51	33.68	1104820.25	23.36

c
Pseurotin D peak area values

Sample	Apex RT	Start RT	End RT	Area	%Area	Height	%Height
WT-1	9.05	9.03	9.08	380251.118	4.77	210161.937	6.16
WT-2	9.06	9.04	9.08	364951.769	4.92	203190.467	6.06
WT-3	9.06	9.03	9.08	387574.864	4.85	214401.464	6.27
hamE deletion-1	9.05	9.03	9.08	500946.548	5.06	272955.187	6.73
hamE deletion-2	9.06	9.04	9.09	503340.945	5.15	274308.597	6.6
hamE deletion-3	9.06	9.03	9.08	548166.477	4.76	300807.793	6.53
mkkB deletion-1	9.05	9.03	9.08	109687.437	2.28	61954.349	2.74
mkkB deletion-2	9.06	9.04	9.09	112152.931	2.05	63838.591	2.52
mkkB deletion-3	9.06	9.04	9.08	133101.349	2.22	74723.16	2.83
hamE comp-1	9.05	9.03	9.08	247390.019	2.26	137797.831	2.97
hamE comp-2	9.06	9.03	9.08	247585.463	2.16	138837.262	2.87
hamE comp-3	9.06	9.03	9.08	265047.95	2.29	148744.346	2.97
mkkB comp-1	9.05	9.03	9.08	255720.945	2.4	143318.547	3.18
mkkB comp-2	9.06	9.03	9.08	264325.161	2.36	148292.558	3.16
mkkB comp-3	9.06	9.04	9.09	278323.953	2.52	156099.718	3.3

Figure 5.15. LC-MS detection of the levels of pseurotin A and pseurotin D produced by deletion and complementation strains. Strains were inoculated in triplicate in 40ml of liquid GMM (5 million spores/ml) and incubated for 48 hours at 37°C. Average peak area values were plotted as a percentage of the wild type ± s.d. *P*-values were calculated by performing unpaired Student's *t*-tests (**$P<0.01$; ***$P<0.001$). (a) Peak area values of pseurotin A (b) Graphical representation of the pseurotin A levels in each strain. (c) Peak area values of pseurotin D (d) Graphical representation of the pseurotin D levels in each strain.

a

Fumagillin peak area values

Sample	Apex RT	Start RT	End RT	Area	%Area	Height	%Height
WT-1	13.63	13.6	13.66	1590606.91	19.95	659368.837	19.34
WT-2	13.64	13.61	13.67	1570726.01	21.17	654960.797	19.53
WT-3	13.64	13.61	13.67	1605068.26	20.09	665869.978	19.46
hamE deletion-1	13.63	13.6	13.67	1670386.63	16.88	650686.25	16.05
hamE deletion-2	13.65	13.62	13.68	1639709.01	16.79	648423.613	15.61
hamE deletion-3	13.64	13.61	13.67	1834220.25	15.91	733564.928	15.92
mkkB deletion-1	13.63	13.6	13.66	1032302.04	21.47	476382.04	21.04
mkkB deletion-2	13.64	13.61	13.67	1132824.86	20.7	526477.456	20.77
mkkB deletion-3	13.64	13.61	13.67	1128830.4	18.79	518476.131	19.64
hamE comp-1	13.63	13.59	13.66	1946057.04	17.8	754735.148	16.28
hamE comp-2	13.64	13.6	13.67	1993889.2	17.37	773820.583	16.02
hamE comp-3	13.64	13.6	13.67	2020374.36	17.42	788294.924	15.76
mkkB comp-1	13.63	13.6	13.66	1833439.03	17.22	732959.093	16.26
mkkB comp-2	13.64	13.61	13.67	1885196.86	16.83	746252.127	15.89
mkkB comp-3	13.64	13.61	13.68	1929839.07	17.51	759607.453	16.06

b

c

Pyripyropene A peak area values

Sample	Apex RT	Start RT	End RT	Area	%Area	Height	%Height
WT-1	11.33	11.31	11.35	153895.482	1.93	85058.308	2.49
WT-2	11.32	11.29	11.34	158614.798	2.14	87193.057	2.6
WT-3	11.33	11.31	11.36	161126.77	2.02	89161.479	2.61
hamE deletion-1	11.32	11.3	11.35	179888.318	1.82	99535.898	2.46
hamE deletion-2	11.31	11.28	11.33	195781.35	2.01	108400.882	2.61
hamE deletion-3	11.33	11.31	11.35	192390.543	1.67	107849.542	2.34
mkkB deletion-1	11.32	11.3	11.35	69975.325	1.46	38691.063	1.71
mkkB deletion-2	11.31	11.29	11.33	80437.921	1.47	44428.047	1.75
mkkB deletion-3	11.33	11.31	11.36	85349.053	1.42	47554.274	1.8
hamE comp-1	11.32	11.3	11.35	80369.712	0.74	45109.112	0.97
hamE comp-2	11.31	11.29	11.34	81607.641	0.71	46079.399	0.95
hamE comp-3	11.33	11.31	11.35	84031.152	0.72	47837.628	0.96
mkkB comp-1	11.33	11.3	11.35	80275.629	0.75	44694.158	0.99
mkkB comp-2	11.32	11.29	11.34	86962.241	0.78	48444.605	1.03
mkkB comp-3	11.33	11.31	11.36	88916.51	0.81	49817.485	1.05

d

Figure 5.16. LC-MS detection of the levels of fumagillin and pyripyropene A produced by deletion and complementation strains. Culturing of strains and statistical calculations are as described in the **Figure 5.15** figure legend. (**$P<0.01$; ***$P<0.001$). (a) Peak area values of fumagillin. (b) Graphical representation of the fumagillin levels in each strain. (c) Peak area values of pyripyropene A (d) Graphical representation of the pyripyropene A levels in each strain.

5.5. The pheromone module may assemble in the cytoplasm and MpkB enters the nucleus

Confocal microscopy imaging was performed to determine the sub-cellular localisations of the pheromone module proteins *in vivo*, using the GFP-tagged proteins and a DAPI stain for the nuclei (**Figure 5.17.**). Strains from panels (a-d) were inoculated in 400μl of liquid GMM which contained appropriate supplements. Each of these strains was cultured for various durations (24 hours or less) at 30˚C. Strains were imaged initially without DAPI staining to observe the localisations of these proteins in living material. Samples were later fixed and stained with DAPI to compare the localisations of these proteins with respect to the nuclei.

Confocal microscopy imaging revealed that SteC-GFP displayed cytoplasmic fluorescence that was uniform throughout hyphae. This fusion protein was also shown to be excluded from interphase nuclei. (**Figure 4.17. (a)**). MkkB-GFP fluorescence was uniformly distributed throughout fungal hyphae. It was observed that this fusion protein is mostly cytoplasmic and is excluded from interphase nuclei and vacuoles. This protein was also observed to be enriched at the central portion of some septa and hyphal tips (**Figure 4.17. (b)**). MpkB-GFP exhibited mostly cytoplasmic distribution throughout fungal hyphae that was fairly uniform. However, MpkB was also observed to be slightly more concentrated in interphase nuclei and at the hyphal apices (**Figure 4.17. (c)**). SteD-GFP fluorescence was faint and mostly uniform throughout the fungal hyphae. This fusion protein was found to be cytoplasmic and is excluded from interphase nuclei and vacuoles (**Figure 4.17. (d)**).

To observe the sub-cellular localisation of HamE *in vivo,* immunostaining was performed, using the HamE-HA strain. This strain was cultured on sterile coverslips submerged in Sabouraud medium with required supplements. The strain was left to incubate at 30˚C for 16 hours without agitation. DAPI staining was used to stain the nuclei blue and the two images were merged to show the localisation of the HamE protein with respect to the nuclei in the fungal hyphae. It was observed that the HamE protein becomes enriched at the hyphal tips and the plasma membrane and is absent from the nuclei (**Figure 4.17. (e)**). Overall, these data complement findings in both *A. nidulans* (Bayram and Braus, 2012, Frawley et al., 2018) and *A. flavus* (Frawley et al., 2020a), suggesting that a conserved mechanism of complex assembly and signalling exists in *A. fumigatus.*
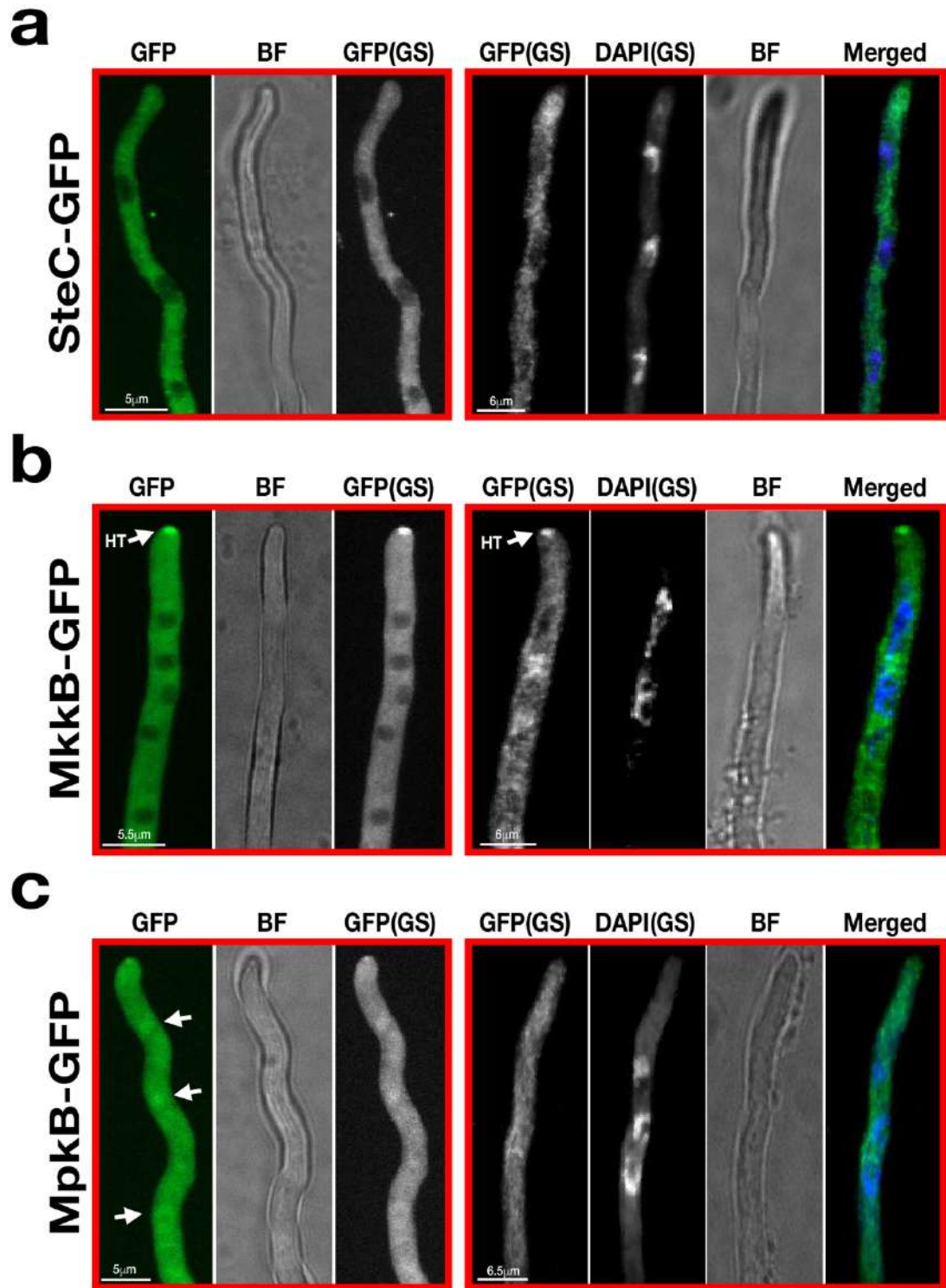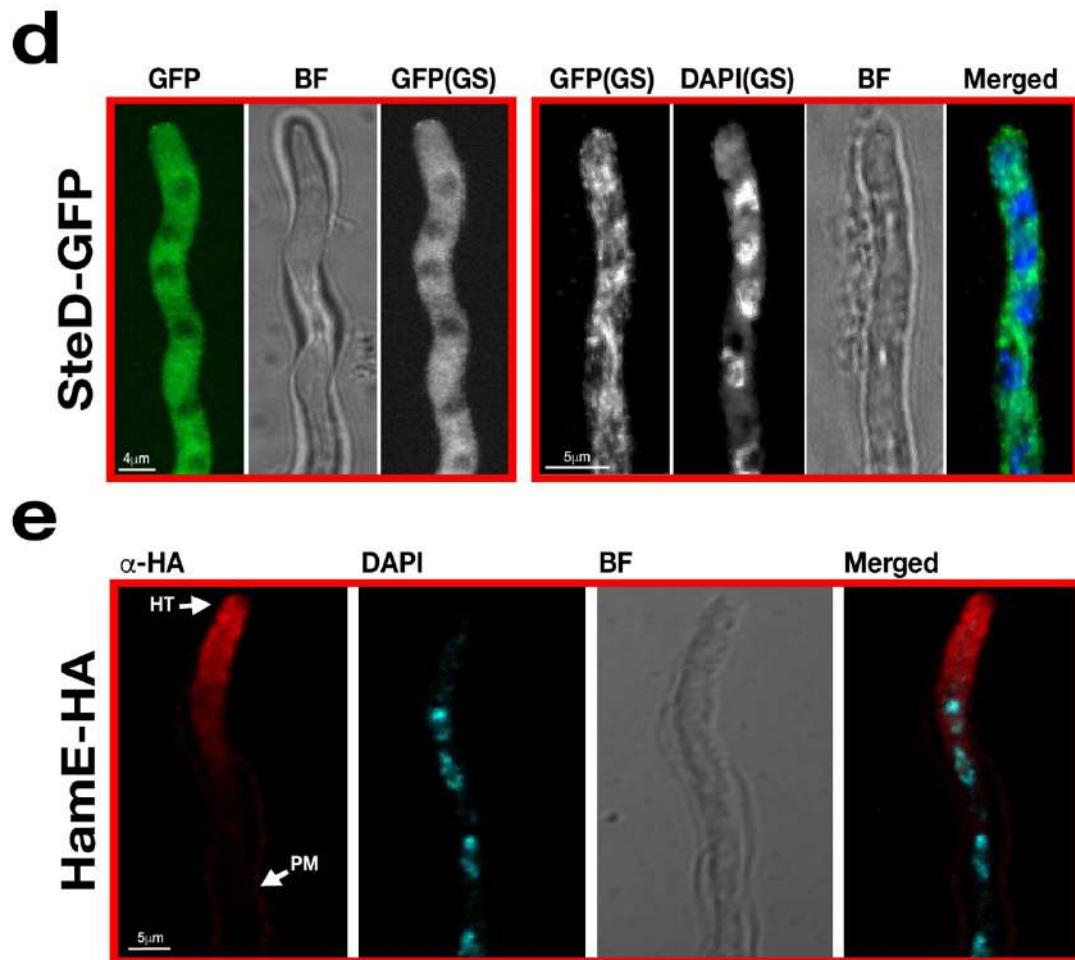
Figure 5.17. Sub-cellular localisations of the pheromone module proteins *in vivo*. (a) Sub-cellular localisation of SteC-GFP. Strains from panels a-d were incubated at 30°C for various durations in 400μL of liquid GMM, containing appropriate supplements. 'BF' (brightfield images). 'GS' (grayscale images). To visualise the nuclei, DAPI staining was performed. White arrows depict the accumulation of fusion protein in the nuclei. 'HT' refers to accumulation of protein at hyphal tips. (b) Sub-cellular localisation of MkkB-GFP. (c) Sub-cellular localisation of MpkB-GFP. (d) Sub-cellular localisation of SteD-GFP. (e) Sub-cellular localisation of HamE-HA. The HamE-HA strain was inoculated ($5x10^3$ spores) on sterile coverslips, covered in 450μL of Sabouraud medium, containing supplements. This strain were left to incubate at 30 °C for 16 hours.

5.6. Summary of main findings and chapter conclusions

5.6.1. The pheromone module is conserved in *A. fumigatus* and may exist as a pentameric complex

In this chapter, orthologs of all five members of the *A. nidulans* pheromone module were found to exist in *A. fumigatus*. These proteins were shown to exhibit high similarity to the respective *A. nidulans* proteins (**Figure 5.1.**), signifying their evolutionary conservation and importance. However, it was apparent that the provided protein sequence for SteC in *A. fumigatus* was considerably larger than the respective SteC protein in *A. nidulans*. Sequence alignment of the two proteins led to the proposal that an alternative stop codon exists in the *A. fumigatus* SteC sequence (**Appendix C: Figure S3**). Tagging from this newly proposed stop codon resulted in successful transformation, confirming that the sequence provided on ASPGD is incorrect.

Immunoprecipitations and LC-MS/MS analysis revealed that a pentameric complex may be formed in *A. fumigatus* (**Figure 5.2.)**. This complex consists of the MAP3K SteC (Afu5g06420), the MAP2K MkkB (Afu3g05900), the MAPK MpkB (Afu6g12820), the adaptor protein SteD (Afu6g17130) and potentially the scaffold HamE (Afu5g13970). However, HamE was only shown to interact with MkkB in MkkB immunoprecipitations and this reaction was not confirmed reciprocally. Perhaps this interaction is transient and thus, further experiments would be required to fully confirm that HamE exists as a member of the complex.

5.6.2. Each member of the pheromone module contributes to the regulation of asexual sporulation and radial growth rate

The *A. fumigatus steC, mkkB, mpkB, steD* and *hamE* genes were deleted to monitor the influence of the respective proteins in the regulation of fungal development. It was observed that each mutant displayed significant reductions in asexual reproduction, (**Figures 5.3. and 5.4.**) and vegetative growth rate (**Figure 5.5.**). Each gene was then complemented to restore gene functionality. It was observed that the complementation of each gene restored the ability of these strains to undergo normal asexual sporulation and vegetative growth, as the phenotypes of each strain resembled the wild type. Overall, these data provide evidence that each of the five proteins tested all contribute in a similar

manner to regulate the development of *A. fumigatus,* which could support the hypothesis that these proteins all form a complex and function within the same signalling pathway.

5.6.3. The pheromone module proteins regulate various cell stress responses

To assess whether the pheromone module proteins contribute to the regulation of various cell stress responses, each mutant strain was cultured in the presence of multiple cell stressors. It was observed that each mutant exhibited increased sensitivity to the cell wall stress agent Congo Red (**Figure 5.6.**) and the oxidative stressor H_2O_2 (**Figure 5.8.**). In the presence of the osmotic stress agent NaCl, mutant strains did not display any significant reductions in growth. However, it was observed that in the presence of 0.5M and 1M NaCl, the *steC, mkkB, mpkB* and *steD* mutants exhibited significantly increased levels of sporulation in comparison to the wild type strain, while the *hamE* mutant resembled the wild type (**Figures 5.10. and 5.12.**). Complementation of each gene resulted in the restoration of the wild type phenotypes in the presence of all stress agents tested. Complementation strains grew more than the respective mutants in the presence of all Congo Red (**Figure 5.7.**) and H_2O_2 (**Figure 5.9.**) concentrations. Interestingly, the complementation strains also exhibited reduced sporulation in the presence of NaCl, thus resembling the wild type (**Figures 5.11. and 5.13.**).

Overall, these data suggest that signalling *via* the pheromone module pathway may positively regulate the cell wall stress pathway and oxidative stress response. It can also be proposed that inactivation of pheromone module pathway signalling may positively increase sporulation in the presence of osmotic stress agents. However, HamE does not contribute to this mechanism of regulation and may not be implicated in the osmotic stress response.

5.6.4. The production of a myriad of SMs is dependent on the pheromone module

To determine whether the pheromone module proteins are involved in the regulation of secondary metabolism, LC-MS analysis was performed to detect the levels of various metabolites produced by the mutant and complementation strains (**Figures 5.14., 5.15. and 5.16.**). It was observed that the deletion of any of the pheromone module proteins

results in dramatic reductions in gliotoxin production (**Figure 5.14.**), whereas the complementation of each pheromone module gene restores the ability of these strains to produce gliotoxin and the levels of production resemble those observed for the wild type strain. The levels of pseurotin A (**Figure 5.15. (b)**), pseurotin D (**Figure 5.15. (d)**), fumagillin (**Figure 5.16. (b)**) and pyripyropene A (**Figure 5.16. (d)**) were determined in both the *mkkB* and *hamE* mutants and the respective complementation strains. Interestingly, it was observed that while MkkB is critical for the positive regulation of all four of these compounds, the deletion of *hamE* elicited an increase in production of all of these compounds, aside from fumagillin, which exhibited similar trends to the wild type levels.

In summary, these data suggest that MkkB is critical for the positive regulation of various metabolites and this is likely *via* its interactions within the pheromone module complex. However, the roles of HamE are less clear, as this protein exhibits both positive and negative regulatory roles with regards to SM production. It is possible that HamE functions within the pheromone module to regulate gliotoxin production but perhaps functions independently of this complex to module the production of various metabolites.

5.6.5. The pheromone module may assemble in the cytoplasm and MpkB translocates into the nucleus

In order to determine the sub-cellular localisations of the pheromone module proteins *in vivo*, confocal microscopy imaging was utilised. It was evident that both the SteC-GFP and SteD-GFP fusion proteins were uniformly distributed throughout the cytoplasm of fungal hyphae and both were excluded from interphase nuclei (**Figure 5.17. (a) and (d)**). The MkkB-GFP fusion protein was found to be mostly cytoplasmic but was also enriched at the apices of hyphal tips and at some, but not all septa (**Figure 5.17. (b)**). MpkB-GFP was observed to be dispersed throughout the cytoplasm but was also enriched at the hyphal apices and was the only protein that was localised within interphase nuclei (**Figure 5.17. (c)**). Lastly, *via* immunostaining, the sub-cellular localisation of the HamE-HA fusion protein was determined. It was apparent that this protein becomes highly enriched at the hyphal tips and at the plasma membrane (**Figure 5.17. (e)**).

Taken together, these data suggest that HamE, MkkB and MpkB may accumulate and physically interact at the hyphal tips. It is possible that these three proteins then interact with both SteC and SteD in the cytoplasm to form a pentameric complex. Assembly of this complex could allow for kinase phosphorylation and translocation of MpkB into the nucleus.

5.6.6. Overall conclusions

To summarise the findings from this chapter, orthologs of each of the five *A. nidulans* pheromone module proteins were found to exist in the opportunistic pathogenic fungus *A. fumigatus*. This chapter provides evidence that these five proteins may form a pentameric pheromone module complex, similar to what is observed in *A. nidulans* (Frawley et al., 2018, Bayram et al., 2012). This complex consists of the three kinases SteC, MkkB and MpkB, the adaptor protein SteD and the scaffold protein HamE. The kinases MkkB and MpkB may accumulate and interact with HamE at the hyphal tips, in response to pheromone signalling between neighbouring hyphae. Signal detection could lead to the interaction of this trimer with the cytoplasmic SteC-SteD dimer to form a pentameric complex that allows for efficient kinase phosphorylation and MpkB activation. Presumably, MpkB then translocates into the nucleus, where it interacts with various transcription factors to regulate a myriad of biological processes, such as vegetative growth, asexual sporulation, stress responses and secondary metabolism (**Figure 5.18.**). However, the exact molecular mechanism of signal transduction from hyphal tip to the nuclear envelope, as well as the direct targets of MpkB in the nucleus are currently unknown. The direct role(s) of HamE in the pheromone module are also not fully understood as this protein appears to be required for the positive regulation of various SMs and these trends were not observed in the *mkkB* mutant, suggesting that HamE may also act independently of the pheromone module to regulate secondary metabolism.

Overall, in this chapter, the molecular roles of the pheromone module pathway in *A. fumigatus* were characterised. Consequently, this provides insight on how filamentous fungi regulate their development and secondary metabolism in response to environmental cues. The data from this chapter may contribute to strategies for combatting fungal infections caused by *A. fumigatus*. This species is a prolific producer of SMs like the immunosuppressant gliotoxin and causes lethality in immunocompromised individuals. By identifying a central signalling mechanism for the regulation of both fungal development and production of SMs, this, in turn, may allow for more selective and efficient treatments for patients with invasive aspergillosis.
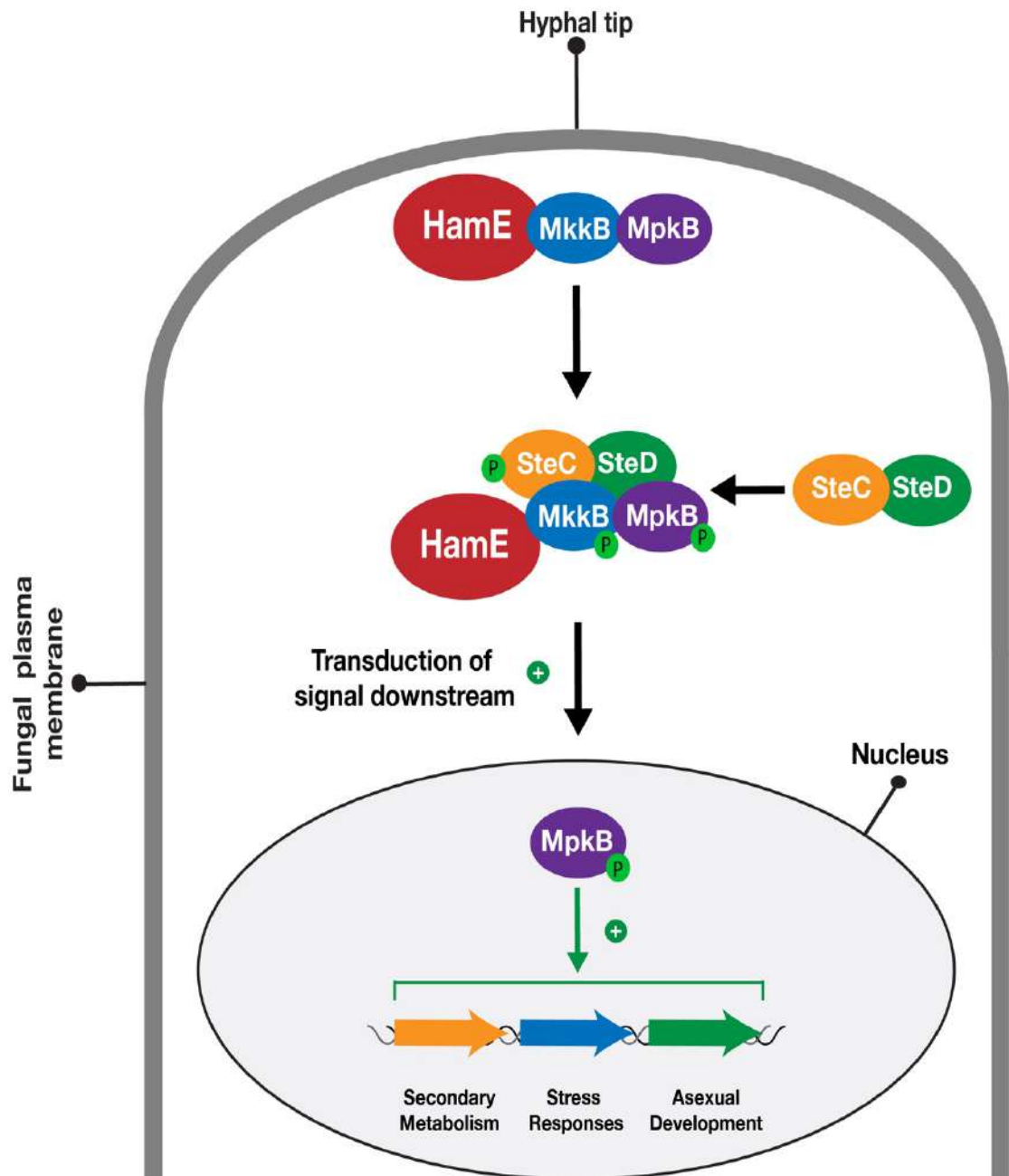
Figure 5.18. Illustration of the *A. fumigatus* pheromone module and it's roles in regulating development, stress responses and secondary metabolism. MkkB, MpkB and HamE localise to the hyphal tips. These three proteins interact with the SteC-SteD dimer in the cytoplasm to form a pentameric complex which results in MpkB activation and transduction of a signal downstream to the nucleus. MpkB translocates into the nucleus, where presumably it interacts with transcription factors to positively regulate asexual sporulation, vegetative growth, stress responses and production of various SMs. 'P' represents phosphate groups.

5.7. Author contributions and declarations

The majority of data from this chapter has been taken from Frawley *et al*. (2020b) and the authors declare that there is no conflict of interest. The majority of experiments were performed by Dean Frawley. Exceptions are the following: (i) Isolation of metabolites and LC-MS analysis (of all compounds except gliotoxin). This was performed by Dr. Maria Stroe, under the supervision of Prof. Axel Brakhage at the Leibniz-institute for natural product research and infection biology (ii) Confocal microscopy imaging of GFP-tagged *A*. *fumigatus* strains. This was performed by Prof. Berl Oakley at the Department of Molecular Biosciences, University of Kansas, United States of America.

Chapter 6

General Discussion and Overall

Conclusions

6.1. Pheromone module orthologs are highly conserved in eukaryotes

MAP kinase cascades are highly conserved signalling pathways in eukaryotic organisms, ranging from yeast to humans. These pathways are required for the regulation of a myriad of biological processes, such as cell proliferation, metabolism and stress responses, to name a few (Schaeffer and Weber, 1999, Widmann et al., 1999, Marshall, 1994). The pheromone module is a highly conserved MAP kinase pathway that has been extensively studied in yeast (Bardwell, 2005). This pathway consists of the three kinases Ste11, Ste7 and Fus3, which become tethered to the membrane *via* the adaptor protein Ste50 and scaffold protein Ste5. This leads to sequential phosphorylation of each kinase, translocation of Fus3 into the nucleus and activation of transcription factors that ultimately regulate cell fusion and sexual reproduction in response to pheromone detection (Pryciak and Huntress, 1998, Good et al., 2009, Wu et al., 1999, Wong Sak Hoi and Dumas, 2010).

6.1.1. Orthologous genes in *H. sapiens*

Since the discovery of the pheromone module in yeast, orthologous genes have been shown to be highly conserved in eukaryotes. In the human genome, genes encoding the three kinases *raf-1, mek-1* and *erk-1* exist (Roberts and Der, 2007). These genes correspond to the yeast *ste11, ste7* and *fus3* genes respectively. There are no orthologs of *ste5* present in the genomes of humans and filamentous fungal species (Rispail et al., 2009). Instead, the human genome possesses the *ksr1* gene, which encodes a scaffold protein to bind these kinases (Roberts and Der, 2007). By performing pairwise sequence alignment of yeast and human protein sequences using the Smith-Waterman algorithm (Madeira et al. 2019), the percentages of sequence similarity between each respective protein were calculated. It was found that Raf-1 exhibits 39.8% sequence similarity (SS) to Ste11, while Mek-1 and Erk-1 exhibit 53% and 67.2% SS to Ste7 and Fus3 respectively. The human genome does not encode an ortholog of yeast *ste50.*

6.1.2. Orthologous genes in *N. crassa*

Orthologs of the pheromone module genes have been identified in the filamentous fungus *N. crassa*. The genome of this species consists of genes that encode the three kinases *nrc-1, mek-2* and *mak-2* (orthologs of yeast *ste11, ste7* and *fus3*), the adaptor protein *ste50* (ortholog of yeast *ste50*) and the scaffold *ham5*, which does not exist in yeast (Jonkers et al., 2014, Dettmann et al., 2014). Nrc-1 exhibits 43% SS to yeast Ste11 and 40.8% SS to human Raf-1. Mek-2 exhibits 56.7% SS to yeast Ste7 and 58.4% SS to human Mek-1. Mak-2 exhibits 78.2% SS to yeast Fus3 and 74.6% SS to human Erk-1. Lastly, *N. crassa* Ste50 exhibits 37.4% SS to yeast Ste50.

6.1.3. Orthologous genes in *A. nidulans*

In *Aspergillus* species, orthologs of the pheromone module genes are highly conserved and were initially detected in *A. nidulans* (Bayram et al., 2012, Teague et al., 1986, Wei et al., 2003, Paoletti et al., 2007). These genes are denoted as AN2269 (SteC), AN3422 (MkkB), AN3719 (MpkB) and AN7252 (SteD). These genes correspond to the yeast *ste11, ste7, fus3 and ste50* genes. SteC exhibits 44% SS to yeast Ste11, 39.2% SS to human Raf-1 and 63.9% SS to *N. crassa* Nrc-1. MkkB exhibits 56.4% SS to yeast Ste7, 56.9% SS to human Mek-1 and 59.5% SS to *N. crassa* Mek-2. MpkB exhibits 78.8% SS to yeast Fus3, 71.8% SS to human Erk-1 and 98% SS to *N. crassa* Mak-2. SteD exhibits 41.6% SS to yeast Ste50 and 60.5% SS to *N. crassa* Ste50. Orthologs of yeast Ste5 do not exist in the genomes of *Aspergillus* species. However, orthologs of *N. crassa* Ham-5 have been shown to be highly conserved in the genomes of filamentous fungal species (Jamet-Vierny et al., 2007, Rispail et al., 2009). In Chapter 3, the *A. nidulans* gene AN2701 and respective protein were characterised (Frawley et al., 2018). The AN2701 gene was found to be an ortholog of *N. crassa ham5* and these two proteins share 51.2% SS.

6.1.4. Orthologous genes in *A. flavus*

There have been no studies on the pheromone module genes in the saprophytic fungus *A. flavus*. However, in Chapter 4 of this thesis, orthologs of *A. nidulans* SteC (AFLA_048880), MkkB (AFLA_103480), MpkB (AFLA_034170), SteD

(AFLA_002340) and HamE (AFLA_095770) were identified (Frawley et al., 2020a). *A. flavus* SteC exhibits 45.9% SS to yeast Ste11, 37.4% SS to human Raf-1, 67.1% SS to *N. crassa* Nrc-1 and 87% SS to *A. nidulans* SteC. *A. flavus* MkkB exhibits 56.2% SS to yeast Ste7, 57.7% SS to human Mek-1, 67.4% SS to *N. crassa* Mek-2 and 85.2% SS to *A. nidulans* MkkB. *A. flavus* MpkB exhibits 78.8% SS to yeast Fus3, 73.7% SS to human Erk-1, 97.7% SS to *N. crassa* Mak-2 and 99.7% SS to *A. nidulans* MpkB. *A. flavus* SteD exhibits 37.5% SS to yeast Ste50, 63.7% SS to *N. crassa* Ste50 and 83% SS to *A. nidulans* SteD. Lastly, *A. flavus* HamE exhibits 50.7% SS to *N. crassa* Ham5 and 75.2% SS to *A. nidulans* HamE.

6.1.5. Orthologous genes in *A. fumigatus*

Aside from the recent study on the MpkB ortholog in the opportunistic human pathogen *A. fumigatus* (Manfiolli et al., 2019), there have been no studies on the pheromone module genes in this species. In Chapter 5 of this thesis, orthologs of the remaining pheromone module genes were identified in *A. fumigatus* (Frawley et al., 2020b). *A. fumigatus* SteC (Afu5g06420) exhibits 44.1% SS to yeast Ste11, 39.6% SS to human Raf-1, 64.6% SS to *N. crassa* Nrc-1, 85.8% SS to *A. nidulans* SteC and 87.7% SS to *A. flavus* SteC. *A. fumigatus* MkkB (Afu3g05900) exhibits 55.3% SS to yeast Ste7, 59.1% SS to human Mek-1, 64.1% SS to *N. crassa* Mek-2, 84.1% SS to *A. nidulans* MkkB and 92.8% SS to *A. flavus* MkkB. *A. fumigatus* MpkB exhibits 79.1% SS to yeast Fus3, 72% SS to human Erk-1, 98% SS to *N. crassa* Mak-2, 99.2% SS to *A. nidulans* MpkB and 99.4% SS to *A. flavus* MpkB. *A. fumigatus* SteD exhibits 40.7% SS to yeast Ste50, 63.6% SS to *N. crassa* Ste50, 85.3% SS to *A. nidulans* SteD and 87.6% SS to *A. flavus* SteD. Lastly, *A. fumigatus* HamE exhibits 50.9% SS to *N. crassa* Ham5, 75.5% SS to *A. nidulans* HamE and 78.8% SS to *A. flavus* HamE.

6.1.6. The pheromone module orthologs are significantly similar in *Aspergillus* species.

Taken together, these results highlight the conservation of the pheromone module genes in eukaryotes, suggesting that they may perform essential and similar roles in various organisms, such as those mentioned above. It is evident that orthologs of yeast Ste11 are

not as highly conserved in each of the species mentioned in this discussion section, as the range of SS for these orthologous proteins is between 39.8%-45.9%. However, it is evident that these values are significantly higher between orthologs of Ste11 in filamentous fungal species, suggesting that these proteins may play unique roles in these species that they do not perform in yeast. Ste7 orthologs are more highly conserved in eukaryotes. Each ortholog of Ste7 exhibits between 53%-56.7% SS to the yeast protein. In *Aspergillus* species, the respective MkkB ortholog is highly conserved and is between 85.2%-92.8% similar across the three species mentioned above. The most highly conserved pheromone module protein is the terminal kinase Fus3. Orthologs of Fus3 share between 67.2%-79.1% SS with the yeast protein. In filamentous fungi, this protein is highly conserved and the protein sequence is 97.7%-99.7% similar between these species. An ortholog of the yeast *ste50* gene does not exist in the human genome, however, it does exist in the genomes of other fungi. The levels of similarity of the Ste50 orthologs are low in comparison to the other pheromone module proteins, suggesting that Ste50 proteins may exert various functions depending on the species. Each Ste50 ortholog exhibits between 37.4%-41.6% SS to the yeast protein. In *Aspergillus* species, the conservation of the respective Ste50 ortholog is considerably higher and these proteins exhibit between 83%-87.6% SS. The *hamE* gene and it's orthologs are also highly conserved in filamentous fungal genomes but not in yeast or humans. Between *Aspergillus* species, it was found that HamE orthologs exhibit between 75.2%-78.8% SS.

6.1.7. Functional domains of the pheromone module proteins are highly conserved in eukaryotes

The pheromone module genes in each eukaryotic organism mentioned above encode proteins that possess highly conserved functional domains. Particularly in fungal species, certain domains and motifs are conserved across unicellular yeast and multicellular filamentous fungi. In humans, these domains are not as highly conserved. However, these proteins share many similarities with the fungal orthologs overall. **Figure 6.1.** provides a schematic illustrating the pheromone module proteins and their functional domains in fungal species, signifying the high degree of conservation across the fungal kingdom. It can be observed that yeast Ste11 and its orthologs all possess a SAM domain at the N-terminal and a protein kinase domain at the C-terminal. Each Ste11 ortholog also possesses an RA domain, however, this domain is not detected in the yeast Ste11

sequence. Yeast Ste7 and Fus3 and all respective orthologs possess protein kinase domains. Together, with the SteC orthologs, this provides strong evidence to suggest that these three proteins in each organism form a classic three-tiered kinase cascade. Yeast Ste50 and its orthologs all possess a SAM domain at the N-terminal and an RA domain at the C-terminal. This implicates that these proteins interact with SteC *via* SAM domain binding (Kim and Bowie, 2003) and are associated with Ras proteins, which are GTPases that are often involved in cell signalling (Ponting and Benjamin, 1996). The *N. crassa* Ham5 protein and its respective orthologs in *Aspergillus* species all possess WD40 domains, which are characteristic scaffolding domains that enable protein-protein interactions (Xu and Min, 2011). This would suggest that these proteins are implicated in the regulation of signalling pathways and the assembly of protein complexes. The *N. crassa* Ham5 protein also possesses two putative coiled-coil domains which are not detectable in the *Aspergillus* orthologs. These domains are involved in a diverse range of processes, ranging from the tethering of transport vesicles to the assembly of macromolecular complexes (Truebestein and Leonard, 2016).

Overall, these results, in combination with the conservation of pheromone module gene sequences in eukaryotes suggest that the pheromone module proteins play diverse but similar roles in various organisms, specifically fungi. The conservation of these functional domains provides evidence that these proteins form a MAPK signalling pathway that may be essential for viability in each of these organisms.
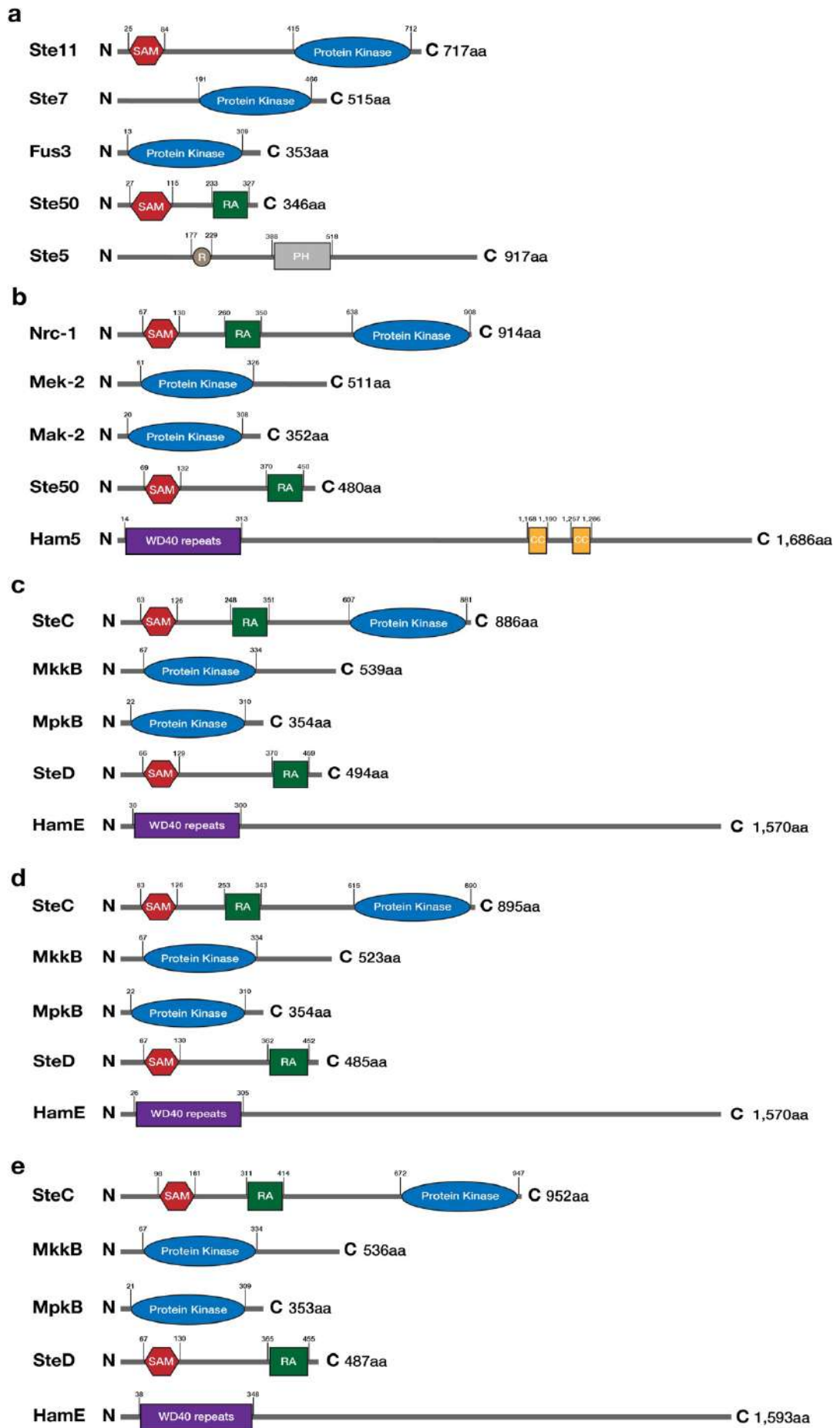
Figure 6.1. Pheromone module proteins in various eukaryotic organisms. (a) The domains of the pheromone module proteins in *S. cerevisiae*. 'PH' refers to pleckstrin-homology domain. 'R' refers to RING-H2 motif. (b) Protein domains in *N. crassa*. 'CC' refers to coiled-coil domains. (c) Protein domains in *A. nidulans*. (d) Protein domains in *A. flavus*. (e) Protein domains in *A. fumigatus*. Detection of protein sizes and domains were performed using a combination of ScanProsite (de Castro et al., 2006) and InterPro software (Mitchell et al., 2019). For *N. crassa* Ham5, protein domains were discovered by (Jonkers et al., 2014). For yeast Ste5, protein domains were discovered by (Garrenton et al., 2006, Inouye et al., 1997).

6.2. The pheromone module proteins form a central signalling hub in eukaryotes that regulates a diverse array of biological processes

It has been shown in various eukaryotic organisms that the pheromone module proteins assemble to form a MAP kinase signalling pathway. As mentioned above, the yeast pheromone module is a pentameric complex, consisting of three kinases, an adaptor protein and a scaffold protein, which function in transducing a signal downstream to the nucleus to activate transcription factors like Ste12. This, in turn regulates cell fusion and sexual development (Bardwell, 2005). This pathway has become a paradigm for MAP kinase signalling in eukaryotes and since it's discovery, a myriad of MAP kinase pathways have been characterised in various eukaryotic organisms (Frawley et al., 2018, Li et al., 2005, Lev et al., 1999, Paoletti et al., 2007).

In humans, a pathway orthologous to the pheromone module is assembled, often in response to growth factors. This pathway consists of the Raf-1 MAP3K, the Mek-1 MAP2K and the Erk-1 MAPK, as well as the KSR-1 scaffold. Binding of the kinases to the KSR-1 scaffold results in signal specificity and sequential phosphorylation of each kinase. This results in the activation of Erk-1 and various transcription factors in the nucleus, leading to the subsequent regulation of a diverse array of biological processes, such as cell proliferation and survival. Dysregulation of this MAPK pathway has been implicated in the progression of various cancers and thus, this pathway is considered an important target for anti-cancer therapies (Chang et al., 2003, Roberts and Der, 2007).

In *N. crassa,* as described previously, a pentameric complex consisting of the Nrc-1, Mek-2 and Mak-2 kinases, the Ste50 adaptor and the Ham5 scaffold is assembled in response to pheromone signalling between neighbouring hyphae (Jonkers et al., 2014, Dettmann et al., 2014). The three kinases associate with Ste50, which leads to Ste50-mediated activation of Nrc-1 (Dettmann et al., 2014). This tetrameric complex then associates with Ham5 and the entire complex localises to puncta at opposing hyphal tips during chemotropic interactions and undergoes repeated cycles of assembly and disassembly, in which the complex assembles in one hyphal tip, disassembles and then assembles in the opposite hyphal tip (Jonkers et al., 2014). The assembly of this complex results in the sequential phosphorylation of each kinase, resulting in activation of Mak-2. Mak-2 phosphorylation results in activation of PP-1 in the nucleus (Dettmann et al., 2014), a transcription factor similar to yeast Ste12 that regulates germling and hyphal fusion, sexual development and SM production (Leeder et al., 2013, Li et al., 2005).

6.2.1. The pheromone module is required for the regulation of development in *Aspergillus* species

6.2.1.1. Assembly and signalling of the *A. nidulans* pheromone module

As described in Chapter 3 of this thesis, the *A. nidulans* pheromone module is a pentameric complex consisting of the three kinases SteC, MkkB and MpkB, the adaptor protein SteD and the newly identified scaffold protein HamE (**Figure 3.19.**) (Bayram et al., 2012, Frawley et al., 2018). The HamE scaffold was found to be an ortholog of *N. crassa* Ham5 and exhibited significant similarities to this protein. Both proteins possess multiple phosphorylation sites (**Figure 3.2. (b)**) and WD40 domains at the N-terminal (**Figure 3.2. (a) and (c)**) (Jonkers et al., 2014, Dettmann et al., 2014). The relative abundance of HamE at various stages of development also revealed that this protein is readily produced and degraded during different stages of growth (**Figure 3.4. (a)**). Taken together, these data suggest that HamE is a scaffold protein and is a direct target of regulation. This could implicate HamE in higher order regulatory processes such as positive and negative feedback loops in the pheromone module, as is the case for yeast Ste5 (Strickfaden et al., 2007, Bhattacharyya et al., 2006).

It is postulated that the pheromone module pathway is assembled in response to the detection of pheromones, released by hyphae undergoing chemotropic interactions (Bayram et al., 2012, Frawley et al., 2018). Proteins of this complex were observed to be enriched at specific sites such as the hyphal tips, plasma membrane and nuclear envelope, while MpkB was found to translocate into the nucleus (**Figures 3.3. and 3.4.**) (Bayram et al., 2012). This provides evidence that this pathway is involved in the detection of stimuli and transduction of a signal downstream to the nucleus. SteD associates with all three kinases, (Bayram et al., 2012) whereas the HamE scaffold was only found to interact with MkkB and MpkB (**Figure 3.1. (a)**). Although the deletion of *hamE* did not impose any effects on the sub-cellular localisation of the complex components (**Figure 3.17.**) or assembly of the complex (**Figure 3.18.**), the levels of phosphorylation intensity of the kinases were dramatically reduced (**Figure 3.16.**). Significantly fewer phosphorylated residues were detected on MkkB in a *hamE* mutant (**Figure 3.16. (b)**). Also, the intensity of MpkB phosphorylation at Threonine 182 and Tyrosine 184 was dramatically reduced during all stages of development (**Figure 3.16. (a)**), signifying a reduction in MpkB activation. This complements the reduced levels of Mak-2 phosphorylation observed in a *N. crassa ham5* mutant (Dettmann et al., 2014). Overall, these data suggest that HamE exhibits an active regulatory role and it is possible that HamE is required to catalytically unlock MpkB for phosphorylation by MkkB, which is evident for the Ste5 scaffold in yeast (Good et al., 2009). This could explain why the tetrameric complex can assemble in a *hamE* mutant (**Figure 3.18.**) but MpkB phosphorylation is inefficient and transcription factor activation does not occur.

6.2.1.2. The *A. nidulans* pheromone module regulates vegetative growth, as well as asexual and sexual reproduction

The pheromone module was shown to be essential for the regulation of various *A. nidulans* developmental programmes. With regards to vegetative hyphal growth, it was observed that the deletion of *steC, mkkB, mpkB* and *steD* resulted in 20-30% reductions in colony size, whereas the deletion of *hamE* did not hinder the rate of growth (**Figures 3.5. and 3.7.**). These data provide support for the findings in *N. crassa* (Dettmann et al., 2014), where it was observed that the deletion of *mak-2* and *ste-50* resulted in reduced mycelial extension rates, whereas the *ham-5* mutant displayed a reduction in growth rate but it was not as severe as the phenotypes observed for the other two mutants. It was also apparent

that the deletion of any of the pheromone module genes results in dramatic reductions in sporulation. All single and double mutants exhibited a 50-60% decrease in asexual conidiation, in comparison to the wild type strain (**Figures 3.6. and 3.8.**). Lastly, it was evident that the pheromone module proteins are essential for the regulation of sexual reproduction. It was found that all single and double mutants exhibited a pale phenotype (**Figure 3.5.**) and were incapable of producing cleistothecia (**Figures 3.6. and 3.9.**), which are sexual reproductive structures. In each of the mutant strains, only premature aggregates of Hulle cells known as nests were formed (**Figure 3.6.**), signifying that these mutants were sterile. These data complement results observed for the *ham5* mutant in *N. crassa*, which were shown to produce reduced levels (20% of the wild type) of sexual reproductive structures known as protoperithecia (Dettmann et al., 2014).

In *A. nidulans*, the presence and absence of light induces asexual and sexual development respectively (Adams et al., 1998, Purschwitz et al., 2008). In order to regulate development in response to light signals, activation of the SteA transcription factor and assembly of the velvet complex (VeA-VelB-LaeA) is required (Bayram et al., 2008). SteA is required for the positive regulation of fruiting body formation but is not essential for the production of Hulle cells (Vallim et al., 2000). It has been shown in *A. nidulans* that phosphorylation and activation of MpkB results in translocation of this kinase into the nucleus where it activates SteA and VeA (Bayram et al., 2012). In the *A. nidulans* mutants in this study, impaired MpkB phosphorylation could result in reduced phosphorylation and activation of SteA and VeA, which consequently may result in altered signalling dynamics in response to light signals, resulting in impaired fungal development. Inefficient activation of SteA could also explain why these mutants are incapable of producing mature cleistothecia but retain the ability to produce Hulle cells.

6.2.1.3. Conservation of the pheromone module in *A. flavus*

Genes encoding the pheromone module proteins have been found to be highly conserved within filamentous fungal genomes (Rispail et al., 2009). This led to the hypothesis that other filamentous fungi such as *A. flavus* may utilise the pheromone module to regulate their development and secondary metabolism. Chapter 4 of this thesis highlighted the identification of a conserved pheromone module pathway in the saprophytic fungus *A. flavus*. This pathway was shown to consist of orthologs of SteC, MkkB and MpkB, as

well as the SteD adaptor, which assemble to form a tetrameric complex (**Figures 4.2. and 4.19.**) (Frawley et al., 2020a). Each of the orthologous pheromone module proteins in *A. flavus* are highly similar to the respective *A. nidulans* proteins and possess high levels of sequence similarity and conserved functional domains and motifs (**Figures 4.1. and 6.1.**). This provides evidence that these proteins may function in a similar manner to what is observed in *A. nidulans*.

This complex was observed to be potentially composed of two sub-complexes. MkkB and MpkB were found to be enriched at the hyphal tips (**Figure 4.17. (b) and (c)**) and MpkB was also found to be localised in the nucleus. *Via* MS experiments, these two proteins were shown to physically interact (**Figure 4.2.**). Thus, it is possible that they form a dimer that becomes enriched at the tips of hyphae, potentially in response to pheromone signalling between neighbouring hyphae undergoing chemotropic interactions. The SteC kinase and SteD adaptor were found to interact (**Figure 4.2.**) and both of these proteins exhibit a cytoplasmic distribution throughout the hyphae (**Figure 4.17 (a) and (d)**). It can be proposed that these proteins also form a dimer in the cytoplasm. Based on MS data, it is known that the four proteins associate with one another (**Figure 4.2.**). Thus, it can be suggested that the MkkB-MpkB dimer physically interacts with the SteC-SteD dimer to form a tetrameric cytoplasmic complex. Assembly of the complex likely results in kinase phosphorylation and translocation of MpkB into the nucleus, similar to what is observed in *A. nidulans* (Bayram et al., 2012). Presumably, MpkB would then interact with various transcription factors to regulate a myriad of biological processes, as is observed in other fungal species (Bayram et al., 2012, van Drogen et al., 2001, Li et al., 2005, Dettmann et al., 2014).

Interestingly, HamE was not found to interact with any members of the pathway (**Appendix B: Table S8**) and was shown to accumulate at the hyphal tips (**Figure 4.18. (a)**). However, the distribution of HamE at the hyphal tips was different from that observed for both MkkB and MpkB. This suggests that HamE may be involved in responding to signalling between hyphae but may not act as a scaffold in the *A. flavus* pheromone module. This is unlike what is observed in other fungal species like *A. nidulans* (Frawley et al., 2018) and *N. crassa* (Jonkers et al., 2014, Dettmann et al., 2014), where HamE acts as a scaffold, regulating kinase phosphorylation and signal transduction to the nucleus. Perhaps the adaptor SteD is exerting a scaffolding role in this MAPK

pathway as it was found to bind all three kinases (**Figure 4.2.**), although further testing would be required to confirm this claim.

6.2.1.4. The *A. flavus* pheromone module regulates asexual conidiation and sclerotia formation

In *A. flavus*, it has been shown that the pheromone module proteins are required for the regulation of both asexual sporulation and sexual sclerotia formation, but are not involved in the regulation of vegetative growth (Frawley et al., 2020a). Similarly to what is observed in *A. nidulans,* the presence and absence of light induces asexual and sexual development in *A. flavus* respectively (Adams et al., 1998, Purschwitz et al., 2008, Amaike and Keller, 2011). In the presence of light, each of the *A. flavus* kinase mutants, as well as the *steD* mutant, exhibited dramatic reductions in asexual sporulation (**Figures 4.3. and 4.4.**), which complement the findings in *A. nidulans* (Bayram et al., 2012, Frawley et al., 2018)*.* Additionally, the relative expression levels of the asexual development genes *flbC* and *abaA* were significantly downregulated in an *mkkB* mutant (**Figure 4.6.**). Interestingly, the deletion of *hamE* did not result in any significant defects in sporulation with regards to the wild type (**Figures 4.3. and 4.4.**). This largely supports a previous study of the role of *ham* genes on fusion processes in *A. flavus* where the loss of *hamE* had relatively small contributions to sporulation but a large impact on sclerotia (Zhao et al., 2017).

In the absence of light, it was observed that all mutants, including the *hamE* mutant, resulted in the complete inhibition of sexual sclerotia formation (**Figures 4.7. and 4.8.**). This is similar to what is observed in both *A. nidulans* (Frawley et al., 2018, Bayram et al., 2012) and *N. crassa* (Dettmann et al., 2014)*,* whereby the deletion of various pheromone module genes and *hamE/ham5* results in reduced levels of cleistothecia and protoperithecia respectively. Furthermore, in *A. flavus,* it was shown that the relative expression levels of the sexual development genes *veA* and *nsdD* were significantly downregulated in an *mkkB* mutant (**Figure 4.9.**). Together, these phenotypical data provide further evidence for the existence of a tetrameric complex consisting of the three kinases and the adaptor SteD, as each of these mutants displayed highly similar asexual and sexual phenotypes. However, contradictory to what is observed in *A. nidulans* (Frawley et al., 2018) and *N. crassa* (Dettmann et al., 2014)*,* the pheromone module

proteins are not required for the regulation of vegetative growth (**Figure 4.5.**). Another exception is that HamE is likely not required for the regulation of asexual sporulation and may function independently of the pheromone module to regulate sclerotia production. Perhaps HamE is also required for the response to chemotropic signals, in a manner that is unique to *A. flavus*. It is possible that HamE may be required as a scaffold during the later stages of sclerotia formation. However, the mechanism of HamE-dependent signalling to the nucleus, as well as the direct functions of HamE are not fully understood.

6.2.1.5. Conservation of the pheromone module in *A. fumigatus*

Chapter 5 of this thesis highlighted the identification of a conserved pheromone module in the opportunistic human pathogen *A. fumigatus*. Evidence suggests that this a pentameric complex, consisting of the three kinases SteC, MkkB and MpkB, the adaptor SteD and the scaffold HamE, similar to what is observed in *A. nidulans* (**Figures 5.2. and 5.18.**) (Frawley et al., 2018). Each of these orthologous pheromone module proteins exhibit significant sequence similarity to the respective *A. nidulans* and *A. flavus* proteins (**Figure 6.1.**). This suggests that a conserved mechanism of pheromone signalling may be utilised by *A. fumigatus* to regulate it's development.

Based on confocal microscopy experiments, the sub-cellular localisation of each pheromone module protein *in vivo* exhibits similarities to what is observed in *A. flavus*. *A. fumigatus* MkkB and MpkB were found to be distributed uniformly throughout the fungal hyphae, however, it was also evident that both proteins, as well as HamE were enriched at the hyphal tips (**Figure 5.17. (b), (c) and (e)**). MpkB was also observed to be localised in interphase nuclei. HamE, MkkB and MpkB have been shown to physically interact *via* MS experiments (**Figure 5.2.**). Thus, it can be postulated that these three proteins form a trimer at the hyphal apices. This is similar to what is observed in *A. flavus*, but complements the interactome data observed in *A. nidulans* more accurately, as HamE was not shown to interact with the pheromone module proteins in *A. flavus* (Frawley et al., 2020a). Both SteC and SteD were observed to be localised throughout the hyphae and were not enriched at the hyphal tips (**Figure 5.17. (a) and (d)**). These two proteins have also been shown to physically interact (**Figure 5.2.**) and thus, it can proposed that these two proteins form a cytoplasmic dimer, as is the case in *A. flavus*. Based on MS data, it is known that these five proteins in *A. fumigatus* interact or at least transiently associate with

one another (**Figure 5.2.**). Thus, these data suggest that the HamE-MkkB-MpkB trimeric complex may associate with the SteC-SteD dimer in the cytoplasm in response to pheromone signalling to form a pentameric complex. Assembly of this complex is likely required for the efficient activation and translocation of MpkB into the nucleus, where it activates various transcription factors (**Figure 5.18**), similar to what is observed in both *A. nidulans* (Frawley et al., 2018, Bayram et al., 2012) and *A. flavus* (Frawley et al., 2020a).

6.2.1.6. The *A. fumigatus* pheromone module regulates vegetative growth, asexual sporulation and stress responses

In *A. fumigatus*, the pheromone module proteins have been shown to be critical for the regulation of various methods of fungal growth, including vegetative growth, asexual sporulation and responses to various cell stresses (Frawley et al., 2020b). Deletion of any of the five pheromone module genes results in significant reductions in hyphal extension rate in comparison to the wild type strain, with the *hamE* mutant displaying the highest degree of reduction (**Figures 5.3. and 5.5.**). For the *A. fumigatus* deletion strains, the average percentage range of colony diameters in comparison to the wild type was between 83.22%-94.61% (**Figure 5.5.**). Aside from the *hamE* mutant phenotype, these data support the findings in *A. nidulans,* where the deletion of either *steC, mkkB, mpkB* o*r steD* results in a dramatic reduction in vegetative growth (Frawley et al., 2018). These results also provide support for the reduced mycelial extension rates observed in *N. crassa* pheromone module mutants (Dettmann et al., 2014). However, these results contradict the findings in *A. flavus* since no reductions in the rates of hyphal extension were observed in any of these mutants (Frawley et al., 2020a). These data also do not support what was found in the study on MpkB in *A. fumigatus,* in which the deletion of *mpkB* did not cause any defects in radial growth rate (Manfiolli et al., 2019). Each pheromone module mutant also exhibited significantly reduced levels of asexual sporulation (**Figures 5.3. and 5.4.**), similar to what is observed in both *A. nidulans* (Bayram et al., 2012, Frawley et al., 2018) and *A. flavus* (Frawley et al., 2020a), with the exception of the *A. flavus hamE* mutant, which did not show any defects in asexual reproduction. When expressed as a percentage of the sporulation levels of the wild type strain, the levels of sporulation of each mutant ranged between 10.16% and 27.02% (**Figure 5.4.**).

Lastly, the pheromone module proteins were found to be essential for the regulation of cellular stress responses. Fungi like *A. fumigatus* utilise multiple MAPK pathways to respond to various cell stressors, such as cell wall, osmotic and oxidative stresses (Rispail et al., 2009, Hamel et al., 2012). In *A. fumigatus,* the CWI pathway is activated in response to cell wall stress agents and signals *via* the MAPK MpkA (van de Veerdonk et al., 2017, Valiante et al., 2015). The HOG pathway is required for the response to osmotic stressors and signals *via* the MAPK SakA (Martinez-Montanes et al., 2010, de Nadal and Posas, 2015, Du et al., 2006). Lastly, the HOG pathway, in cooperation with the MAPK MpkC have been shown to regulate cellular responses to osmotic, oxidative and cell wall stresses (Bruder Nascimento et al., 2016). Each pheromone module mutant displayed significantly increased sensitivity to the cell wall stress agent Congo Red (**Figures 5.6. and 5.7.**), which provides evidence that these proteins may play a role in cell wall biosynthesis or maintenance. This does not fully support the findings by (Manfiolli et al., 2019), in which the presence of Congo Red did not impair vegetative growth. However, the addition of the cell wall perturbing agent caspofungin caused significant reductions in the radial growth rates of the *mpkB* mutant. Each mutant also exhibited increased sensitivity to the oxidative stressor H_2O_2. In the presence of this stress agent, sporulation was drastically reduced in all mutants, in comparison to the wild type strain (**Figures 5.8. and 5.9.**), suggesting that these proteins may function in regulating signalling directly or indirectly in response to oxidative stress. This complements results observed by (Manfiolli et al., 2019), where it was found that the *A. fumigatus mpkB* mutant exhibited increased sensitivity to H_2O_2.

In response to osmotic stress agents like NaCl, the pheromone module proteins, with the exception of the *hamE* mutant did not exhibit impaired growth but instead produced more spores and displayed a darker pigmentation in comparison to the wild type (**Figures 5.10-5.13.**). This could indicate that SteC, MkkB, MpkB and SteD may play a role in negatively regulating sporulation in the presence of osmotic stressors. Many MAPK pathways incorporate multiple common proteins, leading to module cross-talk (Saito, 2010). For example, in yeast, cross-talk exists between the pheromone module and HOG pathway. These two pathways cannot both be active at any one time, signifying that these pathways are insulated from one another. This was demonstrated by stimulating yeast cells simultaneously with both pheromones and osmostress stimuli and observing that cells could only respond to one stimulus at any given time (McClean et al., 2007). It was also shown that when the *fus3* gene is deleted, Hog1 is capable of becoming activated

by pheromone stimuli. Perhaps in *A. fumigatus,* the deletion of the pheromone module genes results in increased activation of the osmotic stress response pathway, resulting in increased resistance to osmotic stressors. It has also been shown that submerged cultures of an *mpkB* mutant in both *A. fumigatus* (Manfiolli et al., 2019) and *A. nidulans* (Kang et al., 2013, Paoletti et al., 2007) produce conidiophores, suggesting that this protein may be critical for both inducing and repressing asexual sporulation, depending on the culturing conditions. Overall, these data provide evidence that the pheromone module proteins contribute to cellular responses to stress, particularly cell wall and oxidative stress. It is likely that there is also cross-talk between the pheromone module pathway and osmotic stress response pathway, however, the exact mechanism of this interplay is not fully understood.

6.3. The production of various SMs is dependent on the pheromone module

As discussed previously in section 1.6., filamentous fungal species such as those belonging to the genus *Aspergillus* are of significant importance due to their potential to produce a myriad of SMs. Fungal SMs can exert a wide range of properties and can impose either beneficial or detrimental effects with regards to human and plant health. It is has been shown in certain *Aspergillus* species that the regulation of SM production is often co-ordinated with the developmental state of the organism, specifically the sexual development cycle (Bayram et al., 2008, Calvo et al., 2002, Yu and Keller, 2005). This co-ordination is mediated *via* the trimeric velvet complex, which assembles in the nucleus in the absence of light. The light-responsive protein VeA interacts with VelB and this heterodimer translocates into the nucleus to interact with LaeA (Bok and Keller, 2004). In the presence of light, nuclear accumulation of this complex is reduced (Bayram and Braus, 2012). Both VeA and VelB are required for the regulation of sexual fruiting body formation, while LaeA is necessary for the production of Hulle cells as well as the regulation of asexual sporulation in the presence of light (Bayram et al., 2008, Sarikaya Bayram et al., 2010).

The coupling of both development and SM production allows fungal species to be readily adaptable to new environments and aids in self-protection against competitors. Although the velvet complex is critical in co-ordinating both fungal growth and secondary metabolism, a myriad of factors are also involved in this complex mechanism of

regulation. For example, MAPK pathways have been implicated in the control of both development and secondary metabolism. These pathways are essential for detecting and responding to environmental stimuli and transducing a signal downstream to the nucleus to initiate appropriate responses. In some cases, this involves the modulation of velvet complex assembly, which subsequently regulates both fungal growth and SM production (Bayram and Braus, 2012).

6.3.1. The *A. nidulans* pheromone module is required for the regulation of various SM genes

Chapter 3 highlighted the characterisation of the pheromone module in *A. nidulans* and provided evidence suggesting that this pentameric complex is required for the transduction of a signal downstream to the nucleus, resulting in SteA and VeA activation and the regulation of fungal development. Given that each pheromone module mutant exhibited defects in sexual development, the roles of these proteins with regards to the regulation of secondary metabolism was assessed. *A. nidulans* is capable of producing over 40 SMs, that can exhibit beneficial as well as deleterious effects. Examples of SMs produced by *A. nidulans* include the carcinogenic ST, the antibiotic PN and the anti-tumour agent TQ (Inglis et al., 2013, Bayram and Braus, 2012, Bok et al., 2006).

It has been shown that the pheromone module in *A. nidulans* is required for the positive regulation of a variety of SMs (Bayram et al., 2012, Frawley et al., 2018). This is likely due to the interactions of MpkB with VeA in the nucleus, which presumably leads to VeA phosphorylation and velvet complex assembly. It was found that in each pheromone module mutant and double mutant strain, the relative expression levels of the velvet complex genes were significantly decreased (**Figure 3.10.**). For the *veA* gene, all mutants displayed similar levels of reduction, ranging from 58%-72%, in comparison to the wild type strain. Expression levels of the *laeA* gene were decreased, with mutants exhibiting reductions of 47%-64%. Lastly, the *velB* gene also displayed reduced expression levels, ranging from 32%-61%.

It was also found that ST, PN and TQ are likely regulated *via* pheromone module signalling and velvet complex assembly. Detection of ST *via* HPLC revealed that in each mutant, there is a 87.5%-97% reduction in the levels of this carcinogen (**Figure 3.11.**). To

further support this, the genes of the ST cluster were significantly downregulated in each pheromone module mutant (**Figure 3.12.**). *aflR* levels exhibited a 63%-86% reduction in all mutants. *stcQ* also exhibited significantly reduced expression levels (59%-91% reduction). Lastly, *stcE* levels displayed reductions ranging from 65%-88%. It was also observed that expression of genes belonging to the PN cluster were considerably decreased in all single and double deletion strains (**Figure 3.13**). In all mutant strains, *acvA, aatA* and *ipnA* exhibited reductions in expression ranging from 62-85%, 56-77% and 71%-89%, respectively. Lastly, the *tdiA* and *tdiB* genes of the TQ cluster exhibited dramatic reductions in expression. Levels of *tdiA* showed a 88%-95% reduction, while the levels of *tdiB* expression were also significantly reduced, ranging from 90-94% (**Figure 3.14.**).

Overall, these data provide evidence that the pheromone module proteins are required for the positive regulation of a wide variety of SMs, likely *via* the modulation of velvet complex activation or assembly. To date, it is not known in other fungi whether the pheromone module regulates secondary metabolism. No SMs are produced by yeast, hence why the velvet complex is unique to filamentous fungi (Bayram and Braus, 2012). It has been shown recently that *N. crassa* contains 10 putative SM gene clusters and is capable of producing various SMs such as ergothioneine (Bello et al., 2012), coprogen (Toth et al., 2009) and carotenoids and this is regulated *via* the velvet complex (Bayram et al., 2019). However, it is not known whether the pheromone module is required for velvet complex assembly or activation in this organism.

6.3.2. The pheromone module in *A. flavus* regulates production of aflatoxin B1 and a myriad of other SMs

Chapter 4 of this thesis highlighted the identification of the pheromone module in *A. flavus* and provided evidence of the involvement of this pathway in the regulation of asexual sporulation and sclerotia formation. Due to the findings in *A. nidulans* (Chapter 3)*,* which revealed that the pheromone module positively regulates the production of SMs, the influence of this pathway in the regulation of SM production in *A. flavus* was investigated. The *A. flavus* genome can potentially encode for at least 56 SMs and only 8 have been studied in detail (Georgianna et al., 2010, Marui et al., 2011). Examples of biologically relevant SMs produced by *A. flavus* were discussed in Chapter 4. These include aflatoxin

B1 (Amare and Keller, 2014), leporin B (Cary et al., 2015), CPA (Chang et al., 2009), aspergillicin A and aspergillicin F (Kikuchi et al., 2015, Capon et al., 2003, Greco et al., 2019) and ditryptophenaline (Barrow and Sedlock, 1994, Saruwatari et al., 2014).

It has been shown that the pheromone module proteins in *A. flavus* are critical mediators of SM regulation. The levels of the six compounds mentioned above were detected in each mutant strain. With the exception of aflatoxin B1, it was found that the *steC, mkkB, mpkB* and *steD* mutants exhibit very similar metabolic profiles that differ significantly from the wild type and *hamEΔ* strain (**Figure 4.13.**). Aflatoxin B1 levels were not detectable in any of the mutant strains (**Figure 4.10. (a)**). This complements the findings in *A. nidulans,* whereby the deletion of any of the five pheromone module genes results in reduced levels of the aflatoxin precursor ST (Chapter 3). It has been shown that sclerotia are capable of containing aflatoxin, as well as many other SMs and that sclerotial development is positively correlated with aflatoxin production (Wicklow and Shotwell, 1983, Brown et al., 2009, Gloer, 1995). Studies have also found evidence for the co-regulation of both sclerotia development and SM biosynthesis *via* similar genetic mechanisms (Calvo et al., 2002, Calvo, 2008). This could explain why each of these mutants are incapable of producing aflatoxin or forming sclerotia. The production of leporin B (**Figure 4.10. (d)**), CPA (**Figure 4.11. (a)**), aspergillicin A (**Figure 4.11. (d)**) and aspergillicin F (**Figure 4.12. (a)**) was increased in the *steC, mkkB, mpkB* and *steD* mutants, whereas the deletion of *hamE* did not result in any significant differences. With regards to ditryptophenaline production (**Figure 4.12. (d)**), there were no significant changes observed in any of the mutants with respect to the wild type strain.

To support these metabolomics data, the expression levels of a myriad of SM genes were also assessed in both the wild type and *mkkB* mutant, cultured for various lengths of time (**Figures 4.14-4.16.**). The *mkkB* mutant was chosen because MkkB is the central kinase in the proposed pheromone module and it is critical for MpkB activation. Thus, it was postulated that the changes observed for this mutant are representative of the changes that would be observed for all pheromone module mutant strains. It was observed that after 48 hours of incubation, the expression levels of aflatoxin B1 genes such as *aflR, aflP, aflA, aflD* and *aflC* exhibited no significant differences in the *mkkB* mutant, while a significant 39% decrease in expression of the *aflM* gene was detected (**Figure 4.14. (a)**). After 72 hours of incubation, it was observed that multiple aflatoxin genes were downregulated in the *mkkB* mutant (**Figure 4.15. (a)**). For example, expression of *aflM,*

aflA and *aflD* exhibited a 30%, 42% and 58% decrease respectively. The backbone genes of leporin B (*lepA*), CPA (*cpaA*), aspergillicin A/aspergillicin F (*agiA*) and ditryptophenaline (*dtpA*) were also tested after 48 hours of incubation. It was found that the relative expression levels of *lepA*, *agiA* and *dtpA* were significantly upregulated in the *mkkB* mutant, while the *cpaA* gene was not detectable at this time point (**Figure 4.14. (b)**).

Taken together, these data suggest that the deletion of either *steC, mkkB, mpkB* or *steD* results in the complete inhibition of aflatoxin B1 production and an increase in leporin B, CPA, aspergillicin A and aspergillicin F production. As is observed in *A. nidulans* (Chapter 3)*,* this could potentially be due to the modulation of velvet complex activity *via* pheromone module signalling as the velvet complex genes are highly conserved in *A. flavus* (Section 1.9.2). Interestingly, while the deletion of *hamE* results in a complete loss of aflatoxin B1 production, it exhibits no significant differences with respect to production of the five other compounds tested. This could suggest that HamE does not function as a member of the pheromone module in *A. flavus* to regulate SM production but it may independently regulate aflatoxin production *via* a separate mechanism. This is unlike what is observed in *A. nidulans,* as the deletion of any of the five pheromone module genes results in very similar metabolic profiles in this species. Perhaps HamE is acted upon by unique regulators. A previous study showed *hamE* was regulated by NosA, a transcription factor involved in sexual development in *A. nidulans* (Vienken and Fischer, 2006) *via* LaeA activation (Zhao et al., 2017). This has not been shown for the other four members of the pheromone module pathway in *A. flavus*.

6.3.3. Production of gliotoxin and various other SMs is dependent on the *A. fumigatus* pheromone module

Chapter 5 of this thesis investigated the roles of the pheromone module with regards to the regulation of various developmental programmes in *A. fumigatus*. Based on findings from Chapters 3 and 4, it was proposed that the pheromone module may regulate SM production in *A. fumigatus*. As mentioned in Chapter 5, *A. fumigatus* is capable of producing a myriad of SMs, such as gliotoxin (Hof and Kupfahl, 2009, Ghazaei, 2017), pseurotin A (Maiya et al., 2007, Ishikawa et al., 2009), pseurotin D (Ishikawa and Ninomiya, 2008), fumagillin (Sin et al., 1997, Mc et al., 1951) and pyripyropene A (Horikoshi et al., 2017). The levels of each of these compounds were detected in

pheromone module mutant strains to determine whether these proteins are required for the regulation of SM production.

With regards to gliotoxin production, it was found that production of this compound was significantly decreased in each mutant strain. The range of decrease detected was between 63-80% (**Figure 5.14.**). For the other four compounds mentioned above, the levels of each were detected in crude extracts from the wild type strain, the *hamE* mutant, the *mkkB* mutant and the respective complementation strains. As described for the metabolomics work in *A. flavus* (Chapter 4 and Section 6.3.2.), the *mkkB* mutant was chosen for these experiments as it is a central kinase in the pheromone module. The *hamE* mutant was also chosen in order to assess whether this protein could exhibit any unique biological roles that are separate to those observed for the remaining pheromone module proteins, as is observed in *A. flavus* (Chapter 4). It was evident that the *hamE* mutant and the *mkkB* mutant exhibited different trends in production of all four compounds tested (**Figures 5.15. and 5.16.**). It was observed that pseurotin A production (**Figure 5.15. (b)**) exhibits a 63% increase in the *hamE* mutant and a 65% decrease in the *mkkB* mutant. Pseurotin D levels showed a similar trend (**Figure 5.15. (d)**). A 37% increase in production of this compound was detected in the *hamE* mutant, while a 69% decrease was observed in the *mkkB* mutant. Fumagillin production (**Figure 5.16. (b)**) showed no significant differences between the wild type and *hamE* mutant, whereas a 31% decrease was evident in the *mkkB* mutant. Lastly, the levels of pyripyropene A (**Figure 5.16. (d)**) were slightly increased in the *hamE* mutant (20% increase), whereas production of this compound was significantly decreased in the *mkkB* mutant (50% decrease).

Taken together, these data suggest that the pheromone module proteins contribute to the positive regulation of SM production, which complement the findings observed in both *A. nidulans* (Bayram et al., 2012, Frawley et al., 2018) and *A. flavus* (Frawley et al., 2020a). However, these data also propose that HamE may exert regulatory roles that are independent of the pheromone module signalling pathway, which supports results observed in the experiments with *A. flavus* mutants (Frawley et al., 2020a). The velvet complex proteins have been found to exist in *A. fumigatus* and have been shown to regulate both development and secondary metabolism in this species (Park et al., 2012). However, little is known regarding the mechanisms of signal detection and transduction that precede activation of the velvet complex. Conservation of the pheromone module pathway in this species may regulate both development and secondary metabolism in *A.*

fumigatus via modulation of velvet complex assembly, as is observed in *A. nidulans* (Chapter 3).

6.4. Overall conclusions and future work

In conclusion, this thesis has provided evidence of the identification and characterisation of a highly conserved MAP kinase pathway known as the pheromone module in three *Aspergillus* species. This pathway is critical for the detection of pheromone signals between hyphae and for transducing a signal downstream to the nucleus to modulate transcription factor activity and various biological responses. In *A. nidulans,* the pheromone module was found to be a pentameric complex that is critical for the regulation of vegetative, asexual and sexual reproduction, as well as the production of various SMs. In *A. flavus,* this pathway was shown to be a tetrameric complex that is essential for regulating asexual sporulation, sexual sclerotia formation and SM production. Lastly, in *A. fumigatus,* evidence suggested that this pathway consists of five proteins. This complex is indispensable for the regulation of asexual sporulation, vegetative growth, response to exogenous stresses and secondary metabolism. A comparative illustration of the pheromone module pathway in each *Aspergillus* species is presented in **Figure 6.2.**

Identification of a central MAPK signalling hub in the genus *Aspergillus* has aided in elucidating the regulation of MAP kinase signalling and the structure of MAP kinase pathways in filamentous fungal species. Consequently, this provides insight on how filamentous fungi utilise MAPK pathways to regulate their development and secondary metabolism in response to environmental cues. With regards to pathogenic fungi like *A. flavus* and *A. fumigatus,* identification of the pheromone module may allow for more selective and efficient anti-fungal therapies to be established, as novel drug targets could be potentially identified. This, in turn, could result in the prevention of crop spoilage due to mycotoxin contamination and infections caused by *Aspergillus* species, such as invasive aspergillosis.

However, although a conserved mechanism of MAPK signalling has been shown to be utilised by *Aspergillus* species, information regarding the stimuli required for activation of these pathways and the direct targets of regulation in the nucleus is sparse. It is likely that a combination of GTPases and receptors contribute to the activation of this

MAPK pathway, which is supported by the fact that the MpkB interactome provided evidence of interactions with various upstream regulators. These interactome data also propose that MpkB either directly or indirectly interacts with a myriad of transcriptional activators, repressors and nuclear proteins. However, the majority of these proteins are hypothetical and uncharacterised and so, information regarding the molecular roles of these proteins is limited. Thus, by utilising a combination of gene editing, LC-MS/MS and qPCR techniques, future research may help provide insight on the chemical messengers and receptors required to induce complex activation, the mechanisms of signalling to the nucleus, the genes regulated *via* pheromone module signalling and the biological consequences of this pathway.

213
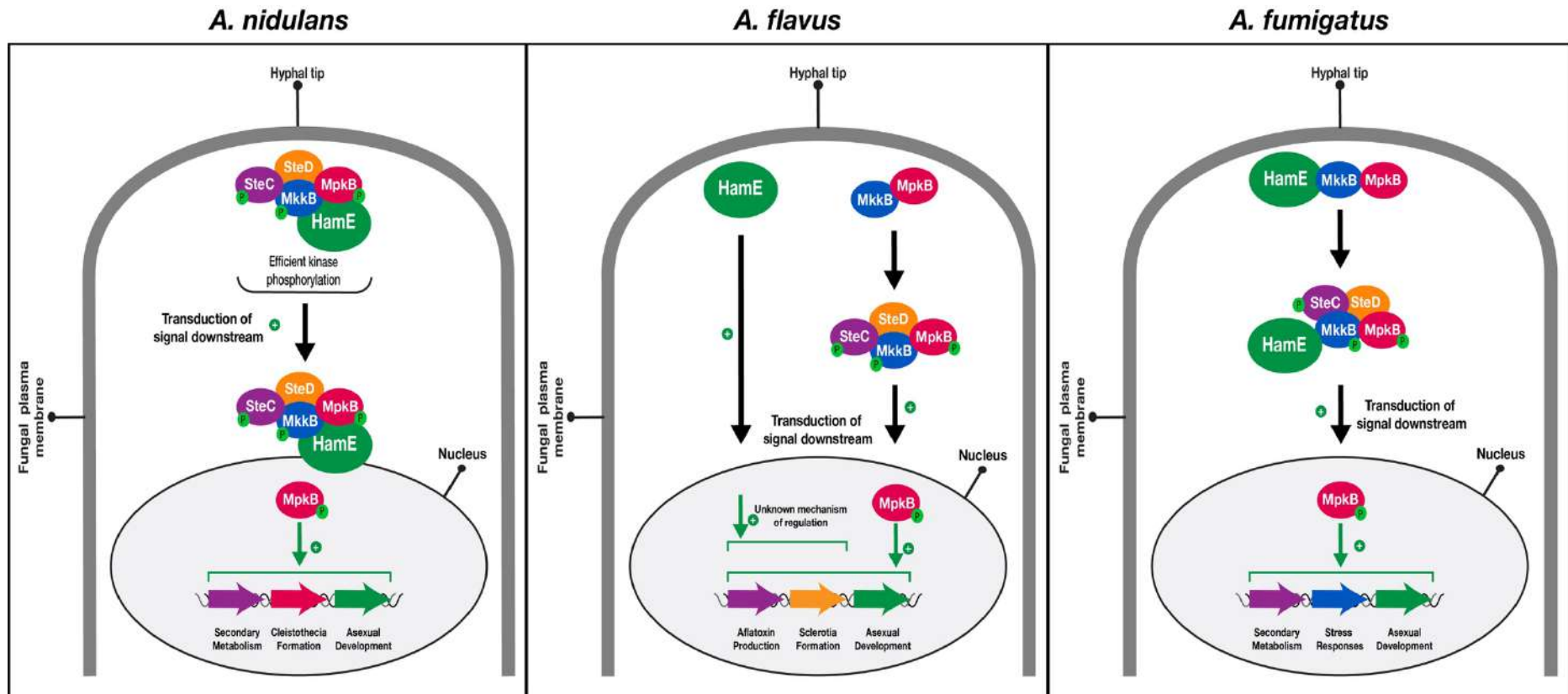
Figure 6.2. Schematics of the pheromone module pathway in *A. nidulans, A. flavus* and *A. fumigatus.* The *A. nidulans* pheromone module consists of the three kinases SteC, MkkB and MpkB, the adaptor protein SteD and the scaffold HamE. These 5 proteins co-localise to regions like the hyphal tip and plasma membrane. HamE mediates efficient kinase phosphorylation, resulting in MpkB activation and migration of the entire complex to the nuclear envelope. MpkB translocates into the nucleus and interacts with transcription factors like SteA and VeA to regulate various biological processes such as asexual sporulation, cleistothecia development, vegetative growth and the production of various SMs. The *A. flavus* pheromone module consists of the three kinases and SteD. The MkkB-MpkB dimer localises to the hyphal tip and interacts with the cytoplasmic SteC-SteD dimer to form a tetrameric complex. MpkB becomes phosphorylated and enters the nucleus where it positively regulates aflatoxin production, asexual sporulation and sclerotia development. HamE also localises to the hyphal tip and regulates aflatoxin production and sclerotia development but the mechanism of regulation is unknown. The *A. fumigatus* pheromone module consists of the three kinases, SteD adaptor and possibly the HamE scaffold. MkkB, MpkB and HamE localise at hyphal tips and interact with the cytoplasmic SteC-SteD dimer in the cytoplasm. MpkB translocates into the nucleus and positively regulates asexual sporulation, vegetative growth, stress responses and production of various SMs such as gliotoxin.

Bibliography

ABAD, A., FERNANDEZ-MOLINA, J. V., BIKANDI, J., RAMIREZ, A., MARGARETO, J., SENDINO, J., HERNANDO, F. L., PONTON, J., GARAIZAR, J. & REMENTERIA, A. 2010. What makes *Aspergillus fumigatus* a successful pathogen? Genes and molecules involved in invasive aspergillosis. *Rev Iberoam Micol,* 27**,** 155-82.

ADAMS, D. R., RON, D. & KIELY, P. A. 2011. RACK1, A multifaceted scaffolding protein: Structure and function. *Cell Commun Signal,* 9**,** 22.

ADAMS, T. H., WIESER, J. K. & YU, J. H. 1998. Asexual sporulation in *Aspergillus nidulans. Microbiol Mol Biol Rev,* 62**,** 35-54.

ALAZI, E. & RAM, A. F. J. 2018. Modulating Transcriptional Regulation of Plant Biomass Degrading Enzyme Networks for Rational Design of Industrial Fungal Strains. *Front Bioeng Biotechnol,* 6**,** 133.

ALDABBOUS, M. S., ROCA, M. G., STOUT, A., HUANG, I. C., READ, N. D. & FREE, S. J. 2010. The *ham-5, rcm-1* and *rco-1* genes regulate hyphal fusion in *Neurospora crassa. Microbiology,* 156**,** 2621-9.

ALTSCHUL, S. F., GISH, W., MILLER, W., MYERS, E. W. & LIPMAN, D. J. 1990. Basic local alignment search tool. *J Mol Biol,* 215**,** 403-10.

AMAIKE, S. & KELLER, N. P. 2011. *Aspergillus flavus. Annu Rev Phytopathol,* 49**,** 107-33.

AMARE, M. G. & KELLER, N. P. 2014. Molecular mechanisms of *Aspergillus flavus* secondary metabolism and development. *Fungal Genet Biol,* 66**,** 11-8.

ANDRIANOPOULOS, A. & TIMBERLAKE, W. E. 1991. ATTS, a new and conserved DNA binding domain. *Plant Cell.* United States.

ATOUI, A., BAO, D., KAUR, N., GRAYBURN, W. S. & CALVO, A. M. 2008. *Aspergillus nidulans* natural product biosynthesis is regulated by mpkB, a putative pheromone response mitogen-activated protein kinase. *Appl Environ Microbiol,* 74**,** 3596-600.

AVALOS, J. & CARMEN LIMON, M. 2015. Biological roles of fungal carotenoids. *Curr Genet,* 61**,** 309-24.

BALLOY, V. & CHIGNARD, M. 2009. The innate immune response to *Aspergillus fumigatus. Microbes Infect,* 11**,** 919-27.

BARDWELL, L. 2005. A walk-through of the yeast mating pheromone response pathway. *Peptides,* 26**,** 339-50.

BARROW, C. J. & SEDLOCK, D. M. 1994. 1'-(2-Phenyl-ethylene)-ditryptophenaline, a new dimeric diketopiperazine from *Aspergillus flavus. J Nat Prod,* 57**,** 1239-44.

BAYRAM, O., BAYRAM, O. S., AHMED, Y. L., MARUYAMA, J., VALERIUS, O., RIZZOLI, S. O., FICNER, R., IRNIGER, S. & BRAUS, G. H. 2012. The *Aspergillus nidulans* MAPK module AnSte11-Ste50-Ste7-Fus3 controls development and secondary metabolism. *PLoS Genet,* 8**,** e1002816.

BAYRAM, O. & BRAUS, G. H. 2012. Coordination of secondary metabolism and development in fungi: the velvet family of regulatory proteins. *FEMS Microbiol Rev,* 36**,** 1-24.

BAYRAM, O., KRAPPMANN, S., NI, M., BOK, J. W., HELMSTAEDT, K., VALERIUS, O., BRAUS-STROMEYER, S., KWON, N. J., KELLER, N. P., YU, J. H. & BRAUS, G. H. 2008. VelB/VeA/LaeA complex coordinates light signal with fungal development and secondary metabolism. *Science,* 320**,** 1504-6.

BAYRAM, O. S., DETTMANN, A., KARAHODA, B., MOLONEY, N. M., ORMSBY, T., MCGOWAN, J., CEA-SANCHEZ, S., MIRALLES-DURAN, A., BRANCINI, G. T. P., LUQUE, E. M., FITZPATRICK, D. A., CANOVAS, D., CORROCHANO, L. M., DOYLE, S., SELKER, E. U., SEILER, S. & BAYRAM, O. 2019. Control of Development, Secondary Metabolism and Light-Dependent Carotenoid Biosynthesis by the Velvet Complex of *Neurospora crassa. Genetics,* 212**,** 691-710.

BELLO, M. H., BARRERA-PEREZ, V., MORIN, D. & EPSTEIN, L. 2012. The *Neurospora crassa* mutant *NcDeltaEgt-1* identifies an ergothioneine biosynthetic gene and demonstrates that ergothioneine enhances conidial survival and protects against peroxide toxicity during conidial germination. *Fungal Genet Biol,* 49**,** 160-72.

BERLIN, V. & YANOFSKY, C. 1985. Isolation and characterization of genes differentially expressed during conidiation of *Neurospora crassa. Mol Cell Biol,* 5**,** 849-55.

BERTHIER, E., LIM, F. Y., DENG, Q., GUO, C. J., KONTOYIANNIS, D. P., WANG, C. C., RINDY, J., BEEBE, D. J., HUTTENLOCHER, A. & KELLER, N. P. 2013. Low-volume toolbox for the discovery of immunosuppressive fungal secondary metabolites. *PLoS Pathog,* 9**,** e1003289.

BHATNAGAR-MATHUR, P., SUNKARA, S., BHATNAGAR-PANWAR, M., WALIYAR, F. & SHARMA, K. K. 2015. Biotechnological advances for combating *Aspergillus flavus* and aflatoxin contamination in crops. *Plant Sci,* 234**,** 119-32.

BHATTACHARYYA, R. P., REMENYI, A., GOOD, M. C., BASHOR, C. J., FALICK, A. M. & LIM, W. A. 2006. The Ste5 scaffold allosterically modulates signaling output of the yeast mating pathway. *Science,* 311**,** 822-6.

BILLS, G. F. & GLOER, J. B. 2016. Biologically Active Secondary Metabolites from the Fungi. *Microbiol Spectr,* 4.

BOK, J. W., BALAJEE, S. A., MARR, K. A., ANDES, D., NIELSEN, K. F., FRISVAD, J. C. & KELLER, N. P. 2005. LaeA, a regulator of morphogenetic fungal virulence factors. *Eukaryot Cell,* 4**,** 1574-82.

BOK, J. W. & KELLER, N. P. 2004. LaeA, a regulator of secondary metabolism in *Aspergillus* spp. *Eukaryot Cell,* 3**,** 527-35.

BOK, J. W., NOORDERMEER, D., KALE, S. P. & KELLER, N. P. 2006. Secondary metabolic gene cluster silencing in *Aspergillus nidulans. Mol Microbiol,* 61**,** 1636-45.

BORSELLO, T. & FORLONI, G. 2007. JNK signalling: a possible target to prevent neurodegeneration. *Curr Pharm Des,* 13**,** 1875-86.

BOYLAN, M. T., MIRABITO, P. M., WILLETT, C. E., ZIMMERMAN, C. R. & TIMBERLAKE, W. E. 1987. Isolation and physical characterization of three essential conidiation genes from *Aspergillus nidulans. Mol Cell Biol,* 7**,** 3113-8.

BRAKHAGE, A. A. & SCHROECKH, V. 2011. Fungal secondary metabolites - strategies to activate silent gene clusters. *Fungal Genet Biol,* 48**,** 15-22.

BRAUS, G. H., KRAPPMAN, S. & ECKERT, S. E. 2002. Sexual development in ascomycetes. Fruit body formation of *Aspergillus nidulans.,* New York, *Molecular biology of fungi development.*

BRAUTIGAN, D. L. 2013. Protein Ser/Thr phosphatases--the ugly ducklings of cell signalling. *Febs j,* 280**,** 324-45.

BREWSTER, J. L., DE VALOIR, T., DWYER, N. D., WINTER, E. & GUSTIN, M. C. 1993. An osmosensing signal transduction pathway in yeast. *Science,* 259**,** 1760-3.

BROWN, M. D. & SACKS, D. B. 2009. Protein scaffolds in MAP kinase signalling. *Cell Signal,* 21**,** 462-9.

BROWN, S. H., SCOTT, J. B., BHAHEETHARAN, J., SHARPEE, W. C., MILDE, L., WILSON, R. A. & KELLER, N. P. 2009. Oxygenase coordination is required for morphological transition and the host-fungus interaction of *Aspergillus flavus. Mol Plant Microbe Interact,* 22**,** 882-94.

BRUDER NASCIMENTO, A. C., DOS REIS, T. F., DE CASTRO, P. A., HORI, J. I., BOM, V. L., DE ASSIS, L. J., RAMALHO, L. N., ROCHA, M. C., MALAVAZI, I., BROWN, N. A., VALIANTE, V., BRAKHAGE, A. A., HAGIWARA, D. & GOLDMAN, G. H. 2016. Mitogen activated protein kinases SakA(HOG1) and MpkC collaborate for *Aspergillus fumigatus* virulence. *Mol Microbiol,* 100**,** 841-59.

BUCHSBAUM, R. J., CONNOLLY, B. A. & FEIG, L. A. 2002. Interaction of Rac exchange factors Tiam1 and Ras-GRF1 with a scaffold for the p38 mitogen-activated protein kinase cascade. *Mol Cell Biol,* 22**,** 4073-85.

BUDAY, L. & TOMPA, P. 2010. Functional classification of scaffold proteins and related molecules. *Febs j,* 277**,** 4348-55.

BULJAN, M., CHALANCON, G., DUNKER, A. K., BATEMAN, A., BALAJI, S., FUXREITER, M. & BABU, M. M. 2013. Alternative splicing of intrinsically disordered regions and rewiring of protein interactions. *Curr Opin Struct Biol,* 23, 443-50.

CABRERA-VERA, T. M., VANHAUWE, J., THOMAS, T. O., MEDKOVA, M., PREININGER, A., MAZZONI, M. R. & HAMM, H. E. 2003. Insights into G protein structure, function, and regulation. *Endocr Rev,* 24**,** 765-81.

CALVO, A. M. 2008. The VeA regulatory system and its role in morphological and chemical development in fungi. *Fungal Genet Biol,* 45**,** 1053-61.

CALVO, A. M., BOK, J., BROOKS, W. & KELLER, N. P. 2004. *veA* is required for toxin and sclerotial production in *Aspergillus parasiticus. Appl Environ Microbiol,* 70**,** 4733-9.

CALVO, A. M. & CARY, J. W. 2015. Association of fungal secondary metabolism and sclerotial biology. *Front Microbiol,* 6**,** 62.

CALVO, A. M., WILSON, R. A., BOK, J. W. & KELLER, N. P. 2002. Relationship between secondary metabolism and fungal development. *Microbiol Mol Biol Rev,* 66**,** 447-59, table of contents.

CAPON, R. J., SKENE, C., STEWART, M., FORD, J., O'HAIR, R. A., WILLIAMS, L., LACEY, E., GILL, J. H., HEILAND, K. & FRIEDEL, T. 2003. Aspergillicins A-E: five novel depsipeptides from the marine-derived fungus *Aspergillus carneus. Org Biomol Chem,* 1**,** 1856-62.

CARY, J. W., HARRIS-COWARD, P. Y., EHRLICH, K. C., MACK, B. M., KALE, S. P., LAREY, C. & CALVO, A. M. 2012. NsdC and NsdD affect *Aspergillus flavus* morphogenesis and aflatoxin production. *Eukaryot Cell,* 11**,** 1104-11.

CARY, J. W., UKA, V., HAN, Z., BUYST, D., HARRIS-COWARD, P. Y., EHRLICH, K. C., WEI, Q., BHATNAGAR, D., DOWD, P. F., MARTENS, S. L., CALVO, A. M., MARTINS, J. C., VANHAECKE, L., COENYE, T., DE SAEGER, S. & DI MAVUNGU, J. D. 2015. An *Aspergillus flavus* secondary metabolic gene cluster containing a hybrid PKS-NRPS is necessary for synthesis of the 2-pyridones, leporins. *Fungal Genet Biol,* 81**,** 88-97.

CHANG, F., STEELMAN, L. S., LEE, J. T., SHELTON, J. G., NAVOLANIC, P. M., BLALOCK, W. L., FRANKLIN, R. A. & MCCUBREY, J. A. 2003. Signal transduction mediated by the Ras/Raf/MEK/ERK pathway from cytokine receptors to transcription factors: potential targeting for therapeutic intervention. *Leukemia,* 17**,** 1263-93.

CHANG, P. K., HORN, B. W. & DORNER, J. W. 2009. Clustered genes involved in cyclopiazonic acid production are next to the aflatoxin biosynthesis gene cluster in *Aspergillus flavus. Fungal Genet Biol,* 46**,** 176-82.

CHANG, P. K., SCHARFENSTEIN, L. L., EHRLICH, K. C. & DIANA DI MAVUNGU, J. 2016. The *Aspergillus flavus* fluP-associated metabolite promotes sclerotial production. *Fungal Biol,* 120**,** 1258-68.

CHANG, P. K., SCHARFENSTEIN, L. L., LI, P. & EHRLICH, K. C. 2013. *Aspergillus flavus* VelB acts distinctly from VeA in conidiation and may coordinate with FluG to modulate sclerotial production. *Fungal Genet Biol,* 58-59**,** 71-9.

CHANG, P. K., SCHARFENSTEIN, L. L., LI, R. W., ARROYO-MANZANARES, N., DE SAEGER, S. & DIANA DI MAVUNGU, J. 2017. *Aspergillus flavus aswA*, a gene homolog of *Aspergillus nidulans oefC*, regulates sclerotial development and biosynthesis of sclerotium-associated secondary metabolites. *Fungal Genet Biol,* 104**,** 29-37.

CHANG, P. K., SCHARFENSTEIN, L. L., MACK, B. & EHRLICH, K. C. 2012. Deletion of the *Aspergillus flavus* orthologue of *A. nidulans fluG* reduces conidiation and promotes production of sclerotia but does not abolish aflatoxin biosynthesis. *Appl Environ Microbiol,* 78**,** 7557-63.

CHEN, R. E. & THORNER, J. 2007. Function and regulation in MAPK signaling pathways: lessons learned from the yeast *Saccharomyces cerevisiae. Biochim Biophys Acta,* 1773**,** 1311-40.

CHOI, J. & KIM, S. H. 2017. A genome Tree of Life for the Fungi kingdom. *Proc Natl Acad Sci U S A,* 114**,** 9391-9396.

CHOI, K. Y., SATTERBERG, B., LYONS, D. M. & ELION, E. A. 1994. Ste5 tethers multiple protein kinases in the MAP kinase cascade required for mating in *S. cerevisiae. Cell,* 78**,** 499-512.

CLASQUIN, M. F., MELAMUD, E. & RABINOWITZ, J. D. 2012. LC-MS data processing with MAVEN: a metabolomic analysis and visualization engine. *Curr Protoc Bioinformatics,* Chapter 14**,** Unit14.11.

CLUTTERBUCK, A. J. 1969. A mutational analysis of conidial development in *Aspergillus nidulans. Genetics,* 63**,** 317-27.

COLEY-SMITH, J. R. & COOKE, R. C. 1971. Survival and germination of fungal sclerotia. Annu. Rev. Phytopathol.

COWAN, C. A. & HENKEMEYER, M. 2001. The SH2/SH3 adaptor Grb4 transduces B-ephrin reverse signals. *Nature,* 413**,** 174-9.

CUEVAS, B. D., ABELL, A. N. & JOHNSON, G. L. 2007. Role of mitogen-activated protein kinase kinase kinases in signal integration. *Oncogene,* 26**,** 3159-71.

CUI, C. B., KAKEYA, H. & OSADA, H. 1997. Novel mammalian cell cycle inhibitors, cyclotroprostatins A-D, produced by *Aspergillus fumigatus, w*hich can inhibit mammalian cell cycle at G2/M phase. *Tetrahedron.*

CZAJA, W., MILLER, K. Y. & MILLER, B. L. 2011. Complex mechanisms regulate developmental expression of the *matA* (HMG) mating type gene in homothallic *Aspergillus nidulans. Genetics,* 189**,** 795-808.

DA SILVA FERREIRA, M. E., KRESS, M. R., SAVOLDI, M., GOLDMAN, M. H., HARTL, A., HEINEKAMP, T., BRAKHAGE, A. A. & GOLDMAN, G. H. 2006. The *akuB*(*KU80*) mutant deficient for nonhomologous end joining is a powerful tool for analyzing pathogenicity in *Aspergillus fumigatus. Eukaryot Cell,* 5**,** 207-11.

DAGENAIS, T. R. & KELLER, N. P. 2009. Pathogenesis of *Aspergillus fumigatus* in Invasive Aspergillosis. *Clin Microbiol Rev,* 22**,** 447-65.

DANG, C. K., CHAUVET, E. & GESSNER, M. O. 2005. Magnitude and variability of process rates in fungal diversity-litter decomposition relationships. *Ecol Lett,* 8**,** 1129-37.

DASGUPTA, A., FULLER, K. K., DUNLAP, J. C. & LOROS, J. J. 2016. Seeing the world differently: variability in the photosensory mechanisms of two model fungi. *Environ Microbiol,* 18**,** 5-20.

DAVIS, R. J. 2000. Signal transduction by the JNK group of MAP kinases. *Cell,* 103**,** 239-52.

DE CASTRO, E., SIGRIST, C. J., GATTIKER, A., BULLIARD, V., LANGENDIJK-GENEVAUX, P. S., GASTEIGER, E., BAIROCH, A. & HULO, N. 2006. ScanProsite: detection of PROSITE signature matches and ProRule-associated functional and structural residues in proteins. *Nucleic Acids Res,* 34**,** W362-5.

DE NADAL, E. & POSAS, F. 2015. Osmostress-induced gene expression--a model to understand how stress-activated protein kinases (SAPKs) regulate transcription. *Febs j,* 282**,** 3275-85.

DE VRIES, R. P. & VISSER, J. 2001. *Aspergillus* enzymes involved in degradation of plant cell wall polysaccharides. *Microbiol Mol Biol Rev,* 65**,** 497-522, table of contents.

DETTMANN, A., HEILIG, Y., VALERIUS, O., LUDWIG, S. & SEILER, S. 2014. Fungal communication requires the MAK-2 pathway elements STE-20 and RAS-2, the NRC-1 adapter STE-50 and the MAP kinase scaffold HAM-5. *PLoS Genet,* 10**,** e1004762.

DHANASEKARAN, D. N., KASHEF, K., LEE, C. M., XU, H. & REDDY, E. P. 2007. Scaffold proteins of MAP-kinase modules. *Oncogene,* 26**,** 3185-202.

DHINGRA, S., ANDES, D. & CALVO, A. M. 2012. VeA regulates conidiation, gliotoxin production, and protease activity in the opportunistic human pathogen *Aspergillus fumigatus. Eukaryot Cell,* 11**,** 1531-43.

DHINGRA, S., LIND, A. L., LIN, H. C., TANG, Y., ROKAS, A. & CALVO, A. M. 2013. The fumagillin gene cluster, an example of hundreds of genes under *veA* control in *Aspergillus fumigatus. PLoS One,* 8**,** e77147.

DIKICIOGLU, D., PIR, P. & OLIVER, S. G. 2013. Predicting complex phenotype-genotype interactions to enable yeast engineering: *Saccharomyces cerevisiae* as a model organism and a cell factory. *Biotechnol J,* 8**,** 1017-34.

DORTER, I. & MOMANY, M. 2016. Fungal Cell Cycle: A Unicellular versus Multicellular Comparison. *Microbiol Spectr,* 4.

DOWNWARD, J. 2001. The ins and outs of signalling. *Nature,* 411**,** 759-62.

DOYLE, D. A., LEE, A., LEWIS, J., KIM, E., SHENG, M. & MACKINNON, R. 1996. Crystal structures of a complexed and peptide-free membrane protein-binding domain: molecular basis of peptide recognition by PDZ. *Cell,* 85**,** 1067-76.

DU, C., SARFATI, J., LATGE, J. P. & CALDERONE, R. 2006. The role of the *sakA* (*hog1*) and *tcsB* (*sln1*) genes in the oxidant adaptation of *Aspergillus fumigatus. Med Mycol,* 44**,** 211-8.

DUFF, D. & LONG, A. 2017. Roles for RACK1 in cancer cell migration and invasion. *Cell Signal,* 35**,** 250-255.

DURAN, R. M., CARY, J. W. & CALVO, A. M. 2007. Production of cyclopiazonic acid, aflatrem, and aflatoxin by *Aspergillus flavus* is regulated by *veA*, a gene necessary for sclerotial formation. *Appl Microbiol Biotechnol,* 73**,** 1158-68.

DYER, P. S. & O'GORMAN, C. M. 2011. A fungal sexual revolution: *Aspergillus* and *Penicillium* show the way. *Curr Opin Microbiol,* 14**,** 649-54.

DYER, P. S. & O'GORMAN, C. M. 2012. Sexual development and cryptic sexuality in fungi: insights from *Aspergillus* species. *FEMS Microbiol Rev,* 36**,** 165-92.

ELIAS, G. M. & NICOLL, R. A. 2007. Synaptic trafficking of glutamate receptors by MAGUK scaffolding proteins. *Trends Cell Biol,* 17**,** 343-52.

ELION, E. A. 2000. Pheromone response, mating and cell biology. *Curr Opin Microbiol,* 3**,** 573-81.

ELION, E. A. 2001. The Ste5p scaffold. *J Cell Sci,* 114**,** 3967-78.

ETXEBESTE, O., GARZIA, A., ESPESO, E. A. & UGALDE, U. 2010. *Aspergillus nidulans* asexual development: making the most of cellular modules. *Trends Microbiol,* 18**,** 569-76.

EVANS, B. S., ROBINSON, S. J. & KELLEHER, N. L. 2011. Surveys of non-ribosomal peptide and polyketide assembly lines in fungi and prospects for their analysis *in vitro* and *in vivo. Fungal Genet Biol,* 48**,** 49-61.

FAUSTINELLI, P. C., WANG, X. M., PALENCIA, E. R. & ARIAS, R. S. 2016. Genome Sequences of Eight *Aspergillus flavus* spp. and One *A. parasiticus* sp., Isolated from Peanut Seeds in Georgia. *Genome Announc,* 4.

FEDOROVA, N. D., KHALDI, N., JOARDAR, V. S., MAITI, R., AMEDEO, P., ANDERSON, M. J., CRABTREE, J., SILVA, J. C., BADGER, J. H., ALBARRAQ, A., ANGIUOLI, S., BUSSEY, H., BOWYER, P., COTTY, P. J., DYER, P. S., EGAN, A., GALENS, K., FRASER-LIGGETT, C. M., HAAS, B. J., INMAN, J. M., KENT, R., LEMIEUX, S., MALAVAZI, I., ORVIS, J., ROEMER, T., RONNING, C. M., SUNDARAM, J. P., SUTTON, G., TURNER, G., VENTER, J. C., WHITE, O. R., WHITTY, B. R., YOUNGMAN, P., WOLFE, K. H., GOLDMAN, G. H., WORTMAN, J. R., JIANG, B., DENNING, D. W. & NIERMAN, W. C. 2008. Genomic islands in the pathogenic filamentous fungus *Aspergillus fumigatus. PLoS Genet,* 4**,** e1000046.

FENG, W. & ZHANG, M. 2009. Organization and dynamics of PDZ-domain-related supramodules in the postsynaptic density. *Nat Rev Neurosci,* 10**,** 87-99.

FINKING, R. & MARAHIEL, M. A. 2004. Biosynthesis of nonribosomal peptides. *Annu Rev Microbiol,* 58**,** 453-88.

FONG, H. K., HURLEY, J. B., HOPKINS, R. S., MIAKE-LYE, R., JOHNSON, M. S., DOOLITTLE, R. F. & SIMON, M. I. 1986. Repetitive segmental structure of the transducin beta subunit: homology with the *CDC4* gene and identification of related mRNAs. *Proc Natl Acad Sci U S A,* 83**,** 2162-6.

FOURY, F. 1997. Human genetic diseases: a cross-talk between man and yeast. *Gene,* 195**,** 1-10.

FRAWLEY, D., GRECO, C., OAKLEY, B., ALHUSSAIN, M. M., FLEMING, A. B., KELLER, N. P. & BAYRAM, O. 2020a. The tetrameric pheromone module SteC-MkkB-MpkB-SteD regulates asexual sporulation, sclerotia formation and aflatoxin production in *Aspergillus flavus. Cell Microbiol,* 22(6), e13192.

FRAWLEY, D., KARAHODA, B., SARIKAYA BAYRAM, O. & BAYRAM, O. 2018. The HamE scaffold positively regulates MpkB phosphorylation to promote development and secondary metabolism in *Aspergillus nidulans. Sci Rep,* 8**,** 16588.

FRAWLEY, D., STROE, M. C., OAKLEY, B. R., HEINEKAMP, T., STRAßBURGER , M., FLEMING, A. B., BRAKHAGE, A. A. & BAYRAM, Ö. 2020b. The Pheromone Module SteC-MkkB-MpkB-SteD-HamE Regulates Development, Stress Responses and Secondary Metabolism in *Aspergillus fumigatus. Front. Microbiol,* 11, 811.

FU, C., IYER, P., HERKAL, A., ABDULLAH, J., STOUT, A. & FREE, S. J. 2011. Identification and characterization of genes required for cell-to-cell fusion in *Neurospora crassa. Eukaryot Cell,* 10**,** 1100-9.

GALAGAN, J. E., CALVO, S. E., CUOMO, C., MA, L. J., WORTMAN, J. R., BATZOGLOU, S., LEE, S. I., BASTURKMEN, M., SPEVAK, C. C., CLUTTERBUCK, J., KAPITONOV, V., JURKA, J., SCAZZOCCHIO, C., FARMAN, M., BUTLER, J., PURCELL, S., HARRIS, S., BRAUS, G. H., DRAHT, O., BUSCH, S., D'ENFERT, C., BOUCHIER, C., GOLDMAN, G. H., BELL-PEDERSEN, D., GRIFFITHS-JONES, S., DOONAN, J. H., YU, J., VIENKEN, K., PAIN, A., FREITAG, M., SELKER, E. U., ARCHER, D. B., PENALVA, M. A., OAKLEY, B. R., MOMANY, M., TANAKA, T., KUMAGAI, T., ASAI, K., MACHIDA, M., NIERMAN, W. C., DENNING, D. W., CADDICK, M., HYNES, M., PAOLETTI, M., FISCHER, R., MILLER, B., DYER, P., SACHS, M. S., OSMANI, S. A. & BIRREN, B. W. 2005. Sequencing of *Aspergillus nidulans* and comparative analysis with *A. fumigatus* and *A. oryzae. Nature,* 438**,** 1105-15.

GARDINER, D. M., WARING, P. & HOWLETT, B. J. 2005. The epipolythiodioxopiperazine (ETP) class of fungal toxins: distribution, mode of action, functions and biosynthesis. *Microbiology,* 151**,** 1021-32.

GARRENTON, L. S., YOUNG, S. L. & THORNER, J. 2006. Function of the MAPK scaffold protein, Ste5, requires a cryptic PH domain. *Genes Dev,* 20**,** 1946-58.

GARRINGTON, T. P. & JOHNSON, G. L. 1999. Organization and regulation of mitogen-activated protein kinase signaling pathways. *Curr Opin Cell Biol,* 11**,** 211-8.

GARZIA, A., ETXEBESTE, O., HERRERO-GARCIA, E., FISCHER, R., ESPESO, E. A. & UGALDE, U. 2009. *Aspergillus nidulans* FlbE is an upstream developmental activator of conidiation functionally associated with the putative transcription factor FlbB. *Mol Microbiol,* 71**,** 172-84.

GARZIA, A., ETXEBESTE, O., HERRERO-GARCIA, E., UGALDE, U. & ESPESO, E. A. 2010. The concerted action of bZip and cMyb transcription factors FlbB and FlbD induces *brlA* expression and asexual development in *Aspergillus nidulans. Mol Microbiol,* 75**,** 1314-24.

GAUTHIER, T., WANG, X., SIFUENTES DOS SANTOS, J., FYSIKOPOULOS, A., TADRIST, S., CANLET, C., ARTIGOT, M. P., LOISEAU, N., OSWALD, I. P. & PUEL, O. 2012. Trypacidin, a spore-borne toxin from *Aspergillus fumigatus*, is cytotoxic to lung cells. *PLoS One,* 7**,** e29906.

GEISER, D. M. 2009. Sexual structures in *Aspergillus*: morphology, importance and genomics. *Med Mycol,* 47 Suppl 1**,** S21-6.

GEORGIANNA, D. R., FEDOROVA, N. D., BURROUGHS, J. L., DOLEZAL, A. L., BOK, J. W., HOROWITZ-BROWN, S., WOLOSHUK, C. P., YU, J., KELLER, N. P. & PAYNE, G. A. 2010. Beyond aflatoxin: four distinct expression patterns and functional roles associated with *Aspergillus flavus* secondary metabolism gene clusters. *Mol Plant Pathol,* 11**,** 213-26.

GHAZAEI, C. 2017. Molecular Insights into Pathogenesis and Infection with *Aspergillus fumigatus. Malays J Med Sci,* 24**,** 10-20.

GLOER, J. B. 1995. Antiinsectan natural products from fungal sclerotia. *Acc. Chem. Res.*

GOOD, M., TANG, G., SINGLETON, J., REMENYI, A. & LIM, W. A. 2009. The Ste5 scaffold directs mating signaling by catalytically unlocking the Fus3 MAP kinase for activation. *Cell,* 136**,** 1085-97.

GOOD, M. C., ZALATAN, J. G. & LIM, W. A. 2011. Scaffold proteins: hubs for controlling the flow of cellular information. *Science,* 332**,** 680-6.

GRECO, C., PFANNENSTIEL, B. T., LIU, J. C. & KELLER, N. P. 2019. Depsipeptide Aspergillicins Revealed by Chromatin Reader Protein Deletion. *ACS Chem Biol,* 14**,** 1121-1128.

HAMEL, L. P., NICOLE, M. C., DUPLESSIS, S. & ELLIS, B. E. 2012. Mitogen-activated protein kinase signaling in plant-interacting fungi: distinct messages from conserved messengers. *Plant Cell,* 24**,** 1327-51.

HAN, K. H., HAN, K. Y., YU, J. H., CHAE, K. S., JAHNG, K. Y. & HAN, D. M. 2001. The *nsdD* gene encodes a putative GATA-type transcription factor necessary for sexual development of *Aspergillus nidulans. Mol Microbiol,* 41**,** 299-309.

HANEEF, M., CESERACCIU, L., CANALE, C., BAYER, I. S., HEREDIA-GUERRERO, J. A. & ATHANASSIOU, A. 2017. Advanced Materials From Fungal Mycelium: Fabrication and Tuning of Physical Properties. *Sci Rep,* 7**,** 41292.

HAO, N., NAYAK, S., BEHAR, M., SHANKS, R. H., NAGIEC, M. J., ERREDE, B., HASTY, J., ELSTON, T. C. & DOHLMAN, H. G. 2008. Regulation of cell signaling dynamics by the protein kinase-scaffold Ste5. *Mol Cell,* 30**,** 649-56.

HARRIS, B. Z. & LIM, W. A. 2001. Mechanism and role of PDZ domains in signaling complex assembly. *J Cell Sci,* 114**,** 3219-31.

HARRIS, S. D. 1997. The duplication cycle in *Aspergillus nidulans. Fungal Genet Biol,* 22**,** 1-12.

HARRIS, S. D. 2008. Branching of fungal hyphae: regulation, mechanisms and comparison with other branching systems. *Mycologia,* 100**,** 823-32.

HARRIS, S. D. 2009. The Spitzenkorper: a signalling hub for the control of fungal development? *Mol Microbiol,* 73**,** 733-6.

HARRIS, S. D. 2019. Hyphal branching in filamentous fungi. *Dev Biol,* 451**,** 35-39.

HARTWELL, L. H. 2002. Nobel Lecture. Yeast and cancer. *Biosci Rep,* 22**,** 373-94.

HEDAYATI, M. T., PASQUALOTTO, A. C., WARN, P. A., BOWYER, P. & DENNING, D. W. 2007. *Aspergillus flavus*: human pathogen, allergen and mycotoxin producer. *Microbiology,* 153**,** 1677-92.

HELMSCHROTT, C., SASSE, A., SAMANTARAY, S., KRAPPMANN, S. & WAGENER, J. 2013. Upgrading fungal gene expression on demand: improved systems for doxycycline-dependent silencing in *Aspergillus fumigatus. Appl Environ Microbiol,* 79**,** 1751-4.

HERMANN, T. E., KURTZ, M. B. & CHAMPE, S. P. 1983. Laccase localized in hulle cells and cleistothecial primordia of *Aspergillus nidulans. J Bacteriol,* 154**,** 955-64.

HOF, H. & KUPFAHL, C. 2009. Gliotoxin in *Aspergillus fumigatus*: an example that mycotoxins are potential virulence factors. *Mycotoxin Res,* 25**,** 123-31.

HOFF, B., KAMEREWERD, J., SIGL, C., MITTERBAUER, R., ZADRA, I., KURNSTEINER, H. & KUCK, U. 2010. Two components of a velvet-like complex control hyphal morphogenesis, conidiophore development, and penicillin biosynthesis in *Penicillium chrysogenum. Eukaryot Cell,* 9**,** 1236-50.

HORIKOSHI, R., GOTO, K., MITOMI, M., OYAMA, K., SUNAZUKA, T. & OMURA, S. 2017. Identification of pyripyropene A as a promising insecticidal compound in a microbial metabolite screening. *J Antibiot (Tokyo),* 70**,** 272-276.

HORN, B. W., DORNER, J. W., GREENE, R. L., BLANKENSHIP, P. D. & COLE, R. J. 1994. Effect of *Aspergillus parasiticus* soil inoculum on invasion of peanut seeds. *Mycopathologia,* 125**,** 179-91.

HORN, B. W., GELL, R. M., SINGH, R., SORENSEN, R. B. & CARBONE, I. 2016. Sexual Reproduction in *Aspergillus flavus* Sclerotia: Acquisition of Novel Alleles from Soil Populations and Uniparental Mitochondrial Inheritance. *PLoS One,* 11**,** e0146169.

HORN, B. W., MOORE, G. G. & CARBONE, I. 2009. Sexual reproduction in *Aspergillus flavus. Mycologia,* 101**,** 423-9.

HORN, B. W., SORENSEN, R. B., LAMB, M. C., SOBOLEV, V. S., OLARTE, R. A., WORTHINGTON, C. J. & CARBONE, I. 2014. Sexual reproduction in *Aspergillus flavus* sclerotia naturally produced in corn. *Phytopathology,* 104**,** 75-85.

HSU, W., ZENG, L. & COSTANTINI, F. 1999. Identification of a domain of Axin that binds to the serine/threonine protein phosphatase 2A and a self-binding domain. *J Biol Chem,* 274**,** 3439-45.

INGLIS, D. O., BINKLEY, J., SKRZYPEK, M. S., ARNAUD, M. B., CERQUEIRA, G. C., SHAH, P., WYMORE, F., WORTMAN, J. R. & SHERLOCK, G. 2013. Comprehensive annotation of secondary metabolite biosynthetic genes and gene clusters of *Aspergillus nidulans, A. fumigatus, A. niger* and *A. oryzae. BMC Microbiol,* 13**,** 91.

INOUYE, C., DHILLON, N. & THORNER, J. 1997. Ste5 RING-H2 domain: role in Ste4-promoted oligomerization for yeast pheromone signaling. *Science,* 278**,** 103-6.

ISHIKAWA, M. & NINOMIYA, T. 2008. Chemical modification of pseurotin A: one-pot synthesis of synerazol and pseurotin E and determination of absolute stereochemistry of pseurotin E. *J Antibiot (Tokyo).* Japan.

ISHIKAWA, M., NINOMIYA, T., AKABANE, H., KUSHIDA, N., TSUJIUCHI, G., OHYAMA, M., GOMI, S., SHITO, K. & MURATA, T. 2009. Pseurotin A and its analogues as inhibitors of immunoglobulin E [correction of immunoglobuline E] production. *Bioorg Med Chem Lett,* 19**,** 1457-60.

JAGODZIK, P., TAJDEL-ZIELINSKA, M., CIESLA, A., MARCZAK, M. & LUDWIKOW, A. 2018. Mitogen-Activated Protein Kinase Cascades in Plant Hormone Signaling. *Front Plant Sci,* 9**,** 1387.

JAMET-VIERNY, C., DEBUCHY, R., PRIGENT, M. & SILAR, P. 2007. IDC1, a pezizomycotina-specific gene that belongs to the PaMpk1 MAP kinase transduction cascade of the filamentous fungus *Podospora anserina. Fungal Genet Biol,* 44**,** 1219-30.

JIN, J. & PAWSON, T. 2012. Modular evolution of phosphorylation-based signalling systems. *Philos Trans R Soc Lond B Biol Sci,* 367**,** 2540-55.

JONKERS, W., LEEDER, A. C., ANSONG, C., WANG, Y., YANG, F., STARR, T. L., CAMP, D. G., 2ND, SMITH, R. D. & GLASS, N. L. 2014. HAM-5 functions as a MAP kinase scaffold during cell fusion in *Neurospora crassa. PLoS Genet,* 10**,** e1004783.

JURICK, W. M., 2ND & ROLLINS, J. A. 2007. Deletion of the adenylate cyclase (sac1) gene affects multiple developmental pathways and pathogenicity in *Sclerotinia sclerotiorum. Fungal Genet Biol,* 44**,** 521-30.

KALE, S. P., MILDE, L., TRAPP, M. K., FRISVAD, J. C., KELLER, N. P. & BOK, J. W. 2008. Requirement of LaeA for secondary metabolism and sclerotial production in *Aspergillus flavus. Fungal Genet Biol,* 45**,** 1422-9.

KANG, J. Y., CHUN, J., JUN, S. C., HAN, D. M., CHAE, K. S. & JAHNG, K. Y. 2013. The MpkB MAP kinase plays a role in autolysis and conidiation of *Aspergillus nidulans. Fungal Genet Biol,* 61**,** 42-9.

KATRITCH, V., CHEREZOV, V. & STEVENS, R. C. 2013. Structure-function of the G protein-coupled receptor superfamily. *Annu Rev Pharmacol Toxicol,* 53**,** 531-56.

KELKAR, N., GUPTA, S., DICKENS, M. & DAVIS, R. J. 2000. Interaction of a mitogen-activated protein kinase signaling module with the neuronal protein JIP3. *Mol Cell Biol,* 20**,** 1030-43.

KELLER, N. P., TURNER, G. & BENNETT, J. W. 2005. Fungal secondary metabolism - from biochemistry to genomics. *Nat Rev Microbiol,* 3**,** 937-47.

KENNEDY, J., AUCLAIR, K., KENDREW, S. G., PARK, C., VEDERAS, J. C. & HUTCHINSON, C. R. 1999. Modulation of polyketide synthase activity by accessory proteins during lovastatin biosynthesis. *Science,* 284**,** 1368-72.

KEW, M. C. 2013. Aflatoxins as a cause of hepatocellular carcinoma. *J Gastrointestin Liver Dis,* 22**,** 305-10.

KIKUCHI, H., HOSHIKAWA, T., FUJIMURA, S., SAKATA, N., KURATA, S., KATOU, Y. & OSHIMA, Y. 2015. Isolation of a Cyclic Depsipetide, Aspergillicin F, and Synthesis of Aspergillicins with Innate Immune-Modulating Activity. *J Nat Prod,* 78**,** 1949-56.

KIM, A. H., YANO, H., CHO, H., MEYER, D., MONKS, B., MARGOLIS, B., BIRNBAUM, M. J. & CHAO, M. V. 2002. Akt1 regulates a JNK scaffold during excitotoxic apoptosis. *Neuron,* 35**,** 697-709.

KIM, C. A. & BOWIE, J. U. 2003. SAM domains: uniform structure, diversity of function. *Trends Biochem Sci,* 28**,** 625-8.

KIM, E. & SHENG, M. 2004. PDZ domain proteins of synapses. *Nat Rev Neurosci,* 5**,** 771-81.

KIM, H. R., CHAE, K. S., HAN, K. H. & HAN, D. M. 2009. The *nsdC* gene encoding a putative C2H2-type transcription factor is a key activator of sexual development in *Aspergillus nidulans*. *Genetics,* 182**,** 771-83.

KLICH, M. A. 2007. *Aspergillus flavus*: the major producer of aflatoxin. *Mol Plant Pathol,* 8**,** 713-22.

KOLCH, W. 2005. Coordinating ERK/MAPK signalling through scaffolds and inhibitors. *Nat Rev Mol Cell Biol,* 6**,** 827-37.

KORNAU, H. C., SCHENKER, L. T., KENNEDY, M. B. & SEEBURG, P. H. 1995. Domain interaction between NMDA receptor subunits and the postsynaptic density protein PSD-95. *Science,* 269**,** 1737-40.

KRANZ, J. E., SATTERBERG, B. & ELION, E. A. 1994. The MAP kinase Fus3 associates with and phosphorylates the upstream signaling component Ste5. *Genes Dev,* 8**,** 313-27.

KRISAK, L., STRICH, R., WINTERS, R. S., HALL, J. P., MALLORY, M. J., KREITZER, D., TUAN, R. S. & WINTER, E. 1994. SMK1, a developmentally regulated MAP kinase, is required for spore wall assembly in *Saccharomyces cerevisiae*. *Genes Dev,* 8**,** 2151-61.

KUES, U. & FISCHER, R. 2006. Asexual sporulation in mycelial fungi, *The Mycota: Growth, differentiation and sexuality*, Springer-Verlag.

KUMAR, P., MAHATO, D. K., KAMLE, M., MOHANTA, T. K. & KANG, S. G. 2016. Aflatoxins: A Global Concern for Food Safety, Human Health and Their Management. *Front Microbiol,* 7**,** 2170.

KWON, N. J., GARZIA, A., ESPESO, E. A., UGALDE, U. & YU, J. H. 2010. FlbC is a putative nuclear C2H2 transcription factor regulating development in *Aspergillus nidulans*. *Mol Microbiol,* 77**,** 1203-19.

KYRIAKIS, J. M. & AVRUCH, J. 2001. Mammalian mitogen-activated protein kinase signal transduction pathways activated by stress and inflammation. *Physiol Rev,* 81**,** 807-69.

LAGERSTROM, M. C. & SCHIOTH, H. B. 2008. Structural diversity of G protein-coupled receptors and significance for drug discovery. *Nat Rev Drug Discov,* 7**,** 339-57.

LATGE, J. P. 1999. *Aspergillus fumigatus* and aspergillosis. *Clin Microbiol Rev,* 12**,** 310-50.

LATGE, J. P. 2001. The pathobiology of *Aspergillus fumigatus*. *Trends Microbiol,* 9**,** 382-9.

LEE, B. N. & ADAMS, T. H. 1994. The *Aspergillus nidulans fluG* gene is required for production of an extracellular developmental signal and is related to prokaryotic glutamine synthetase I. *Genes Dev,* 8**,** 641-51.

LEEDER, A. C., JONKERS, W., LI, J. & GLASS, N. L. 2013. Early colony establishment in *Neurospora crassa* requires a MAP kinase regulatory network. *Genetics,* 195**,** 883-98.

LEEUW, T., WU, C., SCHRAG, J. D., WHITEWAY, M., THOMAS, D. Y. & LEBERER, E. 1998. Interaction of a G-protein beta-subunit with a conserved sequence in Ste20/PAK family protein kinases. *Nature,* 391**,** 191-5.

LEV, S., SHARON, A., HADAR, R., MA, H. & HORWITZ, B. A. 1999. A mitogen-activated protein kinase of the corn leaf pathogen *Cochliobolus heterostrophus* is involved in conidiation, appressorium formation, and pathogenicity: diverse roles for mitogen-activated protein kinase homologs in foliar pathogens. *Proc Natl Acad Sci U S A,* 96**,** 13542-7.

LEWIS, L., ONSONGO, M., NJAPAU, H., SCHURZ-ROGERS, H., LUBER, G., KIESZAK, S., NYAMONGO, J., BACKER, L., DAHIYE, A. M., MISORE, A., DECOCK, K. & RUBIN, C. 2005. Aflatoxin contamination of commercial maize products during an outbreak of acute aflatoxicosis in eastern and central Kenya. *Environ Health Perspect,* 113**,** 1763-7.

LI, D., BOBROWICZ, P., WILKINSON, H. H. & EBBOLE, D. J. 2005. A mitogen-activated protein kinase pathway essential for mating and contributing to vegetative growth in *Neurospora crassa*. *Genetics,* 170**,** 1091-104.

LIM, W. A. & PAWSON, T. 2010. Phosphotyrosine signaling: evolving a new cellular communication system. *Cell,* 142**,** 661-7.

LUO, W. & LIN, S. C. 2004. Axin: a master scaffold for multiple signaling pathways. *Neurosignals,* 13**,** 99-113.

MA, D., COOK, J. G. & THORNER, J. 1995. Phosphorylation and localization of Kss1, a MAP kinase of the *Saccharomyces cerevisiae* pheromone response pathway. *Mol Biol Cell,* 6**,** 889-909.

MADEIRA, F., PARK, Y. M., LEE, J., BUSO, N., GUR, T., MADHUSOODANAN, N., BASUTKAR, P., TIVEY, A. R. N., POTTER, S. C., FINN, R. D. & LOPEZ, R. 2019. The EMBL-EBI search and sequence analysis tools APIs in 2019.

MADEO, F., ENGELHARDT, S., HERKER, E., LEHMANN, N., MALDENER, C., PROKSCH, A., WISSING, S. & FROHLICH, K. U. 2002. Apoptosis in yeast: a new model system with applications in cell biology and medicine. *Curr Genet,* 41**,** 208-16.

MAGALHAES, A. C., DUNN, H. & FERGUSON, S. S. 2012. Regulation of GPCR activity, trafficking and localization by GPCR-interacting proteins. *Br J Pharmacol,* 165**,** 1717-1736.

MAGER, W. H. & WINDERICKX, J. 2005. Yeast as a model for medical and medicinal research. *Trends Pharmacol Sci,* 26**,** 265-73.

MAH, J. H. & YU, J. H. 2006. Upstream and downstream regulation of asexual development in *Aspergillus fumigatus*. *Eukaryot Cell,* 5**,** 1585-95.

MAIYA, S., GRUNDMANN, A., LI, X., LI, S. M. & TURNER, G. 2007. Identification of a hybrid PKS/NRPS required for pseurotin A biosynthesis in the human pathogen *Aspergillus fumigatus*. *Chembiochem,* 8**,** 1736-43.

MANFIOLLI, A. O., SIQUEIRA, F. S., DOS REIS, T. F., VAN DIJCK, P., SCHREVENS, S., HOEFGEN, S., FOGE, M., STRASSBURGER, M., DE ASSIS, L. J., HEINEKAMP, T., ROCHA, M. C., JANEVSKA, S., BRAKHAGE, A. A., MALAVAZI, I., GOLDMAN, G. H. & VALIANTE, V. 2019. Mitogen-Activated Protein Kinase Cross-Talk Interaction Modulates the Production of Melanins in *Aspergillus fumigatus*. *MBio,* 10.

MAO, J., WANG, J., LIU, B., PAN, W., FARR, G. H., 3RD, FLYNN, C., YUAN, H., TAKADA, S., KIMELMAN, D., LI, L. & WU, D. 2001. Low-density lipoprotein receptor-related protein-5 binds to Axin and regulates the canonical Wnt signaling pathway. *Mol Cell,* 7**,** 801-9.

MARSHALL, C. J. 1994. MAP kinase kinase kinase, MAP kinase kinase and MAP kinase. *Curr Opin Genet Dev,* 4**,** 82-9.

MARSHALL, C. J. 1995. Specificity of receptor tyrosine kinase signaling: transient versus sustained extracellular signal-regulated kinase activation. *Cell,* 80**,** 179-85.

MARSHALL, M. A. & TIMBERLAKE, W. E. 1991. *Aspergillus nidulans wetA* activates spore-specific gene expression. *Mol Cell Biol,* 11**,** 55-62.

MARTIN, B. R. 2014. The next frontier of post-translational modifications. *Biopolymers,* 101**,** 131-2.

MARTINEZ-MONTANES, F., PASCUAL-AHUIR, A. & PROFT, M. 2010. Toward a genomic view of the gene expression program regulated by osmostress in yeast. *Omics,* 14**,** 619-27.

MARUI, J., YAMANE, N., OHASHI-KUNIHIRO, S., ANDO, T., TERABAYASHI, Y., SANO, M., OHASHI, S., OHSHIMA, E., TACHIBANA, K., HIGA, Y., NISHIMURA, M., KOIKE, H. & MACHIDA, M. 2011. Kojic acid biosynthesis in *Aspergillus oryzae* is regulated by a Zn(II)(2)Cys(6) transcriptional activator and induced by kojic acid at the transcriptional level. *J Biosci Bioeng,* 112**,** 40-3.

MASCHMEYER, G., HAAS, A. & CORNELY, O. A. 2007. Invasive aspergillosis: epidemiology, diagnosis and management in immunocompromised patients. *Drugs,* 67**,** 1567-601.

MAZZONI, C., ZAROV, P., RAMBOURG, A. & MANN, C. 1993. The SLT2 (MPK1) MAP kinase homolog is involved in polarized cell growth in *Saccharomyces cerevisiae*. *J Cell Biol,* 123**,** 1821-33.

MC, C. M., CALLENDER, M. E. & LAWLIS, J. F., JR. 1951. Fumagillin (H-3), a new antibiotic with amebicidal properties. *Science,* 113**,** 202-3.

MCALPIN, C. E. 2004. Synnema and sclerotium production in *Aspergillus caelatus* and the influence of substrate composition on their development in selected strains. *Mycologia,* 96**,** 937-47.

MCCLEAN, M. N., MODY, A., BROACH, J. R. & RAMANATHAN, S. 2007. Cross-talk and decision making in MAP kinase pathways. *Nat Genet,* 39**,** 409-14.

MCCORMICK, A., LOEFFLER, J. & EBEL, F. 2010. *Aspergillus fumigatus*: contours of an opportunistic human pathogen. *Cell Microbiol,* 12**,** 1535-43.

MILLER, B. L., MILLER, K. Y. & TIMBERLAKE, W. E. 1985. Direct and indirect gene replacements in *Aspergillus nidulans*. *Mol Cell Biol,* 5**,** 1714-21.

MIMS, C. W., RICHARDSON, E. A. & TIMBERLAKE, W. E. 1988. Ultrastructural analysis of conidiophore development in the fungus *Aspergillus nidulans* using freeze-substitution. *Protoplasma.*

MITCHELL, A. L., ATTWOOD, T. K., BABBITT, P. C., BLUM, M., BORK, P., BRIDGE, A., BROWN, S. D., CHANG, H. Y., EL-GEBALI, S., FRASER, M. I., GOUGH, J., HAFT, D. R., HUANG, H., LETUNIC, I., LOPEZ, R., LUCIANI, A., MADEIRA, F., MARCHLER-BAUER, A., MI, H., NATALE, D. A., NECCI, M., NUKA, G., ORENGO, C., PANDURANGAN, A. P., PAYSAN-LAFOSSE, T., PESSEAT, S., POTTER, S. C., QURESHI, M. A., RAWLINGS, N. D., REDASCHI, N., RICHARDSON, L. J., RIVOIRE, C., SALAZAR, G. A., SANGRADOR-VEGAS, A., SIGRIST, C. J. A., SILLITOE, I., SUTTON, G. G., THANKI, N., THOMAS, P. D., TOSATTO, S. C. E., YONG, S. Y. & FINN, R. D. 2019. InterPro in 2019: improving coverage, classification and access to protein sequence annotations. *Nucleic Acids Res,* 47**,** D351-d360.

MOONEY, J. L. & YAGER, L. N. 1990. Light is required for conidiation in *Aspergillus nidulans*. *Genes Dev,* 4**,** 1473-82.

MORRIS, N. R. & ENOS, A. P. 1992. Mitotic gold in a mold: *Aspergillus* genetics and the biology of mitosis. *Trends Genet,* 8**,** 32-7.

MORRISON, D. K. & DAVIS, R. J. 2003. Regulation of MAP kinase signaling modules by scaffold proteins in mammals. *Annu Rev Cell Dev Biol,* 19**,** 91-118.

MULLER, J., CACACE, A. M., LYONS, W. E., MCGILL, C. B. & MORRISON, D. K. 2000. Identification of B-KSR1, a novel brain-specific isoform of KSR1 that functions in neuronal signaling. *Mol Cell Biol,* 20**,** 5529-39.

MURPHY, L. O. & BLENIS, J. 2006. MAPK signal specificity: the right place at the right time. *Trends Biochem Sci,* 31**,** 268-75.

NEBREDA, A. R. & PORRAS, A. 2000. p38 MAP kinases: beyond the stress response. *Trends Biochem Sci,* 25**,** 257-60.

NI, M. & YU, J. H. 2007. A novel regulator couples sporogenesis and trehalose biogenesis in *Aspergillus nidulans*. *PLoS One,* 2**,** e970.

O'GORMAN, C. M., FULLER, H. & DYER, P. S. 2009. Discovery of a sexual cycle in the opportunistic fungal pathogen *Aspergillus fumigatus*. *Nature,* 457**,** 471-4.

OJEDA-LOPEZ, M., CHEN, W., EAGLE, C. E., GUTIERREZ, G., JIA, W. L., SWILAIMAN, S. S., HUANG, Z., PARK, H. S., YU, J. H., CANOVAS, D. & DYER, P. S. 2018. Evolution of asexual and sexual reproduction in the *aspergilli*. *Stud Mycol,* 91**,** 37-59.

PAN, C. Q., SUDOL, M., SHEETZ, M. & LOW, B. C. 2012. Modularity and functional plasticity of scaffold proteins as p(l)acemakers in cell signaling. *Cell Signal,* 24**,** 2143-65.

PANDEY, A., ROCA, M. G., READ, N. D. & GLASS, N. L. 2004. Role of a mitogen-activated protein kinase pathway during conidial germination and hyphal fusion in *Neurospora crassa*. *Eukaryot Cell,* 3**,** 348-58.

PAOLETTI, M., RYDHOLM, C., SCHWIER, E. U., ANDERSON, M. J., SZAKACS, G., LUTZONI, F., DEBEAUPUIS, J. P., LATGE, J. P., DENNING, D. W. & DYER, P. S. 2005. Evidence for sexuality in the opportunistic fungal pathogen *Aspergillus fumigatus*. *Curr Biol,* 15**,** 1242-8.

PAOLETTI, M., SEYMOUR, F. A., ALCOCER, M. J., KAUR, N., CALVO, A. M., ARCHER, D. B. & DYER, P. S. 2007. Mating type and the genetic basis of self-fertility in the model fungus *Aspergillus nidulans*. *Curr Biol,* 17**,** 1384-9.

PAOLI, M. 2001. Protein folds propelled by diversity. *Prog Biophys Mol Biol,* 76**,** 103-30.

PARK, H. S., BAYRAM, O., BRAUS, G. H., KIM, S. C. & YU, J. H. 2012. Characterization of the velvet regulators in *Aspergillus fumigatus*. *Mol Microbiol,* 86**,** 937-53.

PARK, H. S., NAM, T. Y., HAN, K. H., KIM, S. C. & YU, J. H. 2014. VelC positively controls sexual development in *Aspergillus nidulans*. *PLoS One,* 9**,** e89883.

PARK, H. S. & YU, J. H. 2012. Genetic control of asexual sporulation in filamentous fungi. *Curr Opin Microbiol,* 15**,** 669-77.

PERIS, D., PEREZ-TORRADO, R., HITTINGER, C. T., BARRIO, E. & QUEROL, A. 2018. On the origins and industrial applications of *Saccharomyces cerevisiae* x *Saccharomyces kudriavzevii* hybrids. *Yeast,* 35**,** 51-69.

PERRIN, R. M., FEDOROVA, N. D., BOK, J. W., CRAMER, R. A., WORTMAN, J. R., KIM, H. S., NIERMAN, W. C. & KELLER, N. P. 2007. Transcriptional regulation of chemical diversity in *Aspergillus fumigatus* by LaeA. *PLoS Pathog,* 3**,** e50.

PONTING, C. P. & BENJAMIN, D. R. 1996. A novel family of Ras-binding domains. *Trends Biochem Sci,* 21**,** 422-5.

PRYCIAK, P. M. & HUNTRESS, F. A. 1998. Membrane recruitment of the kinase cascade scaffold protein Ste5 by the Gbetagamma complex underlies activation of the yeast pheromone response pathway. *Genes Dev,* 12**,** 2684-97.

PURSCHWITZ, J., MULLER, S., KASTNER, C., SCHOSER, M., HAAS, H., ESPESO, E. A., ATOUI, A., CALVO, A. M. & FISCHER, R. 2008. Functional and physical interaction of blue- and red-light sensors in *Aspergillus nidulans*. *Curr Biol,* 18**,** 255-9.

QI, M. & ELION, E. A. 2005. MAP kinase pathways. *J Cell Sci,* 118**,** 3569-72.

REYES-DOMINGUEZ, Y., BOK, J. W., BERGER, H., SHWAB, E. K., BASHEER, A., GALLMETZER, A., SCAZZOCCHIO, C., KELLER, N. & STRAUSS, J. 2010. Heterochromatic marks are associated with the repression of secondary metabolism clusters in *Aspergillus nidulans*. *Mol Microbiol,* 76**,** 1376-86.

RINCON, M. & DAVIS, R. J. 2009. Regulation of the immune response by stress-activated protein kinases. *Immunol Rev,* 228**,** 212-24.

RIQUELME, M., AGUIRRE, J., BARTNICKI-GARCIA, S., BRAUS, G. H., FELDBRUGGE, M., FLEIG, U., HANSBERG, W., HERRERA-ESTRELLA, A., KAMPER, J., KUCK, U., MOURINO-PEREZ, R. R., TAKESHITA, N. & FISCHER, R. 2018. Fungal Morphogenesis, from the Polarized Growth of Hyphae to Complex Reproduction and Infection Structures. *Microbiol Mol Biol Rev,* 82.

RIQUELME, M. & SANCHEZ-LEON, E. 2014. The Spitzenkorper: a choreographer of fungal growth and morphogenesis. *Curr Opin Microbiol,* 20**,** 27-33.

RISPAIL, N., SOANES, D. M., ANT, C., CZAJKOWSKI, R., GRUNLER, A., HUGUET, R., PEREZ-NADALES, E., POLI, A., SARTOREL, E., VALIANTE, V., YANG, M., BEFFA, R., BRAKHAGE, A. A., GOW, N. A., KAHMANN, R., LEBRUN, M. H., LENASI, H., PEREZ-MARTIN, J., TALBOT, N. J., WENDLAND, J. & DI PIETRO, A. 2009. Comparative genomics of MAP kinase and calcium-calcineurin signalling components in plant and human pathogenic fungi. *Fungal Genet Biol,* 46**,** 287-98.

ROBERTS, P. J. & DER, C. J. 2007. Targeting the Raf-MEK-ERK mitogen-activated protein kinase cascade for the treatment of cancer. *Oncogene,* 26**,** 3291-310.

ROCHE, C. M., LOROS, J. J., MCCLUSKEY, K. & GLASS, N. L. 2014. *Neurospora crassa*: looking back and looking forward at a model microbe. *Am J Bot,* 101**,** 2022-35.

ROMSDAHL, J. & WANG, C. C. C. 2019. Recent advances in the genome mining of *Aspergillus* secondary metabolites (covering 2012-2018). *Medchemcomm,* 10**,** 840-866.

RUBINFELD, B., TICE, D. A. & POLAKIS, P. 2001. Axin-dependent phosphorylation of the adenomatous polyposis coli protein mediated by casein kinase 1epsilon. *J Biol Chem,* 276**,** 39037-45.

RUSHING, B. R. & SELIM, M. I. 2019. Aflatoxin B1: A review on metabolism, toxicity, occurrence in food, occupational exposure, and detoxification methods. *Food Chem Toxicol,* 124**,** 81-100.

SACKS, D. B. 2006. The role of scaffold proteins in MEK/ERK signalling. *Biochem Soc Trans,* 34**,** 833-6.

SAITO, H. 2010. Regulation of cross-talk in yeast MAPK signaling pathways. *Curr Opin Microbiol,* 13**,** 677-83.

SALAZAR-CEREZO, S., MARTINEZ-MONTIEL, N., GARCIA-SANCHEZ, J., PEREZ, Y. T. R. & MARTINEZ-CONTRERAS, R. D. 2018. Gibberellin biosynthesis and metabolism: A convergent route for plants, fungi and bacteria. *Microbiol Res,* 208**,** 85-98.

SANCHEZ, J. F., SOMOZA, A. D., KELLER, N. P. & WANG, C. C. 2012. Advances in *Aspergillus* secondary metabolite research in the post-genomic era. *Nat Prod Rep,* 29**,** 351-71.

SARIKAYA BAYRAM, O., BAYRAM, O., VALERIUS, O., PARK, H. S., IRNIGER, S., GERKE, J., NI, M., HAN, K. H., YU, J. H. & BRAUS, G. H. 2010. LaeA control of velvet family regulatory proteins for light-dependent development and fungal cell-type specificity. *PLoS Genet,* 6**,** e1001226.

SARUWATARI, T., YAGISHITA, F., MINO, T., NOGUCHI, H., HOTTA, K. & WATANABE, K. 2014. Cytochrome P450 as dimerization catalyst in diketopiperazine alkaloid biosynthesis. *Chembiochem,* 15**,** 656-9.

SATOH, S., DAIGO, Y., FURUKAWA, Y., KATO, T., MIWA, N., NISHIWAKI, T., KAWASOE, T., ISHIGURO, H., FUJITA, M., TOKINO, T., SASAKI, Y., IMAOKA, S., MURATA, M., SHIMANO, T., YAMAOKA, Y. & NAKAMURA, Y. 2000. AXIN1 mutations in hepatocellular carcinomas, and growth suppression in cancer cells by virus-mediated transfer of AXIN1. *Nat Genet,* 24**,** 245-50.

SCHAEFFER, H. J. & WEBER, M. J. 1999. Mitogen-activated protein kinases: specific messages from ubiquitous messengers. *Mol Cell Biol,* 19**,** 2435-44.

SCHLAEPFER, D. D. & HUNTER, T. 1998. Integrin signalling and tyrosine phosphorylation: just the FAKs? *Trends Cell Biol,* 8**,** 151-7.

SCHLESSINGER, J. 2000. Cell signaling by receptor tyrosine kinases. *Cell,* 103**,** 211-25.

SCHLESSINGER, J. 2014. Receptor tyrosine kinases: legacy of the first two decades. *Cold Spring Harb Perspect Biol,* 6.

SCHOORLEMMER, J. & GOLDFARB, M. 2001. Fibroblast growth factor homologous factors are intracellular signaling proteins. *Curr Biol,* 11**,** 793-7.

SEWALL, T. C., MIMS, C. W. & TIMBERLAKE, W. E. 1990a. *abaA* controls phialide differentiation in *Aspergillus nidulans*. *Plant Cell,* 2**,** 731-9.

SEWALL, T. C., MIMS, C. W. & TIMBERLAKE, W. E. 1990b. Conidium differentiation in *Aspergillus nidulans* wild-type and wet-white (*wetA*) mutant strains. *Dev Biol,* 138**,** 499-508.

SHAW, A. S. & FILBERT, E. L. 2009. Scaffold proteins and immune-cell signalling. *Nat Rev Immunol,* 9**,** 47-56.

SHENG, M. & HOOGENRAAD, C. C. 2007. The postsynaptic architecture of excitatory synapses: a more quantitative view. *Annu Rev Biochem,* 76**,** 823-47.

SIN, N., MENG, L., WANG, M. Q., WEN, J. J., BORNMANN, W. G. & CREWS, C. M. 1997. The anti-angiogenic agent fumagillin covalently binds and inhibits the methionine aminopeptidase, MetAP-2. *Proc Natl Acad Sci U S A,* 94**,** 6099-103.

SKIETERSKA, K., RONDOU, P. & VAN CRAENENBROECK, K. 2017. Regulation of G Protein-Coupled Receptors by Ubiquitination. *Int J Mol Sci,* 18.

SMITH, D. J., EARL, A. J. & TURNER, G. 1990. The multifunctional peptide synthetase performing the first step of penicillin biosynthesis in *Penicillium chrysogenum* is a 421,073 dalton protein similar to *Bacillus brevis* peptide antibiotic synthetases. *Embo j,* 9**,** 2743-50.

SONG, X., WANG, S. & LI, L. 2014. New insights into the regulation of Axin function in canonical Wnt signaling pathway. *Protein Cell,* 5**,** 186-93.

SPIKES, S., XU, R., NGUYEN, C. K., CHAMILOS, G., KONTOYIANNIS, D. P., JACOBSON, R. H., EJZYKOWICZ, D. E., CHIANG, L. Y., FILLER, S. G. & MAY, G. S. 2008. Gliotoxin production in *Aspergillus fumigatus* contributes to host-specific differences in virulence. *J Infect Dis,* 197**,** 479-86.

STEINBERG, G. 2007. Hyphal growth: a tale of motors, lipids, and the Spitzenkorper. *Eukaryot Cell,* 6**,** 351-60.

STEURY, M. D., MCCABE, L. R. & PARAMESWARAN, N. 2017. G Protein-Coupled Receptor Kinases in the Inflammatory Response and Signaling. *Adv Immunol,* 136**,** 227-277.

STRICKFADEN, S. C., WINTERS, M. J., BEN-ARI, G., LAMSON, R. E., TYERS, M. & PRYCIAK, P. M. 2007. A mechanism for cell-cycle regulation of MAP kinase signaling in a yeast differentiation pathway. *Cell,* 128**,** 519-31.

SZEWCZYK, E. & KRAPPMANN, S. 2010. Conserved regulators of mating are essential for *Aspergillus fumigatus* cleistothecium formation. *Eukaryot Cell,* 9**,** 774-83.

TAHERI-TALESH, N., XIONG, Y. & OAKLEY, B. R. 2012. The functions of myosin II and myosin V homologs in tip growth and septation in *Aspergillus nidulans*. *PLoS One,* 7**,** e31218.

TAKEDA, S., KADOWAKI, S., HAGA, T., TAKAESU, H. & MITAKU, S. 2002. Identification of G protein-coupled receptor genes from the human genome sequence. *FEBS Lett,* 520**,** 97-101.

TATEBAYASHI, K., YAMAMOTO, K., TANAKA, K., TOMIDA, T., MARUOKA, T., KASUKAWA, E. & SAITO, H. 2006. Adaptor functions of Cdc42, Ste50, and Sho1 in the yeast osmoregulatory HOG MAPK pathway. *Embo j,* 25**,** 3033-44.

TEAGUE, M. A., CHALEFF, D. T. & ERREDE, B. 1986. Nucleotide sequence of the yeast regulatory gene STE7 predicts a protein homologous to protein kinases. *Proc Natl Acad Sci U S A,* 83**,** 7371-5.

TEMPLETON, A. J., DIEZ-GONZALEZ, L., ACE, O., VERA-BADILLO, F., SERUGA, B., JORDAN, J., AMIR, E., PANDIELLA, A. & OCANA, A. 2014. Prognostic relevance of receptor tyrosine kinase expression in breast cancer: a meta-analysis. *Cancer Treat Rev,* 40**,** 1048-55.

TERHEM, R. B. & VAN KAN, J. A. 2014. Functional analysis of hydrophobin genes in sexual development of *Botrytis cinerea*. *Fungal Genet Biol,* 71**,** 42-51.

TOTH, V., ANTAL, K., GYEMANT, G., MISKEI, M., POCSI, I. & EMRI, T. 2009. Optimization of coprogen production in *Neurospora crassa*. *Acta Biol Hung,* 60**,** 321-8.

TRUEBESTEIN, L. & LEONARD, T. A. 2016. Coiled-coils: The long and short of it. *Bioessays,* 38**,** 903-16.

TUDZYNSKI, P., HOLTER, K., CORREIA, T., ARNTZ, C., GRAMMEL, N. & KELLER, U. 1999. Evidence for an ergot alkaloid gene cluster in *Claviceps purpurea*. *Mol Gen Genet,* 261**,** 133-41.

TURGEON, B. G. & YODER, O. C. 2000. Proposed nomenclature for mating type genes of filamentous ascomycetes. *Fungal Genet Biol,* 31**,** 1-5.

VAGA, S., BERNARDO-FAURA, M., COKELAER, T., MAIOLICA, A., BARNES, C. A., GILLET, L. C., HEGEMANN, B., VAN DROGEN, F., SHARIFIAN, H., KLIPP, E., PETER, M., SAEZ-RODRIGUEZ, J. & AEBERSOLD, R. 2014. Phosphoproteomic analyses reveal novel cross-modulation mechanisms between two signaling pathways in yeast. *Mol Syst Biol,* 10**,** 767.

VALIANTE, V., MACHELEIDT, J., FOGE, M. & BRAKHAGE, A. A. 2015. The *Aspergillus fumigatus* cell wall integrity signaling pathway: drug target, compensatory pathways, and virulence. *Front Microbiol,* 6**,** 325.

VALLIM, M. A., MILLER, K. Y. & MILLER, B. L. 2000. *Aspergillus* SteA (sterile12-like) is a homeodomain-C2/H2-Zn+2 finger transcription factor required for sexual reproduction. *Mol Microbiol,* 36**,** 290-301.

VAN DE VEERDONK, F. L., GRESNIGT, M. S., ROMANI, L., NETEA, M. G. & LATGE, J. P. 2017. *Aspergillus fumigatus* morphology and dynamic host interactions. *Nat Rev Microbiol,* 15**,** 661-674.

VAN DROGEN, F., STUCKE, V. M., JORRITSMA, G. & PETER, M. 2001. MAP kinase dynamics in response to pheromones in budding yeast. *Nat Cell Biol,* 3**,** 1051-9.

VARGA, J., SZIGETI, G., BARANYI, N., KOCSUBE, S., O'GORMAN, C. M. & DYER, P. S. 2014. *Aspergillus*: sex and recombination. *Mycopathologia,* 178**,** 349-62.

VIENKEN, K. & FISCHER, R. 2006. The Zn(II)2Cys6 putative transcription factor NosA controls fruiting body formation in *Aspergillus nidulans*. *Mol Microbiol,* 61**,** 544-54.

WEI, H., REQUENA, N. & FISCHER, R. 2003. The MAPKK kinase SteC regulates conidiophore morphology and is essential for heterokaryon formation and sexual development in the homothallic fungus *Aspergillus nidulans*. *Mol Microbiol,* 47**,** 1577-88.

WEI, H., SCHERER, M., SINGH, A., LIESE, R. & FISCHER, R. 2001. *Aspergillus nidulans* alpha-1,3 glucanase (mutanase), *mutA*, is expressed during sexual development and mobilizes mutan. *Fungal Genet Biol,* 34**,** 217-27.

WHITEWAY, M. S., WU, C., LEEUW, T., CLARK, K., FOUREST-LIEUVIN, A., THOMAS, D. Y. & LEBERER, E. 1995. Association of the yeast pheromone response G protein beta gamma subunits with the MAP kinase scaffold Ste5p. *Science,* 269**,** 1572-5.

WHITMARSH, A. J., CAVANAGH, J., TOURNIER, C., YASUDA, J. & DAVIS, R. J. 1998. A mammalian scaffold complex that selectively mediates MAP kinase activation. *Science,* 281**,** 1671-4.

WICKLOW, D. T. & SHOTWELL, O. L. 1983. Intrafungal distribution of aflatoxins among conidia and sclerotia of *Aspergillus flavus* and *Aspergillus parasiticus*. *Can J Microbiol,* 29**,** 1-5.

WIDMANN, C., GIBSON, S., JARPE, M. B. & JOHNSON, G. L. 1999. Mitogen-activated protein kinase: conservation of a three-kinase module from yeast to human. *Physiol Rev,* 79**,** 143-80.

WIEMANN, P., BROWN, D. W., KLEIGREWE, K., BOK, J. W., KELLER, N. P., HUMPF, H. U. & TUDZYNSKI, B. 2010. FfVel1 and FfLae1, components of a velvet-like complex in *Fusarium fujikuroi*, affect differentiation, secondary metabolism and virulence. *Mol Microbiol,* 77**,** 972-94.

WIESER, J., LEE, B. N., FONDON, J., 3RD & ADAMS, T. H. 1994. Genetic requirements for initiating asexual development in *Aspergillus nidulans*. *Curr Genet,* 27**,** 62-9.

WILLETTS, H. J. & BULLOCK, S. 1992. Developmental biology of sclerotia. Mycol. Res.

WONG SAK HOI, J. & DUMAS, B. 2010. Ste12 and Ste12-like proteins, fungal transcription factors regulating development and pathogenicity. *Eukaryot Cell,* 9**,** 480-5.

WU, C., LEBERER, E., THOMAS, D. Y. & WHITEWAY, M. 1999. Functional characterization of the interaction of Ste50p with Ste11p MAPKKK in *Saccharomyces cerevisiae*. *Mol Biol Cell,* 10**,** 2425-40.

XU, C. & MIN, J. 2011. Structure and function of WD40 domain proteins. *Protein Cell,* 2**,** 202-14.

XU, G., JANSEN, G., THOMAS, D. Y. & RAMEZANI RAD, M. 1996. Ste50p sustains mating pheromone-induced signal transduction in the yeast *Saccharomyces cerevisiae*. *Mol Microbiol,* 20**,** 773-83.

YAEGASHI, J., OAKLEY, B. R. & WANG, C. C. 2014. Recent advances in genome mining of secondary metabolite biosynthetic gene clusters and the development of heterologous expression systems in *Aspergillus nidulans*. *J Ind Microbiol Biotechnol,* 41**,** 433-42.

YASUDA, J., WHITMARSH, A. J., CAVANAGH, J., SHARMA, M. & DAVIS, R. J. 1999. The JIP group of mitogen-activated protein kinase scaffold proteins. *Mol Cell Biol,* 19**,** 7245-54.

YOSHIOKA, K. 2004. Scaffold proteins in mammalian MAP kinase cascades. *J Biochem,* 135**,** 657-61.

YU, J., CLEVELAND, T. E., NIERMAN, W. C. & BENNETT, J. W. 2005. *Aspergillus flavus* genomics: gateway to human and animal health, food safety, and crop resistance to diseases. *Rev Iberoam Micol,* 22**,** 194-202.

YU, J. H. 2010. Regulation of Development in *Aspergillus nidulans* and *Aspergillus fumigatus*. *Mycobiology,* 38**,** 229-37.

YU, J. H. & KELLER, N. 2005. Regulation of secondary metabolism in filamentous fungi. *Annu Rev Phytopathol,* 43**,** 437-58.

ZARRINPAR, A., BHATTACHARYYA, R. P., NITTLER, M. P. & LIM, W. A. 2004. Sho1 and Pbs2 act as coscaffolds linking components in the yeast high osmolarity MAP kinase pathway. *Mol Cell,* 14**,** 825-32.

ZENG, L., FAGOTTO, F., ZHANG, T., HSU, W., VASICEK, T. J., PERRY, W. L., 3RD, LEE, J. J., TILGHMAN, S. M., GUMBINER, B. M. & COSTANTINI, F. 1997. The mouse Fused locus encodes Axin, an inhibitor of the Wnt signaling pathway that regulates embryonic axis formation. *Cell,* 90**,** 181-92.

ZHANG, M. & WANG, W. 2003. Organization of signaling complexes by PDZ-domain scaffold proteins. *Acc Chem Res,* 36**,** 530-8.

ZHANG, Y., NEO, S. Y., WANG, X., HAN, J. & LIN, S. C. 1999. Axin forms a complex with MEKK1 and activates c-Jun NH(2)-terminal kinase/stress-activated protein kinase through domains distinct from Wnt signaling. *J Biol Chem,* 274**,** 35247-54.

ZHAO, X., KIM, Y., PARK, G. & XU, J. R. 2005. A mitogen-activated protein kinase cascade regulating infection-related morphogenesis in *Magnaporthe grisea*. *Plant Cell,* 17**,** 1317-29.

ZHAO, X., SPRAKER, J. E., BOK, J. W., VELK, T., HE, Z. M. & KELLER, N. P. 2017. A Cellular Fusion Cascade Regulated by LaeA Is Required for Sclerotial Development in *Aspergillus flavus*. *Front Microbiol,* 8**,** 1925.

ZIAEE, A., ZIA, M. & GOLI, M. 2018. Identification of saprophytic and allergenic fungi in indoor and outdoor environments. *Environ Monit Assess,* 190**,** 574.

Appendix A

Supplementary Data Relevant

to Chapter 3
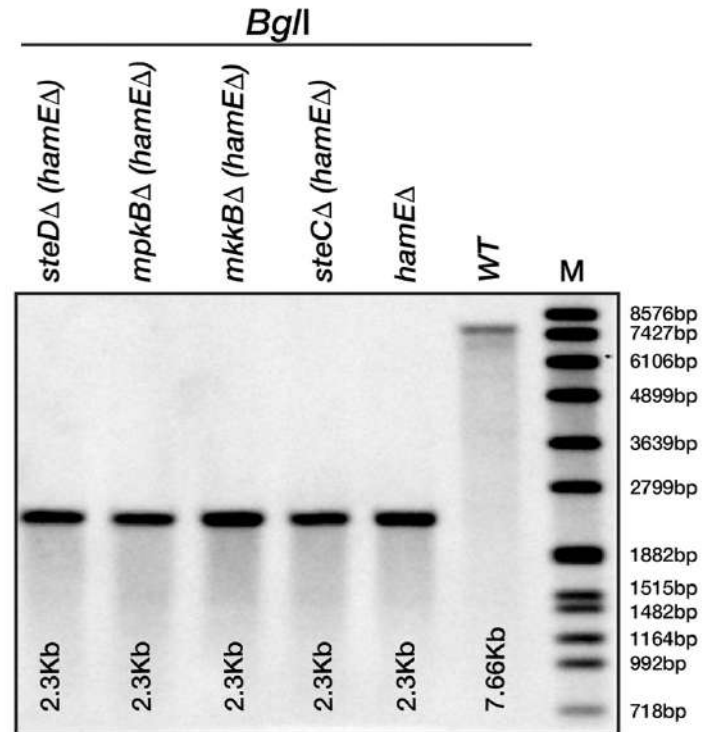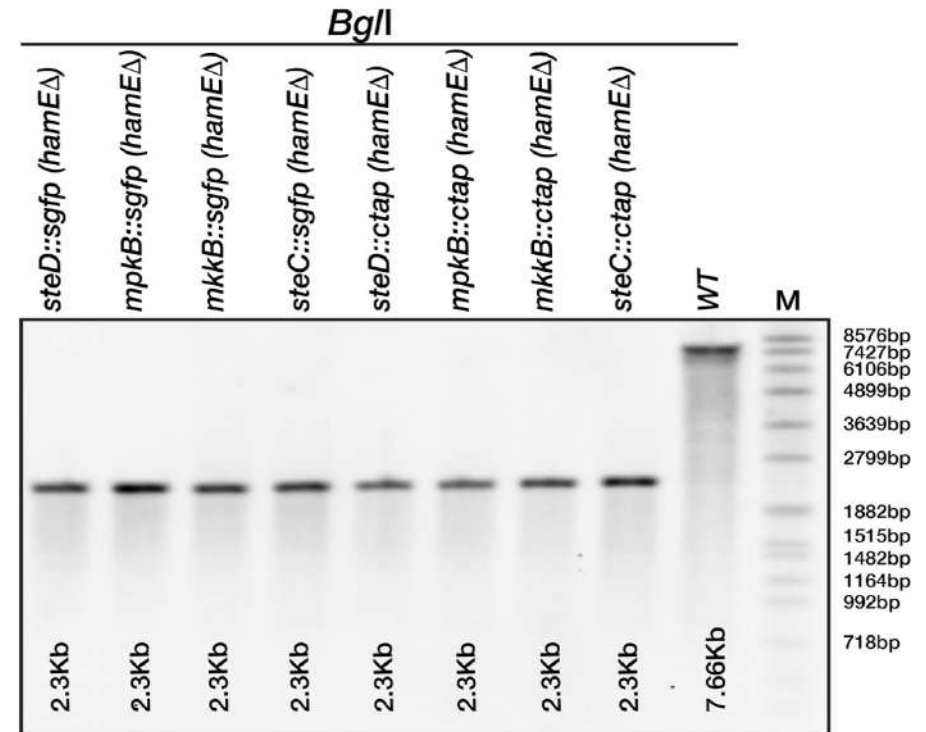
Figure S1: Southern hybridizations of the *hamEΔ* genomic region in *A. nidulans* strains (a) Southern hybridizations of the *hamEΔ* genomic region in kinase deletion background strains. M: Molecular marker in basepairs (bp). Sizes of the bands are shown for the wild type strain and the deletion strains and are in accordance with theoretical maps. The *Bgl*I restriction enzyme was used to digest genomic DNA and a 5' UTR DIG-labelled probe was used for detection. (b) Southern hybridizations of the *hamEΔ* genomic region in *ctap* and *sgfp* fused kinase backgrounds.
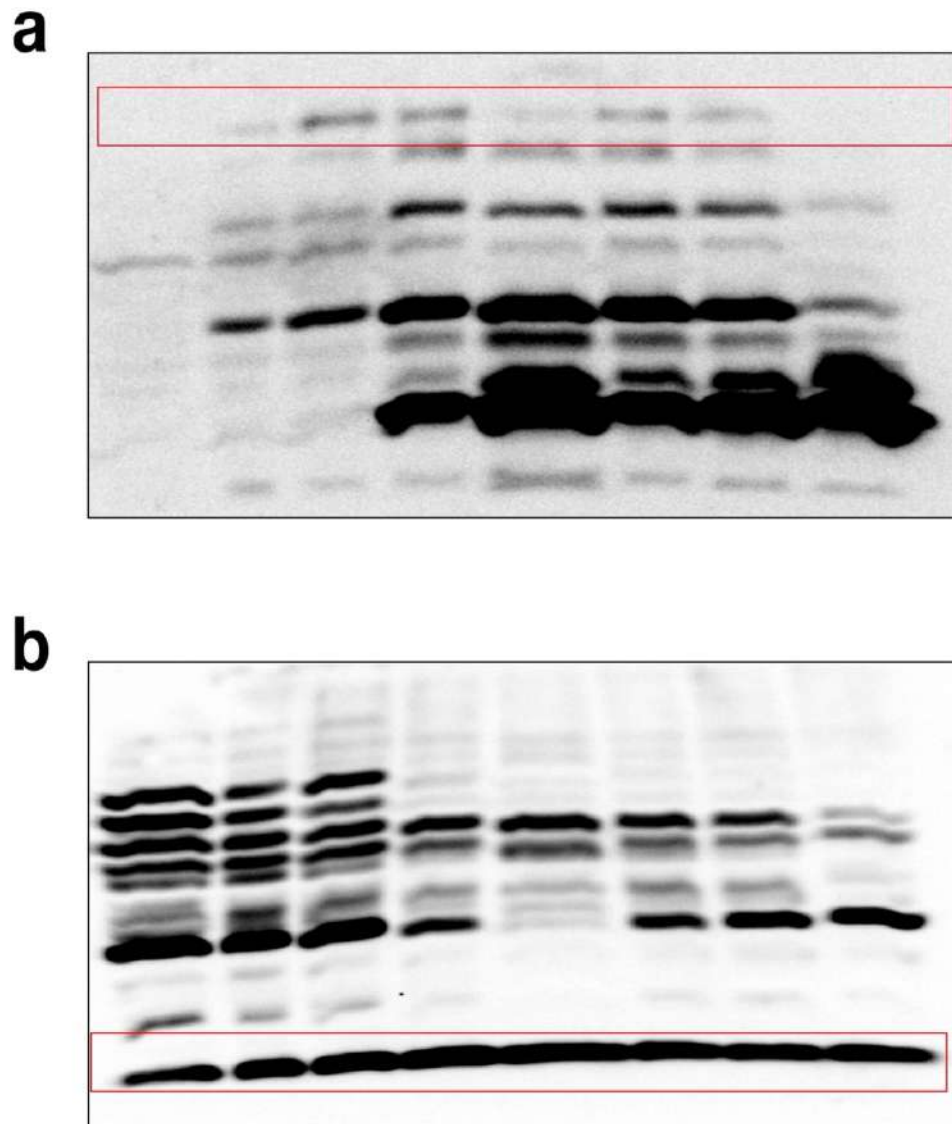
Figure S2: Full length western blot membranes used to generate Figure 3.4. (a) Full length blot of sGFP-tagged HamE during different stages of development. Highlighted red box represents the portion of the blot that was cropped for use in the figure. (b) Full length blot of the SkpA loading control. The highlighted red box represents the section of the blot that was cropped for use in the figure.
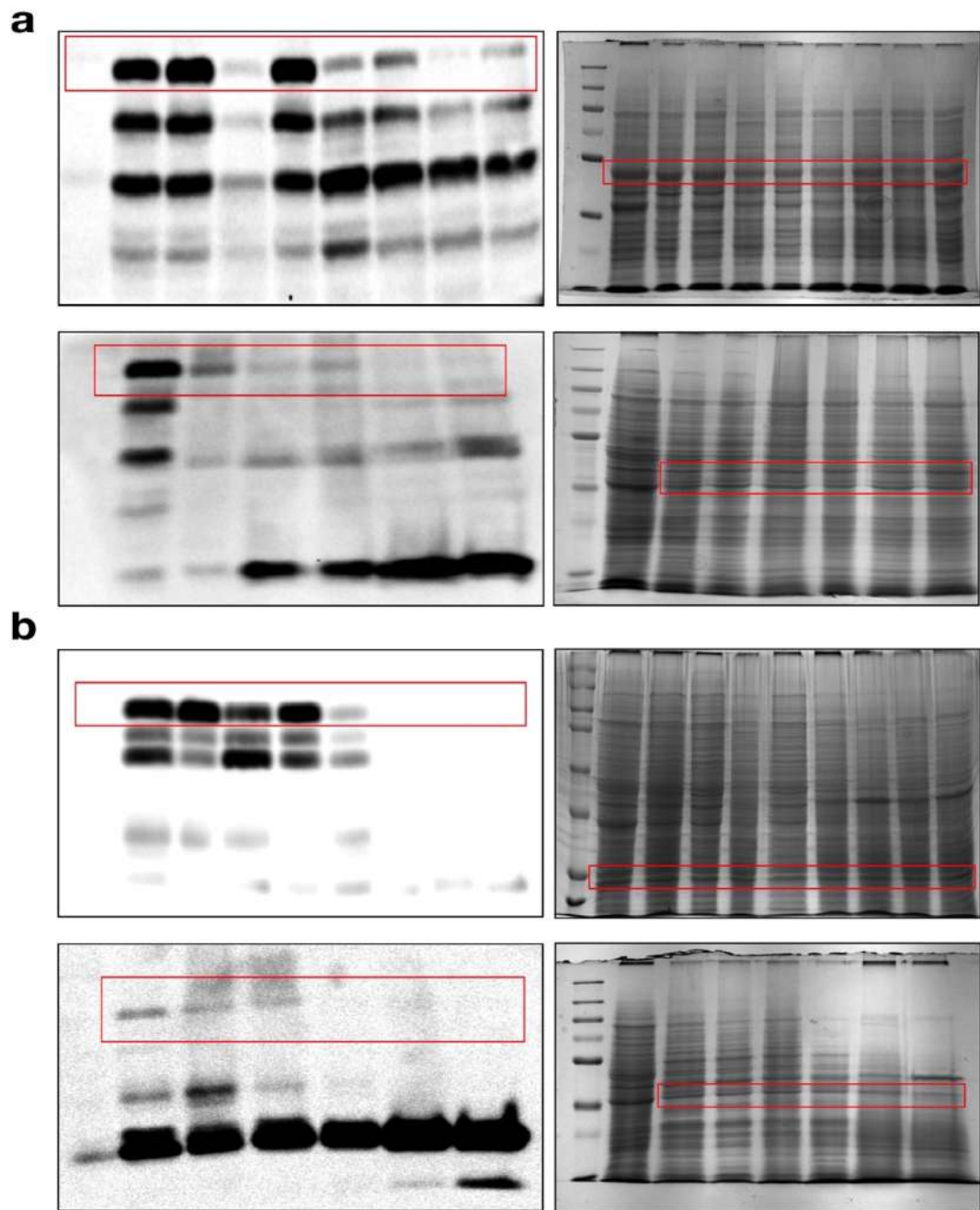
Figure S3: Full length western blot membranes and coomassie stained gels used to generate the SteC and MkkB-GFP panels in Figure 3.15. (a) Full blots and coomassie staining images used to generate the SteC-GFP panels. (b) Full blots and coomassie staining images used to generate the MkkB-GFP panels.
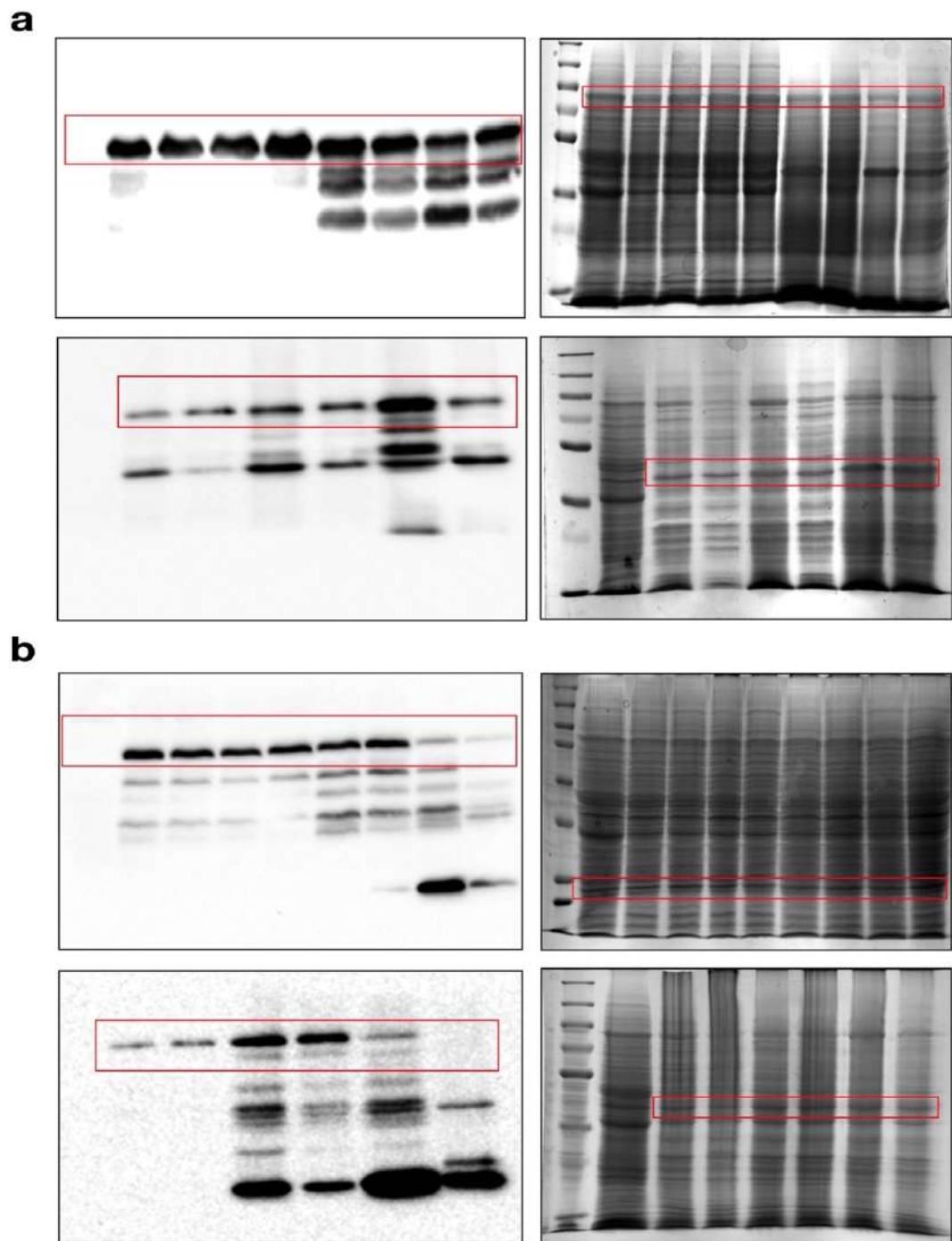
Figure S4: Full length western blot membranes and coomassie stained gels used to generate the MpkB and SteD-GFP panels in Figure 3.15. (a) Full blots and coomassie staining images used to generate the MpkB-GFP panels. (b) Full blots and coomassie staining images used to generate the SteD-GFP panels.
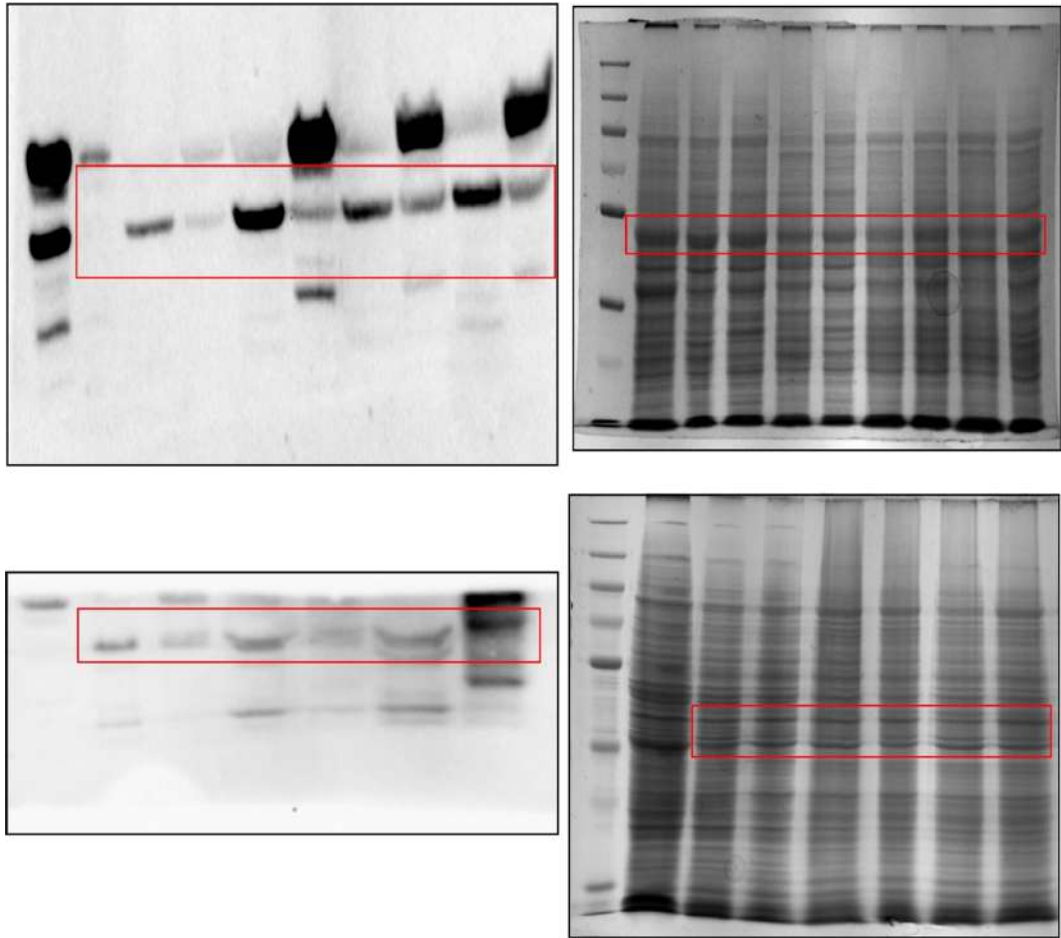
Figure S5: Full length western blot membranes and coomassie stained gels used to generate part (a) of Figure 3.16. The highlighted red boxes represent the sections of the blots/gels that were cropped for use in the figure.

Table S1: SteC-TAP interacting proteins during 24 hours of vegetative growth. Columns highlighted in yellow represent pheromone module proteins. AN2701 represents HamE.

Accession	Description	Score	Coverage	# Proteins	Unique Peptides	# Peptides	# PSMs	# AAs	MW [kDa]	calc. pI
AN2269	steC AspGDID:ASPL0000047432 COORDS:ChrVII_A_nidulans_FGSC_A4:3394519-33917	398.77	68.28	3	45	45	124	886	97.7	7.84
AN7252	steD AspGDID:ASPL0000068680 COORDS:ChrIV_A_nidulans_FGSC_A4:526909-528499	177.55	73.48	1	27	27	57	494	54.3	5.82
AN2701	AN2701 AspGDID:ASPL0000036914 COORDS:ChrVI_A_nidulans_FGSC_A4:3104669-310	96.67	25.22	1	30	30	37	1570	171.6	9.52
AN2068	AN2068 AspGDID:ASPL0000048811 COORDS:ChrVII_A_nidulans_FGSC_A4:2753420-2757504W, trar	31.62	18.39	1	16	16	16	1305	141.4	6.99
AN6988	AN6988 AspGDID:ASPL0000064945 COORDS:ChrIV_A_nidulans_FGSC_A4:1383661-1384960W, tran	11.53	17.74	2	4	5	6	389	43.4	8.18
AN3422	ste7 AspGDID:ASPL0000040884 COORDS:ChrVI_A_nidulans_FGSC_A4:772852-774627	8.74	19.67	1	6	6	7	539	58.9	9.26
AN0948	AN0948 AspGDID:ASPL0000060008 COORDS:ChrVIII_A_nidulans_FGSC_A4:1982457-1984990W, tra	8.24	4.25	1	2	2	3	753	84.2	7.30
AN8182	aspC AspGDID:ASPL0000010754 COORDS:ChrII_A_nidulans_FGSC_A4:1048209-1046907C, translate	5.27	14.81	2	5	5	5	351	40.8	7.39
AN4547	AN4547 AspGDID:ASPL0000072207 COORDS:ChrIII_A_nidulans_FGSC_A4:1694126-1691097C, trans	5.13	5.89	1	3	3	3	917	100.6	5.55
AN6082	AN6082 AspGDID:ASPL0000005199 COORDS:ChrI_A_nidulans_FGSC_A4:1315000-1314445C, transla	4.99	29.25	1	2	2	2	106	11.4	9.83
AN1122	AN1122 AspGDID:ASPL0000057044 COORDS:ChrVIII_A_nidulans_FGSC_A4:1450792-1451666W, tra	2.86	12.44	1	2	2	2	217	24.2	9.92
AN8403	AN8403 AspGDID:ASPL0000029804 COORDS:ChrV_A_nidulans_FGSC_A4:374556-375556W, translat	2.83	3.21	1	1	1	1	280	28.7	9.55
AN2980	AN2980 AspGDID:ASPL0000041158 COORDS:ChrVI_A_nidulans_FGSC_A4:2188481-2189262W, tran	2.81	9.17	1	1	1	1	109	12.3	11.22
AN12491	AN12491 AspGDID:ASPL0000403457 COORDS:ChrI_A_nidulans_FGSC_A4:3575960-3573772C, trans	2.60	4.89	1	1	1	1	266	28.1	10.14
AN1066	AN1066 AspGDID:ASPL0000053780 COORDS:ChrVIII_A_nidulans_FGSC_A4:1627620-1626735C, tra	2.57	8.21	1	1	1	1	268	30.0	9.10
AN8874	AN8874 AspGDID:ASPL0000044708 COORDS:ChrVII_A_nidulans_FGSC_A4:596174-593664C, transla	2.31	1.26	1	1	1	1	794	88.2	6.84
AN3070	AN3070 AspGDID:ASPL0000038764 COORDS:ChrVI_A_nidulans_FGSC_A4:1946042-1944467C, trans	2.17	2.96	1	1	1	1	473	51.8	6.20
AN1700	AN1700 AspGDID:ASPL0000047917 COORDS:ChrVII_A_nidulans_FGSC_A4:1661294-1657645C, tran	2.03	2.57	1	2	2	2	1128	123.6	4.97
AN0673	AN0673 AspGDID:ASPL0000060421 COORDS:ChrVIII_A_nidulans_FGSC_A4:2827801-2826199C, tra	1.98	2.06	1	1	1	1	388	43.7	6.39
AN1967	ppoA AspGDID:ASPL0000045184 COORDS:ChrVII_A_nidulans_FGSC_A4:2425862-2422295C, transla	1.97	1.02	1	1	1	1	1081	120.7	6.24
AN12477	AN12477 AspGDID:ASPL0000395426 COORDS:ChrII_A_nidulans_FGSC_A4:3885169-3881258C, tran	1.92	1.09	1	1	1	1	1013	113.5	5.43
AN0866	AN0866 AspGDID:ASPL0000059656 COORDS:ChrVIII_A_nidulans_FGSC_A4:2232313-2229877C, tra	1.91	1.71	1	1	1	1	702	77.9	7.59
AN4222	AN4222 AspGDID:ASPL0000016741 COORDS:ChrII_A_nidulans_FGSC_A4:1700210-1700927W, trans	1.90	20.74	1	3	3	3	135	15.6	10.54
AN4936	prp4 AspGDID:ASPL0000072111 COORDS:ChrIII_A_nidulans_FGSC_A4:501679-504118W, translated	1.75	0.90	1	1	1	1	780	88.6	7.91
AN1177	AN1177 AspGDID:ASPL0000052724 COORDS:ChrVIII_A_nidulans_FGSC_A4:1288872-1291941W, tra	1.66	0.84	1	1	1	1	950	105.7	5.55
AN6900	tpiA AspGDID:ASPL0000001144 COORDS:ChrI_A_nidulans_FGSC_A4:3517593-3518737W, translated	0.00	6.02	1	1	1	1	249	27.1	6.13
AN2488	AN2488 AspGDID:ASPL0000047088 COORDS:ChrVII_A_nidulans_FGSC_A4:4109983-4110663W, trar	0.00	12.14	1	1	1	1	173	19.7	8.84
AN0118	nudA AspGDID:ASPL0000062573 COORDS:ChrVIII_A_nidulans_FGSC_A4:4538250-4551348W, trans	0.00	0.14	1	1	1	1	4345	491.8	5.97
AN0688	AN0688 AspGDID:ASPL0000053784 COORDS:ChrVIII_A_nidulans_FGSC_A4:2786646-2789142W, tra	0.00	3.51	1	2	2	2	684	74.5	6.37
AN2296	AN2296 AspGDID:ASPL0000043720 COORDS:ChrVII_A_nidulans_FGSC_A4:3475231-3478036W, trar	0.00	1.04	1	1	1	1	862	95.0	6.62
AN6329	AN6329 AspGDID:ASPL0000002722 COORDS:ChrI_A_nidulans_FGSC_A4:516784-507119C, translate	0.00	0.25	1	1	1	1	3187	356.7	7.08

Table S2: MkkB-TAP interacting proteins during 24 hours of vegetative growth

Accession	Description	Score	Coverage	# Proteins	Unique Peptides	# Peptides	# PSMs	# AAs	MW [kDa]	calc. pI
AN3422	ste7 AspGDID:ASPL0000040884 COORDS:ChrVI_A_nidulans_FGSC_A4:772852-774627W, translated using c	302.92	72.17	1	29	29	119	539	58.9	9.26
AN2701	AN2701 AspGDID:ASPL0000036914 COORDS:ChrVI_A_nidulans_FGSC_A4:3104669-3109566W, translated u	190.19	39.04	1	43	43	60	1570	171.6	9.52
AN2269	steC AspGDID:ASPL0000047432 COORDS:ChrVII_A_nidulans_FGSC_A4:3394519-3391706C, translated usin	164.44	54.18	1	36	36	50	886	97.7	7.84
AN3719	mpkB AspGDID:ASPL00000010103 COORDS:ChrII_A_nidulans_FGSC_A4:3287538-3288820W, translated usin	94.84	78.53	1	18	18	25	354	41.0	6.90
AN11173	AN11173 AspGDID:ASPL0000037145 COORDS:ChrVI_A_nidulans_FGSC_A4:562397-560740C, translated using codon table	93.16	70.95		1	20	20	26	420	47.4	6.54
AN7252	steD AspGDID:ASPL0000068680 COORDS:ChrIV_A_nidulans_FGSC_A4:526909-528499W, translated using c	90.63	69.03	1	22	22	32	494	54.3	5.82
AN4182	nimX AspGDID:ASPL0000011155 COORDS:ChrII_A_nidulans_FGSC_A4:1845106-1843914C, translated using codon table 1 (	20.44	29.10	1	7	7	8	323	36.8	7.28
AN5666	mpkA AspGDID:ASPL0000028487 COORDS:ChrV_A_nidulans_FGSC_A4:2038483-2039584W, translated using codon table 1	5.19	9.70	1	2	2	2	330	37.9	4.96
AN4563	ckiA AspGDID:ASPL0000072181 COORDS:ChrIII_A_nidulans_FGSC_A4:1656470-1657827W, translated using codon table 1	3.43	7.03	1	2	2	2	370	42.6	9.55
AN6701	AN6701 AspGDID:ASPL0000003259 COORDS:ChrI_A_nidulans_FGSC_A4:2901645-2900755C, translated using codon table	2.75	7.29	1	1	1	1	247	26.4	9.39
AN7659	AN7659 AspGDID:ASPL0000065093 COORDS:ChrIV_A_nidulans_FGSC_A4:2294510-2296239W, translated using codon tabl	2.71	4.40	1	1	1	1	477	52.4	6.57
AN10778	AN10778 AspGDID:ASPL0000008271 COORDS:ChrI_A_nidulans_FGSC_A4:975084-973327C, translated using codon table 1	2.40	2.39	1	1	1	1	545	57.4	9.31
AN4523	prp8 AspGDID:ASPL0000077099 COORDS:ChrIII_A_nidulans_FGSC_A4:1775943-1766887C, translated using codon table 1	2.37	0.65	1	1	1	1	2940	338.9	8.31
AN2150	AN2150 AspGDID:ASPL0000045530 COORDS:ChrVII_A_nidulans_FGSC_A4:3036747-3038720W, translated using codon tab	2.34	3.54	1	1	1	1	594	66.1	7.14
AN4085	AN4085 AspGDID:ASPL0000015687 COORDS:ChrII_A_nidulans_FGSC_A4:2142705-2145033W, translated using codon table	1.95	2.60	1	1	1	1	616	69.0	4.81
AN0140	AN0140 AspGDID:ASPL0000062071 COORDS:ChrVIII_A_nidulans_FGSC_A4:4475446-4474013C, translated using codon tab	1.87	2.57	1	1	1	1	428	46.6	6.86
AN7030	bemA AspGDID:ASPL0000064539 COORDS:ChrIV_A_nidulans_FGSC_A4:1256525-1258694W, translated using codon table	0.00	3.25	1	1	1	1	616	68.1	7.65
AN2493	AN2493 AspGDID:ASPL0000050594 COORDS:ChrVII_A_nidulans_FGSC_A4:4128076-4125973C, translated using codon tabl	0.00	4.68	1	1	1	1	663	73.1	5.17
AN5865	AN5865 AspGDID:ASPL0000000466 COORDS:ChrI_A_nidulans_FGSC_A4:1972670-1974875W, translated using codon table	0.00	1.52	1	1	1	1	656	74.3	9.11
AN6329	AN6329 AspGDID:ASPL0000002722 COORDS:ChrI_A_nidulans_FGSC_A4:516784-507119C, translated using codon table 1 (	0.00	0.25	1	1	1	1	3187	356.7	7.08
AN3420	AN3420 AspGDID:ASPL0000040053 COORDS:ChrVI_A_nidulans_FGSC_A4:780303-781940W, translated using codon table 1	0.00	1.90	1	1	1	1	527	60.0	8.57
AN6700	AN6700 AspGDID:ASPL0000007308 COORDS:ChrI_A_nidulans_FGSC_A4:2897960-2894554C, translated using codon table	0.00	0.82	1	1	1	1	1103	121.3	6.10
AN1966	hulE AspGDID:ASPL0000049675 COORDS:ChrVII_A_nidulans_FGSC_A4:2421142-2408808C, translated using codon table 1	0.00	0.70	1	1	1	1	4019	447.8	5.05

Table S3: MpkB-TAP interacting proteins during 24 hours of vegetative growth

Accession	Description	Score	Coverage	# Proteins	Unique Peptides	# Peptides	# PSMs	# AAs	MW [kDa]	calc. pI
AN3719	mpkB AspGDID:ASPL0000010103 COORDS:ChrII_A_nidulans_FGSC_A4:3	379.68	82.20	1	25	25	125	354	41.0	6.90
AN2701	AN2701 AspGDID:ASPL0000036914 COORDS:ChrVI_A_nidulans_FGSC_A4	213.77	46.56	1	50	50	72	1570	171.6	9.52
AN6560	AN6560 AspGDID:ASPL0000000623 COORDS:ChrI_A_nidulans_FGSC_A4:2460021-24	140.60	57.73	1	19	19	47	459	49.2	10.52
AN8862	myoV AspGDID:ASPL0000071197 COORDS:ChrIII_A_nidulans_FGSC_A4:2568236-25	136.69	36.97	1	42	42	52	1569	179.0	6.99
AN3422	ste7 AspGDID:ASPL0000040884 COORDS:ChrVI_A_nidulans_FGSC_A4:77	111.40	56.96	1	21	21	34	539	58.9	9.26
AN2290	steA AspGDID:ASPL0000050963 COORDS:ChrVII_A_nidulans_FGSC_A4:3458964-345	55.26	31.21	1	16	16	20	692	76.6	6.93
AN5982	torA AspGDID:ASPL0000006879 COORDS:ChrI_A_nidulans_FGSC_A4:1599573-15922	37.31	11.91	1	21	21	21	2385	269.3	7.08
AN6010	sgdE AspGDID:ASPL0000007208 COORDS:ChrI_A_nidulans_FGSC_A4:1520285-1518	32.33	26.73	1	13	13	14	666	72.3	6.04
AN5746	acuN AspGDID:ASPL0000028218 COORDS:ChrV_A_nidulans_FGSC_A4:1820581-182	27.86	26.94	1	9	9	10	438	47.5	5.57
AN2047	CaM AspGDID:ASPL0000051423 COORDS:ChrVII_A_nidulans_FGSC_A4:2693663-269	27.43	56.38	1	8	9	12	149	17.0	4.27
AN5603	AN5603 AspGDID:ASPL0000026783 COORDS:ChrV_A_nidulans_FGSC_A4:2257109-2	25.84	12.07	1	11	11	11	1218	134.1	6.62
AN4743	racA AspGDID:ASPL0000073163 COORDS:ChrIII_A_nidulans_FGSC_A4:1120752-112	15.13	26.63	1	4	4	5	199	22.2	7.72
AN4182	nimX AspGDID:ASPL0000011155 COORDS:ChrII_A_nidulans_FGSC_A4:1845106-184	14.54	22.60	1	5	5	5	323	36.8	7.28
AN1967	ppoA AspGDID:ASPL0000045184 COORDS:ChrI_A_nidulans_FGSC_A4:2425862-24	14.00	9.90	1	8	8	8	1081	120.7	6.24
AN5168	AN5168 AspGDID:ASPL0000030834 COORDS:ChrV_A_nidulans_FGSC_A4:1374007-1	13.35	9.62	1	9	9	11	1299	142.8	6.48
AN1558	myoA AspGDID:ASPL0000043272 COORDS:ChrV_A_nidulans_FGSC_A4:1171032-11	13.30	9.21	1	9	9	10	1249	137.0	9.39
AN2062	bipA AspGDID:ASPL0000045915 COORDS:ChrVII_A_nidulans_FGSC_A4:2730139-272	12.28	8.46	1	5	5	6	674	73.7	4.97
AN6330	AN6330 AspGDID:ASPL0000004211 COORDS:ChrI_A_nidulans_FGSC_A4:505935-503	11.66	9.95	1	6	6	6	844	93.7	6.68
AN5169	AN5169 AspGDID:ASPL0000027409 COORDS:ChrV_A_nidulans_FGSC_A4:1378128-1	11.55	8.51	1	5	5	5	823	91.5	8.18
AN4859	pmaA AspGDID:ASPL0000077585 COORDS:ChrIII_A_nidulans_FGSC_A4:748768-745	10.08	7.27	2	5	5	5	990	108.7	5.36
AN3664	AN3664 AspGDID:ASPL0000015483 COORDS:ChrII_A_nidulans_FGSC_A4:3450340-3	8.61	13.18	1	5	5	5	516	62.7	9.07
AN0214	AN0214 AspGDID:ASPL0000056619 COORDS:ChrVIII_A_nidulans_FGSC_A4:4273702	8.04	7.17	1	6	6	6	976	108.2	5.47
AN7570	tubB AspGDID:ASPL0000065841 COORDS:ChrIV_A_nidulans_FGSC_A4:1979601-197	7.27	8.43	2	1	3	3	451	50.0	5.11
AN7953	AN7953 AspGDID:ASPL0000013400 COORDS:ChrII_A_nidulans_FGSC_A4:316180-31	7.09	20.12	1	4	4	4	338	38.6	6.16
AN4544	AN4544 AspGDID:ASPL0000075073 COORDS:ChrIII_A_nidulans_FGSC_A4:1706426-	6.81	7.41	1	4	4	4	702	76.0	6.81
AN1263	AN1263 AspGDID:ASPL0000057622 COORDS:ChrVIII_A_nidulans_FGSC_A4:1016078	6.54	7.13	1	2	2	2	449	48.8	6.47
AN7030	bemA AspGDID:ASPL0000064539 COORDS:ChrIV_A_nidulans_FGSC_A4:1256525-12	5.99	7.63	1	3	3	3	616	68.1	7.65
AN4474	AN4474 AspGDID:ASPL0000076079 COORDS:ChrIII_A_nidulans_FGSC_A4:1932392-	5.53	32.81	1	3	3	3	128	14.2	10.43
AN2436	aclB AspGDID:ASPL0000051301 COORDS:ChrVII_A_nidulans_FGSC_A4:3947892-395	4.67	7.02	1	3	3	3	655	71.5	8.05
AN0768	AN0768 AspGDID:ASPL0000059306 COORDS:ChrVIII_A_nidulans_FGSC_A4:2530403	4.48	5.89	1	3	3	3	492	54.7	6.01
AN5226	acpA AspGDID:ASPL0000028397 COORDS:ChrV_A_nidulans_FGSC_A4:1553659-1552	4.47	9.73	1	2	2	2	298	31.6	6.09
AN5442	cpyA AspGDID:ASPL0000030746 COORDS:ChrV_A_nidulans_FGSC_A4:2803189-2804	4.45	7.79	1	3	3	3	552	62.0	5.05
AN6089	AN6089 AspGDID:ASPL0000003680 COORDS:ChrI_A_nidulans_FGSC_A4:1294502-12	4.38	9.18	1	4	4	4	588	61.8	5.63
AN5790	AN5790 AspGDID:ASPL0000029618 COORDS:ChrV_A_nidulans_FGSC_A4:1696926-16	4.36	6.61	1	2	2	2	439	47.9	8.94
AN2435	aclA AspGDID:ASPL0000045833 COORDS:ChrVII_A_nidulans_FGSC_A4:3945971-394	4.34	6.80	1	3	3	3	485	53.0	6.18
AN0554	aldA AspGDID:ASPL0000055794 COORDS:ChrVIII_A_nidulans_FGSC_A4:3188631-31	4.30	8.45	1	3	3	3	497	54.1	6.62
AN4479	nikA AspGDID:ASPL0000074067 COORDS:ChrIII_A_nidulans_FGSC_A4:1917993-191	4.07	3.08	1	1	1	1	1297	142.7	5.41
AN5740	rhoA AspGDID:ASPL0000033387 COORDS:ChrV_A_nidulans_FGSC_A4:1836572-1835	4.07	29.02	1	4	4	4	193	21.7	6.67
AN1369	AN1369 AspGDID:ASPL0000060179 COORDS:ChrII_A_nidulans_FGSC_A4:726428-	4.06	5.01	1	1	1	1	459	50.6	4.51
AN2936	AN2936 AspGDID:ASPL0000039697 COORDS:ChrVI_A_nidulans_FGSC_A4:2343393-2	4.05	2.28	1	2	2	2	1095	124.0	5.59
AN1599	pbcR AspGDID:ASPL0000042603 COORDS:ChrVII_A_nidulans_FGSC_A4:1296287-12	3.96	6.29	1	1	1	1	700	77.8	5.58
AN1980	AN1980 AspGDID:ASPL0000048719 COORDS:ChrVII_A_nidulans_FGSC_A4:2451771-	3.55	3.62	1	1	1	1	883	97.3	5.22
AN7984	AN7984 AspGDID:ASPL0000011950 COORDS:ChrII_A_nidulans_FGSC_A4:397432-39	3.41	2.98	1	1	1	1	503	54.4	7.15
AN3172	AN3172 AspGDID:ASPL0000040942 COORDS:ChrII_A_nidulans_FGSC_A4:1592512-1	3.11	8.87	1	2	2	3	293	31.6	4.91
AN9204	ngn6 AspGDID:ASPL0000041086 COORDS:ChrVI_A_nidulans_FGSC_A4:112265-1116	3.05	19.29	1	1	1	1	197	22.8	7.06
AN0451	AN0451 AspGDID:ASPL0000062676 COORDS:ChrVII_A_nidulans_FGSC_A4:3511999	3.05	5.58	1	1	1	1	215	24.3	6.44
AN0310	AN0310 AspGDID:ASPL0000062261 COORDS:ChrVIII_A_nidulans_FGSC_A4:3951375	2.96	2.80	1	1	1	1	535	59.3	4.61
AN3075	oefC AspGDID:ASPL0000036798 COORDS:ChrVI_A_nidulans_FGSC_A4:1925548-192	2.88	5.49	1	1	1	1	637	71.8	6.29
AN1171	kin1 AspGDID:ASPL0000056639 COORDS:ChrVIII_A_nidulans_FGSC_A4:1308284-13	2.71	2.55	1	2	2	2	1059	117.4	9.77
AN4639	AN4639 AspGDID:ASPL0000073481 COORDS:ChrIII_A_nidulans_FGSC_A4:1447462-	2.68	3.86	1	3	3	3	1424	160.2	7.12
AN4013	AN4013 AspGDID:ASPL0000017916 COORDS:ChrIII_A_nidulans_FGSC_A4:2343271-2	2.54	1.16	1	1	1	1	860	95.5	7.24
AN1250	AN1250 AspGDID:ASPL0000059123 COORDS:ChrVIII_A_nidulans_FGSC_A4:1053105	2.49	2.09	1	1	1	1	622	70.5	10.26
AN2000	ubi4 AspGDID:ASPL0000049163 COORDS:ChrVII_A_nidulans_FGSC_A4:2515485-251	2.46	20.98	2	1	1	1	305	34.3	7.53
AN0866	AN0866 AspGDID:ASPL0000059656 COORDS:ChrVIII_A_nidulans_FGSC_A4:2232313	2.43	1.71	1	1	1	1	702	77.9	7.59
AN5066	AN5066 AspGDID:ASPL0000072873 COORDS:ChrIII_A_nidulans_FGSC_A4:99921-98	2.38	5.71	1	1	1	1	245	27.8	7.20
AN8403	AN8403 AspGDID:ASPL0000029804 COORDS:ChrV_A_nidulans_FGSC_A4:374556-37	2.34	3.21	1	1	1	1	280	28.7	9.55
AN1222	sasA AspGDID:ASPL0000052344 COORDS:ChrVIII_A_nidulans_FGSC_A4:1146168-11	2.33	9.79	1	2	2	2	388	42.2	5.50
AN1718	AN1718 AspGDID:ASPL0000042635 COORDS:ChrII_A_nidulans_FGSC_A4:1707417-	2.29	20.25	1	3	3	3	242	26.6	9.86
AN10130	AN10130 AspGDID:ASPL0000058475 COORDS:ChrVIII_A_nidulans_FGSC_A4:195724	2.26	10.87	1	1	1	1	92	10.2	10.18
AN1847	AN1847 AspGDID:ASPL0000051760 COORDS:ChrVIII_A_nidulans_FGSC_A4:2053414-	2.23	15.28	1	2	2	2	288	31.9	9.94
AN12475	AN12475 AspGDID:ASPL0000378904 COORDS:ChrVII_A_nidulans_FGSC_A4:324170	2.20	3.95	1	1	1	1	354	37.7	8.66
AN4936	prp4 AspGDID:ASPL0000072111 COORDS:ChrIII_A_nidulans_FGSC_A4:501679-5041	2.17	0.90	1	1	1	1	780	88.6	7.91
AN10736	AN10736 AspGDID:ASPL0000004051 COORDS:ChrI_A_nidulans_FGSC_A4:1994433-1	2.15	4.23	1	1	1	1	473	52.4	10.35

Table S3 (continued): MpkB-TAP interacting proteins during 24 hours of vegetative growth

ID	Description									
AN10736	AN10736 AspGDID:ASPL0000004051 COORDS:ChrI_A_nidulans_FGSC_A4:1994433-1995975W, translated using codon table 1 (473 amino	2.15	4.23	1	1	1	1	473	52.4	10.35
AN0411	AN0411 AspGDID:ASPL0000060507 COORDS:ChrVIII_A_nidulans_FGSC_A4:3637903-3638922W, translated using codon table 1 (192 amir	2.12	4.69	1	1	1	1	192	21.7	6.20
AN9407	fasA AspGDID:ASPL0000056625 COORDS:ChrVIII_A_nidulans_FGSC_A4:538683-532978C, translated using codon table 1 (1860 amino aci	2.12	0.54	1	1	1	1	1860	204.9	6.02
AN4281	rabO AspGDID:ASPL0000016908 COORDS:ChrII_A_nidulans_FGSC_A4:1520443-1521522W, translated using codon table 1 (201 amino ac	2.12	5.47	4	1	1	1	201	22.3	5.27
AN1175	AN1175 AspGDID:ASPL0000057791 COORDS:ChrVII_A_nidulans_FGSC_A4:1295736-1294630C, translated using codon table 1 (331 amin	2.10	3.02	1	1	1	1	331	37.4	5.91
AN2286	alcC AspGDID:ASPL0000042717 COORDS:ChrVII_A_nidulans_FGSC_A4:3446591-3445392C, translated using codon table 1 (352 amino ac	2.08	7.10	1	2	2	2	352	37.1	7.05
AN4501	artA AspGDID:ASPL0000074811 COORDS:ChrIII_A_nidulans_FGSC_A4:1848751-1847737C, translated using codon table 1 (261 amino ac	2.05	6.90	2	2	2	2	261	29.1	4.79
AN11008	AN11008 AspGDID:ASPL0000065685 COORDS:ChrIV_A_nidulans_FGSC_A4:2593040-2591532C, translated using codon table 1 (483 amino	2.01	4.14	1	1	1	1	483	53.0	8.75
AN2007	AN2007 AspGDID:ASPL0000047555 COORDS:ChrVII_A_nidulans_FGSC_A4:2543261-2542697C, translated using codon table 1 (116 amino	1.98	7.76	1	1	1	1	116	12.9	11.44
AN7258	AN7258 AspGDID:ASPL0000063859 COORDS:ChrIV_A_nidulans_FGSC_A4:514976-514042C, translated using codon table 1 (269 amino ac	1.96	6.69	1	1	1	1	269	29.5	10.08
AN5715	AN5715 AspGDID:ASPL0000029491 COORDS:ChrV_A_nidulans_FGSC_A4:1907272-1908090W, translated using codon table 1 (119 amino	1.94	20.17	1	2	2	2	119	13.5	10.87
AN5626	facA AspGDID:ASPL0000032980 COORDS:ChrV_A_nidulans_FGSC_A4:2172227-2169930C, translated using codon table 1 (670 amino acid	1.88	1.64	1	1	1	1	670	74.2	6.47
AN4563	ckiA AspGDID:ASPL0000072181 COORDS:ChrIII_A_nidulans_FGSC_A4:1656470-1657827W, translated using codon table 1 (370 amino ac	1.87	2.70	1	1	1	1	370	42.6	9.55
AN4168	AN4168 AspGDID:ASPL0000012058 COORDS:ChrII_A_nidulans_FGSC_A4:1894672-1893232C, translated using codon table 1 (410 amino	1.81	2.20	1	1	1	1	410	44.2	8.44
AN0118	nudA AspGDID:ASPL0000062573 COORDS:ChrVIII_A_nidulans_FGSC_A4:4538250-4551348W, translated using codon table 1 (4345 amino	1.80	0.14	1	1	1	1	4345	491.8	5.97
AN6681	AN6681 AspGDID:ASPL0000008688 COORDS:ChrI_A_nidulans_FGSC_A4:2833110-2831178C, translated using codon table 1 (543 amino a	1.78	2.21	1	1	1	1	543	61.3	6.76
AN3706	AN3706 AspGDID:ASPL0000012467 COORDS:ChrII_A_nidulans_FGSC_A4:3321661-3320973C, translated using codon table 1 (153 amino	1.77	7.84	1	1	1	1	153	17.6	9.82
AN4339	AN4339 AspGDID:ASPL0000077725 COORDS:ChrIII_A_nidulans_FGSC_A4:2345261-2342874C, translated using codon table 1 (782 amino	1.77	1.15	1	1	1	1	782	88.4	5.17
AN10620	AN10620 AspGDID:ASPL0000077491 COORDS:ChrII_A_nidulans_FGSC_A4:422542-423821W, translated using codon table 1 (375 amino	1.74	2.93	1	1	1	1	375	43.7	9.51
AN0140	AN0140 AspGDID:ASPL0000062071 COORDS:ChrVII_A_nidulans_FGSC_A4:4475446-4474013C, translated using codon table 1 (428 amino	1.71	4.91	1	2	2	2	428	46.6	6.86
AN7031	AN7031 AspGDID:ASPL0000068288 COORDS:ChrIV_A_nidulans_FGSC_A4:1252436-1254095W, translated using codon table 1 (515 amino	1.69	1.55	1	1	1	1	515	57.8	9.50
AN9320	AN9320 AspGDID:ASPL0000052150 COORDS:ChrVIII_A_nidulans_FGSC_A4:272723-269559C, translated using codon table 1 (1054 amino	1.67	0.76	1	1	1	1	1054	116.9	5.76
AN4532	AN4532 AspGDID:ASPL0000073527 COORDS:ChrIII_A_nidulans_FGSC_A4:1742160-1741099C, translated using codon table 1 (295 amino	1.65	3.39	1	1	1	1	295	33.0	5.57
AN5167	AN5167 AspGDID:ASPL0000026563 COORDS:ChrV_A_nidulans_FGSC_A4:1364294-1368255W, translated using codon table 1 (1166 amino	1.64	0.94	1	1	1	1	1166	128.5	7.88
AN8369	AN8369 AspGDID:ASPL0000027602 COORDS:ChrV_A_nidulans_FGSC_A4:258022-266816W, translated using codon table 1 (2815 amino a	1.61	0.25	1	1	1	1	2815	317.7	7.06
AN3223	pfkA AspGDID:ASPL0000034836 COORDS:ChrVI_A_nidulans_FGSC_A4:1415541-1418027W, translated using codon table 1 (795 amino ac	0.00	1.51	1	1	1	1	795	87.2	7.37
AN3088	AN3088 AspGDID:ASPL0000034820 COORDS:ChrVI_A_nidulans_FGSC_A4:1881529-1880871C, translated using codon table 1 (161 amino	0.00	11.18	1	1	1	1	161	16.3	7.75
AN2316	AN2316 AspGDID:ASPL0000047751 COORDS:ChrVII_A_nidulans_FGSC_A4:3536168-3535400C, translated using codon table 1 (197 amino	0.00	13.20	1	2	2	2	197	22.2	9.74
AN8903	AN8903 AspGDID:ASPL0000044037 COORDS:ChrVIII_A_nidulans_FGSC_A4:508308-510359W, translated using codon table 1 (628 amino	0.00	1.91	1	1	1	1	628	69.4	7.42
AN6630	AN6630 AspGDID:ASPL0000008445 COORDS:ChrI_A_nidulans_FGSC_A4:2679580-2680339W, translated using codon table 1 (203 amino	0.00	6.90	1	1	1	1	203	22.0	4.94
AN4513	kipB AspGDID:ASPL0000076343 COORDS:ChrIII_A_nidulans_FGSC_A4:1814947-1811922C, translated using codon table 1 (989 amino ac	0.00	1.11	1	1	1	1	989	108.6	9.91
AN2037	AN2037 AspGDID:ASPL0000050407 COORDS:ChrV_A_nidulans_FGSC_A4:2664455-2663383C, translated using codon table 1 (336 amino	0.00	2.08	1	1	1	1	336	36.3	6.71
AN9327	AN9327 AspGDID:ASPL0000062577 COORDS:ChrVIII_A_nidulans_FGSC_A4:296631-295565C, translated using codon table 1 (337 amino	0.00	4.15	1	1	1	1	337	38.6	5.72
AN7547	uncA AspGDID:ASPL0000069504 COORDS:ChrIV_A_nidulans_FGSC_A4:1911470-1916437W, translated using codon table 1 (1630 amino	0.00	2.70	1	1	1	1	1630	182.7	6.76
AN6241	AN6241 AspGDID:ASPL0000008519 COORDS:ChrI_A_nidulans_FGSC_A4:784939-787015W, translated using codon table 1 (659 amino aci	0.00	1.67	1	1	1	1	659	73.6	6.65
AN6210	AN6210 AspGDID:ASPL0000001018 COORDS:ChrI_A_nidulans_FGSC_A4:903774-905786W, translated using codon table 1 (631 amino ac	0.00	1.11	1	1	1	1	631	70.2	8.43
AN6007	AN6007 AspGDID:ASPL0000004985 COORDS:ChrI_A_nidulans_FGSC_A4:1525129-1529306W, translated using codon table 1 (1293 amino	0.00	0.62	1	1	1	1	1293	144.4	6.14
AN5879	AN5879 AspGDID:ASPL0000003052 COORDS:ChrI_A_nidulans_FGSC_A4:1934189-1933563C, translated using codon table 1 (169 amino a	0.00	4.73	1	1	1	1	169	18.3	5.02
AN5811	AN5811 AspGDID:ASPL0000003493 COORDS:ChrI_A_nidulans_FGSC_A4:2171926-2172935W, translated using codon table 1 (294 amino	0.00	4.08	1	1	1	1	294	32.9	5.47
AN4280	AN4280 AspGDID:ASPL0000011755 COORDS:ChrII_A_nidulans_FGSC_A4:1522722-1523800W, translated using codon table 1 (320 amino	0.00	3.44	1	1	1	1	320	34.8	9.92
AN4018	AN4018 AspGDID:ASPL0000015477 COORDS:ChrII_A_nidulans_FGSC_A4:2328688-2326267C, translated using codon table 1 (772 amino	0.00	1.04	1	1	1	1	772	85.6	5.15
AN3729	fksA AspGDID:ASPL0000011003 COORDS:ChrII_A_nidulans_FGSC_A4:3255844-3261673W, translated using codon table 1 (1905 amino ac	0.00	0.68	1	1	1	1	1905	218.3	7.96
AN1964	AN1964 AspGDID:ASPL0000048771 COORDS:ChrVII_A_nidulans_FGSC_A4:2404820-2405920W, translated using codon table 1 (237 amin	0.00	3.38	1	1	1	1	237	27.1	10.73
AN1660	AN1660 AspGDID:ASPL0000041941 COORDS:ChrVII_A_nidulans_FGSC_A4:1537476-1532132C, translated using codon table 1 (1764 amir	0.00	1.93	1	1	1	1	1764	194.7	7.39
AN1163	AN1163 AspGDID:ASPL0000062455 COORDS:ChrVIII_A_nidulans_FGSC_A4:1336458-1334056C, translated using codon table 1 (800 amin	0.00	1.25	1	1	1	1	800	88.6	6.84
AN0870	AN0870 AspGDID:ASPL0000052900 COORDS:ChrVIII_A_nidulans_FGSC_A4:2217373-2218540W, translated using codon table 1 (314 amino	0.00	3.82	1	1	1	1	314	32.9	9.36
AN0445	AN0445 AspGDID:ASPL0000051953 COORDS:ChrVIII_A_nidulans_FGSC_A4:3532607-3533558W, translated using codon table 1 (203 amin	0.00	4.93	1	1	1	1	203	24.0	11.31
AN1333	tctexA AspGDID:ASPL0000062581 COORDS:ChrVIII_A_nidulans_FGSC_A4:802696-803365W, translated using codon table 1 (141 amino a	0.00	8.51	1	1	1	1	141	14.8	5.45
AN3931	pilB AspGDID:ASPL0000011213 COORDS:ChrII_A_nidulans_FGSC_A4:2614920-2613608C, translated using codon table 1 (399 amino acids	0.00	7.77	1	1	1	1	399	44.5	5.94
AN4085	AN4085 AspGDID:ASPL0000015687 COORDS:ChrII_A_nidulans_FGSC_A4:2142705-2145033W, translated using codon table 1 (616 amino	0.00	3.73	1	1	1	1	616	69.0	4.81
AN5666	mpkA AspGDID:ASPL0000028487 COORDS:ChrV_A_nidulans_FGSC_A4:2038483-2039584W, translated using codon table 1 (330 amino ac	0.00	9.70	1	2	2	2	330	37.9	4.96
AN1701	AN1701 AspGDID:ASPL0000043270 COORDS:ChrVII_A_nidulans_FGSC_A4:1661764-1663128W, translated using codon table 1 (454 amin	0.00	2.42	1	1	1	1	454	50.9	5.19
AN10550	AN10550 AspGDID:ASPL0000070489 COORDS:ChrIII_A_nidulans_FGSC_A4:2356897-2359346W, translated using codon table 1 (797 amir	0.00	1.51	1	1	1	1	797	87.5	7.09
AN6717	mdhA AspGDID:ASPL0000006775 COORDS:ChrI_A_nidulans_FGSC_A4:2957682-2958968W, translated using codon table 1 (340 amino ac	0.00	5.59	1	1	1	3	340	35.7	8.78
AN5482	ran AspGDID:ASPL0000033427 COORDS:ChrV_A_nidulans_FGSC_A4:2669233-2668207C, translated using codon table 1 (215 amino acids	0.00	9.77	1	2	2	2	215	24.2	7.39
AN2014	AN2014 AspGDID:ASPL0000041933 COORDS:ChrVII_A_nidulans_FGSC_A4:2568677-2566568C, translated using codon table 1 (649 amino	0.00	1.69	1	1	1	1	649	71.0	8.18
AN5583	asIA AspGDID:ASPL0000031423 COORDS:ChrV_A_nidulans_FGSC_A4:2327378-2328452W, translated using codon table 1 (306 amino ac	0.00	3.27	1	1	1	1	306	35.5	8.35
AN8770	AN8770 AspGDID:ASPL0000077969 COORDS:ChrIII_A_nidulans_FGSC_A4:2876101-2873327C, translated using codon table 1 (905 amino	0.00	4.42	1	1	1	1	905	99.1	8.12
AN2736	AN2736 AspGDID:ASPL0000037083 COORDS:ChrVI_A_nidulans_FGSC_A4:2978805-2981502W, translated using codon table 1 (862 amino	0.00	3.02	1	1	1	1	862	95.5	5.83
AN9329	AN9329 AspGDID:ASPL0000057364 COORDS:ChrVIII_A_nidulans_FGSC_A4:303670-300464C, translated using codon table 1 (877 amino	0.00	0.91	1	1	1	1	877	99.2	6.55
AN1377	rgsC AspGDID:ASPL0000054438 COORDS:ChrVIII_A_nidulans_FGSC_A4:695781-691759C, translated using codon table 1 (1257 amino ac	0.00	0.80	1	1	1	1	1257	140.9	7.56
AN7865	bglJ AspGDID:ASPL0000013688 COORDS:ChrII_A_nidulans_FGSC_A4:56735-54216C, translated using codon table 1 (781 amino acids) Ur	0.00	3.59	1	1	1	1	781	85.1	6.39
AN3881	AN3881 AspGDID:ASPL0000014088 COORDS:ChrII_A_nidulans_FGSC_A4:2793888-2790376C, translated using codon table 1 (1170 amino	0.00	0.94	1	1	1	1	1170	130.9	6.60
AN3739	snxA AspGDID:ASPL0000011897 COORDS:ChrII_A_nidulans_FGSC_A4:3221793-3219888C, translated using codon table 1 (425 amino acid	0.00	3.53	1	1	1	1	425	44.8	6.95
AN7254	AN7254 AspGDID:ASPL0000069340 COORDS:ChrIV_A_nidulans_FGSC_A4:520523-523263W, translated using codon table 1 (814 amino a	0.00	0.98	1	1	1	1	814	89.4	5.12

Table S4: HamE-TAP interacting proteins during 24 hours of vegetative growth

Accession	Description	Score	Coverage	# Proteins	Unique Peptides	# Peptides	# PSMs	# AAs	MW [kDa]	calc. pI
AN2701	AN2701 AspGDID:ASPL0000036914 COORDS:ChrVI_A_nidulans_FGSC_A4:3104669-3109566W, translated using codon ta	172.46	46.50	1	45	45	58	1570	171.6	9.52
AN3422	ste7 AspGDID:ASPL0000040884 COORDS:ChrVI_A_nidulans_FGSC_A4:772852-774627W, translated using codon table 1	17.18	28.39	1	10	10	11	539	58.9	9.26
AN2526	AN2526 AspGDID:ASPL0000041782 COORDS:ChrVII_A_nidulans_FGSC_A4:4236654-4235452C, translated using codon table 1 (400 amino	9.35	14.00	1	4	4	4	400	44.3	8.87
AN0688	AN0688 AspGDID:ASPL0000053784 COORDS:ChrVIII_A_nidulans_FGSC_A4:2786646-2789142W, translated using codon table 1 (684 amin	8.02	8.63	1	6	6	7	684	74.5	6.37
AN6563	AN6563 AspGDID:ASPL0000006513 COORDS:ChrI_A_nidulans_FGSC_A4:2468078-2466458C, translated using codon table 1 (411 amino a	7.55	11.92	1	3	3	4	411	46.2	6.58
AN6700	AN6700 AspGDID:ASPL0000007308 COORDS:ChrI_A_nidulans_FGSC_A4:2897960-2894554C, translated using codon table 1 (1103 amino	5.70	2.54	1	2	2	3	1103	121.3	6.10
AN6900	tpiA AspGDID:ASPL0000001144 COORDS:ChrI_A_nidulans_FGSC_A4:3517593-3518737W, translated using codon table 1 (249 amino acids	5.34	6.02	1	1	1	2	249	27.1	6.13
AN2936	AN2936 AspGDID:ASPL0000039697 COORDS:ChrVI_A_nidulans_FGSC_A4:2343393-2346882W, translated using codon table 1 (1095 amin	4.83	2.56	1	2	2	2	1095	124.0	5.59
AN7459	hxkA AspGDID:ASPL0000069760 COORDS:ChrIV_A_nidulans_FGSC_A4:1609646-1608307C, translated using codon table 1 (426 amino aci	3.40	8.22	1	3	3	3	426	46.9	5.24
AN5716	AN5716 AspGDID:ASPL0000033419 COORDS:ChrV_A_nidulans_FGSC_A4:1906499-1904312C, translated using codon table 1 (666 amino a	2.32	2.85	1	1	1	2	666	71.7	6.40
AN3719	mpkB AspGDID:ASPL0000010103 COORDS:ChrII_A_nidulans_FGSC_A4:3287538-3288820W, translated using codon tabl	2.25	4.52	1	2	2	2	354	41.0	6.90
AN5168	AN5168 AspGDID:ASPL0000030834 COORDS:ChrV_A_nidulans_FGSC_A4:1374007-1369735C, translated using codon table 1 (1299 amino	2.17	1.08	1	1	1	1	1299	142.8	6.48
AN4743	racA AspGDID:ASPL0000073163 COORDS:ChrIII_A_nidulans_FGSC_A4:1120752-1121676W, translated using codon table 1 (199 amino ac	2.09	11.56	1	2	2	2	199	22.2	7.72
AN11173	AN11173 AspGDID:ASPL0000037145 COORDS:ChrVI_A_nidulans_FGSC_A4:562397-560740C, translated using codon table 1 (420 amino a	2.07	6.67	1	2	2	2	420	47.4	6.54
AN4523	prp8 AspGDID:ASPL0000077099 COORDS:ChrIII_A_nidulans_FGSC_A4:1775943-1766887C, translated using codon table 1 (2940 amino a	2.02	1.12	1	2	2	2	2940	338.9	8.31
AN0866	AN0866 AspGDID:ASPL0000059656 COORDS:ChrVIII_A_nidulans_FGSC_A4:2232313-2229877C, translated using codon table 1 (702 amin	1.91	1.42	1	1	1	1	702	77.9	7.59
AN5747	AN5747 AspGDID:ASPL0000032311 COORDS:ChrV_A_nidulans_FGSC_A4:1819371-1818026C, translated using codon table 1 (393 amino a	1.84	8.91	1	2	3	3	393	44.2	5.81
AN6036	AN6036 AspGDID:ASPL0000002523 COORDS:ChrI_A_nidulans_FGSC_A4:1444044-1446557W, translated using codon table 1 (762 amino a	1.76	7.35	1	4	4	4	762	84.7	4.97
AN1966	hulE AspGDID:ASPL0000049675 COORDS:ChrVII_A_nidulans_FGSC_A4:2421142-2408808C, translated using codon table 1 (4019 amino a	1.76	0.30	1	1	1	1	4019	447.8	5.05
AN7706	AN7706 AspGDID:ASPL0000065384 COORDS:ChrIV_A_nidulans_FGSC_A4:2440922-2439332C, translated using codon table 1 (328 amino	1.75	6.71	1	2	2	2	328	36.3	9.25
AN6906	AN6906 AspGDID:ASPL0000003842 COORDS:ChrI_A_nidulans_FGSC_A4:3528221-3526545C, translated using codon table 1 (475 amino a	0.00	3.16	1	1	1	1	475	50.5	5.27
AN5217	pilA AspGDID:ASPL0000031781 COORDS:ChrV_A_nidulans_FGSC_A4:1524093-1525284W, translated using codon table 1 (347 amino acids	0.00	6.05	1	2	2	2	347	39.3	5.68
AN3782	AN3782 AspGDID:ASPL0000017892 COORDS:ChrII_A_nidulans_FGSC_A4:3070621-3072315W, translated using codon table 1 (564 amino	0.00	3.37	1	1	1	1	564	63.1	6.99
AN5907	AN5907 AspGDID:ASPL0000006696 COORDS:ChrI_A_nidulans_FGSC_A4:1844323-1844796W, translated using codon table 1 (157 amino a	0.00	8.28	1	1	1	1	157	16.9	7.28
AN5717	kapI AspGDID:ASPL0000030160 COORDS:ChrV_A_nidulans_FGSC_A4:1903567-1899930C, translated using codon table 1 (1095 amino aci	0.00	1.10	1	1	1	1	1095	121.1	4.79
AN5525	acoA AspGDID:ASPL0000027768 COORDS:ChrV_A_nidulans_FGSC_A4:2516549-2519412W, translated using codon table 1 (783 amino acid	0.00	1.79	1	1	1	1	783	84.9	6.74
AN10944	AN10944 AspGDID:ASPL0000068168 COORDS:ChrIV_A_nidulans_FGSC_A4:1714200-1716760W, translated using codon table 1 (791 amin	0.00	1.64	1	1	1	1	791	88.4	6.70
AN10561	AN10561 AspGDID:ASPL0000075585 COORDS:ChrIII_A_nidulans_FGSC_A4:1929771-1929018C, translated using codon table 1 (196 amin	0.00	7.14	1	1	1	1	196	19.2	10.59
AN3347	AN3347 AspGDID:ASPL0000039045 COORDS:ChrVI_A_nidulans_FGSC_A4:1016611-1018631W, translated using codon table 1 (527 amino	0.00	2.47	1	1	1	1	527	56.5	7.65
AN6717	mdhA AspGDID:ASPL0000006775 COORDS:ChrI_A_nidulans_FGSC_A4:2957682-2958968W, translated using codon table 1 (340 amino aci	0.00	5.59	1	1	1	1	340	35.7	8.78
AN4563	ckiA AspGDID:ASPL0000072181 COORDS:ChrIII_A_nidulans_FGSC_A4:1656470-1657827W, translated using codon table 1 (370 amino aci	0.00	5.14	1	2	2	2	370	42.6	9.55
AN7625	AN7625 AspGDID:ASPL0000068586 COORDS:ChrIV_A_nidulans_FGSC_A4:2179774-2178579C, translated using codon table 1 (382 amino	0.00	3.14	1	1	1	1	382	41.4	6.37
AN10182	AN10182 AspGDID:ASPL0000055955 COORDS:ChrVIII_A_nidulans_FGSC_A4:759975-761121W, translated using codon table 1 (345 amino	0.00	2.90	1	1	1	1	345	37.4	4.89
AN3026	copA AspGDID:ASPL0000037303 COORDS:ChrVI_A_nidulans_FGSC_A4:2072274-2068223C, translated using codon table 1 (1211 amino a	0.00	0.91	1	1	1	1	1211	135.2	6.19
AN4272	AN4272 AspGDID:ASPL0000011761 COORDS:ChrII_A_nidulans_FGSC_A4:1556010-1553127C, translated using codon table 1 (824 amino a	0.00	1.09	1	1	1	1	824	93.4	8.68
AN7884	AN7884 AspGDID:ASPL0000010516 COORDS:ChrII_A_nidulans_FGSC_A4:118328-139584W, translated using codon table 1 (7015 amino a	0.00	0.19	1	1	1	1	7015	773.0	5.81
AN10223	AN10223 AspGDID:ASPL0000050719 COORDS:ChrVII_A_nidulans_FGSC_A4:1631540-1632512W, translated using codon table 1 (223 amin	0.00	4.04	2	1	1	1	223	24.6	6.14

Table S5: Phosphorylated residues detected for HamE during 24 hours of vegetative growth

HamE-TAP (Veg24)	HamE-TAP (Veg24)
1st replicate (coverage=39.11%)	2nd replicate (coverage=43.18%)
425 (S)	425 (S)
707 (S)	707 (S)
711 (S)	711 (S)
	786 (S)
	881 (S)
	973 (S)
	1199 (S)
	1202 (S)

Table S6: Phosphorylated residues detected for SteC during 24 hours of vegetative growth in the presence of HamE

SteC-TAP (Veg24)	SteC-TAP (Veg24)	SteC-TAP (Veg24)	SteC-TAP (Veg24)	SteC-TAP (Veg24)
1st rep (coverage=64.67%)	2nd rep (coverage=70.65%)	3rd rep (coverage=68.17%)	4th rep (coverage=70.32%)	Total phosphorylation sites detected
32 (T)	30 (S)	43(T)	42(Y)	30 (S)
44 (S)	31 (S)	44(S)	43(T)	31 (S)
48 (S)	32 (T)	46(T)	44(S)	32 (T)
51 (S)	44 (S)	150(S)	46(T)	42(Y)
150 (S)	48 (S)	153(S)	51 (S)	43(T)
153 (S)	51 (S)	197(S)	150(S)	44(S)
197 (S)	150 (S)	233(S)	182(S)	46(T)
309 (S)	181 (T)	464(S)	186(S)	48 (S)
398 (T)	182 (S)	467(S)	197(S)	51 (S)
535 (S)	197 (S)	535(S)	233(S)	150(S)
784 (S)	309 (S)	575(S)	400(S)	153(S)
	418 (S)		535(S)	181 (T)
	426 (S)		784(S)	182 (S)
	535 (S)			197 (S)
				233(S)
				309 (S)
				398 (T)
				400(S)
				418 (S)
				426 (S)
				464(S)
				467(S)
				535(S)
				575(S)
				784 (S)

Table S7: Phosphorylated residues detected for SteC during 24 hours of vegetative growth in the absence of HamE

SteC-TAP (*hamE* deletion-Veg24)	SteC-TAP (*hamE* deletion-Veg24)	SteC-TAP (*hamE* deletion-Veg24)	SteC-TAP (*hamE* deletion-Veg24)	SteC-TAP (*hamE* deletion-Veg24)
1st replicate (coverage=62.19%)	2nd replicate (coverage=57.56%)	3rd replicate (coverage=70.88%)	4th replicate (coverage=61.96%)	**Total sites detected**
51 (S)	30 (S)	43(T)	43(T)	30 (S)
197 (S)	31 (S)	44(S)	44(S)	31 (S)
535 (S)	32 (T)	46(T)	46(T)	32 (T)
	44 (S)	150(S)	150(S)	43(T)
	48 (S)	181(T)	181(T)	44(S)
	51 (S)	182(S)	182(S)	46(T)
	535 (S)	186(S)	186(S)	48 (S)
		197(S)	197(S)	51 (S)
		233(S)	233(S)	150(S)
		398(T)	400(S)	181(T)
		467(S)	535(S)	182(S)
		535(S)		186(S)
		784(S)		197(S)
				233(S)
				398(T)
				400(S)
				467(S)
				535(S)
				784(S)

Table S8: Phosphorylated residues detected for MkkB during 24 hours of vegetative growth in the presence of HamE

MkkB-TAP (Veg24)	MkkB-TAP (Veg24)	MkkB-TAP (Veg24)	MkkB-TAP (Veg24)	MkkB-TAP (Veg24)
1st replicate (coverage=62.34%)	2nd replicate (coverage=58.07%)	3rd replicate (coverage=66.6%)	4th replicate (coverage=72.73%)	**Total sites detected**
213 (T)	359 (S)	275(S)	26(S)	26(S)
215 (T)	360 (Y)	359(S)	27(T)	27(T)
218 (S)		372(T)	28(S)	28(S)
275 (S)		375(S)	29(T)	29(T)
359 (S)		383(S)	31(S)	31(S)
360 (Y)		470(S)	35(S)	35(S)
			213(T)	213(T)
			215(T)	215(T)
			218(S)	218(S)
			222(T)	222(T)
			268(S)	268(S)
			275(S)	275(S)
			359(S)	359(S)
			383(S)	360 (Y)
				372(T)
				375(S)
				383(S)
				470(S)

Table S9: Phosphorylated residues detected for MkkB during 24 hours of vegetative growth in the absence of HamE

MkkB-TAP (*hamE* deletion-Veg24)	MkkB-TAP (*hamE* deletion-Veg24)	MkkB-TAP (*hamE* deletion-Veg24)	MkkB-TAP (*hamE* deletion-Veg24)	MkkB-TAP (*hamE* deletion-Veg24)
1st replicate (coverage=64.75%)	2nd replicate (coverage=69.76%)	3rd replicate (coverage=77.18%)	4th replicate (coverage=72.54%)	**Total sites detected**
	383 (S)	268(S)	268(S)	268(S)
		275(S)	275(S)	275(S)
		383(S)	383(S)	383(S)
		470(S)		470(S)
		472(T)		472(T)

Table S10: Phosphorylated residues detected for MpkB during 24 hours of vegetative growth in the presence and absence of HamE

MpkB-TAP (Veg24)	MpkB-TAP (Veg24)	MpkB-TAP (Veg24)	MpkB-TAP (Veg24)
1st replicate (coverage=79.38%)	2nd replicate (coverage=82.2%)	3rd replicate (coverage=86.44%)	4th replicate (coverage=83.05%)
	15 (S)	15 (S)	184 (Y)
	184 (Y)	184 (Y)	
MpkB-TAP (*hamE* deletion-Veg24)	MpkB-TAP (*hamE* deletion-Veg24)	MpkB-TAP (*hamE* deletion-Veg24)	MpkB-TAP (*hamE* deletion-Veg24)
1st replicate (coverage=74.29%)	2nd replicate (coverage=79.38%)	3rd replicate (coverage=84.18%)	4th replicate (coverage=85.31%)
184 (Y)		182(T)	15 (S)
		184(Y)	184 (Y)

Table S11: SteC-TAP interacting proteins during 24 hours of vegetative growth in the absence of HamE

Accession	Description	Score	Coverage	# Proteins	Unique Peptides	# Peptides	# PSMs	# AAs	MW [kDa]	calc. pI
AN2269	steC AspGDID:ASPL0000047432 COORDS:ChrVII_A_nidulans_FGSC	301.86	62.08	1	42	42	105	886	97.7	7.84
AN7252	steD AspGDID:ASPL0000068680 COORDS:ChrIV_A_nidulans_FGSC	184.08	64.78	1	25	25	59	494	54.3	5.82
AN8870	AN8870 AspGDID:ASPL0000071167 COORDS:ChrIII_A_nidulans_FGSC_A4:25	41.30	48.83	1	13	13	15	256	29.1	10.04
AN5979	AN5979 AspGDID:ASPL0000004567 COORDS:ChrI_A_nidulans_FGSC_A4:160	22.40	59.71	1	8	8	9	139	16.1	9.94
AN5716	AN5716 AspGDID:ASPL0000033419 COORDS:ChrV_A_nidulans_FGSC_A4:190	18.71	24.47	1	11	11	12	666	71.7	6.40
AN5931	AN5931 AspGDID:ASPL0000006660 COORDS:ChrI_A_nidulans_FGSC_A4:177	17.80	17.58	1	6	7	7	563	60.9	9.23
AN6731	sdeA AspGDID:ASPL0000005877 COORDS:ChrI_A_nidulans_FGSC_A4:30022	17.72	28.35	1	7	8	8	455	51.6	9.01
AN7540	AN7540 AspGDID:ASPL0000063813 COORDS:ChrIV_A_nidulans_FGSC_A4:18	15.18	28.67	1	9	9	9	586	64.8	5.38
AN5715	AN5715 AspGDID:ASPL0000029491 COORDS:ChrV_A_nidulans_FGSC_A4:190	14.48	37.82	1	4	4	6	119	13.5	10.87
AN5132	AN5132 AspGDID:ASPL0000033818 COORDS:ChrV_A_nidulans_FGSC_A4:124	14.02	26.14	1	5	5	5	306	33.0	9.89
AN0314	AN0314 AspGDID:ASPL0000051982 COORDS:ChrVIII_A_nidulans_FGSC_A4:	13.96	11.61	1	9	9	9	956	108.8	7.01
AN1345	AN1345 AspGDID:ASPL0000058023 COORDS:ChrVIII_A_nidulans_FGSC_A4:7	13.26	44.83	1	5	5	5	145	15.8	10.39
AN4859	pmaA AspGDID:ASPL0000077585 COORDS:ChrIII_A_nidulans_FGSC_A4:748	13.04	16.97	1	12	12	12	990	108.7	5.36
AN7258	AN7258 AspGDID:ASPL0000063859 COORDS:ChrIV_A_nidulans_FGSC_A4:51	12.55	24.54	1	4	4	5	269	29.5	10.08
AN11008	AN11008 AspGDID:ASPL0000065685 COORDS:ChrIV_A_nidulans_FGSC_A4:2	12.28	20.08	1	7	7	7	483	53.0	8.75
AN8274	AN8274 AspGDID:ASPL0000012182 COORDS:ChrII_A_nidulans_FGSC_A4:13	12.00	18.79	1	4	4	5	314	33.6	9.67
AN8874	AN8874 AspGDID:ASPL0000044708 COORDS:ChrVII_A_nidulans_FGSC_A4:5	10.76	11.46	1	6	6	7	794	88.2	6.84
AN0776	AN0776 AspGDID:ASPL0000053603 COORDS:ChrV_A_nidulans_FGSC_A4:2	10.57	39.13	1	6	6	6	184	20.6	10.83
AN10681	AN10681 AspGDID:ASPL0000026338 COORDS:ChrV_A_nidulans_FGSC_A4:26	8.62	27.87	1	5	5	5	122	13.9	10.35
AN5167	AN5167 AspGDID:ASPL0000026563 COORDS:ChrV_A_nidulans_FGSC_A4:13	8.59	6.35	1	6	6	8	1166	128.5	7.88
AN1964	AN1964 AspGDID:ASPL0000048771 COORDS:ChrVII_A_nidulans_FGSC_A4:2	8.22	21.94	1	4	4	4	237	27.1	10.73
AN3706	AN3706 AspGDID:ASPL0000012467 COORDS:ChrI_A_nidulans_FGSC_A4:33	7.95	22.88	1	3	3	4	153	17.6	9.82
AN0252	AN0252 AspGDID:ASPL0000052676 COORDS:ChrVIII_A_nidulans_FGSC_A4:	7.84	28.38	1	5	5	5	296	31.9	7.83
AN2992	AN2992 AspGDID:ASPL0000034768 COORDS:ChrVI_A_nidulans_FGSC_A4:21	7.82	22.14	1	4	4	4	280	31.2	8.91
AN2047	CaM AspGDID:ASPL0000051423 COORDS:ChrVII_A_nidulans_FGSC_A4:2693	7.51	24.83	1	4	4	4	149	17.0	4.27
AN6182	aspC AspGDID:ASPL0000010754 COORDS:ChrII_A_nidulans_FGSC_A4:10487	7.35	19.94	1	5	5	5	351	40.8	7.39
AN5713	cct7 AspGDID:ASPL0000028827 COORDS:ChrV_A_nidulans_FGSC_A4:191300	7.35	16.87	1	6	6	6	563	60.8	6.48
AN11565	AN11565 AspGDID:ASPL0000063719 COORDS:ChrIV_A_nidulans_FGSC_A4:1	6.48	24.75	1	2	2	3	101	11.1	10.18
AN0359	sgcA AspGDID:ASPL0000058305 COORDS:ChrVIII_A_nidulans_FGSC_A4:379	6.31	8.94	1	5	5	5	738	84.2	5.29
AN12491	AN12491 AspGDID:ASPL0000403457 COORDS:ChrI_A_nidulans_FGSC_A4:35	6.29	16.54	1	3	3	3	266	28.1	10.14
AN6060	AN6060 AspGDID:ASPL0000002483 COORDS:ChrI_A_nidulans_FGSC_A4:138	6.26	8.91	1	10	10	10	1447	154.6	9.31
AN4547	AN4547 AspGDID:ASPL0000072207 COORDS:ChrIII_A_nidulans_FGSC_A4:16	6.25	10.25	1	7	7	7	917	100.6	5.55
AN8705	AN8705 AspGDID:ASPL0000070541 COORDS:ChrIV_A_nidulans_FGSC_A4:30	5.85	17.74	1	2	2	3	62	6.9	11.77
AN2426	H4.2 AspGDID:ASPL0000050285 COORDS:ChrVII_A_nidulans_FGSC_A4:3917	5.56	29.13	1	1	3	3	103	11.4	11.36
AN8712	AN8712 AspGDID:ASPL0000074179 COORDS:ChrIV_A_nidulans_FGSC_A4:30	4.97	13.42	1	2	2	2	149	17.3	5.19
AN2316	AN2316 AspGDID:ASPL0000047751 COORDS:ChrVII_A_nidulans_FGSC_A4:3	4.91	27.92	1	4	4	4	197	22.2	9.74
AN7350	AN7350 AspGDID:ASPL0000069068 COORDS:ChrIV_A_nidulans_FGSC_A4:21	4.80	7.94	1	3	3	3	428	46.3	9.10
AN1851	AN1851 AspGDID:ASPL0000049731 COORDS:ChrVII_A_nidulans_FGSC_A4:2	4.66	11.36	1	5	5	5	581	62.6	5.03
AN3422	ste7 AspGDID:ASPL0000040884 COORDS:ChrVI_A_nidulans_FGSC	4.47	20.96	1	8	8	9	539	58.9	9.26
AN4794	AN4794 AspGDID:ASPL0000073357 COORDS:ChrIII_A_nidulans_FGSC_A4:97	4.06	17.24	1	4	4	4	261	29.4	9.96
AN7003	AN7003 AspGDID:ASPL0000067118 COORDS:ChrIV_A_nidulans_FGSC_A4:13	3.62	12.83	1	3	3	3	226	25.6	10.55
AN0357	AN0357 AspGDID:ASPL0000052094 COORDS:ChrVIII_A_nidulans_FGSC_A4:	3.62	16.77	1	5	5	6	316	34.9	8.22
AN11411	AN11411 AspGDID:ASPL0000011385 COORDS:ChrIII_A_nidulans_FGSC_A4:2	3.39	26.79	1	2	2	2	56	6.7	10.21
AN10416	AN10416 AspGDID:ASPL0000039794 COORDS:ChrVI_A_nidulans_FGSC_A4:6	2.44	23.49	1	4	4	4	149	16.7	10.37
AN5520	AN5520 AspGDID:ASPL0000029714 COORDS:ChrV_A_nidulans_FGSC_A4:255	2.32	12.50	1	3	3	3	264	29.4	10.29
AN9468	AN9468 AspGDID:ASPL0000000085 COORDS:ChrI_A_nidulans_FGSC_A4:166	2.30	11.19	1	2	2	2	143	15.9	10.18
AN0465	AN0465 AspGDID:ASPL0000052975 COORDS:ChrVIII_A_nidulans_FGSC_A4:	2.30	13.43	1	2	2	2	201	22.8	11.15
AN3629	AN3629 AspGDID:ASPL0000009569 COORDS:ChrII_A_nidulans_FGSC_A4:35	2.04	5.23	1	2	2	2	363	41.5	9.20
AN1055	AN1055 AspGDID:ASPL0000061577 COORDS:ChrVIII_A_nidulans_FGSC_A4:	1.94	4.17	1	2	2	2	552	58.1	9.14
AN1166	AN1166 AspGDID:ASPL0000060399 COORDS:ChrVIII_A_nidulans_FGSC_A4:	1.77	8.59	1	2	2	2	198	22.1	10.17
AN4803	AN4803 AspGDID:ASPL0000071451 COORDS:ChrIII_A_nidulans_FGSC_A4:94	1.74	11.40	1	3	3	3	193	22.2	10.10
AN1608	AN1608 AspGDID:ASPL0000050167 COORDS:ChrVII_A_nidulans_FGSC_A4:1	1.63	14.77	1	3	3	3	176	18.5	9.52
AN4402	AN4402 AspGDID:ASPL0000077985 COORDS:ChrIII_A_nidulans_FGSC_A4:21	0.00	8.80	1	2	2	2	284	29.9	9.01
AN4259	AN4259 AspGDID:ASPL0000017804 COORDS:ChrII_A_nidulans_FGSC_A4:159	0.00	5.45	1	2	2	2	459	49.8	4.97
AN1215	AN1215 AspGDID:ASPL0000061166 COORDS:ChrVIII_A_nidulans_FGSC_A4:	0.00	5.33	1	3	3	3	544	59.8	7.15
AN4038	AN4038 AspGDID:ASPL0000017318 COORDS:ChrII_A_nidulans_FGSC_A4:22	0.00	5.04	1	3	3	3	1072	118.8	5.74
AN4908	AN4908 AspGDID:ASPL0000070619 COORDS:ChrIII_A_nidulans_FGSC_A4:58	0.00	3.43	1	3	3	3	1225	135.6	6.15
AN3070	AN3070 AspGDID:ASPL0000038764 COORDS:ChrVI_A_nidulans_FGSC_A4:19	0.00	6.34	1	3	3	3	473	51.8	6.20
AN2775	AN2775 AspGDID:ASPL0000035752 COORDS:ChrVI_A_nidulans_FGSC_A4:28	0.00	3.50	1	2	2	2	658	71.4	9.17
AN2907	AN2907 AspGDID:ASPL0000034005 COORDS:ChrVI_A_nidulans_FGSC_A4:24	0.00	8.91	1	2	2	2	449	51.3	5.41

Table S12: MkkB-TAP interacting proteins during 24 hours of vegetative growth in the absence of HamE

Accession	Description	Score	Coverage	# Proteins	Unique Peptides	Peptides	# PSMs	# AAs	MW [kDa]	calc. pI
AN2269	steC AspGDID:ASPL0000047432 COORDS:ChrVII_A_nidulans_FGSC_A4:3394519-3391706C, translated using codon table 1 (88	302.95	71.90	1	44	44	96	886	97.7	7.84
AN3422	ste7 AspGDID:ASPL0000040884 COORDS:ChrVI_A_nidulans_FGSC_A4:772852-774627W, translated using codon table 1 (539	218.21	74.77	1	29	29	88	539	58.9	9.26
AN7252	steD AspGDID:ASPL0000068680 COORDS:ChrIV_A_nidulans_FGSC_A4:526909-528499W, translated using codon table 1 (494	171.89	72.06	1	24	24	53	494	54.3	5.82
AN1025	AN1025 AspGDID:ASPL0000059836 COORDS:ChrVIII_A_nidulans_FGSC_A4:1766255-1762759C, translated using codon table 1 (1067 amino acid	70.89	31.58	1	23	23	26	1067	118.0	6.55
AN3719	mpkB AspGDID:ASPL0000010103 COORDS:ChrII_A_nidulans_FGSC_A4:3287538-3288820W, translated using codon table 1 (3	22.80	36.44	1	10	10	11	354	41.0	6.90
AN5931	AN5931 AspGDID:ASPL0000006660 COORDS:ChrI_A_nidulans_FGSC_A4:1770987-1773596W, translated using codon table 1 (563 amino acids) U	19.67	23.62	1	10	11	11	563	60.9	9.23
AN8870	AN8870 AspGDID:ASPL0000071167 COORDS:ChrIII_A_nidulans_FGSC_A4:2544176-2543164C, translated using codon table 1 (256 amino acids)	16.82	33.20	1	6	6	7	256	29.1	10.04
AN1851	AN1851 AspGDID:ASPL0000049731 COORDS:ChrVII_A_nidulans_FGSC_A4:2066695-2068624W, translated using codon table 1 (581 amino acids	15.77	20.14	1	9	9	10	581	62.6	5.03
AN4547	AN4547 AspGDID:ASPL0000072207 COORDS:ChrIII_A_nidulans_FGSC_A4:1694126-1691097C, translated using codon table 1 (917 amino acids)	10.96	6.76	1	5	5	5	917	100.6	5.55
AN5979	AN5979 AspGDID:ASPL0000004567 COORDS:ChrI_A_nidulans_FGSC_A4:1608051-1607409C, translated using codon table 1 (139 amino acids) U	10.96	38.13	1	4	4	4	139	16.1	9.94
AN2530	hsp30 AspGDID:ASPL0000049895 COORDS:ChrVII_A_nidulans_FGSC_A4:4245415-4244870C, translated using codon table 1 (181 amino acids) V	9.22	23.76	1	4	4	4	181	20.3	6.57
AN5435	AN5435 AspGDID:ASPL0000027283 COORDS:ChrV_A_nidulans_FGSC_A4:2826313-2828135W, translated using codon table 1 (490 amino acids)	7.74	9.18	1	3	3	3	490	52.1	6.57
AN1007	niiA AspGDID:ASPL0000053621 COORDS:ChrVIII_A_nidulans_FGSC_A4:1822109-1818402C, translated using codon table 1 (1104 amino acids) V	7.46	6.97	1	7	7	7	1104	122.6	6.15
AN1964	AN1964 AspGDID:ASPL0000048771 COORDS:ChrVII_A_nidulans_FGSC_A4:2404820-2405920W, translated using codon table 1 (237 amino acids)	7.37	17.30	1	4	4	5	237	27.1	10.73
AN10681	AN10681 AspGDID:ASPL0000026338 COORDS:ChrV_A_nidulans_FGSC_A4:2652978-2653935W, translated using codon table 1 (122 amino acids)	6.43	28.69	1	4	4	4	122	13.9	10.35
AN5206	lysB AspGDID:ASPL0000026903 COORDS:ChrV_A_nidulans_FGSC_A4:1483680-1484947W, translated using codon table 1 (360 amino acids) Veri	6.07	14.72	1	4	4	4	360	38.3	5.90
AN8705	AN8705 AspGDID:ASPL0000070541 COORDS:ChrIII_A_nidulans_FGSC_A4:3063860-3063288C, translated using codon table 1 (62 amino acids) U	5.64	17.74	1	2	2	2	62	6.9	11.77
AN3134	AN3134 AspGDID:ASPL0000038552 COORDS:ChrVI_A_nidulans_FGSC_A4:1722811-1720942C, translated using codon table 1 (538 amino acids)	5.42	11.90	1	6	6	6	538	58.9	6.21
AN5715	AN5715 AspGDID:ASPL0000029491 COORDS:ChrV_A_nidulans_FGSC_A4:1907272-1908090W, translated using codon table 1 (119 amino acids)	5.37	17.65	1	2	2	2	119	13.5	10.87
AN0776	AN0776 AspGDID:ASPL0000053603 COORDS:ChrVIII_A_nidulans_FGSC_A4:2502223-2501208C, translated using codon table 1 (184 amino acids	5.35	15.76	1	3	3	3	184	20.6	10.83
AN12491	AN12491 AspGDID:ASPL0000403457 COORDS:ChrI_A_nidulans_FGSC_A4:3575960-3573772C, translated using codon table 1 (266 amino acids)	5.21	8.27	1	2	2	2	266	28.1	10.14
AN11411	AN11411 AspGDID:ASPL0000011385 COORDS:ChrII_A_nidulans_FGSC_A4:3309578-3310189W, translated using codon table 1 (56 amino acids)	4.31	26.79	1	2	2	2	56	6.7	10.21
AN1345	AN1345 AspGDID:ASPL0000058023 COORDS:ChrVII_A_nidulans_FGSC_A4:775408-775967W, translated using codon table 1 (145 amino acids)	4.25	15.17	1	2	2	2	145	15.8	10.39
AN3706	AN3706 AspGDID:ASPL0000012467 COORDS:ChrII_A_nidulans_FGSC_A4:3321661-3320973C, translated using codon table 1 (153 amino acids)	4.25	27.45	1	4	4	4	153	17.6	9.82
AN0922	AN0922 AspGDID:ASPL0000062974 COORDS:ChrVIII_A_nidulans_FGSC_A4:2067861-2069582W, translated using codon table 1 (516 amino acids	3.79	10.66	1	4	4	4	516	57.2	5.21
AN0314	AN0314 AspGDID:ASPL0000051982 COORDS:ChrVIII_A_nidulans_FGSC_A4:3941284-3938414C, translated using codon table 1 (956 amino acids	3.66	4.29	1	4	4	4	956	108.8	7.01
AN9509	AN9509 AspGDID:ASPL0000042910 COORDS:ChrVII_A_nidulans_FGSC_A4:3893231-3894115W, translated using codon table 1 (291 amino acids	2.74	13.75	1	2	2	2	291	30.7	6.98
AN7540	AN7540 AspGDID:ASPL0000063813 COORDS:ChrIV_A_nidulans_FGSC_A4:1883120-1884941W, translated using codon table 1 (586 amino acids)	2.39	5.97	1	2	2	2	586	64.8	5.38
AN11008	AN11008 AspGDID:ASPL0000065685 COORDS:ChrIV_A_nidulans_FGSC_A4:2593040-2591532C, translated using codon table 1 (483 amino acids	2.26	12.01	1	4	4	4	483	53.0	8.75
AN4803	AN4803 AspGDID:ASPL0000071451 COORDS:ChrIII_A_nidulans_FGSC_A4:942550-941690C, translated using codon table 1 (193 amino acids) Un	2.19	11.40	1	3	3	3	193	22.2	10.10
AN8874	AN8874 AspGDID:ASPL0000044708 COORDS:ChrVII_A_nidulans_FGSC_A4:596174-593664C, translated using codon table 1 (794 amino acids) U	2.15	3.02	1	2	2	2	794	88.2	6.84
AN4594	AN4594 AspGDID:ASPL0000070889 COORDS:ChrIII_A_nidulans_FGSC_A4:1578408-1577891C, translated using codon table 1 (115 amino acids)	2.07	16.52	1	2	2	2	115	12.9	9.82
AN10734	AN10734 AspGDID:ASPL0000003073 COORDS:ChrI_A_nidulans_FGSC_A4:2076455-2068027C, translated using codon table 1 (2672 amino acids)	2.05	0.94	1	2	2	2	2672	291.6	5.62
AN6181	AN6181 AspGDID:ASPL0000001539 COORDS:ChrI_A_nidulans_FGSC_A4:1007160-1006231C, translated using codon table 1 (106 amino acids) U	1.97	16.04	1	2	2	2	106	12.1	10.32
AN5713	cct7 AspGDID:ASPL0000028827 COORDS:ChrV_A_nidulans_FGSC_A4:1913003-1915026W, translated using codon table 1 (563 amino acids) Unc	1.93	12.43	1	4	4	4	563	60.8	6.48
AN5716	AN5716 AspGDID:ASPL0000033419 COORDS:ChrV_A_nidulans_FGSC_A4:1906499-1904312C, translated using codon table 1 (666 amino acids) U	1.85	4.35	1	2	2	2	666	71.7	6.40
AN4859	pmaA AspGDID:ASPL0000077585 COORDS:ChrIII_A_nidulans_FGSC_A4:748768-745667C, translated using codon table 1 (990 amino acids) Uncl	1.73	2.02	1	2	2	2	990	108.7	5.36
AN4315	AN4315 AspGDID:ASPL0000074597 COORDS:ChrIII_A_nidulans_FGSC_A4:2419780-2417185C, translated using codon table 1 (751 amino acids)	0.00	3.20	1	2	2	2	751	83.0	6.27
AN0359	sgdA AspGDID:ASPL0000058305 COORDS:ChrVII_A_nidulans_FGSC_A4:3797400-3799815W, translated using codon table 1 (738 amino acids) V	0.00	2.98	1	2	2	2	738	84.2	5.29
AN1281	AN1281 AspGDID:ASPL0000052531 COORDS:ChrVIII_A_nidulans_FGSC_A4:963704-962099C, translated using codon table 1 (514 amino acids) U	0.00	8.17	1	3	3	3	514	57.9	8.98
AN10071	AN10071 AspGDID:ASPL0000057098 COORDS:ChrVIII_A_nidulans_FGSC_A4:3918177-3920205W, translated using codon table 1 (650 amino aci	0.00	2.92	1	2	2	2	650	71.8	7.37
AN5520	AN5520 AspGDID:ASPL0000029714 COORDS:ChrV_A_nidulans_FGSC_A4:2531411-2530236C, translated using codon table 1 (264 amino acids) U	0.00	8.71	1	2	2	2	264	29.4	10.29
AN3070	AN3070 AspGDID:ASPL0000038764 COORDS:ChrVI_A_nidulans_FGSC_A4:1946042-1944467C, translated using codon table 1 (473 amino acids)	0.00	4.86	1	2	2	2	473	51.8	6.20
AN8836	cla4 AspGDID:ASPL0000070493 COORDS:ChrIII_A_nidulans_FGSC_A4:2643492-2646117W, translated using codon table 1 (845 amino acids) Un	0.00	4.97	1	3	3	3	845	93.2	8.91
AN5602	AN5602 AspGDID:ASPL0000030224 COORDS:ChrV_A_nidulans_FGSC_A4:2273125-2274358W, translated using codon table 1 (349 amino acids)	0.00	5.73	1	2	2	2	349	38.9	5.50

Table S13: MpkB-TAP interacting proteins during 24 hours of vegetative growth in the absence of HamE

Accession	Description	Score	Coverage	Proteins	Unique Peptides	Peptides	# PSMs	# AAs	MW [kDa]	calc. pI
AN6560	AN6560 AspGDID:ASPL0000000623 COORDS:ChrI_A_nidulans_FGSC_A4:2460021-2461457W, translated using codon table 1 (459 a	257.20	60.57	1	24	24	77	459	49.2	10.52
AN3719	mpkB AspGDID:ASPL00000010103 COORDS:ChrII_A_nidulans_FGSC_A4:3287538-3288820W, translated using codon	217.62	80.51	1	23	23	78	354	41.0	6.90
AN8862	myoV AspGDID:ASPL0000071197 COORDS:ChrII_A_nidulans_FGSC_A4:2568236-2573235W, translated using codon table 1 (1569 a	166.30	48.12	1	54	54	61	1569	179.0	6.99
AN5603	AN5603 AspGDID:ASPL0000026783 COORDS:ChrV_A_nidulans_FGSC_A4:2257109-2260929W, translated using codon table 1 (1218	132.01	43.19	1	32	32	39	1218	134.1	6.62
AN2290	steA AspGDID:ASPL0000050963 COORDS:ChrVII_A_nidulans_FGSC_A4:3458964-3456622C, translated using codon	104.92	50.72	1	22	22	33	692	76.6	6.93
AN2142	kapA AspGDID:ASPL0000045550 COORDS:ChrVII_A_nidulans_FGSC_A4:3012006-3013947W, translated using codon table 1 (553 am	68.52	55.33	1	19	19	26	553	60.6	5.11
AN4544	AN4544 AspGDID:ASPL0000075073 COORDS:ChrIII_A_nidulans_FGSC_A4:1706426-1708534W, translated using codon table 1 (702 a	57.45	39.03	1	19	19	22	702	76.0	6.81
AN5167	AN5167 AspGDID:ASPL0000026563 COORDS:ChrV_A_nidulans_FGSC_A4:1364294-1368255W, translated using codon table 1 (1166	53.60	25.81	1	22	22	25	1166	128.5	7.88
AN6304	AN6304 AspGDID:ASPL0000003395 COORDS:ChrI_A_nidulans_FGSC_A4:609686-607104C, translated using codon table 1 (843 amino	51.24	28.23	1	17	17	20	843	92.4	6.80
AN5982	torA AspGDID:ASPL0000006879 COORDS:ChrI_A_nidulans_FGSC_A4:1599573-1592218C, translated using codon table 1 (2385 amin	49.32	18.11	1	31	31	32	2385	269.3	7.08
AN4706	myoB AspGDID:ASPL0000075283 COORDS:ChrII_A_nidulans_FGSC_A4:1230057-1222630C, translated using codon table 1 (2404	48.71	12.65	1	25	25	26	2404	276.7	6.49
AN10756	AN10756 AspGDID:ASPL0000005758 COORDS:ChrI_A_nidulans_FGSC_A4:1674642-1678733W, translated using codon table 1 (1313	47.51	26.35	1	22	22	26	1313	146.4	7.09
AN1213	AN1213 AspGDID:ASPL0000054825 COORDS:ChrVIII_A_nidulans_FGSC_A4:1181878-1178568C, translated using codon table 1 (994	46.43	28.47	1	23	23	24	994	109.1	6.27
AN4859	pmaA AspGDID:ASPL0000077585 COORDS:ChrII_A_nidulans_FGSC_A4:748768-745667C, translated using codon table 1 (990 amino	43.38	27.27	2	17	17	21	990	108.7	5.36
AN4639	AN4639 AspGDID:ASPL0000073481 COORDS:ChrIII_A_nidulans_FGSC_A4:1447462-1452030W, translated using codon table 1 (1424	40.67	20.01	1	18	18	20	1424	160.2	7.12
AN3422	ste7 AspGDID:ASPL0000040884 COORDS:ChrVI_A_nidulans_FGSC_A4:772852-774627W, translated using codon tab	38.91	35.25	1	15	15	17	539	58.0	9.26
AN8870	AN8870 AspGDID:ASPL0000071167 COORDS:ChrIII_A_nidulans_FGSC_A4:2544176-2543164C, translated using codon table 1 (256 a	24.96	38.67	1	9	9	10	256	29.1	10.04
AN5979	AN5979 AspGDID:ASPL0000004567 COORDS:ChrI_A_nidulans_FGSC_A4:1608051-1607409C, translated using codon table 1 (139 am	23.52	59.71	1	7	7	9	139	16.1	9.94
AN4267	AN4267 AspGDID:ASPL0000017798 COORDS:ChrII_A_nidulans_FGSC_A4:1570713-1567771C, translated using codon table 1 (938 a	20.60	12.69	1	8	8	11	938	100.4	7.42
AN4435	AN4435 AspGDID:ASPL0000077445 COORDS:ChrVII_A_nidulans_FGSC_A4:2061136-2058007C, translated using codon table 1 (980 a	19.94	16.12	1	13	13	13	980	109.1	8.95
AN7252	steD AspGDID:ASPL0000068680 COORDS:ChrIV_A_nidulans_FGSC_A4:526909-528499W, translated using codon ta	18.60	15.79	1	5	5	7	494	54.3	5.82
AN2070	AN2070 AspGDID:ASPL0000045907 COORDS:ChrVII_A_nidulans_FGSC_A4:2762644-2760686C, translated using codon table 1 (652 a	18.20	24.08	1	12	12	13	652	70.2	9.66
AN0406	AN0406 AspGDID:ASPL0000052822 COORDS:ChrVIII_A_nidulans_FGSC_A4:3661137-3663071W, translated using codon table 1 (609	18.04	23.48	1	9	9	9	609	65.2	9.16
AN10751	AN10751 AspGDID:ASPL0000008014 COORDS:ChrI_A_nidulans_FGSC_A4:1993352-1994401W, translated using codon table 1 (321 a	13.05	20.25	1	4	4	5	321	37.5	9.57
AN5132	AN5132 AspGDID:ASPL0000033818 COORDS:ChrV_A_nidulans_FGSC_A4:1240763-1241955W, translated using codon table 1 (306 am	12.78	35.29	1	6	6	6	306	33.0	9.89
AN3706	AN3706 AspGDID:ASPL0000012467 COORDS:ChrII_A_nidulans_FGSC_A4:3321661-3320973C, translated using codon table 1 (153 a	12.60	41.18	1	5	5	6	153	17.6	9.82
AN10689	AN10689 AspGDID:ASPL0000029447 COORDS:ChrV_A_nidulans_FGSC_A4:2546580-2549095W, translated using codon table 1 (748	11.89	16.98	1	9	9	10	748	82.0	9.95
AN6125	nudE AspGDID:ASPL0000007192 COORDS:ChrI_A_nidulans_FGSC_A4:1186781-1184960C, translated using codon table 1 (586 amino	11.83	8.36	1	4	4	5	586	64.6	9.85
AN5931	AN5931 AspGDID:ASPL0000006660 COORDS:ChrI_A_nidulans_FGSC_A4:1770987-1773596W, translated using codon table 1 (563 am	10.18	16.16	1	6	7	7	563	60.9	9.23
AN1964	AN1964 AspGDID:ASPL0000048771 COORDS:ChrVII_A_nidulans_FGSC_A4:2404820-2405920W, translated using codon table 1 (237	9.88	20.25	1	3	3	4	237	27.1	10.73
AN1345	AN1345 AspGDID:ASPL0000058023 COORDS:ChrI_A_nidulans_FGSC_A4:775408-775967W, translated using codon table 1 (145 a	8.90	31.03	1	3	3	3	145	15.8	10.39
AN10853	hbrB AspGDID:ASPL0000001268 COORDS:ChrI_A_nidulans_FGSC_A4:2969482-2966688C, translated using codon table 1 (904 amino	8.31	7.19	1	4	4	5	904	97.8	8.94
AN6339	pod6 AspGDID:ASPL0000003634 COORDS:ChrI_A_nidulans_FGSC_A4:479694-477237C, translated using codon table 1 (785 amino a	7.49	6.88	1	4	4	5	785	86.2	4.64
AN3819	AN3819 AspGDID:ASPL0000011591 COORDS:ChrII_A_nidulans_FGSC_A4:2961435-2960161C, translated using codon table 1 (424 a	7.03	10.14	1	3	3	3	424	46.1	4.92
AN0776	AN0776 AspGDID:ASPL0000053603 COORDS:ChrVII_A_nidulans_FGSC_A4:2502223-2501208C, translated using codon table 1 (184	6.94	20.65	1	4	4	4	184	20.6	10.83
AN0252	AN0252 AspGDID:ASPL0000052676 COORDS:ChrVIII_A_nidulans_FGSC_A4:4138380-4139599W, translated using codon table 1 (296	6.91	17.91	1	4	4	4	296	31.9	7.83
AN11008	AN11008 AspGDID:ASPL0000065685 COORDS:ChrIV_A_nidulans_FGSC_A4:2593040-2591532C, translated using codon table 1 (483	6.48	20.50	1	6	6	7	483	53.0	8.75
AN11411	AN11411 AspGDID:ASPL0000011385 COORDS:ChrII_A_nidulans_FGSC_A4:3309578-3310189W, translated using codon table 1 (56 a	6.46	28.57	1	3	3	3	56	6.7	10.21
AN10681	AN10681 AspGDID:ASPL0000026338 COORDS:ChrV_A_nidulans_FGSC_A4:2652978-2653935W, translated using codon table 1 (122 a	6.07	21.31	1	4	4	4	122	13.9	10.35
AN12491	AN12491 AspGDID:ASPL0000403457 COORDS:ChrI_A_nidulans_FGSC_A4:3575960-3573772C, translated using codon table 1 (266 a	5.74	8.27	1	2	2	2	266	28.1	10.14
AN9468	AN9468 AspGDID:ASPL0000000085 COORDS:ChrII_A_nidulans_FGSC_A4:1661637-1662566W, translated using codon table 1 (143 ar	5.67	16.78	1	3	3	3	143	15.9	10.18
AN7258	AN7258 AspGDID:ASPL0000063859 COORDS:ChrIV_A_nidulans_FGSC_A4:514976-514042C, translated using codon table 1 (269 ami	5.13	24.91	1	5	5	5	269	29.5	10.08
AN5715	AN5715 AspGDID:ASPL0000029491 COORDS:ChrV_A_nidulans_FGSC_A4:1907272-1908090W, translated using codon table 1 (119 a	5.12	25.21	1	3	3	3	119	13.5	10.87
AN2979	AN2979 AspGDID:ASPL0000039874 COORDS:ChrVI_A_nidulans_FGSC_A4:2192709-2194003W, translated using codon table 1 (382 a	4.97	7.59	1	2	2	2	382	42.3	9.51
AN7877	AN7877 AspGDID:ASPL0000015573 COORDS:ChrI_A_nidulans_FGSC_A4:94602-93359C, translated using codon table 1 (383 amino	4.73	6.53	1	2	2	2	383	43.3	9.60
AN6307	AN6307 AspGDID:ASPL0000000161 COORDS:ChrI_A_nidulans_FGSC_A4:602555-601168C, translated using codon table 1 (360 amin	4.52	10.56	1	3	3	3	360	40.0	7.02
AN5716	AN5716 AspGDID:ASPL0000033419 COORDS:ChrV_A_nidulans_FGSC_A4:1906499-1904312C, translated using codon table 1 (666 a	4.47	10.06	1	4	4	4	666	71.7	6.40
AN1847	AN1847 AspGDID:ASPL0000051760 COORDS:ChrVII_A_nidulans_FGSC_A4:2053414-2052484C, translated using codon table 1 (288 a	4.25	12.50	1	3	3	3	288	31.9	9.94
AN8704	AN8704 AspGDID:ASPL0000074183 COORDS:ChrIII_A_nidulans_FGSC_A4:3065640-3064819C, translated using codon table 1 (160 a	4.22	11.25	1	2	2	2	160	17.9	11.22
AN10736	AN10736 AspGDID:ASPL0000004051 COORDS:ChrVII_A_nidulans_FGSC_A4:1994433-1995975W, translated using codon table 1 (473 a	4.21	6.55	1	2	2	2	473	52.4	10.35
AN1097	nnk1 AspGDID:ASPL0000058612 COORDS:ChrVIII_A_nidulans_FGSC_A4:1521366-1523303W, translated using codon table 1 (645 a	4.15	5.12	1	3	3	3	645	71.7	5.77
AN11789	AN11789 AspGDID:ASPL0000099841 COORDS:ChrV_A_nidulans_FGSC_A4:1911605-1912390W, translated using codon table 1 (261 a	4.14	12.26	1	3	3	3	261	30.6	8.92
AN4803	AN4803 AspGDID:ASPL0000071451 COORDS:ChrIII_A_nidulans_FGSC_A4:942550-941690C, translated using codon table 1 (193 ami	4.01	7.77	1	2	2	2	193	22.2	10.10
AN4402	AN4402 AspGDID:ASPL0000077985 COORDS:ChrII_A_nidulans_FGSC_A4:2150995-2149676C, translated using codon table 1 (284 a	3.68	20.77	1	5	5	5	284	29.9	9.01
AN10975	AN10975 AspGDID:ASPL0000067132 COORDS:ChrIV_A_nidulans_FGSC_A4:2170511-2171497W, translated using codon table 1 (289	3.15	6.23	1	1	1	1	289	31.7	6.71
AN6892	ptcA AspGDID:ASPL0000008393 COORDS:ChrI_A_nidulans_FGSC_A4:3494532-3492776C, translated using codon table 1 (566 amino	2.79	2.83	1	1	1	1	566	60.5	5.71
AN11178	AN11178 AspGDID:ASPL0000035207 COORDS:ChrVI_A_nidulans_FGSC_A4:338117-336398C, translated using codon table 1 (552 am	2.26	2.54	1	1	1	1	552	62.2	9.23
AN1250	AN1250 AspGDID:ASPL0000059123 COORDS:ChrVIII_A_nidulans_FGSC_A4:1053105-1055030W, translated using codon table 1 (622	2.24	2.09	1	1	1	1	622	70.5	10.26
AN3468	H2A.X AspGDID:ASPL0000038151 COORDS:ChrVI_A_nidulans_FGSC_A4:632619-633175W, translated using codon table 1 (132 amino	2.07	6.82	1	1	1	1	132	14.0	10.55
AN20019	oxlB AspGDID:ASPL0000090295 COORDS:mito_A_nidulans_FGSC_A4:32464-33225W, translated using codon table 4 (253 amino acid	2.04	13.44	1	3	3	3	253	29.2	4.83
AN5347	AN5347 AspGDID:ASPL0000027592 COORDS:ChrV_A_nidulans_FGSC_A4:3082742-3079684C, translated using codon table 1 (942 a	1.82	2.44	1	2	2	2	942	101.9	7.59
AN5787	AN5787 AspGDID:ASPL0000027670 COORDS:ChrV_A_nidulans_FGSC_A4:1706350-1701976C, translated using codon table 1 (1390 a	1.66	4.32	1	3	3	3	1390	151.9	7.23
AN3729	ficsA AspGDID:ASPL0000011003 COORDS:ChrII_A_nidulans_FGSC_A4:3255844-3261673W, translated using codon table 1 (1905 ami	1.61	3.25	1	4	4	4	1905	218.3	7.96
AN6241	AN6241 AspGDID:ASPL0000008519 COORDS:ChrI_A_nidulans_FGSC_A4:784939-787015W, translated using codon table 1 (659 amin	0.00	3.64	1	2	2	2	659	73.6	6.65
AN2269	steC AspGDID:ASPL0000047432 COORDS:ChrVII_A_nidulans_FGSC_A4:3394519-3391706C, translated using codon	0.00	5.87	1	3	3	3	886	97.7	7.84
AN0445	AN0445 AspGDID:ASPL0000051953 COORDS:ChrI_A_nidulans_FGSC_A4:3532607-3533558W, translated using codon table 1 (203	0.00	3.45	1	1	1	1	203	24.0	11.31
AN10752	AN10752 AspGDID:ASPL0000004032 COORDS:ChrI_A_nidulans_FGSC_A4:1960272-1961578W, translated using codon table 1 (383 a	0.00	3.13	1	1	1	1	383	45.1	10.20
AN11565	AN11565 AspGDID:ASPL0000063719 COORDS:ChrIV_A_nidulans_FGSC_A4:1725476-1724868C, translated using codon table 1 (101	0.00	13.86	1	1	1	2	101	11.1	10.18
AN5003	AN5003 AspGDID:ASPL0000071119 COORDS:ChrIII_A_nidulans_FGSC_A4:315809-313840C, translated using codon table 1 (637 ami	0.00	3.45	1	2	2	2	637	69.2	9.07
AN6523	sepA AspGDID:ASPL0000002931 COORDS:ChrI_A_nidulans_FGSC_A4:2368685-2363251C, translated using codon table 1 (1762 ami	0.00	1.42	1	1	1	1	1762	193.9	6.23
AN0214	AN0214 AspGDID:ASPL0000056619 COORDS:ChrVIII_A_nidulans_FGSC_A4:4273702-4270684C, translated using codon table 1 (976	0.00	4.51	1	4	4	4	976	108.2	5.47

Table S14. *A. nidulans* strains created or used in this study

Strain	Genotype	Plasmid used	Reference
AGB551	*nkuAΔ::argB, pyrG89, pyroA4, veA+*	Not applied	(Bayram et al., 2012)
AGB586	*mkkBΔ::ptrA, nkuAΔ::argB, pyrG89, pyroA4, veA1*	Fusion PCR	(Bayram et al., 2012)
AGB590	*mkkB::sgfp::natR; nkuAΔ::argB, pyroA4, pyrG89, veA1*	Fusion PCR	(Bayram et al., 2012)
AGB591	*mrfp::h2A-pyrG; mkkB::sgfp::natR; nkuAΔ::argB, pyroA4, pyrG89, veA1*	pME3858 in AGB590	(Bayram et al., 2012)
AGB597	*mkkB::ctap::natR; nkuAΔ::argB, pyroA4, pyrG89, veA+*	Fusion PCR	(Bayram et al., 2012)
AGB650	*steDΔ::ptrA , nkuAΔ::argB, pyrG89, pyroA4, veA+*	Fusion PCR	(Bayram et al., 2012)
AGB654	*mpkB::sgfp::natR; nkuAΔ::argB, pyrG89, pyroA4, veA+*	Fusion PCR	(Bayram et al., 2012)
AGB655	*pgpdA::mrfp::h2A-pyrG; mpkB::sgfp::natR; nkuAΔ::argB, pyrG89, pyroA4, veA+*	pME3858 in AGB654	(Bayram et al., 2012)
AGB656	*mpkB::ctap::natR; nkuAΔ::argB, pyroA4, pyrG89, veA+*	Fusion PCR	(Bayram et al., 2012)
AGB657	*steD::sgfp::natR; nkuAΔ::argB, pyroA4, pyrG89, veA+*	Fusion PCR	(Bayram et al., 2012)
AGB659	*steD::ctap::natR; nkuAΔ::argB, pyroA4, pyrG89, veA+*	Fusion PCR	(Bayram et al., 2012)
SteC-GFP	*steC::sgfp::natR; nkuAΔ::argB, pyroA4, pyrG89, veA+*	pOB478 in AGB551	This Study
SteC-TAP	*steC::ctap::natR; nkuAΔ::argB, pyroA4, pyrG89, veA+*	pOB479 in AGB551	This Study
SteC-DEL	*steCΔ::ptrA, nkuAΔ::argB, pyrG89, pyroA4, veA+*	pOB483 in AGB551	This Study
MpkB-DEL	*mpkBΔ::ptrA, nkuAΔ::argB, pyrG89, pyroA4, veA+*	Fusion PCR	This Study
HamE DEL-1	*hamEΔ::pyroA; nkuAΔ::argB, pyrG89, pyroA4, veA+*	pOB451 in AGB551	This Study
HamE-GFP	*hamE::sgfp::natR; pyrG89, pyroA4, veA+*	pOB456 in AGB551	This Study
HamE-GFP-mRFP	*hamE::sgfp::natR; ^PgpdA::mrfp::h2A::AfpyroA, pyrG89, pyroA4, veA+*	pOB340 in HamE-GFP	This Study
HamE-TAP	*hamE::ctap::natR; pyrG89, pyroA4, veA+*	pOB457 in AGB551	This Study
c-yfp-HamE, n-yfp-SteC	*^PniiA::n-yfp::steC; ^PniiD::c-yfp::hamE-pyrG; ^PgpdA::mrfp::h2A natR; pyroA4, pyrG89, nkuAΔ::argB, veA+*	pOB216 in AGB551	This Study
ANDF1	*steC::ctap::natR; hamEΔ::pyroA; nkuAΔ::argB, pyroA4, pyrG89, veA+*	pOB451 in SteC-TAP	This Study
ANDF2	*mkkB::ctap::natR; hamEΔ::pyroA; nkuAΔ::argB, pyroA4, pyrG89, veA+*	pOB451 in AGB597	This Study
ANDF3	*mpkB::ctap::natR; hamEΔ::pyroA; nkuAΔ::argB, pyroA4, pyrG89, veA+*	pOB451 in AGB656	This Study
ANDF4	*steD::ctap::natR; hamEΔ::pyroA; nkuAΔ::argB, pyrG89, pyroA4, veA+*	pOB451 in AGB659	This Study
ANDF5	*steC::sgfp::natR; hamEΔ::pyroA; nkuAΔ::argB, pyrG89, pyroA4, veA+*	pOB451 in SteC-GFP	This Study
ANDF6	*mrfp::h2A-pyrG; mkkB::sgfp::natR; hamEΔ::pyroA, nkuAΔ::argB, pyroA4, pyrG89, veA+*	pOB451 in AGB590	This Study
ANDF7	*pgpdA::mrfp::h2A-pyrG; mpkB::sgfp::natR; hamEΔ::pyroA, nkuAΔ::argB, pyrG89, pyroA4, veA+*	pOB451 in AGB654	This Study
ANDF8	*steD::sgfp::natR; hamEΔ::pyroA, nkuAΔ::argB, pyrG89, pyroA4, veA+*	pOB451 in AGB657	This Study
ANDF9	*steCΔ::ptrA, hamEΔ::pyroA, nkuAΔ::argB, pyrG89, pyroA4, veA+*	pOB451 in SteC DEL	This Study
ANDF10	*mkkBΔ::ptrA, hamEΔ::pyroA, nkuAΔ::argB, pyrG89, pyroA4, veA+*	pOB451 in AGB586	This Study

ANDF11	mpkBΔ::ptrA, hamEΔ::pyroA, nkuAΔ::argB, pyrG89, pyroA4, veA+	pOB451 in MpkB DEL	This Study
ANDF12	steDΔ::ptrA, hamEΔ::pyroA, nkuAΔ::argB, pyrG89, pyroA4, veA+	pOB451 in AGB650	This Study
ANDF13	hamEΔ::ptrA; pyrG89, pyroA4, nkuAΔ::argB, veA+	pOB341 in AGB551	This Study
ANDF14	hamEΔ::ptrA; mrfp::h2A-pyroA; pyrG89, pyroA4, nkuAΔ::argB, veA+	pOB207 in ANDF13	This Study
ANDF15	steC::sgfp::natR; hamEΔ::ptrA, nkuAΔ::argB, pyroA4, pyrG89, veA+	pOB341 in SteC-GFP	This Study
ANDF16	steD::sgfp::natR; hamEΔ::ptrA, nkuAΔ::argB, pyrG89, pyroA4, veA+	pOB341 in AGB657	This Study
ANDF17	steC::sgfp::natR; ᵖgpdA::mrfp::h2A::AfpyroA, pyroA4, pyrG89, veA+	pOB340 in SteC-GFP	This Study
ANDF18	steD::sgfp::natR; ᵖgpdA::mrfp::h2A::AfpyroA, nkuAΔ::argB, pyrG89, pyroA4, veA+	pOB340 in SteD-GFP	This Study
ANDF19	steC::sgfp::natR; hamEΔ::ptrA, ᵖgpdA::mrfp::h2A::AfpyroA, pyroA4, pyrG89, veA+	pOB341 in ANDF15	This Study
ANDF20	steD::sgfp::natR; hamEΔ::ptrA, ᵖgpdA::mrfp::h2A::AfpyroA, nkuAΔ::argB, pyrG89, pyroA4, veA+	pOB341 in ANDF16	This Study

Table S15. Plasmids created or used in this study

Plasmid	Description	Reference
pUC19	*E. coli* cloning plasmid with *bla* (ampicillin resistance gene) gene	Thermo Fisher
pOB207	*pgpdA::mrfp::h2A::pyroA* (histone 2A) in *Kpn*I site of pSK379	This Study
pOB340	*bioA5ORF::AfpyroA::pgpdA::mrfp::bioA3ORF* (histone 2A) with *bla* (*E.coli*) and *AfpyroA* (*A. nidulans*)	This Study
pOB341	*hamE* (AN2701) deletion *with ptrA* in *Sma*I site of pUC19	This Study
pOB451	*hamE* (AN2701) deletion *with pyroA* in *Sma*I site of pUC19	This Study
pOB456	*hamE::sgfp::natR* cassette with *Pme*I site in *Sma*I site of pUC19	This Study
pOB457	*hamE::ctap::natR* cassette with *Pme*I site in *Sma*I site of pUC19	This Study
pOB478	*steC::sgfp::natR* cassette with *Pme*I site in *Sma*I site of pUC19	This Study
pOB479	*steC::ctap::natR* cassette with *Pme*I site in *Sma*I site of pUC19	This Study
pOB483	*steC* deletion with *ptrA* in *Sma*I site of pUC19	This Study
pME3858	*pgpdA::mrfp::h2A* (histone 2A) with *pyrG* marker	(Bayram et al., 2012)
pOB216	*c-yfp hamE* in *Swa*I site of pOB133 (*n-yfp-steC*)	This Study

Table S16. Oligonucleotides created or used in this study

Designation	Sequence in 5' > 3' direction	Size (basepairs)
3422-A (*mkkB* 5UTR forward)	CTC GGG CGC TCA TCG TGT GTT G	22
3422-B (*mkkB* 5UTR nest)	CTT GCA ATG GGA CAA GCG ACG	21
3422-C (*mkkB* 5UTR reverse with *ptrA* tail)	CTT TTA CAT TTC GTT ACC AAT GGG ATC CCG TAA TCA ATT GGC GAC GGC GAC TGA AGA TTG	60
3422-D (*mkkB* 3UTR forward with *ptrA* tail)	CAA GAA AGA CAG TAT AAT ACA AAC AAA GAT GCA AGA CCT CTA AAC TAT TCA TGG GCC CC	59
3422-E (*mkkB* 3UTR nest)	CCA CTA GCC GAT GAA CGA GTA TTC	24
3422-F (*mkkB* 3UTR reverse)	GAG CCT CTG TTG TAG TGG GTA GAG	24
OZG314 (*mkkB* 3UTR forward with tail for natR)	GCA GGC GCT CTA CAT GAG CAT GCC CTG CCC CTG ACC TCT AAA CTA TTC ATG GGC CCC	57
OZG380 (*mkkB* 5UTR reverse with GFP tail)	GCC CTT GCT CAC CAT ACC ACC GCT ACC ACC GAG GGC CCC CAT ATG GTC GCC GC	54
OZG382 (*mkkB* 5UTR reverse with TAP tail)	CTT TTT CCA TCT TCT CTT ACC ACC GCT ACC ACC GAG GGC CCC CAT ATG GTC GCC GC	56
OZG443 (*mpkB* 5UTR forward)	CCC AGA AGT CCC AGG CCA GTT C	22
OZG444 (*mpkB* 5UTR nest)	CAA GAG ATC ATT CTT GAG GCA AAA G	25
OZG445 (*mpkB* 5UTR reverse with *ptrA* tail)	CAT TTC GTT ACC AAT GGG ATC CCG TAA TCA ATT CTG CTG CAC CAT GTT GAC TGG	54
OZG446 (*mpkB* 3UTR forward with *ptrA* tail)	GAC AGT ATA ATA CAA ACA AAG ATG CAA GAT GTC ATC ACA GTT CTG ATT TAC GAG	54
OZG447 (*mpkB* 3UTR nest)	GCT GAC GGC AAT ATA GAA TCA TAC	24
OZG448 (*mpkB* 3UTR reverse)	CGA GGC GTT TGG GGA CAC GCT GAG	24
OZG470 (*steD* 5UTR forward)	GAC CAT CCA GAG GCG GTA ACG	21
OZG471 (*steD* 5UTR nest)	GTC GAA GAA TTT GCA TAT CGA TTA TC	26
OZG472 (*steD* 5UTR reverse with tail for *ptrA*)	CAT TTC GTT ACC AAT GGG ATC CCG TAA TCA ATT GAC GAG AGC GAG CTG ACG AC	53
OZG473 (*steD* 3UTR forward with tail for *ptrA*)	GAC AGT ATA ATA CAA ACA AAG ATG CAA GAA ACC ATC GCA GGG GCA TAT GC	50
OZG474 (*steD* 3UTR nest)	CGC GTG ATC TTT CAC GTA ACC G	22
OZG475 (*steD* 3UTR reverse)	CTC CGT AGG TGG AAT CCA AAC AG	23
OZG560 (*mpkB* 5UTR reverse with tail for GFP)	GCC CTT GCT CAC CAT ACC ACC GCT ACC ACC CCG CAT GAT CTC CTC GTA AAT CAG	54

243

OZG561 (*mpkB* 5UTR reverse with tail for TAP)	CTT TTT CCA TCT TCT CTT ACC ACC GCT ACC ACC CCG CAT GAT CTC CTC GTA AAT CAG	57
OZG562 (*mpkB* 3UTR forward with tail for natR)	GCG CTC TAC ATG AGC ATG CCC TGC CCC TGA AGA ATC AAG TGT CGA ATC TTG GAG TTG	57
OZG564 (*steD* 5UTR reverse with tail for GFP)	GCC CTT GCT CAC CAT ACC ACC GCT ACC ACC TAA AAC TCC GCC GGG AAG GTT G	52
OZG565 (*steD* 5UTR reverse with tail for TAP)	CTT TTT CCA TCT TCT CTT ACC ACC GCT ACC ACC TAA AAC TCC GCC GGG AAG GTT G	55
OZG566 (*steD* 3UTR forward with tail for natR)	GCG CTC TAC ATG AGC ATG CCC TGC CCC TGA AGG CAT GCG ACT TGG ATG AAG C	52
OZG928 (*hamE* 5UTR forward with tail for pUC19)	TTC GAG CTC GGT ACC CGT TTA AAC CGC AGC TGG TGG ACT TGG AAC	45
OZG929 (*hamE* 5UTR reverse with tail for ptrA)	GAT CCC GTA ATC AAT TAA TTC CGC CCG AAT CCG TGA C	37
OZG931 (*hamE* 3UTR reverse with tail for pUC19)	ACT CTA GAG GAT CCC CGT TTA AAC ACT GAC ACA TCT GCA GCG CAA G	46
OZG948 (*hamE* 5UTR reverse with tail for pyroA)	CAG CAT CTG ATG TCC AAT TCC GCC CGA ATC CGT GAC	36
OZG949 (*hamE* 3UTR forward with tail for pyroA)	GCC TCC TCT CAG ACA GGC TGA CTG CCT TTT GCT ACT CAC	39
OZG983 (*hamE* 5UTR reverse with tail for TAP/GFP)	ACC ACC GCT ACC ACC TAT ACG ACC ATC AGC ATC AGG AG	38
OZG984 (*hamE* 3UTR forward with tail for natR)	ATG CCC TGC CCC TGA CTT CCG TTT TAA TCT TTT TTC TTC TTT GCT G	46
OZG1019 (*steC* 5UTR with tail for pUC19)	TTC GAG CTC GGT ACC CGT TTA AAC CTG GGA ATC GGA GCG TGT TG	44
OZG1020 (*steC* 5UTR reverse with tail for GFP & TAP linker)	TAC CAC CGC TAC CAC CGG TAA GTG TTG TAG CAA GGA AG	38
OZG1021 (*steC* 3UTR forward with tail for natR)	CAT GCC CTG CCC CTG AAA TCC TTT ACG ATG TCG GAT AGA C	40
OZG1022 (*steC* 3UTR with tail for pUC19)	ACT CTA GAG GAT CCC CGT TTA AAC CAG CGT TTA ATT CAA CTT GAG CAT G	49
OZG1023 (*steC* 5UTR reverse with tail for ptrA)	GGA TCC CGT AAT CAA TTG GAT TAG TAG ATG GGC GTA TAG	39
OZG1024 (*steC* 3UTR forward with tail for ptrA)	CAA ACA AAG ATG CAA GAT GAA ATC CTT TAC GAT GTC GGA TAG	42
OSBRT1 (*laeA* 5UTR)	CAC AAC CAC TAC AGC TAC CAC	21
OSBRT2 (*laeA* 3UTR)	GCA ACC GCG TAT CTG GTC G	19
OSBRT7 (*ipnA* 5UTR)	GAG AGT AGC CCA GCA AAT CG	20
OSBRT8 (*ipnA* 3UTR)	GGC ACG AAT CGC AAG GTC C	19
OSBRT9 (*acvA* 5UTR)	GAC AAG GAC AAC CGT GAT G	19
OSBRT10 (*acvA* 3UTR)	GCA CAC CAT TAC TGC TAG AGG	21

OSBRT11 (*aatA* 5UTR)	CCA TTG ACT TCG CAA CTG GC	20
OSBRT12 (*aatA* 3UTR)	CGT ACG AGT GTT GAG CAT GAC	21
OSBRT13 (*tdiA* 5UTR)	CGA TGC CTG GAG TGC GAA TG	20
OSBRT14 (*tdiA* 3UTR)	GCC GTT GCT GTC AAT GAA CG	20
OSBRT15 (*tdiB* 5UTR)	GCT ACC TGC ACA CGA GCA GC	20
OSBRT16 (*tdiB* 3UTR)	GCG CTC TCA AAG TTC CGC TC	20
OSBRT57 (*aflR* 5UTR)	CCT TCG CTT CTT GAG GGT ATG G	22
OSBRT58 (*aflR* 3UTR)	GCA GTA GGA GTG GCT TGT GGT G	22
OSBRT68 (*stcE* 5UTR)	GCA TCT CGA TGT AGT GAT CG	20
OSBRT69 (*stcE* 3UTR)	CTA GTC GCC TGG AAC AGT AG	20
OSBRT70 (*stcQ* 5UTR)	GGT TGT AGC GTC TTT GCA ACG	21
OSBRT71 (*stcQ* 3UTR)	GAA CAT CGT TGC AGA ACG TGG	21
OSBRT76 (*veA* 5UTR)	CGA TCC AGA GCC TCT CAG AG	20
OSBRT77 (*veA* 3UTR)	GGT CAT CAT GAC CGA ACG AC	20
OSBRT78 (*velB* 5UTR)	CCT CCC ACA ATC GGA TAT TGC	21
OSBRT79 (*velB* 3UTR)	GGG ATC TTG ATT CCT TGG TTC	21
BK280 (*benA* 5UTR)	GAT GGC TGC CTC TGA CTT C	19
BK281 (*benA* 3UTR)	GCA TCT GGT CCT CAA CCT C	19

Appendix B

Supplementary Data Relevant

to Chapter 4

a PstI

M | WT | steCΔ | steC::sgfp

8576bp
7427bp
6106bp
4899bp
3639bp
2799bp
1882bp
1515bp
1482bp
1164bp
992bp
718bp

3.45Kb | 5.03Kb | 6.52Kb

b BssHII

M | WT | mkkBΔ | mkkB::sgfp

8576bp
7427bp
6106bp
4899bp
3639bp
2799bp
1882bp
1515bp
1482bp
1164bp
992bp
718bp

4.29Kb | 2.34Kb | 2.34Kb

c SalI

M | WT | mpkBΔ | mpkB::sgfp

8576bp
7427bp
6106bp
4899bp
3639bp
2799bp
1882bp
1515bp
1482bp
1164bp
992bp
718bp

5.99Kb | 3.25Kb | 3.25Kb

d ScaI

M | WT | steDΔ | steD::sgfp

8576bp
7427bp
6106bp
4899bp
3639bp
2799bp
1882bp
1515bp
1482bp
1164bp
992bp

5.17Kb | 2.94Kb | 6.06Kb

e

WT | SteD-GFP

α-GFP 81kDa

247

Figure S1. Confirmation of deletions and tagged *A. flavus* strains *via* southern blotting (a) Southern hybridizations of *steCΔ* and *steC::sgfp*. M: Molecular marker in basepairs (bp). Sizes of the bands shown for the wild type TJES19.1 strain, the deletion strain and the tagged strain are in accordance with theoretical maps. The *Pst*I restriction enzyme was used to digest genomic DNA and a 3' UTR DIG-labelled probe was used for detection. (b) Southern hybridizations of *mkkBΔ* and *mkkB::sgfp*. The *Bss*HII restriction enzyme was used to digest genomic DNA and a 3' UTR DIG-labelled probe was used for detection. (c) Southern hybridizations of *mpkBΔ* and *mpkB::sgfp*. The *Sal*I restriction enzyme was used to digest genomic DNA and a 3' UTR DIG-labelled probe was used for detection. (d) Southern hybridizations of *steDΔ* and *steD::sgfp*. The faint upper band corresponds to the predicted size for *steD::sgfp*. The *Sca*I restriction enzyme was used to digest genomic DNA and a 5' UTR DIG-labelled probe was used for detection. (e) Western blot detecting the presence of the functional SteD-GFP fusion protein *via* an α-GFP antibody. The size of the tagged protein is 81kDa as predicted.
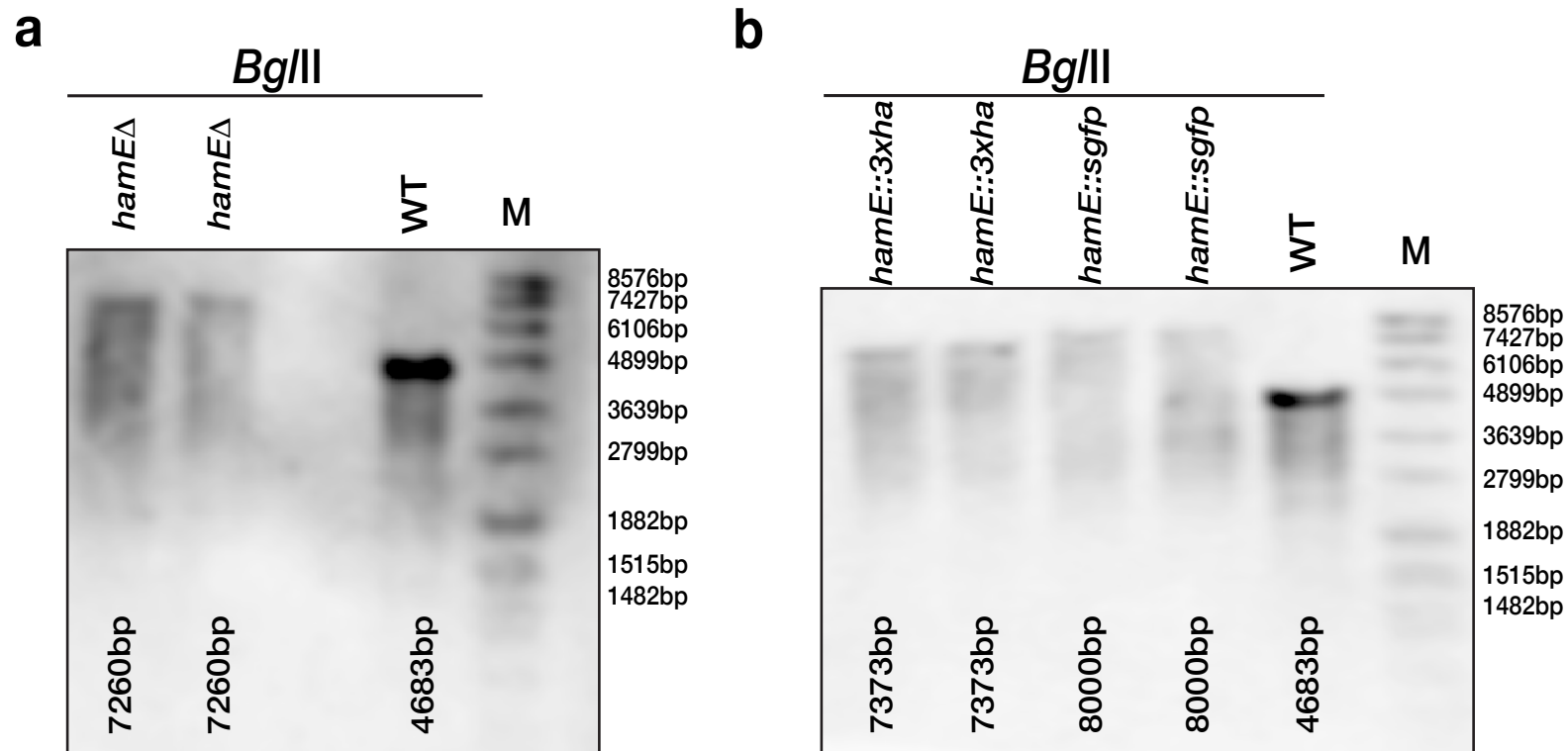
Figure S2. Confirmation of *A. flavus hamE* deletions and tagged *hamE* strains *via* southern blotting. (a) Southern hybridizations of two *hamEΔ* clones. M: Molecular marker in basepairs (bp). Sizes of the bands shown for the wild type TJES19.1 strain, the deletion strain and the tagged strain are in accordance with theoretical maps. The *Bgl*II restriction enzyme was used to digest genomic DNA and a 3' UTR DIG-labelled probe was used for detection. (b) Southern hybridizations of two *hamE::sgfp* and two *hamE::3xha* clones. The *Bgl*II restriction enzyme was used to digest genomic DNA and a 3' UTR DIG-labelled probe was used for detection.
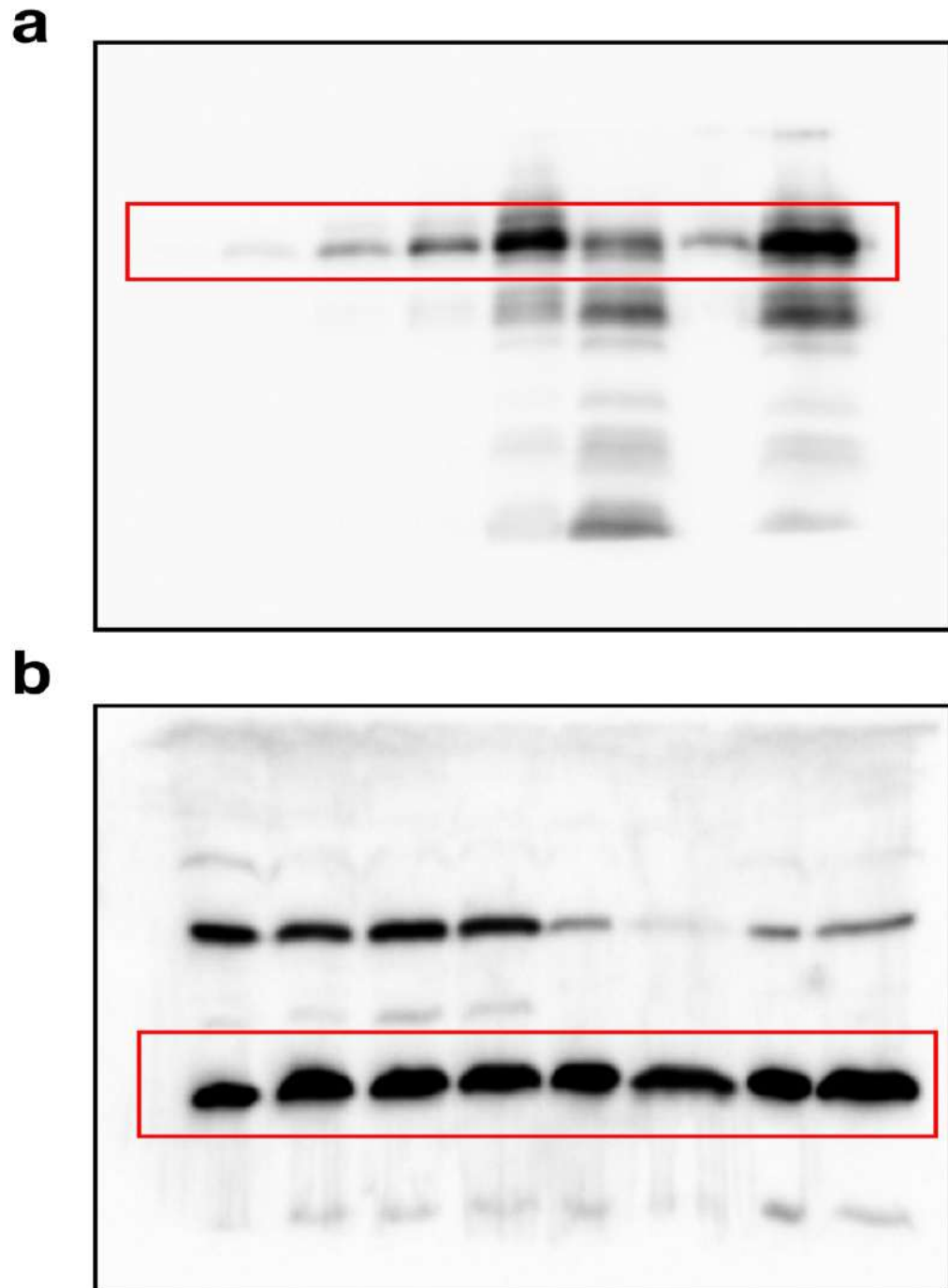
Supplementary Figure S3. Full length western blot membranes used to generate Figure 4.18. (a) Full length blot of HA-tagged HamE during different stages of development. Highlighted red box represents the portion of the blot that was cropped for use in the figure. (b) Full length blot of the SkpA loading control. The highlighted red box represents the section of the blot that was cropped for use in the figure

Table S1: Fungal strains created or used in this study

Strain	Genotype	Plasmid used	Reference
TJES19.1	*Wild type, nku70Δ::argB, pyrG89*	Not applied	N. Keller Lab
AFLDF1	*hamEΔ::pyrG; nku70Δ, pyrG89*	pDF1 in TJES19.1	This Study
AFLDF2	*hamE::sgfp::pyrG; nku70Δ, pyrG89*	pDF2 in TJES19.1	This Study
AFLDF3	*hamE::3xha::pyrG; nku70Δ, pyrG89*	pDF3 in TJES19.1	This Study
AFLDF11	*steCΔ::phleO, nku70Δ, pyrG89*	pDF30 in TJES19.1	This Study
AFLDF12	*mkkBΔ::phleO, nku70Δ, pyrG89*	pDF31 in TJES19.1	This Study
AFLDF13	*mpkBΔ::phleO, nku70Δ, pyrG89*	pDF32 in TJES19.1	This Study
AFLDF14	*steDΔ::phleO, nku70Δ, pyrG89*	pDF33 in TJES19.1	This Study
AFLDF15	*steC::sgfp::phleO, nku70Δ, pyrG89*	pDF34 in TJES19.1	This Study
AFLDF16	*mkkB::sgfp::phleO, nku70Δ, pyrG89*	pDF35 in TJES19.1	This Study
AFLDF17	*mpkB::sgfp::phleO, nku70Δ, pyrG89*	pDF36 in TJES19.1	This Study
AFLDF18	*steD::sgfp::phleO, nku70Δ, pyrG89*	pDF37 in TJES19.1	This Study
AFLDF23	*$_p$hamE::hamE::hamE$_t$, gpdA::phleO, hamEΔ::pyrG, nku70Δ, pyrG89*	pDF38 in AFLDF1	This Study
AFLDF24	*$_p$steC::steC::steC$_t$::pyrG, steCΔ::phleO, nku70Δ, pyrG89*	pDF39 in AFLDF11	This Study
AFLDF25	*$_p$mkkB::mkkB::mkkB$_t$::pyrG, mkkBΔ::phleO, nku70Δ, pyrG89*	pDF40 in AFLDF12	This Study
AFLDF26	*$_p$mpkB::mpkB::mpkB$_t$::pyrG, mpkBΔ::phleO, nku70Δ, pyrG89*	pDF41 in AFLDF13	This Study
AFLDF27	*$_p$steD::steD::steD$_t$::pyrG, steDΔ::phleO, nku70Δ, pyrG89*	pDF42 in AFLDF14	This Study
AFLDF29	*steCΔ::pyrG, nku70Δ, pyrG89*	pDF51 in TJES19.1	This Study
AFLDF30	*mkkBΔ::pyrG, nku70Δ, pyrG89*	pDF52 in TJES19.1	This Study
AFLDF31	*mpkBΔ:: pyrG, nku70Δ, pyrG89*	pDF53 in TJES19.1	This Study
AFLDF32	*steDΔ::pyrG, nku70Δ, pyrG89*	pDF54 in TJES19.1	This Study

Table S2: Plasmids created or used in this study

Plasmid	Description	Reference
pUC19	*E. coli* cloning plasmid with *bla* (ampicillin resistance) gene	Thermo Fisher
pAN8-1	*gpdA::phleO* resistance cassette	This Study
pOSB113	*Pme*I::*AfpyrG*::*Swa*I inserted in *Sma*I site of pUC19	This Study
pDF1	*hamE* deletion with *pyrG* in *Sma*I site of pUC19	This Study

pDF2	*hamE::sgfp::pyrG* cassette in *Sma*I site of pUC19	This Study
pDF3	*hamE::3xha::pyrG* cassette in *Sma*I site of pUC19	This Study
pDF30	*steC* deletion with *phleO* in *Sma*I site of pUC19	This Study
pDF31	*mkkB* deletion with *phleO* in *Sma*I site of pUC19	This Study
pDF32	*mpkB* deletion with *phleO* in *Sma*I site of pUC19	This Study
pDF33	*steD* deletion with *phleO* in *Sma*I site of pUC19	This Study
pDF34	*steC::sgfp::phleO* cassette in *Sma*I site of pUC19	This Study
pDF35	*mkkB::sgfp::phleO* cassette in *Sma*I site of pUC19	This Study
pDF36	*mpkB::sgfp::phleO* cassette in *Sma*I site of pUC19	This Study
pDF37	*steD::sgfp::phleO* cassette in *Sma*I site of pUC19	This Study
pDF38	*hamE* genomic locus in *Stu*I site of pAN8-1	This Study
pDF39	*steC* genomic locus in *Swa*I site of pOSB113	This Study
pDF40	*mkkB* genomic locus in *Swa*I site of pOSB113	This Study
pDF41	*mpkB* genomic locus in *Swa*I site of pOSB113	This Study
pDF42	*steD* genomic locus in *Swa*I site of pOSB113	This Study

Table S3: Oligonucleotides created or used in this study

Designation	Sequence in 5' > 3' direction	Size (basepairs)
DF01 (pDF1 5' UTR FWD, with pUC19 tail)	TTC GAG CTC GGT ACC CCT ACC GTT CCT TCT CCC TTC C	37
DF02 (pDF1 5' UTR REV, with *pyrG* tail)	GAG CAT TGT TTG AGG CGC TTC CGG TTG CAC CGG CA	35
DF03 (pDF1 3' UTR FWD, with *pyrG* tail)	GCC TCC TCT CAG ACA GCT ATT CGC CGA TCT TCG CTT TG	38
DF04 (pDF1 3' UTR REV, with pUC19 tail)	ACT CTA GAG GAT CCC CGA AGA GGT TCG CGG TTG CTG	36
DF05 (pDF1 5' FWD **nest oligo**)	CTC AAT CCG CCT CGT ACT AC	20
DF06 (pDF1 3' REV **nest oligo**)	CGA GTG TTT ATG CGG TCT ATA AAG	24
DF07 (pDF2/3 *hamE* ORF FWD with pUC19 tail)	TTC GAG CTC GGT ACC CGA ATA CCA TCT CCA GCG GCT G	37
DF08 (pDF2/3 ORF FWD **nest oligo**)	GAC CGA TCT GAC AGT CGC AAT G	22
DF09 (pDF2/3 *hamE* ORF REV with tail for GFP/HA linker)	CAC CGC TAC CAC CTC CGA TGC GAC CGT CGG CGA C	34
DF10 (pDF2/3 3' UTR FWD with tail for *pyrG*)	GCC TCC TCT CAG ACA GGT CAT TTT AAT TCT ATT CGC CGA TC	41
DF11 (pDF2/3 3' UTR REV **nest oligo**)	GGA GAT TAT ACA GGC CGC GAA G	22

DF12 (pDF2/3 3' UTR REV with pUC19 tail)	ACT CTA GAG GAT CCC CCA GGA AGT CGG AGT TGT ATC C	37
DF143 (pDF30 5' FWD with pUC19 tail)	TTC GAG CTC GGT ACC CCC ATC AAG AAG AAC GCC AGA C	37
DF144 (pDF30/34 3' REV with pUC19 tail)	ACT CTA GAG GAT CCC CCG ACC ACA TTG CTA TCC AGA TC	38
DF145 (pDF30 5' REV with *gpdA* promoter tail)	TTG ATG GTC GTT GTA GGG TTG AAA GGG GAA GCA ACC	36
DF146 (pDF30/34 3' FWD with *phleO* tail)	CGA GGA GCA GGA CTG AAA CCA GCC TGG TTG GAT GTG	36
DF147 (pDF30 5' FWD **nest oligo**)	GGA GCT AGC AGT TGT CAG C	19
DF148 (pDF30/34 3' REV **nest oligo**)	GAT CGT GGT CCT CTA CAC C	19
DF149 (pDF31 5' FWD with pUC19 tail)	TTC GAG CTC GGT ACC CCT ACG TCG CTT TCT CTT CTC C	37
DF150 (pDF31/35 3' REV with pUC19 tail)	ACT CTA GAG GAT CCC CCG TAT ATA GTG GTC CTC TGG TG	38
DF151 (pDF31 5' REV with *gpdA* promoter tail)	TTG ATG GTC GTT GTA GGG TTG GAC GGC AGA TTT ACT C	37
DF152 (pDF31/35 3' FWD with *phleO* tail)	CGA GGA GCA GGA CTG AGT AAA TAG AGT ACA TCA CTA TCG C	40
DF153 (pDF31 5' FWD **nest oligo**)	CCT CAT CGT CAT CAT CAT CAT C	22
DF154 (pDF31/35 3' REV **nest oligo**)	CGT TCG ATC CCA ACC ACT AAC	21
DF155 (pDF32 5' FWD with pUC19 tail)	TTC GAG CTC GGT ACC CGG ACC CTG AGA TTG CCT ATG	36
DF156 (pDF32/36 3' REV with pUC19 tail)	ACT CTA GAG GAT CCC CGG ACT CGA CAG AGC TAC TAC	36
DF157 (pDF32 5' REV with *gpdA* promoter tail)	TTG ATG GTC GTT GTA GAT TCG TGG ACT GTC CGA ACT AG	38
DF158 (pDF32/36 3' FWD with *phleO* tail)	CGA GGA GCA GGA CTG AGC TTG CAT GGA CAG CT TGT C	37
DF159 (pDF32 5' FWD **nest oligo**)	GAG GTA CCT GAC TCC ATT ATG G	22
DF160 (pDF32/36 3' REV **nest oligo**)	CCT TCA ACA CCT CCT CGA CC	20
DF161 (pDF33 5' FWD with pUC19 tail)	TTC GAG CTC GGT ACC CGG TGG ATT CTG ACA GCG GAG	36
DF162 (pDF33/37 3' REV with pUC19 tail)	ACT CTA GAG GAT CCC CGA GCG TCG CAG TAC TCT CAA C	37
DF163 (pDF33 5' REV with *gpdA* promoter tail)	TTG ATG GTC GTT GTA GGG TGG TAG CGA ACA ATT TCT CG	38
DF164 (pDF33/37 3' FWD with *phleO* tail)	CGA GGA GCA GGA CTG ATC TGT CTG TTA CGG ACG TCG	36
DF165 (pDF33 5' FWD **nest oligo**)	GTG GGT ATT GAT TGG CGT TGG	21
DF166 (pDF33/37 3' REV **nest oligo**)	CTC CAC CTC AGC AAG ATG AC	20
DF167 (pDF34 5' FWD with pUC19 tail)	TTC GAG CTC GGT ACC CCC AAG CGA CGC ATA TCA ATG C	37
DF168 (pDF34 5' REV with tail for linker)	CAC CGC TAC CAC CTC CTG CAA TTG GCG TGG CGA GG	35
DF169 (pDF34 5' FWD **nest oligo**)	GTG CTG AAT ACG GAG CGA CAC	21

DF170 (pDF35 5' FWD with pUC19 tail)	TTC GAG CTC GGT ACC CAT GGC CGA CCA ATT CAA AGC TC	38
DF171 (pDF35 5' REV with tail for linker)	CAC CGC TAC CAC CTC CGC GTT GCC ATG GTG TTC C	34
DF172 (pDF35 5' FWD **nest oligo**)	CTG GAG ATC GGA CTG GAG TTC	21
DF173 (pDF36 5' FWD with pUC19 tail)	TTC GAG CTC GGT ACC CCT GTG GAT TCG CTC GAT GTT TG	38
DF174 (pDF36 5' REV with tail for linker)	CAC CGC TAC CAC CTC CCC GCA TGA TCT CCT CGT AG	35
DF175 (pDF36 5' FWD **nest oligo**)	CGA ATC GTT TGA CAG CAG ACA C	22
DF176 (pDF37 5' FWD with pUC19 tail)	TTC GAG CTC GGT ACC CGT CCA TGT GGC ACA CTC TC	35
DF177 (pDF37 5' REV with tail for linker)	CAC CGC TAC CAC CTC CTA GCA CTC CGC CGG GTA GAT TG	38
DF178 (pDF37 5' FWD **nest oligo**)	GTG TCG TGT CGG TCC TTA TC	20
DF247 (pDF38 5' forward primer with tail for pAN8-1)	CCC AAG ACC GAC AAG GAG GGC TGC AGT GTG AAG AAA C	37
DF248 (pDF38 3' reverse primer with tail for pAN8-1)	GCG TTC TGG AGG GAG GCG AAC TAG ATG CGA TGG TCA C	37
DF249 (pDF39 5' forward primer with tail for pOSB113)	AGC TCG GTA CCC ATT TGG ACG CAC CTC ATT ATG GAG	36
DF250 (pDF39 3' reverse primer with tail for pOSB113)	TTG AGG CGA ATT ATT TCC ATC TGA TCC CTC TTC CC	35
DF251 (pDF40 5' forward primer with tail for pOSB113)	AGC TCG GTA CCC ATT TCA GCA CCC TGA TGA GCT TC	35
DF252 (pDF40 3' reverse primer with tail for pOSB113)	TTG AGG CGA ATT ATT TCG ATC CAA CCA CT AAC GC	35
DF253 (pDF41 5' forward primer with tail for pOSB113)	AGC TCG GTA CCC ATT TGT AGA TAC CGG ACC CTG AG	35
DF254 (pDF41 3' reverse primer with tail for pOSB113)	TTG AGG CGA ATT ATT TCG AGC TGG TTG ACC GTG AAA TC	38
DF255 (pDF42 5' forward primer with tail for pOSB113)	AGC TCG GTA CCC ATT TGT GGA TTC TGA CAG CGG AG	35
DF256 (pDF42 3' reverse primer with tail for pOSB113)	TTG AGG CGA ATT ATT TCT CTG AAG ACG ATG GCA CTG	36
DF302 (*veA* cDNA FWD)	CAA CCT CTC TCA ATC ATC CAG	21
DF303 (*veA* cDNA REV)	CTT CGT ACG ACC GCT TGG	18
DF304 (*velB* cDNA FWD)	GTT CAC GCG CAA CCT CAT C	19
DF305 (*velB* cDNA REV)	CCT TCA GTC CGT ACA CTC AG	20
DF306 (*fluG* cDNA FWD)	CAA CAT GTA CTT CGC CAT CG	20
DF307 (*fluG* cDNA REV)	GGT AAT TTG GCG GCA TCG TG	20
DF308 (*wetA* cDNA FWD)	GCT CAC GCT AAA TAT GTT GAC G	22
DF309 (*wetA* cDNA REV)	GCA TGG CTA ATC CGT TCT TG	20
aflA-F (AFLA qPCR) (Chang et al., 2012)	CCT ATA AGT GCT TCA AAG ATC GTG ATC G	28

aflA-R (AFLA qPCR) (Chang et al., 2012)	CGT ACA TGG ATG ACA CGT TGT CCC AG	26
aflC-F (AFLA qPCR) (Chang et al., 2012)	CCT ATT CTA GCC GCC TTT CTT GAC	24
aflC-R (AFLA qPCR) (Chang et al., 2012)	CAT GTT GCC AGA TTC CTC ATA TTC C	25
aflD-F (AFLA qPCR) (Chang et al., 2012)	TGT ATG CTC CCG TCC TAC TGT TTC	24
aflD-R (AFLA qPCR) (Chang et al., 2012)	TGT AGT CTC CTT AGT CGC TTC ATC	24
aflM-F (AFLA qPCR) (Chang et al., 2012)	GCG GAG AAA GTG GTT GAA CAG ATC	24
aflM-R (AFLA qPCR) (Chang et al., 2012)	CAG CGA ACA AAG GTG TCA ATA GCC	24
aflP-F (AFLA qPCR) (Chang et al., 2012)	CGA TGT CTA TCT TCT CCG ATC TAT TC	26
aflP-R (AFLA qPCR) (Chang et al., 2012)	TCT CAG TCT CCA GTC TAT TAT CTA CC	26
brlA-F (AFLA qPCR) (Chang et al., 2012)	TAT CCA GAC ATT CAA GAC GCA CAG	24
brlA-R (AFLA qPCR) (Chang et al., 2012)	GAT AAT AGA GGG CAA GTT CTC CAA AG	26
abaA-F (AFLA qPCR) (Chang et al., 2012)	GAG TGG CAG ACC GAA TGT ATG TTG	24
abaA-R (AFLA qPCR) (Chang et al., 2012)	TAG TGG TAG GCA TTG GGT GAG TTG	24
BK276 (AFL *skpA* cDNA FWD)	CGA TGT TAG TCT TGC CTT GC	20
BK277 (AFL *skpA* cDNA RVS)	GAC CAG ATG AAA CTC AAG CTG	21
BK465 (AFLA *laeA* cDNA F)	CAC AAC TCT CGT GAT ACA ATC C	22
BK466 (AFLA *laeA* cDNA R)	GTA CCA GCG AGC AAC CTT TC	20
BK471 (AFLA *nsdC* cDNA F)	CAG CCA TTC TAG CAA CCA TAA C	22
BK472 (AFLA *nsdC* cDNA R)	TCT CGC TCA CGA TTC TGA TC	20
BK473 (AFLA *nsdD* cDNA F)	CAA TGT ACC AAG ACG AAT ACA AG	23
BK474 (AFLA *nsdD* cDNA R)	TGT CTC AGC TCG GTT ACA AC	20
BK585 (AFLA *flbA* cDNA F)	CAC TGC GCA ACA GCT TGG	18
BK586 (AFLA *flbA* cDNA R)	GAT CGA ATC ACT TGA CAT CAA C	22
BK587 (AFLA *flbB* cDNA F)	CTG ACA ACG CTG CTC AAC C	19
BK588 (AFLA *flbB* cDNA R)	CTT TAC GTC ATC TCT GGT CAA C	22
BK589 (AFLA *flbC* cDNA F)	CAT GAT GAG CCA GTT CAG TTC	21
BK590 (AFLA *flbC* cDNA R)	CAC CAG TGT GAC TGT ACA TG	20
BK591 (AFLA *flbD* cDNA F)	CCT AGG ACC GTC TCA TCG	18
BK592 (AFLA *flbD* cDNA F)	GTT GTC GGA CTT CTT CGA GC	20
BK593 (AFLA *flbE* cDNA F)	GCG TTG ACA GAG ATG CGA G	19
BK594 (AFLA *flbE* cDNA R)	ACA TCA TAC TTT CAT CGT CGT C	22
BK609_AFCL4F	CAA GTC AGC ATG GTT GAC ATT C	22
BK610_AFCL4R	TCG TCG CAT CTT GTT CCG AG	20

255

BK617_AFCL8F	GTT GAT ATT CTG AAC CCA GAT G	22
BK618_AFCL8R	GGC AGC CAA CTC ATC AAG G	19
BK647_AFCL23F	CAG CGA GCG ATA TCT GGA G	19
BK648_AFCL23R	AGG ATC GCA TTC AAG GCA TC	20
BK709_AFCL54F	CGT CCT ACT TAA TCC CAC AC	20
BK710_AFCL54R	CTC GTC CAT GAC TGT ATC TG	20

Table S4: SteC-GFP (CADAFLAP00010880) interacting proteins at 24 hours of vegetative growth. Proteins of interest are highlighted in yellow.

SteD (CADAFLAP00010300), MpkB (CADAFLAP00002792).

Table S4: *Aspergillus flavus* SteC-GFP interacting proteins (Vegetative growth-24 hours)

Accession	Description	Score	Coverage	# Proteins	# Unique Peptides	# Peptides	# PSMs	# AAs	MW [kDa]	calc. pI
CADAFLAP00010880	pep:known supercontig:JCVI-afl1-v2.0:EQ963483:278171:281036:1 gene:CADAFLAG00010880 transcript:CADAFLAT00010880 description: MAP kinase kinase kinase St	166.82	51.96	1	30	30	43	895	98.9	8.35
CADAFLAP00010300	pep:known supercontig:JCVI-afl1-v2.0:EQ963482:495063:496660:-1 gene:CADAFLAG00010300 transcript:CADAFLAT00010300 description: Protein kinase regulator Ste	89.78	48.25	1	15	15	22	485	53.9	6.00
CADAFLAP00003740	pep:known supercontig:JCVI-afl1-v2.0:EQ963474:1563476:1566818:1 gene:CADAFLAG00003740 transcript:CADAFLAT00003740 description: Glycogen phosphorylase GlpV/Gph1, putative	58.96	23.89	1	13	13	14	879	99.7	6.06
CADAFLAP00009051	pep:known supercontig:JCVI-afl1-v2.0:EQ963480:1241438:1243239:1 gene:CADAFLAG00009051 transcript:CADAFLAT00009051 description: Solid-state culture expressed protein (Aos23), puta	43.01	35.64	1	12	12	13	550	57.0	7.14
CADAFLAP00012901	pep:known supercontig:JCVI-afl1-v2.0:EQ963486:140443:144341:-1 gene:CADAFLAG00012901 transcript:CADAFLAT00012901 description: 5-oxo-L-prolinase, putative	39.91	12.42	1	11	11	12	1280	138.6	5.95
CADAFLAP00002576	pep:known supercontig:JCVI-afl1-v2.0:EQ963473:2502671:2504536:1 gene:CADAFLAG00002576 transcript:CADAFLAT00002576 description: FAD binding domain protein	33.30	20.10	1	8	8	10	587	65.8	7.80
CADAFLAP00001170	pep:known supercontig:JCVI-afl1-v2.0:EQ963472:3123769:3125798:1 gene:CADAFLAG00001170 transcript:CADAFLAT00001170 description: DEAD box RNA helicase HelA, putative	32.17	17.38	1	8	8	9	656	72.7	9.94
CADAFLAP00006440	pep:known supercontig:JCVI-afl1-v2.0:EQ963477:995640:997061:-1 gene:CADAFLAG00006440 transcript:CADAFLAT00006440 description: Formaldehyde dehydrogenase	30.38	28.16	1	6	6	7	380	40.3	6.73
CADAFLAP00007224	pep:known supercontig:JCVI-afl1-v2.0:EQ963478:641683:643939:1 gene:CADAFLAG00007224 transcript:CADAFLAT00007224 description: CTP synthase	21.81	15.35	1	6	6	6	593	65.9	6.57
CADAFLAP00011127	pep:known supercontig:JCVI-afl1-v2.0:EQ963483:994025:997698:1 gene:CADAFLAG00011127 transcript:CADAFLAT00011127 description: Putative uncharacterized protein	21.60	10.68	1	6	6	6	899	100.0	8.50
CADAFLAP00006062	pep:known supercontig:JCVI-afl1-v2.0:EQ963476:2518574:2520387:-1 gene:CADAFLAG00006062 transcript:CADAFLAT00006062 description: Probable Xaa-Pro aminopeptidase pepP	19.88	11.56	1	4	4	4	467	51.6	5.80
CADAFLAP00005791	pep:known supercontig:JCVI-afl1-v2.0:EQ963476:1725709:1728027:1 gene:CADAFLAG00005791 transcript:CADAFLAT00005791 description: Fatty acid activator Faa4, putative	19.72	15.04	1	5	5	5	698	76.3	7.56
CADAFLAP00001377	pep:known supercontig:JCVI-afl1-v2.0:EQ963472:3693037:3694319:-1 gene:CADAFLAG00001377 transcript:CADAFLAT00001377 description: Regulatory protein SUAPRGA1	19.65	29.68	1	4	4	4	310	34.8	4.67
CADAFLAP00010782	pep:known supercontig:JCVI-afl1-v2.0:EQ963482:1923985:1926988:1 gene:CADAFLAG00010782 transcript:CADAFLAT00010782 description: NADH-ubiquinone oxidoreductase, subunit G, puta	19.27	15.60	1	5	5	5	737	80.8	6.51
CADAFLAP00002458	pep:known supercontig:JCVI-afl1-v2.0:EQ963473:2174554:2175988:1 gene:CADAFLAG00002458 transcript:CADAFLAT00002458 description: Oxysterol binding protein (Osh5), putative	18.70	20.58	1	7	7	7	413	45.8	6.76
CADAFLAP00010364	pep:known supercontig:JCVI-afl1-v2.0:EQ963482:666798:667988:1 gene:CADAFLAG00010364 transcript:CADAFLAT00010364 description: N,N-dimethylglycine oxidase	18.54	16.92	1	5	5	5	396	43.1	5.68
CADAFLAP00002306	pep:known supercontig:JCVI-afl1-v2.0:EQ963473:1745130:1746774:1 gene:CADAFLAG00002306 transcript:CADAFLAT00002306 description: Alcohol dehydrogenase, zinc-containing, putative	17.97	22.25	1	5	5	5	346	37.7	6.44
CADAFLAP00002511	pep:known supercontig:JCVI-afl1-v2.0:EQ963473:2306586:2309501:1 gene:CADAFLAG00002511 transcript:CADAFLAT00002511 description: Proteasome component Prs2, putative	17.22	8.86	1	5	5	5	666	74.4	6.68
CADAFLAP00004269	pep:known supercontig:JCVI-afl1-v2.0:EQ963475:301343:302978:-1 gene:CADAFLAG00004269 transcript:CADAFLAT00004269 description: Phosphoserine aminotransferase	17.18	17.38	1	5	5	5	420	46.0	6.14
CADAFLAP00000615	pep:known supercontig:JCVI-afl1-v2.0:EQ963472:1608276:1609022:-1 gene:CADAFLAG00000615 transcript:CADAFLAT00000615 description: Putative uncharacterized protein	16.53	48.10	1	3	3	4	79	8.7	9.70
CADAFLAP00004416	pep:known supercontig:JCVI-afl1-v2.0:EQ963475:691946:693316:1 gene:CADAFLAG00004416 transcript:CADAFLAT00004416 description: Guanine deaminase, putative	16.47	12.06	1	3	3	4	456	49.8	5.26
CADAFLAP00007467	pep:known supercontig:JCVI-afl1-v2.0:EQ963478:1327020:1331214:-1 gene:CADAFLAG00007467 transcript:CADAFLAT00007467 description: Protein transport protein (SEC31), putative	16.46	6.81	1	6	6	6	1263	135.7	6.46
CADAFLAP00013460	pep:known supercontig:JCVI-afl1-v2.0:EQ963487:323434:325053:1 gene:CADAFLAG00013460 transcript:CADAFLAT00013460 description: Ran exchange factor Prp20/Pim1, putative	15.10	14.34	1	5	5	5	523	55.4	7.84
CADAFLAP00011807	pep:known supercontig:JCVI-afl1-v2.0:EQ963484:952298:953870:1 gene:CADAFLAG00011807 transcript:CADAFLAT00011807 description: Phosphoserine phosphatase	14.57	18.38	1	3	3	3	468	51.4	5.67
CADAFLAP00003701	pep:known supercontig:JCVI-afl1-v2.0:EQ963474:1446236:1447417:-1 gene:CADAFLAG00003701 transcript:CADAFLAT00003701 description: Coatomer subunit epsilon, putative	14.49	24.07	1	3	3	3	295	31.6	4.61
CADAFLAP00006284	pep:known supercontig:JCVI-afl1-v2.0:EQ963477:578138:579490:-1 gene:CADAFLAG00006284 transcript:CADAFLAT00006284 description: Carbamoyl-phosphate synthase, small subunit	14.41	10.22	1	3	3	4	450	49.1	7.33
CADAFLAP00007312	pep:known supercontig:JCVI-afl1-v2.0:EQ963478:884527:885757:1 gene:CADAFLAG00007312 transcript:CADAFLAT00007312 description: BAR domain protein	14.32	13.77	1	2	2	3	305	33.5	5.19
CADAFLAP00002828	pep:known supercontig:JCVI-afl1-v2.0:EQ963473:3173108:3175535:-1 gene:CADAFLAG00002828 transcript:CADAFLAT00002828 description: Translation initiation factor eif-2b epsilon subunit,	13.98	10.09	1	3	3	3	704	78.2	4.77
CADAFLAP00005860	pep:known supercontig:JCVI-afl1-v2.0:EQ963476:1897595:1902056:1 gene:CADAFLAG00005860 transcript:CADAFLAT00005860 description: Eukaryotic translation initiation factor subunit eIF-	13.81	6.10	1	5	5	5	1376	147.7	9.38
CADAFLAP00010662	pep:known supercontig:JCVI-afl1-v2.0:EQ963482:1616917:1620814:1 gene:CADAFLAG00010662 transcript:CADAFLAT00010662 description: Ubiquitin carboxyl-terminal hydrolase	13.42	6.19	1	4	4	4	1115	128.6	5.71
CADAFLAP00008803	pep:known supercontig:JCVI-afl1-v2.0:EQ963480:550393:551622:-1 gene:CADAFLAG00008803 transcript:CADAFLAT00008803 description: ARP2/3 complex 20 kDa subunit (P20-ARC), putative	13.28	30.77	1	4	4	4	169	19.6	7.50
CADAFLAP00005126	pep:known supercontig:JCVI-afl1-v2.0:EQ963475:2606598:2609389:-1 gene:CADAFLAG00005126 transcript:CADAFLAT00005126 description: Translation initiation regulator (Gcn20), putative	13.28	6.52	1	3	3	3	751	83.0	6.27
CADAFLAP00008984	pep:known supercontig:JCVI-afl1-v2.0:EQ963480:1060277:1063706:-1 gene:CADAFLAG00008984 transcript:CADAFLAT00008984 description: Protein kinase c	13.27	8.13	1	4	4	4	1008	112.4	7.81
CADAFLAP00003681	pep:known supercontig:JCVI-afl1-v2.0:EQ963474:1394000:1394902:1 gene:CADAFLAG00003681 transcript:CADAFLAT00003681 description: Prohibitin complex subunit Phb1, putative	12.70	19.29	1	4	4	4	280	30.9	9.01
CADAFLAP00003048	pep:known supercontig:JCVI-afl1-v2.0:EQ963473:3788828:3790033:-1 gene:CADAFLAG00003048 transcript:CADAFLAT00003048 description: Cell division control protein 2 kinase, putative	12.63	15.00	1	4	4	4	320	36.3	7.87
CADAFLAP00011080	pep:known supercontig:JCVI-afl1-v2.0:EQ963483:847581:849011:-1 gene:CADAFLAG00011080 transcript:CADAFLAT00011080 description: GTP binding protein, putative	12.59	14.00	1	3	3	3	350	38.2	8.95
CADAFLAP00002799	pep:known supercontig:JCVI-afl1-v2.0:EQ963473:3102956:3103825:-1 gene:CADAFLAG00002799 transcript:CADAFLAT00002799 description: Dienelactone hydrolase family protein	12.30	22.13	1	3	3	3	244	26.9	6.37
CADAFLAP00009858	pep:known supercontig:JCVI-afl1-v2.0:EQ963481:1303727:1305754:-1 gene:CADAFLAG00009858 transcript:CADAFLAT00009858 description: Protoporphyrinogen oxidase, putative	12.13	6.87	1	2	2	2	597	65.9	8.06
CADAFLAP00004361	pep:known supercontig:JCVI-afl1-v2.0:EQ963475:547130:548172:1 gene:CADAFLAG00004361 transcript:CADAFLAT00004361 description: HAD superfamily hydrolase, putative	11.86	15.70	1	3	3	3	293	32.3	5.58
CADAFLAP00001659	pep:known supercontig:JCVI-afl1-v2.0:EQ963472:4442484:4444810:-1 gene:CADAFLAG00001659 transcript:CADAFLAT00001659 description: Glycerol-3-phosphate dehydrogenase, mitochondr	11.61	6.20	1	4	4	4	710	77.5	6.76
CADAFLAP00009908	pep:known supercontig:JCVI-afl1-v2.0:EQ963481:1447501:1448657:-1 gene:CADAFLAG00009908 transcript:CADAFLAT00009908 description: S-methyl-5'-thioadenosine phosphorylase	11.61	12.05	1	2	2	2	365	40.3	7.83
CADAFLAP00009916	pep:known supercontig:JCVI-afl1-v2.0:EQ963481:1465611:1466733:-1 gene:CADAFLAG00009916 transcript:CADAFLAT00009916 description: NADH-ubiquinone oxidoreductase 304 kDa subun	11.60	13.64	1	3	3	3	352	40.2	9.17
CADAFLAP00012843	pep:known supercontig:JCVI-afl1-v2.0:EQ963485:1782769:1785991:-1 gene:CADAFLAG00012843 transcript:CADAFLAT00012843 description: Actin binding protein, putative	11.44	10.27	1	3	3	3	526	56.0	9.10
CADAFLAP00005777	pep:known supercontig:JCVI-afl1-v2.0:EQ963476:1678698:1680170:-1 gene:CADAFLAG00005777 transcript:CADAFLAT00005777 description: ATP-dependent (S)-NAD(P)H-hydrate dehydratase	11.06	9.56	1	2	2	2	366	39.4	6.70
CADAFLAP00008304	pep:known supercontig:JCVI-afl1-v2.0:EQ963479:1226718:1228096:-1 gene:CADAFLAG00008304 transcript:CADAFLAT00008304 description: Vacuolar ATP synthase subunit c	10.96	10.34	1	3	3	3	387	43.7	7.27
CADAFLAP00003671	pep:known supercontig:JCVI-afl1-v2.0:EQ963474:1367376:1367860:-1 gene:CADAFLAG00003671 transcript:CADAFLAT00003671 description: Putative uncharacterized protein	10.96	24.65	1	2	2	3	142	15.4	6.95
CADAFLAP00006825	pep:known supercontig:JCVI-afl1-v2.0:EQ963477:1992461:1994977:1 gene:CADAFLAG00006825 transcript:CADAFLAT00006825 description: Polyubiquitin binding protein (Doa1/Ufd3), putative	10.95	5.70	1	4	4	4	789	84.8	5.10
CADAFLAP00011749	pep:known supercontig:JCVI-afl1-v2.0:EQ963484:800622:801017:-1 gene:CADAFLAG00011749 transcript:CADAFLAT00011749 description: Putative uncharacterized protein	10.87	22.90	1	2	2	2	131	14.9	9.23
CADAFLAP00013021	pep:known supercontig:JCVI-afl1-v2.0:EQ963486:451616:453602:1 gene:CADAFLAG00013021 transcript:CADAFLAT00013021 description: Reticulon-like protein	10.70	12.83	1	3	3	3	343	38.4	5.55
CADAFLAP00010388	pep:known supercontig:JCVI-afl1-v2.0:EQ963482:732204:736369:1 gene:CADAFLAG00010388 transcript:CADAFLAT00010388 description: Phospholipase D (PLD), putative	10.51	3.59	1	3	3	3	1309	145.2	6.58
CADAFLAP00004403	pep:known supercontig:JCVI-afl1-v2.0:EQ963475:656317:657289:1 gene:CADAFLAG00004403 transcript:CADAFLAT00004403 description: Tip120, putative	10.41	15.95	1	2	2	2	301	32.2	7.55
CADAFLAP00011075	pep:known supercontig:JCVI-afl1-v2.0:EQ963483:831054:832618:-1 gene:CADAFLAG00011075 transcript:CADAFLAT00011075 description: Uridine nucleosidase Urh1, putative	10.25	17.60	1	3	3	3	375	40.2	5.59
CADAFLAP00000968	pep:known supercontig:JCVI-afl1-v2.0:EQ963472:2582911:2584123:-1 gene:CADAFLAG00000968 transcript:CADAFLAT00000968 description: Branched-chain amino acid aminotransferase	9.92	14.44	1	3	3	3	381	41.2	6.27
CADAFLAP00012900	pep:known supercontig:JCVI-afl1-v2.0:EQ963486:137809:140008:1 gene:CADAFLAG00012900 transcript:CADAFLAT00012900 description: 5'-nucleotidase, putative	9.78	7.51	1	3	3	3	666	74.1	6.64
		9.57	4.36	1	2	2	2	803	85.3	6.19
	pep:known supercontig:JCVI-afl1-v2.0:EQ963473:3767161:3769228:1 gene:CADAFLAG00003038 transcript:CADAFLAT00003038 description: Probable HECT-type ubiquitin ligase-interacting protein creD	9.49	6.63	1	2	2	2	603	67.1	6.65
		9.48	11.61	1	2	2	2	267	29.2	6.58
		9.45	10.54	1	3	3	3	408	46.0	5.72
	pep:known supercontig:JCVI-afl1-v2.0:EQ963474:1749061:1749645:-1 gene:CADAFLAG00003808 transcript:CADAFLAT00003808 description: Mismatched base pair and cruciform DNA recognition protein, putative	9.43	21.14	1	3	3	3	175	18.0	5.63
		9.43	10.24	1	2	2	2	381	43.2	6.55
		9.22	39.74	1	2	2	2	78	8.7	6.52
	pep:known supercontig:JCVI-afl1-v2.0:EQ963473:1417524:1418881:-1 gene:CADAFLAG00002181 transcript:CADAFLAT00002181 description: Anthranilate phosphoribosyltransferase, putative	9.14	9.74	1	2	2	2	431	46.5	6.20
		9.10	8.85	1	2	2	2	373	42.2	5.31
		8.83	10.65	1	3	3	3	338	37.1	6.13
		8.78	14.52	1	3	3	3	420	45.7	5.95
		8.77	7.47	1	3	3	3	843	93.3	6.52
		8.69	35.16	1	2	2	2	128	14.4	5.49
		8.65	21.14	1	3	3	3	175	19.7	6.27
	pep:known supercontig:JCVI-afl1-v2.0:EQ963474:1898503:1900756:-1 gene:CADAFLAG00003867 transcript:CADAFLAT00003867 description: DNA replication licensing factor Mcm2, putative	8.64	6.62	1	4	4	4	710	79.2	7.21
		8.30	25.00	1	2	2	3	108	11.5	9.70

257

		14.41	10.22	1	3	3	4	450	49.1	7.33
	pep:known supercontig:JCVI-afl1-v2.0:EQ963473:3173108:3175535::-1 gene:CADAFLAG00002828 transcript:CADAFLAT00002828 description: Translation initiation factor eif-2b epsilon subunit, putative	14.32	13.77	1	2	2	3	305	33.5	5.19
		13.98	10.09	1	3	3	3	704	78.2	4.77
	pep:known supercontig:JCVI-afl1-v2.0:EQ963473:1897595:1902056::-1 gene:CADAFLAG00005860 transcript:CADAFLAT00005860 description: Eukaryotic translation initiation factor subunit eIF-4F, putative	13.81	6.10	1	5	5	5	1376	147.7	9.38
		13.42	6.19	1	4	4	4	1115	128.6	5.71
	pep:known supercontig:JCVI-afl1-v2.0:EQ963480:550393:551622::-1 gene:CADAFLAG00008803 transcript:CADAFLAT00008803 description: ARP2/3 complex 20 kDa subunit (P20-ARC), putative	13.28	30.77	1	4	4	4	169	19.6	7.50
	pep:known supercontig:JCVI-afl1-v2.0:EQ963475:2606598:2609389::-1 gene:CADAFLAG00005126 transcript:CADAFLAT00005126 description: Translation initiation regulator (Gcn20), putative	13.28	6.52	1	3	3	3	751	83.0	6.27
		13.27	8.13	1	4	4	4	1008	112.4	7.81
		12.70	19.29	1	4	4	4	280	30.9	9.01
	pep:known supercontig:JCVI-afl1-v2.0:EQ963473:3788828:3790033::-1 gene:CADAFLAG00003048 transcript:CADAFLAT00003048 description: Cell division control protein 2 kinase, putative	12.63	15.00	1	4	4	4	320	36.3	7.87
		12.59	14.00	1	3	3	3	350	38.2	8.95
		12.30	22.13	1	3	3	3	244	26.9	6.37
	pep:known supercontig:JCVI-afl1-v2.0:EQ963472:4442484:4444810::-1 gene:CADAFLAG00001659 transcript:CADAFLAT00001659 description: Glycerol-3-phosphate dehydrogenase, mitochondrial	12.13	6.87	1	3	3	3	597	65.9	8.06
		11.86	15.70	1	3	3	3	293	32.3	5.58
		11.61	6.20	1	4	4	4	710	77.5	6.76
	pep:known supercontig:JCVI-afl1-v2.0:EQ963481:1465611:1466733::-1 gene:CADAFLAG00009916 transcript:CADAFLAT00009916 description: NADH-ubiquinone oxidoreductase 304 kDa subunit	11.61	12.05	1	2	2	2	365	40.3	7.83
		11.60	13.64	1	3	3	3	352	40.2	9.17
		11.44	10.27	1	3	3	3	526	56.0	9.10
	pep:known supercontig:JCVI-afl1-v2.0:EQ963476:1678698:1680170::-1 gene:CADAFLAG00005777 transcript:CADAFLAT00005777 description: ATP-dependent (S)-NAD(P)H-hydrate dehydratase	11.06	9.56	1	2	2	2	366	39.4	6.70
		10.96	10.34	1	3	3	3	387	43.7	7.27
		10.96	24.65	1	2	2	2	142	15.4	6.95
	pep:known supercontig:JCVI-afl1-v2.0:EQ963477:1992461:1994977::-1 gene:CADAFLAG00006825 transcript:CADAFLAT00006825 description: Polyubiquitin binding protein (Doa1/Ufd3), putative	10.95	5.70	1	4	4	4	789	84.8	5.10
		10.87	22.90	1	2	2	2	131	14.9	9.23
		10.70	12.83	1	3	3	3	343	38.4	5.55
		10.51	3.59	1	3	3	3	1309	145.2	6.58
		10.41	15.95	1	2	2	2	301	32.2	7.55
		10.25	17.60	1	3	3	3	375	40.2	5.59
		9.92	14.44	1	3	3	3	381	41.2	6.27

Table S4 (continued)

Gene ID	Description										
CADAFLAP00008267	pep:known supercontig:JCVI-afl1-v2.0:EQ963479:1122051:1123491::-1 gene:CADAFLAG00008267 transcript:CADAFLAT00008267 description: Adhesion regulating molecule, putative	9.61	11.98	1	2	2	2	384	41.4	4.61
CADAFLAP00009842	pep:known supercontig:JCVI-afl1-v2.0:EQ963481:1244015:1246504::-1 gene:CADAFLAG00009842 transcript:CADAFLAT00009842 description: Aconitate hydratase, mitochondrial	9.57	4.36	1	2	2	2	803	85.3	6.19
CADAFLAP00003038	pep:known supercontig:JCVI-afl1-v2.0:EQ963473:3767161:3769228::-1 gene:CADAFLAG00003038 transcript:CADAFLAT00003038 description: Probable HECT-type ubiquitin ligase-interacting pro	9.49	6.63	1	2	2	2	603	67.1	6.65
CADAFLAP00010455	pep:known supercontig:JCVI-afl1-v2.0:EQ963482:950511:951570::-1 gene:CADAFLAG00010455 transcript:CADAFLAT00010455 description: Proteasome subunit alpha type	9.48	11.61	1	2	2	2	267	29.2	6.58
CADAFLAP00008026	pep:known supercontig:JCVI-afl1-v2.0:EQ963479:465865:467269::-1 gene:CADAFLAG00008026 transcript:CADAFLAT00008026 description: 12-oxophytodienoate reductase, putative	9.45	10.54	1	3	3	3	408	46.0	5.72
CADAFLAP00003808	pep:known supercontig:JCVI-afl1-v2.0:EQ963474:1749061:1749645::-1 gene:CADAFLAG00003808 transcript:CADAFLAT00003808 description: Mismatched base pair and cruciform DNA recogni	9.43	21.14	1	3	3	3	175	18.0	5.63
CADAFLAP00011217	pep:known supercontig:JCVI-afl1-v2.0:EQ963483:1249886:1251157::-1 gene:CADAFLAG00011217 transcript:CADAFLAT00011217 description: Actin-related protein ArpA	9.43	10.24	1	2	2	2	381	43.2	6.55
CADAFLAP00008425	pep:known supercontig:JCVI-afl1-v2.0:EQ963479:1564296:1564956::-1 gene:CADAFLAG00008425 transcript:CADAFLAT00008425 description: Putative uncharacterized protein	9.22	39.74	1	2	2	2	78	8.7	8.72
CADAFLAP00002181	pep:known supercontig:JCVI-afl1-v2.0:EQ963473:1417524:1418881::-1 gene:CADAFLAG00002181 transcript:CADAFLAT00002181 description: Anthranilate phosphoribosyltransferase, putative	9.14	9.74	1	2	2	2	431	46.5	6.20
CADAFLAP00011797	pep:known supercontig:JCVI-afl1-v2.0:EQ963484:926296:927457::-1 gene:CADAFLAG00011797 transcript:CADAFLAT00011797 description: Salicylate hydroxylase, putative	9.10	8.85	1	2	2	2	373	42.2	5.31
CADAFLAP00008034	pep:known supercontig:JCVI-afl1-v2.0:EQ963479:485114:487530::-1 gene:CADAFLAG00008034 transcript:CADAFLAT00008034 description: Putative uncharacterized protein	8.83	10.65	1	3	3	3	338	37.1	6.13
CADAFLAP00004474	pep:known supercontig:JCVI-afl1-v2.0:EQ963475:845682:847178::1 gene:CADAFLAG00004474 transcript:CADAFLAT00004474 description: PWWP domain protein	8.78	14.52	1	2	2	2	420	45.7	5.95
CADAFLAP00003394	pep:known supercontig:JCVI-afl1-v2.0:EQ963474:605078:607776::1 gene:CADAFLAG00003394 transcript:CADAFLAT00003394 description: HET-C domain protein	8.77	7.47	1	3	3	3	843	93.3	6.52
CADAFLAP00006407	pep:known supercontig:JCVI-afl1-v2.0:EQ963477:918562:918948::-1 gene:CADAFLAG00006407 transcript:CADAFLAT00006407 description: Putative uncharacterized protein	8.69	35.16	1	2	2	2	128	14.4	5.49
CADAFLAP00008944	pep:known supercontig:JCVI-afl1-v2.0:EQ963480:940008:940692:1 gene:CADAFLAG00008944 transcript:CADAFLAT00008944 description: Peptide methionine sulfoxide reductase	8.65	21.14	1	3	3	3	175	19.7	6.27
CADAFLAP00003867	pep:known supercontig:JCVI-afl1-v2.0:EQ963474:1898503:1900756::-1 gene:CADAFLAG00003867 transcript:CADAFLAT00003867 description: DNA replication licensing factor Mcm2, putative	8.64	6.62	1	4	4	4	710	79.2	7.21
CADAFLAP00009746	pep:known supercontig:JCVI-afl1-v2.0:EQ963481:986842:987750::1 gene:CADAFLAG00009746 transcript:CADAFLAT00009746 description: Peptidyl-prolyl cis-trans isomerase	8.30	25.00	1	2	2	2	108	11.5	9.70
CADAFLAP00009947	pep:known supercontig:JCVI-afl1-v2.0:EQ963481:1550350:1551234:1 gene:CADAFLAG00009947 transcript:CADAFLAT00009947 description: 60S ribosomal protein L6, putative	8.23	15.42	1	2	2	2	253	27.6	9.80
CADAFLAP00003167	pep:known supercontig:JCVI-afl1-v2.0:EQ963473:4130531:4131708:1 gene:CADAFLAG00003167 transcript:CADAFLAT00003167 description: Proteasome subunit alpha type	8.22	9.73	1	2	2	2	298	31.7	5.27
CADAFLAP00003085	pep:known supercontig:JCVI-afl1-v2.0:EQ963473:3903691:3905019::-1 gene:CADAFLAG00003085 transcript:CADAFLAT00003085 description: Proteasome subunit beta type	8.16	12.16	1	2	2	2	296	32.9	7.05
CADAFLAP00010535	pep:known supercontig:JCVI-afl1-v2.0:EQ963483:1195811:1196158:1 gene:CADAFLAG00010535 transcript:CADAFLAT00010535 description: Putative uncharacterized protein	8.10	45.98	1	2	2	2	87	8.7	7.05
CADAFLAP00000161	pep:known supercontig:JCVI-afl1-v2.0:EQ963472:409331:410787::-1 gene:CADAFLAG00000161 transcript:CADAFLAT00000161 description: Putative uncharacterized protein	8.01	10.30	1	2	2	3	466	47.8	7.18
CADAFLAP00009141	pep:known supercontig:JCVI-afl1-v2.0:EQ963480:1500139:1500786::1 gene:CADAFLAG00009141 transcript:CADAFLAT00009141 description: Peptidyl-prolyl cis-trans isomerase	7.94	16.36	1	2	2	2	165	18.0	6.32
CADAFLAP00006826	pep:known supercontig:JCVI-afl1-v2.0:EQ963477:1995128:1996212::-1 gene:CADAFLAG00006826 transcript:CADAFLAT00006826 description: NAD(P)H-hydrate epimerase	7.74	16.35	1	2	2	2	263	28.6	7.43
CADAFLAP00011573	pep:known supercontig:JCVI-afl1-v2.0:EQ963484:320996:323696:1 gene:CADAFLAG00011573 transcript:CADAFLAT00011573 description: Cysteinyl-tRNA synthetase	7.54	6.41	1	4	4	4	874	98.4	6.62
CADAFLAP00006242	pep:known supercontig:JCVI-afl1-v2.0:EQ963477:470492:472355::-1 gene:CADAFLAG00006242 transcript:CADAFLAT00006242 description: Amidophosphoribosyltransferase	7.50	6.53	1	3	3	3	582	63.6	6.33
CADAFLAP00007065	pep:known supercontig:JCVI-afl1-v2.0:EQ963478:237548:238102:1 gene:CADAFLAG00007065 transcript:CADAFLAT00007065 description: Putative uncharacterized protein	7.35	23.42	1	2	2	2	111	12.7	7.06
CADAFLAP00010805	pep:known supercontig:JCVI-afl1-v2.0:EQ963483:47236:47573:1 gene:CADAFLAG00010805 transcript:CADAFLAT00010805 description: Mitochondrial intermembrane space translocase subunit	7.31	30.68	1	2	2	3	88	10.0	6.28
CADAFLAP00002792	**pep:known supercontig:JCVI-afl1-v2.0:EQ963473:3088919:3090923:1 gene:CADAFLAG00002792 transcript:CADAFLAT00002792 description: MAP kinase FUS3/KSS1**	**7.26**	**7.63**	**1**	**2**	**2**	**2**	**354**	**40.9**	**6.90**
CADAFLAP00013268	pep:known supercontig:JCVI-afl1-v2.0:EQ963486:1092894:1093344:1 gene:CADAFLAG00013268 transcript:CADAFLAT00013268 description: Putative uncharacterized protein	7.11	25.00	1	2	2	2	92	10.3	6.97
CADAFLAP00008676	pep:known supercontig:JCVI-afl1-v2.0:EQ963480:221696:222278::-1 gene:CADAFLAG00008676 transcript:CADAFLAT00008676 description: Cofilin, actophorin, putative	7.09	16.22	1	2	2	2	148	16.3	6.01
CADAFLAP00002687	pep:known supercontig:JCVI-afl1-v2.0:EQ963473:2795573:2796487::-1 gene:CADAFLAG00002687 transcript:CADAFLAT00002687 description: BAP31 domain protein, putative	7.04	10.95	1	2	2	2	210	24.0	8.90
CADAFLAP00010075	pep:known supercontig:JCVI-afl1-v2.0:EQ963481:1922719:1925901::1 gene:CADAFLAG00010075 transcript:CADAFLAT00010075 description: Actin cortical patch component, putative	7.01	3.95	1	2	2	2	684	74.2	9.07
CADAFLAP00006077	pep:known supercontig:JCVI-afl1-v2.0:EQ963478:7597:9346:1 gene:CADAFLAG00006077 transcript:CADAFLAT00006077 description: Purine nucleoside phosphorylase	7.01	9.09	1	2	2	2	319	34.6	6.58
CADAFLAP00007336	pep:known supercontig:JCVI-afl1-v2.0:EQ963478:945598:947133:1 gene:CADAFLAG00007336 transcript:CADAFLAT00007336 description: CobW domain protein	6.94	11.36	1	2	2	2	405	44.5	4.72
CADAFLAP00004669	pep:known supercontig:JCVI-afl1-v2.0:EQ963475:1379799:1381959:1 gene:CADAFLAG00004669 transcript:CADAFLAT00004669 description: NADPH--cytochrome P450 reductase	6.92	3.60	1	4	4	4	695	76.6	5.33
CADAFLAP00001078	pep:known supercontig:JCVI-afl1-v2.0:EQ963472:2873794:2875058:1 gene:CADAFLAG00001078 transcript:CADAFLAT00001078 description: Dihydroorotase, homodimeric type	6.92	7.16	1	2	2	2	363	40.1	6.30
CADAFLAP00010967	pep:known supercontig:JCVI-afl1-v2.0:EQ963483:514516:516342:1 gene:CADAFLAG00010967 transcript:CADAFLAT00010967 description: Flavin-binding monooxygenase-like protein	6.87	4.93	1	2	2	2	588	65.5	6.65
CADAFLAP00001406	pep:known supercontig:JCVI-afl1-v2.0:EQ963472:3748487:3752788:1 gene:CADAFLAG00001406 transcript:CADAFLAT00001406 description: Nuclear import and export protein Msn5, putative	6.73	1.87	1	2	2	2	1230	139.2	5.67
CADAFLAP00007381	pep:known supercontig:JCVI-afl1-v2.0:EQ963478:1088879:1089270:1 gene:CADAFLAG00007381 transcript:CADAFLAT00007381 description: Mitochondrial intermembrane space translocase su	6.60	26.79	1	2	2	2	112	12.0	10.78
CADAFLAP00000646	pep:known supercontig:JCVI-afl1-v2.0:EQ963472:1687478:1688735::1 gene:CADAFLAG00000646 transcript:CADAFLAT00000646 description: Methylenetetrahydrofolate dehydrogenase	6.54	7.49	1	2	2	2	334	37.3	6.68
CADAFLAP00004733	pep:known supercontig:JCVI-afl1-v2.0:EQ963475:1563224:1564186::-1 gene:CADAFLAG00004733 transcript:CADAFLAT00004733 description: SNARE protein Ykt6, putative	6.53	13.47	1	2	2	2	245	27.5	6.55
CADAFLAP00006823	pep:known supercontig:JCVI-afl1-v2.0:EQ963477:1985186:1986763:1 gene:CADAFLAG00006823 transcript:CADAFLAT00006823 description: RNA binding protein	6.51	12.11	1	3	3	3	322	36.2	9.41
CADAFLAP00001461	pep:known supercontig:JCVI-afl1-v2.0:EQ963473:3885396:3886384::-1 gene:CADAFLAG00001461 transcript:CADAFLAT00001461 description: Pyruvate dehydrogenase complex component Pdx	6.46	10.65	1	2	2	2	291	31.1	9.20
CADAFLAP00002299	pep:known supercontig:JCVI-afl1-v2.0:EQ963473:1719311:1720439::1 gene:CADAFLAG00002299 transcript:CADAFLAT00002299 description: NifU-related protein	6.34	15.20	1	2	2	2	329	36.0	5.55
CADAFLAP00002574	pep:known supercontig:JCVI-afl1-v2.0:EQ963473:2495287:2495957::-1 gene:CADAFLAG00002574 transcript:CADAFLAT00002574 description: Actin-related protein 2/3 complex subunit 5	6.33	13.99	1	2	2	2	193	20.4	6.00
CADAFLAP00001871	pep:known supercontig:JCVI-afl1-v2.0:EQ963473:535706:536644::-1 gene:CADAFLAG00001871 transcript:CADAFLAT00001871 description: ARP2/3 complex subunit Arc18, putative	6.20	12.77	1	3	3	3	188	21.0	7.99
CADAFLAP00002744	pep:known supercontig:JCVI-afl1-v2.0:EQ963473:2952676:2953540::-1 gene:CADAFLAG00002744 transcript:CADAFLAT00002744 description: 60S ribosomal protein L31e	6.12	16.26	1	2	2	2	123	14.1	10.21
CADAFLAP00002240	pep:known supercontig:JCVI-afl1-v2.0:EQ963473:1573422:1574996:1 gene:CADAFLAG00002240 transcript:CADAFLAT00002240 description: Rhodanese domain protein	6.07	10.38	1	2	2	2	212	23.2	9.07
CADAFLAP00005036	pep:known supercontig:JCVI-afl1-v2.0:EQ963475:235536:237072::-1 gene:CADAFLAG00005036 transcript:CADAFLAT00005036 description: Methionine aminopeptidase 2-1	5.95	6.74	1	2	2	2	445	48.5	6.76
CADAFLAP00001898	pep:known supercontig:JCVI-afl1-v2.0:EQ963473:603914:604438::-1 gene:CADAFLAG00001898 transcript:CADAFLAT00001898 description: UPF0047 domain protein	5.87	24.83	1	3	3	3	145	16.4	6.38
CADAFLAP00001493	pep:known supercontig:JCVI-afl1-v2.0:EQ963472:3968502:3971678::-1 gene:CADAFLAG00001493 transcript:CADAFLAT00001493 description: PX domain protein	5.82	3.03	1	2	2	2	892	101.3	5.33
CADAFLAP00005762	pep:known supercontig:JCVI-afl1-v2.0:EQ963476:1621252:1628532:1 gene:CADAFLAG00005762 transcript:CADAFLAT00005762 description: TOR pathway phosphatidylinositol 3-kinase TorA	5.78	1.09	1	2	2	2	2384	269.5	7.08
CADAFLAP00000449	pep:known supercontig:JCVI-afl1-v2.0:EQ963472:1175704:1181844::-1 gene:CADAFLAG00000449 transcript:CADAFLAT00000449 description: Guanyl-nucleotide exchange factor (Sec7), putativ	5.74	1.20	1	2	2	2	1994	224.4	5.72
CADAFLAP00010469	pep:known supercontig:JCVI-afl1-v2.0:EQ963482:993055:993270::-1 gene:CADAFLAG00010469 transcript:CADAFLAT00010469 description: Putative uncharacterized protein	5.72	33.80	1	2	2	2	71	7.7	7.18
CADAFLAP00012037	pep:known supercontig:JCVI-afl1-v2.0:EQ963484:1516200:1516935::-1 gene:CADAFLAG00012037 transcript:CADAFLAT00012037 description: DsDNA-binding protein PDCD5, putative	5.68	17.65	1	2	2	2	136	15.5	5.17
CADAFLAP00001457	pep:known supercontig:JCVI-afl1-v2.0:EQ963472:3874883:3876676::-1 gene:CADAFLAG00001457 transcript:CADAFLAT00001457 description: Aspartyl aminopeptidase	5.66	5.62	1	2	2	2	498	54.0	6.37
CADAFLAP00008184	pep:known supercontig:JCVI-afl1-v2.0:EQ963473:889741:891417:1 gene:CADAFLAG00008184 transcript:CADAFLAT00008184 description: Nuclear and cytoplasmic polyadenylated RNA-binding	5.53	5.24	1	2	2	2	477	51.7	7.58
CADAFLAP00002001	pep:known supercontig:JCVI-afl1-v2.0:EQ963473:901632:902625:1 gene:CADAFLAG00002001 transcript:CADAFLAT00002001 description: Small nuclear ribonucleoprotein SmD3, putative	5.47	16.38	1	2	2	2	116	12.9	11.44
CADAFLAP00010626	pep:known supercontig:JCVI-afl1-v2.0:EQ963482:1502685:1503835::1 gene:CADAFLAG00010626 transcript:CADAFLAT00010626 description: NAP family protein	5.44	7.47	1	2	2	2	348	39.9	4.48
CADAFLAP00002754	pep:known supercontig:JCVI-afl1-v2.0:EQ963473:2982953:2983879::1 gene:CADAFLAG00002754 transcript:CADAFLAT00002754 description: 3,4-dihydroxy-2-butanone 4-phosphate synthase	5.39	9.36	1	2	2	2	235	25.2	4.98
CADAFLAP00010821	pep:known supercontig:JCVI-afl1-v2.0:EQ963483:80720:81979::-1 gene:CADAFLAG00010821 transcript:CADAFLAT00010821 description: Homoserine kinase	5.26	6.23	1	2	2	2	353	37.9	5.77
CADAFLAP00011532	pep:known supercontig:JCVI-afl1-v2.0:EQ963484:205870:206792::-1 gene:CADAFLAG00011532 transcript:CADAFLAT00011532 description: AhpC/TSA family thioredoxin peroxidase, putative	4.87	7.49	1	2	2	2	267	29.6	9.09
CADAFLAP00003113	pep:known supercontig:JCVI-afl1-v2.0:EQ963473:3989780:3990215::-1 gene:CADAFLAG00003113 transcript:CADAFLAT00003113 description: Putative uncharacterized protein	4.57	18.33	1	2	2	2	120	12.9	10.74
CADAFLAP00000750	pep:known supercontig:JCVI-afl1-v2.0:EQ963472:1990995:1993641::-1 gene:CADAFLAG00000750 transcript:CADAFLAT00000750 description: Vesicular fusion ATPase, putative	4.46	3.18	1	2	2	2	848	93.4	6.42
CADAFLAP00010081	pep:known supercontig:JCVI-afl1-v2.0:EQ963481:1941579:1943563:1 gene:CADAFLAG00010081 transcript:CADAFLAT00010081 description: Heterogeneous nuclear ribonucleoprotein HRP1	4.43	7.42	1	2	2	2	445	48.8	9.36
CADAFLAP00005642	pep:known supercontig:JCVI-afl1-v2.0:EQ963476:1292428:1292950:1 gene:CADAFLAG00005642 transcript:CADAFLAT00005642 description: 40S ribosomal protein S10a	4.18	12.93	1	2	2	2	116	13.1	9.82
CADAFLAP00004298	pep:known supercontig:JCVI-afl1-v2.0:EQ963475:380813:382855::-1 gene:CADAFLAG00004298 transcript:CADAFLAT00004298 description: Dihydroxy acid dehydratase Ilv3, putative	4.03	3.74	1	2	2	2	615	65.5	6.99
CADAFLAP00010689	pep:known supercontig:JCVI-afl1-v2.0:EQ963482:1685104:1690608::-1 gene:CADAFLAG00010689 transcript:CADAFLAT00010689 description: PHD transcription factor (Rum1), putative	3.90	2.46	1	2	2	2	1704	192.4	6.32
CADAFLAP00013327	pep:known supercontig:JCVI-afl1-v2.0:EQ963486:1261810:1264943:1 gene:CADAFLAG00013327 transcript:CADAFLAT00013327 description: U5 snRNP component Snu114, putative	3.73	3.00	1	2	2	2	801	88.7	5.02
CADAFLAP00008680	pep:known supercontig:JCVI-afl1-v2.0:EQ963480:234111:231996:1 gene:CADAFLAG00008680 transcript:CADAFLAT00008680 description: Thioredoxin, putative	3.68	12.82	1	2	2	2	156	17.3	9.22
CADAFLAP00002929	pep:known supercontig:JCVI-afl1-v2.0:EQ963473:3445050:3447364:1 gene:CADAFLAG00002929 transcript:CADAFLAT00002929 description: Signal transducing adapter molecule, putative	3.64	9.41	1	3	3	3	627	69.5	5.91
CADAFLAP00008965	pep:known supercontig:JCVI-afl1-v2.0:EQ963480:992648:1002540:1 gene:CADAFLAG00008965 transcript:CADAFLAT00008965 description: Dynein heavy chain	3.42	0.73	1	2	2	2	3277	372.0	6.42
CADAFLAP00007470	pep:known supercontig:JCVI-afl1-v2.0:EQ963478:1333279:1334206:1 gene:CADAFLAG00007470 transcript:CADAFLAT00007470 description: Cytochrome c oxidase polypeptide vib	3.35	19.57	1	2	2	2	92	11.0	7.37
CADAFLAP00007158	pep:known supercontig:JCVI-afl1-v2.0:EQ963478:466117:467411::-1 gene:CADAFLAG00007158 transcript:CADAFLAT00007158 description: 37S ribosomal protein S5	3.29	5.57	1	2	2	2	413	46.4	8.59
CADAFLAP00002636	pep:known supercontig:JCVI-afl1-v2.0:EQ963473:2654987:2664610::-1 gene:CADAFLAG00002636 transcript:CADAFLAT00002636 description: Ccr4-Not transcription complex subunit (NOT1), pu	0.00	1.63	1	2	2	2	2394	266.7	5.92

Table S5: MkkB-GFP (CADAFLAP00012084) interacting proteins at 24 hours of vegetative growth. Proteins of interest are highlighted in yellow.

SteC (CADAFLAP00010880), SteD (CADAFLAP00010300).

Table S5: *Aspergillus flavus* MkkB-GFP interacting proteins (Vegetative growth-24 hours)

Accession	Description	Score	Coverage	# Proteins	# Unique Peptides	# Peptides	# PSMs	# AAs	MW [kDa]	calc. pI
CADAFLAP00010880	pep:known supercontig:JCVI-afl1-v2.0:EQ963483:278171:281036:1 gene:CADAFLAG00010880 transcript:CADAFLAT00010880 description: MAP kinase kinase kinas	393.00	66.93	1	46	46	91	895	98.9	8.35
CADAFLAP00012084	pep:known supercontig:JCVI-afl1-v2.0:EQ963484:1641926:1643675:-1 gene:CADAFLAG00012084 transcript:CADAFLAT00012084 description: MAP kinase kinase St	380.25	73.80	1	29	29	90	523	57.4	9.22
CADAFLAP00010300	pep:known supercontig:JCVI-afl1-v2.0:EQ963482:495063:496660:-1 gene:CADAFLAG00010300 transcript:CADAFLAT00010300 description: Protein kinase regulato	219.07	70.93	1	21	21	50	485	53.9	6.00
CADAFLAP00003857	pep:known supercontig:JCVI-afl1-v2.0:EQ963474:1870591:1873300:-1 gene:CADAFLAG00003857 transcript:CADAFLAT00003857 description: Rho GTPase activator Rga, putative	128.04	38.25	1	27	27	36	868	96.3	6.96
CADAFLAP00001170	pep:known supercontig:JCVI-afl1-v2.0:EQ963472:3123769:3125798:1 gene:CADAFLAG00001170 transcript:CADAFLAT00001170 description: DEAD box RNA helicase HelA, putative	43.69	26.07	1	12	12	13	656	72.7	9.94
CADAFLAP00006284	pep:known supercontig:JCVI-afl1-v2.0:EQ963477:578138:579490:-1 gene:CADAFLAG00006284 transcript:CADAFLAT00006284 description: Carbamoyl-phosphate synthase, small subunit	30.61	24.89	1	7	7	8	450	49.1	7.33
CADAFLAP00003858	pep:known supercontig:JCVI-afl1-v2.0:EQ963474:1873364:1874157:-1 gene:CADAFLAG00003858 transcript:CADAFLAT00003858 description: GTPase activator protein, putative	26.70	32.30	1	5	5	7	226	24.6	5.92
CADAFLAP00003740	pep:known supercontig:JCVI-afl1-v2.0:EQ963474:1563476:1566818:1 gene:CADAFLAG00003740 transcript:CADAFLAT00003740 description: Glycogen phosphorylase GlpV/Gph1, putative	17.59	7.28	1	3	3	4	879	99.7	6.06
CADAFLAP00006823	pep:known supercontig:JCVI-afl1-v2.0:EQ963477:1985186:1986763:1 gene:CADAFLAG00006823 transcript:CADAFLAT00006823 description: RNA binding protein, putative	15.33	24.53	1	6	6	6	322	36.2	9.41
CADAFLAP00002483	pep:known supercontig:JCVI-afl1-v2.0:EQ963473:2237209:2238210:1 gene:CADAFLAG00002483 transcript:CADAFLAT00002483 description: FHA domain protein SNIP1, putative	14.99	18.32	1	4	4	4	333	38.9	10.35
CADAFLAP00003394	pep:known supercontig:JCVI-afl1-v2.0:EQ963474:605078:607776:1 gene:CADAFLAG00003394 transcript:CADAFLAT00003394 description: HET-C domain protein	13.83	9.13	1	4	4	4	843	93.3	6.52
CADAFLAP00003048	pep:known supercontig:JCVI-afl1-v2.0:EQ963473:3788828:3790033:-1 gene:CADAFLAG00003048 transcript:CADAFLAT00003048 description: Cell division control protein 2 kinase, putative	13.45	15.00	1	4	4	4	320	36.3	7.87
CADAFLAP00002576	pep:known supercontig:JCVI-afl1-v2.0:EQ963473:2502671:2504536:-1 gene:CADAFLAG00002576 transcript:CADAFLAT00002576 description: FAD binding domain protein	12.65	11.24	1	4	4	4	587	65.8	7.80
CADAFLAP00000629	pep:known supercontig:JCVI-afl1-v2.0:EQ963472:1645094:1646704:1 gene:CADAFLAG00000629 transcript:CADAFLAT00000629 description: Putative uncharacterized protein	11.47	10.64	1	3	3	3	470	51.7	8.38
CADAFLAP00003808	pep:known supercontig:JCVI-afl1-v2.0:EQ963474:1749061:1749645:-1 gene:CADAFLAG00003808 transcript:CADAFLAT00003808 description: Mismatched base pair and cruciform DNA rec	10.15	26.29	1	3	3	3	175	18.0	5.63
CADAFLAP00009051	pep:known supercontig:JCVI-afl1-v2.0:EQ963480:1241438:1243239:1 gene:CADAFLAG00009051 transcript:CADAFLAT00009051 description: Solid-state culture expressed protein (Aos23),	9.83	11.64	1	3	3	3	550	57.0	7.14
CADAFLAP00005791	pep:known supercontig:JCVI-afl1-v2.0:EQ963476:1725709:1728027:1 gene:CADAFLAG00005791 transcript:CADAFLAT00005791 description: Fatty acid activator Faa4, putative	8.83	5.30	1	2	2	2	698	76.3	7.56
CADAFLAP00002001	pep:known supercontig:JCVI-afl1-v2.0:EQ963473:901632:902625:1 gene:CADAFLAG00002001 transcript:CADAFLAT00002001 description: Small nuclear ribonucleoprotein SmD3, putative	8.07	25.00	1	3	3	3	116	12.9	11.44
CADAFLAP00005730	pep:known supercontig:JCVI-afl1-v2.0:EQ963476:1538600:1539188:1 gene:CADAFLAG00005730 transcript:CADAFLAT00005730 description: Putative uncharacterized protein	7.99	27.18	1	2	2	2	103	11.6	9.06
CADAFLAP00002744	pep:known supercontig:JCVI-afl1-v2.0:EQ963473:2952676:2953540:-1 gene:CADAFLAG00002744 transcript:CADAFLAT00002744 description: 60S ribosomal protein L31e	6.20	17.07	1	2	2	2	123	14.1	10.21
CADAFLAP00011080	pep:known supercontig:JCVI-afl1-v2.0:EQ963483:847581:849011:-1 gene:CADAFLAG00011080 transcript:CADAFLAT00011080 description: GTP binding protein, putative	6.13	7.43	1	2	2	2	350	38.2	8.95
CADAFLAP00005642	pep:known supercontig:JCVI-afl1-v2.0:EQ963476:1292428:1292950:1 gene:CADAFLAG00005642 transcript:CADAFLAT00005642 description: 40S ribosomal protein S10a	5.34	16.38	1	2	2	2	116	13.1	9.82
CADAFLAP00011127	pep:known supercontig:JCVI-afl1-v2.0:EQ963483:994025:997698:1 gene:CADAFLAG00011127 transcript:CADAFLAT00011127 description: Putative uncharacterized protein	5.14	3.00	1	2	2	2	899	100.0	8.50

Table S6: MpkB-GFP (CADAFLAP00002792) interacting proteins at 24 hours of vegetative growth. Proteins of interest are highlighted in yellow.

MkkB (CADAFLAP00012084), SteD (CADAFLAP00010300), SteA (CADAFLAP00010857).

Table S6: *Aspergillus flavus* MpkB-GFP interacting proteins (Vegetative growth-24 hours)

Accession	Description	Score	Coverage	# Proteins	# Unique Peptides	# Peptides	# PSMs	# AAs	MW [kDa]	calc. pI
CADAFLAP00002792	pep:known supercontig:JCVI-afl1-v2.0:EQ963473:3088919:3090923:1 gene:CADAFLAG00002792 transcript:CADAFLAT00002792 description: MAP kinase FUS3/K	228.08	79.38	1	21	21	59	354	40.9	6.90
CADAFLAP00002108	pep:known supercontig:JCVI-afl1-v2.0:EQ963473:1202066:1206761:1 gene:CADAFLAG00002108 transcript:CADAFLAT00002108 description: Putative uncharacterized protein	136.24	32.19	1	28	28	37	1429	157.6	7.02
CADAFLAP00006151	pep:known supercontig:JCVI-afl1-v2.0:EQ963477:223151:224638:1 gene:CADAFLAG00006151 transcript:CADAFLAT00006151 description: Putative uncharacterized protein	95.02	60.76	1	17	17	27	474	50.6	10.43
CADAFLAP00012084	pep:known supercontig:JCVI-afl1-v2.0:EQ963484:1641926:1643675:-1 gene:CADAFLAG00012084 transcript:CADAFLAT00012084 description: MAP kinase kinase	59.22	46.85	1	15	15	17	523	57.4	9.22
CADAFLAP00001276	pep:known supercontig:JCVI-afl1-v2.0:EQ963472:3429809:3431853:-1 gene:CADAFLAG00001276 transcript:CADAFLAT00001276 description: C2H2 transcription factor, putative	50.34	35.05	1	14	14	18	662	71.4	9.14
CADAFLAP00012901	pep:known supercontig:JCVI-afl1-v2.0:EQ963486:140443:144341:-1 gene:CADAFLAG00012901 transcript:CADAFLAT00012901 description: 5-oxo-L-prolinase, putative	35.56	20.86	1	16	16	17	1280	138.6	5.95
CADAFLAP00007224	pep:known supercontig:JCVI-afl1-v2.0:EQ963478:641683:643939:1 gene:CADAFLAG00007224 transcript:CADAFLAT00007224 description: CTP synthase	30.90	22.09	1	9	9	9	593	65.9	6.57
CADAFLAP00010857	pep:known supercontig:JCVI-afl1-v2.0:EQ963483:205022:207438:1 gene:CADAFLAG00010857 transcript:CADAFLAT00010857 description: Sexual development t	28.01	18.03	1	9	9	11	699	77.6	6.79
CADAFLAP00001170	pep:known supercontig:JCVI-afl1-v2.0:EQ963472:3123769:3125798:1 gene:CADAFLAG00001170 transcript:CADAFLAT00001170 description: DEAD box RNA helicase HelA, putative	25.26	17.84	1	8	8	9	656	72.7	9.94
CADAFLAP00010300	pep:known supercontig:JCVI-afl1-v2.0:EQ963482:495063:496660:-1 gene:CADAFLAG00010300 transcript:CADAFLAT00010300 description: Protein kinase regula	22.48	18.56	1	6	6	7	485	53.9	6.00
CADAFLAP00007210	pep:known supercontig:JCVI-afl1-v2.0:EQ963478:607933:610014:1 gene:CADAFLAG00007210 transcript:CADAFLAT00007210 description: Protein-tyrosine phosphatase, putative	20.39	14.29	1	6	6	6	693	75.4	8.95
CADAFLAP00003740	pep:known supercontig:JCVI-afl1-v2.0:EQ963474:1563476:1566818:1 gene:CADAFLAG00003740 transcript:CADAFLAT00003740 description: Glycogen phosphorylase GlpV/Gph1, putati	19.19	7.51	1	3	3	4	879	99.7	6.06
CADAFLAP00000441	pep:known supercontig:JCVI-afl1-v2.0:EQ963472:1144900:1146066:1 gene:CADAFLAG00000441 transcript:CADAFLAT00000441 description: Glutamine-serine rich protein MS8, putative	15.86	13.38	1	2	2	3	314	33.4	9.60
CADAFLAP00006284	pep:known supercontig:JCVI-afl1-v2.0:EQ963477:578138:579490:-1 gene:CADAFLAG00006284 transcript:CADAFLAT00006284 description: Carbamoyl-phosphate synthase, small subun	15.72	16.67	1	5	5	5	450	49.1	7.33
CADAFLAP00002576	pep:known supercontig:JCVI-afl1-v2.0:EQ963473:2502671:2504536:-1 gene:CADAFLAG00002576 transcript:CADAFLAT00002576 description: FAD binding domain protein	15.01	13.63	1	5	5	6	587	65.8	7.80
CADAFLAP00002483	pep:known supercontig:JCVI-afl1-v2.0:EQ963473:2237209:2238210:1 gene:CADAFLAG00002483 transcript:CADAFLAT00002483 description: FHA domain protein SNIP1, putative	14.84	19.52	1	4	4	4	333	38.9	10.35
CADAFLAP00005791	pep:known supercontig:JCVI-afl1-v2.0:EQ963476:1725709:1728027:1 gene:CADAFLAG00005791 transcript:CADAFLAT00005791 description: Fatty acid activator Faa4, putative	11.26	7.02	1	3	3	3	698	76.3	7.56
CADAFLAP00006823	pep:known supercontig:JCVI-afl1-v2.0:EQ963477:1985186:1986763:1 gene:CADAFLAG00006823 transcript:CADAFLAT00006823 description: RNA binding protein, putative	11.19	26.09	1	6	6	6	322	36.2	9.41
CADAFLAP00005978	pep:known supercontig:JCVI-afl1-v2.0:EQ963476:2232364:2234268:-1 gene:CADAFLAG00005978 transcript:CADAFLAT00005978 description: ATP-dependent RNA helicase Mrh4, putati	11.07	9.78	1	3	3	3	634	70.5	9.91
CADAFLAP00003394	pep:known supercontig:JCVI-afl1-v2.0:EQ963474:605078:607776:1 gene:CADAFLAG00003394 transcript:CADAFLAT00003394 description: HET-C domain protein	10.90	9.85	1	4	4	4	843	93.3	6.52
CADAFLAP00003867	pep:known supercontig:JCVI-afl1-v2.0:EQ963474:1898503:1900756:-1 gene:CADAFLAG00003867 transcript:CADAFLAT00003867 description: DNA replication licensing factor Mcm2, pu	10.88	13.52	1	6	6	6	710	79.2	7.21
CADAFLAP00011080	pep:known supercontig:JCVI-afl1-v2.0:EQ963483:847581:849011:-1 gene:CADAFLAG00011080 transcript:CADAFLAT00011080 description: GTP binding protein, putative	10.81	17.14	1	4	4	4	350	38.2	8.95
CADAFLAP00002001	pep:known supercontig:JCVI-afl1-v2.0:EQ963473:901632:902625:1 gene:CADAFLAG00002001 transcript:CADAFLAT00002001 description: Small nuclear ribonucleoprotein SmD3, putati	7.70	25.00	1	3	3	3	116	12.9	11.44
CADAFLAP00005642	pep:known supercontig:JCVI-afl1-v2.0:EQ963476:1292428:1292950:1 gene:CADAFLAG00005642 transcript:CADAFLAT00005642 description: 40S ribosomal protein S10a	7.58	23.28	1	3	3	3	116	13.1	9.82
CADAFLAP00009141	pep:known supercontig:JCVI-afl1-v2.0:EQ963480:1500139:1500786:1 gene:CADAFLAG00009141 transcript:CADAFLAT00009141 description: Peptidyl-prolyl cis-trans isomerase	5.35	15.76	1	2	2	2	165	18.0	6.32
CADAFLAP00003048	pep:known supercontig:JCVI-afl1-v2.0:EQ963473:3788828:3790033:-1 gene:CADAFLAG00003048 transcript:CADAFLAT00003048 description: Cell division control protein 2 kinase, puta	5.25	12.19	1	3	3	3	320	36.3	7.87
CADAFLAP00010795	pep:known supercontig:JCVI-afl1-v2.0:EQ963483:17183:19179:-1 gene:CADAFLAG00010795 transcript:CADAFLAT00010795 description: CDK9, putative	5.19	4.46	1	1	1	2	538	60.1	9.82
CADAFLAP00005537	pep:known supercontig:JCVI-afl1-v2.0:EQ963476:1047542:1048079:-1 gene:CADAFLAG00005537 transcript:CADAFLAT00005537 description: Small nuclear ribonucleoprotein (LSM7), p	5.12	16.54	1	2	2	2	133	14.2	6.58
CADAFLAP00003085	pep:known supercontig:JCVI-afl1-v2.0:EQ963473:3903691:3905019:-1 gene:CADAFLAG00003085 transcript:CADAFLAT00003085 description: Proteasome subunit beta type	4.70	8.45	1	2	2	2	296	32.9	7.05
CADAFLAP00007319	pep:known supercontig:JCVI-afl1-v2.0:EQ963478:896797:899363:1 gene:CADAFLAG00007319 transcript:CADAFLAT00007319 description: Nucleolar GTP-binding protein (Nog1), putativ	4.59	3.62	1	3	3	3	801	90.6	8.43
CADAFLAP00002511	pep:known supercontig:JCVI-afl1-v2.0:EQ963473:2306586:2309501:1 gene:CADAFLAG00002511 transcript:CADAFLAT00002511 description: Proteasome component Prs2, putative	4.57	3.45	1	2	2	2	666	74.4	6.68
CADAFLAP00011800	pep:known supercontig:JCVI-afl1-v2.0:EQ963484:934734:935058:1 gene:CADAFLAG00011800 transcript:CADAFLAT00011800 description: Putative uncharacterized protein	4.31	41.27	1	2	2	2	63	7.1	5.81
CADAFLAP00005001	pep:known supercontig:JCVI-afl1-v2.0:EQ963475:2253344:2254534:1 gene:CADAFLAG00005001 transcript:CADAFLAT00005001 description: Putative uncharacterized protein	4.30	14.90	1	4	4	4	396	44.2	5.54
CADAFLAP00002687	pep:known supercontig:JCVI-afl1-v2.0:EQ963473:2795573:2796487:-1 gene:CADAFLAG00002687 transcript:CADAFLAT00002687 description: BAP31 domain protein, putative	3.96	10.48	1	2	2	2	210	24.0	8.90
CADAFLAP00004902	pep:known supercontig:JCVI-afl1-v2.0:EQ963475:2001395:2003925:1 gene:CADAFLAG00004902 transcript:CADAFLAT00004902 description: Elongation factor G, mitochondrial	3.76	3.25	1	2	2	2	799	88.8	6.62
CADAFLAP00010364	pep:known supercontig:JCVI-afl1-v2.0:EQ963482:666798:667988:1 gene:CADAFLAG00010364 transcript:CADAFLAT00010364 description: N,N-dimethylglycine oxidase	3.61	7.83	1	2	2	2	396	43.1	5.68
CADAFLAP00003857	pep:known supercontig:JCVI-afl1-v2.0:EQ963474:1870591:1873300:-1 gene:CADAFLAG00003857 transcript:CADAFLAT00003857 description: Rho GTPase activator Rga, putative	2.80	4.61	1	2	2	2	868	96.3	6.96
CADAFLAP00008425	pep:known supercontig:JCVI-afl1-v2.0:EQ963479:1564296:1564956:1 gene:CADAFLAG00008425 transcript:CADAFLAT00008425 description: Putative uncharacterized protein	2.68	39.74	1	2	2	2	78	8.7	6.52
CADAFLAP00008803	pep:known supercontig:JCVI-afl1-v2.0:EQ963480:550393:551622:-1 gene:CADAFLAG00008803 transcript:CADAFLAT00008803 description: ARP2/3 complex 20 kDa subunit (P20-ARC),	2.66	11.24	1	2	2	2	169	19.6	7.50
CADAFLAP00009051	pep:known supercontig:JCVI-afl1-v2.0:EQ963480:1241438:1243239:1 gene:CADAFLAG00009051 transcript:CADAFLAT00009051 description: Solid-state culture expressed protein (Aos2	2.30	8.73	1	2	2	2	550	57.0	7.14

Table S7: SteD-GFP (CADAFLAP00010300) interacting proteins at 24 hours of vegetative growth. Proteins of interest are highlighted in yellow.

SteC (CADAFLAP00010880), MkkB (CADAFLAP00012084), MpkB (CADAFLAP00002792).

Table S7: *Aspergillus flavus* SteD-GFP interacting proteins (Vegetative growth-24 hours)

Accession	Description	Score	Coverage	# Proteins	# Unique Peptides	# Peptides	# PSMs	# AAs	MW [kDa]	calc. pI
CADAFLAP00010880	pep:known supercontig:JCVI-afl1-v2.0:EQ963483:278171:281036:1 gene:CADAFLAG00010880 transcript:CADAFLAT00010880 description: MAP kinase kinase kinase Ste11	267.27	62.57	1	42	42	64	895	98.9	8.35
CADAFLAP00010300	pep:known supercontig:JCVI-afl1-v2.0:EQ963482:495063:496660:-1 gene:CADAFLAG00010300 transcript:CADAFLAT00010300 description: Protein regulator Ste50	134.38	54.02	1	17	17	32	485	53.9	6.00
CADAFLAP00001170	pep:known supercontig:JCVI-afl1-v2.0:EQ963472:3123769:3125798:1 gene:CADAFLAG00001170 transcript:CADAFLAT00001170 description: DEAD box RNA helicase HelA, putative	43.30	27.44	1	12	12	13	656	72.7	9.94
CADAFLAP00003857	pep:known supercontig:JCVI-afl1-v2.0:EQ963474:1870591:1873300:-1 gene:CADAFLAG00003857 transcript:CADAFLAT00003857 description: Rho GTPase activator Rga, putative	30.42	11.52	1	8	8	12	868	96.3	6.96
CADAFLAP00012084	pep:known supercontig:JCVI-afl1-v2.0:EQ963484:1641926:1643675:-1 gene:CADAFLAG00012084 transcript:CADAFLAT00012084 description: MAP kinase kinase Ste7	29.62	24.09	1	8	8	8	523	57.4	9.22
CADAFLAP00003740	pep:known supercontig:JCVI-afl1-v2.0:EQ963474:1563476:1566818:1 gene:CADAFLAG00003740 transcript:CADAFLAT00003740 description: Glycogen phosphorylase GlpV/Gph1, putative	27.09	12.29	1	5	5	5	879	99.7	6.06
CADAFLAP00012901	pep:known supercontig:JCVI-afl1-v2.0:EQ963486:140443:144341:-1 gene:CADAFLAG00012901 transcript:CADAFLAT00012901 description: 5-oxo-L-prolinase, putative	25.27	10.08	1	8	8	8	1280	138.6	5.95
CADAFLAP00007224	pep:known supercontig:JCVI-afl1-v2.0:EQ963478:641683:643939:1 gene:CADAFLAG00007224 transcript:CADAFLAT00007224 description: CTP synthase	25.09	20.40	1	8	8	8	593	65.9	6.57
CADAFLAP00002576	pep:known supercontig:JCVI-afl1-v2.0:EQ963473:2502671:2504536:-1 gene:CADAFLAG00002576 transcript:CADAFLAT00002576 description: FAD binding domain protein	23.38	13.80	1	6	6	8	587	65.8	7.80
CADAFLAP00006284	pep:known supercontig:JCVI-afl1-v2.0:EQ963477:578138:579490:-1 gene:CADAFLAG00006284 transcript:CADAFLAT00006284 description: Carbamoyl-phosphate synthase, small subunit	21.70	22.44	1	6	6	6	450	49.1	7.33
CADAFLAP00003394	pep:known supercontig:JCVI-afl1-v2.0:EQ963474:605078:607776:1 gene:CADAFLAG00003394 transcript:CADAFLAT00003394 description: HET-C domain protein	21.34	13.76	1	6	6	7	843	93.3	6.52
CADAFLAP00003048	pep:known supercontig:JCVI-afl1-v2.0:EQ963473:3788828:3790033:-1 gene:CADAFLAG00003048 transcript:CADAFLAT00003048 description: Cell division control protein 2 kinase, putative	21.27	29.06	1	7	7	7	320	36.3	7.87
CADAFLAP00005791	pep:known supercontig:JCVI-afl1-v2.0:EQ963476:1725709:1728027:1 gene:CADAFLAG00005791 transcript:CADAFLAT00005791 description: Fatty acid activator Faa4, putative	19.71	9.46	1	5	5	5	698	76.3	7.56
CADAFLAP00002483	pep:known supercontig:JCVI-afl1-v2.0:EQ963473:2237209:2238210:1 gene:CADAFLAG00002483 transcript:CADAFLAT00002483 description: FHA domain protein SNIP1, putative	18.55	24.32	1	6	6	6	333	38.9	10.35
CADAFLAP00008336	pep:known supercontig:JCVI-afl1-v2.0:EQ963479:1308050:1309810:1 gene:CADAFLAG00008336 transcript:CADAFLAT00008336 description: GTP binding protein, putative	17.73	13.79	1	4	4	4	544	60.2	6.35
CADAFLAP00005978	pep:known supercontig:JCVI-afl1-v2.0:EQ963476:2232364:2234268:-1 gene:CADAFLAG00005978 transcript:CADAFLAT00005978 description: ATP-dependent RNA helicase Mrh4, putative	16.32	11.83	1	5	5	5	634	70.5	9.91
CADAFLAP00011127	pep:known supercontig:JCVI-afl1-v2.0:EQ963483:994025:997698:1 gene:CADAFLAG00011127 transcript:CADAFLAT00011127 description: Putative uncharacterized protein	16.09	9.01	1	6	6	6	899	100.0	8.50
CADAFLAP00000441	pep:known supercontig:JCVI-afl1-v2.0:EQ963472:1144900:1146066:1 gene:CADAFLAG00000441 transcript:CADAFLAT00000441 description: Glutamine-serine rich protein MS8, putative	15.48	13.38	1	2	2	3	314	33.4	9.60
CADAFLAP00008676	pep:known supercontig:JCVI-afl1-v2.0:EQ963480:221696:222278:-1 gene:CADAFLAG00008676 transcript:CADAFLAT00008676 description: Cofilin, actophorin, putative	14.98	47.97	1	5	5	5	148	16.3	6.01
CADAFLAP00000629	pep:known supercontig:JCVI-afl1-v2.0:EQ963472:1645094:1646704:1 gene:CADAFLAG00000629 transcript:CADAFLAT00000629 description: Putative uncharacterized protein	13.95	12.77	1	4	4	4	470	51.7	8.38
CADAFLAP00006242	pep:known supercontig:JCVI-afl1-v2.0:EQ963477:470492:472355:-1 gene:CADAFLAG00006242 transcript:CADAFLAT00006242 description: Amidophosphoribosyltransferase	13.07	11.68	1	4	4	4	582	63.6	6.33
CADAFLAP00006823	pep:known supercontig:JCVI-afl1-v2.0:EQ963477:1985196:1986763:1 gene:CADAFLAG00006823 transcript:CADAFLAT00006823 description: RNA binding protein, putative	12.75	22.05	1	5	5	5	322	36.2	9.41
CADAFLAP00003858	pep:known supercontig:JCVI-afl1-v2.0:EQ963474:1873364:1874157:-1 gene:CADAFLAG00003858 transcript:CADAFLAT00003858 description: GTPase activator protein, putative	12.48	20.80	1	3	3	3	226	24.6	5.92
CADAFLAP00002792	pep:known supercontig:JCVI-afl1-v2.0:EQ963473:3088919:3090923:1 gene:CADAFLAG00002792 transcript:CADAFLAT00002792 description: MAP kinase FUS3/KSS1	12.41	14.69	1	4	4	4	354	40.9	6.90
CADAFLAP00008387	pep:known supercontig:JCVI-afl1-v2.0:EQ963479:1465953:1467236:1 gene:CADAFLAG00008387 transcript:CADAFLAT00008387 description: UPF0261 domain protein	12.39	9.37	1	3	3	4	427	46.0	5.58
CADAFLAP00003867	pep:known supercontig:JCVI-afl1-v2.0:EQ963474:1898503:1900756:-1 gene:CADAFLAG00003867 transcript:CADAFLAT00003867 description: DNA replication licensing factor Mcm2, putative	12.11	10.14	1	5	5	5	710	79.2	7.21
CADAFLAP00011217	pep:known supercontig:JCVI-afl1-v2.0:EQ963483:1249886:1251157:-1 gene:CADAFLAG00011217 transcript:CADAFLAT00011217 description: Actin-related protein ArpA	12.01	15.49	1	4	4	4	381	43.2	6.55
CADAFLAP00005001	pep:known supercontig:JCVI-afl1-v2.0:EQ963475:2253344:2254534:1 gene:CADAFLAG00005001 transcript:CADAFLAT00005001 description: Putative uncharacterized protein	10.06	20.45	1	5	5	5	396	44.2	5.54
CADAFLAP00002511	pep:known supercontig:JCVI-afl1-v2.0:EQ963476:2306586:2309501:1 gene:CADAFLAG00002511 transcript:CADAFLAT00002511 description: Proteasome component Prs2, putative	10.00	7.06	1	4	4	4	666	74.4	6.68
CADAFLAP00011080	pep:known supercontig:JCVI-afl1-v2.0:EQ963483:847581:849011:-1 gene:CADAFLAG00011080 transcript:CADAFLAT00011080 description: GTP binding protein, putative	9.82	11.14	1	3	3	3	350	38.2	8.95
CADAFLAP00003626	pep:known supercontig:JCVI-afl1-v2.0:EQ963474:1225760:1226524:-1 gene:CADAFLAG00003626 transcript:CADAFLAT00003626 description: Blue light-inducible protein Bli-3	9.01	14.35	1	3	3	3	216	23.2	4.96
CADAFLAP00001477	pep:known supercontig:JCVI-afl1-v2.0:EQ963472:3929090:3930683:1 gene:CADAFLAG00001477 transcript:CADAFLAT00001477 description: PWI domain mRNA processing protein, putative	8.95	8.59	1	4	4	4	489	57.6	11.62
CADAFLAP00002001	pep:known supercontig:JCVI-afl1-v2.0:EQ963473:901632:902625:1 gene:CADAFLAG00002001 transcript:CADAFLAT00002001 description: Small nuclear ribonucleoprotein SmD3, putative	7.94	25.00	1	3	3	3	116	12.9	11.44
CADAFLAP00005642	pep:known supercontig:JCVI-afl1-v2.0:EQ963476:1292428:1292950:1 gene:CADAFLAG00005642 transcript:CADAFLAT00005642 description: 40S ribosomal protein S10a	7.77	23.28	1	3	3	3	116	13.1	9.82
CADAFLAP00010537	pep:known supercontig:JCVI-afl1-v2.0:EQ963482:1200499:1202833:1 gene:CADAFLAG00010537 transcript:CADAFLAT00010537 description: DNA replication licensing factor Mcm5, putative	7.47	4.03	1	2	2	2	719	80.0	6.98
CADAFLAP00002651	pep:known supercontig:JCVI-afl1-v2.0:EQ963473:2701866:2704755:1 gene:CADAFLAG00002651 transcript:CADAFLAT00002651 description: Pre-RNA splicing factor Srp2, putative	6.70	14.67	1	4	4	4	300	35.2	9.48
CADAFLAP00012900	pep:known supercontig:JCVI-afl1-v2.0:EQ963486:137809:140008:1 gene:CADAFLAG00012900 transcript:CADAFLAT00012900 description: 5'-nucleotidase, putative	6.66	4.80	1	2	2	2	666	74.1	6.64
CADAFLAP00009832	pep:known supercontig:JCVI-afl1-v2.0:EQ963481:1218936:1220902:-1 gene:CADAFLAG00009832 transcript:CADAFLAT00009832 description: Metacaspase CasA	6.51	6.77	1	2	2	2	399	44.2	6.89
CADAFLAP00007237	pep:known supercontig:JCVI-afl1-v2.0:EQ963478:667671:669936:-1 gene:CADAFLAG00007237 transcript:CADAFLAT00007237 description: Casein kinase I, putative	6.04	7.94	1	3	3	3	403	45.8	9.54
CADAFLAP00003808	pep:known supercontig:JCVI-afl1-v2.0:EQ963474:1749061:1749645:-1 gene:CADAFLAG00003808 transcript:CADAFLAT00003808 description: Mismatched base pair and cruciform DNA recognition	5.86	17.71	1	2	2	2	175	18.0	5.63
CADAFLAP00009136	pep:known supercontig:JCVI-afl1-v2.0:EQ963480:1484583:1486832:-1 gene:CADAFLAG00009136 transcript:CADAFLAT00009136 description: YjeF_N domain protein	5.84	4.94	1	2	2	2	709	76.5	8.48
CADAFLAP00009878	pep:known supercontig:JCVI-afl1-v2.0:EQ963481:1372109:1373705:1 gene:CADAFLAG00009878 transcript:CADAFLAT00009878 description: Peptidyl-prolyl cis-trans isomerase	5.65	5.96	1	2	2	2	470	51.3	4.56
CADAFLAP00001451	pep:known supercontig:JCVI-afl1-v2.0:EQ963472:3866039:3866667:-1 gene:CADAFLAG00001451 transcript:CADAFLAT00001451 description: Putative uncharacterized protein	5.42	15.86	1	2	2	2	145	16.1	10.21
CADAFLAP00000107	pep:known supercontig:JCVI-afl1-v2.0:EQ963472:266328:267181:-1 gene:CADAFLAG00000107 transcript:CADAFLAT00000107 description: Putative uncharacterized protein	5.25	13.79	1	3	3	3	261	28.8	8.37
CADAFLAP00003388	pep:known supercontig:JCVI-afl1-v2.0:EQ963474:589791:590672:-1 gene:CADAFLAG00003388 transcript:CADAFLAT00003388 description: Mitotic spindle checkpoint protein (Mad2B), putative	5.20	6.48	1	2	2	2	293	32.2	7.34
CADAFLAP00002744	pep:known supercontig:JCVI-afl1-v2.0:EQ963473:2952676:2953540:-1 gene:CADAFLAG00002744 transcript:CADAFLAT00002744 description: 60S ribosomal protein L31e	5.19	15.45	1	2	2	2	123	14.1	10.21
CADAFLAP00000449	pep:known supercontig:JCVI-afl1-v2.0:EQ963472:1175704:1181844:-1 gene:CADAFLAG00000449 transcript:CADAFLAT00000449 description: Guanyl-nucleotide exchange factor (Sec7), putative	4.50	1.10	1	2	2	2	1994	224.4	5.72
CADAFLAP00000750	pep:known supercontig:JCVI-afl1-v2.0:EQ963472:1990995:1993641:-1 gene:CADAFLAG00000750 transcript:CADAFLAT00000750 description: Vesicular fusion ATPase, putative	3.75	2.24	1	2	2	2	848	93.4	6.42
CADAFLAP00009051	pep:known supercontig:JCVI-afl1-v2.0:EQ963480:1241438:1243239:1 gene:CADAFLAG00009051 transcript:CADAFLAT00009051 description: Solid-state culture expressed protein (Aos23), putative	3.75	8.91	1	2	2	3	550	57.0	7.14

Table S8: HamE-HA (CADAFLAP00009262) interacting proteins at 24 hours of vegetative growth.

Table S8: *Aspergillus flavus* HamE-HA interacting proteins (Vegetative growth-24 hours)

Accession	Description	Score	Coverage	# Proteins	# Unique Peptides	# Peptides	# PSMs	# AAs	MW [kDa]	calc. pI
CADAFLAP00009262	pep:known supercontig:JCVI-afl1-v2.0:EQ963480:1787067:1792028:1 gene:CADAFLAG00009262 transcript:CADAFLAT00009262 description: WD domain, G-be	128.02	35.54	1	36	36	43	1570	171.8	9.11
CADAFLAP00008286	pep:known supercontig:JCVI-afl1-v2.0:EQ963479:1181504:1183066:-1 gene:CADAFLAG00008286 transcript:CADAFLAT00008286 description: Tubulin beta, putative	59.97	51.88	1	9	16	17	453	50.5	5.49
CADAFLAP00006001	pep:known supercontig:JCVI-afl1-v2.0:EQ963479:2299764:2302136:-1 gene:CADAFLAG00006001 transcript:CADAFLAT00006001 description: Malic enzyme	36.12	33.59	1	14	14	14	658	72.8	6.71
CADAFLAP00005566	pep:known supercontig:JCVI-afl1-v2.0:EQ963476:1123416:1124536:-1 gene:CADAFLAG00005566 transcript:CADAFLAT00005566 description: Glyceraldehyde-3-phosphate dehydroge	30.81	46.11	1	10	11	11	334	36.0	7.17
CADAFLAP00009285	pep:known supercontig:JCVI-afl1-v2.0:EQ963480:1853396:1853898:1 gene:CADAFLAG00009285 transcript:CADAFLAT00009285 description: Putative uncharacterized protein	24.19	52.78	1	5	5	7	108	12.3	5.15
CADAFLAP00008365	pep:known supercontig:JCVI-afl1-v2.0:EQ963479:1396108:1399261:-1 gene:CADAFLAG00008365 transcript:CADAFLAT00008365 description: RNase L inhibitor of the ABC superfamil	21.28	17.05	1	8	8	8	604	68.0	8.24
CADAFLAP00006035	pep:known supercontig:JCVI-afl1-v2.0:EQ963479:2438623:2440482:-1 gene:CADAFLAG00006035 transcript:CADAFLAT00006035 description: Serine hydroxymethyltransferase	19.96	36.21	1	11	12	12	533	58.4	8.50
CADAFLAP00002717	pep:known supercontig:JCVI-afl1-v2.0:EQ963473:2873371:2874130:-1 gene:CADAFLAG00002717 transcript:CADAFLAT00002717 description: Superoxide dismutase	18.81	47.14	1	6	6	7	210	23.2	7.24
CADAFLAP00005500	pep:known supercontig:JCVI-afl1-v2.0:EQ963476:937194:939853:-1 gene:CADAFLAG00005500 transcript:CADAFLAT00005500 description: Eukaryotic translation initiation factor 3 su	18.28	13.70	1	8	8	8	861	97.1	5.35
CADAFLAP00008409	pep:known supercontig:JCVI-afl1-v2.0:EQ963479:1516901:1517936:-1 gene:CADAFLAG00008409 transcript:CADAFLAT00008409 description: Glycerol dehydrogenase Gcy1, putative	16.26	39.93	1	8	8	8	298	33.5	7.55
CADAFLAP00013316	pep:known supercontig:JCVI-afl1-v2.0:EQ963486:1226650:1228407:-1 gene:CADAFLAG00013316 transcript:CADAFLAT00013316 description: Choline oxidase (CodA), putative	16.19	16.42	1	6	6	6	542	60.1	6.61
CADAFLAP00009844	pep:known supercontig:JCVI-afl1-v2.0:EQ963481:1249119:1250065:1 gene:CADAFLAG00009844 transcript:CADAFLAT00009844 description: 60S acidic ribosomal protein P1	16.13	25.64	1	4	4	4	234	24.9	7.43
CADAFLAP00010322	pep:known supercontig:JCVI-afl1-v2.0:EQ963482:549464:550065:1 gene:CADAFLAG00010322 transcript:CADAFLAT00010322 description: 60S ribosomal protein L37a	15.43	39.13	1	4	4	4	92	10.1	10.45
CADAFLAP00010522	pep:known supercontig:JCVI-afl1-v2.0:EQ963482:1158813:1161211:-1 gene:CADAFLAG00010522 transcript:CADAFLAT00010522 description: Vacuolar ATP synthase catalytic subunit	13.63	15.33	1	6	6	6	698	76.1	5.36
CADAFLAP00005782	pep:known supercontig:JCVI-afl1-v2.0:EQ963476:1687295:1691114:-1 gene:CADAFLAG00005782 transcript:CADAFLAT00005782 description: Carbamoyl-phosphate synthase, large s	13.09	10.04	1	8	9	9	1175	129.2	5.68
CADAFLAP00008895	pep:known supercontig:JCVI-afl1-v2.0:EQ963480:806443:808343:1 gene:CADAFLAG00008895 transcript:CADAFLAT00008895 description: Inosine-5'-monophosphate dehydrogenase	12.54	15.38	1	6	6	6	546	58.0	6.70
CADAFLAP00000856	pep:known supercontig:JCVI-afl1-v2.0:EQ963472:2295061:2296250:1 gene:CADAFLAG00000856 transcript:CADAFLAT00000856 description: ARP2/3 complex 34 kDa subunit , putati	12.14	27.50	1	7	7	7	320	36.9	6.87
CADAFLAP00003961	pep:known supercontig:JCVI-afl1-v2.0:EQ963474:2172634:2174527:-1 gene:CADAFLAG00003961 transcript:CADAFLAT00003961 description: T-complex protein 1, gamma subunit (C	12.11	12.06	1	5	5	5	539	58.9	6.13
CADAFLAP00001117	pep:known supercontig:JCVI-afl1-v2.0:EQ963472:2972890:2974702:-1 gene:CADAFLAG00001117 transcript:CADAFLAT00001117 description: Glutathione oxidoreductase Glr1, putati	11.22	14.77	1	4	4	4	562	60.9	7.65
CADAFLAP00002685	pep:known supercontig:JCVI-afl1-v2.0:EQ963473:2790116:2791670:-1 gene:CADAFLAG00002685 transcript:CADAFLAT00002685 description: Phosphatidylinositol transporter, putativ	11.15	21.54	1	7	7	7	325	36.7	5.82
CADAFLAP00001370	pep:known supercontig:JCVI-afl1-v2.0:EQ963472:3674411:3678461:1 gene:CADAFLAG00001370 transcript:CADAFLAT00001370 description: Coatomer subunit alpha, putative	11.09	7.43	1	5	5	5	1212	135.5	6.16
CADAFLAP00000784	pep:known supercontig:JCVI-afl1-v2.0:EQ963472:2077201:2078611:-1 gene:CADAFLAG00000784 transcript:CADAFLAT00000784 description: ATP synthase subunit gamma	10.89	22.56	1	4	4	4	297	32.3	8.50
CADAFLAP00013452	pep:known supercontig:JCVI-afl1-v2.0:EQ963487:296577:297908:-1 gene:CADAFLAG00013452 transcript:CADAFLAT00013452 description: Proteasome regulatory particle subunit Rp	10.16	13.88	1	4	4	4	389	43.4	7.90
CADAFLAP00001169	pep:known supercontig:JCVI-afl1-v2.0:EQ963472:3121243:3122277:-1 gene:CADAFLAG00001169 transcript:CADAFLAT00001169 description: Oxidoreductase, zinc-binding dehydroge	10.10	19.48	1	4	4	4	344	37.5	7.50
CADAFLAP00009840	pep:known supercontig:JCVI-afl1-v2.0:EQ963481:1238520:1242143:1 gene:CADAFLAG00009840 transcript:CADAFLAT00009840 description: Importin beta-3 subunit, putative	9.96	7.95	1	5	5	5	1095	121.5	4.79
CADAFLAP00010809	pep:known supercontig:JCVI-afl1-v2.0:EQ963483:53550:55891:1 gene:CADAFLAG00010809 transcript:CADAFLAT00010809 description: Peptide chain release factor eRF/aRF, subunit	9.16	18.66	1	6	6	6	434	48.5	5.31
CADAFLAP00011645	pep:known supercontig:JCVI-afl1-v2.0:EQ963484:503711:504206:-1 gene:CADAFLAG00011645 transcript:CADAFLAT00011645 description: Putative uncharacterized protein	8.57	54.17	1	7	7	7	144	17.0	5.43
CADAFLAP00005638	pep:known supercontig:JCVI-afl1-v2.0:EQ963476:1282856:1284624:1 gene:CADAFLAG00005638 transcript:CADAFLAT00005638 description: Dihydrolipoyl dehydrogenase	8.33	15.82	1	6	6	6	512	54.6	7.78
CADAFLAP00010775	pep:known supercontig:JCVI-afl1-v2.0:EQ963482:1901307:1902958:-1 gene:CADAFLAG00010775 transcript:CADAFLAT00010775 description: Secretion related GTPase SrgB/Ypt1	7.86	22.89	1	4	4	4	201	22.3	5.27
CADAFLAP00000923	pep:known supercontig:JCVI-afl1-v2.0:EQ963472:2466299:2468724:-1 gene:CADAFLAG00000923 transcript:CADAFLAT00000923 description: Eukaryotic translation initiation factor 3	7.79	8.37	1	6	6	6	741	84.2	5.25
CADAFLAP00004909	pep:known supercontig:JCVI-afl1-v2.0:EQ963475:2019328:2020275:1 gene:CADAFLAG00004909 transcript:CADAFLAT00004909 description: RAB GTPase Ypt5, putative	7.69	15.60	1	3	3	3	218	23.8	8.54
CADAFLAP00006759	pep:known supercontig:JCVI-afl1-v2.0:EQ963476:1791555:1793057:1 gene:CADAFLAG00006759 transcript:CADAFLAT00006759 description: Squalene monooxygenase Erg1	7.64	7.08	1	3	3	3	480	53.0	8.51
CADAFLAP00002799	pep:known supercontig:JCVI-afl1-v2.0:EQ963473:3102956:3103825:-1 gene:CADAFLAG00002799 transcript:CADAFLAT00002799 description: Dienelactone hydrolase family protein	7.57	22.13	1	3	3	3	244	26.9	6.37
CADAFLAP00001324	pep:known supercontig:JCVI-afl1-v2.0:EQ963472:3562709:3563713:-1 gene:CADAFLAG00001324 transcript:CADAFLAT00001324 description: Eukaryotic translation initiation factor 3	7.54	24.70	1	4	4	5	251	28.0	4.82
CADAFLAP00011162	pep:known supercontig:JCVI-afl1-v2.0:EQ963483:1090790:1092713:1 gene:CADAFLAG00011162 transcript:CADAFLAT00011162 description: Histidyl-tRNA synthetase, mitochondrial	7.53	8.67	1	4	4	4	600	65.8	7.99
CADAFLAP00007026	pep:known supercontig:JCVI-afl1-v2.0:EQ963478:120473:122284:1 gene:CADAFLAG00007026 transcript:CADAFLAT00007026 description: Eukaryotic translation initiation factor 3 sul	7.13	4.97	1	2	2	2	583	64.8	5.34
CADAFLAP00002241	pep:known supercontig:JCVI-afl1-v2.0:EQ963473:1574431:1578642:-1 gene:CADAFLAG00002241 transcript:CADAFLAT00002241 description: Mitochondrial translation initiation facto	6.91	3.26	1	2	2	2	1073	118.7	6.00
CADAFLAP00003834	pep:known supercontig:JCVI-afl1-v2.0:EQ963474:1806089:1806957:1 gene:CADAFLAG00003834 transcript:CADAFLAT00003834 description: ThiJ/PfpI family protein	6.80	17.27	1	3	3	3	249	27.1	6.54
CADAFLAP00007163	pep:known supercontig:JCVI-afl1-v2.0:EQ963478:472774:474322:-1 gene:CADAFLAG00007163 transcript:CADAFLAT00007163 description: Arp2/3 complex subunit (Arp3), putative	6.50	23.79	1	5	5	5	433	47.2	6.70
CADAFLAP00001604	pep:known supercontig:JCVI-afl1-v2.0:EQ963472:4306240:4307413:-1 gene:CADAFLAG00001604 transcript:CADAFLAT00001604 description: Eukaryotic translation initiation factor 3	6.45	10.72	1	3	3	3	345	37.2	4.93
CADAFLAP00012024	pep:known supercontig:JCVI-afl1-v2.0:EQ963484:1491125:1491868:-1 gene:CADAFLAG00012024 transcript:CADAFLAT00012024 description: Translation initiation factor SUI1, putati	6.37	32.46	1	3	3	3	114	13.0	8.60
CADAFLAP00000917	pep:known supercontig:JCVI-afl1-v2.0:EQ963472:2448876:2450191:-1 gene:CADAFLAG00000917 transcript:CADAFLAT00000917 description: Phospho-2-dehydro-3-deoxyheptonate a	6.27	11.80	1	3	3	3	373	40.6	6.90
CADAFLAP00002953	pep:known supercontig:JCVI-afl1-v2.0:EQ963473:3511515:3512529:1 gene:CADAFLAG00002953 transcript:CADAFLAT00002953 description: Putative uncharacterized protein	6.26	23.91	1	4	4	4	276	31.3	5.91
CADAFLAP00010841	pep:known supercontig:JCVI-afl1-v2.0:EQ963483:149516:150784:-1 gene:CADAFLAG00010841 transcript:CADAFLAT00010841 description: Eukaryotic translation initiation factor 6	6.24	23.89	1	3	3	3	247	26.6	4.91
CADAFLAP00001127	pep:known supercontig:JCVI-afl1-v2.0:EQ963472:3011479:3011835:-1 gene:CADAFLAG00001127 transcript:CADAFLAT00001127 description: Ribosomal protein S28e	6.04	36.76	1	3	3	3	68	7.7	10.76
CADAFLAP00007933	pep:known supercontig:JCVI-afl1-v2.0:EQ963479:232251:233963:-1 gene:CADAFLAG00007933 transcript:CADAFLAT00007933 description: Phosphoglucomutase, putative	6.02	5.79	1	3	3	3	570	62.2	5.82
CADAFLAP00011816	pep:known supercontig:JCVI-afl1-v2.0:EQ963484:968882:970564:1 gene:CADAFLAG00011816 transcript:CADAFLAT00011816 description: Proteasome regulatory particle subunit (Rp	6.02	7.23	1	3	3	3	498	57.5	7.75
CADAFLAP00010167	pep:known supercontig:JCVI-afl1-v2.0:EQ963482:146207:148003:-1 gene:CADAFLAG00010167 transcript:CADAFLAT00010167 description: Benzoate 4-monooxygenase cytochrome P	5.83	13.48	1	4	4	4	408	45.5	5.82
CADAFLAP00011743	pep:known supercontig:JCVI-afl1-v2.0:EQ963484:788375:790628:1 gene:CADAFLAG00011743 transcript:CADAFLAT00011743 description: Ran GTPase activating protein 1 (RNA1 pro	5.51	6.71	1	2	2	2	417	46.1	4.75
CADAFLAP00001950	pep:known supercontig:JCVI-afl1-v2.0:EQ963473:744976:746915:1 gene:CADAFLAG00001950 transcript:CADAFLAT00001950 description: T-complex protein 1, theta subunit, putativ	5.50	7.04	1	3	3	3	568	61.0	5.19
CADAFLAP00003018	pep:known supercontig:JCVI-afl1-v2.0:EQ963473:3699245:3700840:1 gene:CADAFLAG00003018 transcript:CADAFLAT00003018 description: Proteasome regulatory particle subunit (	5.46	17.72	1	5	5	5	491	54.2	6.65
CADAFLAP00005798	pep:known supercontig:JCVI-afl1-v2.0:EQ963476:1751196:1752476:-1 gene:CADAFLAG00005798 transcript:CADAFLAT00005798 description: Eukaryotic translation initiation factor 3	5.45	11.85	1	3	3	3	287	31.5	8.59
CADAFLAP00008848	pep:known supercontig:JCVI-afl1-v2.0:EQ963480:675821:677104:-1 gene:CADAFLAG00008848 transcript:CADAFLAT00008848 description: Phospholipase, putative	5.36	16.94	1	4	4	4	242	26.8	5.21
CADAFLAP00002206	pep:known supercontig:JCVI-afl1-v2.0:EQ963473:1480608:1481613:1 gene:CADAFLAG00002206 transcript:CADAFLAT00002206 description: Putative uncharacterized protein	5.32	8.07	1	2	2	2	285	32.6	6.44
CADAFLAP00010812	pep:known supercontig:JCVI-afl1-v2.0:EQ963483:61167:62950:1 gene:CADAFLAG00010812 transcript:CADAFLAT00010812 description: Pseudouridylate synthase family protein	5.28	14.14	1	4	4	4	488	54.8	8.76
CADAFLAP00002744	pep:known supercontig:JCVI-afl1-v2.0:EQ963473:2952676:2953540:-1 gene:CADAFLAG00002744 transcript:CADAFLAT00002744 description: 60S ribosomal protein L31e	5.21	23.58	1	3	3	3	123	14.1	10.21
CADAFLAP00007231	pep:known supercontig:JCVI-afl1-v2.0:EQ963478:656101:659152:-1 gene:CADAFLAG00007231 transcript:CADAFLAT00007231 description: Coatomer subunit gamma	5.03	4.37	1	3	3	3	915	100.6	5.43
CADAFLAP00009991	pep:known supercontig:JCVI-afl1-v2.0:EQ963481:1656671:1659115:1 gene:CADAFLAG00009991 transcript:CADAFLAT00009991 description: Putative uncharacterized protein	4.97	7.62	1	4	4	4	709	75.1	9.48
CADAFLAP00013021	pep:known supercontig:JCVI-afl1-v2.0:EQ963486:451616:453602:1 gene:CADAFLAG00013021 transcript:CADAFLAT00013021 description: Reticulon-like protein	4.95	10.50	1	2	2	2	343	38.4	5.55
CADAFLAP00006060	pep:known supercontig:JCVI-afl1-v2.0:EQ963476:2514161:2516680:-1 gene:CADAFLAG00006060 transcript:CADAFLAT00006060 description: Leukotriene A4 hydrolase	4.85	8.26	1	3	3	3	666	75.7	6.61
	pep:known supercontig:JCVI-afl1-v2.0:EQ963477:680029:681198:-1 gene:CADAFLAG00006323 transcript:CADAFLAT00006323 description: Nucleoside-diphosphate-sugar epimerase, putative	4.80	11.70	1	2	2	2	342	37.5	6.28
		4.71	5.44	1	2	2	2	423	48.2	5.72
	pep:known supercontig:JCVI-afl1-v2.0:EQ963475:2125051:2127154:-1 gene:CADAFLAG00004952 transcript:CADAFLAT00004952 description: ATP dependent RNA helicase (Dbp1), putative	4.66	2.96	1	2	2	2	676	71.9	8.70
	pep:known supercontig:JCVI-afl1-v2.0:EQ963472:2265985:2266770:-1 gene:CADAFLAG00000845 transcript:CADAFLAT00000845 description: NADH-quinone oxidoreductase Pst2, putative	4.62	30.54	1	3	3	3	203	21.8	6.73
		4.49	2.59	1	2	2	2	928	103.2	5.64
	pep:known supercontig:JCVI-afl1-v2.0:EQ963477:1063385:1065153:-1 gene:CADAFLAG00006466 transcript:CADAFLAT00006466 description: ATP dependent RNA helicase (Dbp5), putative	4.36	4.52	1	2	2	2	487	53.3	5.58
		4.29	13.08	1	3	3	3	390	42.9	7.99
	pep:known supercontig:JCVI-afl1-v2.0:EQ963472:1238498:1239936:1 gene:CADAFLAG00000470 transcript:CADAFLAT00000470 description: Stearic acid desaturase (SdeA), putative	4.23	8.33	1	3	3	3	456	51.9	9.01
		4.04	10.94	1	5	5	5	631	71.0	7.75
		3.89	4.89	1	2	2	2	573	64.7	6.33
	pep:known supercontig:JCVI-afl1-v2.0:EQ963481:1111013:1112723:-1 gene:CADAFLAG00009797 transcript:CADAFLAT00009797 description: Proteasome regulatory particle subunit Rpt5, putative	3.87	5.41	1	2	2	2	462	51.4	5.03
		3.77	3.33	1	2	2	2	872	96.0	4.77
		3.63	27.45	1	3	3	3	102	11.0	7.12
		3.51	9.23	1	3	3	3	509	56.6	7.72

ID	Description									
	pep:known supercontig:JCVI-afl1-v2.0:EQ963... description: Eukaryotic translation initiation factor 3 subunit D	7.13	1.97	1				585	64.8	5.57
	pep:known supercontig:JCVI-afl1-v2.0:EQ963473:1574431:1578642:-1 gene:CADAFLAG00002241 transcript:CADAFLAT00002241 description: Mitochondrial translation initiation factor IF-2, putative	6.91	3.26	1	2	2	2	1073	118.7	6.00
		6.80	17.27	1	3	3	3	249	27.1	6.54
	pep:known supercontig:JCVI-afl1-v2.0:EQ963478:472774:474322:-1 gene:CADAFLAG00007163 transcript:CADAFLAT00007163 description: Arp2/3 complex subunit (Arp3), putative	6.50	23.79	1	5	5	5	433	47.2	6.70
	pep:known supercontig:JCVI-afl1-v2.0:EQ963472:4306240:4307413:-1 gene:CADAFLAG00001604 transcript:CADAFLAT00001604 description: Eukaryotic translation initiation factor 3 subunit F	6.45	10.72	1	3	3	3	345	37.2	4.93
	pep:known supercontig:JCVI-afl1-v2.0:EQ963484:1491125:1491868:-1 gene:CADAFLAG00012024 transcript:CADAFLAT00012024 description: Translation initiation factor SUI1, putative	6.37	32.46	1	3	3	3	114	13.0	8.60
	pep:known supercontig:JCVI-afl1-v2.0:EQ963472:2448876:2450191:-1 gene:CADAFLAG00000917 transcript:CADAFLAT00000917 description: Phospho-2-dehydro-3-deoxyheptonate aldolase	6.27	11.80	1	3	3	3	373	40.6	6.90
		6.26	23.91	1	4	4	4	276	31.3	5.91
	pep:known supercontig:JCVI-afl1-v2.0:EQ963483:149516:150784:-1 gene:CADAFLAG00010841 transcript:CADAFLAT00010841 description: Eukaryotic translation initiation factor 6	6.24	23.89	1	3	3	3	247	26.6	4.91
		6.04	36.76	1	3	3	3	68	7.7	10.76
		6.02	5.79	1	3	3	3	570	62.2	5.82
	pep:known supercontig:JCVI-afl1-v2.0:EQ963481:968882:970564:1 gene:CADAFLAG00011816 transcript:CADAFLAT00011816 description: Proteasome regulatory particle subunit (RpnE), putative	6.02	7.23	1	3	3	3	498	57.5	7.75
	pep:known supercontig:JCVI-afl1-v2.0:EQ963482:146207:148003:-1 gene:CADAFLAG00010167 transcript:CADAFLAT00010167 description: Benzoate 4-monooxygenase cytochrome P450, putative	5.83	13.48	1	4	4	4	408	45.5	5.82
	pep:known supercontig:JCVI-afl1-v2.0:EQ963484:789375:790628:1 gene:CADAFLAG00011743 transcript:CADAFLAT00011743 description: Ran GTPase activating protein 1 (RNA1 protein)	5.51	6.71	1	2	2	2	417	46.1	4.75
	pep:known supercontig:JCVI-afl1-v2.0:EQ963473:744976:746915:1 gene:CADAFLAG00001950 transcript:CADAFLAT00001950 description: T-complex protein 1, theta subunit, putative	5.50	7.04	1	3	3	3	568	61.0	5.19
	pep:known supercontig:JCVI-afl1-v2.0:EQ963473:3699245:3700840:1 gene:CADAFLAG00003018 transcript:CADAFLAT00003018 description: Proteasome regulatory particle subunit (RpnG), putative	5.46	17.72	1	5	5	5	491	54.2	6.65
	pep:known supercontig:JCVI-afl1-v2.0:EQ963476:1751196:1752476:-1 gene:CADAFLAG00005798 transcript:CADAFLAT00005798 description: Eukaryotic translation initiation factor 3 subunit G	5.45	11.85	1	3	3	3	287	31.5	8.59
		5.36	16.94	1	4	4	4	242	26.8	5.21
		5.32	8.07	1	2	2	2	285	32.6	6.44
		5.28	14.14	1	4	4	4	488	54.8	8.76
		5.21	23.58	1	3	3	3	123	14.1	10.21
		5.03	4.37	1	3	3	3	915	100.6	5.43
		4.97	7.62	1	4	4	4	709	75.1	9.48
		4.95	10.50	1	2	2	2	343	38.4	5.55

Table S8 (continued)

ID	Description									
CADAFLAP00009938	pep:known supercontig:JCVI-afl1-v2.0:EQ963481:1529840:1530820:-1 gene:CADAFLAG00009938 transcript:CADAFLAT00009938 description: Proteasome subunit alpha type	4.83	15.29	1	2	2	2	255	28.2	5.91
CADAFLAP00006323	pep:known supercontig:JCVI-afl1-v2.0:EQ963477:680029:681198:-1 gene:CADAFLAG00006323 transcript:CADAFLAT00006323 description: Nucleoside-diphosphate-sugar epimerase,	4.80	11.70	1	2	2	2	342	37.5	6.28
CADAFLAP00011248	pep:known supercontig:JCVI-afl1-v2.0:EQ963483:1342686:1344281:1 gene:CADAFLAG00011248 transcript:CADAFLAT00011248 description: MAP kinase MpkA	4.71	5.44	1	2	2	2	423	48.2	5.72
CADAFLAP00004952	pep:known supercontig:JCVI-afl1-v2.0:EQ963475:2125051:2127154:-1 gene:CADAFLAG00004952 transcript:CADAFLAT00004952 description: ATP dependent RNA helicase (Dbp1), p	4.66	2.96	1	2	2	2	676	71.9	8.70
CADAFLAP00000845	pep:known supercontig:JCVI-afl1-v2.0:EQ963472:2265985:2266770:-1 gene:CADAFLAG00000845 transcript:CADAFLAT00000845 description: NADH-quinone oxidoreductase Pst2, pu	4.62	30.54	1	3	3	3	203	21.8	6.73
CADAFLAP00008279	pep:known supercontig:JCVI-afl1-v2.0:EQ963479:1161208:1164297:-1 gene:CADAFLAG00008279 transcript:CADAFLAT00008279 description: Coatomer subunit beta	4.49	2.59	1	2	2	2	928	103.2	5.64
CADAFLAP00006466	pep:known supercontig:JCVI-afl1-v2.0:EQ963477:1063385:1065153:1 gene:CADAFLAG00006466 transcript:CADAFLAT00006466 description: ATP dependent RNA helicase (Dbp5), pu	4.36	4.52	1	2	2	2	487	53.3	5.58
CADAFLAP00013276	pep:known supercontig:JCVI-afl1-v2.0:EQ963486:1112563:1113901:1 gene:CADAFLAG00013276 transcript:CADAFLAT00013276 description: Putative uncharacterized protein	4.29	13.08	1	3	3	3	390	42.9	7.99
CADAFLAP00000470	pep:known supercontig:JCVI-afl1-v2.0:EQ963472:1238498:1239936:1 gene:CADAFLAG00000470 transcript:CADAFLAT00000470 description: Stearic acid desaturase (SdeA), putative	4.23	8.33	1	3	3	3	456	51.9	9.01
CADAFLAP00006674	pep:known supercontig:JCVI-afl1-v2.0:EQ963477:1577624:1580010:-1 gene:CADAFLAG00006674 transcript:CADAFLAT00006674 description: Glutaminyl-tRNA synthetase	4.04	10.94	1	5	5	5	631	71.0	7.75
CADAFLAP00005039	pep:known supercontig:JCVI-afl1-v2.0:EQ963475:2361603:2363845:-1 gene:CADAFLAG00005039 transcript:CADAFLAT00005039 description: Asparagine synthetase	3.89	4.89	1	2	2	2	573	64.7	6.33
CADAFLAP00009797	pep:known supercontig:JCVI-afl1-v2.0:EQ963481:1111013:1112723:1 gene:CADAFLAG00009797 transcript:CADAFLAT00009797 description: Proteasome regulatory particle subunit R	3.87	5.41	1	2	2	2	462	51.4	5.03
CADAFLAP00001155	pep:known supercontig:JCVI-afl1-v2.0:EQ963472:3083165:3086306:-1 gene:CADAFLAG00001155 transcript:CADAFLAT00001155 description: Importin beta-1 subunit	3.77	3.33	1	2	2	2	872	96.0	4.77
CADAFLAP00011004	pep:known supercontig:JCVI-afl1-v2.0:EQ963483:640845:641323:1 gene:CADAFLAG00011004 transcript:CADAFLAT00011004 description: Glutaredoxin Grx1, putative	3.63	27.45	1	3	3	3	102	11.0	7.12
CADAFLAP00000650	pep:known supercontig:JCVI-afl1-v2.0:EQ963472:1696659:1698268:1 gene:CADAFLAG00000650 transcript:CADAFLAT00000650 description: Putative uncharacterized protein	3.51	9.23	1	3	3	3	509	56.6	7.72
CADAFLAP00001502	pep:known supercontig:JCVI-afl1-v2.0:EQ963472:4007647:4008540:-1 gene:CADAFLAG00001502 transcript:CADAFLAT00001502 description: Glutathione S-transferase, putative	3.51	14.59	1	5	5	5	281	31.1	5.78
CADAFLAP00004887	pep:known supercontig:JCVI-afl1-v2.0:EQ963475:1968607:1969839:-1 gene:CADAFLAG00004887 transcript:CADAFLAT00004887 description: Zinc-containing alcohol dehydrogenase,	3.51	9.12	1	2	2	2	351	37.6	7.17
CADAFLAP00010073	pep:known supercontig:JCVI-afl1-v2.0:EQ963481:1916427:1918943:1 gene:CADAFLAG00010073 transcript:CADAFLAT00010073 description: NAD+ dependent glutamate dehydroger	3.49	7.25	1	4	4	4	800	90.9	6.79
CADAFLAP00007046	pep:known supercontig:JCVI-afl1-v2.0:EQ963478:184590:186588:-1 gene:CADAFLAG00007046 transcript:CADAFLAT00007046 description: Oxidoreductase, putative	3.30	5.79	1	3	3	3	639	72.3	4.56
CADAFLAP00002339	pep:known supercontig:JCVI-afl1-v2.0:EQ963473:1828986:1829568:1 gene:CADAFLAG00002339 transcript:CADAFLAT00002339 description: Dynein light chain type 1, putative	2.93	39.36	1	3	3	3	94	11.1	6.67
CADAFLAP00011602	pep:known supercontig:JCVI-afl1-v2.0:EQ963484:377737:379608:1 gene:CADAFLAG00011602 transcript:CADAFLAT00011602 description: Isoflavone reductase family protein	2.89	6.98	1	2	2	2	358	40.7	6.43
CADAFLAP00006133	pep:known supercontig:JCVI-afl1-v2.0:EQ963477:173614:176180:-1 gene:CADAFLAG00006133 transcript:CADAFLAT00006133 description: Bifunctional purine biosynthetic protein Ad	2.74	2.94	1	2	2	2	817	86.5	5.45
CADAFLAP00005042	pep:known supercontig:JCVI-afl1-v2.0:EQ963475:2369636:2371542:1 gene:CADAFLAG00005042 transcript:CADAFLAT00005042 description: Coenzyme A synthetase, putative	2.71	5.04	1	2	2	2	516	56.1	9.09
CADAFLAP00005537	pep:known supercontig:JCVI-afl1-v2.0:EQ963476:1047542:1048079:-1 gene:CADAFLAG00005537 transcript:CADAFLAT00005537 description: Small nuclear ribonucleoprotein (LSM7)	2.66	16.54	1	2	2	2	133	14.2	6.58
CADAFLAP00006169	pep:known supercontig:JCVI-afl1-v2.0:EQ963477:268906:269576:-1 gene:CADAFLAG00006169 transcript:CADAFLAT00006169 description: 1,2-dihydroxy-3-keto-5-methylthiopentene	2.64	12.92	1	2	2	2	178	20.8	5.67
CADAFLAP00002714	pep:known supercontig:JCVI-afl1-v2.0:EQ963473:2864020:2866678:-1 gene:CADAFLAG00002714 transcript:CADAFLAT00002714 description: Phosphoribosyl-AMP cyclohydrolase, pu	2.49	6.92	1	4	4	4	867	92.2	5.47
CADAFLAP00008304	pep:known supercontig:JCVI-afl1-v2.0:EQ963479:1226718:1228096:-1 gene:CADAFLAG00008304 transcript:CADAFLAT00008304 description: Vacuolar ATP synthase subunit c	2.35	5.68	1	2	2	2	387	43.7	7.27
CADAFLAP00000129	pep:known supercontig:JCVI-afl1-v2.0:EQ963472:319068:321233:-1 gene:CADAFLAG00000129 transcript:CADAFLAT00000129 description: Cyclopropane-fatty-acyl-phospholipid synt	2.33	8.67	1	4	4	4	519	58.8	6.73
CADAFLAP00003723	pep:known supercontig:JCVI-afl1-v2.0:EQ963474:1512903:1516959:1 gene:CADAFLAG00003723 transcript:CADAFLAT00003723 description: Anthranilate synthase multifunctional pr	2.31	2.11	1	2	2	2	1043	113.4	8.12
CADAFLAP00006345	pep:known supercontig:JCVI-afl1-v2.0:EQ963477:743198:744966:-1 gene:CADAFLAG00006345 transcript:CADAFLAT00006345 description: Proteasome regulatory particle subunit Rp	2.25	6.26	1	2	2	2	463	51.6	5.85
CADAFLAP00004416	pep:known supercontig:JCVI-afl1-v2.0:EQ963475:691946:693316:1 gene:CADAFLAG00004416 transcript:CADAFLAT00004416 description: Guanine deaminase, putative	2.24	8.11	1	2	2	2	456	49.8	5.26
CADAFLAP00000909	pep:known supercontig:JCVI-afl1-v2.0:EQ963472:2426090:2427299:-1 gene:CADAFLAG00000909 transcript:CADAFLAT00000909 description: Ras GTPase Rab11, putative	2.22	9.95	1	2	2	2	211	23.5	5.48
CADAFLAP00010535	pep:known supercontig:JCVI-afl1-v2.0:EQ963482:1195811:1196158:1 gene:CADAFLAG00010535 transcript:CADAFLAT00010535 description: Putative uncharacterized protein	2.14	60.92	1	3	3	3	87	8.7	7.05
CADAFLAP00003653	pep:known supercontig:JCVI-afl1-v2.0:EQ963474:1308050:1312938:-1 gene:CADAFLAG00003653 transcript:CADAFLAT00003653 description: Pentafunctional AROM polypeptide 3-de	2.10	5.89	1	5	5	5	1578	171.2	6.67
CADAFLAP00007020	pep:known supercontig:JCVI-afl1-v2.0:EQ963478:107244:108734:1 gene:CADAFLAG00007020 transcript:CADAFLAT00007020 description: Eukaryotic translation initiation factor 3 su	1.99	4.08	1	2	2	2	466	50.7	5.24
CADAFLAP00004720	pep:known supercontig:JCVI-afl1-v2.0:EQ963475:1519350:1520299:1 gene:CADAFLAG00004720 transcript:CADAFLAT00004720 description: Translation elongation factor eEF-1B gar	1.95	9.38	1	2	2	2	224	24.6	6.23
CADAFLAP00005750	pep:known supercontig:JCVI-afl1-v2.0:EQ963476:1592217:1593782:-1 gene:CADAFLAG00005750 transcript:CADAFLAT00005750 description: Eukaryotic translation initiation factor 3	1.93	3.99	1	2	2	2	476	54.7	5.34
CADAFLAP00002109	pep:known supercontig:JCVI-afl1-v2.0:EQ963473:1207651:1208771:1 gene:CADAFLAG00002109 transcript:CADAFLAT00002109 description: Aha1 domain family	1.81	6.97	1	2	2	2	330	36.9	5.48
CADAFLAP00001427	pep:known supercontig:JCVI-afl1-v2.0:EQ963472:3798311:3800081:-1 gene:CADAFLAG00001427 transcript:CADAFLAT00001427 description: Translational initiation factor 2 beta	1.73	8.79	1	2	2	2	307	33.8	8.79
CADAFLAP00012077	pep:known supercontig:JCVI-afl1-v2.0:EQ963484:1621938:1624159:1 gene:CADAFLAG00012077 transcript:CADAFLAT00012077 description: Eukaryotic translation initiation factor su	1.68	3.96	1	1	2	2	682	74.9	9.38
CADAFLAP00008944	pep:known supercontig:JCVI-afl1-v2.0:EQ963480:940008:940692:1 gene:CADAFLAG00008944 transcript:CADAFLAT00008944 description: Peptide methionine sulfoxide reductase	1.65	14.29	1	2	2	2	175	19.7	6.27
CADAFLAP00008920	pep:known supercontig:JCVI-afl1-v2.0:EQ963480:872998:874265:-1 gene:CADAFLAG00008920 transcript:CADAFLAT00008920 description: Proteasome regulatory particle subunit (R	0.00	5.67	1	2	2	2	335	37.3	6.28
CADAFLAP00002458	pep:known supercontig:JCVI-afl1-v2.0:EQ963473:2174554:2175988:1 gene:CADAFLAG00002458 transcript:CADAFLAT00002458 description: Oxysterol binding protein (Osh5), putati	0.00	10.17	1	4	4	4	413	45.8	6.76
CADAFLAP00002796	pep:known supercontig:JCVI-afl1-v2.0:EQ963473:3096104:3097373:1 gene:CADAFLAG00002796 transcript:CADAFLAT00002796 description: Proteasome regulatory particle subunit (	0.00	6.30	1	2	2	2	381	43.5	5.33
CADAFLAP00012061	pep:known supercontig:JCVI-afl1-v2.0:EQ963484:1577213:1579827:-1 gene:CADAFLAG00012061 transcript:CADAFLAT00012061 description: Proteasome regulatory particle subunit	0.00	3.69	1	2	2	2	623	69.1	6.67
CADAFLAP00009878	pep:known supercontig:JCVI-afl1-v2.0:EQ963481:1372109:1373705:1 gene:CADAFLAG00009878 transcript:CADAFLAT00009878 description: Peptidyl-prolyl cis-trans isomerase	0.00	7.87	1	2	2	2	470	51.3	4.56
CADAFLAP00003541	pep:known supercontig:JCVI-afl1-v2.0:EQ963474:1010727:1012683:1 gene:CADAFLAG00003541 transcript:CADAFLAT00003541 description: Methionyl-tRNA synthetase	0.00	8.16	1	4	4	4	625	71.0	6.39
CADAFLAP00004855	pep:known supercontig:JCVI-afl1-v2.0:EQ963475:1898378:1902093:-1 gene:CADAFLAG00004855 transcript:CADAFLAT00004855 description: 26S proteasome regulatory subunit Rpr	0.00	1.41	1	2	2	2	1135	124.6	5.02
CADAFLAP00004456	pep:known supercontig:JCVI-afl1-v2.0:EQ963475:797060:798720:-1 gene:CADAFLAG00004456 transcript:CADAFLAT00004456 description: F-actin capping protein alpha subunit, put	0.00	11.36	1	2	2	2	273	30.0	5.15
CADAFLAP00008434	pep:known supercontig:JCVI-afl1-v2.0:EQ963479:1585122:1588613:-1 gene:CADAFLAG00008434 transcript:CADAFLAT00008434 description: Importin beta-4 subunit, putative	0.00	5.43	1	4	4	4	1087	120.4	4.72
CADAFLAP00005000	pep:known supercontig:JCVI-afl1-v2.0:EQ963476:2251824:2252942:1 gene:CADAFLAG00005000 transcript:CADAFLAT00005000 description: Ornithine carbamoyltransferase	0.00	5.11	1	2	2	2	372	40.4	8.16
CADAFLAP00011573	pep:known supercontig:JCVI-afl1-v2.0:EQ963484:320996:323696:1 gene:CADAFLAG00011573 transcript:CADAFLAT00011573 description: Cysteinyl-tRNA synthetase	0.00	4.23	1	3	3	3	874	98.4	6.62
CADAFLAP00008051	pep:known supercontig:JCVI-afl1-v2.0:EQ963479:530733:531930:1 gene:CADAFLAG00008051 transcript:CADAFLAT00008051 description: RNA-binding La domain protein	0.00	5.79	1	2	2	2	380	42.9	7.08
CADAFLAP00003930	pep:known supercontig:JCVI-afl1-v2.0:EQ963474:2086654:2089005:-1 gene:CADAFLAG00003930 transcript:CADAFLAT00003930 description: Nucleolar protein nop5	0.00	6.40	1	2	2	2	578	63.3	7.21
CADAFLAP00000730	pep:known supercontig:JCVI-afl1-v2.0:EQ963472:1925515:1927778:1 gene:CADAFLAG00000730 transcript:CADAFLAT00000730 description: Oligopeptidase family protein	0.00	5.29	1	3	3	3	718	78.8	6.42
CADAFLAP00010469	pep:known supercontig:JCVI-afl1-v2.0:EQ963482:993055:993270:-1 gene:CADAFLAG00010469 transcript:CADAFLAT00010469 description: Putative uncharacterized protein	0.00	26.76	1	2	2	2	71	7.7	7.18
CADAFLAP00009051	pep:known supercontig:JCVI-afl1-v2.0:EQ963480:1241438:1243239:1 gene:CADAFLAG00009051 transcript:CADAFLAT00009051 description: Solid-state culture expressed protein (A	0.00	12.73	1	3	3	3	550	57.0	7.14

Appendix C

Supplementary Data Relevant

to Chapter 5
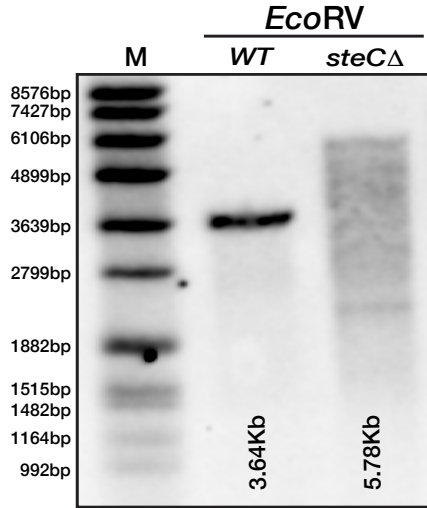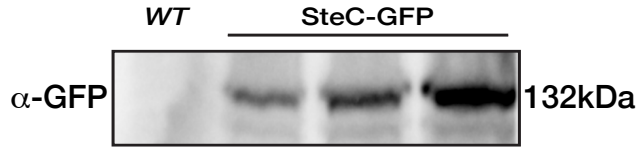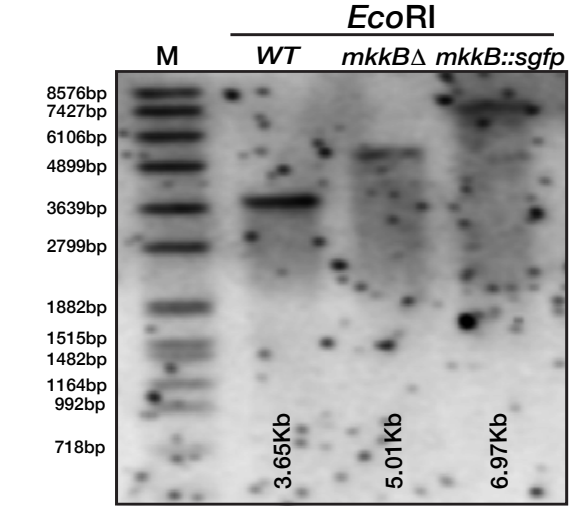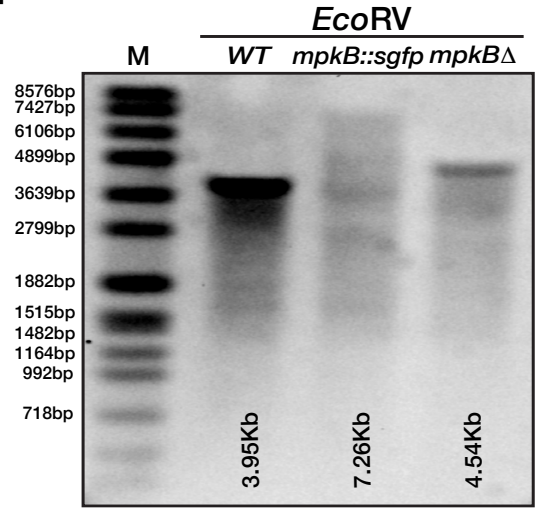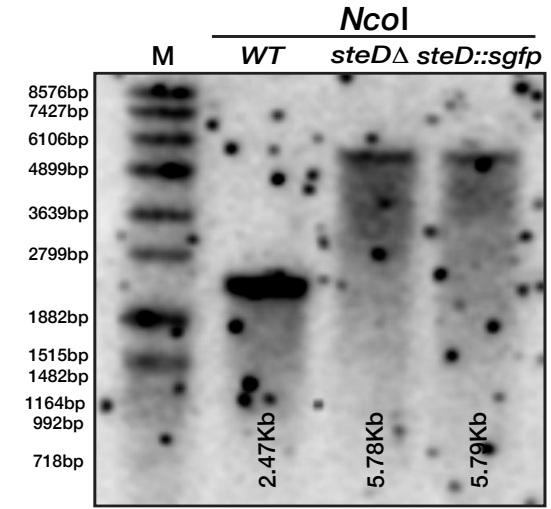
Figure S1. Confirmation of deletions and tagged *A. fumigatus* strains *via* southern blotting (a) Southern hybridizations of *steC*Δ. M: Molecular marker in basepairs (bp). Sizes of the bands shown for the wild type CEA17 strain and the deletion strain are in accordance with theoretical maps. The *Eco*RV restriction enzyme was used to digest genomic DNA and a 3' UTR DIG-labelled probe was used for detection. (b) Western blot detecting the presence of the functional SteC-GFP fusion protein in three *A. fumigatus* clones *via* an α-GFP antibody. The size of the tagged protein is 132kDa as predicted. (c) Southern hybridizations of *mkkB*Δ and *mkkB::sgfp*. The *Eco*RI restriction enzyme was used to digest genomic DNA and a 3' UTR DIG-labelled probe was used for detection. (d) Southern hybridizations of *mpkB*Δ and *mpkB::sgfp*. The *Eco*RV restriction enzyme was used to digest genomic DNA and a 5' UTR DIG-labelled probe was used for detection. (e) Southern hybridizations of *steD*Δ and *steD::sgfp*. The *Nco*I restriction enzyme was used to digest genomic DNA and a 3' UTR DIG-labelled probe was used for detection.

Figure S2: Confirmation of *A. fumigatus hamE* deletions and tagged *hamE* strains *via* southern blotting. Southern hybridizations of two *hamE* deletion, *hamE::sgfp* and *hamE::3xha* clones. M: Molecular marker in basepairs (bp). Sizes of the bands shown for each strain are in accordance with theoretical maps. The *Sca*I restriction enzyme was used to digest genomic DNA and a 3' UTR probe was used for detection.

c

```
# Length: 920
# Identity:     718/920 (78.0%)
# Similarity:   789/920 (85.8%)
# Gaps:          38/920 ( 4.1%)
# Score: 3623.0
#
#
#=======================================

EMBOSS_001      1 MLTSK-AYAGPLGLPSSQTPTASYHT-TTQKSSTFSESQTGTVYTSPTKS     48
                  ||.:|  .:.:|||:.||.....:|  .:.||||..||.:|||||
EMBOSS_001     35 MLATKIQLSAPLGMTGSQATAPTYHVGPSHKSSMGASSQDGMLFTSPTES     84

EMBOSS_001     49 EFSEADDGLDAVRSWDENQVISWLHSINCQQYEPLFRANNFNGNNLIECD     98
                  |||  .-|| .|||||||||-|||:||||||-|||-||||||||||||||
EMBOSS_001     85 EFS-LKDGHDAVRSWDEKQVINWLHSINCGQYESLFRANNFNGNNLIECD    133

EMBOSS_001     99 QKILQEMGIKKIGDRVRIFVAIKQLRNKSVVNKKQKNL------------    136
                  ||||||||||:||||||||||||:|||||-|.:|.|:
EMBOSS_001    134 QKILQEMGIKKVGDRVRIFVAIKKLRNKSVNNLRQTNMVSENLSQLEPQL    183

EMBOSS_001    137 ----RQLAALEAAHQQASPDSARSYSARQQTSSAGHASRTGD--YSYGRP    180
                  -||||||----.:-||:|-.:-||:|----.||.-|  ||-|:.
EMBOSS_001    184 TPKKNQLAALEAPTYAPTSDSSRLTNLRQRSSSNRRMSRLVDNGYSTGKS    233

EMBOSS_001    181 TSRPGSPLRPHRYVANSPMDSGRKD--YL----SAGSGAGRNPGTPVE---    222
                  :||||||||.||||||||.|| |.    .:||.-:|||||:.
EMBOSS_001    234 SSRPGSPLRNQRYAANSPMESGRKEGYFAHPSTGGSNSGRNPGTPSDGSH    283

EMBOSS_001    223 --RIGTHSRQNPSLDGMTMGSLLSNAPVIRVIYSGGQTKVLDIKHCKTPD    270
                  :.|.-|||||:|||-.|:.:|.:||||||||:||||||||||||||||
EMBOSS_001    284 GHKGGVHLRQNPSIDGLTMGALPANSPVIRVIYTGGQTKVLDIKHCKTAD    333

EMBOSS_001    271 EIILCVLKKLQLPEHQYRNYCFYVLDGLDPDPSNCRRLSDHELMEICEGF    320
                  |||||||||||||||||||||||||||||-|||||||||.||:||||||:
EMBOSS_001    334 EIILCVLKKLQLPEHQYRNYCFYVLDGLEPDPSNCRRLTDQELMEICEGS    383

EMBOSS_001    321 HRSERGRLILRKIHAGEPDAEEVHRAAQLALDESQQAHMNALSSSNARNQ    370
                  -|||||||||||||||||-.:|:.-||:||||||||--||||||||:|||
EMBOSS_001    384 SRSERGRLILRKIHAGEPDTDELRRASQLALDESQMTHMNALSSSNVRNQ    433

EMBOSS_001    371 MKIQQLTGESWHNIRQPMSPVSSRHNTTPSDHEIRPPQVSER--VSKLRS    418
                  :||||||||.:|:||:||:|.:.:.:.::|-.:|.::...:||  |:||||
EMBOSS_001    434 IKIQQLTGEPWHHIKQPLSPVSARQPQAHNDHDQSLQMSTERPSVAKLRS    483

EMBOSS_001    419 FFGARPPSEMIIHEISSYFPGHQREDIEKTMRMSVRRSQRLSRAASRLSV    468
                  ||||||||||||||::|:||||||||||||||||||:||||||||||||
EMBOSS_001    484 FFGARPPSEMIIHELTSYFPGHQREDIEKTMRMSIRRSQRLSRAASRLSV    533

EMBOSS_001    469 VSNTSYASSLRDAPPIPSIADTWLNNGTPPTRAARPLSVLSTRPGLPSTS    518
                  :|||||||||||||||||||||||||-|.|:||.|||||--.:|.||.|
EMBOSS_001    534 LSNTSYASSLRDAPPIPSIADTWLNPGAPSTRASRPLSV--SRFNLPQTS    581

EMBOSS_001    519 YRDSIASSSLHPLQEESPVEPNRKSYVSFDSGSDDPNNSRHSLLDENASV    568
                  ||||||||||-||||||||-||||||||||||||||:||-||:||||||||
EMBOSS_001    582 YRDSIASSSLQPLQEESPIEPNRKSYVSFDSGSDDPSNSRQSLLDENASV    631

EMBOSS_001    569 AATDGGSFNERLSVLVAEDGEEEDDGLAEFLAGNNFV--NWMKGSLIGEG    616
                  |||||||||||||||||||||||||||-|||-||||.  ||||||||||||
EMBOSS_001    632 AATDGGSFNERLSVLVAEDGEEEDDGLNEFLSGNNFAPKNWMKGSLIGEG    681

EMBOSS_001    617 SFGSVFLALHSITGELMAVKQVEIPSATKGTEFDKRKNSMVEALKHEIDL    666
                  ||||||||||.||||||||||||||||||||||||||||||:||||||:|
EMBOSS_001    682 SFGSVFLALHAITGELMAVKQVEIPSATKGTEFDKRKNSMVTALKHEIEL    731

EMBOSS_001    667 LQGLHHPNIVQYLGTTADDQYLNIFLEYVPGGSIATMLKQYNTFQEPLIK    716
                  |||||||||||||||.|||||||||||||||||||||||||||||||||||
EMBOSS_001    732 LQGLHHPNIVQYLGTSADDQYLNIFLEYVPGGSIATMLKQYNTFQEPLIK    781

EMBOSS_001    717 NFVRQILAGLSYLHSKDIIHRDIKGANVLVDNKGGIKISDFGISKRVEAS    766
                  ||||||||.|||||||.||||||||||:|||||||||||||||||||||||
EMBOSS_001    782 NFVRQILEGLSYLHSRDIIHRDIKGANILVDNKGGIKISDFGISKRVEAS    831

EMBOSS_001    767 TVLGSRAS-NGGGHIHRPSLQGSVYWMAPEVVRQTAHTKKADIWSLGCLV    815
                  ||||.:.|| |||||.||||||||||||||||||||||||||||||||||||
EMBOSS_001    832 TVLGARASGNGGGHLHRPSLQGSVYWMAPEVVRQTAHTKKADIWSLGCLV    881

EMBOSS_001    816 IEMFIGSHPFPDCSQLQAIFAIGSNKARPPAPEHASKDAVAFLDMTFQLD    865
                  :|||||:||||||||||||||||||||-|||||||||||.|:|||||||:|
EMBOSS_001    882 VEMFIGAHPFPDCSQLQAIFAIGSNSARPPAPEHASKEAMAFLDMTFQVD    931

EMBOSS_001    866 HEKRPDADELLKSPFLATTL                               885
                  :|||||.|||||:||||:..|
EMBOSS_001    932 YEKRPSADELLQSPFLSAPL                               951
```

Figure S3: Alignment of *A. nidulans* SteC (AN2269) and *A. fumigatus* SteC (Afu5g06420) protein sequences. (a) Protein sequence of *A. nidulans* SteC (AN2269). (b) Protein sequence of *A. fumigatus* SteC (Afu5g06420). (c) Pairwise sequence alignment of both SteC protein sequences using the Smith-Waterman algorithm (Madeira et al. 2019).

Supplementary Tables

Table S1: Fungal strains created or used in this study

Strain	Genotype	Plasmid used	Reference
CEA17	*Wild type, akuBΔ::pyrG, MAT1-1*	Not applied	(da Silva Ferreira et al., 2006)
CEA17 (*pyrGΔ*)	*Wild type, akuBΔ, pyrGΔ, MAT1-1*	Not applied	Jean-Paul Latge Lab
AFUDF1	*hamEΔ::ptrA, akuBΔ, pyrG+, MAT1-1*	pDF4 in CEA17	This Study
AFUDF2	*hamE::sgfp::hph, akuBΔ, pyrG+, MAT1-1*	pDF5 in CEA17	This Study
AFUDF3	*hamE::3xha::hph, akuBΔ, pyrG+, MAT1-1*	pDF6 in CEA17	This Study
AFUDF12	*steCΔ::pyrG, akuBΔ, pyrGΔ, MAT1-1*	pDF22 in CEA17 (*pyrGΔ*)	This Study
AFUDF13	*mkkBΔ::pyrG, akuBΔ, pyrGΔ, MAT1-1*	pDF23 in CEA17 (*pyrGΔ*)	This Study
AFUDF14	*mpkBΔ::pyrG, akuBΔ, pyrGΔ, MAT1-1*	pDF24 in CEA17 (*pyrGΔ*)	This Study
AFUDF15	*steDΔ::pyrG, akuBΔ, pyrGΔ, MAT1-1*	pDF25 in CEA17 (*pyrGΔ*)	This Study
AFUDF17	*mkkB::sgfp::pyrG, akuB, pyrGΔ, MAT1-1*	pDF27 in CEA17 (*pyrGΔ*)	This Study
AFUDF18	*mpkB::sgfp::pyrG, akuBΔ, pyrGΔ, MAT1-1*	pDF28 in CEA17 (*pyrGΔ*)	This Study
AFUDF19	*steD::sgfp::pyrG, akuBΔ, pyrGΔ, MAT1-1*	pDF29 in CEA17 (*pyrGΔ*)	This Study
AFUDF20	*hamEΔ::ptrA, akuBΔ, pyrGΔ, MAT1-1*	pDF4 in CEA17 (*pyrGΔ*)	This Study
AFUDF26	*gpdA::steC::ptrA, steCΔ::pyrG, akuBΔ, pyrGΔ, MAT1-1*	pDF44 in AFUDF12	This Study
AFUDF27	*gpdA::mkkB::ptrA, mkkBΔ::pyrG, akuBΔ, pyrGΔ, MAT1-1*	pDF45 in AFUDF13	This Study
AFUDF28	*gpdA::mpkB::ptrA, mpkBΔ::pyrG, akuBΔ, pyrGΔ, MAT1-1*	pDF46 in AFUDF14	This Study
AFUDF29	*gpdA::steD::ptrA, steDΔ::pyrG, akuBΔ, pyrGΔ, MAT1-1*	pDF47 in AFUDF15	This Study
AFUDF31	*_phamE::hamE::hamE_t::pyrG, hamEΔ::ptrA, pyrG-, MAT1-1*	pDF49 in AFUDF20	This Study
AFUDF32	*tetO7::Pmin::steC::GFP::ptrA, steCΔ::pyrG, akuBΔ, pyrGΔ, MAT1-1*	pDF50 in AFUDF12	This Study
AFUDF33	*steC::sgfp::pyrG, akuBΔ, pyrGΔ, MAT1-1*	pDF55 in CEA17 (*pyrGΔ*)	This Study

Table S2: Plasmids created or used in this study

Plasmid	Description	Reference
pUC19	*E. coli* cloning plasmid with *bla* (ampicillin resistance) gene	Thermo Fisher
pCH008	Tet-ON module $^P tpiA::rtTA2^S$ -M2::cgrA^t -tetO-^{P}min	(Helmschrott et al., 2013)
pOSB113	*Pme*I::AfpyrG::*Swa*I inserted in *Sma*I site of pUC19	This Study
pSK379	$^P gpdA$-his2A^t and *ptrA* resistance cassette	(Szewczyk and Krappmann, 2010)

pDF4	*hamE* deletion with *ptrA* in *Sma*I site of pUC19	This Study
pDF5	*hamE::sgfp::hph* cassette in *Sma*I site of pUC19	This Study
pDF6	*hamE::3xha::hph* cassette in *Sma*I site of pUC19	This Study
pDF22	*steC* deletion with *pyrG* in *Sma*I site of pUC19	This Study
pDF23	*mkkB* deletion with *pyrG* in *Sma*I site of pUC19	This Study
pDF24	*mpkB* deletion with *pyrG* in *Sma*I site of pUC19	This Study
pDF25	*steD* deletion with *pyrG* in *Sma*I site of pUC19	This Study
pDF27	*mkkB::sgfp::pyrG* in *Sma*I site of pUC19	This Study
pDF28	*mpkB::sgfp::pyrG* in *Sma*I site of pUC19	This Study
pDF29	*steD::sgfp::pyrG* in *Sma*I site of pUC19	This Study
pDF44	*steC* genomic locus in *Pme*I site of pSK379	This Study
pDF45	*mkkB* genomic locus in *Pme*I site of pSK379	This Study
pDF46	*mpkB* genomic locus in *Pme*I site of pSK379	This Study
pDF47	*steD* genomic locus in *Pme*I site of pSK379	This Study
pDF49	*hamE* genomic locus in *Swa*I site of pOSB113	This Study
pDF50	*steC::sgfp::ptrA* in *Pme*I site of pCH008	This Study
pDF55	*steC::sgfp::pyrG* in *Sma*I site of pUC19	This Study

Table S3: Oligonucleotides created or used in this study

Designation	Sequence in 5' > 3' direction	Size (basepairs)
DF13 (pDF4 5' UTR FWD, with pUC19 tail)	TTC GAG CTC GGT ACC CGA AAT GGC AGA AGT CTT CCA CAG	39
DF14 (pDF4 5' UTR REV, with *ptrA* tail)	GAT CCC GTA ATC AAT TTC TTG GGA TCT TGC GGT TGA G	37
DF15 (pDF4 3' UTR FWD, with *ptrA* tail)	AAA CAA AGA TGC AAG ACA CAG TCA CTT CTT TGA CTT GTC	39
DF16 (pDF4/5/6 3' UTR REV, with pUC19 tail)	ACT CTA GAG GAT CCC CCA TTG GCA CGG CGT ACC TG	35
DF17 (pDF4 5' FWD **nest oligo**)	GAA ATG GCA GAA GTC TTC CAC AG	23
DF18 (pDF4/5/6 3' REV **nest oligo**)	GCT GTG AAG CTG TAC TCG AC	20
DF19 (pDF5/6 *hamE* ORF FWD with pUC19 tail)	TTC GAG CTC GGT ACC CCT CAA AGA ACG CTC CGA CAG	36
DF20 (pDF5/6 5' FWD **nest oligo**)	GTG TTC TCC AGC TTC ACC TG	20
DF21 (pDF5/6 5' UTR REV, with tail for linker)	CAC CGC TAC CAC CTC CCA TCC GGC CGT CCG ACA TTT G	37
DF22 (pDF4 3' UTR FWD, with *hph* tail)	GAG GGC AAA GGA ATA GCA CAG TCA CTT CTT TGA CTT GTC	39
DF107 (pDF22 5' UTR REV, with *pyrG* tail)	GAG CAT TGT TTG AGG CAA CAT AAT ACC GGC GTT TTC CC	38

270

DF108 (pDF22 5' UTR FWD, with pUC19 tail)	TTC GAG CTC GGT ACC CGA GAG CGA TAG TTC CAA GTG G	37
DF109 (pDF22/26 3' UTR REV, with pUC19 tail)	ACT CTA GAG GAT CCC CCC TCT TGT TAT GCG GAG TGA G	37
DF110 (pDF22/26 3' UTR FWD, with *pyrG* tail)	GCC TCC TCT CAG ACA GGA TTT GAT ACT TTA TTG ATT GCA T	40
DF111 (pDF22 5' FWD **nest oligo**)	CAG CCA TCG AGT CGT GAT C	19
DF112 (pDF22/26 3' REV **nest oligo**)	GCA CGT GAC CAT CTG AGA C	19
DF113 (pDF23 5' UTR FWD, with pUC19 tail)	TTC GAG CTC GGT ACC CCC TCA TGA ACT TCG CCG TCG	36
DF114 (pDF23/27 3' UTR REV, with pUC19 tail)	ACT CTA GAG GAT CCC CCG TGA TAG CGA CCT TGA CGG	36
DF115 (pDF23 5' UTR REV, with *pyrG* tail)	GAG CAT TGT TTG AGG CGG CTG GGG CGA ACG GAG T	34
DF116 (pDF23/27 3' UTR FWD, with *pyrG* tail)	GCC TCC TCT CAG ACA GCA CCA TAC GTC GGA GCT ACT C	37
DF117 (pDF23 5' FWD **nest oligo**)	GAG TAC GGA GTA TGC TGC TG	20
DF118 (pDF23/27 3' REV **nest oligo**)	GAG TTG GCT TGG CAG GAA C	19
DF119 (pDF24 5' UTR FWD, with pUC19 tail)	TTC GAG CTC GGT ACC CCG ATC GAC GAA GCA GAA CAT TC	38
DF120 (pDF24/28 3' UTR REV, with pUC19 tail)	ACT CTA GAG GAT CCC CCC GAT CAA CTT ACT CTC CGA G	37
DF121 (pDF24 5' UTR REV, with *pyrG* tail)	GAG CAT TGT TTG AGG CGG TTG CTA ACT TTC AGC ATC	36
DF122 (pDF24/28 3' UTR FWD, with *pyrG* tail)	GCC TCC TCT CAG ACA GAG ATT CAG TGG CGT CTC TTG C	37
DF123 (pDF24 5' FWD **nest oligo**)	CGT GTG CCT GTC TTA CCT TAG	21
DF124 (pDF24/28 3' REV **nest oligo**)	GAG CTC AGC AAT CGA GCA ATC	21
DF125 (pDF25 5' UTR FWD, with pUC19 tail)	TTC GAG CTC GGT ACC CCA GAG CGC AGA GAT GTT GAG	36
DF126 (pDF25/29 3' UTR REV, with pUC19 tail)	ACT CTA GAG GAT CCC CCA GTA CCT GAA TAC ACT CGA GC	38
DF127 (pDF25 5' UTR REV, with *pyrG* tail)	GAG CAT TGT TTG AGG CGT CTA TGG AAG GGG CTA G	35
DF128 (pDF25/29 3' UTR FWD, with *pyrG* tail)	GCC TCC TCT CAG ACA GTG CCA ACG TGC GCC TAG AC	35
DF129 (pDF25 5' FWD **nest oligo**)	CGA TGG TGA CGG AGC ATT GAG	21
DF130 (pDF25/29 3' REV **nest oligo**)	CCT TGG TCT CTG GGC TTG TC	20

DF134 (pDF27 5' UTR FWD, with pUC19 tail)	TTC GAG CTC GGT ACC CAT GGC CGA CCA GTT CAA AGC	36
DF135 (pDF27 5' UTR REV, with tail for linker)	CAC CGC TAC CAC CTC CGA CAG CTC CCG TCA TAT CG	35
DF136 (pDF27 5' FWD **nest oligo**)	CCA TTG GAA ACA CCG ACA GC	20
DF137 (pDF28 5' UTR FWD, with pUC19 tail)	TTC GAG CTC GGT ACC CCC AGG CGA CTC TCA CAA TTC	36
DF138 (pDF28 5' UTR REV, with tail for linker)	CAC CGC TAC CAC CTC CCC GCA TGA TTT CTT CGT AGA TC	38
DF139 (pDF28 5' FWD **nest oligo**)	CAC CAA CTC CTG TTC TGA GG	20
DF140 (pDF29 5' UTR FWD, with pUC19 tail)	TTC GAG CTC GGT ACC CGG ATG ACC TCG ACT GCG ATC	36
DF141 (pDF29 5' UTR REV, with tail for linker)	CAC CGC TAC CAC CTC CCA AAA CGC CGC CAG GTA GG	35
DF142 (pDF29 5' FWD **nest oligo**)	CGA CGT CCA CTC CAT TCA TC	20
DF259 (pDF44 5' *steC* ORF FWD, with pSK379 tail)	GCA GAC ATC ACC GTT TAT GTC ATT GAA GCC CAG TGC ATC	39
DF260 (pDF44 3' *steC* ORF REV, with pSK379 tail)	GAT AGA CAT GGC GTT TCT ACC GGA TAT TAA AAC GCC TTT	39
DF261 (pDF45 5' *mkkB* ORF FWD, with pSK379 tail)	GCA GAC ATC ACC GTT TAT GGC CGA CCA GTT CAA AGC	36
DF262 (pDF45 3' *mkkB* ORF REV, with pSK379 tail)	GAT AGA CAT GGC GTT TTT AGA CAG CTC CCG TCA TAT CG	38
DF263 (pDF46 5' *mpkB* ORF FWD, with pSK379 tail)	GCA GAC ATC ACC GTT TAT GGT GCA GCA ACC TCC TC	35
DF264 (pDF46 3' *mpkB* ORF REV, with pSK379 tail)	GAT AGA CAT GGC GTT TCT ACC GCA TGA TTT CTT CGT A	37
DF265 (pDF47 5' *steD* ORF FWD, with pSK379 tail)	GCA GAC ATC ACC GTT TAT GTC TCT GCA TAC ATC CTA CC	38
DF266 (pDF47 3' *steD* ORF REV, with pSK379 tail)	GAT AGA CAT GGC GTT TTC ACA AAA CGC CGC CAG GTA G	37
DF273 (pDF49 *hamE* 5' UTR FWD, with pOSB113 tail)	AGC TCG GTA CCC ATT TGT CTT CCA CAG GGC TGT TG	35
DF274 (pDF49 *hamE* 3' UTR REV, with pOSB113 tail)	TTG AGG CGA ATT ATT TGA AGC TGT ACT CGA CGA TTG AG	38
DF276 (pDF50 5'*steC* ORF FWD, with pCH008 tail)	GCC TGA GTG GCC GTT TAT GTC ATT GAA GCC CAG TGC	36
DF277 (pDF50 3'*steC* ORF REV, with tail for linker)	CTT GCT CAC CAT GTT TCC ACC GCT ACC ACC TCC CCG GAT ATT AAA ACG CCT TT	53

DF293 (pDF55 5' UTR FWD, with pUC19 tail)	TTC GAG CTC GGT ACC CGC GAA GGA TCA AGT AGG TCC	36
DF296 (pDF55 5' UTR REV, with tail for linker)	CAC CGC TAC CAC CTC CCG CCA GCG GTG CAG ACA AAA AT	38
DF298 (pDF55 3' UTR FWD, with tail for *pyrG*)	GCC TCC TCT CAG ACA GGA TGC ACC TGA ATT TCA GAA TT	38
DF299 (pDF55 3' UTR REV, with tail for pUC19)	ACT CTA GAG GAT CCC CCC TTG AGT CAA GCT CTC TAA G	37
DF300 (pDF55 5' FWD **nest oligo**)	CCA GTT CAA ACT GCG TTC GC	20
DF301 (pDF55 3' REV **nest oligo**)	GCA GTT CAA ATG TGC GCA ACC	22

Supplementary Table S4: SteC-GFP (Afu5g06420) interacting proteins at 24 hours of vegetative growth. Proteins of interest are highlighted in yellow. SteC (Afu5g06420), SteD (Afu2g17130).

Table S4: *Aspergillus fumigatus* SteC-GFP interacting proteins (Vegetative growth-24 hours)

Accession	Description	Score	Coverage	# Proteins	# Unique Peptides	# Peptides	# PSMs	# AAs	MW [kDa]	calc. pI
Afu1g07380	Afu1g07380 AspGDID:ASPL0000101904 COORDS:Chr1_A_fumigatus_Af293:2090929-2084331C, translated using codon table 1 (2126 amino acids) Uncharacterized ORF; Putative NADH-dependent glutamate sy	100.61	18.16	1	26	26	28	2126	234.1	6.39
Afu5g06420	Afu5g06420 AspGDID:ASPL0000107718 COORDS:Chr5_A_fumigatus_Af293:1549998-1553242W, translated using codon table 1 (1007 amino acids) Uncharacterized ORF; Ortholog(s)	104.60	31.58	1	22	22	27	1007	111.6	8.60
Afu1g12840	niiA AspGDID:ASPL0000102352 COORDS:Chr1_A_fumigatus_Af293:3393418-3397198W, translated using codon table 1 (1102 amino acids) Uncharacterized ORF; Putative nitrite reductase; nitrogen-regulated g	62.54	22.14	1	19	19	19	1102	123.1	6.62
Afu4g09140	car2 AspGDID:ASPL0000106629 COORDS:Chr4_A_fumigatus_Af293:2388283-2389697W, translated using codon table 1 (450 amino acids) Uncharacterized ORF; L-ornithine aminotransferase; induced by growth	47.84	34.67	1	12	12	13	450	49.1	6.54
Afu6g03440	Afu6g03440 AspGDID:ASPL0000108799 COORDS:Chr6_A_fumigatus_Af293:738342-736781C, translated using codon table 1 (497 amino acids) Uncharacterized ORF; Putative fructosyl amine; transcript induced	52.60	32.19	1	12	12	14	497	54.9	5.76
Afu2g17130	Afu2g17130 AspGDID:ASPL0000104429 COORDS:Chr2_A_fumigatus_Af293:4574963-4576567W, translated using codon table 1 (487 amino acids) Uncharacterized ORF; Ortholog(s) h	47.73	29.16	1	9	9	13	487	53.5	6.14
Afu4g13700	Afu4g13700 AspGDID:ASPL0000107076 COORDS:Chr4_A_fumigatus_Af293:3586027-3588483W, translated using codon table 1 (737 amino acids) Uncharacterized ORF; Ortholog(s) have cytosol localization	24.40	14.79	1	8	8	8	737	84.4	7.09
Afu5g03690	Afu5g03690 AspGDID:ASPL0000107547 COORDS:Chr5_A_fumigatus_Af293:987794-986454C, translated using codon table 1 (424 amino acids) Uncharacterized ORF; Putative phosphatidylinositol trans	32.51	29.25	1	8	8	9	424	46.1	4.84
Afu6g03460	Afu6g03460 AspGDID:ASPL0000108801 COORDS:Chr6_A_fumigatus_Af293:741171-742895W, translated using codon table 1 (574 amino acids) Uncharacterized ORF; Has domain(s) with predicted ATP binding	32.63	19.69	1	8	8	9	574	63.4	6.14
Afu7g01840	Afu7g01840 AspGDID:ASPL0000109979 COORDS:Chr7_A_fumigatus_Af293:496331-491364C, translated using codon table 1 (1522 amino acids) Uncharacterized ORF; Ortholog(s) have Golgi apparatus, cell tip,	23.00	7.56	1	8	8	8	1522	168.4	6.21
Afu1g15000	Afu1g15000 AspGDID:ASPL0000102567 COORDS:Chr1_A_fumigatus_Af293:4029547-4031693W, translated using codon table 1 (643 amino acids) Uncharacterized ORF; Putative isopropylmalate synthase; trans	21.37	13.06	1	7	7	7	643	71.2	5.68
Afu1g07090	Afu1g07090 AspGDID:ASPL0000101875 COORDS:Chr1_A_fumigatus_Af293:2015732-2011032C, translated using codon table 1 (1526 amino acids) Uncharacterized ORF; Ortholog of <i>A. nidulans FGSC A4</i	18.79	6.62	1	7	7	7	1526	164.4	6.65
Afu4g08710	Afu4g08710 AspGDID:ASPL0000106586 COORDS:Chr4_A_fumigatus_Af293:2256334-2255247C, translated using codon table 1 (287 amino acids) Uncharacterized ORF; Putative short chain dehydrogenase; tra	36.56	29.97	1	7	7	9	287	30.9	5.39
Afu5g07000	Afu5g07000 AspGDID:ASPL0000107775 COORDS:Chr5_A_fumigatus_Af293:1735022-1736346W, translated using codon table 1 (360 amino acids) Uncharacterized ORF; Putative NAD binding Rossmann fold oxi	21.06	28.61	1	7	7	7	360	39.9	7.03
Afu8g05440	atp4 AspGDID:ASPL0000110874 COORDS:Chr8_A_fumigatus_Af293:1265282-1266290W, translated using codon table 1 (274 amino acids) Uncharacterized ORF; Mitochondrial ATPase subunit; hypoxia represse	25.46	31.75	1	7	7	7	274	29.7	9.35
Afu2g13040	grpE AspGDID:ASPL0000104018 COORDS:Chr2_A_fumigatus_Af293:3347479-3346582C, translated using codon table 1 (250 amino acids) Uncharacterized ORF; Mitochondrial co-chaperone; protein level decre	20.58	32.40	1	6	6	6	250	28.4	8.25
Afu5g00720	Afu5g00720 AspGDID:ASPL0000107256 COORDS:Chr5_A_fumigatus_Af293:204504-203702C, translated using codon table 1 (248 amino acids) Uncharacterized ORF; Has domain(s) with predicted N-acetyltrans	28.58	35.89	1	6	6	8	248	29.0	5.33
Afu1g06940	Afu1g06940 AspGDID:ASPL0000101862 COORDS:Chr1_A_fumigatus_Af293:1983163-1981801C, translated using codon table 1 (412 amino acids) Uncharacterized ORF; Ortholog(s) have FMN binding, chorisma	18.76	24.03	1	5	5	5	412	44.2	6.54
Afu2g14210	ilv3 AspGDID:ASPL0000104136 COORDS:Chr2_A_fumigatus_Af293:3721264-3723226W, translated using codon table 1 (606 amino acids) Verified ORF; Putative mitochondrial dihydroxy acid dehydratase; hypo	19.39	12.54	1	5	5	5	606	64.7	7.65
Afu2g09490	Afu2g09490 AspGDID:ASPL0000103667 COORDS:Chr2_A_fumigatus_Af293:2422679-2427552W, translated using codon table 1 (1525 amino acids) Uncharacterized ORF; Eukaryotic translation initiation factor s	16.63	6.10	1	5	5	5	1525	163.9	9.36
Afu3g09910	Afu3g09910 AspGDID:ASPL0000105389 COORDS:Chr3_A_fumigatus_Af293:2542185-2543380W, translated using codon table 1 (331 amino acids) Uncharacterized ORF; Ortholog(s) have phosphatidylcholine tra	22.18	22.66	1	5	5	6	331	37.3	5.52
Afu3g10740	Afu3g10740 AspGDID:ASPL0000105472 COORDS:Chr3_A_fumigatus_Af293:2782828-2781858C, translated using codon table 1 (262 amino acids) Uncharacterized ORF; Putative RAB GTPase with a predicted ro	20.69	36.64	1	5	5	6	262	27.6	4.84
Afu5g08830	hexA AspGDID:ASPL0000107954 COORDS:Chr5_A_fumigatus_Af293:2265787-2268175W, translated using codon table 1 (537 amino acids) Verified ORF; Putative woronin body protein; hypoxia repressed prote	12.78	9.12	1	5	5	5	537	61.4	8.79
Afu5g10640	Afu5g10640 AspGDID:ASPL0000108128 COORDS:Chr5_A_fumigatus_Af293:2721762-2723271W, translated using codon table 1 (391 amino acids) Uncharacterized ORF; Ortholog(s) have tyrosine-tRNA ligase a	8.60	12.79	1	5	5	5	391	43.6	6.58
Afu6g03810	Afu6g03810 AspGDID:ASPL0000108636 COORDS:Chr6_A_fumigatus_Af293:840093-839212C, translated using codon table 1 (255 amino acids) Uncharacterized ORF; Putative mitochondrial ATP synthase D cha	19.90	30.59	1	5	5	5	255	28.7	9.04
Afu6g12740	Afu6g12740 AspGDID:ASPL0000109617 COORDS:Chr6_A_fumigatus_Af293:3219940-3220875W, translated using codon table 1 (245 amino acids) Uncharacterized ORF; Dienelactone hydrolase family protein	18.28	27.35	1	5	5	5	245	26.9	6.64
Afu8g04570	Afu8g04570 AspGDID:ASPL0000110792 COORDS:Chr8_A_fumigatus_Af293:1042481-1044659W, translated using codon table 1 (607 amino acids) Uncharacterized ORF; Ortholog(s) have nucleus localization	14.79	12.52	1	5	5	5	607	66.6	5.22
Afu5g05500	Afu5g05500 AspGDID:ASPL0000107629 COORDS:Chr5_A_fumigatus_Af293:1277444-1278887W, translated using codon table 1 (424 amino acids) Uncharacterized ORF; Putative phosphoglycerate deh	20.34	19.58	1	5	5	5	424	45.9	7.01
Afu1g09830	Afu1g09830 AspGDID:ASPL0000102049 COORDS:Chr1_A_fumigatus_Af293:2550807-2551983W, translated using codon table 1 (348 amino acids) Uncharacterized ORF; Ortholog(s) have protein complex scaffo	13.52	22.99	1	5	5	5	348	36.3	5.02
Afu1g09930	gcy1 AspGDID:ASPL0000102059 COORDS:Chr1_A_fumigatus_Af293:2570399-2571627W, translated using codon table 1 (349 amino acids) Uncharacterized ORF; Putative glycerol dehydrogenase; protein level	29.58	26.93	1	5	5	6	349	39.1	8.84
Afu1g11180	hsp78 AspGDID:ASPL0000102181 COORDS:Chr1_A_fumigatus_Af293:2946736-2944343C, translated using codon table 1 (797 amino acids) Heat shock protein/chaperonin; transcript dow	10.19	6.40	1	4	4	4	797	88.3	7.02
Afu1g15780	leu2A AspGDID:ASPL0000102641 COORDS:Chr1_A_fumigatus_Af293:4264889-4263452C, translated using codon table 1 (366 amino acids) Uncharacterized ORF; 3-isopropylmalate dehydrogenase with a predi	12.00	14.48	1	4	4	4	366	39.0	5.49
Afu1g10820	Afu1g10820 AspGDID:ASPL0000102145 COORDS:Chr1_A_fumigatus_Af293:2823301-2822605C, translated using codon table 1 (211 amino acids) Uncharacterized ORF; have adenylylsulfate kinase	13.37	28.91	1	4	4	4	211	23.6	6.96
Afu1g12760	capA AspGDID:ASPL0000102344 COORDS:Chr1_A_fumigatus_Af293:3372016-3373824W, translated using codon table 1 (526 amino acids) Uncharacterized ORF; Adenylate cyclase-associated protein	11.51	9.13	1	4	4	4	526	56.4	6.70
Afu2g13540	Afu2g13540 AspGDID:ASPL0000104069 COORDS:Chr2_A_fumigatus_Af293:3521810-3524345W, translated using codon table 1 (744 amino acids) Uncharacterized ORF; Ortholog(s) have nucleus localization	17.94	10.35	1	4	4	4	744	81.9	6.05
Afu3g11640	Afu3g11640 AspGDID:ASPL0000105562 COORDS:Chr3_A_fumigatus_Af293:3058607-3059789W, translated using codon table 1 (368 amino acids) Uncharacterized ORF; Homoserine dehydrogenase; no human	8.79	13.59	1	4	4	4	368	38.5	5.87
Afu4g08040	Afu4g08040 AspGDID:ASPL0000106518 COORDS:Chr4_A_fumigatus_Af293:2090716-2089786C, translated using codon table 1 (218 amino acids) Uncharacterized ORF; Ortholog(s) have GTP binding activity	16.12	27.52	1	4	5	5	218	23.7	8.54
Afu5g03520	Afu5g03520 AspGDID:ASPL0000107530 COORDS:Chr5_A_fumigatus_Af293:949870-951084W, translated using codon table 1 (323 amino acids) Verified ORF; Immunoreactive secreted protein	10.66	18.27	1	4	4	4	323	35.5	6.47
Afu5g07890	Afu5g07890 AspGDID:ASPL0000107861 COORDS:Chr5_A_fumigatus_Af293:1979250-1978604C, translated using codon table 1 (149 amino acids) Uncharacterized ORF; Putative single-stranded DNA binding pr	16.35	30.87	1	4	4	5	149	16.2	9.69
Afu6g10610	Afu6g10610 AspGDID:ASPL0000109416 COORDS:Chr6_A_fumigatus_Af293:2625814-2626707W, translated using codon table 1 (272 amino acids) Uncharacterized ORF; Putative ribose 5-phosphate isomerase A	13.16	20.59	1	4	4	4	272	28.4	6.25
Afu7g02340	Afu7g02340 AspGDID:ASPL0000110029 COORDS:Chr7_A_fumigatus_Af293:635304-636088W, translated using codon table 1 (168 amino acids) Uncharacterized ORF; Ortholog(s) have role in isoleucine biosynt	15.12	33.93	1	4	4	4	168	18.0	8.82
Afu8g05480	Afu8g05480 AspGDID:ASPL0000110878 COORDS:Chr8_A_fumigatus_Af293:1281139-1279447C, translated using codon table 1 (452 amino acids) Uncharacterized ORF; Ortholog(s) have role in nuclear-transcri	15.82	17.26	1	4	4	4	452	50.0	8.47
Afu1g02150	Afu1g02150 AspGDID:ASPL0000101385 COORDS:Chr1_A_fumigatus_Af293:639645-637892C, translated using codon table 1 (519 amino acids) Uncharacterized ORF; Ortholog(s) have glycerol-3-phosphate deh	14.57	11.75	1	4	4	4	519	56.4	8.19
Afu1g03400	Afu1g03400 AspGDID:ASPL0000101510 COORDS:Chr1_A_fumigatus_Af293:991451-988800C, translated using codon table 1 (769 amino acids) Uncharacterized ORF; Ortholog(s) have cytoplasm localization	15.22	8.45	1	4	4	4	769	85.4	6.29
Afu7g02570	Afu7g02570 AspGDID:ASPL0000110052 COORDS:Chr7_A_fumigatus_Af293:707039-704159C, translated using codon table 1 (892 amino acids) Uncharacterized ORF; Ortholog of <i>A. nidulans FGSC A4</i> :	11.76	9.42	1	4	4	4	892	101.1	5.06
Afu1g06710	Afu1g06710 AspGDID:ASPL0000101839 COORDS:Chr1_A_fumigatus_Af293:1922660-1920607C, translated using codon table 1 (564 amino acids) Uncharacterized ORF; Ortholog(s) have chaperonin-containing	14.63	6.56	1	3	3	5	564	61.0	6.34
	Afu2g12980 AspGDID:ASPL0000104011 COORDS:Chr2_A_fumigatus_Af293:3335985-3331790C, translated using codon table 1 (1263 amino acids) Uncharacterized ORF; Putative protein transport protein; transcript downregulated in response to amphotericin B			1	3	3	3	1263	136.7	6.73
	Afu2g12900 AspGDID:ASPL0000104003 COORDS:Chr2_A_fumigatus_Af293:3308048-3307099C, translated using codon table 1 (271 amino acids) Uncharacterized ORF; Ortholog(s) have urease activity, role in urea catabolic process and cytosol, nucleus localization			1	3	3	3	271	29.2	6.23
	Afu3g10610 AspGDID:ASPL0000105459 COORDS:Chr3_A_fumigatus_Af293:2742124-2744940W, translated using codon table 1 (938 amino acids) Uncharacterized ORF; Ortholog of <i>A. nidulans FGSC A4</i> : AN4929, <i>A. niger CBS 513.88</i> : An02g06220, <i>A. oryzae RIB40</i> : AO090003000605, <i>Aspergillus wentii</i> : Aspwe1_0104958 and <i>Aspergillus sydowii</i> : Aspsy1_0147876			1	3	3	3	938	101.2	8.30
	erg6 AspGDID:ASPL0000106182 COORDS:Chr4_A_fumigatus_Af293:1025739-1024484C, translated using codon table 1 (377 amino acids) Uncharacterized ORF; Putative sterol 24-C-methyltransferase with a predicted role in ergosterol biosynthesis; transcript downregulated in response to amphotericin B; induced by exposure to artemisinin; SrbA-regulated during hypoxia			1	3	3	3	377	42.5	6.43
	argB AspGDID:ASPL0000106433 COORDS:Chr4_A_fumigatus_Af293:1868021-1866906C, translated using codon table 1 (371 amino acids) Verified ORF; Ornathine carbamoyltransferase, enzyme of the arginine biosynthesis pathway; hypoxia induced protein			1	3	3	3	371	40.1	7.90
	ypd1 AspGDID:ASPL0000106742 COORDS:Chr4_A_fumigatus_Af293:2687057-2687688W, translated using codon table 1 (171 amino acids) Uncharacterized ORF; Putative histidine-containing phosphotransfer intermediate protein	23.72	23.98	1	3	3	3	171	19.1	4.89
		14.62	10.61	1	3	3	4	537	56.9	5.19
	Afu5g06780 AspGDID:ASPL0000107754 COORDS:Chr5_A_fumigatus_Af293:1670126-1668765C, translated using codon table 1 (453 amino acids) Uncharacterized ORF; Putative carbamoyl-phosphate synthase; protein induced by hydrogen peroxide			1	3	3	3	453	49.3	7.14
	Afu5g07300 AspGDID:ASPL0000107804 COORDS:Chr5_A_fumigatus_Af293:1814759-1815768W, translated using codon table 1 (260 amino acids) Uncharacterized ORF; Electron transfer flavoprotein, beta subunit	9.05	14.23	1	3	3	3	260	28.2	8.97
	sdh2 AspGDID:ASPL0000108103 COORDS:Chr5_A_fumigatus_Af293:2655836-2654821C, translated using codon table 1 (299 amino acids) Uncharacterized ORF; Iron-sulfur protein subunit of succinate dehydrogenase with a predicted role in the citric acid cycle; transcript up-regulated in conidia exposed to neutrophils; induced by exposure to artemisinin; transcript downregulated by hypoxia			1	3	3	3	299	38.0	8.92
	Afu5g11290 AspGDID:ASPL0000108345 COORDS:Chr5_A_fumigatus_Af293:2892452-2891416C, translated using codon table 1 (364 amino acids) Uncharacterized ORF; Ortholog(s) have D-amino acid oxidase activity and role in D-alanine metabolic process, D-valine metabolic process			1	3	3	3	364	39.5	7.91
	Afu6g02380 AspGDID:ASPL0000108693 COORDS:Chr6_A_fumigatus_Af293:443140-444917W, translated using codon table 1 (571 amino acids) Uncharacterized ORF; Ortholog(s) have ubiquitin-specific protease activity, role in protein deubiquitination and nucleoplasm, proteasome complex localization			1	3	3	3	571	63.5	5.96

Gene	Description										
	Afu1g09830 AspGDID:ASPL0000102049 COORDS:Chr1_A_fumigatus_Af293:2550807-2551983W, translated using codon table 1 (348 amino acids) Uncharacterized ORF; Ortholog(s) have protein complex scaffold activity, role in posttranslational protein targeting to membrane, response to heat and TRC complex, nucleus localization					5			5	348	36.3	5.02
	gcy1 AspGDID:ASPL0000102059 COORDS:Chr1_A_fumigatus_Af293:2570399-2571627W, translated using codon table 1 (349 amino acids) Uncharacterized ORF; Putative glycerol dehydrogenase; protein level decreases upon heat shock; transcript up-regulated in conidia exposed to neutrophils		29.58			5	6	349	39.1	8.84
	hsp78 AspGDID:ASPL0000102181 COORDS:Chr1_A_fumigatus_Af293:2946736-2944343C, translated using codon table 1 (797 amino acids) Uncharacterized ORF; Heat shock protein/chaperonin; transcript downregulated in response to voriconazole		60.48		4	4	4	797	88.3	7.02
	leu2A AspGDID:ASPL0000102641 COORDS:Chr1_A_fumigatus_Af293:4264889-4263452C, translated using codon table 1 (366 amino acids) Uncharacterized ORF; 3-isopropylmalate dehydrogenase with a predicted role in leucine biosynthesis; RNA-regulated during hypoxia	12.00	54.96	1	4	4	4	366	39.0	5.49
	Afu1g10820 AspGDID:ASPL0000102145 COORDS:Chr1_A_fumigatus_Af293:2823301-2822605C, translated using codon table 1 (211 amino acids) Uncharacterized ORF; Ortholog(s) have adenylylsulfate kinase activity	13.37	28.91	1	4	4	4	211	23.6	6.96
		11.51	9.13	1	4	4	4	526	56.4	6.70
		17.94	10.35	1	4	4	4	744	81.9	6.05
	Afu3g11640 AspGDID:ASPL0000105562 COORDS:Chr3_A_fumigatus_Af293:3058607-3059789W, translated using codon table 1 (368 amino acids) Uncharacterized ORF; Homoserine dehydrogenase; no human homolog	8.79	13.59	1	4	4	4	368	38.5	5.87
		16.12	27.52	1	4	5	5	218	23.7	8.54
		10.66	18.27	1	4	4	4	323	35.5	6.47
	Afu5g07890 AspGDID:ASPL0000107861 COORDS:Chr5_A_fumigatus_Af293:1979250-1978604C, translated using codon table 1 (149 amino acids) Uncharacterized ORF; Putative single-stranded DNA binding protein family member	16.35	30.87	1	4	4	5	149	16.2	9.69
	Afu6g10610 AspGDID:ASPL0000109416 COORDS:Chr6_A_fumigatus_Af293:2625814-2626707W, translated using codon table 1 (272 amino acids) Uncharacterized ORF; Putative ribose 5-phosphate isomerase A	13.16	20.59	1	4	4	4	272	28.4	6.25
	Afu7g02340 AspGDID:ASPL0000102029 COORDS:Chr7_A_fumigatus_Af293:635304-636088W, translated using codon table 1 (168 amino acids) Uncharacterized ORF; Ortholog(s) have role in isoleucine biosynthetic process, mitochondrial translation and mitochondrial matrix localization			4	4	4	4	168	18.0	8.82
	Afu8g05480 AspGDID:ASPL0000110878 COORDS:Chr8_A_fumigatus_Af293:1281136-1279477C, translated using codon table 1 (452 amino acids) Uncharacterized ORF; Ortholog(s) have role in nuclear-transcribed mRNA catabolic process, meiosis-specific transcripts, poly(A)+ mRNA export from nucleus and nucleus localization	15.82		4	4	4	4	452	50.0	8.47
	Afu1g02150 AspGDID:ASPL0000101385 COORDS:Chr1_A_fumigatus_Af293:639645-637892C, translated using codon table 1 (519 amino acids) Uncharacterized ORF; Ortholog(s) have glycerol-3-phosphate dehydrogenase [NAD+] activity and role in NADH oxidation, cell-abiotic substrate adhesion, glycerol biosynthetic process, intracellular accumulation of glycerol	14.57	11.75	519	56.4	8.19
		15.22	8.45	1	4	4	4	769	85.4	6.29
	Afu7g02570 AspGDID:ASPL0000110052 COORDS:Chr7_A_fumigatus_Af293:707039-704159C, translated using codon table 1 (892 amino acids) Uncharacterized ORF; Ortholog of <i>A. nidulans FGSC A4</i> : AN9067/tinC, AN2767/hetC, <i>A. fumigatus Af293</i> : Afu2g15840, <i>A. niger CBS 513.88</i> : An15g06140 and <i>A. oryzae RIB40</i> : AO090038000633, AO090012000230									5.06
Afu1g06710	Afu1g06710 AspGDID:ASPL0000101655 COORDS:Chr1_A_fumigatus_Af293:1522000-1526007C, translated using codon table 1 (304 amino acids) Uncharacterized ORF; Ortholog(s) have chaperonin-containing	14.05	6.30		1	3	3	3	304	61.0	6.51
Afu2g11260	luA AspGDID:ASPL0000103841 COORDS:Chr2_A_fumigatus_Af293:2894027-2896466W, translated using codon table 1 (777 amino acids) Uncharacterized ORF; Putative 3-isopropylmalate dehydratase with a pr	13.55	6.44		1	3	4	4	777	84.0	5.94
Afu2g12980	Afu2g12980 AspGDID:ASPL0000104011 COORDS:Chr2_A_fumigatus_Af293:3335985-3331790C, translated using codon table 1 (1263 amino acids) Uncharacterized ORF; Putative protein transport protein; trans	9.50	2.85		1	3	3	3	1263	136.7	6.73
Afu2g12900	Afu2g12900 AspGDID:ASPL0000104003 COORDS:Chr2_A_fumigatus_Af293:3308048-3307099C, translated using codon table 1 (271 amino acids) Uncharacterized ORF; Ortholog(s) have urease activity, role in	10.18	11.44		1	3	3	3	271	29.2	6.23
Afu3g10610	Afu3g10610 AspGDID:ASPL0000105459 COORDS:Chr3_A_fumigatus_Af293:2742124-2744940W, translated using codon table 1 (938 amino acids) Uncharacterized ORF; Ortholog of <i>A. nidulans FGSC A4</i>	4.82	4.05		1	3	3	3	938	101.5	5.82
Afu4g03630	erg6 AspGDID:ASPL0000106182 COORDS:Chr4_A_fumigatus_Af293:1025739-1024484C, translated using codon table 1 (377 amino acids) Uncharacterized ORF; Putative sterol 24-C-methyltransferase with a pr	11.48	13.53		1	3	3	3	377	42.5	6.43
Afu4g07190	argB AspGDID:ASPL0000106433 COORDS:Chr4_A_fumigatus_Af293:1868021-1866906C, translated using codon table 1 (371 amino acids) Verified ORF; Ornathine carbamoyltransferase, enzyme of the arginine	10.59	11.59		1	3	3	3	371	40.1	7.90
Afu4g10280	ypd1 AspGDID:ASPL0000106742 COORDS:Chr4_A_fumigatus_Af293:2687057-2687688W, translated using codon table 1 (171 amino acids) Uncharacterized ORF; Putative histidine-containing phosphotransfer in	8.72	23.98		1	3	3	3	171	19.1	4.89
Afu5g04160	Afu5g04160 AspGDID:ASPL0000107595 COORDS:Chr5_A_fumigatus_Af293:1105009-1106759W, translated using codon table 1 (537 amino acids) Uncharacterized ORF; NTF2 and RRM domain protein	14.62	10.61		1	3	3	4	537	56.9	5.19
Afu5g06780	Afu5g06780 AspGDID:ASPL0000107754 COORDS:Chr5_A_fumigatus_Af293:1670126-1668765C, translated using codon table 1 (453 amino acids) Uncharacterized ORF; Putative carbamoyl-phosphate synthase;	12.01	12.58		1	3	3	3	453	49.3	7.14
Afu5g07300	Afu5g07300 AspGDID:ASPL0000107804 COORDS:Chr5_A_fumigatus_Af293:1814759-1815768W, translated using codon table 1 (260 amino acids) Uncharacterized ORF; Electron transfer flavoprotein, beta subu	9.05	14.23		1	3	3	3	260	28.2	8.97
Afu5g10370	sdh2 AspGDID:ASPL0000108103 COORDS:Chr5_A_fumigatus_Af293:2655836-2654821C, translated using codon table 1 (299 amino acids) Uncharacterized ORF; Iron-sulfur protein subunit of succinate dehydro	8.52	11.37		1	3	3	3	299	33.9	8.92
Afu5g11290	Afu5g11290 AspGDID:ASPL0000108188 COORDS:Chr5_A_fumigatus_Af293:2892452-2891116C, translated using codon table 1 (364 amino acids) Uncharacterized ORF; Ortholog(s) have D-amino-acid oxidase a	9.83	10.44		1	3	3	3	364	39.5	7.91
Afu6g02380	Afu6g02380 AspGDID:ASPL0000108693 COORDS:Chr6_A_fumigatus_Af293:443140-444917W, translated using codon table 1 (571 amino acids) Uncharacterized ORF; Ortholog(s) have ubiquitin-specific proteas	7.35	8.58		1	3	3	3	571	63.2	5.96
Afu6g06325	Afu6g06325 AspGDID:ASPL0000108991 COORDS:Chr6_A_fumigatus_Af293:1334658-1334305C, translated using codon table 1 (98 amino acids) Uncharacterized ORF; Ortholog(s) have RNA binding activity and	3.78	26.53		1	3	3	3	98	10.6	4.72
Afu6g06840	Afu6g06840 AspGDID:ASPL0000109046 COORDS:Chr6_A_fumigatus_Af293:1497495-1497936W, translated using codon table 1 (120 amino acids) Uncharacterized ORF; Transcript up-regulated in conidia expos	11.78	42.50		1	3	3	3	120	13.0	11.05
Afu7g04070	Afu7g04070 AspGDID:ASPL0000110102 COORDS:Chr7_A_fumigatus_Af293:916318-915016C, translated using codon table 1 (369 amino acids) Uncharacterized ORF; Ortholog(s) have 3-deoxy-7-phosphoheptu	14.53	14.63		1	3	3	3	369	40.0	6.74
Afu4g06950	Afu4g06950 AspGDID:ASPL0000106409 COORDS:Chr4_A_fumigatus_Af293:1799230-1797998C, translated using codon table 1 (284 amino acids) Uncharacterized ORF; Putative endoplasmic reticulum (ER) typ	8.79	14.79		1	3	3	3	284	30.9	6.14
Afu1g15960	Afu1g15960 AspGDID:ASPL0000102659 COORDS:Chr1_A_fumigatus_Af293:4331468-4333260W, translated using codon table 1 (554 amino acids) Uncharacterized ORF; Ortholog(s) have flavin adenine dinucleo	10.45	8.66		1	3	3	3	554	60.1	8.70
Afu2g03140	Afu2g03140 AspGDID:ASPL0000103143 COORDS:Chr2_A_fumigatus_Af293:823665-822897C, translated using codon table 1 (211 amino acids) Uncharacterized ORF; Ortholog(s) have peptide-methionine (S)-S	12.20	18.48		1	3	3	4	211	23.6	7.20
Afu2g06040	Afu2g06040 AspGDID:ASPL0000103427 COORDS:Chr2_A_fumigatus_Af293:1706686-1708648W, translated using codon table 1 (612 amino acids) Uncharacterized ORF; Putative actin cortical patch component	9.87	7.03		1	3	3	3	612	65.1	6.42
Afu2g04940	Afu2g04940 AspGDID:ASPL0000103319 COORDS:Chr2_A_fumigatus_Af293:1358892-1357362C, translated using codon table 1 (470 amino acids) Uncharacterized ORF; Ortholog(s) have mRNA binding activity,	7.57	10.21		1	3	3	4	470	49.1	7.72
Afu1g07530	Afu1g07530 AspGDID:ASPL0000101918 COORDS:Chr1_A_fumigatus_Af293:2122230-2121254C, translated using codon table 1 (257 amino acids) Uncharacterized ORF; Ortholog(s) have adenylate kinase activi	8.36	10.51		1	2	2	2	257	28.7	7.88
Afu1g08960	Afu1g08960 AspGDID:ASPL0000101962 COORDS:Chr1_A_fumigatus_Af293:2324414-2325074W, translated using codon table 1 (167 amino acids) Uncharacterized ORF; Ortholog of <i>A. nidulans FGSC A4</i>	6.30	16.17		1	2	2	2	167	17.7	8.88
Afu1g02290	Afu1g02290 AspGDID:ASPL0000101399 COORDS:Chr1_A_fumigatus_Af293:670312-669933C, translated using codon table 1 (106 amino acids) Uncharacterized ORF; Protein of unknown function; calcium down	15.10	29.25		1	2	2	3	106	11.8	4.58
Afu1g02940	Afu1g02940 AspGDID:ASPL0000101464 COORDS:Chr1_A_fumigatus_Af293:841245-842768W, translated using codon table 1 (446 amino acids) Uncharacterized ORF; Ortholog(s) have GTPase activator activity,	7.12	7.17		1	2	2	2	446	49.7	9.26
Afu2g03830	aspf4 AspGDID:ASPL0000103209 COORDS:Chr2_A_fumigatus_Af293:1016683-1017651W, translated using codon table 1 (322 amino acids) Verified ORF; Allergen Asp f 4; higher expression in biofilm vs plankto	9.17	11.18		1	2	2	2	322	34.1	5.35
Afu2g10270	tor AspGDID:ASPL0000103742 COORDS:Chr2_A_fumigatus_Af293:2631516-2624171C, translated using codon table 1 (2384 amino acids) Uncharacterized ORF; Tor kinase, involved in regulation cell wall biosyn	5.48	0.92		1	2	2	2	2384	269.4	6.90
Afu2g14960	Afu2g14960 AspGDID:ASPL0000104211 COORDS:Chr2_A_fumigatus_Af293:3942076-3942959W, translated using codon table 1 (271 amino acids) Uncharacterized ORF; Ortholog(s) have RNA polymerase II act	5.27	7.01		1	2	2	2	271	28.8	4.91
Afu2g04710	Afu2g04710 AspGDID:ASPL0000103297 COORDS:Chr2_A_fumigatus_Af293:1288894-1287776C, translated using codon table 1 (217 amino acids) Uncharacterized ORF; Has domain(s) with predicted heme bind	6.34	11.52		1	2	2	2	217	23.9	5.59
Afu2g12400	Afu2g12400 AspGDID:ASPL0000103954 COORDS:Chr2_A_fumigatus_Af293:3185304-3186292W, translated using codon table 1 (227 amino acids) Uncharacterized ORF; Putative ATP synthase oligomycin sensit	8.20	11.01		1	2	2	2	227	24.4	9.64
Afu3g06640	Afu3g06640 AspGDID:ASPL0000105075 COORDS:Chr3_A_fumigatus_Af293:1644938-1644430C, translated using codon table 1 (82 amino acids) Uncharacterized ORF; Ortholog(s) have structural constituent of	2.57	18.29		1	2	2	2	82	8.9	9.26
Afu3g10630	Afu3g10630 AspGDID:ASPL0000105461 COORDS:Chr3_A_fumigatus_Af293:2747083-2747630W, translated using codon table 1 (123 amino acids) Uncharacterized ORF; Ortholog(s) have mitochondrion localiza	14.16	33.33		1	2	3	3	123	13.6	4.88
Afu3g14665	Afu3g14665 AspGDID:ASPL0000105856 COORDS:Chr3_A_fumigatus_Af293:3889703-3890168W, translated using codon table 1 (132 amino acids) Uncharacterized ORF; Ortholog of <i>Neosartorya fischeri NRR	7.48	22.73		1	2	2	2	132	14.6	4.45
Afu4g07650	cyp6 AspGDID:ASPL0000106480 COORDS:Chr4_A_fumigatus_Af293:1987776-1988776W, translated using codon table 1 (209 amino acids) Uncharacterized ORF; Putative peptidyl-prolyl cis-trans isomerase	6.79	11.96		1	2	2	2	209	22.9	8.28
AfuMt00120	AfuMt00120 AspGDID:ASPL0000366358 COORDS:mito_A_fumigatus_Af293:25862-26623W, translated using codon table 4 (253 amino acids) Uncharacterized ORF; Ortholog(s) have cytochrome-c oxidase activi	5.99	10.67		1	2	2	2	253	29.0	4.77
Afu5g06320	Afu5g06320 AspGDID:ASPL0000107708 COORDS:Chr5_A_fumigatus_Af293:1519087-1518035C, translated using codon table 1 (169 amino acids) Uncharacterized ORF; Ortholog(s) have role in cellular protein	7.22	8.28		1	2	2	2	169	19.1	8.34
Afu5g12130	rab7 AspGDID:ASPL0000108269 COORDS:Chr5_A_fumigatus_Af293:3142524-3143388W, translated using codon table 1 (171 amino acids) Uncharacterized ORF; Rab small monomeric GTPase	6.16	14.04		1	2	2	2	171	19.2	8.12
Afu6g02090	Afu6g02090 AspGDID:ASPL0000108664 COORDS:Chr6_A_fumigatus_Af293:353609-352850C, translated using codon table 1 (232 amino acids) Uncharacterized ORF; Have fungal-type vacuole mem	6.82	9.05		1	2	2	2	232	26.2	8.66
Afu6g03590	mcsA AspGDID:ASPL0000108814 COORDS:Chr6_A_fumigatus_Af293:783347-784866W, translated using codon table 1 (465 amino acids) Verified ORF; Methylcitrate synthase; catalyses the condensation of pro	3.72	6.24		1	2	2	2	465	51.4	8.94
Afu6g13140	Afu6g13140 AspGDID:ASPL0000109656 COORDS:Chr6_A_fumigatus_Af293:3322359-3321489C, translated using codon table 1 (232 amino acids) Uncharacterized ORF; Ortholog(s) have 3,4-dihydroxy-2-butano	6.92	10.34		1	2	2	2	232	25.3	5.03
Afu6g13670	Afu6g13670 AspGDID:ASPL0000109708 COORDS:Chr6_A_fumigatus_Af293:3483620-3485062W, translated using codon table 1 (338 amino acids) Uncharacterized ORF; Ortholog(s) have role in cellular protein	6.17	7.10		1	2	2	2	338	37.7	6.19
Afu4g04410	Afu4g04410 AspGDID:ASPL0000106258 COORDS:Chr4_A_fumigatus_Af293:1247460-1248557W, translated using codon table 1 (319 amino acids) Uncharacterized ORF; Immunoreactive protein; has predicted	9.11	10.03		1	2	2	2	319	33.7	7.37

Table S5: MkkB-GFP (Afu3g05900) interacting proteins at 24 hours of vegetative growth. Proteins of interest are highlighted in yellow. HamE (Afu5g13970), SteC (Afu5g06420), MpkB (Afu6g12820), SteD (Afu2g17130).

Table S5: *Aspergillus fumigatus* MkkB-GFP interacting proteins (Vegetative growth-24 hours)

Accession	Description	Score	Coverage	# Proteins	# Unique Peptides	# Peptides	# PSMs	# AAs	MW [kDa]	calc. pI
Afu3g05900	ste7 AspGDID:ASPL0000105003 COORDS:Chr3_A_fumigatus_Af293:1444958-1446786W, translated using codon table 1 (536 amino acids) Uncharacterized ORF; MAP kinase kinase (	374.55	71.08	1	29	29	87	536	58.5	9.07
Afu5g06420	Afu5g06420 AspGDID:ASPL0000107718 COORDS:Chr5_A_fumigatus_Af293:1549998-1553242W, translated using codon table 1 (1007 amino acids) Uncharacterized ORF; Ortholog(s	350.23	63.26	1	50	50	83	1007	111.6	8.60
Afu1g12680	Afu1g12680 AspGDID:ASPL0000102336 COORDS:Chr1_A_fumigatus_Af293:3351052-3347476C, translated using codon table 1 (1072 amino acids) Uncharacterized ORF; Ortholog(s) have Rho GTPase activato	252.72	51.59	1	43	43	60	1072	117.7	6.77
Afu2g17130	Afu2g17130 AspGDID:ASPL0000104429 COORDS:Chr2_A_fumigatus_Af293:4574963-4576567W, translated using codon table 1 (487 amino acids) Uncharacterized ORF; Ortholog(s)	147.10	62.42	1	22	22	34	487	53.5	6.14
Afu1g07090	Afu1g07090 AspGDID:ASPL0000101875 COORDS:Chr1_A_fumigatus_Af293:2015732-2011032C, translated using codon table 1 (1526 amino acids) Uncharacterized ORF; Ortholog of <i>A. nidulans FGSC A4</	127.99	30.01	1	31	31	33	1526	164.4	6.65
Afu2g02770	Afu2g02770 AspGDID:ASPL0000103107 COORDS:Chr2_A_fumigatus_Af293:716490-719616W, translated using codon table 1 (1008 amino acids) Uncharacterized ORF; Ortholog of <i>A. nidulans FGSC A4</i>	48.48	21.92	1	13	13	14	1008	109.2	10.18
Afu5g13970	Afu5g13970 AspGDID:ASPL0000108448 COORDS:Chr5_A_fumigatus_Af293:3651112-3656167W, translated using codon table 1 (1593 amino acids) Uncharacterized ORF; Ortholog(s	47.80	13.12	1	12	12	13	1593	174.0	9.74
Afu4g11830	Afu4g11830 AspGDID:ASPL0000106891 COORDS:Chr4_A_fumigatus_Af293:3122796-3124999W, translated using codon table 1 (713 amino acids) Uncharacterized ORF; Ortholog(s) have U2-type spliceosomal	41.60	23.98	1	10	10	10	713	83.4	7.12
Afu5g02160	Afu5g02160 AspGDID:ASPL0000107396 COORDS:Chr5_A_fumigatus_Af293:552208-549993C, translated using codon table 1 (613 amino acids) Uncharacterized ORF; Ortholog(s) have nucleolus localization	31.20	17.78	1	7	7	8	613	65.8	7.34
Afu5g02770	Afu5g02770 AspGDID:ASPL0000107457 COORDS:Chr5_A_fumigatus_Af293:729618-731162W, translated using codon table 1 (514 amino acids) Uncharacterized ORF; Ortholog of <i>A. nidulans FGSC A4</i>	27.14	14.98	1	5	5	6	514	56.3	8.53
Afu3g11480	Afu3g11480 AspGDID:ASPL0000105546 COORDS:Chr3_A_fumigatus_Af293:3012552-3013542W, translated using codon table 1 (308 amino acids) Uncharacterized ORF; Putative enoyl-CoA hydratase	26.12	31.17	1	7	7	7	308	33.0	9.26
Afu4g12750	Afu4g12750 AspGDID:ASPL0000106981 COORDS:Chr4_A_fumigatus_Af293:3344997-3342675C, translated using codon table 1 (750 amino acids) Uncharacterized ORF; Ortholog(s) have role in deadenylation-	25.40	16.13	1	9	9	9	750	84.8	6.99
Afu7g03670	Afu7g03670 AspGDID:ASPL0000110062 COORDS:Chr7_A_fumigatus_Af293:783542-785758W, translated using codon table 1 (604 amino acids) Uncharacterized ORF; Ortholog of <i>A. nidulans FGSC A4</i>	25.07	16.89	1	5	5	5	604	65.7	7.14
Afu5g03340	Afu5g03340 AspGDID:ASPL0000107513 COORDS:Chr5_A_fumigatus_Af293:900468-901964W, translated using codon table 1 (498 amino acids) Uncharacterized ORF; Ortholog of <i>A. nidulans FGSC A4</i>	24.09	11.82	1	6	6	7	498	57.0	5.20
Afu4g03160	Afu4g03160 AspGDID:ASPL0000106134 COORDS:Chr4_A_fumigatus_Af293:886361-887395W, translated using codon table 1 (344 amino acids) Uncharacterized ORF; Ortholog(s) have U2-type spliceosomal co	22.99	22.97	1	5	5	6	344	37.8	5.82
Afu3g10240	Afu3g10240 AspGDID:ASPL0000105422 COORDS:Chr3_A_fumigatus_Af293:2649693-2642482C, translated using codon table 1 (2327 amino acids) Uncharacterized ORF; Ortholog(s) have cytosol, nucleus loca	22.86	4.81	1	9	9	9	2327	259.0	5.95
Afu2g15840	Afu2g15840 AspGDID:ASPL0000104301 COORDS:Chr2_A_fumigatus_Af293:4185756-4183151C, translated using codon table 1 (804 amino acids) Uncharacterized ORF; Ortholog of <i>A. nidulans FGSC A4</i	21.26	11.82	1	6	6	6	804	88.6	6.81
Afu6g12600	Afu6g12600 AspGDID:ASPL0000109603 COORDS:Chr6_A_fumigatus_Af293:3185640-3183146C, translated using codon table 1 (704 amino acids) Uncharacterized ORF; Ortholog of <i>A. nidulans FGSC A4</i	19.73	13.78	1	6	6	6	704	76.2	5.55
Afu2g13040	grpE AspGDID:ASPL0000104018 COORDS:Chr2_A_fumigatus_Af293:3347479-3346582C, translated using codon table 1 (250 amino acids) Uncharacterized ORF; Mitochondrial co-chaperone; protein level decre	19.03	26.80	1	5	5	6	250	28.4	8.25
Afu6g06345	Afu6g06345 AspGDID:ASPL0000108995 COORDS:Chr6_A_fumigatus_Af293:1347575-1348344W, translated using codon table 1 (205 amino acids) Uncharacterized ORF; Ortholog(s) have 6,7-dimethyl-8-ribityllu	15.36	42.44	1	4	4	4	205	21.5	6.10
Afu6g12820	mpkB AspGDID:ASPL0000109625 COORDS:Chr6_A_fumigatus_Af293:3233954-3232650C, translated using codon table 1 (353 amino acids) Uncharacterized ORF; Putative mitogen-ac	14.86	18.13	1	5	5	5	353	40.8	6.90
Afu7g04550	Afu7g04550 AspGDID:ASPL0000110148 COORDS:Chr7_A_fumigatus_Af293:1037177-1035943C, translated using codon table 1 (389 amino acids) Uncharacterized ORF; Has domain(s) with predicted ATP bindi	14.84	13.11	1	4	4	4	389	43.2	7.78
Afu6g02620	Afu6g02620 AspGDID:ASPL0000108122 COORDS:Chr6_A_fumigatus_Af293:503629-501127C, translated using codon table 1 (762 amino acids) Uncharacterized ORF; Has domain(s) with predicted 2-dehydropa	14.55	10.50	1	4	4	4	762	82.9	7.46
Afu4g08040	Afu4g08040 AspGDID:ASPL0000106518 COORDS:Chr4_A_fumigatus_Af293:2090716-2089786C, translated using codon table 1 (218 amino acids) Uncharacterized ORF; Ortholog(s) have GTP binding activity	14.36	27.52	1	5	5	5	218	23.7	8.54
Afu3g10740	Afu3g10740 AspGDID:ASPL0000105472 COORDS:Chr3_A_fumigatus_Af293:2782828-2781858C, translated using codon table 1 (262 amino acids) Uncharacterized ORF; Putative RAB GTPase with a predicted r	14.23	24.81	1	4	4	4	262	27.6	4.84
Afu5g12250	Afu5g12250 AspGDID:ASPL0000108281 COORDS:Chr5_A_fumigatus_Af293:3179873-3182548W, translated using codon table 1 (731 amino acids) Uncharacterized ORF; Ortholog(s) have role in cellular respon	13.74	6.98	1	4	4	4	731	83.0	6.23
Afu1g09630	Afu1g09630 AspGDID:ASPL0000102029 COORDS:Chr1_A_fumigatus_Af293:2492509-2488889C, translated using codon table 1 (1056 amino acids) Uncharacterized ORF; Ortholog of <i>A. nidulans FGSC A4</	13.19	4.17	1	3	3	3	1056	114.4	9.54
Afu5g08230	Afu5g08230 AspGDID:ASPL0000107895 COORDS:Chr5_A_fumigatus_Af293:2087574-2086099C, translated using codon table 1 (473 amino acids) Uncharacterized ORF; Has domain(s) with predicted zinc ion b	13.00	15.86	1	4	4	4	473	51.8	8.24
Afu5g07800	Afu5g07800 AspGDID:ASPL0000107852 COORDS:Chr5_A_fumigatus_Af293:1954043-1956749W, translated using codon table 1 (439 amino acids) Uncharacterized ORF; Ortholog of <i>A. nidulans FGSC A4</i	12.96	8.20	1	2	2	2	439	45.7	10.21
Afu1g06710	Afu1g06710 AspGDID:ASPL0000101839 COORDS:Chr1_A_fumigatus_Af293:1922660-1920607C, translated using codon table 1 (564 amino acids) Uncharacterized ORF; Ortholog(s) have chaperonin-containing	12.82	7.27	1	2	2	3	564	61.0	6.34
Afu2g11750	Afu2g11750 AspGDID:ASPL0000103889 COORDS:Chr2_A_fumigatus_Af293:3018382-3020166W, translated using codon table 1 (543 amino acids) Uncharacterized ORF; Ortholog(s) have mitochondrion localiza	12.04	8.66	1	3	3	3	543	57.1	9.41
Afu2g13540	Afu2g13540 AspGDID:ASPL0000104069 COORDS:Chr2_A_fumigatus_Af293:3521810-3524345W, translated using codon table 1 (744 amino acids) Uncharacterized ORF; Ortholog(s) have nucleus localization	11.53	5.65	1	3	3	3	744	81.9	6.05
Afu1g03010	Afu1g03010 AspGDID:ASPL0000101471 COORDS:Chr1_A_fumigatus_Af293:869019-866374C, translated using codon table 1 (881 amino acids) Uncharacterized ORF; Ortholog(s) have U2-type spliceosomal co	9.88	4.31	1	3	3	3	881	100.8	9.95
Afu6g07980	Afu6g07980 AspGDID:ASPL0000109158 COORDS:Chr6_A_fumigatus_Af293:1850730-1849524C, translated using codon table 1 (323 amino acids) Uncharacterized ORF; Ortholog(s) have RNA polymerase II co	9.65	11.76	1	3	3	3	323	36.6	7.59
Afu4g06890	cyp51A AspGDID:ASPL0000106403 COORDS:Chr4_A_fumigatus_Af293:1785331-1783713C, translated using codon table 1 (515 amino acids) Verified ORF; 14-alpha sterol demethylase; commonly mutated in c	9.21	7.38	1	3	3	3	515	58.0	8.53
Afu2g10270	tor AspGDID:ASPL0000103742 COORDS:Chr2_A_fumigatus_Af293:2631516-2624171C, translated using codon table 1 (2384 amino acids) Uncharacterized ORF; Tor kinase, involved in regulation cell wall biosy	8.98	2.06	1	3	3	3	2384	269.4	6.90
Afu1g09840	tim44 AspGDID:ASPL0000102050 COORDS:Chr1_A_fumigatus_Af293:2554479-2552871C, translated using codon table 1 (515 amino acids) Uncharacterized ORF; Mitochondrial inner membrane translocase su	8.75	10.29	1	4	4	4	515	57.7	9.11
Afu6g03590	mcsA AspGDID:ASPL0000108814 COORDS:Chr6_A_fumigatus_Af293:783347-784866W, translated using codon table 1 (465 amino acids) Verified ORF; Methylcitrate synthase; catalyses the condensation of pro	8.06	9.46	1	3	3	3	465	51.4	8.94
Afu6g12740	Afu6g12740 AspGDID:ASPL0000109617 COORDS:Chr6_A_fumigatus_Af293:3219940-3220875W, translated using codon table 1 (245 amino acids) Uncharacterized ORF; Dienelactone hydrolase family protein	7.80	17.96	1	3	3	3	245	26.9	6.64
Afu5g07890	Afu5g07890 AspGDID:ASPL0000107861 COORDS:Chr5_A_fumigatus_Af293:1979250-1978604C, translated using codon table 1 (149 amino acids) Uncharacterized ORF; Putative single-stranded DNA binding pr	6.15	17.45	1	2	2	2	149	16.2	9.69
Afu7g05260	Afu7g05260 AspGDID:ASPL0000110219 COORDS:Chr7_A_fumigatus_Af293:1249230-1250373W, translated using codon table 1 (304 amino acids) Uncharacterized ORF; Has domain(s) with predicted nucleic a	5.91	11.51	1	2	2	2	304	34.4	8.72
Afu5g07370	Afu5g07370 AspGDID:ASPL0000107811 COORDS:Chr5_A_fumigatus_Af293:1844081-1842511C, translated using codon table 1 (500 amino acids) Uncharacterized ORF; Ortholog(s) have metal ion binding, pol	5.62	7.80	1	3	3	3	500	53.8	7.08
Afu1g02510	Afu1g02510 AspGDID:ASPL0000101421 COORDS:Chr1_A_fumigatus_Af293:729361-725524C, translated using codon table 1 (1018 amino acids) Uncharacterized ORF; Has domain(s) with predicted RNA bindin	4.87	3.73	1	2	2	2	1018	112.0	7.34
AfuMt00120	AfuMt00120 AspGDID:ASPL0000366358 COORDS:mito_A_fumigatus_Af293:25862-26623W, translated using codon table 4 (253 amino acids) Uncharacterized ORF; Ortholog(s) have cytochrome-c oxidase activ	4.76	10.67	1	2	2	2	253	29.0	4.77
Afu3g06640	Afu3g06640 AspGDID:ASPL0000105075 COORDS:Chr3_A_fumigatus_Af293:1644938-1644430C, translated using codon table 1 (82 amino acids) Uncharacterized ORF; Ortholog(s) have structural constituent o	2.69	18.29	1	2	2	2	82	8.9	9.26

Table S6: MpkB-GFP (Afu6g12820) interacting proteins at 24 hours of vegetative growth. Proteins of interest are highlighted in yellow. MkkB (Afu3g05900), SteD (Afu2g17130), SteA (Afu5g06190).

Table S6: *Aspergillus fumigatus* MpkB-GFP interacting proteins (Vegetative growth-24 hours)

Accession	Description	Score	Coverage	# Proteins	# Unique Peptides	# Peptides	# PSMs	# AAs	MW [kDa]	calc. pI
Afu6g12820	mpkB AspGDID:ASPL0000109625 COORDS:Chr6_A_fumigatus_Af293:3233954-3232650C, translated using codon table 1 (353 amino acids) Uncharacterized ORF; Putative mitogen-activated p...	230.62	77.34	1	20	20	43	353	40.8	6.90
Afu6g04600	Afu6g04600 AspGDID:ASPL0000108914 COORDS:Chr6_A_fumigatus_Af293:1069099-1067587C, translated using codon table 1 (477 amino acids) Uncharacterized ORF; Ortholog of <i>A. nidulans FGSC A4</i> : AN6560...	175.75	53.25	1	19	19	35	477	50.7	10.23
Afu5g06190	steA AspGDID:ASPL0000107696 COORDS:Chr5_A_fumigatus_Af293:1482488-1484873W, translated using codon table 1 (688 amino acids) Uncharacterized ORF; Putative transcription factor	51.27	21.08	1	11	11	16	688	76.6	6.64
Afu3g09820	dvrA AspGDID:ASPL0000105380 COORDS:Chr3_A_fumigatus_Af293:2515556-2517655W, translated using codon table 1 (679 amino acids) Verified ORF; C2H2 zinc finger domain protein; putative ortholog of C. albicans...	44.68	20.03	1	9	9	12	679	73.2	9.48
Afu1g12680	Afu1g12680 AspGDID:ASPL0000102336 COORDS:Chr1_A_fumigatus_Af293:3351052-3347476C, translated using codon table 1 (1072 amino acids) Uncharacterized ORF; Ortholog(s) have Rho GTPase activator activity	30.93	8.30	1	6	6	8	1072	117.7	6.77
Afu5g02160	Afu5g02160 AspGDID:ASPL0000107396 COORDS:Chr5_A_fumigatus_Af293:552208-549993C, translated using codon table 1 (613 amino acids) Uncharacterized ORF; Ortholog(s) have nucleolus localization	27.37	13.38	1	4	4	5	613	65.8	7.34
Afu1g00460	Afu1g00460 AspGDID:ASPL0000101218 COORDS:Chr1_A_fumigatus_Af293:146969-145247C, translated using codon table 1 (507 amino acids) Uncharacterized ORF; Ortholog(s) have intracellular localization	24.67	19.92	1	7	7	7	507	55.8	6.15
Afu1g03010	Afu1g03010 AspGDID:ASPL0000101471 COORDS:Chr1_A_fumigatus_Af293:869019-866374C, translated using codon table 1 (881 amino acids) Uncharacterized ORF; Ortholog(s) have U2-type spliceosomal complex loca...	23.75	9.65	1	6	6	7	881	100.8	9.95
Afu2g16020	Afu2g16020 AspGDID:ASPL0000104319 COORDS:Chr2_A_fumigatus_Af293:4237810-4239808W, translated using codon table 1 (566 amino acids) Uncharacterized ORF; Putative heat shock protein; transcript induced du...	21.91	15.55	1	4	4	4	566	61.7	6.87
Afu2g03830	aspf4 AspGDID:ASPL0000103209 COORDS:Chr2_A_fumigatus_Af293:1016683-1017651W, translated using codon table 1 (322 amino acids) Verified ORF; Allergen Asp f 4; higher expression in biofilm vs planktonic cells;	20.89	27.64	1	5	5	5	322	34.1	5.35
Afu2g13860	Afu2g13860 AspGDID:ASPL0000104101 COORDS:Chr2_A_fumigatus_Af293:3619597-3620049W, translated using codon table 1 (142 amino acids) Uncharacterized ORF; Histone H4	19.74	23.24	1	4	4	4	142	15.8	10.21
Afu3g10240	Afu3g10240 AspGDID:ASPL0000105422 COORDS:Chr3_A_fumigatus_Af293:2649693-2642482C, translated using codon table 1 (2327 amino acids) Uncharacterized ORF; Ortholog(s) have cytosol, nucleus localization	18.61	3.91	1	7	7	7	2327	259.0	5.95
Afu4g03160	Afu4g03160 AspGDID:ASPL0000106134 COORDS:Chr4_A_fumigatus_Af293:886361-887395W, translated using codon table 1 (344 amino acids) Uncharacterized ORF; Ortholog(s) have U2-type spliceosomal complex, cyt...	16.95	24.13	1	5	5	5	344	37.8	5.82
Afu6g12600	Afu6g12600 AspGDID:ASPL0000109603 COORDS:Chr6_A_fumigatus_Af293:3185640-3183146C, translated using codon table 1 (704 amino acids) Uncharacterized ORF; Ortholog of <i>A. nidulans FGSC A4</i> : AN3693...	16.46	12.93	1	6	6	6	704	76.2	5.55
Afu7g03670	Afu7g03670 AspGDID:ASPL0000110062 COORDS:Chr7_A_fumigatus_Af293:783542-785758W, translated using codon table 1 (604 amino acids) Uncharacterized ORF; Ortholog of <i>A. nidulans FGSC A4</i> : AN8289,	16.17	11.26	1	2	2	3	604	65.7	7.14
Afu5g12250	Afu5g12250 AspGDID:ASPL0000108281 COORDS:Chr5_A_fumigatus_Af293:3179873-3182548W, translated using codon table 1 (731 amino acids) Uncharacterized ORF; Ortholog(s) have role in cellular response to DNA...	16.15	9.99	1	5	5	5	731	83.0	6.23
Afu2g03810	hosA AspGDID:ASPL0000103207 COORDS:Chr2_A_fumigatus_Af293:1012691-1011228C, translated using codon table 1 (487 amino acids) Uncharacterized ORF; Putative histone deacetylase	15.89	14.78	1	3	3	3	487	54.3	6.14
Afu1g07090	Afu1g07090 AspGDID:ASPL0000110875 COORDS:Chr1_A_fumigatus_Af293:2015732-2011032C, translated using codon table 1 (1526 amino acids) Uncharacterized ORF; Ortholog of <i>A. nidulans FGSC A4</i> : AN519...	14.78	4.65	1	4	4	4	1526	164.4	6.65
Afu1g06170	Afu1g06170 AspGDID:ASPL0000101785 COORDS:Chr1_A_fumigatus_Af293:1784284-1782664C, translated using codon table 1 (464 amino acids) Uncharacterized ORF; Ortholog(s) have role in positive regulation of RNA...	14.61	13.15	1	4	4	4	464	51.7	4.97
Afu1g11830	Afu1g11830 AspGDID:ASPL0000106891 COORDS:Chr1_A_fumigatus_Af293:3122796-3124999W, translated using codon table 1 (713 amino acids) Uncharacterized ORF; Ortholog(s) have U2-type spliceosomal complex lo...	14.27	9.12	1	4	4	4	713	83.4	7.12
Afu3g05900	ste7 AspGDID:ASPL0000105003 COORDS:Chr3_A_fumigatus_Af293:1444958-1446786W, translated using codon table 1 (536 amino acids) Uncharacterized ORF; MAP kinase kinase (MAPKK)	14.12	14.74	1	5	5	5	536	58.5	9.07
Afu1g02150	Afu1g02150 AspGDID:ASPL0000101385 COORDS:Chr1_A_fumigatus_Af293:639645-637892C, translated using codon table 1 (519 amino acids) Uncharacterized ORF; Ortholog(s) have glycerol-3-phosphate dehydrogenas...	13.98	12.14	1	4	4	4	519	56.4	8.19
Afu8g05440	atp4 AspGDID:ASPL0000110874 COORDS:Chr8_A_fumigatus_Af293:1265282-1266290W, translated using codon table 1 (274 amino acids) Uncharacterized ORF; Mitochondrial ATPase subunit; hypoxia repressed protein	13.97	25.18	1	4	4	4	274	29.7	9.35
Afu6g13140	Afu6g13140 AspGDID:ASPL0000109656 COORDS:Chr6_A_fumigatus_Af293:3322359-3321489C, translated using codon table 1 (232 amino acids) Uncharacterized ORF; Ortholog(s) have 3,4-dihydroxy-2-butanone-4-pho...	13.77	20.26	1	3	3	3	232	25.3	5.03
Afu2g15840	Afu2g15840 AspGDID:ASPL0000104301 COORDS:Chr2_A_fumigatus_Af293:4185756-4183151C, translated using codon table 1 (804 amino acids) Uncharacterized ORF; Ortholog of <i>A. nidulans FGSC A4</i> : AN906...	13.76	7.71	1	3	3	3	804	88.6	6.81
Afu5g07890	Afu5g07890 AspGDID:ASPL0000107861 COORDS:Chr5_A_fumigatus_Af293:1979250-1978604C, translated using codon table 1 (149 amino acids) Uncharacterized ORF; Putative single-stranded DNA binding protein famil...	13.54	34.90	1	5	5	5	149	16.2	9.69
Afu4g09140	car2 AspGDID:ASPL0000106629 COORDS:Chr4_A_fumigatus_Af293:2388283-2389697W, translated using codon table 1 (450 amino acids) Uncharacterized ORF; L-ornithine aminotransferase; induced by growth on BSA a...	13.22	14.22	1	4	4	4	450	49.1	6.54
Afu8g02620	Afu8g02620 AspGDID:ASPL0000110698 COORDS:Chr8_A_fumigatus_Af293:695141-693100C, translated using codon table 1 (607 amino acids) Uncharacterized ORF; Ortholog of <i>A. nidulans FGSC A4</i> : AN10344,	12.65	7.25	1	3	3	3	607	68.9	4.65
Afu1g06710	Afu1g06710 AspGDID:ASPL0000101839 COORDS:Chr1_A_fumigatus_Af293:1922660-1920607C, translated using codon table 1 (564 amino acids) Uncharacterized ORF; Ortholog(s) have chaperonin-containing T-comple...	12.29	9.93	1	3	3	3	564	61.0	6.34
Afu6g11890	Afu6g11890 AspGDID:ASPL0000109535 COORDS:Chr6_A_fumigatus_Af293:2972392-2969433C, translated using codon table 1 (930 amino acids) Uncharacterized ORF; Putative dynamin GTPase	12.21	6.67	1	4	4	4	930	104.3	6.83
Afu1g10970	Afu1g10970 AspGDID:ASPL0000106519 COORDS:Chr1_A_fumigatus_Af293:2865856-2868959W, translated using codon table 1 (955 amino acids) Uncharacterized ORF; Ortholog(s) have cytosol, plasma membrane local...	11.88	4.92	1	4	4	4	955	106.5	5.71
Afu6g12770	Afu6g12770 AspGDID:ASPL0000109620 COORDS:Chr6_A_fumigatus_Af293:3226794-3225505C, translated using codon table 1 (381 amino acids) Uncharacterized ORF; Ortholog of <i>A. nidulans FGSC A4</i> : AN3716...	11.85	12.60	1	3	3	3	381	43.4	5.40
Afu6g09810	Afu6g09810 AspGDID:ASPL0000109337 COORDS:Chr6_A_fumigatus_Af293:2412063-2410823C, translated using codon table 1 (344 amino acids) Uncharacterized ORF; Ortholog of <i>A. nidulans FGSC A4</i> : AN752...	11.71	21.51	1	3	3	4	344	37.4	8.90
Afu5g06820	Afu5g06820 AspGDID:ASPL0000107758 COORDS:Chr5_A_fumigatus_Af293:1678782-1677790C, translated using codon table 1 (330 amino acids) Uncharacterized ORF; Ortholog of <i>A. niger CBS 513.88</i> : An03g0...	11.65	17.58	1	2	3	4	330	37.7	7.05
Afu6g12740	mcsA AspGDID:ASPL0000108814 COORDS:Chr6_A_fumigatus_Af293:783347-784866W, translated using codon table 1 (465 amino acids) Verified ORF; Methylcitrate synthase; catalyses the condensation of propionyl-CoA...	11.52	11.61	1	4	4	4	465	51.4	8.94
Afu6g12740	Afu6g12740 AspGDID:ASPL0000109617 COORDS:Chr6_A_fumigatus_Af293:3219940-3220875W, translated using codon table 1 (245 amino acids) Uncharacterized ORF; Dienelactone hydrolase family protein	11.11	15.51	1	3	3	3	245	26.9	6.64
Afu3g09030	Afu3g09030 AspGDID:ASPL0000105302 COORDS:Chr3_A_fumigatus_Af293:2303487-2302210C, translated using codon table 1 (310 amino acids) Uncharacterized ORF; Ortholog(s) have role in aerobic respiration, penic...	11.01	15.16	1	3	3	3	310	34.9	4.65
Afu1g12920	glpV AspGDID:ASPL0000102360 COORDS:Chr1_A_fumigatus_Af293:3420644-3417594C, translated using codon table 1 (879 amino acids) Uncharacterized ORF; Putative glycogen phosphorylase; transcript up-regulated	10.78	4.55	1	2	2	2	879	100.2	6.04
Afu5g10640	Afu5g10640 AspGDID:ASPL0000108128 COORDS:Chr5_A_fumigatus_Af293:2721762-2723271W, translated using codon table 1 (391 amino acids) Uncharacterized ORF; Ortholog(s) have tyrosine-tRNA ligase activity, role...	10.72	14.07	1	4	4	4	391	43.6	6.58
Afu4g08040	Afu4g08040 AspGDID:ASPL0000106518 COORDS:Chr4_A_fumigatus_Af293:2090716-2089786C, translated using codon table 1 (218 amino acids) Uncharacterized ORF; Ortholog(s) have GTP binding activity	10.64	24.31	1	3	3	3	218	23.7	8.54
Afu1g09630	Afu1g09630 AspGDID:ASPL0000102029 COORDS:Chr1_A_fumigatus_Af293:2492509-2488889C, translated using codon table 1 (1056 amino acids) Uncharacterized ORF; Ortholog of <i>A. nidulans FGSC A4</i> : AN132...	10.07	3.60	1	2	2	2	1056	114.4	9.54
Afu1g12590	Afu1g12590 AspGDID:ASPL0000102327 COORDS:Chr1_A_fumigatus_Af293:3325919-3324668C, translated using codon table 1 (398 amino acids) Uncharacterized ORF; La protein homolog	10.00	10.55	1	2	2	2	398	44.5	7.90
Afu5g02150	pre6 AspGDID:ASPL0000107395 COORDS:Chr5_A_fumigatus_Af293:548545-547635C, translated using codon table 1 (251 amino acids) Uncharacterized ORF; Putative proteasome component; reacts with rabbit immuno...	9.98	16.73	1	2	2	2	251	27.4	7.94
Afu4g07650	cyp6 AspGDID:ASPL0000106480 COORDS:Chr4_A_fumigatus_Af293:1987776-1988776W, translated using codon table 1 (209 amino acids) Uncharacterized ORF; Putative peptidyl-prolyl cis-trans isomerase	9.84	19.62	1	3	3	3	209	22.9	8.28
Afu5g04550	Afu5g04550 AspGDID:ASPL0000101623 COORDS:Chr5_A_fumigatus_Af293:1287140-1288616W, translated using codon table 1 (309 amino acids) Uncharacterized ORF; Ortholog of <i>A. nidulans FGSC A4</i> : AN101...	9.75	11.00	1	2	2	2	309	34.0	8.51
Afu2g13040	grpE AspGDID:ASPL0000104018 COORDS:Chr2_A_fumigatus_Af293:3347479-3346582C, translated using codon table 1 (250 amino acids) Uncharacterized ORF; Mitochondrial co-chaperone; protein level decreases upon...	9.75	18.80	1	3	3	3	250	28.4	8.25
Afu5g02050	tim44 AspGDID:ASPL0000107385 COORDS:Chr5_A_fumigatus_Af293:2554479-2552871C, translated using codon table 1 (515 amino acids) Uncharacterized ORF; Mitochondrial inner membrane translocase subunit	9.64	8.35	1	3	3	3	515	57.7	9.11
Afu4g06890	cyp51A AspGDID:ASPL0000106403 COORDS:Chr4_A_fumigatus_Af293:1785331-1783713C, translated using codon table 1 (515 amino acids) Verified ORF; 14-alpha sterol demethylase; commonly mutated in drug resista...	9.30	8.54	1	4	4	4	515	58.0	8.53
Afu5g05460	Afu5g05460 AspGDID:ASPL0000107625 COORDS:Chr5_A_fumigatus_Af293:1268981-1268053C, translated using codon table 1 (242 amino acids) Uncharacterized ORF; Cytosine deaminase-uracil phosphoribosyltransfera...	9.28	14.05	1	2	2	2	242	26.9	7.77
Afu5g02910	Afu5g02910 AspGDID:ASPL0000107403 COORDS:Chr5_A_fumigatus_Af293:772100-770907C, translated using codon table 1 (354 amino acids) Uncharacterized ORF; NAP family protein	9.17	12.15	1	3	3	3	354	41.0	4.50
Afu6g03520	Afu6g03520 AspGDID:ASPL0000108807 COORDS:Chr6_A_fumigatus_Af293:765294-764308C, translated using codon table 1 (278 amino acids) Uncharacterized ORF; Putative short-chain dehydrogenase/reductase family...	9.16	19.06	1	4	4	4	278	29.6	6.95
Afu3g09910	Afu3g09910 AspGDID:ASPL0000105389 COORDS:Chr3_A_fumigatus_Af293:2542185-2543380W, translated using codon table 1 (331 amino acids) Uncharacterized ORF; Putative phosphatidylcholine transporter	9.10	16.31	1	2	2	2	331	37.3	5.52
Afu6g03810	Afu6g03810 AspGDID:ASPL0000108836 COORDS:Chr6_A_fumigatus_Af293:840093-839212C, translated using codon table 1 (255 amino acids) Uncharacterized ORF; Putative mitochondrial ATP synthase D chain; hypoxi...	8.99	15.69	1	2	2	2	255	28.7	9.04
Afu7g05870	pre8 AspGDID:ASPL0000110279 COORDS:Chr7_A_fumigatus_Af293:1438165-1439254W, translated using codon table 1 (282 amino acids) Uncharacterized ORF; Putative proteasome subunit; immunoreactive protein; re...	8.79	14.18	1	2	2	2	282	30.4	5.55
Afu8g05480	Afu8g05480 AspGDID:ASPL0000110878 COORDS:Chr8_A_fumigatus_Af293:1281139-1279477C, translated using codon table 1 (452 amino acids) Uncharacterized ORF; Ortholog(s) have role in nuclear-transcribed mRNA...	8.47	11.73	1	3	3	3	452	50.0	8.47
Afu3g10000	pkaR AspGDID:ASPL0000105358 COORDS:Chr3_A_fumigatus_Af293:2570161-2571402W, translated using codon table 1 (413 amino acids) Verified ORF; cAMP-dependent protein kinase regulatory subunit; induced by e...	8.41	7.26	1	3	3	3	413	44.5	5.19
Afu5g04160	Afu5g04160 AspGDID:ASPL0000107595 COORDS:Chr5_A_fumigatus_Af293:1105009-1106759W, translated using codon table 1 (537 amino acids) Uncharacterized ORF; NTF2 and RRM domain protein	8.40	9.50	1	3	3	3	537	56.9	5.19
Afu2g13590	Afu2g13590 AspGDID:ASPL0000104074 COORDS:Chr2_A_fumigatus_Af293:3535026-3535330W, translated using codon table 1 (81 amino acids) Uncharacterized ORF; Transcript up-regulated in conidia exposed to neutr...	8.34	38.27	1	2	2	2	81	9.3	6.79
Afu1g09550	Afu1g09550 AspGDID:ASPL0000105652 COORDS:Chr1_A_fumigatus_Af293:2468785-2469303W, translated using codon table 1 (143 amino acids) Uncharacterized ORF; Ortholog(s) have translation initiation factor activity,	8.10	22.38	1	2	2	2	143	15.3	5.45
Afu3g12560	Afu3g12560 AspGDID:ASPL0000105652 COORDS:Chr3_A_fumigatus_Af293:3334574-3332914C, translated using codon table 1 (428 amino acids) Uncharacterized ORF; Putative allantoicase; induced by gliotoxin exposu...	8.04	13.08	1	3	3	4	428	46.2	6.48
Afu7g01480	Afu7g01480 AspGDID:ASPL0000102144 COORDS:Chr7_A_fumigatus_Af293:382905-383774W, translated using codon table 1 (249 amino acids) Uncharacterized ORF; Putative translation initiation factor activity,	8.02	8.84	1	2	2	2	249	28.0	6.00
Afu3g03280	Afu3g03280 AspGDID:ASPL0000104846 COORDS:Chr3_A_fumigatus_Af293:876157-877704W, translated using codon table 1 (515 amino acids) Uncharacterized ORF; Putative FAD binding monooxygenase; calcium down...	8.00	6.60	1	2	2	2	515	57.3	7.18
Afu5g05500	Afu5g05500 AspGDID:ASPL0000107629 COORDS:Chr5_A_fumigatus_Af293:1277444-1278887W, translated using codon table 1 (424 amino acids) Uncharacterized ORF; Ortholog(s) have phosphoglycerate dehydrogenas...	7.99	6.60	1	2	2	2	424	45.9	7.01
Afu3g10740	Afu3g10740 AspGDID:ASPL0000105472 COORDS:Chr3_A_fumigatus_Af293:2782828-2781858C, translated using codon table 1 (262 amino acids) Uncharacterized ORF; Putative RAB GTPase with a predicted role in regu...	7.96	15.27	1	2	2	2	262	27.6	4.84
Afu2g09490	Afu2g09490 AspGDID:ASPL0000103667 COORDS:Chr2_A_fumigatus_Af293:2422679-2427552W, translated using codon table 1 (1525 amino acids) Uncharacterized ORF; Eukaryotic translation initiation factor subunit eIF...	7.89	2.75	1	2	2	2	1525	163.9	9.36
Afu7g06780	Afu7g06780 AspGDID:ASPL0000110368 COORDS:Chr7_A_fumigatus_Af293:1648499-1649833W, translated using codon table 1 (374 amino acids) Uncharacterized ORF; Has domain(s) with predicted oxidoreductase acti...	7.76	7.22	1	2	2	2	374	41.5	7.43
Afu3g10630	Afu3g10630 AspGDID:ASPL0000105461 COORDS:Chr3_A_fumigatus_Af293:2747083-2747630W, translated using codon table 1 (123 amino acids) Uncharacterized ORF; Ortholog(s) have mitochondrion localization	7.71	33.33	1	2	2	2	123	13.6	4.88
Afu6g07540	Afu6g07540 AspGDID:ASPL0000109114 COORDS:Chr6_A_fumigatus_Af293:1715811-1713540C, translated using codon table 1 (548 amino acids) Uncharacterized ORF; Ortholog(s) have chaperonin-containing T-comple...	7.59	4.56	1	2	2	2	548	59.8	5.52
Afu3g11300	prs2 AspGDID:ASPL0000105528 COORDS:Chr3_A_fumigatus_Af293:2959483-2958408C, translated using codon table 1 (254 amino acids) Uncharacterized ORF; Putative proteasome component	7.23	9.84	1	2	2	2	254	27.9	6.38
Afu1g09930	gcy1 AspGDID:ASPL0000102059 COORDS:Chr1_A_fumigatus_Af293:2570399-2571627W, translated using codon table 1 (349 amino acids) Uncharacterized ORF; Putative glycerol dehydrogenase; protein level decreases...	7.15	8.02	1	2	2	2	349	39.1	8.84
Afu4g04410	Afu4g04410 AspGDID:ASPL0000107811 COORDS:Chr4_A_fumigatus_Af293:1247460-1248557W, translated using codon table 1 (319 amino acids) Uncharacterized ORF; Immunoreactive protein; has predicted 3-hydroxy...	7.10	10.97	1	3	3	3	319	33.7	7.37
Afu5g03520	Afu5g03520 AspGDID:ASPL0000107530 COORDS:Chr5_A_fumigatus_Af293:949870-951084W, translated using codon table 1 (323 amino acids) Verified ORF; Immunoreactive secreted protein	7.10	8.36	1	2	2	2	323	35.5	6.47

Accession	Description	Score	Coverage	...				# AAs	MW [kDa]	calc. pI
hsp78	hsp78 AspGDID:ASPL0000102181 COORDS:Chr1_A_fumigatus_Af293:2946736-2944343C, translated using codon table 1 (797 amino acids) Uncharacterized ORF; Heat shock protein/chaperonin; transcript downregulated in response to voriconazole	6.92	2.76					797	88.3	7.02
AfuMt00120	AfuMt00120 AspGDID:ASPL0000366358 COORDS:mito_A_fumigatus_Af293:25862-26623W, translated using codon table 4 (253 amino acids) Uncharacterized ORF; Ortholog(s) have cytochrome-c oxidase activity, role in aerobic respiration, mitochondrial electron transport, cytochrome c to oxygen and mitochondrial respiratory chain complex IV localization							253	29.0	4.77
Afu8g04810	Afu8g04810 AspGDID:ASPL0000110815 COORDS:Chr8_A_fumigatus_Af293:1104248-1103015C, translated using codon table 1 (336 amino acids) Uncharacterized ORF; Ortholog(s) have role in circadian regulation of gene expression, conidium formation, establishment or maintenance of bipolar cell polarity regulating cell shape and protein phosphorylation, more									7.31
Afu8g05330	Afu8g05330 AspGDID:ASPL0000110863 COORDS:Chr8_A_fumigatus_Af293:1242642-1243783W, translated using codon table 1 (298 amino acids) Uncharacterized ORF; Putative methylenetetrahydrofolate dehydrogenase	6.94	8.39					298	33.0	6.54
Afu1g15960	Afu1g15960 AspGDID:ASPL0000102659 COORDS:Chr1_A_fumigatus_Af293:4331468-4333260W, translated using codon table 1 (554 amino acids) Uncharacterized ORF; Putative flavin adenine disulfide binding, glutathione transferase activity, glutathione-disulfide reductase activity							554	60.1	8.70
fahA	fahA AspGDID:ASPL0000103249 COORDS:Chr2_A_fumigatus_Af293:1174675-1175970W, translated using codon table 1 (431 amino acids) Uncharacterized ORF; Putative fumarylacetoacetate hydrolase;induced by L-tyrosine; immunoreactive protein; repressed by gliotoxin exposure 1							431	46.8	6.39
Afu1g12440	Afu1g12440 AspGDID:ASPL0000101792 COORDS:Chr1_A_fumigatus_Af293:1798799-1797812C, translated using codon table 1 (282 amino acids) Uncharacterized ORF; Ortholog(s) have role in riboflavin biosynthetic process and cytosol, nucleus localization							233	25.2	5.33
		6.89	18.84					138	14.8	10.37
Afu3g13830	Afu3g13830 AspGDID:ASPL0000105776 COORDS:Chr3_A_fumigatus_Af293:3651475-3654802W, translated using codon table 1 (1064 amino acids) Uncharacterized ORF; Ortholog(s) have role in ascospore wall assembly and ascospore wall, cytosol, nucleus localization							1064	121.9	7.65
Afu6g04010	Afu6g04010 AspGDID:ASPL0000108856 COORDS:Chr6_A_fumigatus_Af293:1281139-1279729C, translated using codon table 1 (962 amino acids) Uncharacterized ORF; Ortholog(s) have nuclear pore receptor activity, role in cell cycle, protein import from nucleus and nuclear membrane localization							962	108.4	5.38
aspf9	aspf9 AspGDID:ASPL0000102682 COORDS:Chr1_A_fumigatus_Af293:4404557-4405859W, translated using codon table 1 (395 amino acids) Verified ORF; Cell wall glucanase; allergen Asp f 9; predicted GPI-anchor; binds specifically to IgE antibodies in the sera of allergic bronchopulmonary aspergillosis (ABPA) patients; transcript repressed by H2O2; induced by exposure to artemisinin							40.3		4.78
Afu1g12810	Afu1g12810 AspGDID:ASPL0000102821 COORDS:Chr1_A_fumigatus_Af293:1358892-1357362C, translated using codon table 1 (391 amino acids) Uncharacterized ORF; Ortholog(s) have mRNA binding activity, role in telomere maintenance via telomerase and cytoplasm, nucleus localization							391	44.1	6.96
Afu2g04940	Afu2g04940 AspGDID:ASPL0000103319 COORDS:Chr2_A_fumigatus_Af293:1358902-1357362C, translated using codon table 1 (470 amino acids) Uncharacterized ORF; Ortholog(s) have protein transporter activity and role in ascospore formation, intracellular protein transport, protein retention in Golgi apparatus, retrograde transport, endosome to Golgi							391	49.1	7.72
Afu3g10360	Afu3g10360 AspGDID:ASPL0000105434 COORDS:Chr3_A_fumigatus_Af293:2688254-2685337C, translated using codon table 1 (878 amino acids) Uncharacterized ORF; Ortholog of <i>A. nidulans FGSC A4</i> : AN6389, <i>A. niger CBS 513.88</i> : An11g00410, <i>A. oryzae RIB40</i> : AO090023000186 and <i>Aspergillus wentii</i> : Aspwe1_0039443							878	99.7	5.96
Afu5g08310	Afu5g08310 AspGDID:ASPL0000107903 COORDS:Chr5_A_fumigatus_Af293:2110783-2111831W, translated using codon table 1 (334 amino acids) Uncharacterized ORF; Has domain(s) with predicted nucleic acid binding, nucleotide binding activity	6.89						334	36.5	6.83
Afu7g07370	Afu7g07370 AspGDID:ASPL0000069811 COORDS:Chr4_A_fumigatus_Af293:1844081-1842511C, translated using codon table 1 (500 amino acids) Uncharacterized ORF; Ortholog(s) have metal ion binding, poly(A)-specific ribonuclease activity	4.60						500	53.8	7.08
Afu1g12750	Afu1g12750 AspGDID:ASPL0000016981 COORDS:Chr4_A_fumigatus_Af293:3344997-3342675C, translated using codon table 1 (750 amino acids) Uncharacterized ORF; Ortholog(s) have role in deadenylation-dependent decapping of nuclear-transcribed mRNA and cytosol, nucleus localization							750	84.8	6.99

Table S6 (continued)

Gene ID	Description								
		9.17	12.15	1	3	3	3	354	41.0	4.50
	Afu6g03520 AspGDID:ASPL0000108807 COORDS:Chr6_A_fumigatus_Af293:765294-764308C, translated using codon table 1 (278 amino acids) Uncharacterized ORF; Putative short-chain dehydrogenase/reductase family protein; predicted gene pair with AFUA_4G03680	8.16		1	4	4	4	278	29.6	6.95
	Afu3g09910 AspGDID:ASPL0000105389 COORDS:Chr3_A_fumigatus_Af293:2542185-2543380W, translated using codon table 1 (331 amino acids) Uncharacterized ORF; Ortholog(s) have phosphatidylcholine transporter activity and role in Golgi to plasma membrane transport, ascospore formation, mitotic cytokinesis, phospholipid transport, regulation of filamentous growth	9.13		1	3	3	3	331	37.3	5.52
	Afu6g03810 AspGDID:ASPL0000108836 COORDS:Chr6_A_fumigatus_Af293:840093-839212C, translated using codon table 1 (255 amino acids) Uncharacterized ORF; Putative mitochondrial ATP synthase D chain; hypoxia induced protein	8.99	15.69	1	2	2	2	255	28.7	9.04
pre8	pre8 AspGDID:ASPL0000110279 COORDS:Chr7_A_fumigatus_Af293:1438165-1439254W, translated using codon table 1 (282 amino acids) Uncharacterized ORF; Putative proteasome subunit; immunoreactive protein; reacts with rabbit IgG antisera exposed to A. fumigatus conidia	8.72		1	2	2	2	282	30.4	5.55
	Afu8g05480 AspGDID:ASPL0000110878 COORDS:Chr8_A_fumigatus_Af293:1281139-1279477C, translated using codon table 1 (452 amino acids) Uncharacterized ORF; Ortholog(s) have role in nuclear-transcribed mRNA catabolic process, meiosis-specific transcripts, poly(A)+ mRNA export from nucleus and nucleus localization	8.47		1	3	3	3	452	50.0	8.47
pkaR	pkaR AspGDID:ASPL0000105398 COORDS:Chr3_A_fumigatus_Af293:2570161-2571402W, translated using codon table 1 (413 amino acids) Verified ORF; cAMP-dependent protein kinase regulatory subunit; induced by endothelial cells and human airway epithelial cells; mutants sensitive to storage in water and contain more nuclei than wild-type; up-regulated in neutrophil-exposed conidia	8.41	22.26	2	2	2	2	413	46.5	5.19
		8.40	9.50	1	3	3	3	537	56.9	5.19
Afu2g13590	Afu2g13590 AspGDID:ASPL0000104074 COORDS:Chr2_A_fumigatus_Af293:3535026-3535330W, translated using codon table 1 (81 amino acids) Uncharacterized ORF; Transcript up-regulated in conidia exposed to neutrophils	8.34	38.27	1	2	2	2	81	9.3	6.79
Afu1g09550	Afu1g09550 AspGDID:ASPL0000102021 COORDS:Chr1_A_fumigatus_Af293:2468785-2469303W, translated using codon table 1 (143 amino acids) Uncharacterized ORF; Ortholog(s) have role in dynein-driven meiotic oscillatory nuclear movement, karyogamy involved in conjugation with cellular fusion, reciprocal meiotic recombination	8.30	2.80	1	2	2	2	143	15.3	5.45
	Afu3g12560 AspGDID:ASPL0000105652 COORDS:Chr3_A_fumigatus_Af293:3334574-3332914C, translated using codon table 1 (428 amino acids) Uncharacterized ORF; Putative allantoicase; induced by gliotoxin exposure	8.04	13.08	1	3	3	4	428	46.2	6.48
	Afu7g01480 AspGDID:ASPL0000109943 COORDS:Chr7_A_fumigatus_Af293:382905-383774W, translated using codon table 1 (249 amino acids) Uncharacterized ORF; Ortholog(s) have translation initiation factor activity, role in translational initiation and cytosol, nucleus localization	8.01		1	2	2	2	249	28.0	6.00
	Afu3g03280 AspGDID:ASPL0000104846 COORDS:Chr3_A_fumigatus_Af293:876157-877704W, translated using codon table 1 (515 amino acids) Uncharacterized ORF; Putative FAD binding monooxygenase; calcium downregulated	8.00	6.60	1	3	3	3	515	57.3	7.18
	Afu5g05500 AspGDID:ASPL0000107629 COORDS:Chr5_A_fumigatus_Af293:1277444-1278887W, translated using codon table 1 (424 amino acids) Uncharacterized ORF; Putative phosphoglycerate dehydrogenase activity, role in serine family amino acid biosynthetic process and cytosol localization	7.99		2	3	3	3	424	45.9	7.01
	Afu3g10740 AspGDID:ASPL0000105472 COORDS:Chr3_A_fumigatus_Af293:2782828-2781858C, translated using codon table 1 (262 amino acids) Uncharacterized ORF; Putative RAB GTPase with a predicted role in regulation of endocytosis; transcript downregulated in response to amphotericin B	7.96	15.02	3	3	3	3	262	27.6	4.84
	Afu2g09490 AspGDID:ASPL0000103667 COORDS:Chr2_A_fumigatus_Af293:2422679-2427552W, translated using codon table 1 (1525 amino acids) Uncharacterized ORF; Eukaryotic translation initiation factor eIF-4F	7.89	2.75	1	3	3	3	1525	163.9	9.36
	Afu7g00780 AspGDID:ASPL0000110389 COORDS:Chr7_A_fumigatus_Af293:1648499-1649833W, translated using codon table 1 (374 amino acids) Uncharacterized ORF; Has domain(s) with predicted oxidoreductase activity and role in oxidation-reduction process	7.72		1	2	2	2	374	41.5	7.43
		7.71	33.33	1	2	2	3	123	13.6	4.88
	Afu6g07540 AspGDID:ASPL0000109114 COORDS:Chr6_A_fumigatus_Af293:1715811-1713540C, translated using codon table 1 (548 amino acids) Uncharacterized ORF; Ortholog(s) have chaperonin-containing T-complex localization	7.59	4.56	1	2	2	2	548	59.8	5.52
		7.23	9.84	1	2	2	2	254	27.9	6.38
gcy1	gcy1 AspGDID:ASPL0000102059 COORDS:Chr1_A_fumigatus_Af293:2570399-2571627W, translated using codon table 1 (349 amino acids) Uncharacterized ORF; Putative glycerol dehydrogenase; protein level decreases upon heat shock; transcript up-regulated in conidia exposed to neutrophils	7.15	8.02	2	2	2	2	349	39.1	8.84
Afu4g04410	Afu4g04410 AspGDID:ASPL0000106256 COORDS:Chr4_A_fumigatus_Af293:1247460-1246537W, translated using codon table 1 (319 amino acids) Uncharacterized ORF; Immunoreactive protein; has predicted 3-hydroxy	7.10	10.97	1	3	3	3	319	35.7	7.37
Afu5g03520	Afu5g03520 AspGDID:ASPL0000107530 COORDS:Chr5_A_fumigatus_Af293:949870-951084W, translated using codon table 1 (323 amino acids) Verified ORF; Immunoreactive secreted protein	7.10	8.36	1	2	2	2	323	35.5	6.47
Afu4g06790	Afu4g06790 AspGDID:ASPL0000106393 COORDS:Chr4_A_fumigatus_Af293:1755480-1756006W, translated using codon table 1 (93 amino acids) Uncharacterized ORF; Ubiquinol-cytochrome c reductase complex 14 kDa	7.06	43.01	1	2	2	2	93	11.0	6.32
Afu1g11180	hsp78 AspGDID:ASPL0000102181 COORDS:Chr1_A_fumigatus_Af293:2946736-2944343C, translated using codon table 1 (797 amino acids) Uncharacterized ORF; Heat shock protein/chaperonin; transcript downregulated	6.97	2.76	1	2	2	2	797	88.3	7.02
AfuMt00120	AfuMt00120 AspGDID:ASPL0000366358 COORDS:mito_A_fumigatus_Af293:25862-26623W, translated using codon table 4 (253 amino acids) Uncharacterized ORF; Ortholog(s) have cytochrome-c oxidase activity, role in	6.96	10.67	1	2	2	2	253	29.0	4.77
Afu8g04810	Afu8g04810 AspGDID:ASPL0000110815 COORDS:Chr8_A_fumigatus_Af293:1104248-1103015C, translated using codon table 1 (336 amino acids) Uncharacterized ORF; Ortholog(s) have role in circadian regulation of ge	6.95	8.04	1	2	2	2	336	39.5	7.31
Afu8g05330	Afu8g05330 AspGDID:ASPL0000110863 COORDS:Chr8_A_fumigatus_Af293:1242642-1243783W, translated using codon table 1 (298 amino acids) Uncharacterized ORF; Putative methylenetetrahydrofolate dehydrogenase	6.94	8.39	1	3	3	3	298	33.0	6.54
Afu1g15960	Afu1g15960 AspGDID:ASPL0000102659 COORDS:Chr1_A_fumigatus_Af293:4331468-4333260W, translated using codon table 1 (554 amino acids) Uncharacterized ORF; Ortholog(s) have flavin adenine dinucleotide bindi	6.94	5.05	1	2	2	2	554	60.1	8.70
Afu2g04230	fahA AspGDID:ASPL0000103249 COORDS:Chr2_A_fumigatus_Af293:1174675-1175970W, translated using codon table 1 (431 amino acids) Uncharacterized ORF; Putative fumarylacetoacetate hydrolase:induced by L-tyro	6.93	7.66	1	2	2	2	431	46.8	6.39
Afu1g06240	Afu1g06240 AspGDID:ASPL0000101792 COORDS:Chr1_A_fumigatus_Af293:1798799-1797804C, translated using codon table 1 (233 amino acids) Uncharacterized ORF; Ortholog(s) have riboflavin synthase activity, role i	6.92	9.87	1	2	2	2	233	25.2	5.33
Afu5g01950	Afu5g01950 AspGDID:ASPL0000107375 COORDS:Chr5_A_fumigatus_Af293:500329-499510C, translated using codon table 1 (138 amino acids) Uncharacterized ORF; Ortholog(s) have chromatin binding activity	6.89	18.84	1	3	3	3	138	14.8	10.37
Afu3g13830	Afu3g13830 AspGDID:ASPL0000105776 COORDS:Chr3_A_fumigatus_Af293:3651475-3654802W, translated using codon table 1 (1064 amino acids) Uncharacterized ORF; Ortholog(s) have role in ascospore wall assembly	6.86	4.70	1	2	2	2	1064	121.9	7.65
Afu6g04010	Afu6g04010 AspGDID:ASPL0000108856 COORDS:Chr6_A_fumigatus_Af293:901498-904822W, translated using codon table 1 (962 amino acids) Uncharacterized ORF; Ortholog(s) have importin-alpha export receptor acti	6.75	4.47	1	2	2	2	962	108.4	5.38
Afu1g16190	aspf9 AspGDID:ASPL0000102682 COORDS:Chr1_A_fumigatus_Af293:4404557-4405859W, translated using codon table 1 (395 amino acids) Verified ORF; Cell wall glucanase; allergen Asp f 9; predicted GPI-anchor; binds	6.64	7.85	1	2	2	2	395	40.3	4.78
Afu1g10810	Afu1g10810 AspGDID:ASPL0000102144 COORDS:Chr1_A_fumigatus_Af293:2821017-2822416W, translated using codon table 1 (391 amino acids) Uncharacterized ORF; Ortholog(s) have role in calcium ion transport into	6.41	7.16	1	2	2	2	391	44.1	6.96
Afu2g04940	Afu2g04940 AspGDID:ASPL0000103319 COORDS:Chr2_A_fumigatus_Af293:1358892-1357362C, translated using codon table 1 (470 amino acids) Uncharacterized ORF; Ortholog(s) have mRNA binding activity, role in tel	6.40	9.15	1	3	3	3	470	49.1	7.72
Afu3g10360	Afu3g10360 AspGDID:ASPL0000105434 COORDS:Chr3_A_fumigatus_Af293:2688254-2685337C, translated using codon table 1 (878 amino acids) Uncharacterized ORF; Ortholog(s) have protein transporter activity and r	6.27	2.73	1	2	2	2	878	99.7	5.96
Afu1g03300	Afu1g03300 AspGDID:ASPL0000101500 COORDS:Chr1_A_fumigatus_Af293:955980-958095W, translated using codon table 1 (594 amino acids) Uncharacterized ORF; Ortholog of <i>A. nidulans FGSC A4</i> : AN6389,	6.27	7.41	1	2	2	2	594	66.3	6.54
Afu5g08310	Afu5g08310 AspGDID:ASPL0000107903 COORDS:Chr5_A_fumigatus_Af293:2110783-2111831W, translated using codon table 1 (334 amino acids) Uncharacterized ORF; Has domain(s) with predicted nucleic acid binding	6.25	6.89	1	2	2	2	334	36.5	6.83
Afu5g07370	Afu5g07370 AspGDID:ASPL0000107811 COORDS:Chr5_A_fumigatus_Af293:1844081-1842511C, translated using codon table 1 (500 amino acids) Uncharacterized ORF; Ortholog(s) have metal ion binding, poly(A)-specif	6.16	4.60	1	2	2	2	500	53.8	7.08
Afu4g12750	Afu4g12750 AspGDID:ASPL0000106981 COORDS:Chr4_A_fumigatus_Af293:3344997-3342675C, translated using codon table 1 (750 amino acids) Uncharacterized ORF; Ortholog(s) have role in deadenylation-dependent	6.16	4.40	1	2	2	2	750	84.8	6.99
Afu8g05610	btgE AspGDID:ASPL0000110890 COORDS:Chr8_A_fumigatus_Af293:1318148-1320231W, translated using codon table 1 (616 amino acids) Uncharacterized ORF; Putative cell wall glucanase	6.11	7.63	1	2	2	2	616	63.6	5.64
Afu1g15000	Afu1g15000 AspGDID:ASPL0000102567 COORDS:Chr1_A_fumigatus_Af293:4029547-4031693W, translated using codon table 1 (643 amino acids) Uncharacterized ORF; Putative isopropylmalate synthase; transcript high	6.07	7.31	1	3	3	3	643	71.2	5.68
Afu4g06690	Afu4g06690 AspGDID:ASPL0000106383 COORDS:Chr4_A_fumigatus_Af293:1733950-1731132C, translated using codon table 1 (859 amino acids) Uncharacterized ORF; Ortholog(s) have nucleotide binding, ribonucleosid	6.07	3.03	1	2	2	2	859	96.0	6.67
Afu2g14970	Afu2g14970 AspGDID:ASPL0000104212 COORDS:Chr2_A_fumigatus_Af293:3944757-3943306C, translated using codon table 1 (483 amino acids) Uncharacterized ORF; Gamma-butyrobetaine hydroxylase subfamily prote	6.05	6.83	1	3	3	3	483	56.7	8.29
Afu5g09910	Afu5g09910 AspGDID:ASPL0000108059 COORDS:Chr5_A_fumigatus_Af293:2564144-2563392C, translated using codon table 1 (217 amino acids) Uncharacterized ORF; Putative p-nitroreductase family protein; protein in	6.03	14.29	1	3	3	3	217	24.3	5.91
Afu7g02340	Afu7g02340 AspGDID:ASPL0000110029 COORDS:Chr7_A_fumigatus_Af293:635304-636088W, translated using codon table 1 (168 amino acids) Uncharacterized ORF; Ortholog(s) have role in isoleucine biosynthetic proc	5.98	13.10	1	2	2	2	168	18.0	8.82
Afu5g06320	Afu5g06320 AspGDID:ASPL0000107708 COORDS:Chr5_A_fumigatus_Af293:1519087-1518035C, translated using codon table 1 (169 amino acids) Uncharacterized ORF; Ortholog(s) have role in cellular protein localizatio	5.92	13.02	1	2	2	2	169	19.1	8.34
Afu5g00650	Afu5g00650 AspGDID:ASPL0000107249 COORDS:Chr5_A_fumigatus_Af293:183963-182941C, translated using codon table 1 (340 amino acids) Uncharacterized ORF; Protein of unknown function; transcript induced by e	5.91	5.29	1	2	2	2	340	38.3	6.46
Afu1g14550	sod3 AspGDID:ASPL0000102522 COORDS:Chr1_A_fumigatus_Af293:3887266-3888013W, translated using codon table 1 (210 amino acids) Verified ORF; Putative manganese superoxide dismutase; allergen Asp f 6; reco	5.80	15.24	1	2	2	2	210	23.4	7.74
Afu6g12500	Afu6g12500 AspGDID:ASPL0000109594 COORDS:Chr6_A_fumigatus_Af293:3156604-3155495C, translated using codon table 1 (220 amino acids) Uncharacterized ORF; Ortholog(s) have cytosol, mitochondrion, nucleus	5.80	9.09	1	2	2	2	220	23.7	8.38
Afu6g08850	Afu6g08850 AspGDID:ASPL0000109241 COORDS:Chr6_A_fumigatus_Af293:2101762-2102788W, translated using codon table 1 (313 amino acids) Uncharacterized ORF; Ubiquinone biosynthesis methlytransferase; hypox	5.79	9.90	1	2	2	2	313	35.2	8.70
Afu4g03322	Afu4g03322 AspGDID:ASPL0000365151 COORDS:Chr4_A_fumigatus_Af293:944673-943800C, translated using codon table 1 (257 amino acids) Uncharacterized ORF; Ortholog of <i>A. nidulans FGSC A4</i> : AN7177,	5.78	8.95	1	2	2	2	257	28.9	4.87
Afu2g06040	Afu2g06040 AspGDID:ASPL0000103427 COORDS:Chr2_A_fumigatus_Af293:1706686-1708648W, translated using codon table 1 (612 amino acids) Uncharacterized ORF; Putative actin cortical patch component	5.71	5.56	1	2	2	2	612	65.1	6.42
Afu4g13700	Afu4g13700 AspGDID:ASPL0000107076 COORDS:Chr4_A_fumigatus_Af293:3586027-3588483W, translated using codon table 1 (737 amino acids) Uncharacterized ORF; Ortholog(s) have cytosol localization	5.66	3.26	1	2	2	2	737	84.4	7.09
Afu3g14680	plb3 AspGDID:ASPL0000105858 COORDS:Chr3_A_fumigatus_Af293:3893246-3895138W, translated using codon table 1 (630 amino acids) Uncharacterized ORF; Putative secreted lysophospholipase B; transcript induced	5.64	6.19	1	2	2	2	630	67.4	5.66
Afu2g15490	Afu2g15490 AspGDID:ASPL0000104266 COORDS:Chr2_A_fumigatus_Af293:4088650-4086962C, translated using codon table 1 (562 amino acids) Uncharacterized ORF; Ortholog(s) have intracellular localization	5.52	4.80	1	2	2	2	562	63.1	5.60
Afu2g10920	Afu2g10920 AspGDID:ASPL0000103807 COORDS:Chr2_A_fumigatus_Af293:2813917-2812855C, translated using codon table 1 (294 amino acids) Uncharacterized ORF; Putative enoyl-CoA hydratase/isomerase family pro	5.50	7.82	1	2	2	2	294	31.6	8.56
Afu2g07960	Afu2g07960 AspGDID:ASPL0000103516 COORDS:Chr2_A_fumigatus_Af293:2038888-2047447W, translated using codon table 1 (2674 amino acids) Uncharacterized ORF; Ortholog(s) have role in regulation of translation	5.46	0.93	1	2	2	2	2674	292.0	5.86
Afu4g09110	ccp1 AspGDID:ASPL0000106626 COORDS:Chr4_A_fumigatus_Af293:2379568-2378394C, translated using codon table 1 (366 amino acids) Uncharacterized ORF; Putative cytochrome c peroxidase; protein induced by hea	5.37	6.83	1	2	2	2	366	40.4	8.56
Afu4g11050	Afu4g11050 AspGDID:ASPL0000106815 COORDS:Chr4_A_fumigatus_Af293:2878131-2879794W, translated using codon table 1 (496 amino acids) Uncharacterized ORF; Putative NADH-ubiquinone oxidoreductase, subun	5.25	5.04	1	2	2	2	496	54.5	8.13
Afu5g08830	hexA AspGDID:ASPL0000107954 COORDS:Chr5_A_fumigatus_Af293:2265787-2268175W, translated using codon table 1 (537 amino acids) Verified ORF; Putative woronin body protein; hypoxia repressed protein	5.23	3.35	1	2	2	2	537	61.4	8.79
Afu3g10700	Afu3g10700 AspGDID:ASPL0000105468 COORDS:Chr3_A_fumigatus_Af293:2775082-2775739W, translated using codon table 1 (193 amino acids) Uncharacterized ORF; Ortholog(s) have mRNA binding, structural molec	5.15	13.47	1	2	2	2	193	20.6	5.60
Afu1g06940	Afu1g06940 AspGDID:ASPL0000101862 COORDS:Chr1_A_fumigatus_Af293:1983163-1981801C, translated using codon table 1 (412 amino acids) Uncharacterized ORF; Putative FMN binding, chorismate synthas	4.97	10.19	1	2	2	2	412	44.2	6.54
Afu1g02410	Afu1g02410 AspGDID:ASPL0000101411 COORDS:Chr1_A_fumigatus_Af293:702057-703574W, translated using codon table 1 (469 amino acids) Uncharacterized ORF; Ortholog(s) have ATP-dependent 3'-5' DNA helicase	4.96	4.48	1	2	2	2	469	51.3	5.83
Afu5g10370	sdh2 AspGDID:ASPL0000108103 COORDS:Chr5_A_fumigatus_Af293:2655836-2654821C, translated using codon table 1 (299 amino acids) Uncharacterized ORF; Iron-sulfur protein subunit of succinate dehydrogenase w	4.12	8.36	1	2	2	2	299	33.9	8.92
Afu2g05340	gel4 AspGDID:ASPL0000103358 COORDS:Chr2_A_fumigatus_Af293:1487091-1488862W, translated using codon table 1 (532 amino acids) Verified ORF; Essential 1,3-beta-glucanosyltransferase, GPI-anchored to the plas	3.81	4.14	1	2	2	2	532	57.1	5.01
Afu4g09010	Afu4g09010 AspGDID:ASPL0000106616 COORDS:Chr4_A_fumigatus_Af293:2336585-2339048W, translated using codon table 1 (597 amino acids) Uncharacterized ORF; Ortholog(s) have U1 snRNP localization	3.75	3.02	1	2	2	2	597	68.2	5.26
Afu2g17130	**Afu2g17130 AspGDID:ASPL0000104429 COORDS:Chr2_A_fumigatus_Af293:4574963-4576567W, translated using codon table 1 (487 amino acids) Uncharacterized ORF; Ortholog(s) have prot**	**3.07**	**7.60**	**1**	**2**	**2**	**2**	**487**	**53.5**	**6.14**
Afu2g08440	Afu2g08440 AspGDID:ASPL0000103563 COORDS:Chr2_A_fumigatus_Af293:2168008-2176342W, translated using codon table 1 (2523 amino acids) Uncharacterized ORF; Has domain(s) with predicted ubiquitinyl hydrola	2.60	1.70	1	2	2	2	2523	284.9	5.27
Afu1g16780	Afu1g16780 AspGDID:ASPL0000102743 COORDS:Chr1_A_fumigatus_Af293:4578362-4576093C, translated using codon table 1 (664 amino acids) Uncharacterized ORF; Ortholog(s) have protein serine/threonine kinase a	2.39	5.27	1	2	2	2	664	74.3	9.36
Afu3g04150	Afu3g04150 AspGDID:ASPL0000104931 COORDS:Chr3_A_fumigatus_Af293:1171784-1173124W, translated using codon table 1 (423 amino acids) Uncharacterized ORF; Ortholog(s) have enoyl-[acyl-carrier-protein] redu	2.02	7.80	1	2	2	2	423	46.6	9.25
Afu6g14280	Afu6g14280 AspGDID:ASPL0000109767 COORDS:Chr6_A_fumigatus_Af293:3632901-3631292C, translated using codon table 1 (517 amino acids) Uncharacterized ORF; Protein of unknown function; calcium downregulat	0.00	6.38	1	2	2	2	517	58.4	9.23

Table S7: SteD-GFP (Afu2g17130) interacting proteins at 24 hours of vegetative growth. Proteins of interest are highlighted in yellow. SteC (Afu5g06420).

Table S7: *Aspergillus fumigatus* SteD-GFP interacting proteins (Vegetative growth-24 hours)

Accession	Description	Score	Coverage	# Proteins	# Unique Peptides	# Peptides	# PSMs	# AAs	MW [kDa]	calc. pI
Afu2g17130	Afu2g17130 AspGDID:ASPL0000104429 COORDS:Chr2_A_fumigatus_Af293:4574963-4576567W, translated using codon table 1 (487 amino acids) Uncharacterized ORF; Ortholog(s) have	106.39	53.18	1	16	16	24	487	53.5	6.14
Afu5g06420	Afu5g06420 AspGDID:ASPL0000107718 COORDS:Chr5_A_fumigatus_Af293:1549998-1553242W, translated using codon table 1 (1007 amino acids) Uncharacterized ORF; Ortholog(s) have	101.57	31.68	1	23	23	27	1007	111.6	8.60
Afu1g12680	Afu1g12680 AspGDID:ASPL0000102336 COORDS:Chr1_A_fumigatus_Af293:3351052-3347476C, translated using codon table 1 (1072 amino acids) Uncharacterized ORF; Ortholog(s) have Rho GTPase activator activ	27.47	5.97	1	5	5	6	1072	117.7	6.77
Afu1g03010	Afu1g03010 AspGDID:ASPL0000101471 COORDS:Chr1_A_fumigatus_Af293:869019-866374C, translated using codon table 1 (881 amino acids) Uncharacterized ORF; Ortholog(s) have U2-type spliceosomal complex	25.40	12.37	1	8	8	9	881	100.8	9.95
Afu5g06820	Afu5g06820 AspGDID:ASPL0000107758 COORDS:Chr5_A_fumigatus_Af293:1678782-1677790C, translated using codon table 1 (330 amino acids) Uncharacterized ORF; Ortholog of <i>A. niger CBS 513.88</i> : Ar	22.74	17.58	1	3	3	6	330	37.7	7.05
Afu6g07980	Afu6g07980 AspGDID:ASPL0000109158 COORDS:Chr6_A_fumigatus_Af293:1850730-1849524C, translated using codon table 1 (323 amino acids) Uncharacterized ORF; Ortholog(s) have RNA polymerase II core bin	20.00	21.05	1	6	6	7	323	36.6	7.59
Afu1g06170	Afu1g06170 AspGDID:ASPL0000101785 COORDS:Chr1_A_fumigatus_Af293:1784284-1782664C, translated using codon table 1 (464 amino acids) Uncharacterized ORF; Ortholog(s) have role in positive regulation o	19.79	18.32	1	6	6	6	464	51.7	4.97
Afu4g11830	Afu4g11830 AspGDID:ASPL0000106891 COORDS:Chr8_A_fumigatus_Af293:3122796-3124999W, translated using codon table 1 (713 amino acids) Uncharacterized ORF; Ortholog(s) have U2-type spliceosomal comp	15.89	8.42	1	4	4	5	713	83.4	7.12
Afu1g12920	glpV AspGDID:ASPL0000102360 COORDS:Chr1_A_fumigatus_Af293:3420644-3417594C, translated using codon table 1 (879 amino acids) Uncharacterized ORF; Putative glycogen phosphorylase; transcript up-regu	15.80	4.55	1	2	2	3	879	100.2	6.04
Afu6g03810	Afu6g03810 AspGDID:ASPL0000108836 COORDS:Chr6_A_fumigatus_Af293:840093-839212C, translated using codon table 1 (255 amino acids) Uncharacterized ORF; Putative mitochondrial ATP synthase D chain; h	13.05	20.78	1	3	3	3	255	28.7	9.04
Afu5g00730	Afu5g00730 AspGDID:ASPL0000107257 COORDS:Chr5_A_fumigatus_Af293:208755-205171C, translated using codon table 1 (1067 amino acids) Uncharacterized ORF; Has domain(s) with predicted cation-transport	12.62	6.00	1	4	4	4	1067	117.4	7.72
Afu5g08310	Afu5g08310 AspGDID:ASPL0000107903 COORDS:Chr5_A_fumigatus_Af293:2110783-2111831W, translated using codon table 1 (334 amino acids) Uncharacterized ORF; Has domain(s) with predicted nucleic acid bi	12.36	14.07	1	4	4	4	334	36.5	6.83
Afu6g12740	Afu6g12740 AspGDID:ASPL0000109617 COORDS:Chr6_A_fumigatus_Af293:3219940-3220875W, translated using codon table 1 (245 amino acids) Uncharacterized ORF; Dienelactone hydrolase family protein	10.44	15.51	1	3	3	3	245	26.9	6.64
Afu4g03160	Afu4g03160 AspGDID:ASPL0000106134 COORDS:Chr4_A_fumigatus_Af293:886361-887395W, translated using codon table 1 (344 amino acids) Uncharacterized ORF; Ortholog(s) have U2-type spliceosomal complex	10.14	7.27	1	2	2	3	344	37.8	5.82
Afu1g04210	Afu1g04210 AspGDID:ASPL0000101588 COORDS:Chr1_A_fumigatus_Af293:1202857-1199114C, translated using codon table 1 (1225 amino acids) Uncharacterized ORF; Ortholog(s) have cytosol, nuclear envelope	9.49	3.43	1	3	3	3	1225	139.5	6.44
Afu2g16020	Afu2g16020 AspGDID:ASPL0000104319 COORDS:Chr2_A_fumigatus_Af293:4237810-4239808W, translated using codon table 1 (566 amino acids) Uncharacterized ORF; Putative heat shock protein; transcript induc	9.33	8.83	1	3	3	3	566	61.7	6.87
Afu5g07890	Afu5g07890 AspGDID:ASPL0000107861 COORDS:Chr5_A_fumigatus_Af293:1979250-1978604C, translated using codon table 1 (149 amino acids) Uncharacterized ORF; Putative single-stranded DNA binding protein	8.77	28.86	1	4	4	4	149	16.2	9.69
Afu8g02620	Afu8g02620 AspGDID:ASPL0000110698 COORDS:Chr8_A_fumigatus_Af293:695141-693100C, translated using codon table 1 (607 amino acids) Uncharacterized ORF; Ortholog of <i>A. nidulans FGSC A4</i> : AN1	8.63	4.61	1	2	2	2	607	68.9	4.65
Afu4g06890	cyp51A AspGDID:ASPL0000106403 COORDS:Chr4_A_fumigatus_Af293:1785311-1783713C, translated using codon table 1 (515 amino acids) Verified ORF; 14-alpha sterol demethylase; commonly mutated in drug r	8.54	9.13	1	3	3	3	515	58.0	8.53
Afu4g08040	Afu4g08040 AspGDID:ASPL0000106518 COORDS:Chr4_A_fumigatus_Af293:2090716-2089786C, translated using codon table 1 (218 amino acids) Uncharacterized ORF; Ortholog(s) have GTP binding activity	8.19	14.22	1	2	2	2	218	23.7	8.54
Afu1g06710	Afu1g06710 AspGDID:ASPL0000101839 COORDS:Chr1_A_fumigatus_Af293:1922660-1920607C, translated using codon table 1 (564 amino acids) Uncharacterized ORF; Ortholog(s) have chaperonin-containing T-co	7.87	7.27	1	2	2	2	564	61.0	6.34
Afu5g01950	Afu5g01950 AspGDID:ASPL0000107375 COORDS:Chr5_A_fumigatus_Af293:500329-499510C, translated using codon table 1 (138 amino acids) Uncharacterized ORF; Ortholog(s) have chromatin binding activity	7.73	19.57	1	3	3	3	138	14.8	10.37
Afu1g04160	Afu1g04160 AspGDID:ASPL0000107595 COORDS:Chr1_A_fumigatus_Af293:1105009-1106759W, translated using codon table 1 (537 amino acids) Uncharacterized ORF; NTF2 and RRM domain protein	7.58	9.87	1	2	2	2	537	56.9	5.19
Afu5g06320	Afu5g06320 AspGDID:ASPL0000107708 COORDS:Chr5_A_fumigatus_Af293:1519087-1518035C, translated using codon table 1 (169 amino acids) Uncharacterized ORF; Ortholog(s) have role in cellular protein locali	6.99	13.02	1	2	2	2	169	19.1	8.34
Afu1g09550	Afu1g09550 AspGDID:ASPL0000102021 COORDS:Chr1_A_fumigatus_Af293:2468785-2469303W, translated using codon table 1 (143 amino acids) Uncharacterized ORF; Ortholog(s) have role in dynein-driven meiot	6.92	22.38	1	2	2	2	143	15.3	5.45
Afu8g05440	atp4 AspGDID:ASPL0000110874 COORDS:Chr8_A_fumigatus_Af293:1265282-1266290W, translated using codon table 1 (274 amino acids) Uncharacterized ORF; Mitochondrial ATPase subunit; hypoxia repressed pr	6.82	8.39	1	2	2	2	274	29.7	9.35
Afu1g09840	tim44 AspGDID:ASPL0000112050 COORDS:Chr1_A_fumigatus_Af293:2554479-2552871C, translated using codon table 1 (515 amino acids) Uncharacterized ORF; Mitochondrial inner membrane translocase subunit	6.67	5.83	1	2	2	2	515	57.7	9.11
Afu6g06345	Afu6g06345 AspGDID:ASPL0000108995 COORDS:Chr6_A_fumigatus_Af293:1347575-1348344W, translated using codon table 1 (205 amino acids) Uncharacterized ORF; Ortholog(s) have 6,7-dimethyl-8-ribityllumaz	6.42	19.51	1	2	2	2	205	21.5	6.10
Afu6g08720	Afu6g08720 AspGDID:ASPL0000109228 COORDS:Chr6_A_fumigatus_Af293:2067644-2066477C, translated using codon table 1 (342 amino acids) Uncharacterized ORF; Putative 5'-methylthioadenosine phosphoryla	6.18	7.31	1	2	2	2	342	37.6	7.39
Afu2g12400	Afu2g12400 AspGDID:ASPL0000103954 COORDS:Chr2_A_fumigatus_Af293:3185304-3186292W, translated using codon table 1 (227 amino acids) Uncharacterized ORF; Putative ATP synthase oligomycin sensitivity	6.01	9.25	1	2	2	2	227	24.4	9.64
Afu5g02850	Afu5g02850 AspGDID:ASPL0000107464 COORDS:Chr5_A_fumigatus_Af293:754834-756051W, translated using codon table 1 (324 amino acids) Uncharacterized ORF; Has domain(s) with predicted arylformamidase	5.93	12.65	1	3	3	3	324	36.3	5.21
Afu4g03322	Afu4g03322 AspGDID:ASPL0000365151 COORDS:Chr4_A_fumigatus_Af293:944673-943800C, translated using codon table 1 (257 amino acids) Uncharacterized ORF; Ortholog of <i>A. nidulans FGSC A4</i> : AN7	5.88	8.95	1	2	2	2	257	28.9	4.87
Afu3g10240	Afu3g10240 AspGDID:ASPL0000105422 COORDS:Chr3_A_fumigatus_Af293:2649693-2642482C, translated using codon table 1 (2327 amino acids) Uncharacterized ORF; Ortholog(s) have cytosol, nucleus localizatio	5.87	1.12	1	3	3	3	2327	259.0	5.95
Afu5g07370	Afu5g07370 AspGDID:ASPL0000107811 COORDS:Chr5_A_fumigatus_Af293:1844081-1842511C, translated using codon table 1 (500 amino acids) Uncharacterized ORF; Ortholog(s) have metal ion binding, poly(A)-s	5.76	4.60	1	2	2	2	500	53.8	7.08
Afu5g05680	Afu5g05680 AspGDID:ASPL0000107645 COORDS:Chr5_A_fumigatus_Af293:1322763-1324274W, translated using codon table 1 (464 amino acids) Uncharacterized ORF; Ortholog(s) have translation release factor a	5.72	4.96	1	2	2	2	464	51.9	6.48
Afu2g04710	Afu2g04710 AspGDID:ASPL0000103297 COORDS:Chr2_A_fumigatus_Af293:1288894-1287776C, translated using codon table 1 (217 amino acids) Uncharacterized ORF; Has domain(s) with predicted heme binding a	5.53	10.14	1	2	2	2	217	23.9	5.59
Afu3g11300	prs2 AspGDID:ASPL0000105528 COORDS:Chr3_A_fumigatus_Af293:2959483-2958408C, translated using codon table 1 (254 amino acids) Uncharacterized ORF; Putative proteasome component	5.48	12.99	1	3	3	3	254	27.9	6.38
Afu1g02150	Afu1g02150 AspGDID:ASPL0000101385 COORDS:Chr1_A_fumigatus_Af293:639645-637892C, translated using codon table 1 (519 amino acids) Uncharacterized ORF; Ortholog(s) have glycerol-3-phosphate dehydro	5.35	8.09	1	2	2	2	519	56.4	8.19
Afu1g09930	gcy1 AspGDID:ASPL0000102059 COORDS:Chr1_A_fumigatus_Af293:2570399-2571627W, translated using codon table 1 (349 amino acids) Uncharacterized ORF; Putative glycerol dehydrogenase; protein level decre	5.02	5.73	1	2	2	2	349	39.1	8.84
Afu6g04010	Afu6g04010 AspGDID:ASPL0000108856 COORDS:Chr6_A_fumigatus_Af293:901498-904822W, translated using codon table 1 (962 amino acids) Uncharacterized ORF; Ortholog(s) have importin-alpha export recepto	4.77	3.22	1	2	2	2	962	108.4	5.38
Afu6g03440	Afu6g03440 AspGDID:ASPL0000108799 COORDS:Chr6_A_fumigatus_Af293:738342-736781C, translated using codon table 1 (497 amino acids) Uncharacterized ORF; Putative fructosyl amine; transcript induced by	4.60	4.43	1	2	2	2	497	54.9	5.76
Afu8g03990	Afu8g03990 AspGDID:ASPL0000110734 COORDS:Chr8_A_fumigatus_Af293:855176-851942C, translated using codon table 1 (985 amino acids) Uncharacterized ORF; Have U5 snRNP, cytosol, spliceosom	4.23	3.05	1	2	2	3	985	110.1	5.08
Afu2g13040	grpE AspGDID:ASPL0000104018 COORDS:Chr2_A_fumigatus_Af293:3347479-3346582C, translated using codon table 1 (250 amino acids) Uncharacterized ORF; Mitochondrial co-chaperone; protein level decreases	4.03	11.20	1	2	2	2	250	28.4	8.25
Afu5g03690	Afu5g03690 AspGDID:ASPL0000107547 COORDS:Chr5_A_fumigatus_Af293:987794-986454C, translated using codon table 1 (424 amino acids) Uncharacterized ORF; Have phosphatidylinositol transporte	3.30	7.55	1	2	2	2	424	46.1	4.84
Afu2g09490	Afu2g09490 AspGDID:ASPL0000103667 COORDS:Chr2_A_fumigatus_Af293:2422679-2427552W, translated using codon table 1 (1525 amino acids) Uncharacterized ORF; Eukaryotic translation initiation factor subur	2.86	2.69	1	2	2	2	1525	163.9	9.36
Afu4g07650	cyp6 AspGDID:ASPL0000106480 COORDS:Chr4_A_fumigatus_Af293:1987776-1988776W, translated using codon table 1 (209 amino acids) Uncharacterized ORF; Putative peptidyl-prolyl cis-trans isomerase	2.23	9.09	1	2	2	2	209	22.9	8.28
Afu4g06790	Afu4g06790 AspGDID:ASPL0000106393 COORDS:Chr4_A_fumigatus_Af293:1755480-1756006W, translated using codon table 1 (93 amino acids) Uncharacterized ORF; Ubiquinol-cytochrome c reductase complex 14	2.23	43.01	1	2	2	2	93	11.0	6.32
Afu6g07540	Afu6g07540 AspGDID:ASPL0000109114 COORDS:Chr6_A_fumigatus_Af293:1715811-1713540C, translated using codon table 1 (548 amino acids) Uncharacterized ORF; Ortholog(s) have chaperonin-containing T-co	2.12	3.47	1	2	2	2	548	59.8	5.52

Table S8: HamE-HA (Afu5g13970) interacting proteins at 24 hours of vegetative growth. Proteins of interest are highlighted in yellow.

Table S8: *Aspergillus fumigatus* HamE-HA interacting proteins (Vegetative growth-24 hours)

Accession	Description	Score	Coverage	# Proteins	# Unique Peptides	# Peptides	# PSMs	# AAs	MW [kDa]	calc. pI
Afu5g13970	Afu5g13970 AspGDID:ASPL0000108448 COORDS:Chr5_A_fumigatus_Af293:3651112-3656167W, translated using codon table 1 (1593 amino acids) Uncharacterized ORF; Ortholog(s) have role in	174.79	21.72	1	23	23	48	1593	174.0	9.74
Afu5g01030	Afu5g01030 AspGDID:ASPL0000107285 COORDS:Chr5_A_fumigatus_Af293:267439-266294C, translated using codon table 1 (332 amino acids) Uncharacterized ORF; Putative glyceraldehyde 3-phosphate dehydrogenase; pre	14.30	21.99	1	5	6	6	332	36.1	6.62
Afu5g05710	Afu5g05710 AspGDID:ASPL0000107648 COORDS:Chr5_A_fumigatus_Af293:1330422-1332169W, translated using codon table 1 (487 amino acids) Uncharacterized ORF; Ortholog(s) have pseudouridine synthase activity	13.94	21.36	1	7	7	7	487	54.7	8.59
Afu4g11250	cafA AspGDID:ASPL0000106834 COORDS:Chr4_A_fumigatus_Af293:2943732-2944595W, translated using codon table 1 (287 amino acids) Uncharacterized ORF; Putative carbonic anhydrase; decreased conidiation in the mu	12.54	19.86	1	3	3	3	287	30.8	8.31
Afu3g13400	nop5 AspGDID:ASPL0000105735 COORDS:Chr3_A_fumigatus_Af293:3545829-3547784W, translated using codon table 1 (591 amino acids) Uncharacterized ORF; Putative nucleolar protein	10.70	9.64	1	4	4	4	591	64.5	7.61
Afu2g05650	Afu2g05650 AspGDID:ASPL0000103388 COORDS:Chr2_A_fumigatus_Af293:1582005-1580139C, translated using codon table 1 (604 amino acids) Uncharacterized ORF; Ortholog(s) have asparagine-tRNA ligase activity, role i	10.04	9.27	1	5	5	5	604	68.2	6.14
Afu4g08040	Afu4g08040 AspGDID:ASPL0000106518 COORDS:Chr4_A_fumigatus_Af293:2090716-2089786C, translated using codon table 1 (218 amino acids) Uncharacterized ORF; Ortholog(s) have GTP binding activity	9.79	19.27	1	3	4	4	218	23.7	8.54
Afu4g03860	nip1 AspGDID:ASPL0000106205 COORDS:Chr4_A_fumigatus_Af293:1086172-1088854W, translated using codon table 1 (862 amino acids) Uncharacterized ORF; Eukaryotic translation initiation factor 3 subunit C	9.37	7.77	1	6	6	6	862	97.4	5.14
Afu2g09870	tif35 AspGDID:ASPL0000103703 COORDS:Chr2_A_fumigatus_Af293:2523373-2524473W, translated using codon table 1 (290 amino acids) Uncharacterized ORF; Eukaryotic translation initiation factor 3 subunit G	7.96	16.90	1	3	3	3	290	31.9	8.79
Afu2g03590	Afu2g03590 AspGDID:ASPL0000103186 COORDS:Chr2_A_fumigatus_Af293:956883-956337C, translated using codon table 1 (88 amino acids) Uncharacterized ORF; Putative ribosomal protein S21e; transcript induced by exp	7.42	28.41	1	2	2	3	88	10.0	8.31
Afu6g02830	Afu6g02830 AspGDID:ASPL0000108738 COORDS:Chr6_A_fumigatus_Af293:575599-576182W, translated using codon table 1 (130 amino acids) Uncharacterized ORF; Has domain(s) with predicted oxidoreductase activity, rol	7.23	51.54	1	4	4	4	130	14.4	8.19
Afu6g09990	Afu6g09990 AspGDID:ASPL0000109355 COORDS:Chr6_A_fumigatus_Af293:2459187-2462825W, translated using codon table 1 (1095 amino acids) Uncharacterized ORF; Ortholog(s) have cytosol, nuclear envelope, nuclear n	6.71	5.30	1	5	5	5	1095	121.5	4.73
Afu1g05200	tif32 AspGDID:ASPL0000101689 COORDS:Chr1_A_fumigatus_Af293:1488654-1485294C, translated using codon table 1 (1051 amino acids) Uncharacterized ORF; Eukaryotic translation initiation factor 3 subunit A	6.34	6.47	1	5	5	5	1051	120.2	9.39
Afu5g05680	Afu5g05680 AspGDID:ASPL0000107645 COORDS:Chr5_A_fumigatus_Af293:1322763-1324274W, translated using codon table 1 (464 amino acids) Uncharacterized ORF; Ortholog(s) have translation release factor activity, coo	5.83	5.39	1	2	2	2	464	51.9	6.48
Afu3g11360	Afu3g11360 AspGDID:ASPL0000105534 COORDS:Chr3_A_fumigatus_Af293:2979671-2978196C, translated using codon table 1 (451 amino acids) Uncharacterized ORF; Ortholog(s) have role in ascospore formation, cellular	4.69	7.76	1	3	3	3	451	51.7	5.35
Afu2g04710	Afu2g04710 AspGDID:ASPL0000103297 COORDS:Chr2_A_fumigatus_Af293:1288894-1287776C, translated using codon table 1 (217 amino acids) Uncharacterized ORF; Has domain(s) with predicted heme binding activity	4.47	28.57	1	3	3	3	217	23.9	5.59
Afu2g16020	Afu2g16020 AspGDID:ASPL0000104319 COORDS:Chr2_A_fumigatus_Af293:4237810-4239808W, translated using codon table 1 (566 amino acids) Uncharacterized ORF; Putative heat shock protein; transcript induced during	4.13	4.42	1	2	2	2	566	61.7	6.87
Afu4g10010	Afu4g10010 AspGDID:ASPL0000106715 COORDS:Chr4_A_fumigatus_Af293:2593720-2595242W, translated using codon table 1 (487 amino acids) Uncharacterized ORF; Ortholog(s) have heat shock protein binding activity, r	2.22	5.75	1	2	2	2	487	54.5	5.00
Afu2g11290	Afu2g11290 AspGDID:ASPL0000103844 COORDS:Chr2_A_fumigatus_Af293:2910595-2909786C, translated using codon table 1 (246 amino acids) Uncharacterized ORF; Orotate phosphoribosyltransferase 1; role in pyrimidine	1.88	6.50	1	2	2	2	246	26.0	6.57
Afu2g17000	Afu2g17000 AspGDID:ASPL0000104419 COORDS:Chr2_A_fumigatus_Af293:4544466-4551049W, translated using codon table 1 (2173 amino acids) Uncharacterized ORF; Ortholog of <i>A. nidulans FGSC A4</i> : AN5649,	1.62	4.00	1	5	5	5	2173	224.3	3.99
Afu1g12940	sakA AspGDID:ASPL0000102362 COORDS:Chr1_A_fumigatus_Af293:3428181-3429807W, translated using codon table 1 (366 amino acids) Verified ORF; Putative mitogen-activated protein kinase (MAPK) with predicted roles	0.00	5.19	1	2	2	2	366	41.9	5.60
Afu2g06230	Afu2g06230 AspGDID:ASPL0000103446 COORDS:Chr2_A_fumigatus_Af293:1796803-1795031C, translated using codon table 1 (550 amino acids) Uncharacterized ORF; Ortholog(s) have imidazoleglycerol-phosphate synthas	0.00	3.64	1	2	2	2	550	60.2	5.76
Afu5g05460	Afu5g05460 AspGDID:ASPL0000107625 COORDS:Chr5_A_fumigatus_Af293:1268981-1268053C, translated using codon table 1 (242 amino acids) Uncharacterized ORF; Cytosine deaminase-uracil phosphoribosyltransferase f	0.00	9.50	1	2	2	2	242	26.9	7.77